REPORT ON EQUATORIAL

AERONOMY

Edited by

Fernando de Mendonça

Illustrated Abstracts

PROCEEDINGS OF THE

SECOND INTERNATIONAL SYMPOSIUM

ON

EQUATORIAL AERONOMY

Held at the

Laboratório de Física Espacial
G.O. Comissão Nacional de Atividades Espaciais
Conselho Nacional de Pesquisas

São José dos Campos
São Paulo
Brasil

— 1965 —

Scientific Program Committee

for the II° I.S.E.A.

Prof. R. W. H. Wright, Chairman, (URSI)

Dr. F. de Mendonça, Secretary, (IQSY)
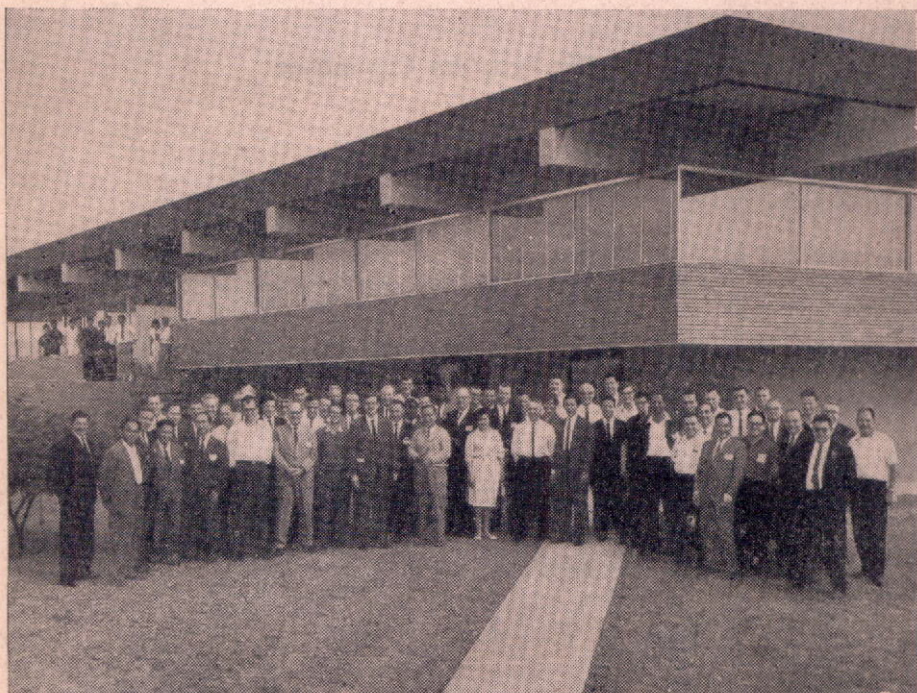
Mr. E. J. Chernosky

Dr. D. T. Farley

Mr. A. Giesecke

Prof. A. J. Lyon

Prof. S. Matsushita

Prof. A. T. Price (IAGA)

Dr. G. Weill (IUGG)

The majority of the participants of the symposium in front of the new auditorium building which was specially designed to provide a functional environment for intense participation of the audience.

The new auditorium shown during one of the sessions

AKNOWLEDGEMENTS

INTRODUCTORY REMARKS

The Second International Symposium on Equatorial Aeronomy took place at the Space Physics Laboratory of the Brazilian Space Commission in São José dos Campos, São Paulo, Brazil, in the period 6-17 of September 1965, and it was sponsored by the following organizations:

— International Association of Geomagnetism and Aeronomy (IAGA)

— International Scientific Radio Union (URSI)

— Comissão Nacional de Atividades Espaciais (CNAE)

— Air Force Cambridge Research Laboratories (AFCRL)

— National Bureau of Standards (NBS-CRPL)

— Consejo Latino Americano de Física Espacial (CLAFE), and

— Voice of America

Close to a hundred invited scientists from twenty countries participated in the discussions and presented over a hundred papers distributed in the eleven topics listed on the table on contents. Each session was led by a "discussion leader" who helped to motivate discussions by playing an active role and conveying to the meeting an atmosphere of factfinding debates. Sessions were started with reviews which were followed by papers interspersed with comments. At the final session, résumés of discussed topics were presented by summarizers.

The Scientific Program Committee decided to present the results of the meetings in two types of publications. The **full papers** are to appear in the **Annale de Geophysique** regular issues of March and June 1966 and the **illustrated abstracts** are presented herein. This decision was made during the Symposium and the participants were requested to draft their abstracts (reviews, short papers and summaries) and provide their slides on loan for reproduction as figures. We must thank the participants for their full cooperation with respect to this request.

Considering that (a) most of the material was provided in handwritten form, (b) many of the slides had to be subjected to redrafting and (c) the authors did not have an opportunity to recheck their work, it is imperative that referencing should be done **only** with the authors' permission.

The main objectives of this report are first to provide the scientific community, in a short time (10 weeks) after the symposium, with the state of knowledge in the various topics encompassed by equatorial aeronomy and second to present investigators in the field, principally the ones working in isolated places, with some elements for planning future research. To attain this end we shall transcribe in the following pages the **Recommendations** adopted at the Symposium, which according to Dr. C.M. Minnis, Secretary of the IQSY Committee, "... come at a particularly appropriate time since they appear near the close of the IQSY programme and provide a guide to some of the directions in which research workers ought to turn their attention from now onwards".

A decision was made based in the general consensus of the participants at the final meeting about holding the Third International Symposium on Equatorial Aeronomy in 1968, possibly in Africa. The desirability of such symposia is possibly best described by Prof. S. Chapman, in his trip report, to NASA and the U. S. Academy of Sciences:

..."In these various fields workers at small universities physics department and observatories in tropical countries can make valuable additions to science, enriching the results given by the much more costly forms of explorations. These equatorial aeronomy symposia give many scattered individuals and small groups a very useful and stimulating opportunity of meeting with American and European and Japanese scientists working in this field"...

Finally, in the preparation of this report one would have to compromise between the issuance date and the amount of small errors that could be tolerated; in view of the objetives perfection was sacrificed.

F. de Mendonça

RECOMMENDATIONS

D-region

1 — The Symposium notes that the knowledge of the value of collisional frequencies and electron densities in the D region near the equator is extremely sparse. The Symposium recommends that experiments designed to remedy this deficiency should be given high priority.

2 — The Symposium notes that the study of VLF transmissions at short range can give considerable information about the structure of the D-region, and that suitable transmitters are available at Panama and in Hawaii. The Symposium recommends that simple observations of the phase and amplitude of the skywave be made at distances of order 100 km using these transmissions in order to determine the differences between the ionized structures in the region and those found at temperate latitudes.

3 — The Symposium notes that LF navigational aid systems have been set up in tropical regions, and that the propagation of sky waves from these regions is different from that found at temperate latitudes, in particular showing great differences with azimuth relative to the earth's magnetic field. The Symposium recommends observations on the skywave at short and medium distances so as to give quantitative measures of these phenomena for practical use and in addition information on the structure of the D-region.

4 — The Symposium draws attention to the desirability of measuring meteorological parameters, in particular temperature and density or pressure, in the D and E regions at low latitudes and associating these with ground based measurements of radio-wave absorption and of the heigth and shape of the E layer.

Ionospheric Absorption

5 — The Symposium notes that there are discrepancies between the A1 pulse absorption values of different longitudes near the magnetic equator, which appear large compared with the experimental errors. The Symposium recommends that every effort be made to investigate them by increasing the number of observing stations. In particular a station is needed in the South American Sector.

6 — The Symposium recommends that A1 absorption measurements be made at a number of sites, in a convenient sector on a line perpendicular to

the magnetic equator, in order to examine further the latitude variation of the equatorial absorption anomaly reported by Flügel.

7 — The Symposium recommends that multifrequency A1 and A2 measurements should be made simultaneously at a number of sites in order to determine the relative contribution to the total absorption of the various ionosphere regions. It will be necessary to use the full waves theory to compute the deviative absorption.

Airglow

8 — The Symposium notes the need for more precise definition of the intensity variations and spatial movements of airglow emissions. The Symposium recommends that studies be carried out using chains of ground stations, aircraft measurements and observations from satellites.

9 — The Symposium notes that the airglow measurements provide a higher spatial resolution of phenomena associated with recombinations than the ionospheric methods. The Symposium recommends that further and more detailed studies be undertaken into the correlation of airglow emission intensities with ionospheric parameters.

10 — The Symposium recommends that studies be made of airglow emissions at magnetically conjugate stations. The stations Maui and Raratonga should be particularly valuable in this respect.

11 — The Symposium recommends that observations on dayglow by ground based and rocket equipment should be extended to equatorial regions.

12 — The Symposium notes the extremely interesting results obtained from observations on the 5577 A and 6300 A lines in the airglow emissions. It recommends that investigations should be extended to other lines, such as 5200 A (NI), 5893 A ($N_a I$), 2972 A (OI) and the O H bands.

E region and Es

13 — The Symposium notes that there is a wide discrepancy between values of the recombination coefficient in the E layer. The Symposium recommends that attention be paid to experiments to resolve this discrepancy.

14 — The Symposium notes that the behavior of the electron density between the peak of the E layer and the bottom of the F layer is poorly understood. The Symposium recommends that theoretical studies should be undertaken with this point in view.

15 — The Symposium recommends that in theoretical studies of the formation of the irregularities in Equatorial Es particular attention should be paid to a non-linear treatment of the problem.

16 — The Symposium recommends that further studies of the Equatorial E_s irregularities, at other equatorial locations, should be made using the Doppler techniques developed at Jicamarca. Observations at multiple frequencies would be extremely desirable.

17 — The Symposium notes that it would be possible to examine the equatorial Es belt by top-side sounding techniques, and recommends that the possibility be examined further.

18 — The Symposium express its regret at the meagre nature of equatorial results from rocket observations presented here. The Symposium recommends that more equatorial data should be obtained from rocket firings, especially of the electron density N_e, and electron temperature T_e profiles.

Current system, electrojet and magnetic effects

19 — The Symposium notes that the magnetic effects of the electrojet phenomena are quite complex. The Symposium recommendts that every effort should be made to increase the number of simultaneous observations of the variations of all three magnetic elements at permanent and temporary stations near the dip equator.

20 — The Symposium notes that there is considerable variations of the equatorial S_q current system ranges with longitude, and that there is evidence of temporal changes in intensity and width of the electrojet. The Symposium recommends that efforts should be made to study a sample length of the electrojet by organized simultaneous observations for a period of one or more months of the variations of H, D, Z at the three permanent stations in Africa, together with two or more temporary stations, all as near the dip equator as possible.

21 — The Symposium notes the large ranges of S_q (H) observed at Nairobi and elsewhere in East Africa, and the observed asymmetry of the ranges along a N-S line crossing the dip equator in several regions. The Symposium recommends that a special effort be made to get simultaneous observations at a number of stations along a roughly N-S line crossing the dip equator in East Africa and also in India and Ceylon. The lines should extend over a latitude range of at least 30°.

22 — The Symposium recommends that the International Association of Geomagnetism and Aeronomy be asked to make recommendations clarifying

many of the terms used in geomagnetism including, for example, the names of the various equators and the different measures used for ranges of the daily variations.

Regular F region

23 — The Symposium notes the need for more information concerning the values of the electron and ion temperatures (T_e, T_i) and electron and ion concentration (N_e, N_i) throughout the F region. It recommends that observations by ground-based, sounding rocket and satellite, should be intensified to provide these data.

24 — The Symposium recommends that experiments should be carried out to measure plasma velocities in the F region.

25 — The Symposium recommends that experiments should be carried out to measure the particle fluxes, particularly electrons in the 10 ev to 20 Kev energy range.

26 — The Symposium notes the need for further morphological studies of the F region based on ground-based, sounding rocket and satellite observations, and including ionospheric and airglow measurements. The Symposium recommends that the large gaps in bottom-side studies in the large ocean area, especially the Pacific, should be studied and filled if at all possible.

27 — The Symposium notes the development of the theoretical studies of the regular equatorial F region which predict equatorial behavior similar to that observed. The Symposium recommends the continuance of this work particularly with a view to achieve better agreement with observations, including both average variations and day-to-day variations.

F region Disturbances and Irregularities

28 — The Symposium recommends further study of the topside irregularities and their relation to the bottom-side irregularities.

29 — The Symposium notes the lack of any in situ measurements of the irregularities and their parameters. It recommends that efforts should be made to design and carry out experiments capable of doing this.

30 — The Symposium recommends that efforts should be made at suitable sites to observe the irregularities responsible for "conjugate ducting" as observed from the topside.

31 — The Symposium recommends that more measurements should be made on the very small scale irregularities often observed in the F region using VHF methods and studying the frequency spectrum.

32 — The Symposium notes the need for more contact between ionospheric workers and those in the field of plasma theory. It recommends that such contact should be encouraged in general, and in particular a theoretical search should be carried out for appropriate plasma instabilities which might explain the formation of F region irregularities.

Ionospheric Drifts

33 — The Symposium notes that the origin of irregularities in the E and F region is poorly understood. It recommends that in order to better understand the significance of the drift observations more effort be put into a theoretical study of the formation of these irregularities.

34 — The Symposium notes the importance of a knowledge of vertical drifts in the equatorial F region, particularly for arriving at a theoretical understanding of the latitudinal electron-density distribution, and recommends that every effort be made to obtain measurements of the vertical drifts.

35 — The Symposium recommends that wherever possible horizontal drifts be studied not only by the spaced antenna techniques but also by simultaneous radar observations of the frequency spectrum of the scattered echoes.

Magnetic and Ionospheric Storms

36 — The Symposium notes that there was no satisfactory theoretical model of a storm. It recommends that further theoretical studies should be carried out on this problem, and, in order to facilitate the testing of such models there is a need for more measurements of ionospheric currents and drifts, and more knowledge of the topside ionosphere, exosphere, and magnetosphere such as may be obtained from rockets and satellites.

37 — The Symposium notes the difficulties inherent in examining magnetic results from restricted data. It recommends that magnetic data need to be examined comprehensively, using all components and many stations before unique interpretations can be obtained.

38 — The Symposium recommends that efforts be made to obtain average storm duration during different parts of the sunspot cycle, and the influence of ionospheric conductivity effects and induction effects on storm-time variations.

Magnetic Pulsations

39 — The Symposium notes the importance of establishing the characteristics of low latitude pulsations, particularly those regular oscillations of shorter period. The Symposium recommends that further measurements of micropulsations in equatorial latitudes be encouraged. Where possible two or more stations should be operated simultaneously so that phase lags on either side, and under, the equatorial electrojet may be determined. Attempts should also be made to relate equatorial pulsations to ionospheric time-varying parameters.

Forthcoming Eclipse

40 — The total eclipe of November 12, 1966 is of extraordinary scientific importance as it is th least this century which will affect the electrojet region in South America and the peculiar characteristics of the atmosphere above the continent. Starting in the Pacific Ocean off the coast of Ecuador, the path of totality crosses Peru, Chile, Bolivia, Argentina, Paraguay and Brazil. Accordingly, the II International Symposium on Equatorial Aeronomy recommends to the International Scientific Unions and to the governments of South America that they give their valued cooperation to the world scientific community interested in making detailed observations of this rare phenomenon. The governments can assist materially by facilitating the anticipated mobilization of international scientists and their equipament within their respective territories and airspace, and by providing support to the scientists and scientific institutions of their own countries.

The Symposium also notes with pleasure the formation of a Working Group of the **CLAFE** (Consejo Latino Americano de Fisica del Espacio) to maximize the effectiveness of observations by scientists of Latin America and to enhance cooperation among the world scientific community.

CONTENTS

XI — LOW LATITUDE MAGNETIC PULSATIONS

I — THE D-REGION AND LOWER

ATMOSPHERE

I — THE D-REGION AND LOWER ATMOSPHERE

(Discussion leader: Raymond W. Wright)

Review Paper

Formation of the Equatorial Ionospheric D region

by

A. C. Aikin

Goddard Space Flight Center — NASA
Greenbelt, Md., U.S.A.

Introduction

The geographic distribution of D Region ionization can be described by considering three zones. These are:

1) The high latitude zone where because of the large magnetic dip angle auroral particles and solar protons impinge on the atmosphere and strongly affect the distribution of ionization. Seasonal changes in the pressure and temperature of the neutral atmosphere are observed. These changes are reflected in such pressure dependent observables as the electron-neutral collision frequency.

2) A middle latitude zone where particle effects occur only during the most extremely disturbed solar conditions. There are still seasonal dependencies as evidenced by Bosolasco and Elene's (1) correlation between stratospheric temperature and radio wave absorption. Beynon and Jones (2) have confirmed this correlation and suggest that it may be the cause of the winter anomaly in the mid-latitude D Region. Aikin et al. (3) have observed directly by means of rocket experiments a change of 50% in collision frequency during a period of one month in the spring of 1963.

3) The equatorial zone should be characterized by the absence of particle ionization and by a stable atmosphere. Under such conditions the discussion of formation of the equatorial D Region may be restricted to the ionizing effect of solar Lyman alpha and X-rays and ionization by cosmic rays.

Sources of Ionization and Their Variations

Thus at middle and equatorial latitudes there are three sources of ionization which need be considered, 2-8A X-rays, Lyman α at 1215.6 A, which ionizes nitric oxide, and cosmic rays. Nicolet and Aikin (4) presented a

comprehensive picture of the formation of the D region taking into account the ion chamber data on solar X-ray variations of the Naval Research Laboratory. These data (5) showed that variations in the solar X-ray flux were responsible for the increase ionization observed during solar flares. Satellite observations show no appreciable increase in Lyman alpha flux during such events. In fact, measurements of Lyman alpha covering most of the last solar cycle using the ion chamber technique do not show variations of more than 100% in the Lyman alpha flux. A value of 4.5 ergs/cm²/sec was obtained by the OSO I satellite in 1963.

In Table I we show the X-ray wavelength bands and the flux values as assumed by Nicolet and Aikin (4). In Figure 1 the modification of the D-region due to such increases in the X-ray flux is shown. Strong flares are also a source of wavelengths shorter than 2 A which may affect the D region below 70 km.

TABLE I

The variation of solar X-ray flux with activity of the sun

Condition of the sun	2A	4A	6A
Solar Minimum	10^{-8}	10^{-7}	10^{-6}
	10^{-7}	10^{-6}	10^{-5}
Solar Maximum	10^{-6}	10^{-5}	10^{-4}
	10^{-5}	10^{-4}	10^{-3}
Flares	10^{-4}	10^{-3}	10^{-2}
	10^{-3}	10^{-2}	10^{-1}

Energies in erg/cm²/sec.

Fig. 1 — The electron density in the D region for different solar conditions.
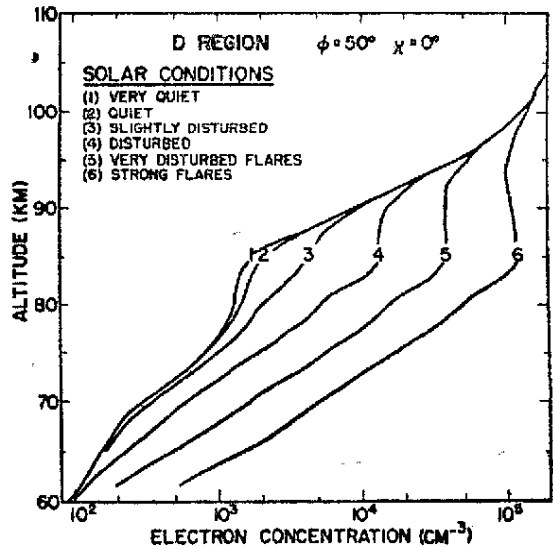
The cosmic ray production function varies by a factor of ten with latitude reaching a minimum value of 23 ion pairs/cm²/atmospheres at the geomagnetic equator. There is also a factor of 2 in variations with sunspot cycle; the minimum flux occuring at the solar sunspot maximum. Figure 2 illustrates the latitude variation of the D-region cosmic ray layer based on the loss process and values given in Table II. This layer, which has its maximum effect below 70 km, strongly affects the reflection and absorption of VLF waves. Thus one would expect VLF propagation across the equator to differ from that at higher latitudes due to the smaller cosmic ray layer at the equator.

TABLE II

Reactions considered in the calculation of the D region models showing the variation of electron density with geomagnetic latitude

Reaction						Symbol	Value
XY	$+$	$h\nu$	$\rightarrow$	X $Yplus$ $+$	e	q	
e	$+$	$2O_2$	$\rightarrow$	O^-_2	$+$ O_2	a	1.5×10^{-35} $n\,(O_2)$ cm⁶/sec
O^-_2	$+$	$h\nu$	$\rightarrow$	O_2	$+$ e	d	0.44 sec⁻¹
O^-_2	$+$	O	$\rightarrow$	O_3	$+$ e	f	10^{-13} cm³/sec
X $Yplus$	$+$	e	$\rightarrow$	X'	$+$ Y'	a_D	N_2 $\quad$ O_2 $\quad$ NO
							6×10^{-7} 4×10^{-7} 3×10^{-8} cm³/sec
X $plus$	$+$	Y^-	$\rightarrow$	X	$+$ Y	a_i	10^{-8} cm³/sec
N^-_3	$+$	O_2	$\rightarrow$	O_2 $plus$	$+$ N_2		2×10^{-10} cm³/sec
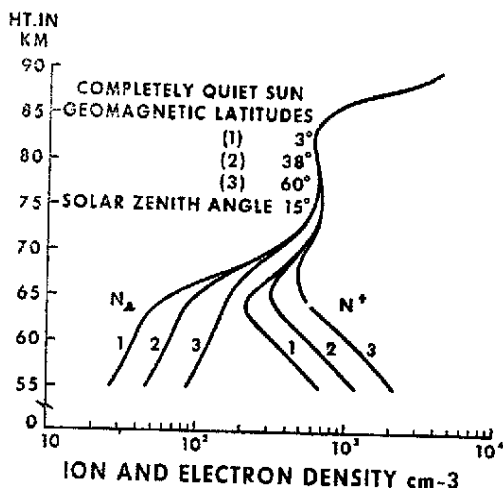
Fig. 2 — The positive ion and electron density distribution for three geomagnetic latitudes

Loss Processes

Based mostly on laboratory measurements the loss processes in the D region are summarized in Table II. The most important processes are

1) three-body attachment of electrons to molecular oxygen.
2) photodetachment from O_2
3) Ion-ion recombination
4) dissociative recombination for positive ions and electrons.

Using all these processes except the charge exchange reaction and the ionization sources discussed earlier, Nicolet and Aikin (4) predicted the ion and electron density distribution for various solar conditions. Figure 3 illustrates the altitude distribution of the various ionic species for a completely quiet sun and with an NO density distribution of 10^{-10} n (M) and an α_{DX} of 3×10^{-9} cm sec^{-1}.

Current Problems

Several recent measurements have shown that the theory presented above is in need of modification. The first of these measurements is the positive ion composition as function of altitude which has been reported by Narcisi and Bailey (6) and is illustrated in Figure 4. Prominent in the mass spectra are 18

plus (presumably water vapor) and 37 plus together with 30 plus and 32 plus, 28 plus which corresponds to N_2 plus is not observed and O_2 plus only becomes comparable to NO plus at 83 km. There are also ions of mass > 44 plus.
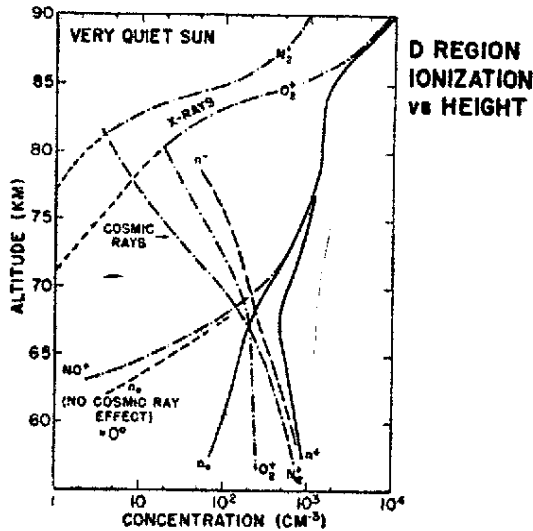
Fig. 3 — The distribution of positive and negative ions and electrons as predicted by Nicolet and Aikin (4)
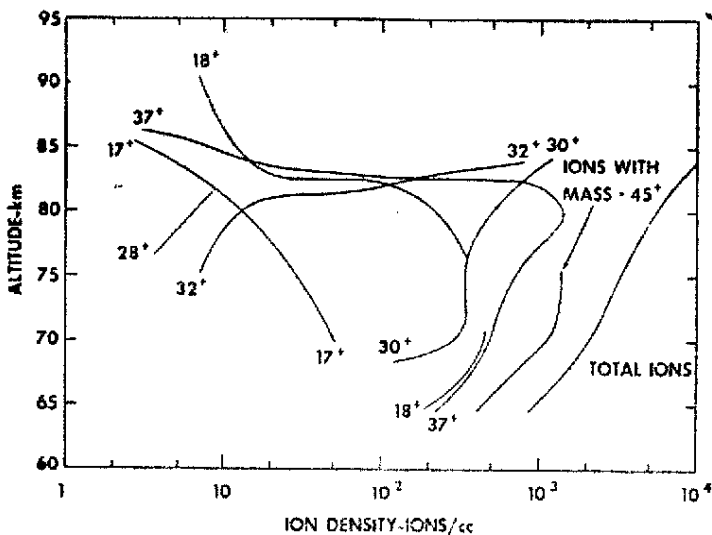
Fig. 4 — Ion composition in the D region as measured by Narcisi and Bailey (6)

The absence of N_2 plus and the [O_2 plus]/[NO plus] ratio of order unity at 85 km can be explained by simply introducing the reactions for charge exchange and ion-atom interchange shown in Table III into a low solar activity model of the D region. The rate coefficients are either consistent with or identical to the laboratory measurements of Ferguson. Even for NO densities as great as 10^9 cm^{-3}, the last two reactions are negligible in comparison with those involving N_2 and O_2. There is as yet no theory which explains the existence of 18 plus and 37 plus in the D region.

TABLE III

Ion-molecule reactions occuring in the D region

Reaction Rate (cm^3 sec^{-1})

N_2 plus	+	O_2	$\rightarrow$	O_2	plus	+	N_2	1 x	10^{-10}
N_2 plus	+	O_2	$\rightarrow$	NO	plus	+	NO	1 x	10^{-16}
N_2 plus	+	NO	$\rightarrow$	NO	plus	+	N_2	4 x	10^{-10}
O_2 plus	+	N_2	$\rightarrow$	NO	plus	+	NO	1 x	10^{-18}
O_2 plus	+	NO	$\rightarrow$	NO	plus	+	O_2	8 x	10^{-10}

The second pertinent experiment involves the observation by Barth (7) of the ultraviolet dayglow spectra of the gamma bands of nitric oxide. The most intense bands were the (2,0) at 2053A, the (1,1) at 2246A, the (0,0) at 2269A, the (0,1) at 2370A and the (0,2) at 2479A. From an analysis of the intensity variation of these bands with height a volume density distribution was deduced. This is illustrated in Fig. 5.

Also illustrated in this figure are the theoretical distributions which would be the result of chemical and ionospheric reactions. In order to derive the theoretical distribution of nitric oxide, it is necessary to consider the various processes as has been done by Nicolet. In Table IV we have listed those processes which are usually considered in any calculation. For sufficiently large amounts of atomic nitrogen the most important processes are

$$N + O_2 \rightarrow NO + O$$

and
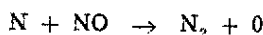
$$N + NO \rightarrow N_2 + O$$

These result in an NO density which is proportional to the molecular oxygen concentration.

TABLE IV

Processes of importance in the distribution of nitric oxide

NO	+	$h\nu$	$\rightarrow$	N	+	0		δNO
NO	+	$h\nu$	$\rightarrow$	NO plus	+	e		I_{NO}
NO plus	+	e	$\rightarrow$	N	+	0		a_{DNO}
N	+	NO	$\rightarrow$	N_2	+	0		b_2
N	+	O_2	$\rightarrow$	NO	+	0		b_1
N_2	+	$h\nu$	$\rightarrow$	N_2 plus	+	e		I_{N2}
N_2 plus	+	e	$\rightarrow$	N	+	N		a_{DN2}

Returning to Table III showing the ionic reactions we note that these can affect the nitric oxide distribution by increasing the density. Calculations have been carried out by Nicolet (8) and his resulting distributions are shown in Figure 5. These distributions compare favorably with those of Barth, and explain Narcisi's and Bailey's spectrometer results. Also shown are possible distribution base on mixing which prevails below the mesopause.
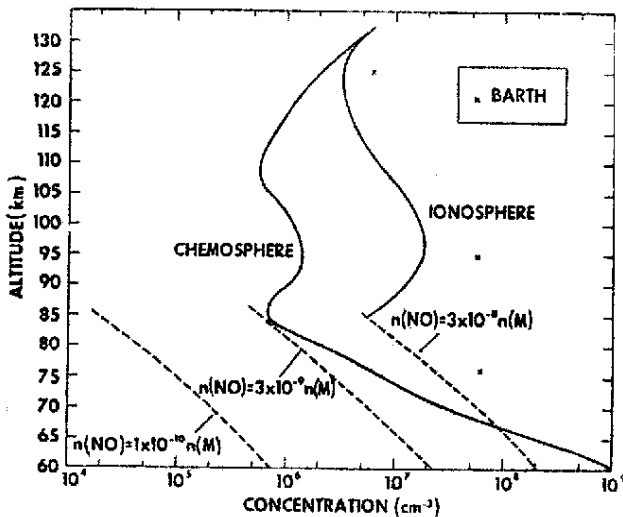
Fig. 5 — The nitric oxide distribution in the 60 to 130 km altitude range

In Figure 6 we illustrate the production functions which would be consistent for each of the distributions given in the previous figure. The cosmic ray and X-ray production functions were chosen to represent a quiet solar period in March 1963 over Wallops Island, Va., geomagnetic latitude 50°. Curve 3 is based on Barth's observations, 2 is consistent with photochemical equilibrium using recent values of rate coefficients, and curve 1 is based on the value used by Nicolet and Aikin which was also illustrated in Fig. 5. It is important to note the cross-over points between the cosmic ray and Lyman alpha production functions. By observing the position of the minimum in the ion and electron density distribution it may be possible to determine the required NO density for a particular solar condition.
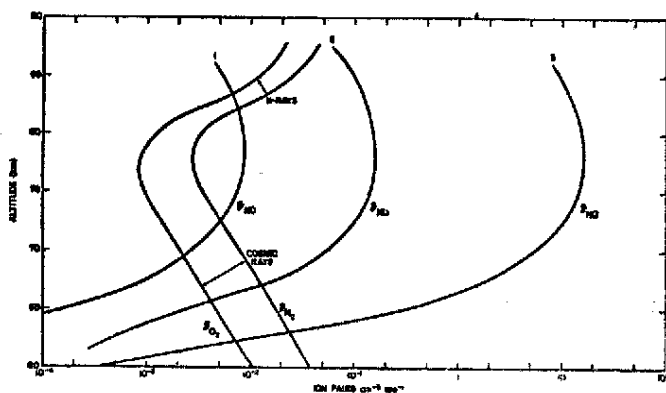
Fig. 6 — Calculated ionization production function versus altitude. Curves labeled 1, 2 and 3 show the effect of Lyman alpha flux on three different nitric oxide distributions

In Figure 7 is shown the electron density distribution for which the production functions shown in Fig. 6 were calculated. This profile was obtained by means of a radio propagation experiment involving transmission to a rocket-borne receiver. There appears a minimum at 70 km which presumably is the cross-over between Lyman alpha and cosmic ray ionization, if the recombination processes are reasonably constant in this altitude range. Another minimum occurs at the level of the mesopause. Chapman and Kendall have recently shown how dust may be trapped at the mesopause level to form a layer. A sufficiently large concentration of dust can affect the electron and ion density distribution by collecting charged particles.

By comparing the electron density at 80 km with the different production functions in Fig. 6 we can arrive at estimates of the effective recombination coefficient required for each of the nitric oxide distributions shown in Fig. 5. These are given in Table V.

TABLE V

Curve	n (NO) cm^{-3}	α (cm^3/sec)
1	4×10^4	2×10^{-8}
2	6×10^5	3×10^{-7}
3	6×10^7	3×10^{-6}
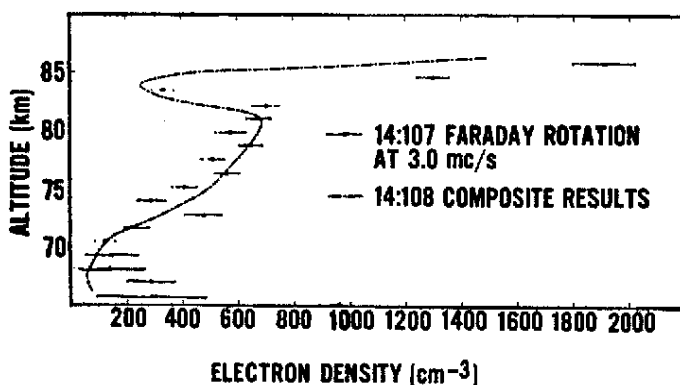
Fig. 7 — Electron density versus altitude for March 8, 1963. Each points is the average electron density in an altitude interval of approximately 1 km. The horizontal bar indicates the uncertainty due to the standard deviation in the scatter of the data used to determine the average value.

If negative ion processes can be neglected, then α is a measure of the dissociative recombination coefficient for NO plus. There are no satisfactory laboratory measurements available. From data at higher altitudes a negative temperature coefficient is indicated. This implies that at 80 km values greater than 10^{-7} cm^3 sec^{-1} might be expected. The Nicolet calculation and Barth's data would require values higher than 10^{-6} cm^3 sec^{-1}. Thus new loss mechanismus must be introduced if the large densities of NO are accepted.

The need for introducing a new set of loss processes is also indicated by studying the formation of the D region around sunrise. Investigations of this type were first carried out by the Cambridge group using VLF wave propagation. By observing the phase and amplitude variations of the received waves they were able to deduce that just after layer sunrise ($\chi = 98°$) a layer centered at about 70 km was formed. The origin of this region is photodetachment of negative ions in the cosmic ray layer. At ground sunrise Lyman alpha is able

to begin penetrating into the D region.   In Figure 8 calculations of this effect
are presented.   Deeks (9) has continued the analysis of VLF data.   His analysis
of phase and amplitude changes have led to the profiles shown in **Figure 9**.
However recent data by Sechrist indicate that on certain occasions the formation
of the cosmic ray layer does not occur until after ground sunrise.
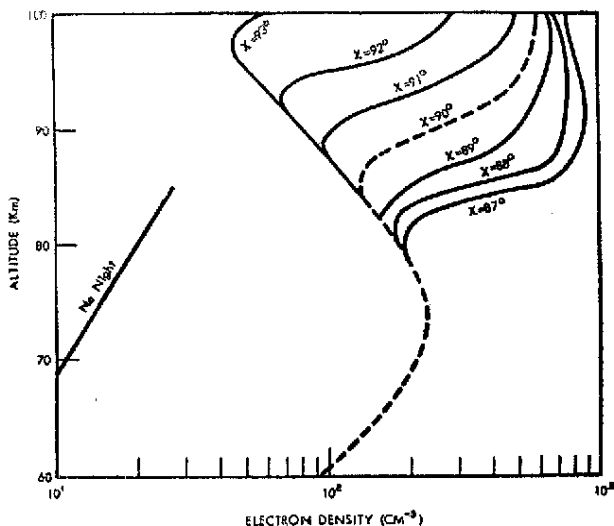
Fig. 8 — Predicted electron density distribution in the D region during sunrise
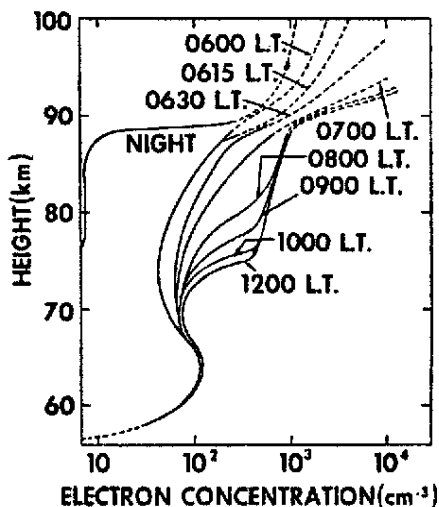
Fig. 9 — Electron density
distribution in the sunrise D-region
as derived from VLF phase
amplitude records by Deeks.

Using a nose-tip probe on a rocket Bowhill and Smith have made a study of the sunrise effect over Wallops Island. The results of their study is given in Fig. 10. If the probe current is an indication of changes in electron density only, then it appears that a negative ion which is photodetached by wavelenghts shorter than 3000 A is required. This evidence is consistent with riometer observations of the diurnal variations of absorption during polar cap events. The results are not in agreement with earlier VLF measurements which indicate that the C layer is formed when light is incident at 70 km.

It has been suggested that negative ions such as O_3^- and NO_2^- may be the dominant species of negative ion. Different processes which may play a role in the formation of such ions are listed in Table VI.

TABLE VI

Negative ion reactions of possible importance in the D region

REACTION	RATE
e + $2O_2$ → O_2^- + O_2	1.4×10^{-30}
e + O → O^- + $h\nu$	1.3×10^{-15}
e + O_2 → O_2^- + $h\nu$	$\ll 10^{-18}$
O_2^- + $h\nu$ → O_2 + e	$\sigma\lambda_{6200} = 1.1 \times 10^{-18}$
	$< \sigma P > = 0.44$
O^- + $h\nu$ → O + e	$\sigma_{4000} < \lambda < 6000 = 6.3 \times 10^{-18}$
	$< \sigma P > = 1.4$
NO_2 + $h\nu$ → NO_2 + e	$\lambda < 5000A$
O_2^- + O_2 → $2O_2$ + e	4×10^{-20}
O_2^- + O → O_3 + e	$\leq 10^{-10}$
NO plus + O_2^- → Neutrals	$10^{-7} - 10^{-8}$
NO plus + NO_3^- → Neutrals	2×10^{-7}
O^- + NO_2 → O + NO_2^-	10^{-10}
O_2^- + O_2 → O_3^- + O	....
O_3^- + O → O_2^- + O_2	....
O_2^- + O → O^- + O_2	....
O^- + $2O_2$ → O_3^- + O_2	9×10^{-31}
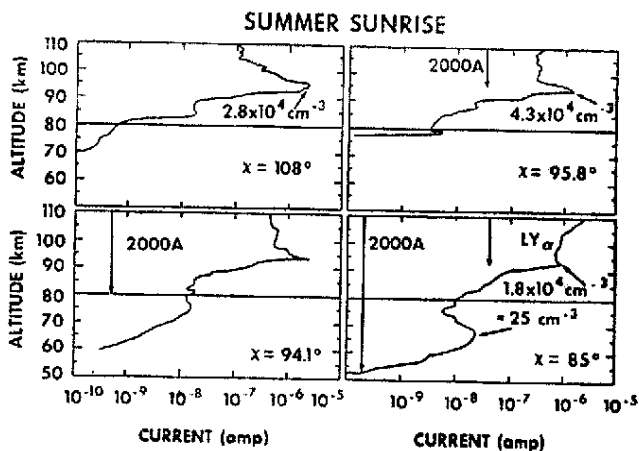
Fig. 10 — Current to a rocket-borne DC probe for different solar zenith angles. Also shown is the depth of penetration of 2 000A and Lyman alpha radiation for each of the solar zenith angles.

Conclusion and Recommendations

The D-region is the least understood of all the ionospheric layers. This is due largely to a deficiency in measurements of quantities such as the electron and positive and negative ion density. To date there have been only two measurements of the positive ion composition and none of the negative ion. There are no electron density profiles determined at equatorial latitudes. In order to have a better understanding of this important portion of the ionosphere emphasis must be placed on experiments to measure these parameters.

REFERENCES

1. Bossolasco, M. and A. Elena — Compt. Rend. T 256 (21), 4491 — 4493, (1963)
2. Beynon, W. J. G. and E. S. O. Jones, Nature, **206**, 4990, 1242 — 1243, (1965)
3. Aikin, A. C., J. A. Kane and J. Troim — J. Geophys. Res. **69** n° 21, 4621, 1964
4. Nicolet, M. and A. C. Aikin, J. Geophys. Res., **65**, 1469 — 1483, (1960)
5. Chubb, T. A., Friedman, H., Kreplin, R. W. and Kupperiam, J. E. — J. Geophys. Res. **62**, 389 (1957)

6. Narcisi, R. S. and A. D. Barley, U. S. Air Force Cambridge Research Laboratories Report 65 — 81, 1965

7. Barth, C. A. — **Space Research V**, North-Holland Publishing Co., 767, (1965)

8. Nicolet, M. — J. Geophys. Res., **70**, (1965)

9. Deeks, D. K. — Internal Memorandum R.S.R.S. (Slough), 1965

10. Bowhill, S. A. and L. G. Smith — **Space Research VI** (to be published)

LOW FREQUENCY BACKGROUND FLUCTUATIONS AT

HUANCAYO, PERU

by

W. Barron and J. Aarons

Air Force Cambridge Research Laboratories
Bedford, Massachussetts — U.S.A.

A. Katz

Boston University
Boston, Massachussetts — U.S.A.

A. A. Giesecke and P. Bandyopadhyay

Instituto Geofísico del Perú
Huancayo — Perú

The observations of ELF signals in the range 5-10,000 Hz is currently the subject of a cooperative program between the Instituto Geofísico del Perú and AFCRL. The aim of the program is to study the diurnal and seasonal variations of the background signal in this range and to investigate the possibilities of detecting long lasting emissions of natural origin in the equatorial zone. Similar equipment was used in a study by Gustafsson, Egeland and Aarons [J.G.R. 65, 2749, 1960].

The experimental equipament used for this study is a slowly sweeping spectrum analyzer with a bandwidth of 2 Hz in the range 5-1000 Hz, and in the range 500-10,000 Hz (its two ranges). A vertical whip antenna of 10 meters is used and the amplifier with a sweep duration of one hour for the two bands records pulses with a time constant of one second.

A typical series of records taken in October, 1964 in the low range (5-1000 Hz) is shown in Fig. 1. During the post midnight hours, the 300-1000 Hz portion of the spectrum showed low amplitude levels; during the post-sunrise period spotty or stormy records are observed. A relatively uniform signal is seen in the late afternoon.
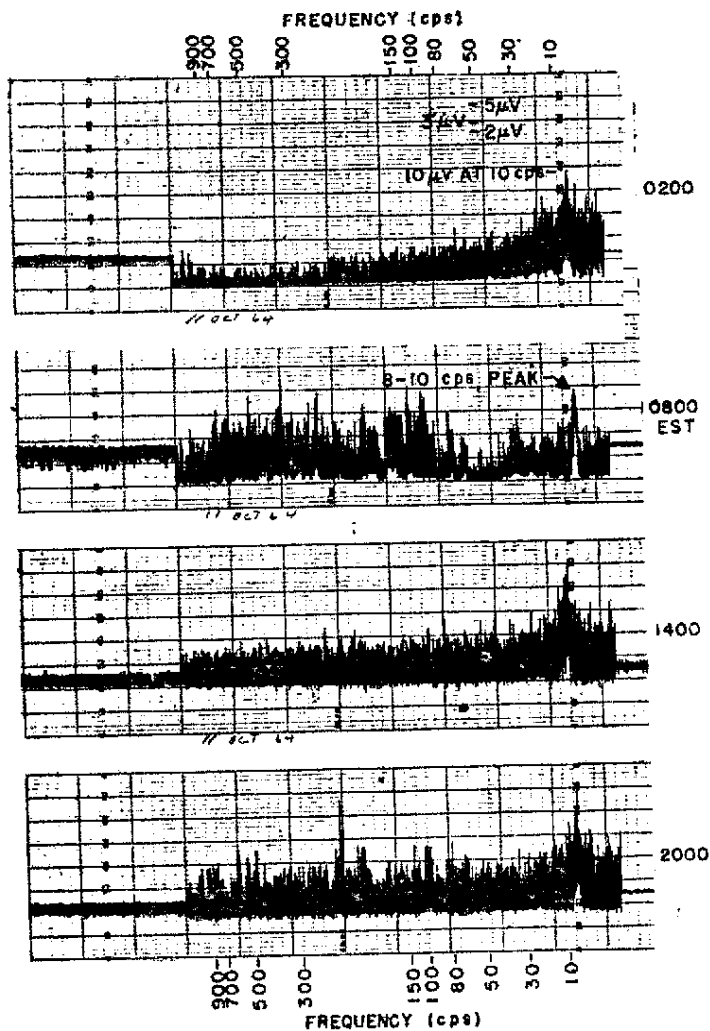
FIG. I TYPICAL LOW FREQUENCY OBSERVATIONS DURING
THE FALL OF 1964 (11 OCTOBER) TAKEN AT
HUANCAYO, PERU

In order to subject the spectral region under observation to closer scrutiny an arbitrary division of the spectrum has been made and Figure 2 illustrates this. In the ranges 200-400 Hz and 400-600 Hz during the hours 0100-0600 there is a minimum. For low frequencies 5-10 Hz, 10-20 Hz and 20-50 Hz the minimum occurs between 0700 and 1000 local time. The maximum for all signals occurs in the late afternoon when local thunderstorms are observed most frequently in the Americas.
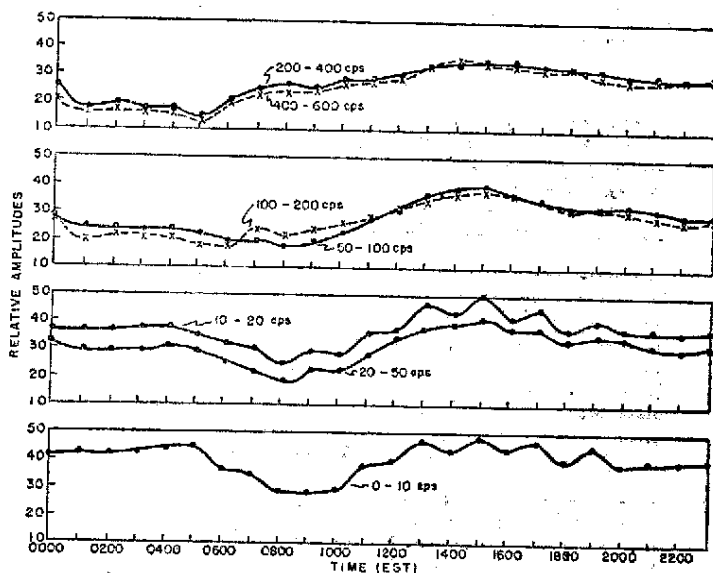
FIG. 2 DIURNAL VARIATION IN SIGNAL AMPLITUDES IN FREQUENCY RANGES: 0-10cps, 10-20 cps, 20-50cps, 50-100cps, 100-200cps, 200-400 cps, AND 400-600 cps FOR OCT. 7-16, 1964 AT HUANCAYO, PERU

Figure 3 using the calibration of the instrument shows the correct amplitude values for a series of days; the spectrum of the received signals is the average over each day listed. The results show consistency but small day-to-day differences. Records taken during the February period show signal enhancements in the high frequency sweep (500-10,000 Hz). These enhancements will be studied in the coming year.

This preliminary report is merely to indicate work in progress. Observations in February 1965 while showing somewhat similar results do not show the identical diurnal pattern; corroboration of a season effect or instrumental problems awaits further records to be taken during the later half of 1965 and the first half of 1966.
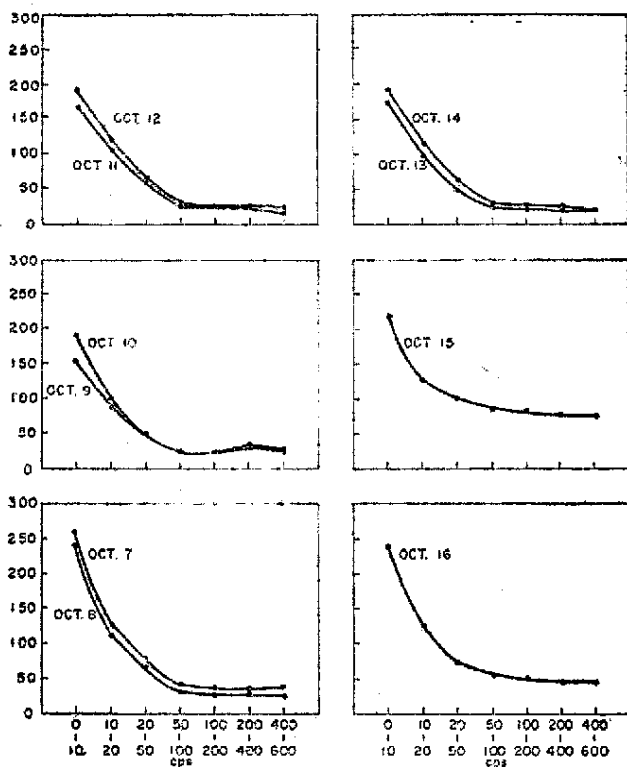
FIG. 3   FREQUENCY SPECTRUM FOR 0-600 cps IN SELECTED RANGES:
0-10 cps, 10-20 cps, 20-50 cps, 50-100 cps, 100-200 cps,
200-400 cps, AND 400-600 cps FOR TEN CONSECUTIVE
DAYS OCT 7-16, 1964 IN HUANCAYO, PERU.

A LASER STUDY OF THE UPPER ATMOSPHERE

by

B. R. Clemesha, G. S. Kent and R. Wright

University of the West Indies, Kingston, Jamaica

Rayleigh scattering of visible light has been used by a number of workers to measure atmospheric density. Elterman in 1951 measured the light scattered from a searchlight beam to obtain density and aerosol profiles up to 70 km. Fiocco and Smullin in 1963 used a laser to do what is essentially the same task, with the added convenience of a pulsed light source. The use of a pulsed light source makes it possible to have the transmitting and receiving beams overlapping at all heights above a few kilometres, the required height range being selected by range gating. The apparatus used by the authors of this note is essentially similar to that used by Fiocso and Smullin, but improvements in laser output and receiving area increase the sensitivity of the equipment by a factor on approximately 100.

The apparatus for this experiment is a pulsed radar operating at a wavelength of 6943 A. The output from a Q-spoiled ruby laser is passed through a diverging lens on to a 20 cm parabolic mirror, in such a may as to produce a parallel beam; this process improves the collimation by a factor of about 20. The emergent beam is directed vertically upwards, and the back-scattered light from the atmosphere collected by a 50 cm mirror. At the focus of the 50 cm mirror is a photo-multiplier, the output from which, consisting of pulses corresponding to photons reaching the photocathode, is amplified and displayed on a CRT. This display is photographed, the photographs subsequently being analysed by counting the number of pulses observed in height intervals of 1.5 km. The essential parameters of the apparatus are given in Table 1.

In addition to Rayleigh scattering from molecules Mie scattering may also be observed. Mie scattering is produced by the aerosol layer which extends from about 15 km to 25 km. Fiocco in 1963 reported observations of scatter from dust particles between 90 and 140 km, and suggested that these may be meteoric in origin. The measurements which we report here show no such scattering, although a signal only 3% of that observed by Fiocco and Smullin would have been detected.

Table 1 — Equipment Parameters

Wavelength	6943 A
Pulse energy	5 joules
Half beam-width	0.1 milliradians
Repetition rate	10 pulses per minute (max)
Receiving bandwidth	20 A
Receiving area	1500 cm^2
Receiving efficiency	1.5%

The results from a series of 100 single pulse measurements are shown in Fig. 1. In this figure the number of echo pulses C, from a given height h, is range normalized by multiplying by h^2, and plotted against h, (note that the Ch^2 axis is logarithmic). Also plotted is the expected theoretical Rayleigh scattering using the standard U.S. atmosphere, modified for 15° north latitude. This theoretical curve is fitted to the experimental results at a height of 30 km. It may be seen that the experimental results fit the theoretical curve well for heights between 25 and 60 km. Below 25 km Mie scattering from aerosols increases the signal by a maximum factor of two. Above 60 km the errors of measurement are such as to render the results of little value. Only one point is more than one standard deviation above the theoretical curve, and this cannot be considered significant.

The measurements described above were made at night; daytime measurements have been made for heights up to 30 km, but above this height the increased noise level due to scattered sunlight gives an unacceptably high noise level. More recent nighttime measurements, not yet fully analyzed, have been made, for which the noise level has been improved. These measurements give appreciably smaller errors at 70 and 80 km, and show that any scattering observed at our latitude (18 degrees north geographic) from above 90 km is not more than 1% of that reported by Fiocco and Smullin. It is of interest to note that these measurements were made at a period of high meteoric activity, and hence should have shown meteoric dust, if present.
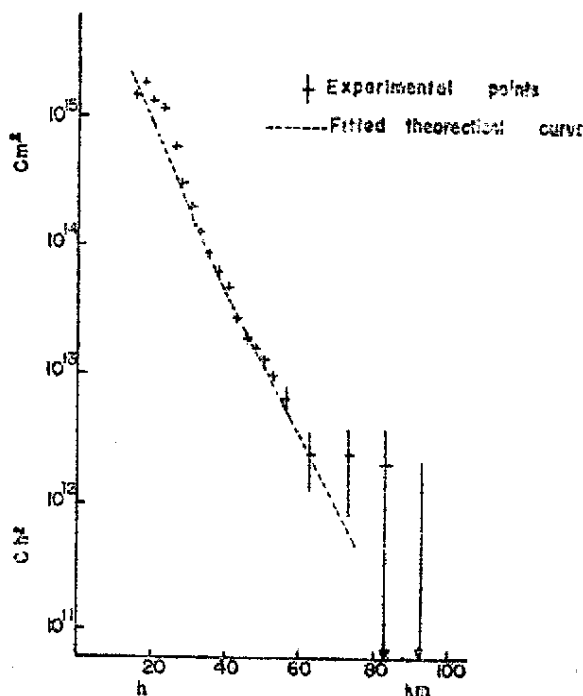
FIG. 1   Experimental variations of Ch^2 with Altitude (C is the count in a $1\frac{1}{2}$ km interval)

The importance of measurements of the sort described in this note lies mainly in the ease and rapidity with which a complete height profile can be obtained. Increases in sensitivity achievable by enlarging the receiving mirror and increasing the laser energy would make it entirely feasible to work at heights up to 110 km. The 15 to 25 km aerosol layer may also be of interest from the point of view of tidal theory. It has been suggested that aerosols might be produced by the oxidation of H_2S by atmospheric ozone. Current theories of atmospheric tides give heating in the ozonosphere as the origin of the semi-diurnal solar tide. In this case a correlation might be found between aerosol concentration and atmospheric tides.

DIURNAL VARIATIONS OF ATOMIC OXYGEN AND OZONE IN

THE MESOSPHERE OVER THE EQUATOR *

Julius London

University of Colorado

and

National Center for Atmospheric Research

Boulder, Colorado

Theory and observations indicate that the production and distribution of ozone in the Stratosphere and Mesosphere result from a combination of photochemical effects and various modes of atmospheric motion. These latter processes are important in proportion to the photochemical relaxation time for ozone. This relaxation time is of the order of years in the troposphere and decreases in the stratosphere to a minimum of about one hour at a height of about 50 km.

In the mesosphere, the relaxation time for ozone increases slowly. It is important to note that in the region of maximum ozone concentration (about 25-30 km near the equator) the relaxation time for ozone is of the order of a few months.

The vertically integrated amount of ozone at the equator, resulting from photochemical processes, is approximately 320×10^{-3} cm (STP), whereas the observed total amount at, for example, Huancayo, Peru is about 250×10^{-3} cm (STP). This excess of theoretical over observed value near the equator is related to the poleward transport of ozone in both hemispheres as a result of atmospheric motions in the lower stratosphere.

The photochemical production of ozone results directly from recombination processes involving atomic oxygen. In the upper mesosphere, atomic oxygen concentrations are larger than those for ozone and consequently time variations of ozone in this region depend sensitively on time changes of the atomic oxygen concentration. The

relevant time dependent photochemical equations for an oxygen atmosphere were solved numerically to determine the diurnal variation of O and O_3 in the upper stratosphere and mesosphere for various latitudes and seasons. Standards values were assumed for the different physical parameters. The reaction time coefficient for $O + O_3$ recombination was assumed to be 5.1×10^{-10} exp $[-3000/T]$. The results for $0°$ latitude are discussed here.

During the night, particularly in the lower mesosphere, O is destroyed by collisional recombination with O_2 and O_3. At sunrise, however, photo dissociation of O_2 quickly restores the atomic oxygen concentration to near equilibrium values.

The computed diurnal pattern of O is shown in Fig. 1 where the variation of O is seen to increase with altitude through the mesosphere. Below 60 km atomic oxygen almost disappears during the night, but reaches maximum values at 60 km of about $10^{11}/cm^3$ during the daytime. At the level of mesopause the indicated diurnal variation of atomic oxygen is quite small.
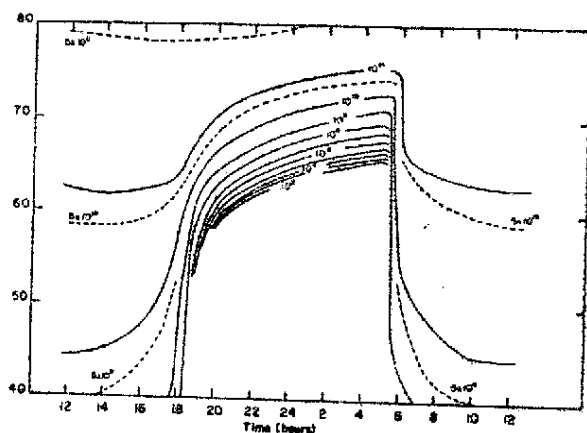
Fig. 1 — Photochemically produced diurnal variation of O at the Equator for an oxygen atmosphere. The ordinate represents height in km and the curves of constant densities are in cm^{-3}.

The daily march of ozone has a phase just opposite to that of atomic oxygen. Immediately after sunrise, O_3 is photo dissociated very rapidly in the mesosphere. It is reformed, however, when sufficient oxygen atoms are present so that the destruction is balanced by recombination processes. After sunset, photodissociation stops and the O_3 concentration increases rapidly at first and then more slowly as the supply of O is used up in recombination. The amplitude of the diurnal variation of O_3 is very small at 50 km but increases with height to a maximum at about 75-80 km. At these levels the ozone concentration is a maximum shortly before sunrise and a minimum shortly thereafter (see Fig. 2). The most rapid increase of ozone occurs at sunset. The total daily range may reach as high as 100 molec/cm³ (i. e., increasing from 10^9/cm³ during the day to 10^{11}/cm³ during the night).
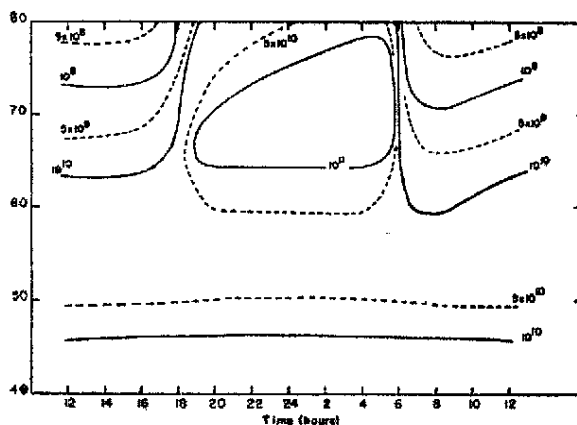
Fig. 2 — Photochemically produced diurnal variation of O_3 at the Equator for an oxygen atmosphere. Ordinate in km and densities in cm⁻³.

Although the largest diurnal O_3 changes take place above 60 km, the primary maximum O_3 concentrations is found in the stratosphere ($\approx 5 \times 10^{12}$/cm³), which at the equator is at a height of about 27-28 km. As a result, total O_3 measurements made at the ground would show on a small percentage variation of the vertically integrated total amount. The computed diurnal variation of total ozone as might

be observed at the ground is shown in Fig. 3. The scale at the left represents the diurnal variation of total ozone which would result from photochemical processes alone. The indicated variation is about 12 x 10⁻³ cm (STP) — or about 5% of the average observed total amount at Huancayo. It is likely that somewhat smaller but similar type of variations could be observed during the time of a total solar eclipse. Total observations (for instance during the solar eclipse in Nov, 1966 across S. America) could reveal an increase of total ozone of the order of a few percent during the time of the eclipse. Observations from high level balloons or from rockets made at first contact and soon after third contact should, of course, show much larger changes in ozone concentrations.
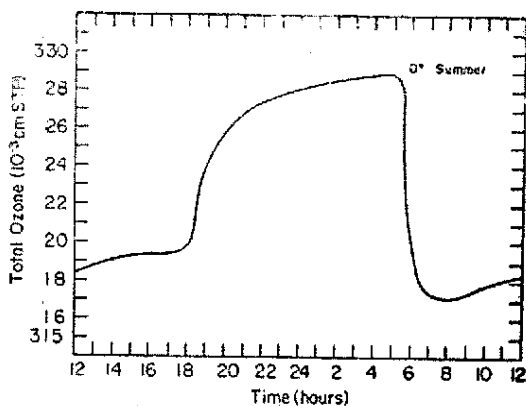
Fig. 3 — Photochemically produced diurnal variation of total O_3 as might be observed from the ground.

EXPERIMENTAL RESULTS ON D-REGION CHEMISTRY

by

G. W. Adams and A. J. Masley

Douglas Missile and Space Systems

Santa Monica, California

Data obtained by other workers have been used to study the gross chemistry of the polar D region. Satellite and balloon measurements of solar cosmic ray energy spectra during the July 1961 solar cosmic ray events were used to calculate $Q(z)$, the rate of production of electron-ion pairs as a function of altitude, while $N(z)$, the electron density profile, was available from multifrequency riometer work in College, Alaska. Having $Q(z)$ and $N(z)$ for six different times, it was possible to determine $\Psi(z)$ in the familiar equation $Q(z) = \Psi(z) N^2(z)$ (Figure 1). Previously reported were the results that (1) the form of the equation was apparently valid, and (2) Ψ depended on n, the number density of neutral air molecules, such that $\Psi(z) = a n^2 + bn$ in the altitude range $40 < z < 80$ km, with $a = 2.5 \times 10^{-37}$, $b = 2.35 \times 10^{-21}$, and n in cm^{-3} (Figure 2).

Two extensions of this work have been done and are reported here. More detailed satellite data have been obtained and used to recalculate the production rate profiles. Using these profiles to recalculate $\Psi(z)$, the validity of the equation $Q(z) = \Psi(z) N^2(z)$ was more strongly confirmed. Since these results were for daytime conditions, an attempt was made to calculate nighttime values for Ψ by using the observed twilight variations in riometer absorption. Preliminary results of this work indicate that no physically meaningful profile for nighttime Ψ is possible, regardless of the assumed height of the effective blocking layer. It may be possible to account for the twilight variations by introducing scattering, but this work has not yet been done.
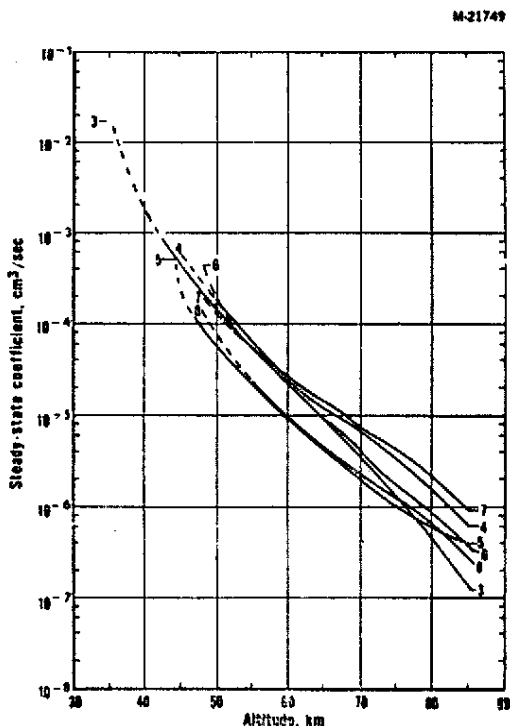
Figure 1 — The results of the six cases of data used to determine Ψ, the steady-state coefficient. The spread in the six cases is very small compared to the differences in the corresponding production rate profiles and in the electron density profiles, indicating that equation $Q(z) = \Psi(z) N^2(z)$ is valid. The differences in the six cases show no observable dependence on Q, N, or the zenith angle of the sun.
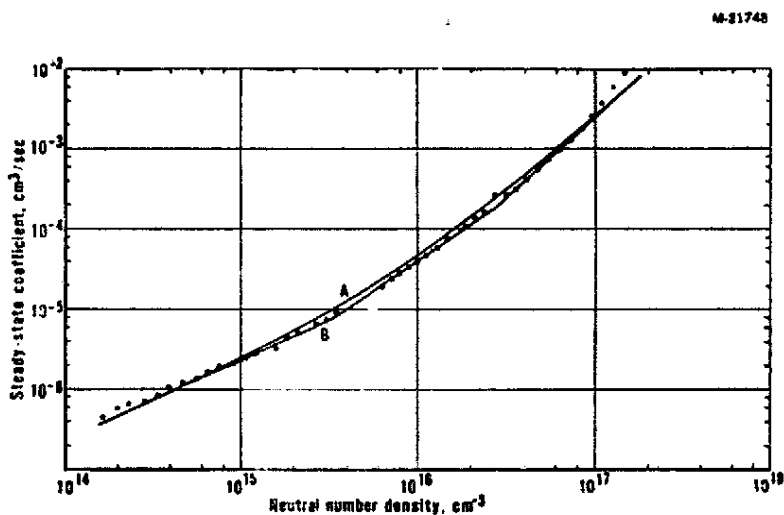
Figure 2 — The average of the six cases for Ψ (shown in Fig. 1) plotted against the number density of neutral air molecules. The data have been fitted with two curves, marked A and B. Curve A is the equation $\Psi = an^2 + b\,n$, discussed in the abstract. Curve B is composed of three straight line segments, but the fit is not significantly better than with curve A.

PLANETARY AND UPPER ATMOSPHERIC GASEOUS ELECTRONIC PROCESSES INVOLVING RADIATION IN THE INFRARED

by

Wilhem Jorgensen

U. S. Army Research Office Durham

Durham, North Carolina, U. S. A.

Abstract: The intent of this paper is to survey the research problems and processes on upper atmospheric gaseous electronic processes which can be studied in equatorial regions by infrared techniques, particularly from terrestrial stations, in the laboratory, or from unsophisticated rocket or balloon facilities. Recent rapid advances in the quantity, quality, and spectral response of infrared detector and components, makes the technique particularly attractive for upper atmospheric research since much of the energy emitted in recombination and relaxation processes is radiated in the infrared. Of particular interest is the development of highly stable tunable lasers which have been shown in principle to permit the application of optical heterodyning techniques to infrared detectors.

IONOSPHERIC CROSS-MODULATION

AT THE GEOMAGNETIC EQUATOR

by

W. K. Klemperer

CRPL, ESSA, Boulder, Colorado

Various experiments to detect radio wave interactions in the lower ionosphere have been carried out using the 22 acre antenna and 4 megawatt transmitter of the Jicamarca Radar Observatory. Although equatorial sporadic-E severely limits observation time, reduction in the amplitude of 3 MHz F layer echoes by as much as 25% is readily obtained from the classical Luxembourg effect. Cross-modulation of 50 MHz cosmic noise has also been observed. In this experiment the lower ionosphere is first heated with a 3 millisecond, 4 megawatt rf pulse. A decrease in sky brightness temperature (about 6,000° K in directions well away from the galactic center) of 30° ± 10° K is observed in daytime with a recovery time on the order of 2 milliseconds. Both the Luxembourg and cosmic noise observations indicate that the interaction height is above 75 km, and essentially no cross-modulation was observed below 65 km. The lower boundary of the D region thus appears to be substantially higher over the geomagnetic equator than in other parts of the world. This is in agreement with theories of D region formation attributing most of the lower level ionization to cosmic ray and solar particle influx, which is significantly less at the geomagnetic equator.

JICAMARCA, PERU
28 NOV 1963
3.0 MC/s

(1)
(2)
(3)

0   75   150 Km   Range
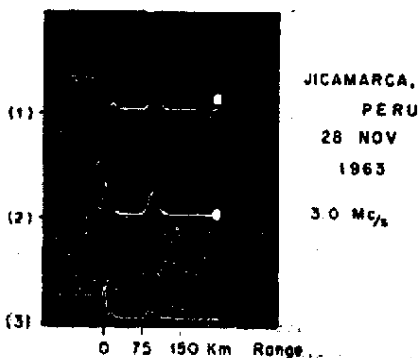
Fig. 1 — Three examples of cross-modulation using E-layer reflections. The bottom trace, which shows a very large amount of cross-modulation, was obtained when the frequency of the wanted wave was near the E layer critical frequency
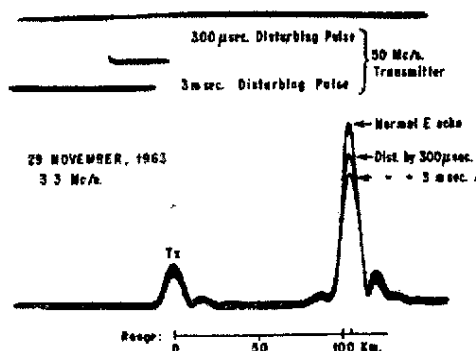
Fig. 2 — An illustration of how the cross modulation changes as the disturbing pulse is lengthened.
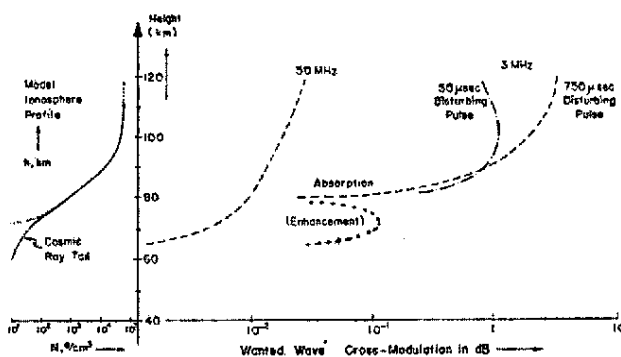
Fig. 3 — The calculate amount of cross-modulation expected under various conditions of "wanted wave" frequency and disturbing pulse length. To the left is the model ionospheric profile used in the calculations. It is thought to be typical of conditions above Jicamarca, Peru at midday. Immediately to the right of this curve is a dashed curve, drawn on the same height scale, which shows the behavior of cross-modulation with height for a 50 MHz wanted wave. To the right of that are curves for a 3 MHz wanted frequency. Between 60 and 80 km, the cross-modulation is positive, i. e. the echo amplitude is enhanced (curve with plus signs) by as much as 0.1 db. Above that height, the cross-modulation is always an increase in absorption.

Examples of Cross-Modulation
F-Layer Echoes
March 1963
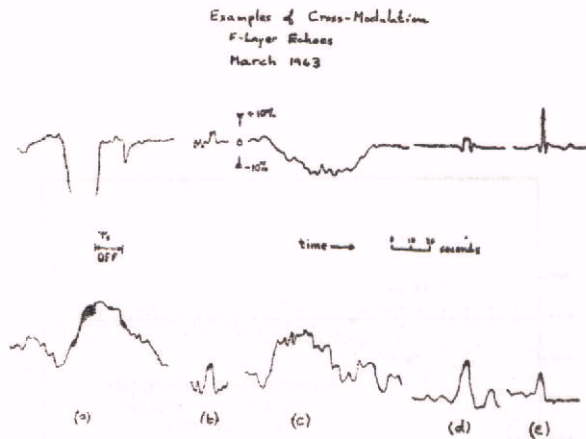
Fig. 4 — A tracing of data taken under conditions of F-layer reflec-
tion. Time goes from left to right, and the upper trace in
each case is a phase detector signal, corresponding to the
lower trace instantaneous echo amplitude. An upward
deflection on the phase detector records corresponds to an
enhancement of the echo amplitude, while a downward
deflection shows absorption. Cases (a) and (c) show absorp-
tion, while (b), (d), and (e) show enhancements. These
latter cases fall on the plus branch of the curves in Fig. 3
(evidence for ionization at about 70 km).

29 NOVEMBER, 1963
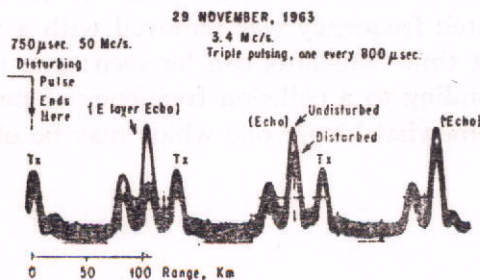
Fig. 5 — An illustration of a technique for measuring the time
constant for heating. Echoes are obtained by passing three
probing pulses through the heated region in rapid succession.
Note that the echo from the lower height shows a faster
recovery time.
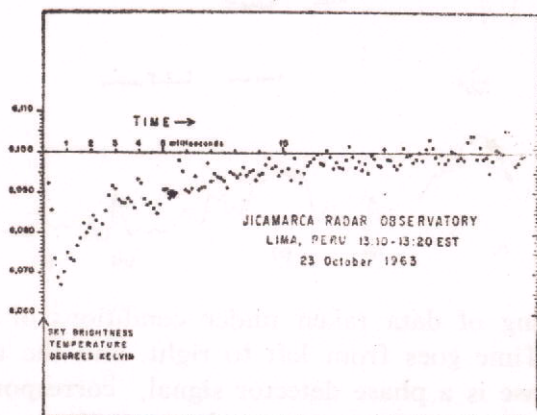
Fig. 6 — A measurement of the change in the cosmic noise level caused
by heating with a 3 millisecond pulse. The transmitted pulse
was at 50 MHz. The cosmic noise was received over a band
2 MHz wide centered on 50 MHz. A 10 kHz band at the
transmitted frequency was removed with a notch filter. Two
apparent time constants can be seen: one of 2 milliseconds,
corresponding to a collision frequency of perhaps $5 . 10^5$ sec^{-1},
and a somewhat longer one which may be of E region origin.

DIFFERENCES BETWEEN TRANSEQUATORIAL AND MIDDLE LATITUDE VLF PROPAGATION

by

C. J. Chilton

NBS, Boulder, Colorado

and

S. M. Radicella

Universidad de Tucuman, Argentina

A comparison is made between the phase and amplitude of the 18kHz signal NBA (Balboa, Panama) recorded at Boulder, Colorado in the northern hemisphere and Tucumán, Argentina, in the southern hemisphere. The normal diurnal and seasonal variations are given and some representative examples of equatorial nighttime phase anomalies (NPA's) not concurrently observed on the mid-latitude path are shown. The approximate geographical and geomagnetic orientations of the two VLF propagation paths are shown in Figure 1.
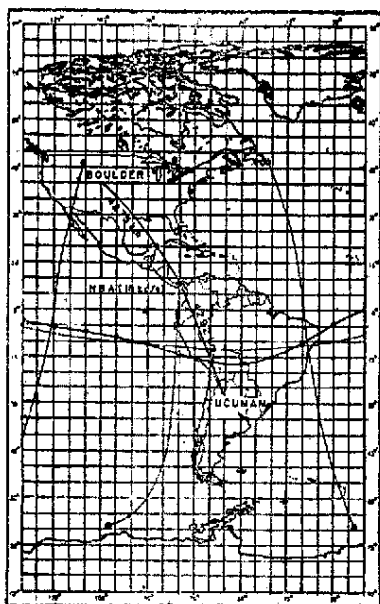
Fig. 1 — The VLF transmission paths: NBA-Boulder and NBA-Tucuman. The basic map showing approximate geomagnetic meridians and the position of the geomagnetic equator at ground level (thin line) and 100-km altitude (thick line) was taken from Dudziak et al[2].

NORMAL DIURNAL AND SEASONAL VARIATION : Monthly averages of the normal diurnal phase and amplitude variations are plotted relative to midpath noon in Fig. 2 and 3. The phase scale is given in degrees of phase retardation relative to the Boulder phase at midpath noon. This was done for convenience of comparison and although the day to night difference in phase appears as a daytime difference this should not necessarily be taken to imply that the nighttime effective heights of reflection are the same for both. The day to night change in phase at Tucuman can be seen to be considerably less, approximately 30% than that observed at Boulder and has remained consistently less from month to month.

The shapes of the daytime amplitude variations for both Boulder and Tucuman are similar and, like the observed difference in time of onset of sunrise and sunset of the phase, can be related to the solar zenith angle variation[1]. The relative amplitude scale is estimated microvolts per meter for the Boulder field strength and 0.5 times the scale values for the Tucuman field strength. Thus the estimated field strengths, both day and night, observed at Boulder appear to be greater than those observed at Tucuman. During the nighttime the field strength at Tucuman is seen to be consistently lower than during the day. This is in direct contrast to the observations made at Boulder where the nighttime field strength is consistently higher than during the day.

The day to night phase change in degrees and calculated effective diurnal change in phase height versus season for Boulder (2 years) and Tucuman (1 year) are given in Fig. 4. The seasonal variation of diurnal phase change for the NBA-Boulder path shows a pronounced semiannual variation with peaks at the equinoxes. This variation observed at Boulder is seen to be consistent from year to year. On the other hand the seasonal variation observed at Tucuman is not as pronounced as that observed at Boulder, but appears to show the same semiannual character. Although this variation is not explainable in terms of the solar illumination of the earth, the apparent difference in the amplitude of the seasonal variation between Boulder and Tucuman could possibly be related to the differences in solar zenith angle variation which existe between the two paths.

Fig. 2 and Fig. 3 — The monthly average phase and amplitude variations of the 18 kHz signal NBA plotted for comparison in hours Universal Time for each path relative to midpath noon.
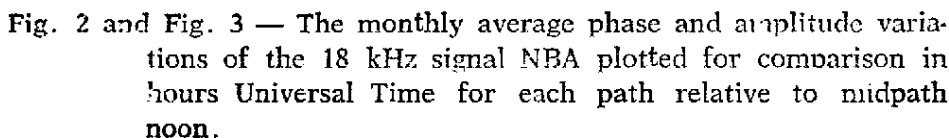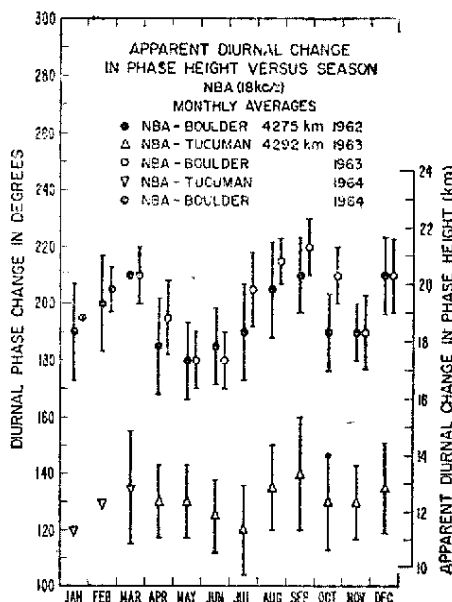
Fig. 4 — The observed diurnal phase change in degrees and the calculated apparent diurnal change in phase height in kilometers versus season for the two paths NBA-Tucuman and NBA-Boulder. The vertical bars give the probable error of an individual measurement.

ANOMALOUS VARIATIONS: As was shown by Chilton, et. al.[1], the nighttime phase and ampliutde at Tucuman are much more disturbed than on the Boulder path. This effect was very often observed during the year on the Tucuman records. It can be shown from a comparison of the data that the Boulder records do not exhibit a similar behavior during the disturbed period. Shown in Fig. 5 is the unusually large nighttime phase anomaly (NPA) which occurred on 8 Sept. 1963. These are photographs of the actual records obtained at Tucuman on the 7, 8 and 9 September 1963. This NPA was not concurrently observed at Boulder. At maximum this change in phase is twice the normal diurnal change in phase observed at Tucuman. Three more examples of NPA's observed at Tucuman on 9 June, 26 August, and 14 September 1963 are presented in Fig. 6.

NIGHTTIME PHASE ANOMALIES

NBA (18 kc/s) BALBOA, PANAMA AT TUCUMAN, ARGENTINA

4292 km

HOURS, UT
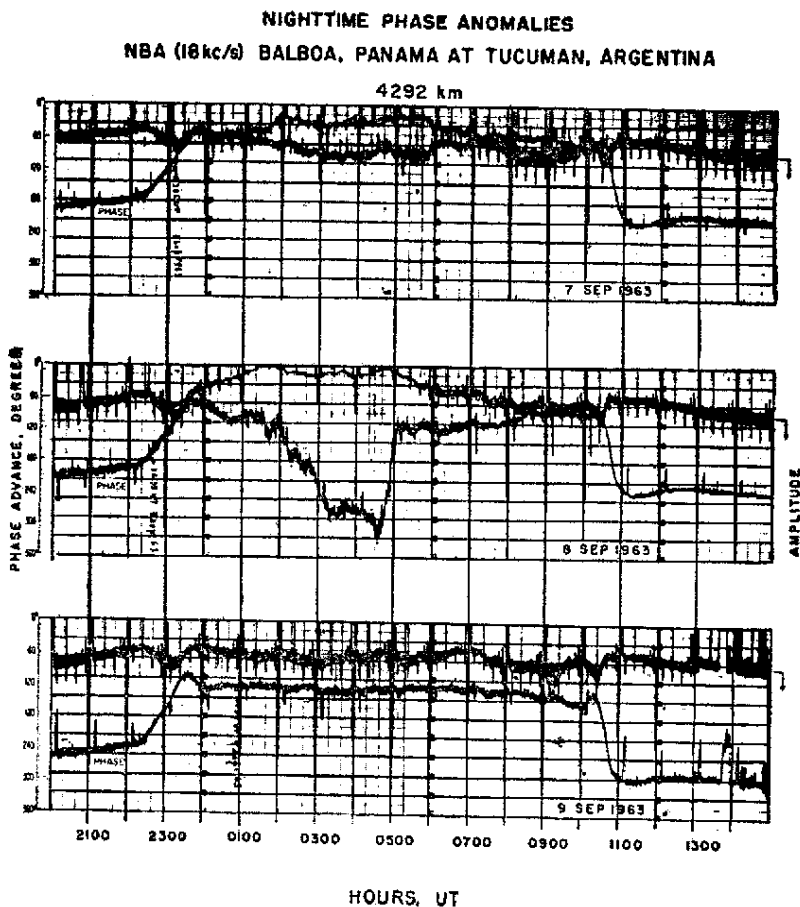
Fig. 5 — Photographs of the actual phase and amplitude recordings made at Tucuman on the 7, 8, and 9 September 1963. On the left the phase scale is one complete cycle at 18 kHz in degrees of phase advance. On the right the relative field strength trace is identified and the direction of an amplitude increase is indicated.

NIGHTTIME PHASE ANOMALIES

NBA (18kc/s) BALBOA, PANAMA AT TUCUMAN, ARGENTINA

4292 km
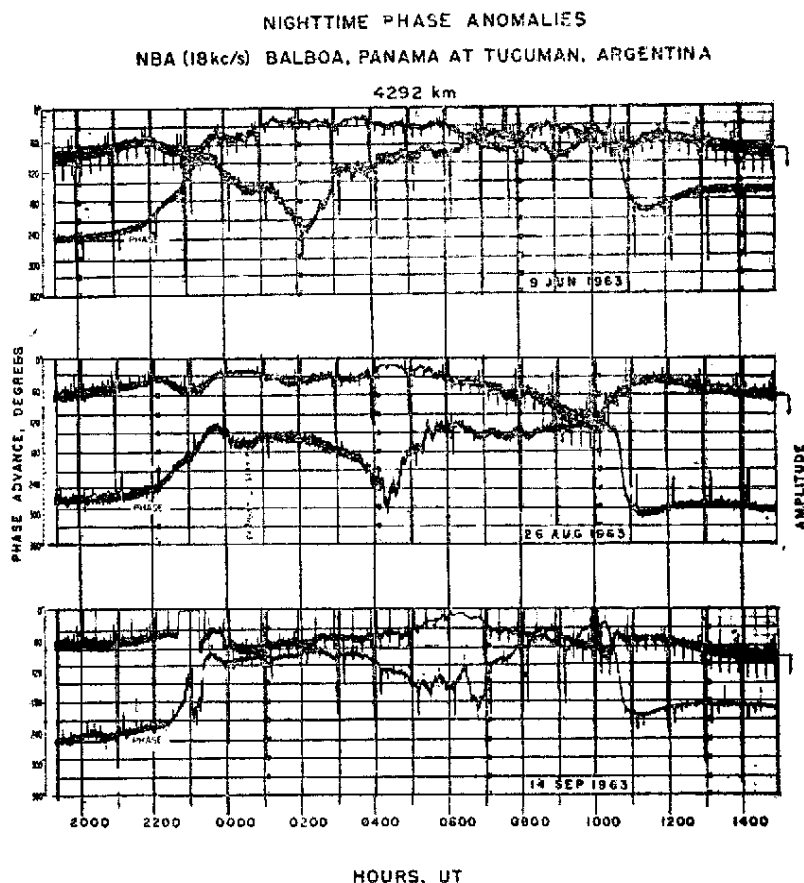
Fig. 6 — Photographs of the phase and amplitude recorded at Tucuman on 9 June, 26 August, and 14 September 1963. On the left the phase scale is one complete cycle at 18 kHz in degrees of phase advance. On the right the relative field strength trace is identified and the direction of an amplitude increase is indicated.

CONCLUSIONS: The normal diurnal and seasonal variations show that there are basic differences between transequatorial and middle latitude VLF propagation characteristics. These differences strongly suggest that the structure of the lower D- region changes with latitude. It is thought that these differences are due to a latitudinal variation in the day-time electron density gradient. The abnormal variations seen on the NBA-Tucuman path and not on the NBA-Boulder path demonstrate that the nighttime equatorial ionosphere is less stable than the nighttime ionosphere at higher latitudes. The explanation and mechanism for this effect is not yet known.

References

1. Chilton, C.J., A.H. Diede and S.M. Radicella, J. Geophy. Res. **69**, N° 7, 1319-1328, 1 April 1964.

2. Dudziak, W. F., D. D. Klenecke, and T. J. Kostigen, Graphic Displays of Geomagnetic Geometry, General Electric Company Rept. RM 63 TMP-2, DASA 1372, 1963.

SUMMARY OF THE SESSION

by

S. Gnanalingam

Applied Physics Section, C.I.S.I.R., Colombo, Ceylon

The sessions began with a review of the D-region by Aikin. This was followed by papers on D-region chemistry, the propagation of VLF radio waves, studies of D-region electron density by ionosphere cross-modulation, low frequency background fluctuations, the determination of atmospheric densities by laser probe and infrared studies of the D-region.

The results of an investigation of the diurnal variation of atomic oxygen and ozone in the mesosphere were presented by London. The vertical distribution of ozone in equatorial regions showed that ozone was in photochemical equilibrium only at levels of about 35-50 km. Above 50 km the time variations of ozone indicated the probability of large diurnal variations. Theoretical studies suggest that the amplitude of these diurnal variations would increase with altitude and reach a maximum of about two orders of magnitude at about 75 km. At these levels the ozone concentration was a maximum shortly before sunrise and a minimum shortly after. The most rapid increase of ozone, however, occurred at sunset. The theory also indicated a secondary maximum of ozone at 60-65 km. With regard to atomic oxygen, the concentration of this constituent decreased with altitude through the mesosphere. Below 60 km, atomic oxygen almost disappeared during the night, but reached maximum values of about 10^{11} per cm^3 in the daytime.

The work of Adams and Masley on the chemistry of the D-region showed that the equation

$$Q(z) = \psi(z) N^2(z)$$

was apparently valid in the daytime in the polar region. It was suggested that this may also be true of the equatorial region. These authors made use of satellite and balloon measurements of solar cosmic ray energy spectra, taken during the July 1961 cosmic ray events, to calculate $Q(z)$; and the multi-frequency riometer work at College, Alaska to determine $N(z)$. They found that ψ varied with the number density n of neutral air molecules according to the relation $\psi = an^2 + bn$. Two extensions of this work, based on more detailed satellite data, have reaffirmed the above relationships. Preliminary results were presented of an analysis of the observed twilight variations in riometer absorption carried out to determine the nighttime values of ψ. These results indicated that no physically meaningful profile for ψ was possible, regardless of the assumed height of the effective blocking layer.

In a paper on atmospheric composition Hanson showed that recent measurements of the ratio of atomic to molecular oxygen could be combined with a knowledge of dissociation, recombination, and molecular diffusion rates to determine an average rate for eddy diffusion, and also to produce an atmospheric model for the lower thermosphere that had a degree of self consistency not present in earlier models. The method consisted of integrating the diffusion equation downwards beginning at 120 km, under the assumption that the eddy diffusion coefficient was independent of altitude. Making used of few available measurements of the ratio of atomic to molecular oxygen, which indicated a value near unity at 120 km, and making allowance for the possibility of recombination in the measuring instruments, it was found that the average eddy diffusion coefficient in the 80 to 120 km altitude range had a value between 6×10^5 and 8×10^6 cm²/sec. Assuming a reasonable value for the coefficient, the analysis showed a broad peak in the atomic oxygen concentration near 90 km. The maximum concentration at this level was within a factor of two of 5×10^{11} atoms/cm³. The total column density of atomic oxygen was found to be of the order of 1.5×10^{18} atoms/cm².

Investigations of the propagation of very low frequency radio waves (18 kHz) over the NBA-Boulder and NBA-Tucuman paths were described by Chilton and Radicella. A marked difference has been noted in the day to night phase change for the two paths, the phase change being greater for the NBA-Boulder path. The seasonal variation of te day-to-night phase for the NBA-Boulder path showed a pronounced semi-annual component, which was consistent from year to year. The seasonal variation observed at Tucuman, however, was not so pronounced, but there appeared to be a small semi-annual component. Considerable fluctuations in the nighttime phase, which were un-correlated with solar or magnetic events have been observed at Tucuman, but these phase anomalies were absent at Boulder. The amplitude variations were also found to be different for the two paths. There was an appreciable diurnal variation in amplitude at Tucuman which showed a tendency for higher field strengths during the day than at night. This diurnal variation was not observed at Boulder. These measurements seem to suggest that there are marked latitudinal variations in the D-region of the ionosphere. It is thought that the variations are due to differences in the electron density gradients over the two paths.

The results of ionospheric cross-modulation experiments carried out by Klemperer at the magnetic equator were presented by Farley. The measurements were made at the Jicamarca Radar Observatory in Peru. The disturbing transmitter operated on 50 MHz, and the cross-modulation was investigated using a 3 MHz "wanted transmitter". Measurements were also made of the cross-modulation on 50 MHz cosmic noise. The limiting value of the measurements was about 1000 electrons/cm³ at 70 km. The main result which emerged was that the D-region was higher at the equator than at temperature latitudes. No appreciable ionization was detected below 60 km.

Aarons described some preliminary observations of ELF signals in the

range 5-10,000 Hz made at Huancayo, Peru. A typical series of records taken in October 1964 in the low range 5-1000Hz showed low amplitude levels in the 300-1000Hz portion of the spectrum during the post-midnight hours. Stormy records were occasionally observed during the post-sunrise period, probably due to local thunderstorms. The maximum for all signals at the low frequencies, however, occurred in the late afternoon, when thunderstorm activity was greatest in the Americas. Records taken in February 1965 showed signal enhancements at certain frequencies in the high range. These are to be investigated in the ensuing months.

A pulsed laser provides a valuable tool for the measurement of atmospheric densities, dust particles and aerosols. The technique is feasible up to 110 km. Experiments using this technique were described by Clemesha. Preliminary measurements of atmospheric density at Kingston Jamaica, gave a good fit to the U.S. standard atmosphere. It was noted that scattering from meteors was absent at this latitude. If any scattering had been present its magnitude would have been less than a hundredth part of the value obtained at higher latitudes by Fiocco and Smullins.

A survey of the research problems and processes which can be studied in equatorial regions by infrared techniques was given by Jorgensen. Recent advances in the quality of infrared detectors made the techniques particularly attractive for upper atmospheric research, since much of the energy emitted in recombination processes was radiated in the infrared.

In conclusion, Piggott drew attention to the fact that pressure changes at low latitudes appeared to be linked with pressure changes at high latitudes, but in opposite phase. He emphasized the importance of meteorological studies being made simultaneously with investigations of the D-region.

II — ABSORPTION IN THE EQUATORIAL

IONOSPHERE

II — ABSORPTION IN THE EQUATORIAL IONOSPHERE

(Discussion leader: W. R. Piggott)

Review Paper

by

N. J. Skinner
Ahmadu Bello University, Zaria, Nigeria

Introduction

When an eletromagnetic wave passes through an ionized medium, energy is dissipated by collisions with neutral particles and electrons set into motion by the wave. At low heights, this collisional frequency can be high, due to the large neutral particle density, and relatively few electrons can cause high absorption.

Measurements of ionospheric absorption are of interest in two ways. Firstly, the radio engineer needs such data in order to calculate the loss for a particular radio circuit at any specified time. He is thereby guided in his choice of frequency and transmitter power necessary to give adequate signal strength at the receiving station. Charts have been given by Piggott (1959) based on experimental data which enable sky wave field strengths to be calculated in tropical regions. Secondly, we are interested in absorption measurements because of the information they give on the structure and behavior of the lowest part of the ionosphere, in particular the D-region. Unfortunately the process is an indirect one and consists in proposing models of the electron density and collisional frequency as functions of height, calculating the absorption and its theoretical variation with wave frequency and sun's zenith distance, and comparing these with the measured variations.

The Relevant Absorption Theory

From the magneto-ionic theory it can be shown that for quasitransverse propagation of radio waves in an ionized medium the absorption index K is given by

$$K = \frac{2 \pi e^2}{m c} \cdot \frac{N \nu}{\mu} \cdot \frac{1}{\nu^2 + \omega^2} \qquad (1)$$

where e and m are the electronic charge and mass respectively,

N is the electron concentration,

ν is the electron collision frequency,

μ is the refractive index of the ionized medium, and ω is the angular frequency of the exploring wave.

This expression is also true for the case of no magnetic field.

Two types of absorption are usually distinguished:

(a) That occurring when $N\nu$ is high and μ is approximately unity — termed non-deviative absorption.

(b) That occurring near the point of reflection where μ approaches zero — termed the deviative absorption.

For the non-deviative absorption it is usually assumed that $\nu^2 \ll \omega^2$ so that the total non-deviative absorption L_{DN} is propational to $\int N\nu$ dh. For a Chapman layer it can be shown that

$$L_{ND} = \frac{A \ (\cos \chi)^{3/2}}{\omega^2} \tag{2}$$

where χ is the sun's zenith angle, and A is a constant.

The deviative absorption in a Chapman layer, L_D, assuming no magnetic field, has been calculated by Jaeger (1947)

$$L_D = (B / \sec \chi) \quad F \ (f/f_c) \tag{3}$$

where B is a constant including the scale height and electron collision frequency, and the tabulated function F (f/f_c) become large when the wave frequency f approaches the critical frequency of the layer f_c.
The total absorption for a wave reflected in the E region expressed as a function of wave frequency for a constant value of χ is therefore.

$$L \ (f) = (A^1/f^2) + B^1 \ F \ (f/f_c) \tag{4}$$

$$(\text{Non-deviative}) \ + \ (\text{Deviative})$$

Several workers have made multi-frequency measurements of total absorption and have used this equation to calculate the deviative and non-deviative contributions.

When the full-wave theory is used to compute deviative absorption assuming a model ionosphere, it is found that the deviative absorption calculated

by the simple method (equation (3)) is too small. For example, Fejer and Vice (1959) showed that corrections must be added to the deviative absorption calculated using ray theory, which amounted to 8 db in total deviative absorption of 59 db at 183 MHz, and to 3 db in 37 db at 2.63 MHz.

Experimental Measurements

Absorption has been studied in the equatorial zone by two main methods. The first employs a vertical incidence pulse reflection technique by which the apparent reflection coefficient of the ionosphere is measured. The integrated absorption over the whole path is proportional to the logarithm of the reflection coefficient This type of measurement is usually termed the A1 method and has been described in detail by Piggott (1953). The other techniques, designated type A2, consists in recording the level of cosmic radio noise at a frequency of about 20 MHz. The noise level is a rather complicated function of sidereal time and the variable absorptivity of the ionosphere and subtraction of the sidereal effect leads to a measurement of the ionospheric absorption. The method was first described by Mitra and Shain (1954).

An additional method of studying absorption is by means of the parameter f-min obtained from normal routine vertical ionospheric soundings. It is the lowest frequency at which echoes are received and is a reliable absorption parameter only when the sensitivity of the sounder is carefully monitored. Values of f-min can be converted to absorption using the A1 or A2 methods.

Type A1 Absorption Measurements At Low Latitudes

Such studies have been made in Africa (Ibadan, Dakar) India (Waltair, Ahmebadad, Delhi and Banaras), Ceylon (Colombo) and the Far East (Singapore). Tables I an II summarize these measurements. The scope of the measurements have varied widely and the variation of absorption with wave frequency, sun's zenith angle, lunar time and solar activity have been studied, (see Table I). In some cases attempts have been made, particularly from the frequency variation, to divide the total measured absorption into "non-deviative" and "deviative" components, that is, absorption beneath the reflecting layer where the refractive index is aproximately unity and absorption near the reflecting point where $\mu \to 0$ respectively, (see Table II). For example, Skinner and Wright (1956) found that the non-deviative absorption at Ibadan varied as $(\cos \chi)^{0.6}/f^{1.2}$ whereas the Appleton-Hartree theory would predict a variation of the form $(\cos \chi)^{3/2}/f^2$. This was interpreted in terms of absorption occurring at levels low in the D-region where $2 \pi f$ is comparable with the collision frequency ν, and it can be shown that an electron density of about 10^3 cm^{-3} at the level where ν is about 10^7 sec^{-1} is required. From their analysis, the deviative absorption in E-layer for a wave frequency of 2.4 MHz was only about 12% of the total absorption.

TABLE I

Summary of experimentally determined variations of absorption with Sun's zenith angle, χ, Solar activity, and Lunar Time

STATION	GEOG. LAT.	MAG. LAT.	OBSERVERS	VARIATION OF ABSORPTION WITH			
				Diurnal $(\cos \chi)^n$	Seasonal	Sunspot Activity R.	Lunar Time
IBADAN	7.5°N	3°S	Skinner & Wright (1954-1964)	$r = 0.62$ (s.s.minimum) $n = 0.63$ (s.s.maximum)	$n = 1.6$ (s.s.minimum) $n = 0.9$ (s.s.maximum)	$L=L_0(1+.0026R)$ (2.4 MHz) $L=L_0(1+.0035R)$ (5.7 MHz)	$L=34 \sin(2t+18°)$ (db) (2.0 MHz) $L=36 \sin(2t+0°)$ (db) (2.4 MHz)
COLOMBO	6.9°N	2.5°S	Ghanalingam & Ratnasiri (1965) Private communication)	$n = 0.90$	$n = 1.7$	$L=L_0(1+.0051R)$	
SINGAPORE	1.2°N	9°S	Skinner (1956) Lange-Hesse (1953)		$n = 1.5$	$L=L_0(1+.003R)$ 27 day periodicity	
DAKAR	14.6°N	10°N	Delobeau & Suchy (1956)			$B = 53+.88R$ $[db \times (MHz)^2]$ non-deviative	
WALTAIR	17.7°N	12°N	Ramana & Ramachandra Rao (1961) Ramana Murty & Ramanchandra Rao (1964.b)	$r = 1.3$ (5.6 MHz) $n = 0.8$ (most prob.)	$n \simeq 2$	$n=1.48(1-.00074R)$ $L=1.42(1+.0092R)$ (5.6 MHz)	
AHMEDABAD	23°N	18°N	Shirke (1959)	$n = 0.75$			
DELHI	28.6°N	24°N	Mitra & Mazumdar (1957) Rao, Mazumdar & Mitra (1962)	$n = 0.62$ (1954) $n = 0.77$	$r = 0.7$		

TABLE II

The variation of absorption with wave frequency

and the relative contributions of the D and E layers to the total absorption

STATION	GEOG. LAT.	MAG. LAT.	OBSERVERS	FREQUENCY LAW	RELATIVE CONTRIBUTIONS OF		al Wave frequency
					D-Region	E-Region	
IBADAN	7.5°N	3°S	Skinner & Wright (1956, 1964)	$L \propto 1/f^{1.2}$ (non-deviative)	~88%	~12%	2.4 MHz
SINGAPORE	1.2°N	9°S	Skinner & Wright (1965)	$L \propto 1/f$ (total absorption)			
WALTAIR	17.7°N	12°N	Ramana Murty & Ramachandra Rao (1964.a) Ramana & Rao (1961)	$L \propto 1/f^{1.5}$ (total absorption) $L \propto 1/f^2$ for $f > 5$ MHz	84-72% varying from month to month	16-28%	2 MHz
DAKAR	14.6°N	10°N	Delobeau & Suchy (1956)	$L \propto 1/(f+f_L)^2$	~77%	~23%	2 MHz
DELHI	28.6°N	24°N	Mitra & Mazumdar (1957) Rao, Mitra & Mazumdar (1962)	$L \propto 1/f^{1.8}$ $f > 5$Mc/s	~88%	~12%	5 MHz

On the other hand, Ramana Murty and Ramachandra Rao (1964.b) in a similar analysis with absorption data for Waltair (India) find that although the total absorption obeys a frequency law of the form $f^{-1.5}$, the non-deviative absorption (obtained by subtracting the calculated deviative absorption from the total measured absorption) follows much more closely an inverse square frequency law. In their view the departure from the inverse square law shown by the total absorption is due to the presence of deviative contribution, which contributes about 20% to the total absorption.

The variations of absorption with lunar time and solar activity provide indirect evidence of the behavior or the D-layer ionization under these influences.

With regard to lunar variation, the only measurements in equatorial regions appear to be those of Skinner and Wright (1964), who find a significant semi-diurnal lunar tide in years of low solar activity. Thus, maximum absorption occurs at 3 hrs. lunar time, which implies that the ionization is at its greatest height at 0.9 hrs., if the lunar variation is due to the vertical movement of the D-layer between levels of different collision frequency. It is interesting that lunar tides in h'Es and h_mF_2 show changes almost in synchronism with this movement.

Rather more work has been done on the dependence of absorption on solar activity. Most workers report a variation of the form:

$$L = Lo (1 + bR)$$

where R is the sunspot number and b is a constant.
Values of b of 2.6 x 10^{-3} for 2.4 MHz and 3.5 x 10^{-3} for 5.7 MHz are reported at Ibadan, based on the years 1953-59, whereas at Colombo, Gnanalingam (private communication) finds values of 5.1 x 10^{-3} for the I. G. Y. and I. Q. S. Y., groups of data.

Type A2 Measurements At Low Latitudes

Riometer measurements have been reported from India (Ahmedabad, Delhi) the Pacific (Johnston Is., Bikini and Hawaii), Huancayo (Peru) and São José dos Campos (Brasil). The work falls into two categories:

a) The study of the regular variations of absorption using data taken over a long period, and

b) the study of short lived absorption events accompanying solar flares, nuclear explosions, etc.

Some attemps have been made to divide the total absorption into D and F2 layer contributions (e.g. Sarada and Mitra, 1960, Ramanathan and Bhonsle,

1959); Sterger and Warwick, 1961). The D region contributions quoted by these workers, of the order of 2— 3 db at noon, appear to be too large.

Several workers (Fredriksen and Dyce, 1962; Sterger and Warwick, 1961; and Ramanathan and Bhonsle, 1959) report abnormal variation of total absorption in the evening hours. In some but not all cases, these correlated with the occurrence of spread F conditions.

Absorption events accompanying large solar flares have been studied by Sarada (1958) at Delhi, and following nuclear explosions by Saha and Mahajan (1964).

Further Research

The major problem to be resolved is the question of the relative contributions of the various ionospheric regions to the total absorption. More multifrequency observations by both A1 and A2 techniques are required and simultaneous measurements by both methods at the same station would be useful. The full wave theory should be used to compute the deviative absorption over a range of frequencies using recent data on the distribution with altitude of N and ν in the deviative absorbing region. Hence the non-deviative absorption can be obtained as a function of frequency and deductions may then be made about the structure of the D region.

References

Delobeau, F. and Suchy, K   1956 J. Atmos. Terr. Phys. **9**. 45

Fejer, J.A. and Vice, R.W.   1959 J. Atmos. Terr. Phys. **16**. 307

Fredricksen, A. and Dyce, R. B.   1960 J. Geophys. Res. **65**. 1177

Jaeger, J.C.   1947 Proc. Phys. Soc. **59**. 87

Lange-Hesse, G.   1953 J. Atmos. Terr. Phys. **3**. 153

Mitra, A. P. and Shain, C.A.   1954 J. Atmos. Terr. Phys. **4**. 204

Mitra, S.N. and Mazumdar, S.C.   1957 J. Atmos. Terr. Phys. **10**. 32

Mitra, A.P. and Sarada, K.A.   1962 "Radio Wave Absorption in the Ionosphere' (ed. Gerson) (Pergamon) p. 347

Piggott, W.R.   1953 Proc. Inst. Elect. Eng. III. **100**. 61

Piggott, W.R.   1959 "The Calculation of Median Sky
                                       Wave Field Strength in Tropical
                                       Regions" Special Report. No. 27.
                                       D.S.I.R.

Ramana, K.V.V. and Rao, B.R.   1961 J. Atmos. Terr. Phys. **22**. 1

Ramana Murty, Y.V. and Ramachandra
    Rao, B.   1964.a. J. Atmos. Terr Phys. **26**. 849

Ramana Murty, Y.V. and Ramachandra
    Rao, B.   1964.b. J. Atmos. Terr. Phys.**26**. 1087

Ramanathan, K.R. and Bhonsle, R.V.   1959 J. Geophys. Res. **64**. 1635

Rao, M.K., Mitra S.N. and Mazumdar,
    S.C.   1962 J. Atmos. Terr. Phys. **24**. 245

Saha, A.K. and Mahajan, K.K.   1964 J. Atmos. Terr. Phys. **26**. 624

Sarada, K.A.   1958 J. Atmos. Terr. Phys. **13**. 192

Sarada, K.A. and Mitra, A.P.   1960 "Some Ionospheric Results Obtain-
                                       ed During the IGY" (Elsevier Press)

Sharma, S.K.   1958 Proc. Phys. Soc. **71**. 1007

Shirke, J.S.   1959 J. Inst. Telecommun. Engrs. India.
                                       5. 115

Skinner, N.J.   1956 Ph.D. Thesis, London University.

Skinner, N.J. and Wright, R.W.   1956 J. Atmos. Terr.Phys. **9**. 103

Skinner, N.J. and Wright, R.W.   1964 J. Atmos. Terr. Phys. **26**. 1221

Steiger, W.R. and Warwick, J.W.   1961 J. Geophys. Res. **66** 57

MULTIFREQUENCY ABSORPTION MEASUREMENTS

FOR IONOSPHERIC STUDIES

by

G. W. Adams, A. D. Goedecke, and A. J. Masley

Douglas Missile and Space Systems

Santa Monica, California, U.S.A.

The multifrequency riometer is being developed as a tool for D-region studies in the polar caps and the auroral zones. Theoretical investigations indicate that it may also prove useful at latitudes below the auroral zones. The multifrequency riometer is used to measure cosmic noise absorption as a function of frequency in the HF and VHF. If all the absorption takes place above 75 km, then the absorption varies inversely as the frequency squared, and the only benefits are an expanded range and greater accuracy. If a significant fraction of the absorption takes place below 75 km, then the absorption-frequency curve is a function of the electron density profile in this region, and the absorption-frequency curve can be used to determine the electron density profile at the same region (the contribution from above 75 km exists as a single term in the solution). The determination of the electron density profile below 75 km is possible because the electron collision frequency here is not negligibly small compared to the radio wave frequency, as it is above 75 km. As a result, the absorption coefficients in this region are not simply related, as is shown in Fig. 1, and the absorption equations can then be solved for the electron density profile.

In the polar caps, the electron density profiles derived during solar cosmic ray events are used to determine the energy spectra of the solar particles. One such spectrum, derived from multifrequency riometer results of other workers, is shown in Fig. 2 as an indication of the accuracy of the technique. Note that the technique gives absolute values; no normalization is required.

The equipment under development is basically a fixed-frequency riometer with switched tuning. A program unit drives the frequency

through 19 steps (8-45 MHz) with the cosmic radio noise power level at each frequency being sampled four times by a digital voltmeter and the data punched into paper tape for direct computer analysis. One full cycle requires 8.7 minutes, and also includes time and other auxiliary information.
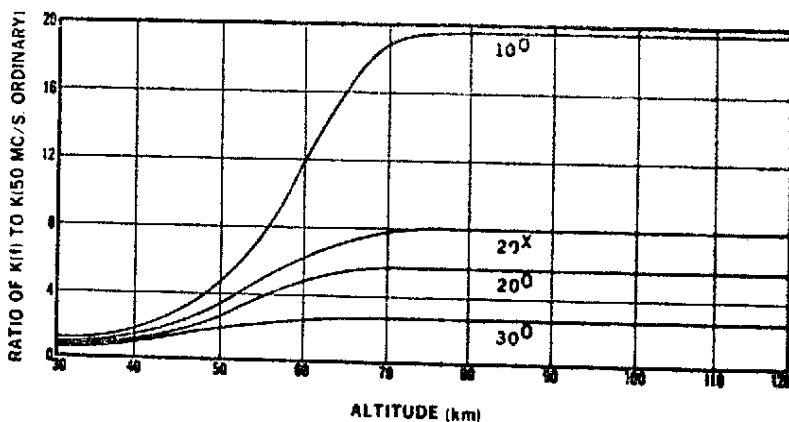
Fig. 1 — The ratios of the absorption coefficients in the lower iono-
sphere to the absorption coefficient for 50 MHz, for several
different frequencies and modes. (20° denotes the ordinary
mode on 20 MHz; 20^x is the extraordinary mode). At
altitudes greater than about 70 km, the ratio is given by the
ratio of the squares of the frequencies. At altitudes below
about 30 km, there is no frequency dependance. In the region
$30 < Z < 70$ km, the absorption coefficients are not simply
related, and electron profile determinations may be done
here.
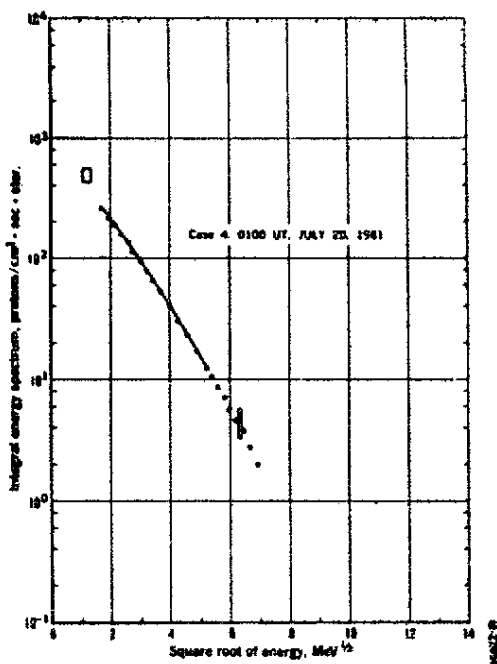
Fig. 2 — A solar cosmic ray energy spectrum determined from multi-frequency riometer data taken during the July 1961 solar cosmic ray events. The dots connected by a line are points calculated from the multifrequency riometer; the two retangles are derived from the Injun 1 satellite data. The good agreement is indicative of the accuracy which can be obtained with the multifrequency riometer technique.

To examine the possible uses of such a technique at latitudes below the auroral zones, we have performed calculations for several electron profiles, two of which are shown in Fig. 3. These profiles are not particular measurements or models, but are typical of mid-latitude daytime profiles. The resultant absorption-frequency curves are shown in Fig. 4. Since the absorption as a function of frequency may be conveniently represented as $A(f) = g(f)/f^2$ (where g (f)

contains the information about the electron density profile), the quantity
A (f) . f² (= g (f)) is plotted instead of A (f). The shallower of the
two electron density profiles gives the upper absorption-frequency
curve, which is almost a straight line at unity (the profiles have been
normalized at 50 MHz). A straight line at unity represents a 1/f²
dependence, indicating no significant absorption below 75 km. The
other electron density profile (the one with more ionization at lower
altitudes) give the lower absorption-frequency curve, which shows a
significant (and measurable) departure from 1/f². The two electron
density profiles therefore represent the boundary of the usefulness of
the multifrequency riometer. We conclude from this that, at mid-
latitudes, the multifrequency riometer will be useful around noon and
during periods of enhanced ionization, such as SID's.
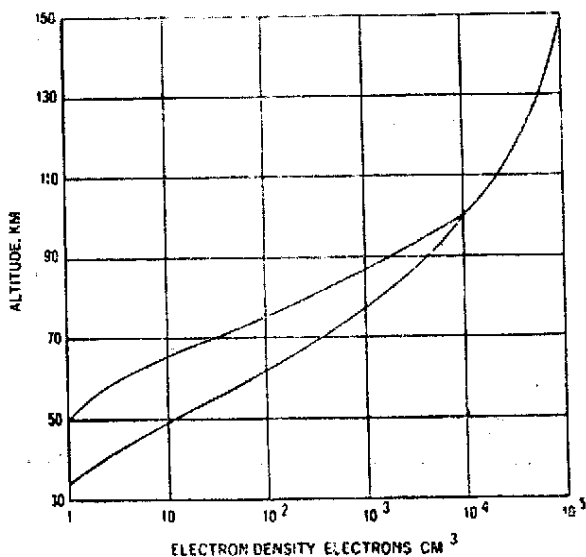
Fig. 3 — Two of the electron density profiles used for this study.
These profiles do not represent any particular measurements
or theoretical models, but are representative of most day-
time mid-latitude measurements. Nicolet and Aikin's model
is roughly bracketed by these two profiles.
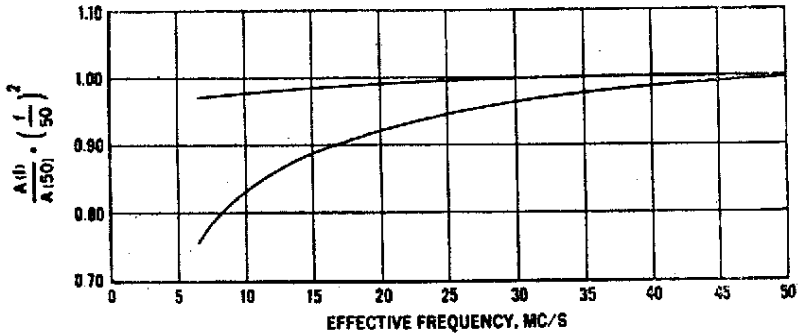
Fig. 4 — The absorption-frequency curves which would result from the electron density profiles in Fig. 3. The quantity on the vertical scale is the absorption (A) times the square of the frequency (f), normalized to unity at 50 MHz. On the horizontal scale is the effective frequency — the frequency ± the gyrofrequency, depending on the mode. Absorption occurring above 70 km gives a straight line at unity; absorption below 70 km gives a curve lying below unity. Here the upper curve (close to unity) corresponds to the shallower electron density profile; the lower curve is for the more intense profile.

COSMIC NOISE ABSORPTION AT HUANCAYO, PERU

by

P. Bandyopadhyay

Huancayo Observatory, Instituto Geofísico del Perú

A 30 MHz riometer has been in operation at Huancayo since July 1961. Thus, by the time of the Starfish explosion (July 9, 1962) we already had about a year of data which made it possible to derive the "quiet-day curve". This same riometer was used (a) to obtain values of absorption and (b) to follow course of decay of the synchrotron noise.

Fig. 1 shows the average diurnal variation of total absorption during the different months of a two-year period. The usual midday peak and an occasional peak (in September and November) are noticeable. The attenuation given by Fig. 1 is the total of contributions from all different regions of the ionosphere. From physical considerations one can expect that the major contributions will be from the D- and the F2-region. We tried to separate these contributions by the Mitra and Shain method which did work with our data. Besides, doubt has been cast on the validity of the method by some recent Russian work.

We have examined at some length the nighttime values of absorption which are almost entirely F-region contribution. These values when plotted against foF2 generally give the kind of curve shown by Fig. 2. The curve shows two things: (a) the magnitude of the F2-layer absorption corresponding to a given foF2 and (b) the rapid increase of absorption with foF2. We checked the magnitude of the absorption using the electron density profiles from Jicamarca (Lima). Four such profiles obtained near midnight are shown in Fig. 3. Using the average profile of the figure (critical frequency 6.0 MHz) and assuming all collisions to be between the electrons and the positive ions we find that the calculated absorption agrees with the observed value for electron temperatures of the order of 550° K.
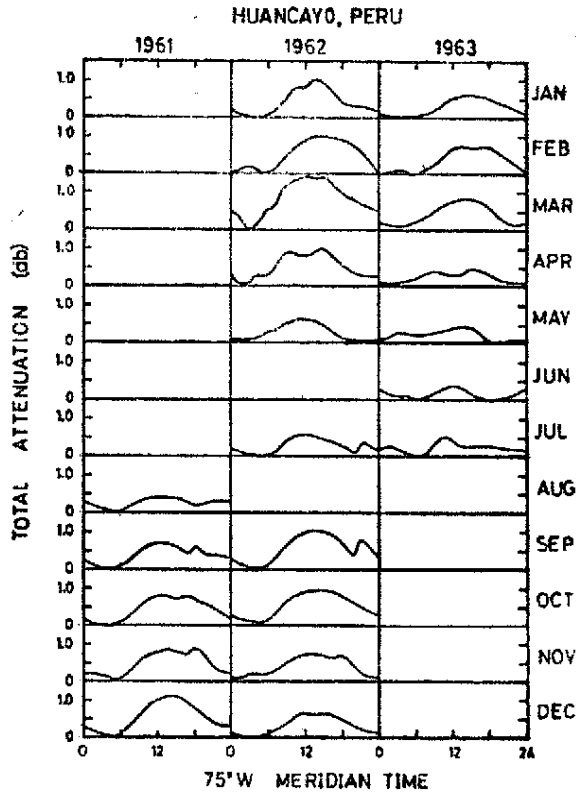
Fig. 1 — Average diurnal variation of total attenuation (monthly averages of hourly values) of cosmic radio noise on 30.5 MHz at Huancayo during some months of 1961-63.
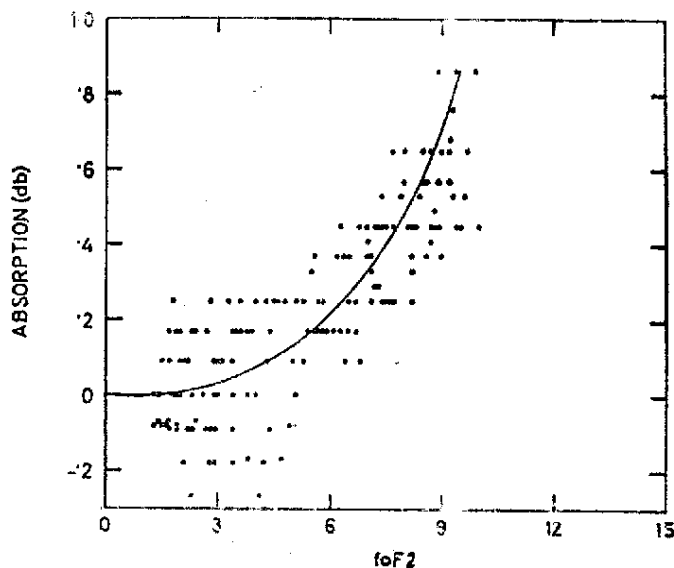
Fig. 2 — A typical plot of nighttime absorption against foF2 at Huancayo. Values for the night hours (19 hr. — 05 hr.) for January, 1963 have been plotted.
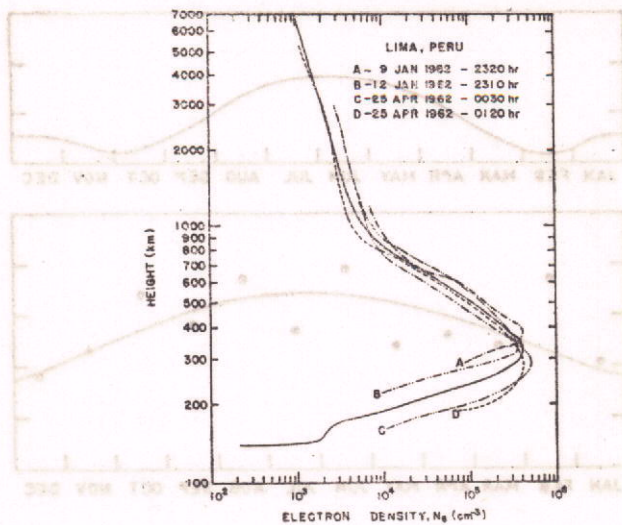
Fig. 3 — Electron density profiles at the magnetic equator, obtained around midnight using the incoherent scatter technique. Curves A, B, C and D, after Bowles et al.; full line curve, smoothed average. Average value of absorption corresponding to these profiles is 0.1 db. This value of absorption can be obtained by calculation using the average profile and Nicolet's expression for collision frequency (between electrons and positive ions) when the electron temperature is taken as 550°K.

Some workers have found that the variation of F2 absorption with foF2 can be fitted by and equation of the type $A = K (foF2)^n$. The values of the exponent n for different places are: 2.0 (Gorki, USSR), 6.0 (Ahmedabad, India), 7.6 (Hornsby, Australia) and 2.0-4.0 (Huancayo, Perú). The Huancayo values suggest a seasonal dependence (Fig. 4).

We find that theoretically it is more reasonable to expect the dependence of absorption on foF2 to be of the type $A = [R - S \log_{10} foF2] (foF2)^4$. The values of S obtained for Huancayo during August 1961 through July 1962 are shown in Fig. 5.
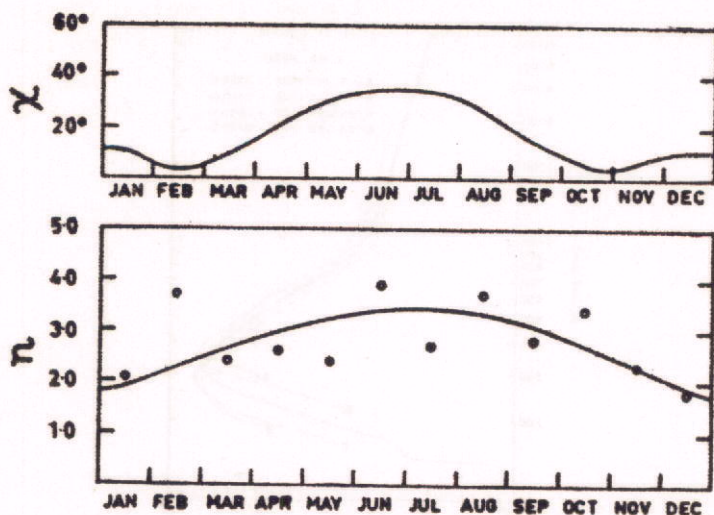
Fig. 4 — Botton figure: the values of the exponent n in the equation
A = K (foF2)ⁿ for the different months at Huancayo. Top
figure: Seasonal variation of midday values of solar zenith
angle χ at Huancayo.
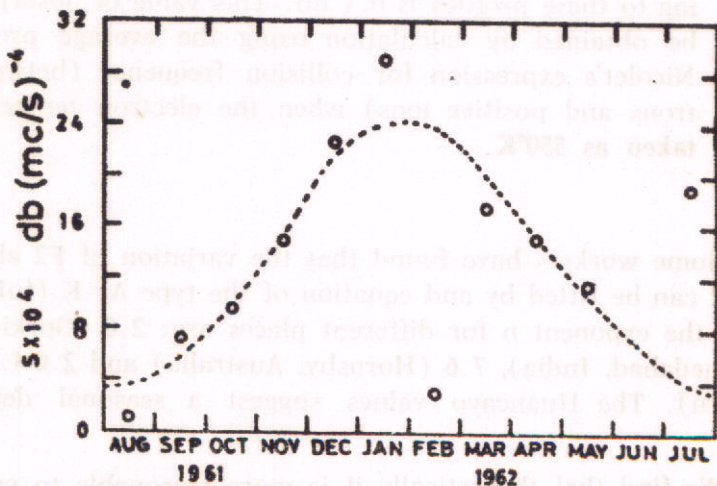
Fig. 5 — Values of S in the equation A = [R − S log₁₀foF2] (foF2)⁴ for
the different months at Huancayo. Broken curve shows the
seasonal variation suggested by the experimental values.

Figs. 6, 7 and 8 show the course of decay of the synchrotron noise generated by the Starfish explosion. The solid line curve in the figures shows a decay of the form $(1 + {}^t/\tau)^{-1}$ which was predicted by Welch and Whitaker. The value of τ used in the figures is 60 days.
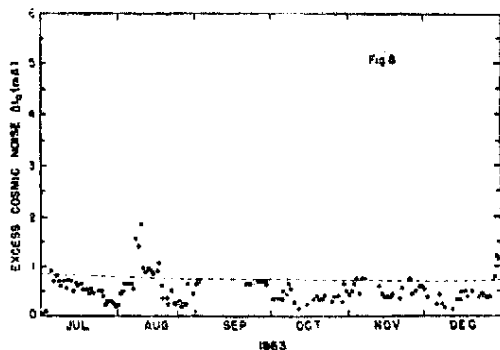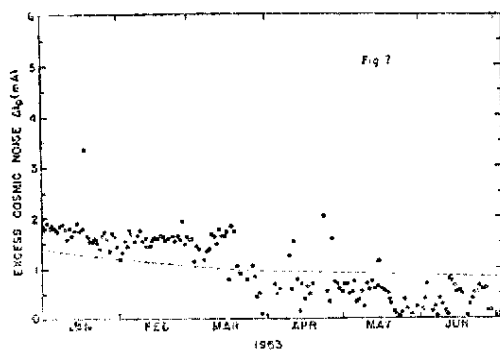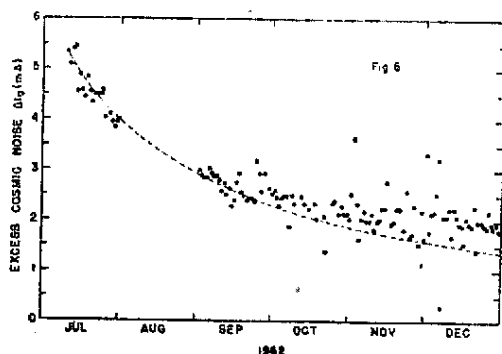
Figs. 6, 7 and 8 — Decay of the excess 30 MHz noise generated by the high altitude nuclear explosion of July 9, 1962. Circles show values of the excess noise in terms of the equivalent noise diode current. Dashed line shows a predicted form of decay of the excess noise.

IONOSPHERIC ABSORPTION MEASUREMENTS

AT COLOMBO, CEYLON

by

S. Gnanalingam and P A. J. Ratnasiri

Ceylon Institute of Scientific and Industrial Research

The paper describes the results of an investigation of iono-spheric absorption at vertical incidence, in the frequency range 2.0 to 2.9 MHz, at Colombo, Ceylon (06° 54'N, 79° 52'E, Dip 5°S). The period of observation was from July 1957 through March 1960, corresponding, to sunspot maximum, and from January 1964 through May 1965, corresponding to sunspot minimum as shown in Fig. 1. The main conclusions are as follows:
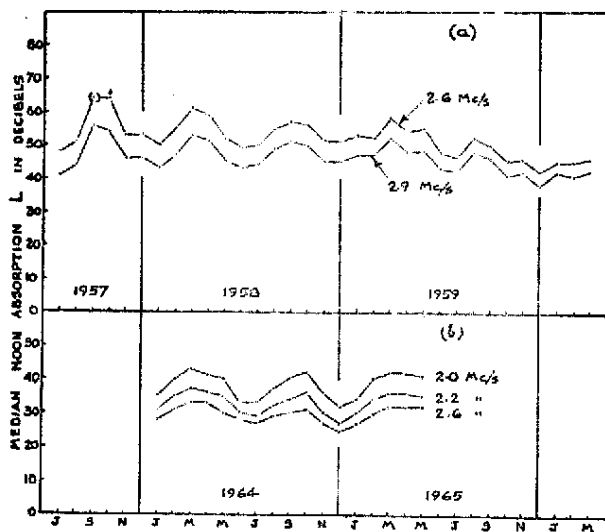
Fig. 1. MONTHLY MEDIAN VALUES OF NOON ABSORPTION DURING THE I. G. Y., I. G. C AND I. Q. S. Y.

1 — The noon absorption on 2.6 MHz increases with solar activity according to the law

$$L \propto (1 + bR_z)$$

for values of R_z up to about 190, above which a saturation effect seems to set in (Fig. 2). The value of the coefficient b is slightly greater at Southern solstice (5.5×10^{-3}) than at Northern solstice (4.8×10^{-3}), in agreement with the observations on 2.4 MHz at Ibadan. The mean annual value of b is 5.1×10^{-3}, and is nearly double the value found at Ibadan. Values of the coefficient b obtained at various stations are summarized in Table I.
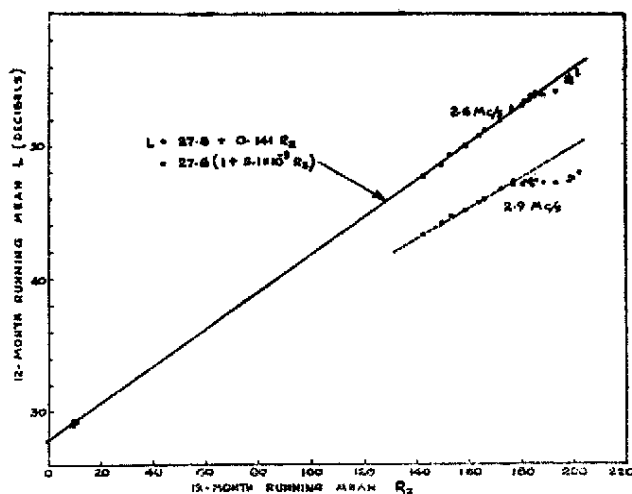
Fig. 2.   VARIATION OF NOON ABSORPTION WITH SUNSPOT NUMBER

TABLE I

Values of the constant b for various stations

Authority	Station	Frequency	Constant b x 10¹
Appleton and Piggott (1954)	Slough	4 MHz	7 - 13
Gnanalingam and Ratnasiri	Colombo	2.6 MHz	5.1
National Bureau of Standards (1948)	Not specified	Not specified	5.0
Piggott (1959)	Slough (Summer) Falkland Islands (Summer) Singapore	A - figure	4.0 ± 0.5
Rawer (1951)	Slough	A - figure	3.5
Skinner and Wright (1964)	Ibadan	5.7 MHz	3.5
Skinner (quoted in Skinner and Wright 1964)	Singapore		3.0
Skinner and Wright (1964)	Ibadan	2.4 MHz	2.6

2 — The seasonal variation of noon absorption at zero sunspot number obeys a law of the form

$$L \propto (\cos \chi)^{1.7}$$

with the exception that the absorption is abnormally low during the period from May to September. This abnormal decrease of absorption, which is observed both at sunspot maximum and at sunspot minimum, may be the result either of a decrease in the D-region electron density, or a decrease in the collisional frequency, possibly due to the ionization moving upwards. It is of interest to note that Appleton reported a similar decrease in the electron density of the E-layer under conditions of constant χ and constant R_z, in the same months. The decrease is attributable partly to the reduction in the incident solar flux resulting from the earth's orbital eccentricity, and the same cause may be at work in the D-region.

3 — The magnitude of the noon absorption on 2.6 MHz is given by the expression

$$L = 31.6 \ (\cos \chi)^{1.7} \ (1 + b \ R_z)$$

decibels for R_z less than 190, where b has the values shown in Fig. 3. In the period from May to September, however, the absorption is less than the figure given by this expression, by amounts varying from 5 to 10% (Fig. 4).

4 — The diurnal variation of absorption with $(\cos \chi)$ is approximately according to the law $L \propto (\cos \chi)^n$ where $n = 0.9$, but there is considerable scatter in the values of n obtained on different days.
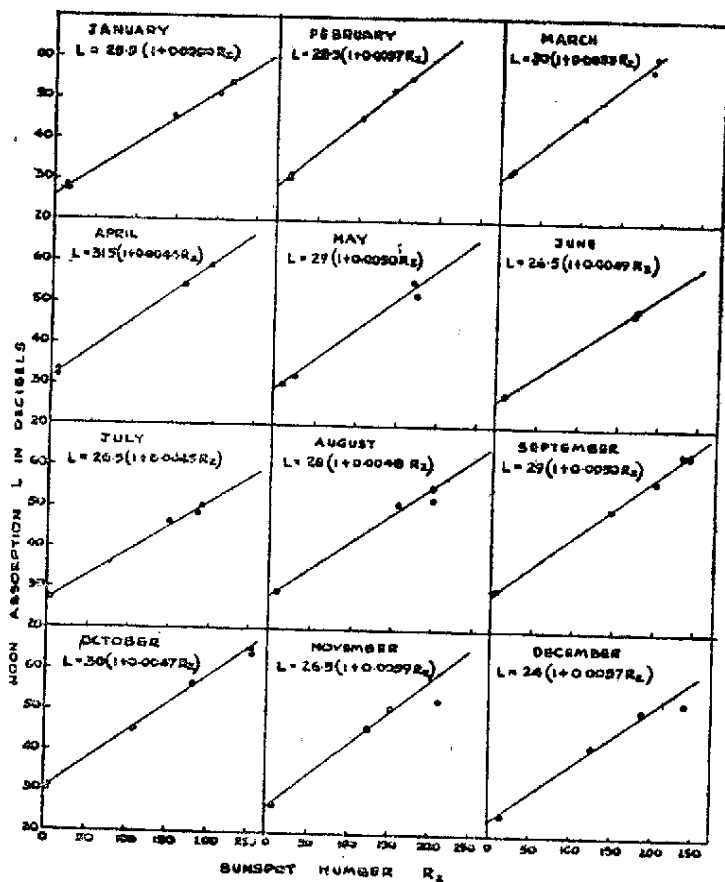
Fig. 3. GRAPHS SHOWING THE VARIATION OF ABSORPTION WITH SUNSPOT NUMBER FOR EACH MONTH
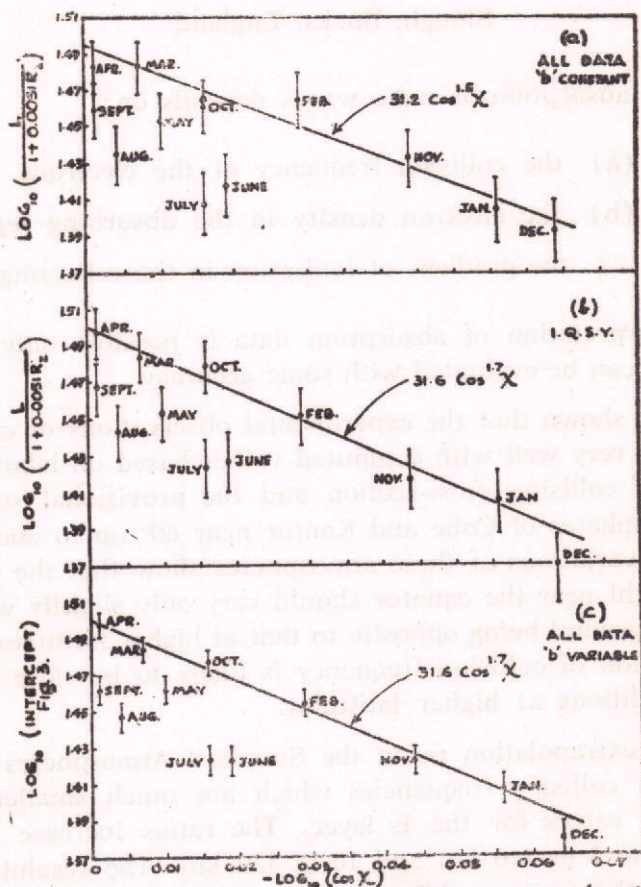
Fig. 4. GRAPHS OF LOG (L/1+bR₂) AGAINST LOG (cos χ).

COLLISION FREQUENCIES IN THE D AND E REGIONS

by

W. R. Piggott

Radio and Space Research Station

Slough, Bucks, England

The absorption of radio waves depends on:

   (a) the collision frequency of the electrons,

   (b) the electron density in the absorbing region, and

   (c) the gradient of ionization in the reflecting region.

Interpretation of absorption data is possible only if at least one of these can be evaluated with some accuracy.

It is shown that the experimental observations of collision frequency agree very well with computed values based on laboratory measurements of collision cross-section and the provisional summer and winter atmospheres of Cobe and Kantor near 60° up to about 80 km. The latitude variations of these atmospheres show that the pressure at constant height near the equator should vary only slightly with season, the sense in general being opposite to that at higher latitudes. Thus the height variation of collision frequency is likely to be close to that for summer conditions at higher latitudes.

The extrapolation using the Standard Atmospheres at greater heights gives collision frequencies which are much smaller than the experimental values for the E layer. The ratios increase from unity near 90 km to 3 at 110 km and 10 at 130 km. The resolution of this difference is the major problem to be solved before reliable interpretations of absorption data can be made. Possible explanations are:

   (a) that the experimental values are misleading, or if not;

   (b) that a minor constituent with very large cross-section for electron collisions is present;

(c) that the electron temperature is much higher (e.g. by a factor 2) than the gas temperature in the E Region.

The available data do not provide any convincing evidence in favor of one of these explanations, some supporting one and some the others. Thus, while satellite and rockets experiments suggest that T_e/T_i may exceed unity, correlations of absorption with stratospheric phenomena suggest the presence of variable amounts of a minor constituent.

The following Figs. 1 to 6 with long captions are self explanatory.
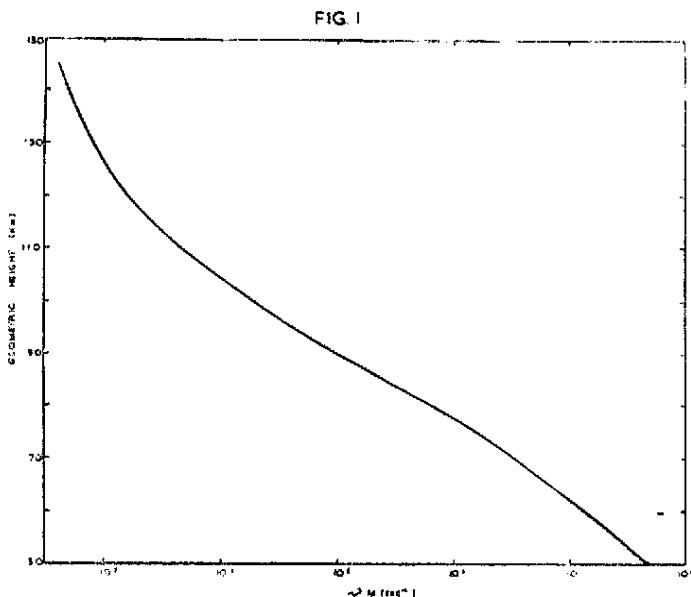
Fig. 1 — Height variation of monoenergetic collision frequency, ν_M, deduced from U. S. Standard Atmosphere 1962 and Pack and Phelp cross-sections for collision.
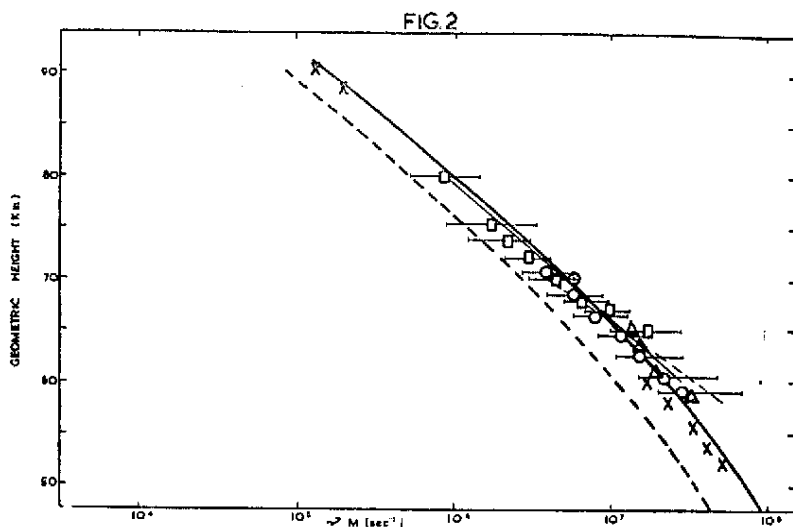
Fig. 2 — Height variations of experimental values of v_M (symbols and thin lines) for summer and autumn months together with theoretical height variation from U. S. Standard Atmosphere 1962 fitted to experimental data. The broken curve shows the corresponding variation fitted to winter data by R M S methods.
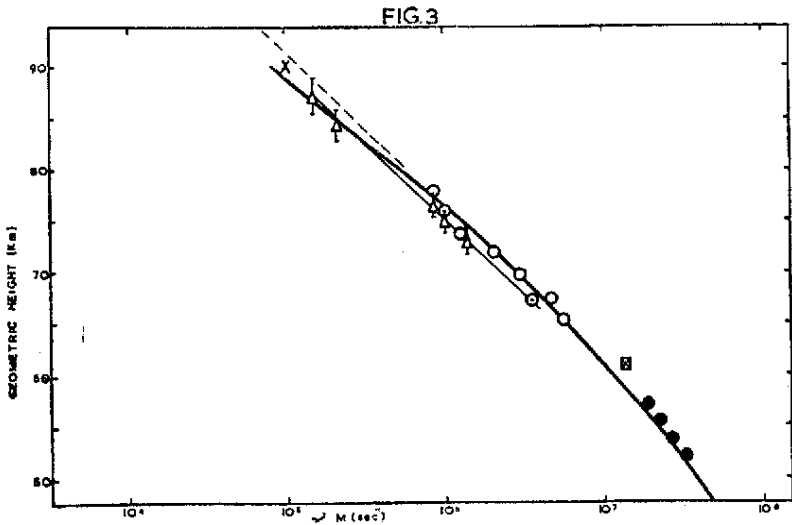
Fig. 3 — Height variations of experimental values of ν_M (symbols and thin lines) for winter and spring months together with theoretical height variation from U. S. Standard Atmosphere 1962 fitted to experimental data by R M S methods.
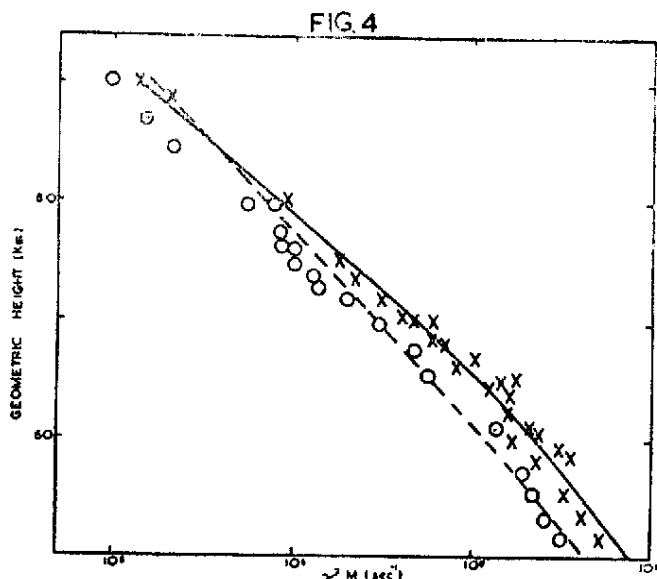
Fig. 4 — Height variations in summer and winter compared with the
corresponding height variations of Cole and Kantor provision-
al subarctic atmospheres in summer and winter. The absolute
value of cross-section has been adjusted so that the summer
curve is fitted to the summer experimental data. The the-
oretical curve of Fig. 1 lies between these curves.
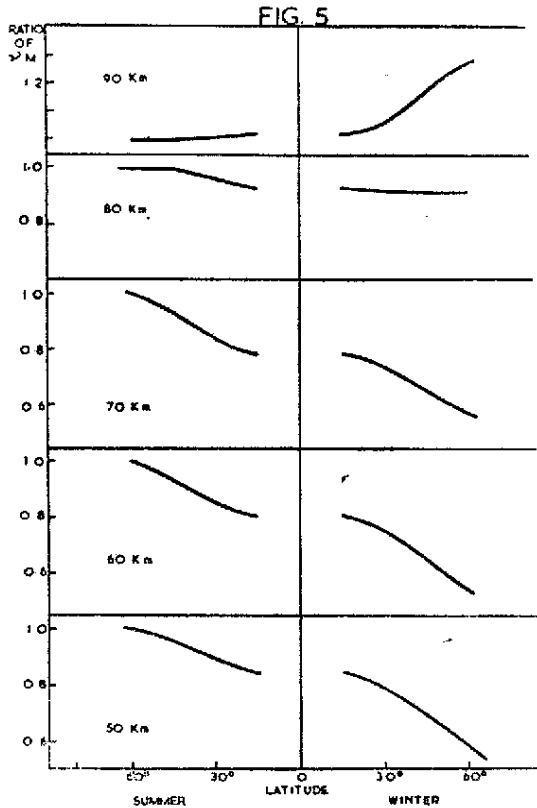
Fig. 5 — Variation of ν_M with latitude. summer and winter, deduced from Cole and Kanton's provisional atmospheres. The ratios at each height are relative to the summer subarctic values of collision frequency shown in Fig. 4.
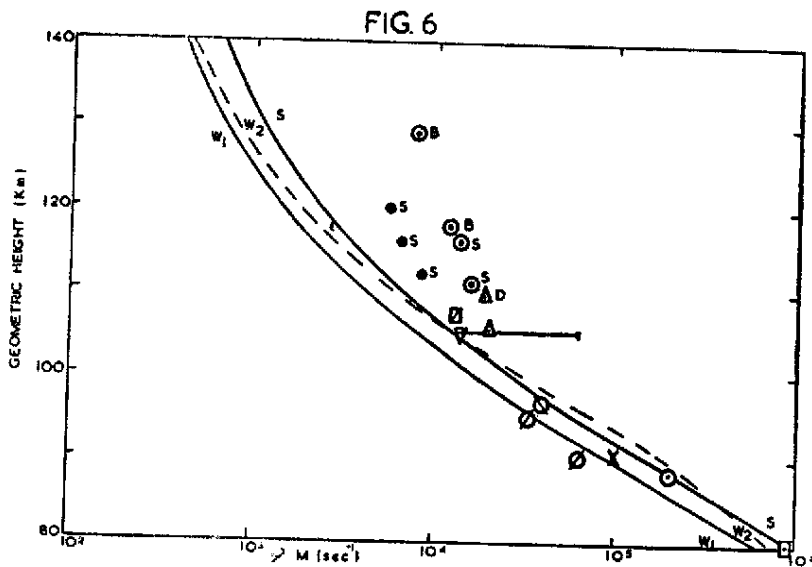
Fig. 6 — Comparison of experimental values of collision frequency (symbols and thin lines) and theoretical values. Curves S and W1 are extrapolations using the U. S. Standard Atmosphere as fitted in Figs. 2 and 3, curve W2 is an estimate based on Cole and Kantor winter values plus satellite data above 150 km. A discrepancy appears above about 95 km which rapidly increases with height.

SOME COMMENTS ON OUTSTANDING PROBLEMS

IN ABSORPTION

by

W. R. Piggott

Radio and Space Research Station

Slough, Bucks, England

There are still important difficulties in the interpretation of absorption data which are not understood even at the equator where the theory of analysis is relatively simple.

The problems are:

a) — Is the large part of the absorption in the D region or in the main E layer?

b) — Are the anomalies in absorption due to changes of ionization density, collision frequency or both?

Internally consistent but widely different interpretations are possible with either large values of collision frequency in the E layer or very small values. Both extremes raise serious difficulties.

If the collision frequency is consistent with the experimental values (large value model) accepted analyses (e.g. Jaeger method or Rawer method) are wrong because the scale height of the collision frequency is much larger than the scale height of the ionized constituents. This completely alters: (a) — the computed frequency variation of the E layer deviative absorption both on frequencies less than and greater than foE; (b) — the predicted diurnal and seasonal variations of absorption at all frequencies; and (c) — the solar cycle variation of the absorption for frequencies reflected in the E layer.

The differences are important, for example, the absorption due to (c) should decrease with increase in solar activity. In addition

this error would cause the deduced amount of absorption low in the D region to be much too high.

For the other extreme it is difficult to obtain sufficient absorption because is small at the levels in the D and lower E layer where the electron density is high.

If the partial reflection, very long and long wave and rocket values of electron density in the D region are correct the HF absorption must be almost entirely above the mesopause (above about 80 km). These show at temperate latitudes, a decrease in D region ionization density with decreasing latitude in rough agreement with the latitude changes in cosmic ray intensity. It is important to discover whether the high absorption normally found near the equator is due to excess ionization or increased collision frequency. This might be studied using rocket or LF short range propagation as well as the frequency variations of virtual height and absorption.

When the seasonal and diurnal variations of absorption obey different laws, as is usual in equatorial regions, this implies corresponding changes in the atmosphere which may alter either the collision frequency or electron density. The morphology of these variations is very important but is little known. Flügel claims that there is a magnetic dip factor with peak absorption near 15° magnetic latitude. Thus, if true, is also very important and needs careful confirmation.

At higher latitudes there is some evidence for solar cycle variations in collision frequency in the E region. If these are confirmed, some of the abnormalities in absorption may be due to collision frequency changes.

Comparisons of the deviative absorption deduced by aproximate methods and by a full phase integral analysis show stricking differences, for example a parabolic layer can give an absorption independent of frequency from 0.3 to 3.0 MHz. The use of aproximate methods should therefore be avoided.

Great care is necessary to distinguish between the absense of ionization and the condition that it does not effect radio waves. Thus

in the region where $v > (\omega \pm \omega_L)$ the complex refractive index varies so that $n^2 - 1 \propto N/v$. Thus equal percentage changes in N and v, such as can be due to pressure perturbation of N and v, do not alter N/v and are invisible. A comparison of partial reflections computed for the case when irregularities are possible in both N and v, shows that the fluctuations in v have little effect until $v \approx (\omega \pm \omega_L)$. For such and larger values of v, fluctuations in v can alter the interpretation of the collision frequency and electron density at low height, as shown by partial reflection techniques, by factors of orders 2 to 3.

SUMMARY OF THE SESSION AND OTHER DISCUSSIONS

by

A. N. Hunter

University College Nairobi, Kenya

Professor N. Skinner gave the review of current knowledge on absorption of radio waves in the equatorial ionosphere. He drew attention to the scarcity of absorption measurements at low latitudes although these are relatively easier to interpret than at higher latitudes because of the approach to quasi-transverse conditions. Such data are of importance to radio engineers but in addition are necessary for the determination of the structure of the lower ionosphere. Measurement of the frequency dependence of absorption is important in estimating the relative contributions of the D and E layers to the total absorption, and the published results show considerable discrepancies which remain to be resolved. Only one measurement of the effect of lunar tides on absorption has been published. Experimentally there is a need for comparison of pulse reflection (A1) measurements with riometer (A2) studies in order to make possible the replacement of the time consuming A1 method by riometer techniques The development of multifrequency riometers offers a powerful tool for absorption studies if the present considerable difficulties in experiment and interpretation can be overcome.

Three papers were presented. A. Gnanalingam and P. Ratnasiri described the results of measurements of ionospheric absorption at vertical incidence in the frequency range 2.0 to 2.9 MHz at Colombo, Ceylon. They find a linear relation between absorption and sunspot number with a slope twice that found in similar studies at Ibadan. Additional stations are required in order to resolve the discrepancy. The seasonal variation in absorption at Colombo at zero sunspot number varies as $(\cos \chi)^{1.7}$, excepting an abnormally low absorption observed for the period May to September; after allowing for the effect of the variation with season of the distance of the earth from the sun, this may be attributed to a decrease either of D region electron density or of collision frequency. It is to be noted that the diurnal variation of absorption varies as $(\cos \chi)^{0.9}$; since the sun cannot distinguish between the seasons, this result in strong evidence for actual changes in the constitution of the lower atmosphere.

P. Bandyopadhyay presented details of 30 MHz riometer measurements in Huancayo since 1961. The observed daily maximum absorption is 0.5 to 1 dB. There is at times an evening peak in addition to the midday peak which has also been observed by other stations. The observed decay of synchrotron radiation noise from the nuclear explosion of July 1962 agrees with the theoretical

time constant of 16 days. The D region absorption has not yet been computed. G. W. Adams gave an account of the use of multi-frequency riometers for which a sensitivity of 0.1 dB was claimed. He pointed out that if absorption occurs at levels below 75 km the frequency dependence of absorption gives information about electron densities in this height range, the usefulness of the method being mainly in daytime hours around noon and during disturbed times which give enhanced D layer ionization.

There was considerable discussion stimulated by the chairman, W. Piggott, both at the session and at a meeting held in the evening.

The principal points which arose during the discussion were: —

1. The importance of further equatorial absorption measurements in order to determine electron densities in the D region.

2. The need to resolve the discrepancy in frequency dependence and solar activity which appears in the records from Colombo, Ibadan and Singapore.

3. Whilst recognizing the potentialities of riometer studies, particularly with multi-frequency instruments, it was thought that these are much more difficult to carry out with the required accuracy of 0.1 dB than is the case with pulse methods; consequently caution should be exercised in the use and interpretation of data from riometers.

W Piggott emphasized that the interpretation of absorption records depends on an accurate determination of at least one of the following quantities: — electron collision frequency in the absorbing region, electron density in the absorbig region and the ionization gradient in the reflection region. He pointed out that extrapolation using standard atmospheres gives collision frequencies which are smaller by a factor of 3 at 90 km and by a factor of 10 at 130 km than those experimentally observed, although the values are reliable below 80 km. This discrepancy must be resolved before absorption data can reliably be interpreted.

About one half the experimental evidence points to absorption occurring almost wholly in the E region and the other half to there being a considerable contribution from the D region. It is clear that there must be some absorption in the D region since there would otherwise be a decrease of absorption with solar activity, which is not in agreement with observation. We must distinguish between the absence of ionization and the absence of an effect on radio waves. In addition, sunspot cycle variations in reflection from the E and F layers are similar and this again points to a dominant D layer absorption. No critical experiments have been devised to resolve these questions.

In computing results from absorption experiments it is important to carry out full wave analyses using phase integral methods on a computer as these can reveal serious errors in the simple approach; there are no methods which are worthwhile, which compromise between such a full wave analysis and the simplest approaches. Local patches in ionization of the order of a few Fresnel zones in extent may completely alter the pattern of absorption measurement.

Evidence from rocket experiments agrees in giving electron densities of less than 1000 per cm³ below 80 km suggesting that HF absorption must be above this height. At temperate latitudes the values obtained for the variation of electron density with height agree roughly with the latitude variation of cosmic ray intensity. Measurements of cross modulation made by D. Farley in another session gave evidence for ionization at the 70 km level but no evidence for appreciable ionization below 60 km at the equator.

Other points of interest included the question as to whether there is a real change of collision frequency with sunspot number; the difference between the results obtained for the upward and downward legs of the solar cycles and the fact that cosmic ionization is much less at equatorial latitudes than at higher latitudes. It was considered that high frequency Doppler data are too indirect for absorption information but that it is important to obtain VLF results over short distances of the order of 150 to 200 km, this latter experiment being technically easy.

It is important to discover whether the high absorption near the equator is due to collision frequency or ionization.

Recent Russian work (Flügel) of considerable interest has suggested that there is magnetic control of absorption near the equator with substantially higher absorption on either side at latitudes of about $\pm 15°$ and so producing an equatorial anomaly which parallels that in foF2. There is some reason to suspect that this effect may be even greater than is suggested by the Russian work and a chain of stations making absorption measurements across the dip equator is suggested in order to establish the true position.

III — THE REGULAR E-REGION AND

EQUATORIAL Es

III — THE REGULAR E-REGION AND EQUATORIAL Es

(Discussion leader: Ken-Ichi Maeda)

Summary of the Review by

D. T. Farley

Jicamarca Radar Observatory, Lima, Peru

The E region is a rather well behaved portion of the ionosphere and appears now to be quite well understood in most respects. A list of references is given in a recent review paper by Bourdeau [1]. Typical electron densities are of the order of 10^5 cm^{-3} during the day and perhaps 10^3 cm^{-3} at night, with reported nighttime values ranging from 10^2 to 10^4. Temperatures are of the order of $200°$ to $500°$K. All the details of the photochemistry of the E region are not as yet completely clear. We do know, however, that O_2 plus, O plus, and N_2 plus are the principal ions produced by photoionization, whereas O_2 plus and NO plus are the most abundant ions actually present. The loss of ions takes place mainly through atom-ion interchange reactions and dissociative recombination.
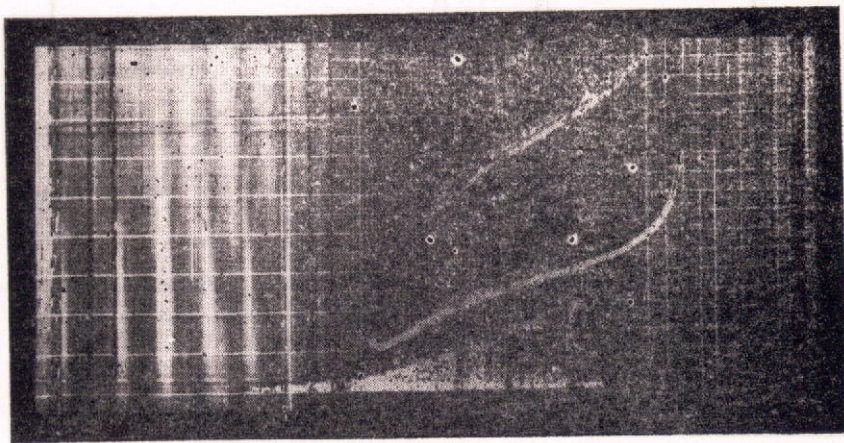
Fig. 1 — A typical equatorial ionogram showing Esq and slant Es.

Neglecting motion terms, the continuity equation for the electron density, N, can be written as

$$dN/dt = q - \alpha N^2$$

where q is the production function and α is the effective recombination coefficient. In equilibrium, then

$$N = (q/\alpha)^{1/2} = (q_o/\alpha)^{1/2} \cos^n \chi$$

The value of q_o is of the order of 3×10^8 cm^{-3} sec^{-1}, n is between 0.5 and 0.6, and α is perhaps [2] of order 10^{-7} cm^{-3} sec^{-1}. The latter value is still somewhat controversial. Assuming it to be correct, however, we find a typical time constant for the daytime E region, $\alpha N/2$, of the order of a minute.
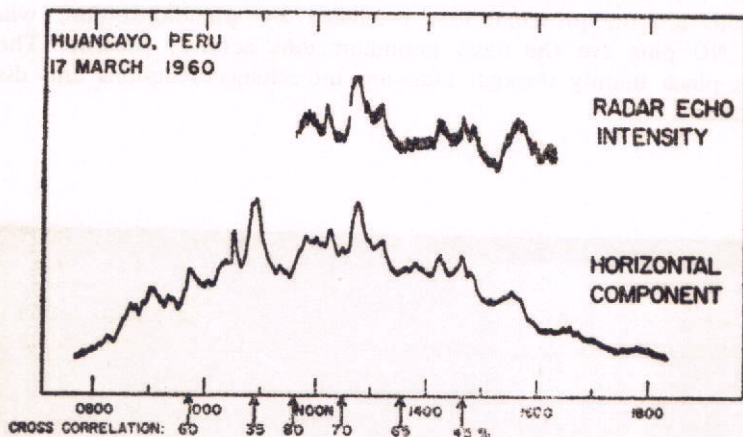
Fig. 2 — An illustration of the very close correlation between the radar echo intensity at 50 MHz and the electrojet strength, as measured by the horizontal component of the magnetic field.

An important feature of the lower E region is that the electron gyrofrequency is greater than the electron collision frequency, whereas the reverse is true for the ions. As a result, the Hall conductivity is large, which at equatorial latitudes gives rise to the equatorial electrojet. Equatorial sporadic-E has long been known to be closely associated with the electrojet. In the last

few years some progress has been made in understanding how this association comes about. VHF observations, mainly at Jicamarca, Peru, have demonstrated that these irregularities are plane waves traveling normal to the magnetic lines of force [3]. Waves having a large component of their velocity parallel to the motion of the electrons in the electrojet travel at approximately the speed of sound in the medium. Some waves are also observed which travel normal to both the magnetic field and the electron streaming velocity. These waves, which are responsible for the echoes seen by a vertically directed radar, are considerably weaker than the oblique ones and travel at all velocities less than or equal to the speed of sound.
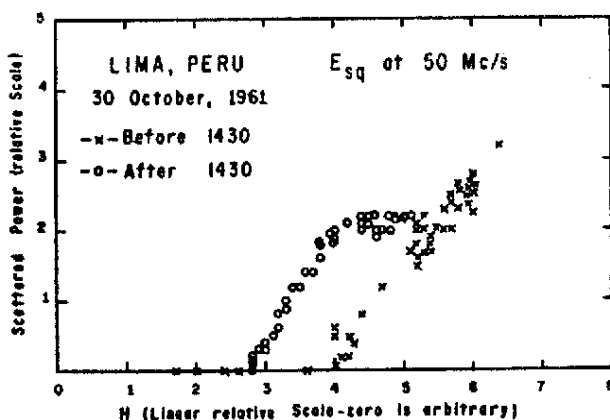
Fig. 3 — An example of the "threshold effect". Strong radar returns are not obtained until the electrojet strength reaches a certain critical value.

It has been shown [4] that the current in the electrojet can cause a plasma instability known as the two-stream instability. The growing waves resulting from this instability can account for nearly all of the observed features of the oblique echoes. The explanation of the overhead echoes is not so clear, however. Perhaps it arises from non-linear processes once the instability is developed.

Several workers have proposed macroscopic instability theories which somewhat oversimplify the plasma physics, but take account of the variation of electron density with height [5]. These theories have difficulty in explaining the small scale irregularities observed on VHF, but may be of importance for the larger scale sizes.

HUANCAYO, PERU (1960)
(Spectra integrated photographically)
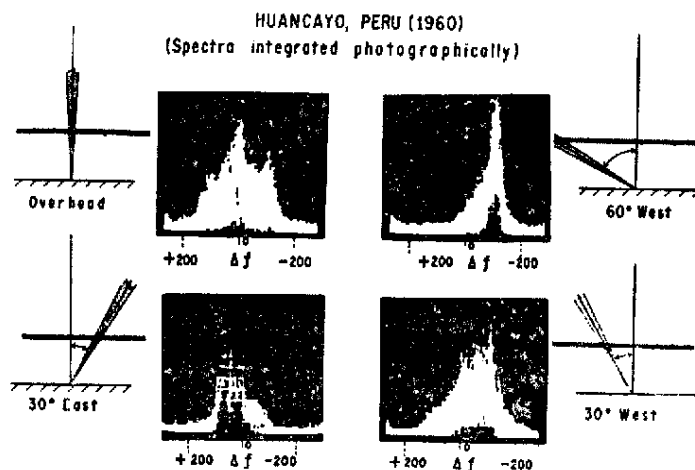
Fig. 4 — Spectra of radar echoes at 50 MHz related to the direction of propaga-
tion. Note that on the westward pointing examples, the spectra have
peaks at the same Doppler shift. This shift corresponds to the sound
velocity.

LIMA, PERU
18 August, 1962
1100-1200 Local Time
RELATIVE SCALE

LEGEND

- - - - - Radar Sensitivity $\left(\frac{V}{R^4}\right)$

—*—*— Relative Echo Power (P_R)

—o—o— Scattering Cross Section
per unit Volume (σ)
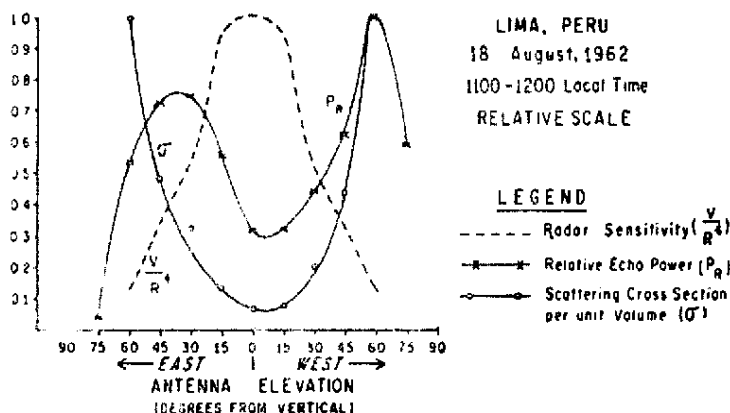
Fig. 5 — The variation of scattering cross-section, for the electrojet irregularities,
with elevation angle. When all the geometrical factors have been
removed, we find that the oblique echoes are much stronger than the
overhead echoes. This is in qualitative agreement with theoretical
predictions.

References

1) — R. E. Bourdeau. **Science, 148**, 585 — 594, 1965.

2) — R. B. Norton, T. E. VanZandt and J. S. Denison, **Proc. Int. Conf. Ionos.** (London), Inst. Phys, and Phys. Soc., London, 1963.

3) — Most of this work is reviewed by K. L. Bowles, B. B. Balsley and R. Cohen (**JGR, 68**, 2485 — 2501, 1963).

4) — D T. Farley, Jr., **JGR, 68**, 6083 —6097, 1963.

5) — F. B. Knox, **JATP, 26**, 239 — 249, 1964.
J. D. Whitehead, **JATP, 25**, 167 — 173, 1963.
K. Maeda, T. Tsuda and H. Maeda, **J. Ionos. and Sp. Res. in Japan, 17**, 147 — 159, 1963.

ROCKET OBSERVATIONS OF THE EQUATORIAL IONOSPHERE

by

L. J. Blumle, A. C. Aikin and J. E. Jackson

Goddard Space Flight Center, NASA.

Greenbelt, Md., U.S.A.

During March 1965, a series of six rockets were launched in the vicinity of the magnetic equator, aproximately 100 km from the coast of Peru for the purpose of measuring the electron density distribution of the equatorial ionosphere to an altitude of 200 km. The rocket payload consisted of a nosetip Langmuir probe and the two-frequency radio propagation experiment (24 and 72 MHz).

Results of the four daytime flights which were launched at a solar zenith angle of approximately 12°, were essentially identical and one (14.181) is illustrated in Fig. 1. This figure illustrates the electron density and Langmuir probe current as a function of altitude. Ionograms obtained at the firing showed equatorial sporadic E at 110 km but there was no evidence of a large increase in density in the altitude region of the electrojet.
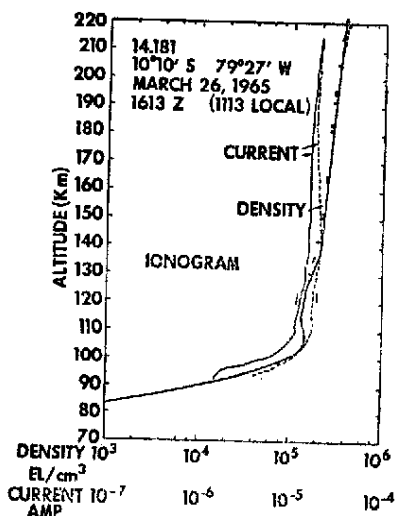
Fig. 1 — Electron density and Langmuir probe current as a function of altitude observed in the daytime equatorial E region. Ionogram N-h data are shown by crosses.

The results of two night flights separated by nine days are shown in Figures 2 and 3. At 2200 LMT the electron density profile has essentially constant density of 10^3 cm^{-3} from 100 to 220 km. At 0140 LMT, the profile has a definite region 30 km thick with a peak density of 10^4 cm^{-3} at 105 km.
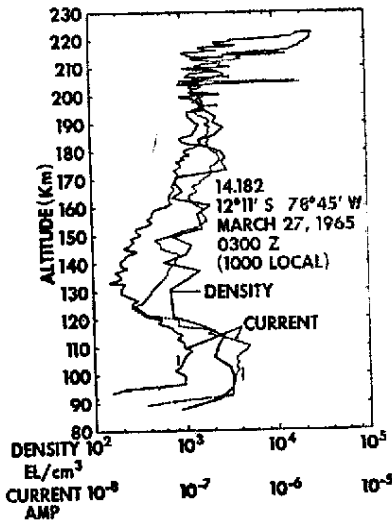
Fig. 2 — Electron density and Langmuir probe current as a function of altitude observed on 14.182 at 2200 LMT.
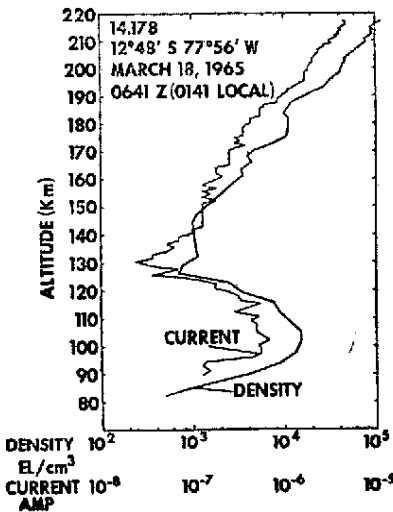
Fig. 3 — Electron density and Langmuir probe current as a function of altitude observed on 14.178 at 0141 LMT.

SOLAR CYCLE AND ANNUAL VARIATIONS OF THE E LAYER

ELECTRON DENSITY AT IBADAN

by

Arthur J. Lyon

University of Ibadan, Nigeria

The Solar Cycle Variations

Figure 1 shows the variation of annual mean foE at noon with mean sunspot number R at Ibadan (a) and at Slough (b). In both cases the data are for the years 1952-64. The least squares regression lines are:

$$(foE)_{Slough} = 2.86 \ (1 + 0.0015R)$$
$$(foE)_{Ibadan} = 3.47 \ (1 + 0.0014R)$$

The coefficients of relative increase with sunspot number are thus very nearly identical at the two stations.
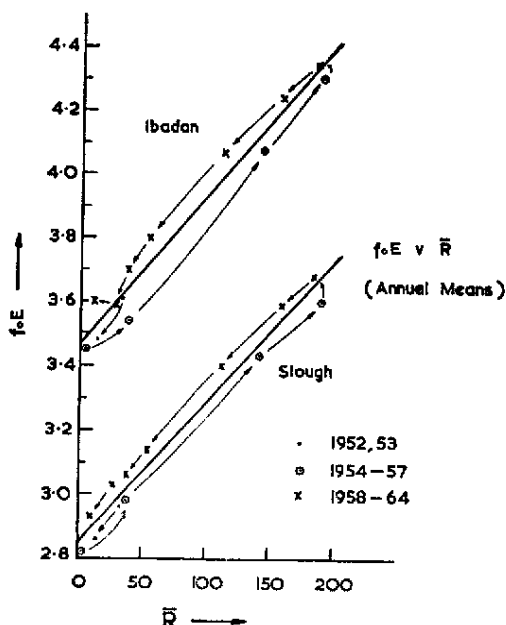
Fig. 1 — Variations of annual mean foE at noon with annual mean sunspot number at Ibadan and at Slough. Circles are for the rising phase and crosses for the falling phase of the cycle, and arrows indicate the direction of change in successive years.

A curious feature of these graphs is that at both stations foE is consistently higher, by about 0.1 MHz, during the falling phase of the solar cycles, 1958-64, than in the preceding rising phase, 1954-57.

The Annual Variations

Figure 2 shows how noon foE (averaged over the whole period 1952-64) varies with month of the year. The variation is clearly similar to that $\cos \chi$ shown below. If however the character figure $(foE)^4 . (\cos \chi)^{-1}$ is plotted against month of the year, the third diagram of Fig. 2 is obtained. It is clear that there is a residual annual variation having a maximum near the December solstice and a minimum near the June solstice. The total range of the variation is about 5% of the mean value.

Because of the uncertainty of the earth's orbit the sun-earth distance varies in such a way that the ionizing flux is about 6.3% greater on January 1st than on July 1st. The residual annual component is thus of the right order of magnitude.
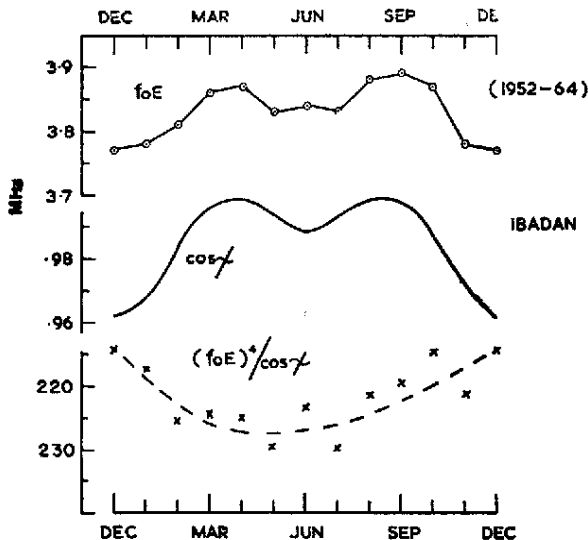
Fig. 2 — Variations through the year of noon foE, noon $\cos \chi$ and the E region "character figure" $(foF)^4/\cos \chi$ at Ibadan.

It is known that foE varies diurnally more nearly as $(\cos \chi)^{0.3}$ than as $(\cos \chi)^{0.25}$ as simple theory requires. In that case q should be proportional to $(foE)^4 / (\cos \chi)^{1.2}$. This quantity is plotted in Fig. 3, which shows that the residual annual change is than about 6.8%, closer to the theoretical value than before. The fit of the points is also improved.
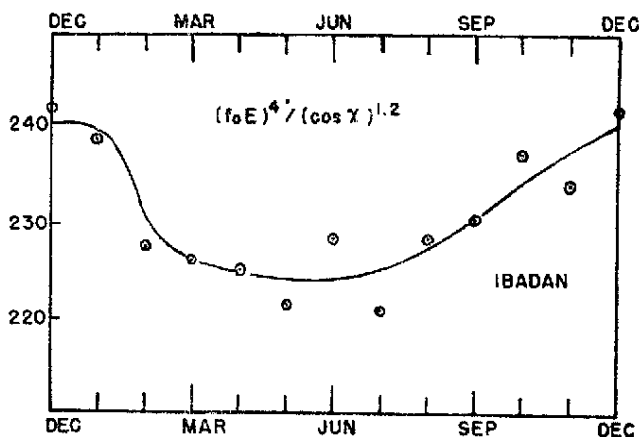
Fig. 3 — Annual variation of the quantity $(foE)^4 / (\cos \chi)^{1.2}$, proportional approximately to the rate of electron production q.

Two conclusions appear to be justified:

1) that noon foE has no seasonal variation, and its variation throughout the year is entirely explained by the variations of $\cos \chi$ and the sun-earth distance, and

2) that the diurnal $\cos \chi$ exponent of about 0.3 is also valid for noon foE as it varies through the year.

It is believed that this is the first time the effect of the earth's orbital eccentricity have been isolated from other seasonal or annual variations in an ionospheric parameter. It is intended to check this finding with data from other stations.

SECOND-ORDER IRREGULARITIES IN THE

EQUATORIAL E-REGION

by

Robert Cohen and Kenneth L. Bowles

Jicamarca Radar Observatory, Lima, Peru

Although the two-stream instability theory of Farley has been quite successful in accounting for many features of the irregularities produced in the equatorial electrojet, greater sensitivity and improved techniques of observing the power spectrum of radio echoes have resulted in the resolution of weaker irregularities not predicted by the theory. In particular, such irregularities are observed (Fig. 1) when the radar is directed vertically (Fig. 2 and 3), and when observing obliquely (Figs. 4 and 5) irregularities are observed that have lower Doppler shifts than are contemplated by the theory.

Experimental spectra are presented that demonstrate the close adherence to the two-stream theory for a well-developed electrojet, and it is shown how the relative contribution of the weaker irregularities can be resolved when the electrojet is not so strong. The shape of the spectrum obtained at vertical incidence is shown to be narrow for a weak electrojet, and to be broadened as the electrojet becomes stronger.

The weaker irregularities probably result from non-linear coupling of the stronger irregularities, as will be demonstrated by Dougherty and Farley (private communication). In particular, that explanation implies that irregularities of small wave numbers result from those of large wave numbers, and would permit the formation of the horizontal irregularities that give rise to the echoes at vertical incidence.
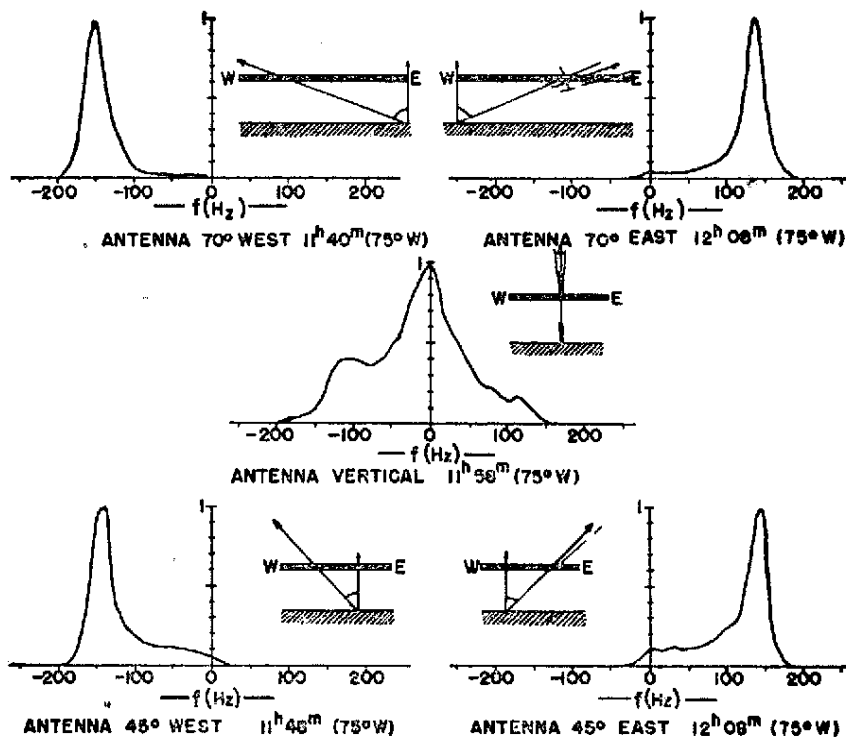
Fig. 1 — Composite of power spectra obtained near noon from electrojet irregularities above Jicamarca, Peru, at various angles, using a frequency of 49.92 MHz.
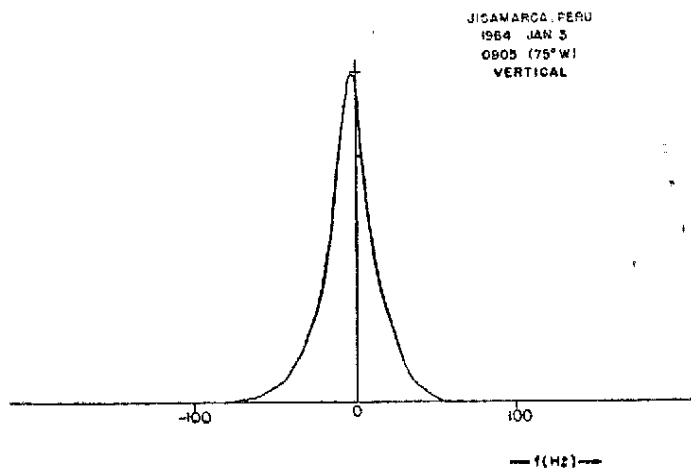
Fig. 2 — Spectrum obtained at vertical incidence for a weak electrojet.
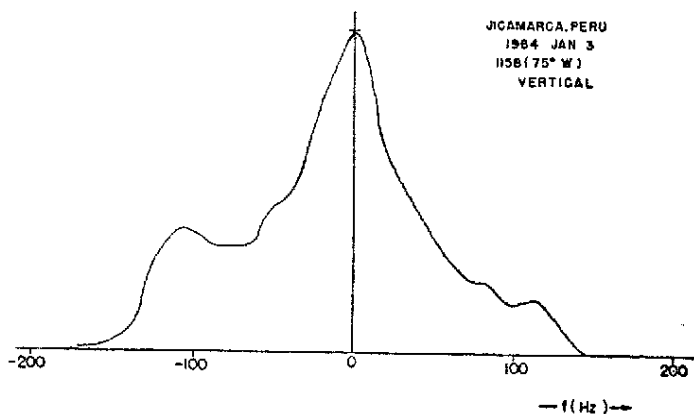
Fig. 3 — Same for a well-developed electrojet.
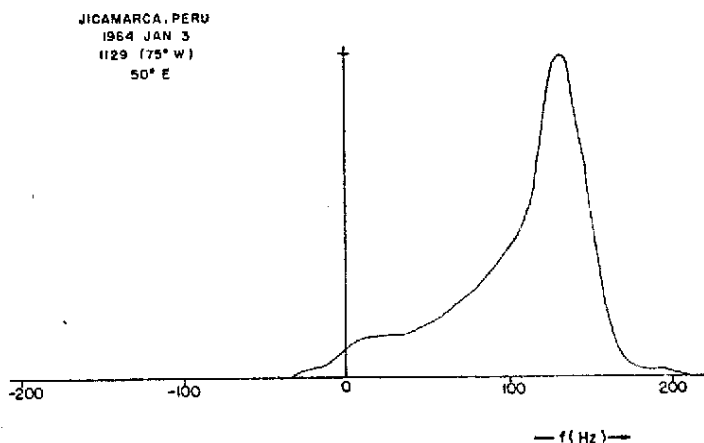
Fig. 4 — Spectrum observed at an off-vertical angle of 50°East for a weak electrojet. Note that the 120 Hz frequency shift of the strong component (corresponding to an acoustic velocity of 300 m/s) is the same as that at 50°E, similar to the comparisons of Fig. 1.
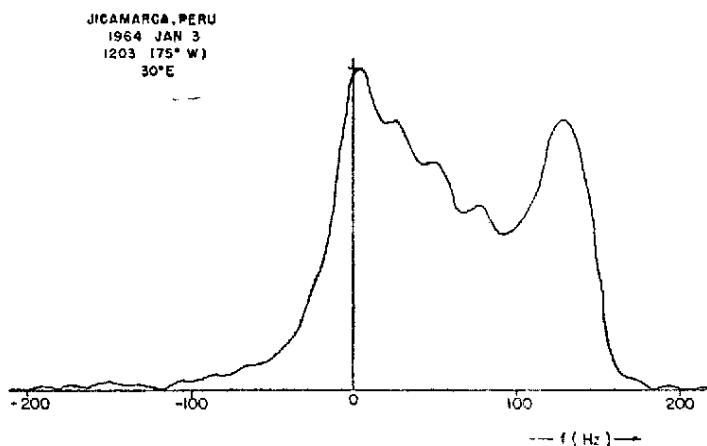
Fig. 5 — Spectrum observed at an off-vertical angle of 30° East for a well developed electrojet.

SOME HIGH FREQUENCY OBSERVATIONS OF EQUATORIAL SPORADIC-E IRREGULARITIES

by

G. S. Kent

University of the West Indies, Jamaica

Results are presented which have been obtained from measurements made on Sporadic-E irregularities over Ibadan, Nigeria (Magnetic Latitude $2\frac{1}{2}°$ S). The main measurements which have been made are on the diffraction pattern formed by reflection on the ground. These have been made by the conventional three spaced receivers method and reduced by a full correlation analysis to find the size and shape of the pattern and its drift velocity. Several frequencies have been used between 3 and 7 MHz.

In addition to this, some preliminary measurements were made on the angle of arrival of the echoes at 7 MHz using directional antennas. These showed the irregularities scattered the incident radiation to very wide angle in the east-west plane and that, under most experimental conditions, the received angular spectrum at the ground would depend mainly on the antennas used.

The measurements on the diffraction pattern showed the irregularities to be elongated along a magnetic north-south axis with dimensions of the order of 300 m in this direction. No estimate was obtained of their east-west size since, as explained above, the angular spectrum and hence the diffraction pattern size in this direction was determined by the experimental parameters. Measurements on the drift velocity of the pattern were made on several days using the range of frequencies from 3 to 7 MHz in fast sucession. Because of the elongation of the pattern these measurements were limited to the east-west component of the true drift. The results obtained on three such days are shown in Fig. 1. The following are the main points which have emerged from this analysis:

1) — The drift velocity is almost always to the west.

2) — The measured velocity is independent of the frequency used in the range 3-7 MHz.

3) — The drift velocity of the irregularities (half that of the diffraction pattern) may vary on different occasions between 0 and 125 m/sec with a mean value of about 80 m/sec.
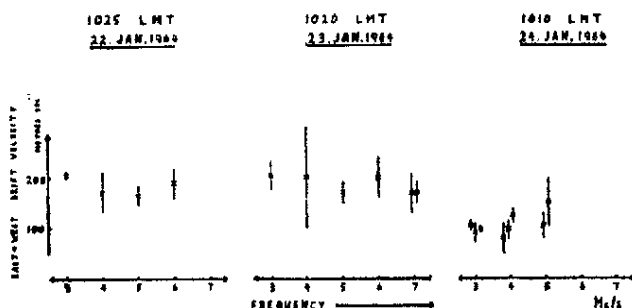
Fig. 1 — East-west component of the true drift (m/s) for three days in January 1964.

A second parameter usually determined from drift analysis is Vc, which is a measure of the random changes in the diffraction pattern as it moves. In contrast to V this is found to be highly frequency dependent, as is shown in Fig. 2. In a companion paper in another section of this report, it is shown how Vc may be interpreted in terms of a randon velocity of motion of the irregularities. When this theory is applied to the experimental results, the variation of V_c with frequency is found to be due to the changes in the refractive index of the medium with frequency. Taking this into account, a mean random velocity of about 150 m/sec may be deduced.

The results given here can be compared to those obtained on the magnetic equator at VHF, from which a plane wave picture of sporadic-E is deduced. These waves have velocities greater than 300 m/sec

with their wave-normals being close to the direction of the electrojet. This picture appears incompatible with the results described here, and it may be concluded either, that the same irregularities are not responsible for scattering at both HF and VHF, or that there is a very rapid change of their characteristics with latitude about the magnetic equator.
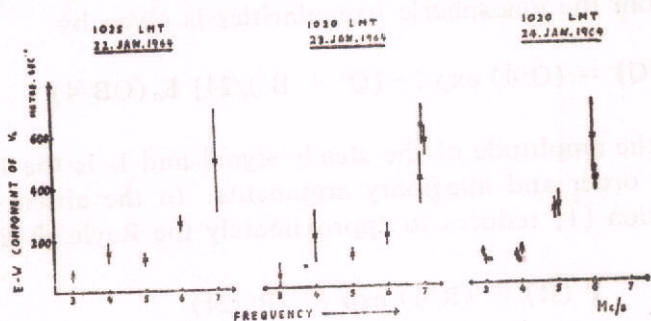
Fig. 2 — East-west component of Vc in m/s for the same observations of Fig. 1. Note the frequency dependence of Vc.

FADING CHARACTERISTICS OF Es REFLECTIONS OVER THE

MAGNETIC EQUATOR IN THUMBA (INDIA)

by

R. G. Rastogi, M. R. Deshpande and N. D. Kaushika

Physical Research Laboratory, Ahmedabad, India

The probability distribution of the amplitude of radio waves reflected from the ionospheric irregularities is given by

$$P(Q) = (Q/4) \exp[-(Q^2 + B^2)/24] \, I_0(QB/4) \qquad (1)$$

where B is the amplitude of the steady signal and I_0 is the Bessel function of zero order and imaginary arguments. In the absence of steady signal, equation (1) reduces to approximately the Rayleigh distribution,

$$P(R) = (R/4) \exp(-R^2/24) \qquad (2)$$

while in the absence of random signal equation (1) reduces to Gaussian distribution.

The fading patterns of Es reflections on 2.2 MHz at Thumba show very large diurnal variation. The fadings are very slow around midday and very fast during morning and evening hours. The amplitude distribution does not correspond to either Rayleigh o Guassian distribution (Fig. 1).

According to Alpert, the relative proportion of steady and random signal can be estimated by the ratio of the mean squares of the amplitude $(R^*)^2$. The value of the ratio $(R^2)^*/(R^*)^2$ is 1.0 for Guassian distribution and $4/\pi$ for Rayleigh distribution. The experimental values of the ratio for Es reflections at Thumba ranges between about 1.3 to 2.2, the mean value being 1.7 (Fig. 2). These results are inconsistent with those derived according to Ratcliffe's theory of isotropic scattering centers having randon phase distribution.
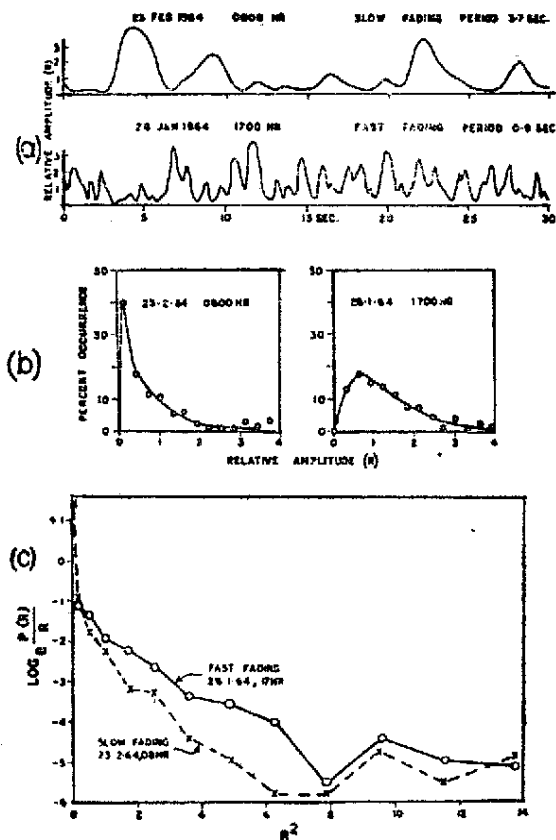
Fig 1 — Sample fading records of Es reflections at Thumba, amplitude probability distribution and their log plots for Rayleigh distribution.

THUMBA JAN FEB 1964·
E REGION 2·2 MC/S·

MEAN = 1·67
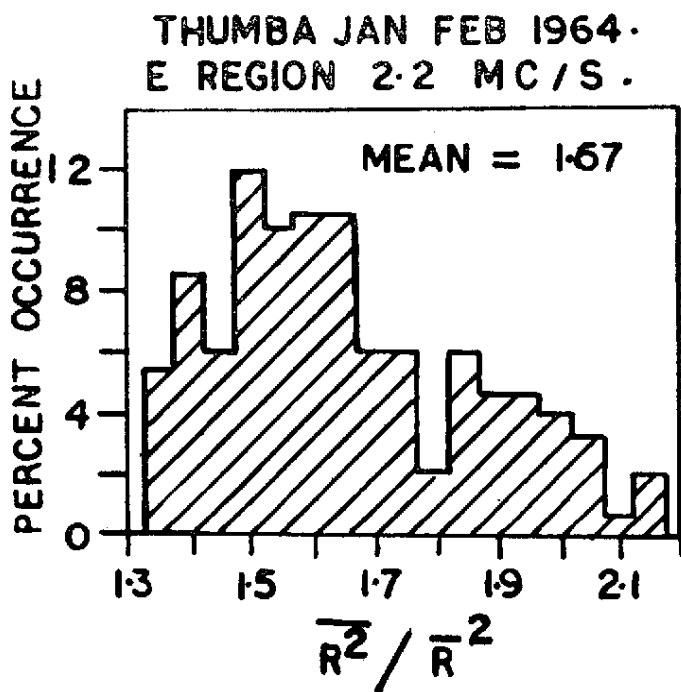
Fig. 2 — Histogram of the values of the ratio of mean squared amplitude and square of mean amplitude of Es reflection over Thumba.

EQUATORIAL Es AND THE ELECTROJET

by

A. J. Lyon and J. O. Oyinloye

University of Ibadan, Nigeria

Correlation Between foEs and H

A study of correlations between the intensity of equatorial Es and the strength of the electrojet is in progress at Ibadan. The monthly medians of foEs for each hour of the day have been averaged over all months of the year for 1958 and for 1964; and the annual mean diurnal variations of H have been calculated in a similar way. Figure 1 shows that in both years foEs reaches its maximum between 10h. and 11h. at nearly the same time as H and so, approximately at least, as the intensity of the electrojet.
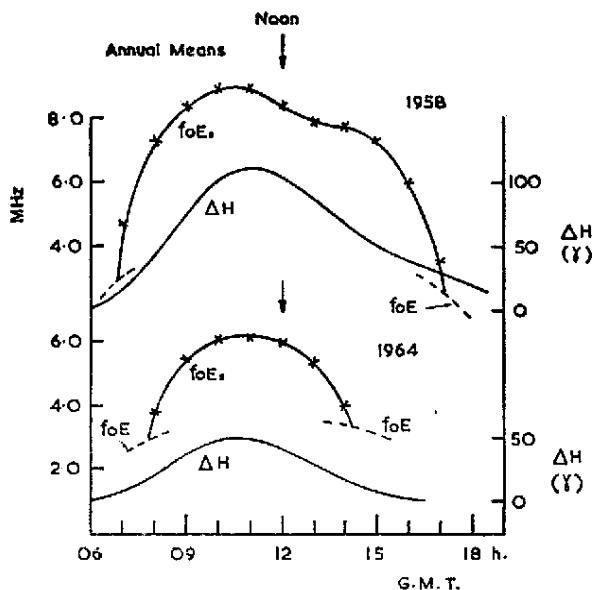
Fig. 1 — Comparision of diurnal variations of foEs (crosses) and of △H, the increase of horizontal field intensity above the nighttime value, for Ibadan at sunspot maximum and at sunspot minimum.

The Es Effective Reflection Coefficient R (Es).

The effective reflection coefficient of Es, R (Es), can be measured with the aid of the pulse reflection (or A1) method used for absorption measurements. The amplitude of Es echoes, A (Es), is of course affected not only by the reflecting or scattering properties of the Es layer but also by the absorption in lower layers. In the present method the latter is eliminated by measuring the amplitude of echoes from the normal E-region, A(E), at a lower frequency (about 2.4 MHz), and at approximately the same height.

It is easy to see that

$$A(Es)/A(E) = K . R (Es) = \alpha,$$

where K is an instrumental constant. Hence the variations of α during the day, or from day to day, will provide a measure of the corresponding changes in R (Es).

In attempting to measure α continuously it is of course necessary to make measurements alternately on E and Es. In view of the relatively slow and smooth variations of A (E) it is usually sufficient to measure it at relatively long intervals, of say 20 or 30 minutes, and to divide measured values of A (Es) by interpolated values of A (E).

Correlation Between R (Es) and H

Cohen and Bowles[1] have reported a remarkable close correlation between variations of H and the intensity of echoes from equatorial Es on 50 MHz. A similar experiment has been attempted at Ibadan on 5.0 MHz using the quantity α which is measured as explained above, and which is proportional to the Es reflection coefficient, R (Es).

Measurements of A (Es) were made as frequently as possible and averaged over periods of 2-5 minutes, and these averages were divided by interpolated values of A (E) to give a series of values of α as shown in Fig. 2. The corresponding variations of H are obtained from a magnetogram.
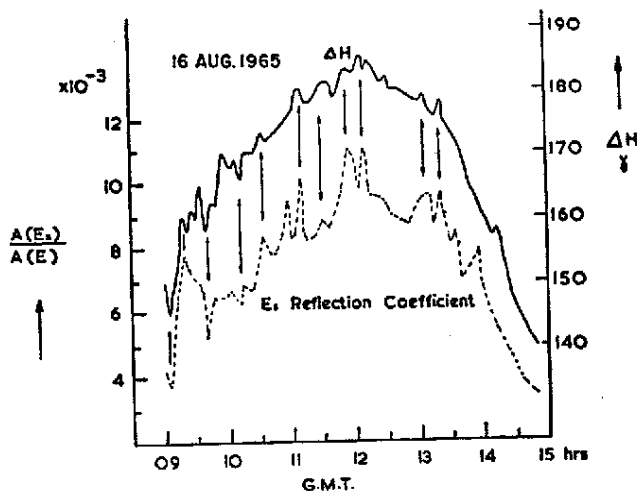
Fig. 2 — Comparison of the diurnal variations of Es reflection coefficient A(Es)/A(E), and H (arbitrary zero) for Ibadan on a particular day. The arrows indicate some of the corresponding features.

There seems to be little doubt in this case that there is a very good correlation. The general trends are similar, the sharp initial rise and final fall occur simultaneously, and both reach a maximum approximately at noon. Moreover many of the finer details correspond.

On two other days, common features occurred but the correlation was not so good, and further work is needed.

Reference:

Cohen, R. and K.L. Bowles, J. Geophys. Res. **68**, 2503, (1963)

NON-LINEAR EFFECTS IN THE ELECTROJET INSTABILITIES

by

J. P. Dougherty

Department of Applied Mathematics and Theoretical Physics,
University of Cambridge

Abstract

The main features of the frequency spectra of equatorial Es, as observed by VHF backscatter, have been explained by Farley in terms of the two-stream instability. The occurrence of scattering at Doppler shifts other than the frequency of the instability can be discussed in some detail by a consideration of the non-linear interaction of the unstable plasma waves. The existence of scattering at vertical incidence can be also be explained in this way.

SUMMARY OF THE SESSION

by

R. B. Norton

CRPL — National Bureau of Standards
Boulder, Colorado — U.S.A.

The most important results presented in this session were observations for both the regular E region and sporadic E. Blumle reported the electron density results obtained by rockets fired from a ship just off the coast of Peru. Several daytime profiles were obtained and showed no surprizing features. These daytime measurements support the scattering theory of equatorial sporadic E since no structure was seen on the profiles obtained from the rocket while at the same time strong sporadic E echos were obtained by an ionosonde. Blumle also presented two nighttime results. One electron density profile, taken at about 2200 LT, showed a peak density in the E region of about 2×10^3 cm^{-3} at 105 km. This peak could possibly be explained by involving scattered Ly β as a nighttime ionization source. Another profile taken at 0141 LT showed a peak density of 10^4 cm^{-3} at 105 km. No explanation for such a density has been given.

Lyon pointed out that a statistical analysis of ionogram data taken at Ibadan showed that the foE variation could be explained solely in terms of a $\cos \chi$ variation and the changing sun-earth distances. This latter effect is small and is normaly mashed by other effect at higher latitudes.

Although no paper were given on the theory of the normal E region, two important points came out in the discussion. First there is still some controversy as to the specific reactions that are important in the E region. This problem is compounded by the possible importance of fast ion-neutral involving minor constituents. Second, although there is ionosphere and laboratory data suggestion that the dissociative recombination coefficient for O_2 plus and NO plus is of the order of 10^{-7} cm^3 sec^{-1}, there is still some doubt that the coefficient is this large specially for NO plus.

Several interesting results were presented for the Jicamarca Radar Observatory. Recent power spectra of echoes from the nighttime E region irregularities above Jicamarca indicate frequency shifts that are opposite to those obtained in the daytime and which may be interpreted in terms of a westward flowing current at night. Such a current had been previously proposed by magneticians. Cohen reported that greater sensitivity of observing the power

spectrum of radio echoes and improved techniques, have resulted in the detection of weak irregularities not predicted by the two stream instability theory as it is presently developed.

These irregularities are seen when the radar is directed upward and, if the electrojet is weak, when the radar is observing obliquely. The Doppler shift for these irregularities is considerably less than for the strong irregularities.

Dougherty suggested that weak irregularities may arise from non-linear coupling of strong irregularities.

Kent reported that some drift measurents made between 3 and 7 MHz at Ibadan by the Mitra method gave much smaller velocities than the ones given by the Jicamarca Observatory for strong irregularities. The suggestion was made that his HF frequency data may refer to the Jicamarca weak irregularities.

IV — THE REGULAR LOW LATITUDE F-REGION:

BOTTOM AND TOP SIDE STUDIES

IV — THE REGULAR LOW LATITUDE F-REGION: BOTTOM AND

TOP SIDE STUDIES

(Discussion leader: Arthur J. Lyon)

Review Paper by

J. W. King

Radio and Space Research Station

Ditton Park, Slough, Buck, England

(paper not available)

DIURNAL VARIATION OF THE QUIET F2 MAXIMUM IONIZATION

ALONG THE NIAMEY MERIDIAN, IN MARCH-APRIL

AND JUNE-JULY 1965

by

P. Vila

GRI, B15, CNET, Seine, France

Detailed bottom side sections of the F2 ionization were obtained utilizing airborne ionospheric soundings along the Niamey Meridian (as shown on Fig. 1) for the March equinox (Fig. 2) and the June solstice (Fig. 3) in periods nearly symmetrical for the magnetic season (Fig. 4). Ionosonde data from Tamanrasset, Ibadan, Bangui and Niamey were also included. Figure 5 displays the magnetic meridian of the study.
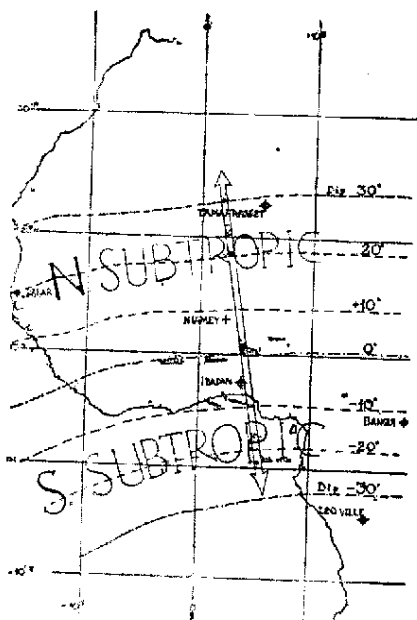
Fig. 1 — Map of the meridian at the heights and stations involved in the work.
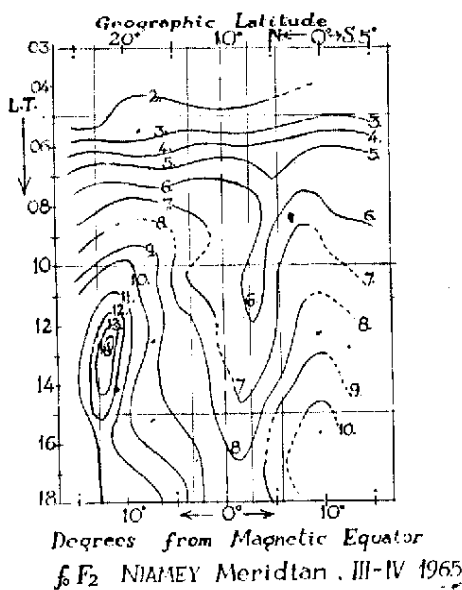
Fig. 2 — Synthetic plot for March equinox with foF2 variation.
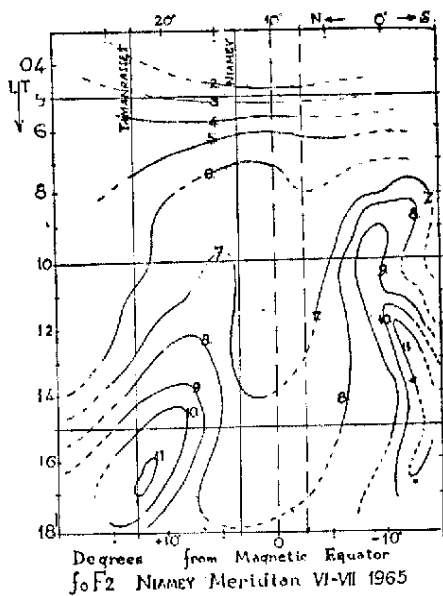
Fig. 3 — Idem for solstice of the previous plot.

MARCH EQUINOX   JUNE SOLSTICE

Dip Equator

Geogr. Equator

Dip Eq
0°N

Dip Eq
0°N

Magnetic Seasons of the Anomaly for the NIAMEY Meridian
------ Iso X lines
X zenith angle of the Sun.
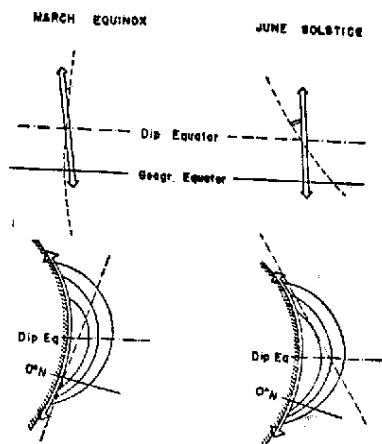
Fig. 4 — Comparison of the magnetic season for the two periods.
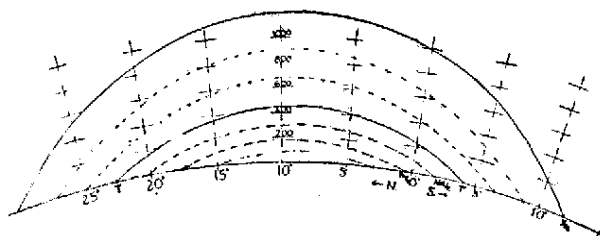
Fig. 5 — The Magnetic Meridian of the study

The maximum ionization crests appeared before 0800 LT, separated by a narrow trough moving northwards at 50 km/hour. The southern crest remained stable while the northern crest moved to the north at 100 km/hour in March and 150 km/hour in July.

The known current systems (Wilkins) do not seem sufficiently developped on the cold side at early hours (0400 to 0800 LT) to support any upward drift of ionization comparable to that of the warm side. The morning cold crest seems only explainable by the additional source

of a conjugate stock of primary photo electrons, of energies 0,3 to 13 eV, which could pile up at levels above 1000 km to 2000 km, travel along field lines imbedded in neutral oxygen atoms at mean temperature 700° K to 1200° K, according to Hanson's cross-section (Space Research II). These temperatures, and the very high electron temperature observed at Jicamarca at 0600, just above the hmF2 line of force seem to account well for the observed accumulation of electrons on both sides at the lower F2 crests themselves.

A continuous F 1½ ledge structure linked the edges at a height of 320 km of the central trough to the F1 (180 km) levels on both inner sides of the crests. This motionless structure lasted until about 1030 LT. In a three-dimensional model of the anomaly, the upper F2 shell above this F 1½ ledge would appear field-aligned from underneath, but wider from the topside. It is suggested that photo-electrons populated this upper F2 shell.

During the maximal phase, the tropical crest under the overhead sun grows at a later time and it is least ionized and much wider in latitude coverage. The more ionized cold crest extending only about 4° in latitude reaches its furthest distance before noon and its peak density is reached about 1300 LT.

This North-South asymmetry can be expressed by the following ratios of ionization (upper limits):

	North	Trough	South
For the Equinox:	3,5	1,0	2,0
For the Solstice:	2,0	1,0	2,5

The very selective enhancement of the F2 ionization inside the magnetic tube of the cold crest could be explained by diffusive equilibrium along lines of force with the F2 ionization being mainly controlled by temperature (Ne $\propto$ $T^{-1/2}$). A complete true height analysis of our sections will be necessary in order to compare them with the other hypotheses which require upward drifts in the equatorial anomaly.

TOP OF THE EQUATORIAL ANOMALY AND CONSTITUTION OF

THE TOPSIDE IONOSPHERE

by

Y. V. Somayajulu

National Physical Laboratory, New Delhi, India

Using the published Alouette Satellite data on the equatorial anomaly and incoherent-scatter data on inferred ion composition in the topside ionosphere, it is shown that the height of the top of the equatorial anomaly is closely related to the transition level of 0 plus to lighter ions. This is interpreted to indicate that the equatorial anomaly forms primarily in the height in which 0 plus is the dominant constituent and is under diffusive control. It is also suggested that the lighter ions may be under chemical control and may not have attained diffusive equilibrium even up to heights of 1,000 km during midday and about 600-700 km during late evening. See Figures 1 through 3.
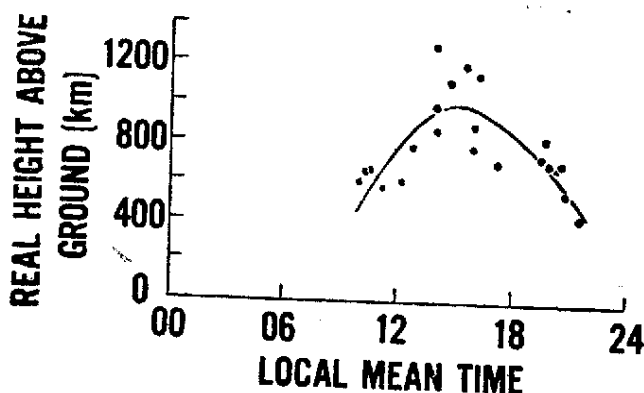
Fig. 1 — Diurnal Variation of the real height above ground of the top of the anomaly.
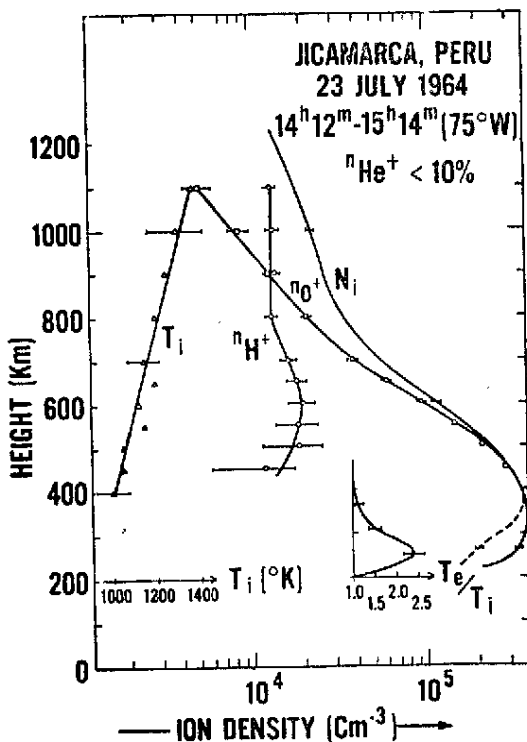
Fig. 2 — Daytime ion composition results inferred by Bowles et al. using incoherent scatter at Jicamarca, which is at the geomagnetic equator.
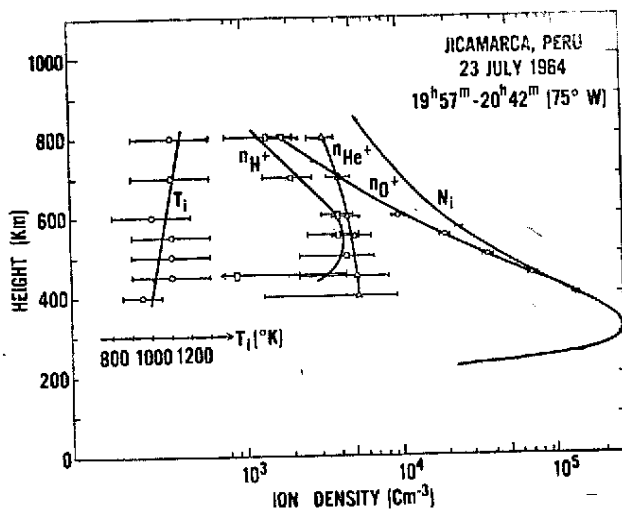
Fig. 3 — Nighttime ion composition results inferred by Bowles et al. using incoherent scatter at Jicamarca.

PRELIMINARY STUDIES OF THE EQUATORIAL ANOMALY

by

J. P. McClure

Jicamarca Radar Observatory

Lima, Peru

The diurnal variation of electron density in the topside ionosphere above the dip equator is observed at Jicamarca. These data are compared with data obtained from topside and conventional ionosondes. Figures 1 shows the Jicamarca data compared with Nmax at Bogota, near the crest of the equatorial anomaly, on a day when the anomaly is well developed.

Temperature and composition measurements made at Jicamarca indicate that in the daytime the electron and ion temperatures are about $300°K$ higher than at night, and that the height of the transition from 0 plus to H plus ions is about 200-300 km higher than at night. This would indicate that the ratio of Nmax at Bogota to the electron density 800-900 km above Jicamarca, on the same field line, should increase in the daytime and decrease to near its original value again at night. Fig. 1 shows that the expected behavior is occuring with approximately the expected magnitude of increase of the ratio, a factor of 3, being observed.

The topside sounder Alouette passed from north to south at about 1500 hours, giving essentially an instantaneous picture of the topside ionosphere along its path. The results were very surprising. Though there was a 3:1 ratio of the densities at the F region maxima at Bogota and Jicamarca, at heights of 500 km and above, there was less than a 50% change in density at any point between the two stations. It is believed that the overlap problem would not affect the accuracy of the topside sounder profiles above 500 km. However, the lack of a substantial "equatorial anomaly" in the topside ionosphere as reported by King and others is definitely contradictory. More comparisons of this type will be made in the near future.
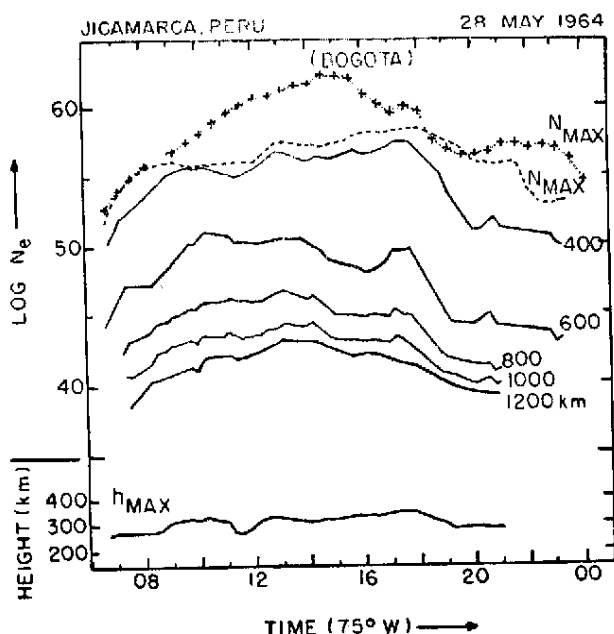
Fig. 1 — Jicamarca electron density variation at fixed heights compared with Nmax at Bogota. Temperature and composition changes from night to day would predict changes in the ratio of Nmax at Bogota and the equatorial density at about 800 km. The observed changes in this ratio are consistent with the observed changes in temperature and composition as measured at Jicamarca.

Figures 2 and 3 show data obtained from the satellite on 15 and 16 October 1964. There is a striking break in the electron density contours at 0200 on 16 October, and at the same time Nmax at Bogota was observed to increase. The break in the contours indicates a change in the electric fields which control the drift and transport of ionization in the F region. It is probable that these electric fields caused the change in Nmax at Bogota, but exactly how they did so is difficult to decide from these data.

Fig 2 — Electron density contours for 15-16 October 1964. Notice the sharp break in the contours at 0200 on 16 October This and the next figure give an indication that ionization was removed from the 800-1000 km region above equator in the hours 0000-0200 on 16 October.
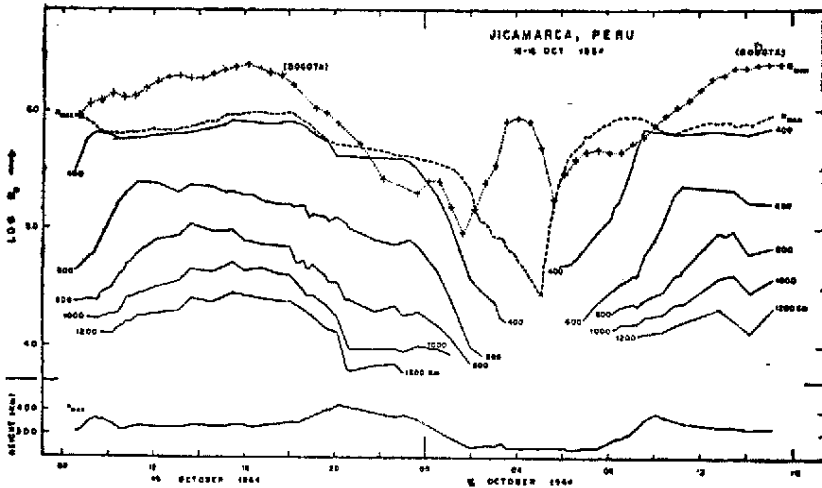
Fig. 3 — Jicamarca and Bogota electron density variations. The cause of the 0200 increase in Nmax at Bogota cannot be definitely ascertained from this data. It begins at a time when the vertical motion of ionization above Jicamarca is suddenly changed. It must be either a redistribution of already existing ionization or an influx of fresh ionization from high above the equator.

A NOTE ON THE MORPHOLOGY OF THE TOPSIDE

EQUATORIAL IONOSPHERE

by

J. O. Thomas*, K. L. Chan, L. Colin and M. Rycroft

NASA Ames Research Center, Moffett Field, California

From ionograms recorded from the Alouette I satellite it is possible to determine the detailed electron density morphology of the topside ionosphere almost from pole to pole. In this illustrated abstract some typical results are presented in the form of curves giving the electron density as a function of latitude at a series of heights between 300 and 1000 km. The scale height, H, of the vertical electron density distribution as defined by

$$H_v = -N/(dN/dH)$$

is also computed and plotted for the same height.

Figures 1 and 2 show the N and H curves for pass number 596 and Fig. 3 and 4 the corresponding quantities for pass number 5427.

The most important new feature of these results can be observed in the form of the curves of Fig. 2 and 4. It is found that H, at the greater altitude shows two distinct maxima between approximately 15° and 30° dip latitudes with a minimum close to the dip equator in between. Lower down the form of the H_v curves is different with minima near $\pm$ 10° dip and a small maximum on the dip equator.

It is shown that the form of the curves at the greater altitudes can be interpreted by means of the formula

---

* Now at Imperial College, University of London

$$1/H_s = (1/H_v) - A/H_o \qquad (1)$$

where

$$H_s = k\,(T_e + T_i)m^{*}_{i}g \quad \text{and} \quad T_e = T_i$$
$$H_v = (-\,1/N)\ \delta N/\delta r\ , \quad H_o = (-\,1/Nr)\delta N/\delta\theta$$
$$r = R_e + h$$
$$A = (\cot\theta)/2$$

in which R_e is the radius of the earth, h the altitude concerned, θ the magnetic (dip) latitude and m^{*}_{i} is the mean ionic mass, k is the Boltzman's constant, and g the acceleration of gravity. It is assumed that at the 900 km level considered below, the electron and ion temperatures in equation (1) are the same. Lower down this assumption cannot be made for converting the observed vertical scale height into a "field aligned scale height", H_s. The quantity H_s can then be interpreted in terms of the ratio of effective temperature to mean ionic mass in the usual way. In Fig. 5 it is shown that when H_s is computed using the above formula and the data of Figs. 1 and 2 for 900 km, the large minimum near the dip equator is removed and H_s changes very little with latitude between $\pm$ 30°. At latitudes above 30°, H_v and H_s are not significantly different.
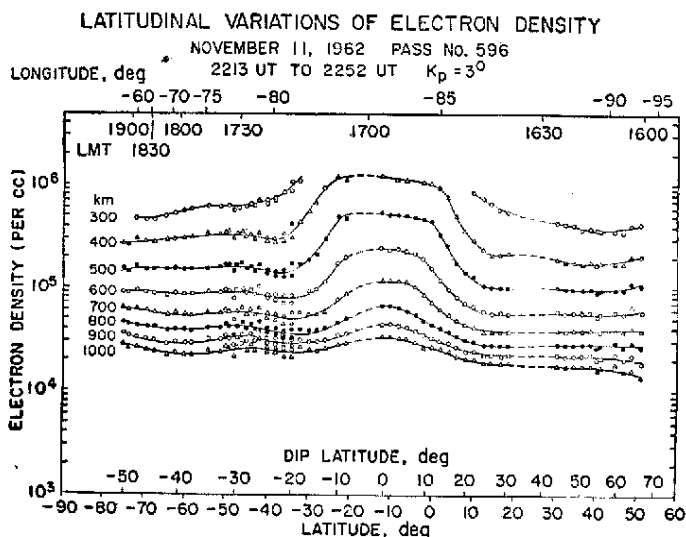
Fig. 1 — The latitudinal variation of electron density for pass 596 of the Alouette satellite.
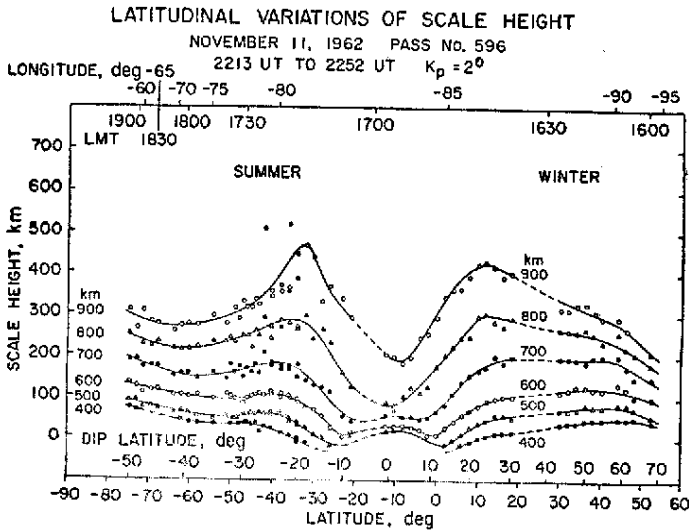
Fig. 2 — The latitudinal variation of scale height, H_v, for pass 596.
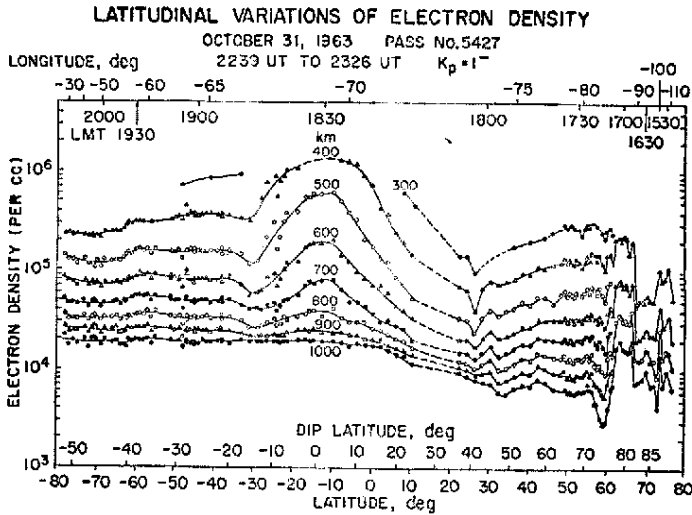
Fig. 3 — The latitudinal variation of electron density for pass 5427.
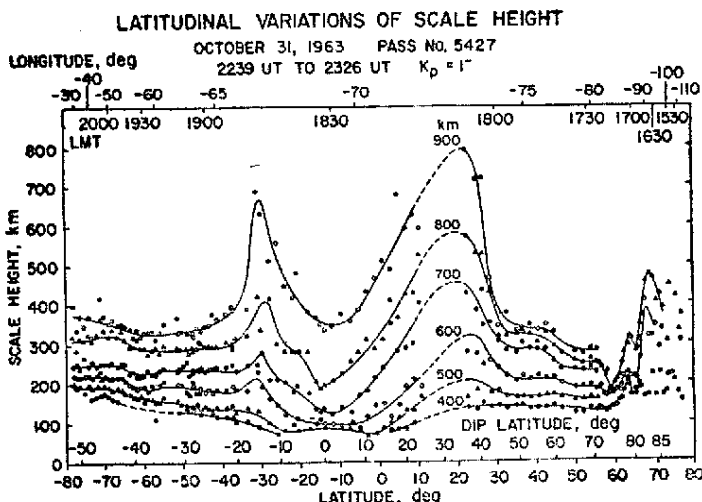
Fig. 4 — The latitudinal variation of scale height, H_v, for pass 5427.
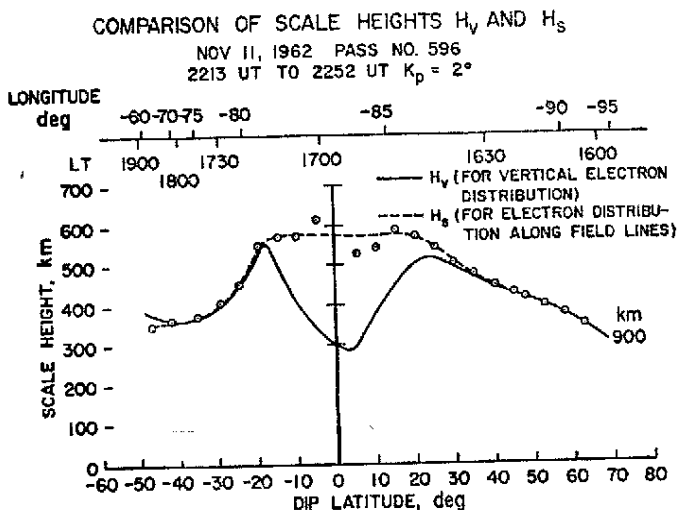
Fig. 5 — The vertical scale height, H_v, for 900 km on pass 596 (see Figs. 1 and 2) has been converted into a field aligned scale heigt, H_s. The large minimum in H_v near the dip equator is removed and H_s may be used to deduce the ratio of effective temperature to mean ionic mass in the usual way.

It is therefore concluded that at the greater altitude referred to, the electron distribution along field lines is the important parameter and that before useful information about temperature and mean ionic mass can be obtained, the vertical scale heights must first be converted into field aligned scale heights using the formula given above.

At the lower altitudes, shown in the curves of Figs. 1-4 it cannot be assumed that $T_e = T_i$ and proper allowance would have to be made for the latitudinal and altitudinal gradients of $T_e + T_i$ and the formula for H_o given above appropriately modified.

ON THE SEASONAL, NON-SEASONAL AND SEMI-ANNUAL VARIATIONS IN THE PEAK ELECTRON DENSITY OF THE F2 LAYER AT NOON IN THE EQUATORIAL ZONE

by

T. Yonezawa

Radio Research Laboratories, Kokubunji, Japan

Using ionospheric data at Huancayo and Kodaikanal which make approximately a pair of antipodal points, the seasonal, non-seasonal and semi-annual variations in the peak electron density of the F2 layer have been derived. In order to obtain the most probable values of foF2 for sunspot numbers of 0, 50, 100, 150, and 200, we have fitted a quadratic form to the noon foF2 versus sunspot number relation at each month as show in Fig. 1, and the ordinates of the quadratic curve for the above sunspot numbers have been taken as the basis of the following analysis.
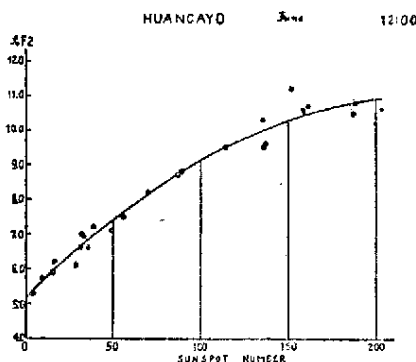
Fig. 1 — Relation between noon foF2 and sunspot number at Huancayo in June.

Figs. 2 (a) and 2 (b) illustrate the seasonal and non-seasonal variations for sunspot numbers 0 and 100. One will notice a component of 1/3 year period as a component of one year period. This means that these variations can be expressed in the following form:

$$N = \{a + b \cos [\pi (t - \beta)/3]\} \cos [(t - \alpha) \pi/6]$$

where t is the time in units of month, and the seasonal and non-seasonal variations are seen to be subjected to amplitude modulation, the quantity (b/a) will be called degree of amplitude modulation in this report.
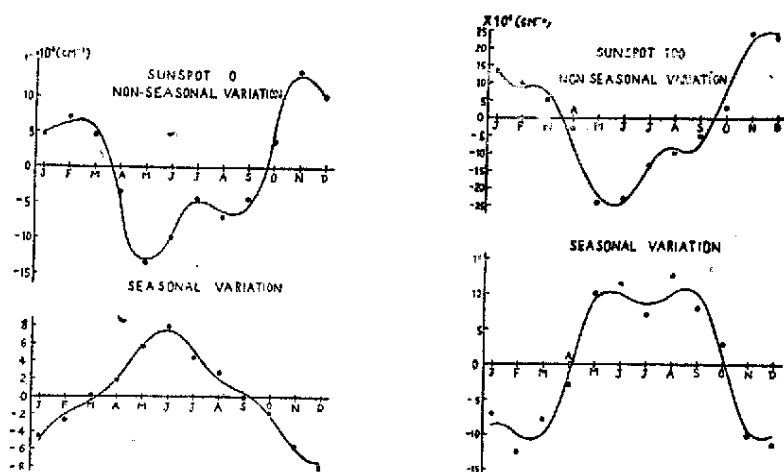
Fig. 2 — Non-seasonal and seasonal variations in the peak electron density of the foF2 layer at noon for
    (a)   Sunspot number 0
    (b)   Sunspot number 100

Figures 3 (a) and 3 (b) show the semi-annual variations plus annual averages at Kodaikanal and Huancayo for sunspot numbers 0 and 100. Figures 4 (a) and 4 (b) show the superposition of the three components plus annual average. As may naturally be expected, the agreements is good between observed and calculated values.
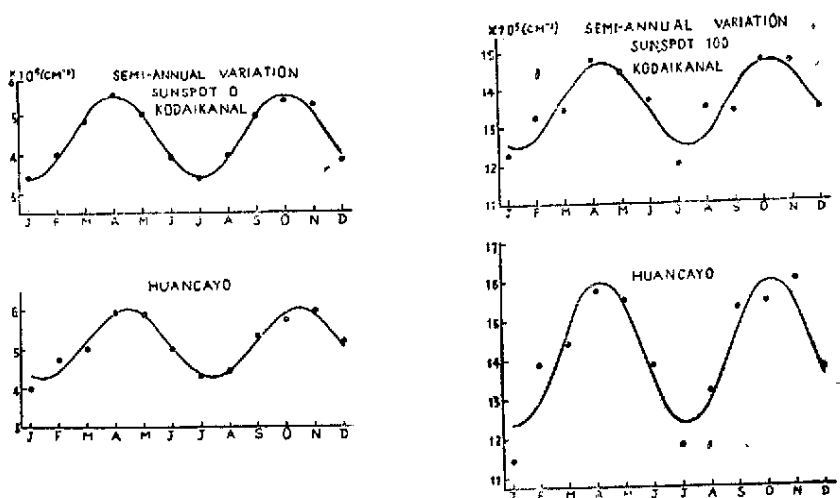
Fig. 3 — Semi-annual variations in the peak electron density of the
F2 layer at noon plus annual averages at Kodaikanal and
Huancayo for

    (a)   Sunspot number 0

    (b)   Sunspot number 100

       The non-seasonal variation becomes a maximum at the beginning of January which is approximately coincident with the time of shortest distance between the earth and the sun (Fig. 5). The seasonal variation is a maximum near June solstice or somewhat later (Fig. 5). The semi-annual variation reaches its maxima in mid-April and mid-October or a little later (Fig. 6). As regards the degree of amplitude modulation of the non-seasonal and seasonal variations, it is very high for the non-seasonal variation and amounts to more than 60% for sunspot number zero and it is also high for the seasonal variation, exceeding 40% in all cases for sunspot numbers from 0 to 200 (Fig. 7). The phase of the amplitude modulation is such that the amplitude becomes a maximum at roughly the same times as the semi-annual variation, or somewhat later, for both the non-seasonal and seasonal variation (Fig. 5). Of the amplitudes of the three components the greatest is the non-seasonal one, amounting to about 30% of the annual average in the case of sunspot number zero and the smallest is the seasonal one being about 10% (Fig. 8).
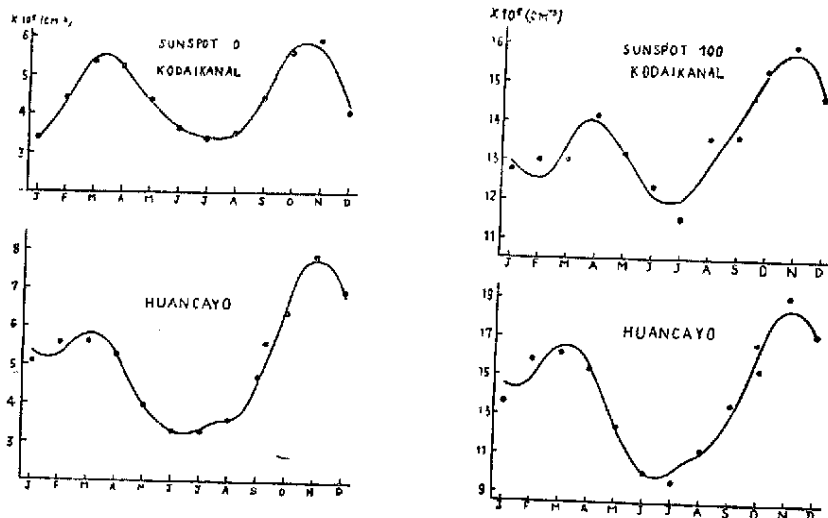
Fig. 4 — Superposition of the non-seasonal, seasonal and semi-annual
variations in the peak electron density of the F2 layer at
noon plus annual averages for

    (a)   Sunspot number 0

    (b)   Sunspot number 100
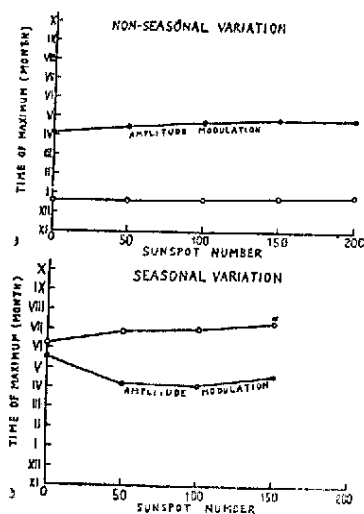
Fig. 5 — Times of maximum of
the non-seasonal and seasonal variations
as functions of sunspot number, together
with those of their amplitudes subject to
semi-annual modulation.
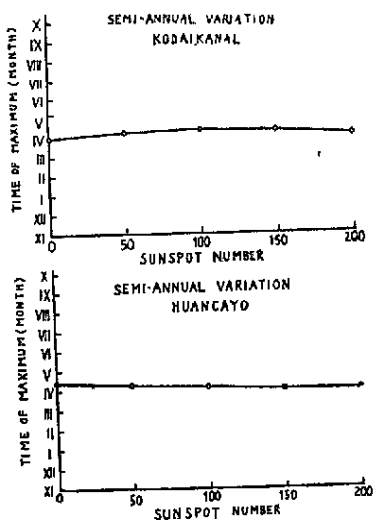
Fig. 6 — Times of maximum of the semi-annual variations for Kodaikanal and Huancayo as functions of sunspot number.
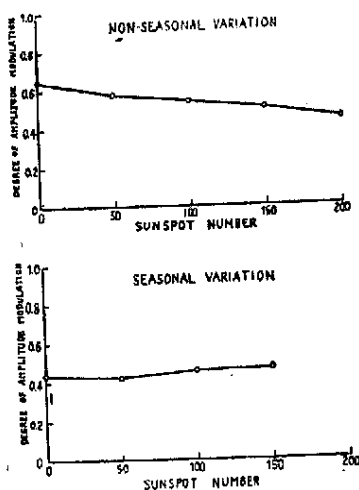
Fig. 7 — Degrees of amplitude modulation of the non-seasonal and seasonal variations as functions of sunspot number.
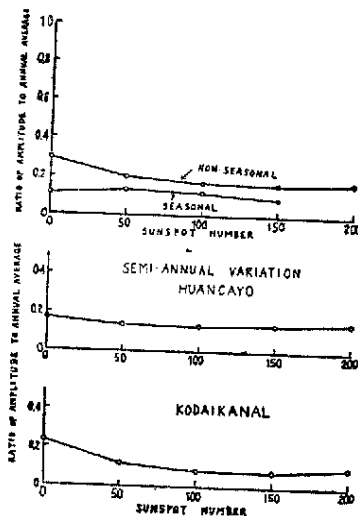
Fig. 8 — Amplitudes of the seasonal, non-seasonal and semi-annual variations relative to the annual variations as functions of sunspot number.

These results may not readily be explicable, but the existence of large non-seasonal variation seems to suggest some form of corpuscular effect, though the detailed mechanism of this effect is not clear at the present stage.

THE F2 REGION AT IBADAN OVER A SUNSPOT CYCLE

Part I — Solar Cycle and Annual Variations

by

Arthur J. Lyon

University of Ibadan, Nigeria

Introduction

The ionospheric station at the University of Ibadan, (geographic latitude 7.4°N, magnetic latitude 2.6°S) was set up in December 1951. It has thus been operating for rather more than a sunspot cycle, and sufficient data have now accumulated for an investigation of general trends over the solar cycle, and also of mean variations throughout the year.

Variations of electron density with R

Figure 1 shows the variations of (a) the smoothed Zurich relative sunspot number (R^*, 13-month running means), (b) foF2 at midday (averages of monthly medians for 09h, 12h, and 15h), and (c) foF2 at midnight (monthly medians for 00h). The general trend at midday clearly follows that of R^*, but there is a marked flattening over the period of sunspot maximum — from mid-1956 to mid-1959. This phenomenon is further illustrated in Fig. 2, which shows a plot of annual means of NmF2 at midday against annual means of R, the unsmoothed sunspot number, (a) for Ibadan, and (b) for Slough. For Slough the variation is linear, and NmF2 continues to increase at the same rate up to the high sunspot values of 1957-58, but for Ibadan the rate of increase for $R^* > 100$ is less than half that for $R^* > 100$. This corresponds to the "flattening" evident in Fig. 1.

The least squares regression line of Nm on R^* for Slough is

$$NmF2 = 0.26 \ (1 + 0.027R^*).$$

For Ibadan the regression line for $R^* > 100$, by visual estimation is

$$NmF2 = 0.60 \, (1 + 0.017R^*)$$
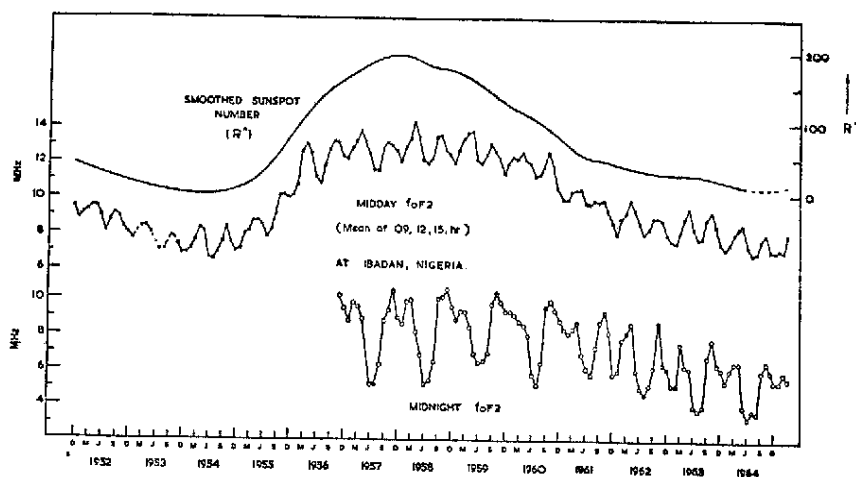
Fig. 1 — Variations of monthly median midday foF2 (crosses) and midnight foF2 (circles) at Ibadan and of smoothed sunspot number, R^*, (continuous line) from 1952 to 1964.
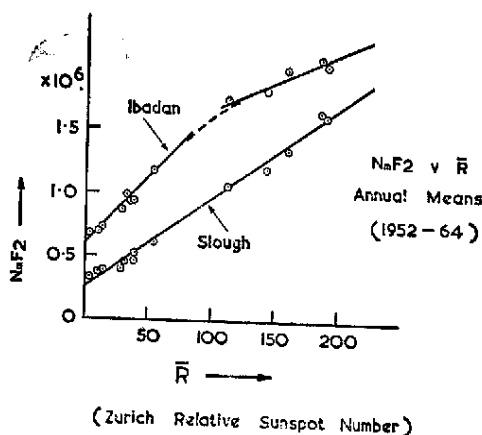
Fig. 2 — Variations of midday NmF2 with mean sunspot number R^* for Ibadan and for Slough. The F2 data are annual means of monthly medians, averaged over 09h, 12h and 15h.

Annual Variations of NmF2

The mean values of NmF2 for successive months, averaged corresponding to R = 0 and R = 200 are shown below, in Figs. 3 (b) and 3 (c).

Annual Variation of NmF2, Ibadan.
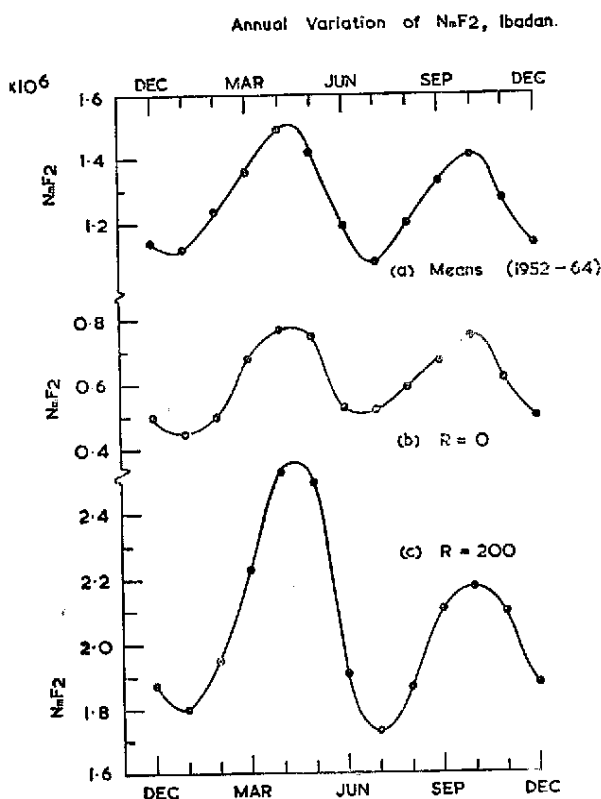
Fig. 3 — Variations throughout the year of midday NmF2 (a) averaged over a sunspot cycle, (b) for zero sunspot number, and (c) for R = 200.

In all the curves of Fig. 3 there are maxima in April and October, and minima in January and July. For the mean curve, Fig. 3 (a), the amplitude of the variation is about $\pm$ 15% of the mean level; and for R = 0, Fig. 3 (b) it is about $\pm$ 25%. A remarkable feature of the annual variation at sunspot maximum (R = 200) is the much higher maximum in April than in October, the values for April and May being particulary high. The amplitude of the semi-annual variation is $\pm$ 20% in the first half of the year and only about $\pm$ 10% in the second half. An examination of individual years shows that this asymmetry between the equinoxes occurs in each of the years 1957, 1958 and 1959, though not in 1956.

Variations of hmF2 with R

Figure 4 shows the variation of annual means of midday hmF2 with R*, midday implying as previously the mean of values for 09, 12 and 15h. The figure shows a linear increase of hmF2 with R* given approximately by

$$hmF2 = 325 + 0.67R^* \text{ km}.$$
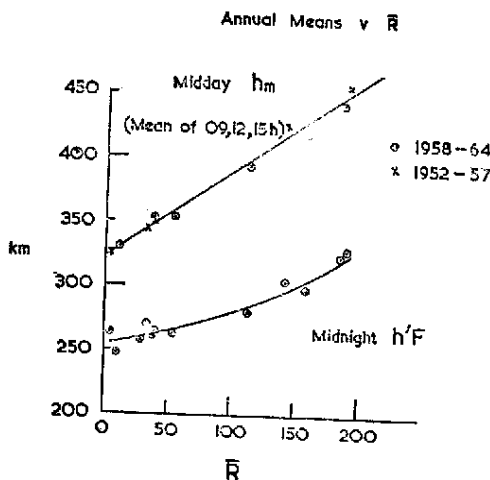
Fig. 4 — Variations of midday hmF2 and midnight h'F with sunspot number. Crosses indicate values obtained by the Appleton-Beynon method but with corrections applied.

Annual Variations of hmF2 and q$_c$

Figure 5 shows the annual variations of hmF2 averaged over the period 1952-64. The main feature appears to be a variation of annual period with a flat minimum from May to August and a rather flat maximum from October to January The amplitude of the variation is ± 8 km or ± 2%; the total range of variation is thus about one quarter of a scale height. The same figure shows that the corresponding variations of M (3000) F2, plotted with values increasing downwards, follows very closed that of hmF2.

The variation of the "quarter-thickness" q$_c$, also shown in Fig. 5, is rather similar to that of hmF2, with a flat minimum in summer and a flat maximum in winter. The variation is a substancial one with an amplitude of ± 12 km or about ± 15%.
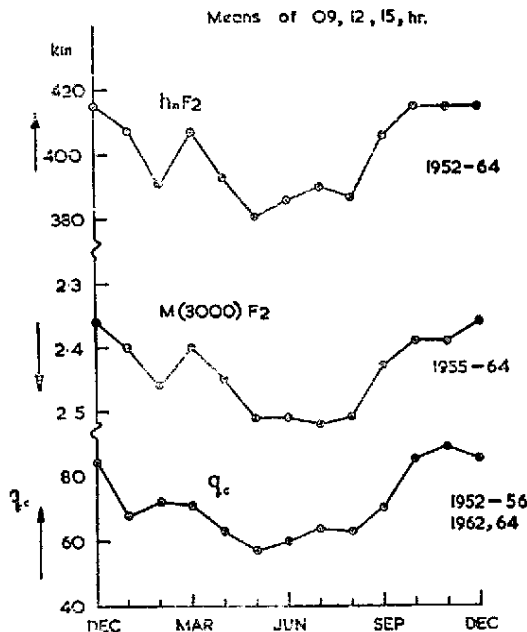
Fig. 5 — Variations throughout the year of midday hmF2, M(3000) F2, and the "quarter-thickness", q$_c$.

Variations at Midnight

The annual variations at midnight of NmF2 are shown in Fig. 6. A variation of semi-annual period is again present but a marked variation of annual period is also clearly present in this case. The two variations are of about equal magnitude, $\pm\ 0.2$ x 10^6 electrons per cm³ or about $\pm\ 25\%$ of the mean value, and have minima together at the June solstice.
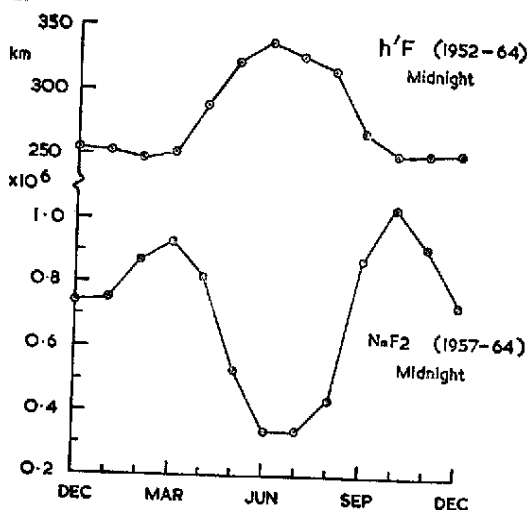
Fig. 6 — Variations throughout the year of midnight h'F and midnight NmF2.

The variation of annual period may be contrasted with that of h'F at midnight which is in antiphase and has a large maximum in June, and a very flat minimum from October to March. Between the September equinox and the March one the mean h'F over the period 1952-64 remains very close to 250 km but it rises to an average value of about 325 km for the summer months, May to August.

THE F2 REGION AT IBADAN OVER A SUNSPOT CYCLE

Part II — Diurnal Variations

by

E. O. Olatunji

Department of Physics

University of Ibadan, Nigeria

The diurnal variations of foF2 and hmF2 for different seasons and phases of the solar cycle are examined in the following five figures.
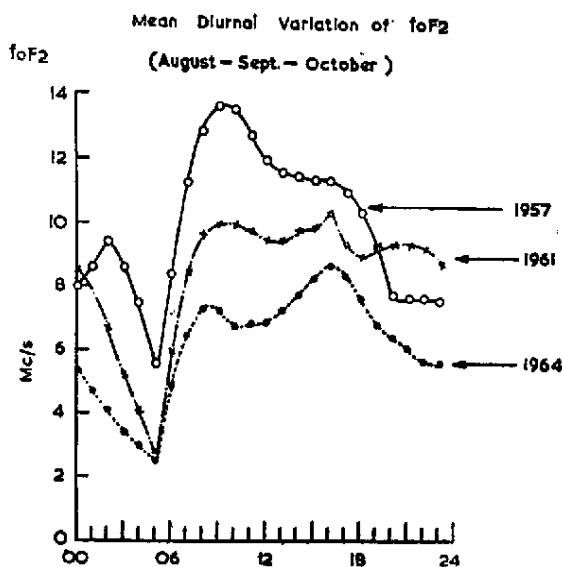
Fig. 1 — Mean diurnal variation of foF2 at Ibadan for the months of Aug., Sept. and Oct. in the years 1957, 1961 and 1964. At sunspot maximum, the diurnal peak of foF2 variation occurs before noon while at sunspot minimum it exhibits a post-noon peak.

Mean Diurnal Variation of foF2

(November — December — January)
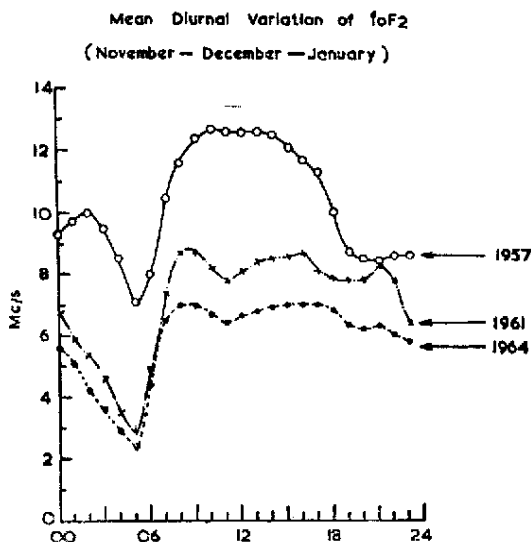
Fig. 2 — Same as Fig. 1 for the months of Nov., Dec. and Jan.

Mean Diurnal Variation of hmF2
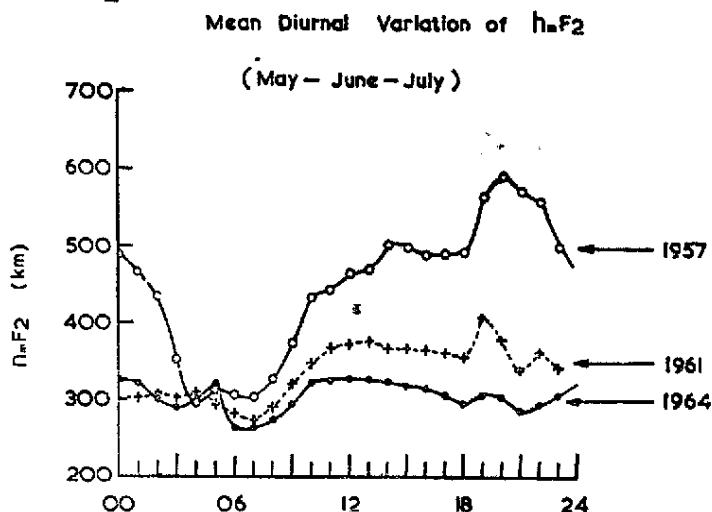
(May — June — July)

Fig. 3 — Mean diurnal variation of hmF2 at Ibadan for May, June and July in the years 1957, 1961 and 1964. These variations show a consistent trend over the solar cycle. Outstanding features are a greater diurnal range and a more pronounced post-sunset increase in hmF2 at sunspot maximum than at sunspot minimum.

Rates of increase of f_oF2 from
05 to 08 hrs LMT.

-⊙···⊙···⊙·· (Mean of 1957, 1961 and 1964)

+——+——+ 1964

-□--□--□- 1957
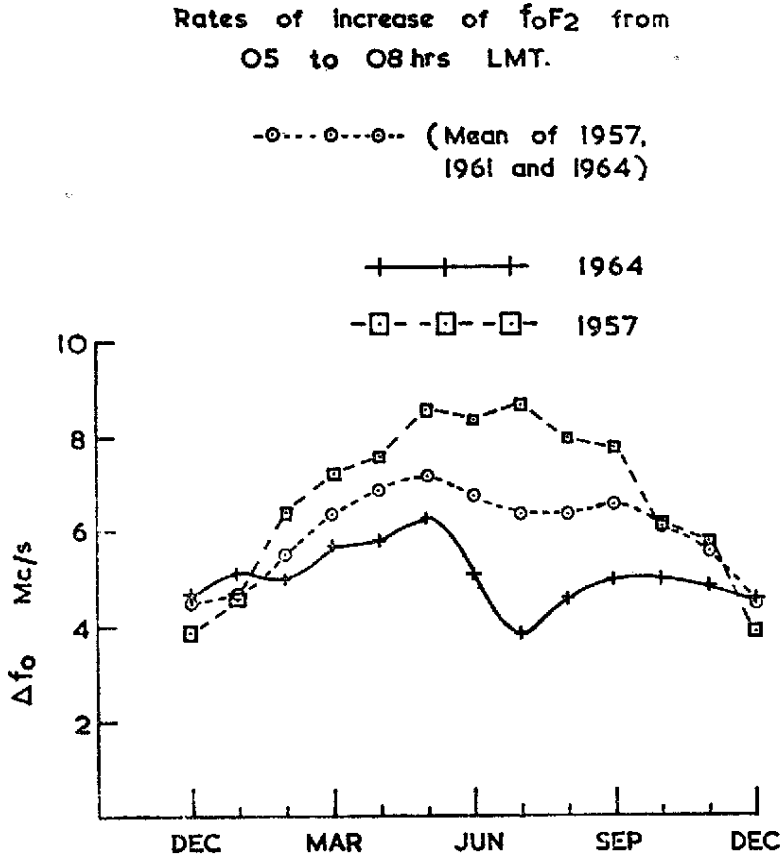
Fig. 4 — Morning rates of increase of foF2. It shows an annual variation at sunspot maximum, while that at sunspot minimum in marked by a semi-annual variation.
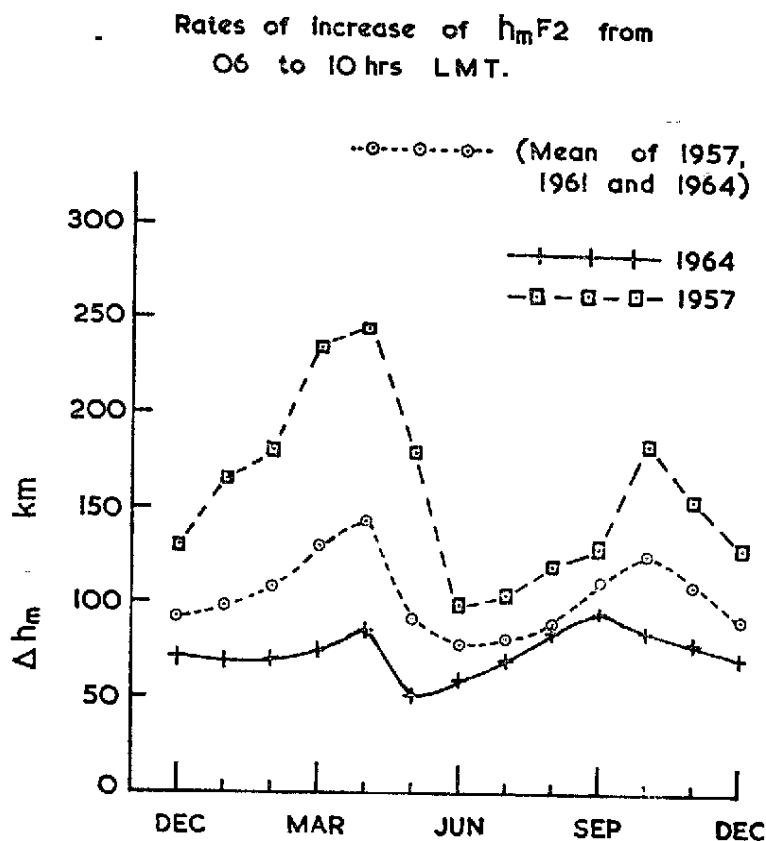
Fig. 5 — Morning rates of increase of hmF2. Note the consistent trend of the semi-annual variation over the solar cycle.

RECENT IDEAS ON THE MORPHOLOGY OF THE

F-REGION OF THE IONOSPHERE

by

J. W. King

Radio and Space Research Station
Ditton Park, Slough, Bucks, England

(paper not available)

LONGITUDINAL VARIATION IN THE EQUATORIAL

F2 REGION OF THE IONOSPHERE

by

R. G. Rastogi and S. Sanatani

Physical Research Laboratory, Ahmedabad, India

The paper describes the difference in annual average daily variation of foF2 at different epochs of solar activity at equatorial stations in American, African and Indian zones. During low sunspot years, two peaks of foF2 were observed at each station at about 09 and 12 hours. With increasing solar activity the morning peak gets more prominent than the evening one. During maximum sunspot year one gets almost single morning peak at Huancayo, but at Kodaikanal both the peaks are significant and another midnight peak is also developed (Fig. 1). At Natal, a station close to the magnetic equator in Eastern Brazil, the variation of foF2 shows a strong single midday maximum which is different from the equatorial type of variation. These variations of foF2 may be due to the very important position of the station on the magnetic equator where the shift of the magnetic equator with universal time is the largest (Fig. 3).
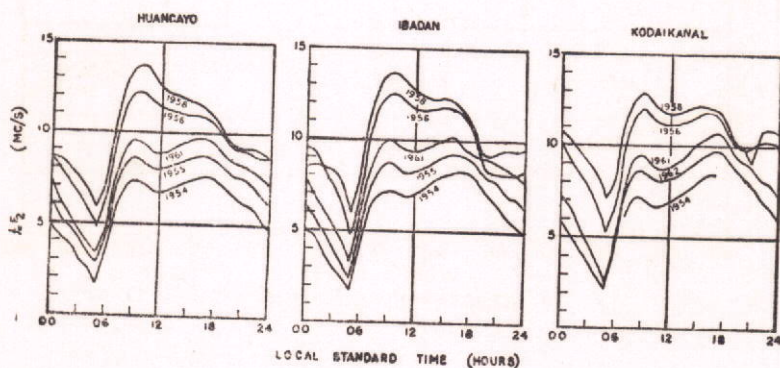
Fig. 1 — Annual mean daily variations of foF2 at Huancayo, Ibadan and Kodaikanal during different years (1934-1962).
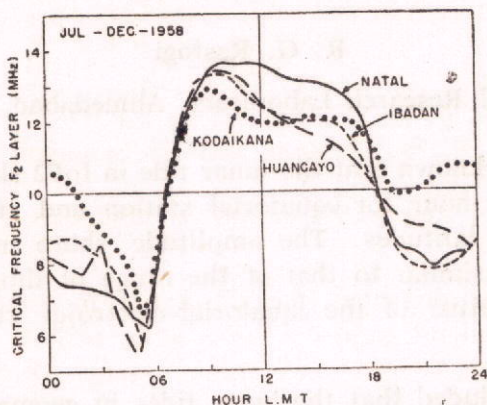
Fig. 2 — Mean daily variation foF2 at the equatorial stations, showing abnormal variation at Natal.
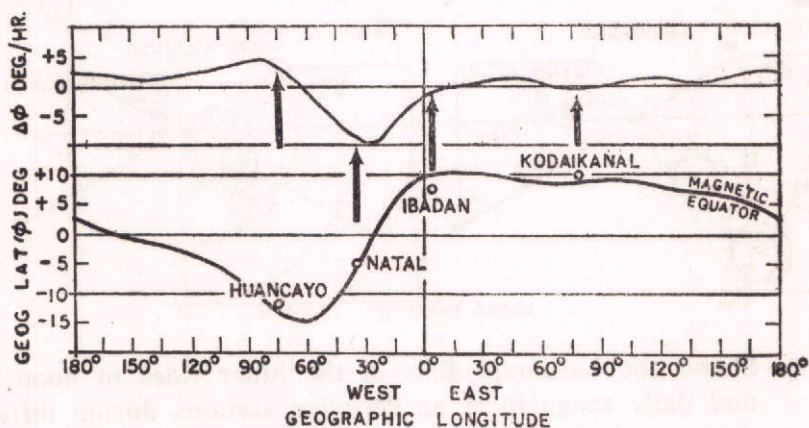
Fig. 3 — Position of the magnetic equator at different longitude and the deviation in the position of the magnetic equator for one hour change in the universal time.

LUNAR TIDES IN foF2 AND H NEAR THE MAGNETIC EQUATOR

by

R. G. Rastogi

Physical Research Laboratory, Ahmedabad, India

It is well known that the lunar tide in foF2 shows a maximum at about 04 lunar hour for equatorial station and at about 10 lunar hour for tropical latitudes. The amplitude sharp maximum on the magnetic equator similar to that of the range of diurnal variation of H which is indicative of the equatorial electrojet current strength. (Figs. 1 to 7).

It is concluded that the lunar tides in geomagnetism and the ionospheric F-region near the magnetic equator are closely related to each others and are associated with the equatorial electrojet currents.
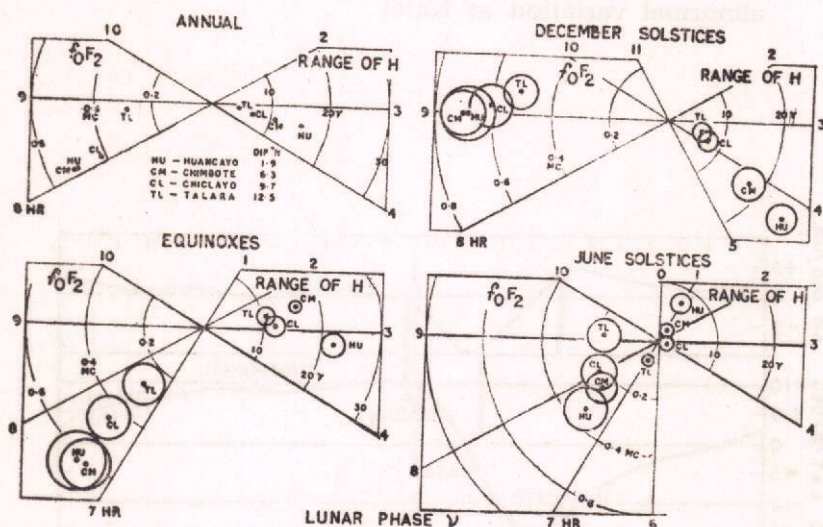
Fig. 1 — Shows the harmonic dials of the lunar tides in noon foF2 and daily range in H at Peruvian stations during different seasons of IGY-IGC. The amplitude of tides in both foF2 or range H increase progressively with decreasing latitude. The phase of lunar tide changes slightly with season, but the difference in phase of tides in foF2, and range H remains almost constant.
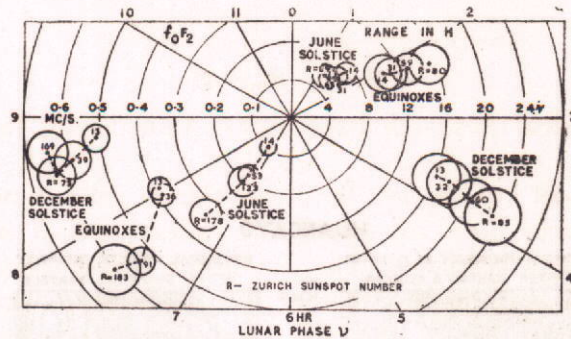
Fig. 2 — Shows the harmonic dials of the lunar tides in noon foF2 and range H at Huancayo during different seasons and different solar ativity. With increasing solar activity the amplitude of tide increases for both foF2 as well as range H keeping almost same phase.
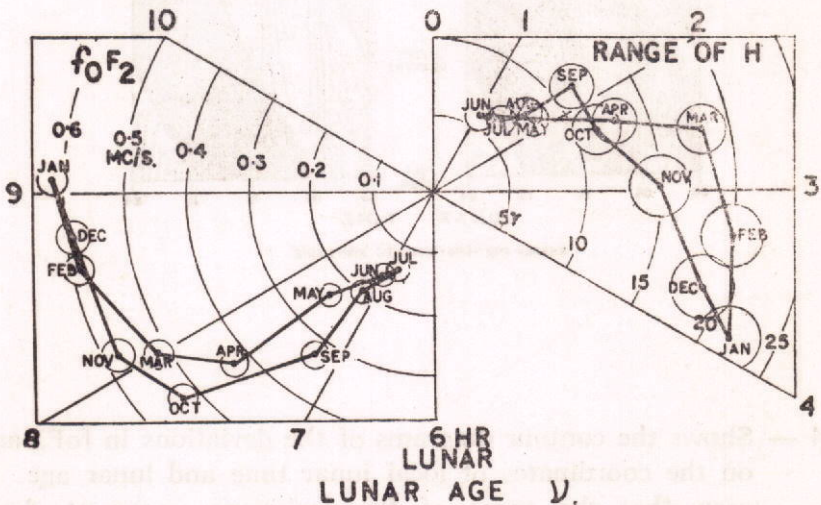
Fig. 3 — Shows the seasons variation of the amplitude and phase of tides in foF2 and range H at Huancayo. The amplitude of tides for both the parameters foF2 and range H is least during June-July and maximum during January. There is a progressive change in the phase of the tidal oscillation such that the phase difference between the oscillation at two parameters for any month remains constant.

HUANCAYO

CRITICAL FREQUENCY OF F₂ LAYER
AFTER RASTOGI & ALURKAR

HORIZONTAL MAGNETIC INTENSITY
AFTER CHAPMAN & BARTELS

LUNAR TIME

SHADED PORTIONS INDICATE NIGHTTIME
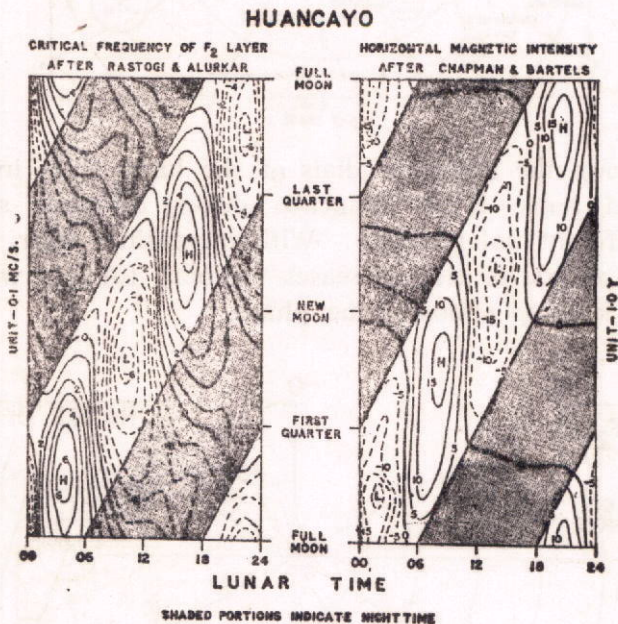
Fig. 4 — Shows the contour diagrams of the deviations in foF2 and H
on the coordinates of local lunar time and lunar age. It is
seen that the most of the deviations occur at daytime
indicating that the magnitude of the lunar tide in foF2 as
well as in H is maximum during the daylight hours. An anti-
phase relation between the tides in foF2 and H is clearly
shown in the diagram.
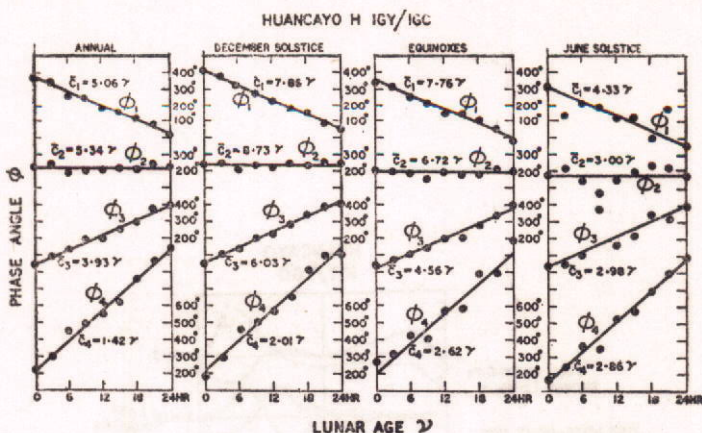
Fig. 5 — Shows the first, second, third and fourth harmonic
components of lunar daily variations in H at Huancayo dur-
ing different lunar age in different seasons of the year. The
curves indicate that the Chapman's phase law is very closely
followed by these variations. The phase of second harmonic
is independent of lunar age.
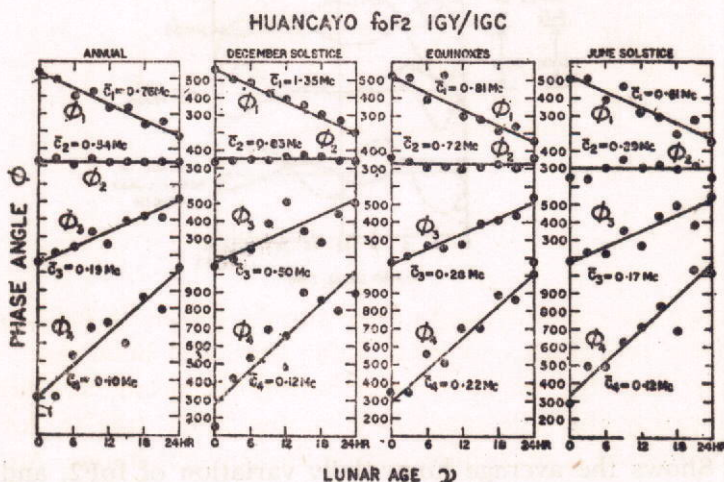
Fig. 6 — Shows similar diagrams for foF2 during IGY-IGC. The
phase of second harmonic is again independent of the lunar
age indicating that the lunar pertubations are predominant-
ly tidal in nature.
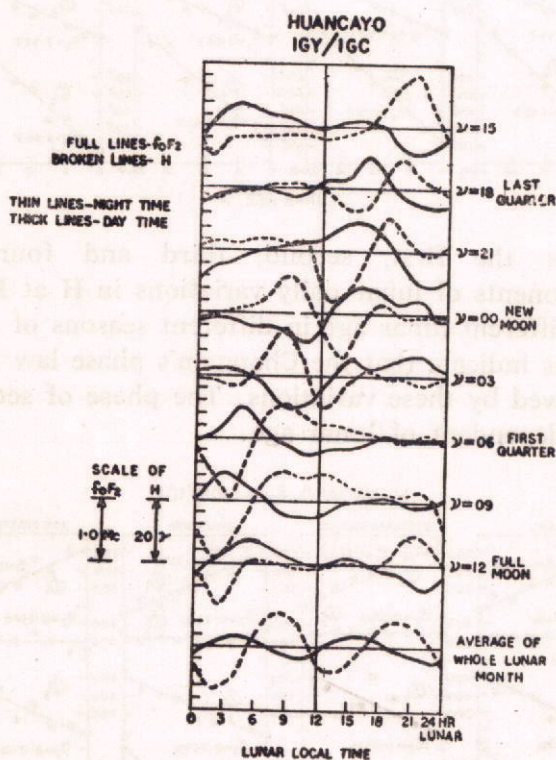
Fig. 7 — Shows the average lunar daily variation of foF2, and H during different lunar age. It is seen that the two variations are almost opposite in phase to each other.

THE ANOMALOUS ENHANCEMENT OF THE F2-REGION ELECTRON DENSITY AT NIGHT IN LOW AND EQUATORIAL LATITUDES

by

Teruo Sato

Meteorology Section

First Research and Development Center

Japan Defence Agency

13 Mita, Meguro, Tokyo

The anomalous enhancement of the F2-region electron density at post-sunset time in low and equatorial latitudes is analyzed, and the cause is studied. Data used here are mainly those in American Zone. The major peak of the electron density enhancement occurs usually at 2000-2400 LT, with different times at various latitudes and generally one or two minor peaks appear between 0000 and 0400 LT. The enhancement phenomenon takes place most remarkably at 15°-17° geomagnetic latitudes (dip angle 32°-35°) throughtout the year, showing the biggest effect in equinoctial season. The boundary latitudes that the enhancement can be recorded is lower in winter (about 20°) than in other seasons (see Fig. 1).

Successive time variations of the foF2 latitudinal distribution or the vertical profiles of the F2 region electron density distribution between Huancayo and Washington show that the anomalous high electron density region (so called equatorial anomaly situated at 15°-20° in daytime) moves towards the equator after sunset and the arrival time at any particular latitude is consistent with the time of the nighttime increase of the electron density at that latitude. The direction of the drift of the ionization, deduced from the geomagnetic variation is downwards and towards the equator horizontally in low and equatorial latitudes during the time concerned (see Figs. 2 to 6). Therefore abnormal increase of the F2-region electron density in these latitudes seems to be explained by the ionization drift theory.
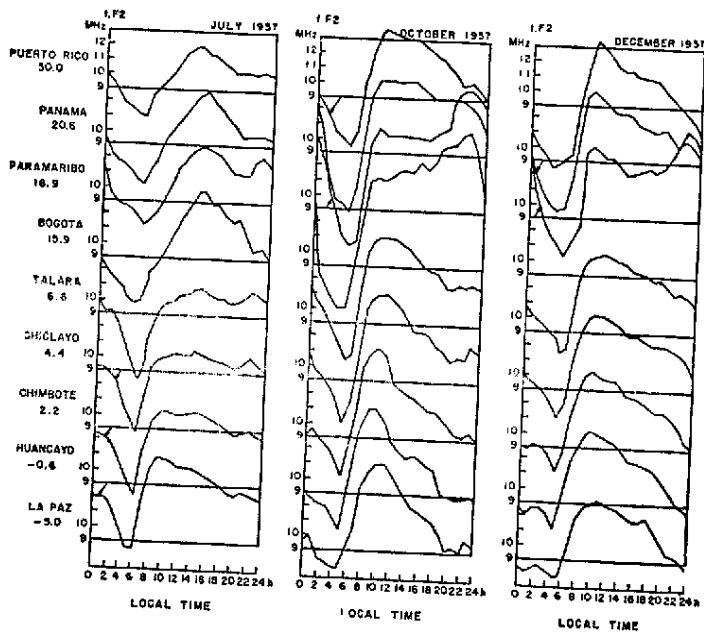
Fig. 1 — Daily variation of monthly median foF2 in July, October and December 1957.
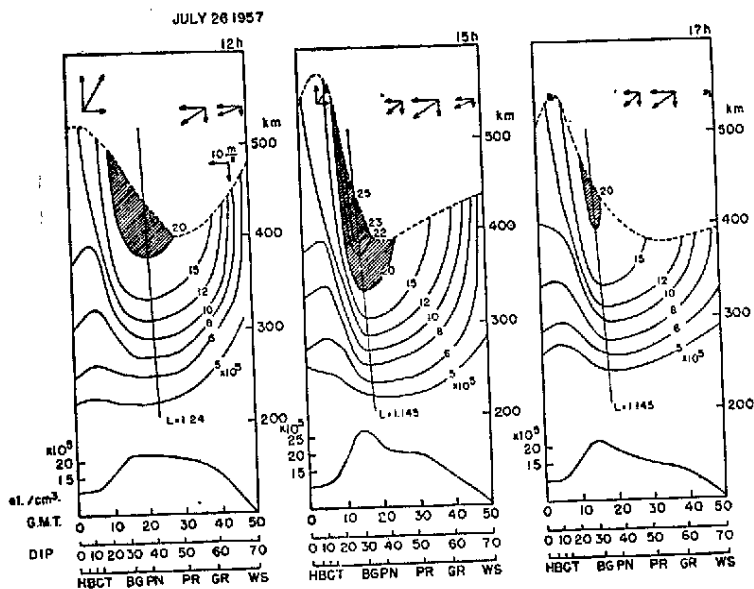
Fig. 2 — Sequential time variation of the vertical profile of electron density in the 350° geomagnetic meridian plane. The lower curves show the maximum electron density distribution, the line contours of the F region density, the dotted lines the height of the maximum electron density, the thin lines the geomagnetic line of force and the arrows the velocity vector of the ionization drift.
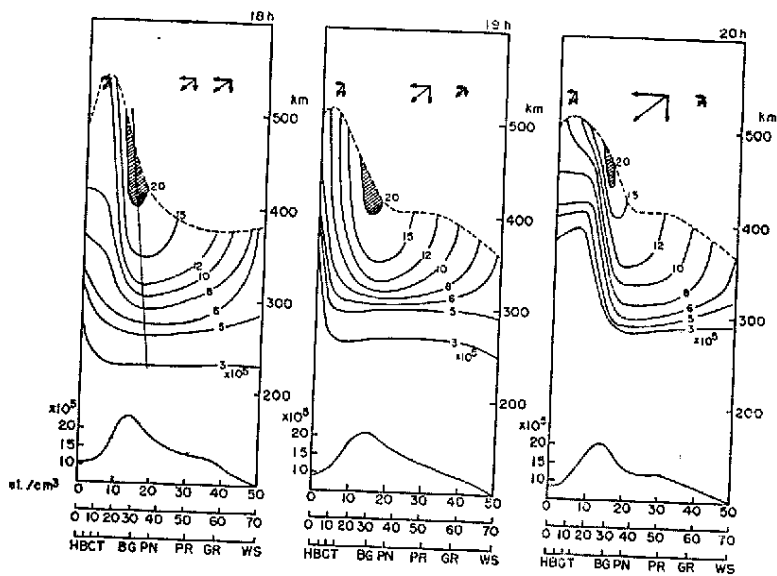
Fig. 3 — Same as Fig. 2
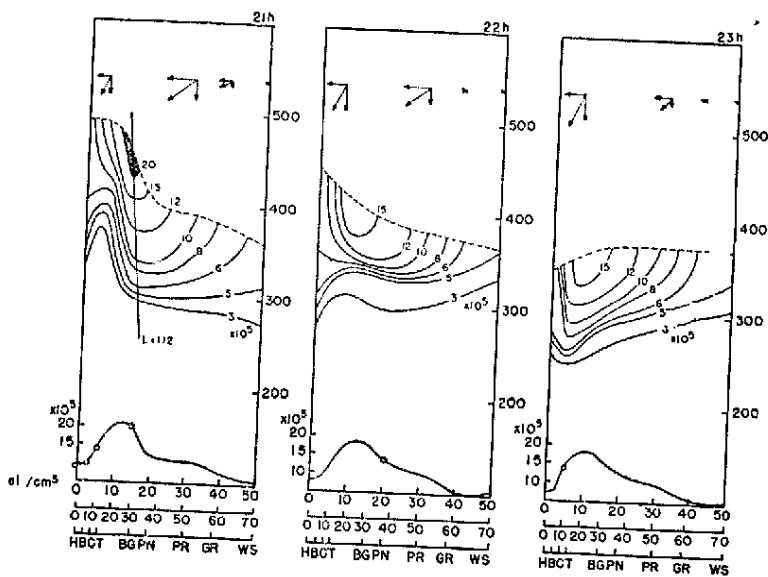
Fig. 4 — Same as Fig. 2
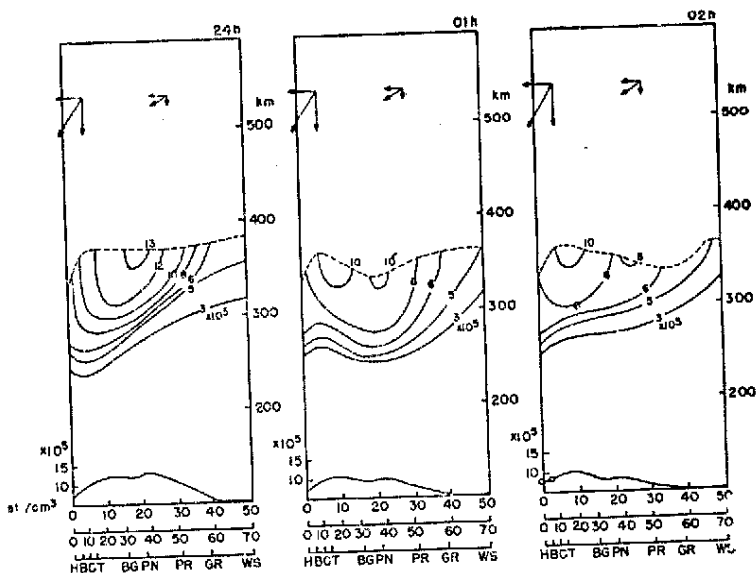
Fig. 5 — Same as Fig. 2
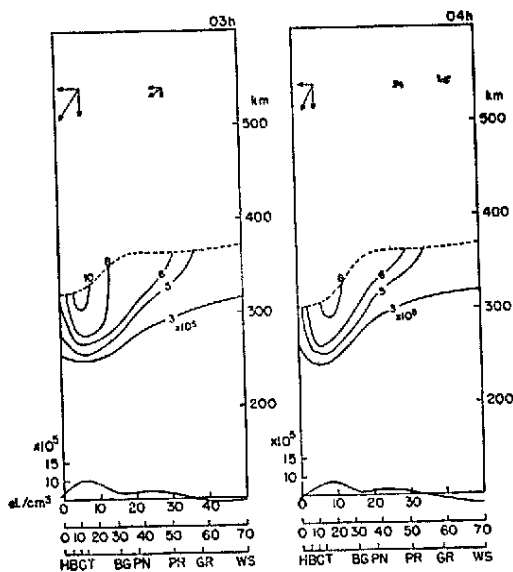
Fig. 6 — Same as Fig. 2

TOTAL ELECTRON CONTENT FROM TRANSMISSIONS OF SATELLITE S66 OBSERVED AT UNIVERSITY COLLEGE NAIROBI

by

A. N. Hunter and A. Webster
University College Nairobi, Kenya

Observations of Faraday rotation of the 20, 40 and 41 MHz transmissions form S-66 (B-EB) have been made since 10 October 1964. The station coordinates are 1.32° S, 36.32° E, with a dip of 26.9° S. The two closest passes, one north-bound and one south-bound, are recorded each day and an ionogram is automatically recorded for each pass. Only the 41 MHz transmissions have been analysed so far.
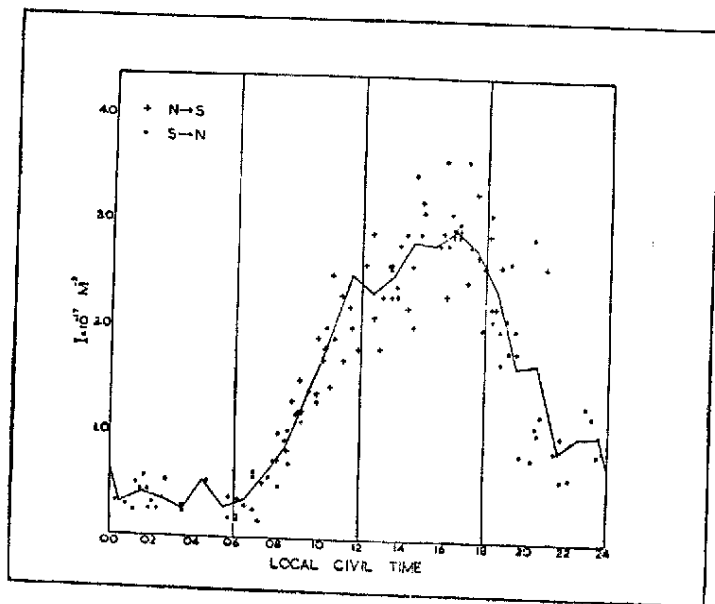
Fig 1 — Gives the hourly medians of total electron content I for the period October 1964 to January 1965 inclusive; the points show north- and south- going passes separately but all are included in the medians. The values were obtained from the fading rate at the zenith together with a constant value of 3000 gammas per degree for the latitude derivative dM/dλ, horizontal gradients are neglected but the records do not, in general, indicate large horizontal gradients in daytime.
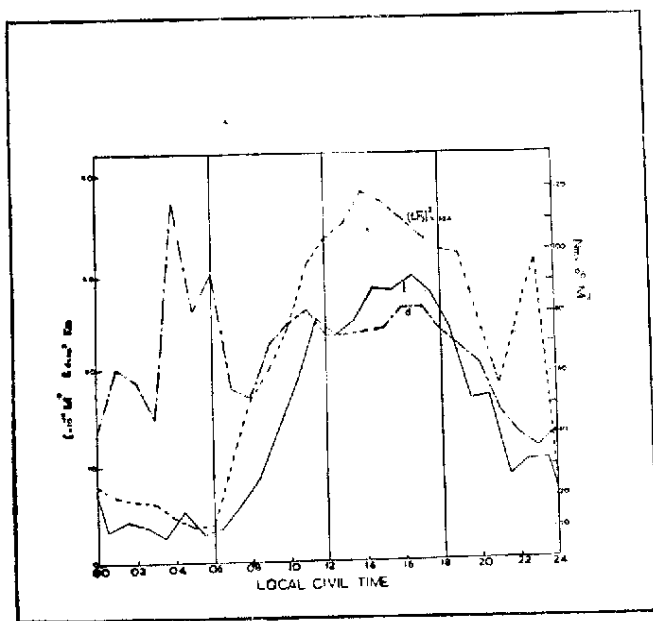
Fig. 2 — Shows the corresponding plot for the density Nm (dotted line) from foF2 taken from the ionogram associated with the recorded satellite passes; is also shows the equivalent layer thickness d (dash-dot line).
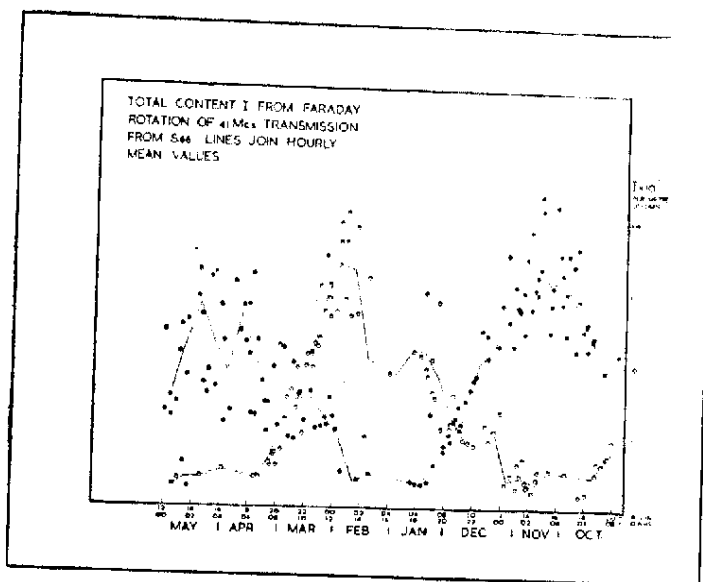
Fig. 3 — Presents the hourly medians of I for the period October 1965 to May 1965. In this case all values have been calculated by a method suggested by E. Golton[1]; in which a mean in taken of the fading rate over a period of 0.5 minute on either side of the transverse propagation point and used as the effective fading rate on the transverse point in order to eliminate effects of horizontal gradients. Value of $dM/d\lambda$ were interpolated from the tables of L. Blumle in which the value of H_t was obtained from a ten-point real height analysis of the corresponding ionograms. South- and north-going passes are separately plotted so that the time advances from right to left.
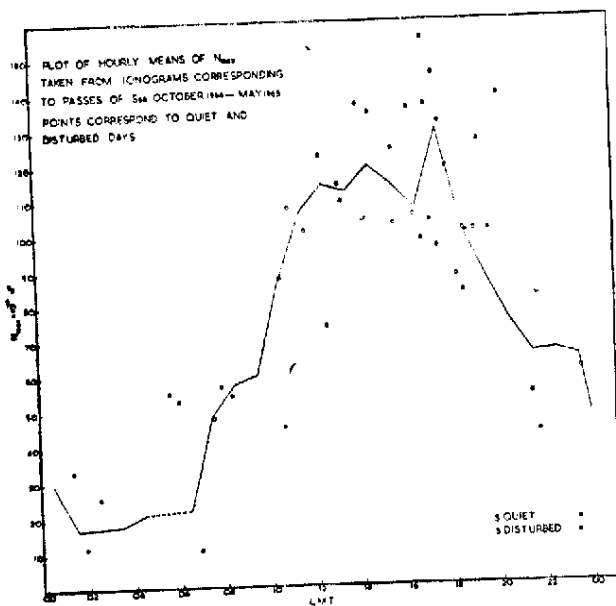
Fig. 4 — Gives the same data as Figure 3 but with hourly medians plotted for all passes.
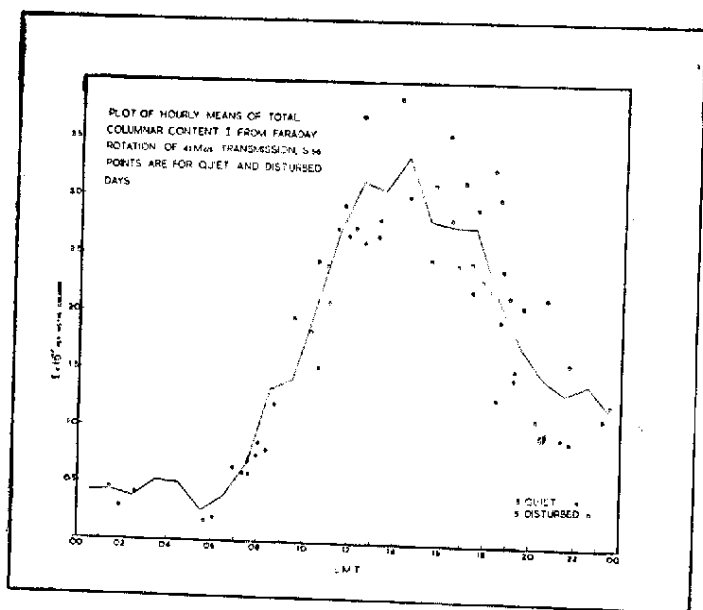
Fig. 5 — Gives the corresponding plot of Nm. Both Fig. 4 and Fig. 5 show quiet and disturbed days only plotted.

Points of interest from the above diurnal variations are:

1 — The ratio of maximum to minimum content is greater than 20; this figure will certainly increase when the 20 MHz records have been analysed for times of low content.

2 — The maximum in I occurs late in the afternoon at a time which is consistent with the expected arrival of the maximum of the equatorial anomaly.

3 — There is a large day-time scatter probably due to perturbations in position of the peak of the equatorial anomaly.

4 — A small peak occurs in I together with a much larger one in at Nm about 2300 hours.

5 — There is no evidence of correlation of either I or Nm with magnetic activity at sunspot minimum.

The transverse propagation region in always clearly on the Nairobi records so that single frequency analysis is usually applicable. Pass 1313 at 1900 hours has been analyzed for latitude distribution of i and the results are shown in Fig. 6 in which the upper and lower curves show the effect of a second timing error and the values of I are plotted against satellite time in minutes. An initial manual analysis with and without second order corrections has been compared with an analysis using a field model prepared by E. Golton on a computer. All the results agree in placing the maximum just north of Nairobi at that time in rough agreement with the anticipated position of the anomaly. The Ross[2] method for second-order correction is difficult to apply at Nairobi because of a discontinuity in the field parameter G and future analysis will be computed by ray-tracing a model ionosphere.
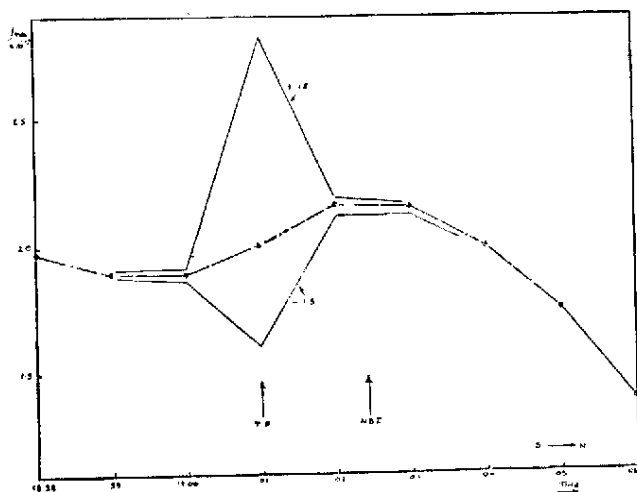
Fig. 6 — Latitude distribution of electron content for pass 1313 aournd 1900 hours.

References

(1) — E. Golton, I.M. 172, September 1964
    Radio and Space Research Station,
    Slough, England. Internal Report.

(2) — W. J. Ross — J. Geophys. Res. Vol. **70.**, 597, Feb. 1965

PRELIMINARY RESULTS OF MEASUREMENTS

OF TOTAL ELECTRON CONTENT AT

ZARIA USING THE S66 SATELLITE

by

N. J. Skinner

Ahmadu Bello University, Zaria, Nigeria

Measurements of Faraday rotation of the 40 and 41 MHz transmissions from the S66 satellite have been made at Zaria in Northern Nigeria (geographic coordinates 11.1° N, 1.60° E, magnetic dip 2.5° N) since 14 November 1964. The total columnar electron content, N_T, has been calculated from the differential rates of fading on the two frequencies.

Figure 1 shows the "diurnal" variation of N_T for observations made during the local winter period 14 November 1964 to 14 February 1965. There is no evidence of a midday biteout such as is observed with peak electron measurements, and maximum occurs at about 1300 GMT.

Figures 2 and 3 show the variations with latitude of N_T for eight satellite passes close to the meridian of Zaria. The geomagnetic anomaly in the latitude variation of N_T is most pronounced in the evening and least evident in the morning period of 0700 to 0800 hours. There is some evidence of asymmetry for the midday measurements with greater ionization on the northern side. Since no corrections have been made for horizontal gradients of electron density, the values of N_T at the extreme latitude must be treated with some caution.

For six daytime transits, ionosonde data has been analyzed to obtain, by integration of the N-h profile, the subpeak, electron content below hmF. This has been subtracted from the corresponding value of N_T to give the topside electron content N_u. Values of NmF, hmF, N_T and N_u are given in Table I. The topside content is found to exceed the sub-peak content by a factor of almost two. For a topside iono-

sphere containing a single ionized constituent (atomic oxigen) the electron density N, would be expected to vary with height h, as

$$N = Nm \exp [-(h-k_m)/2H]$$

where H is the scale height of the neutral atmosphere. Values of H for each of the six transits have been calculated assuming the distribution from the measured values of NmF and N_u, and are given together with values of N_{1000}, the electron density at 1000 km, in Table I. Values of H vary between 64 and 142 km in reasonable agreement with results of other workers using different methods. The model is over-simplified in that at least two ionized constituents are actually present in the topside ionosphere with the atomic hydrogen ion becoming important at altitudes above 800 km. Nevertheless the profiles obtained using simples model are very similar to those obtained for example by workers at Jicamarca using the incoherent scatter technique.
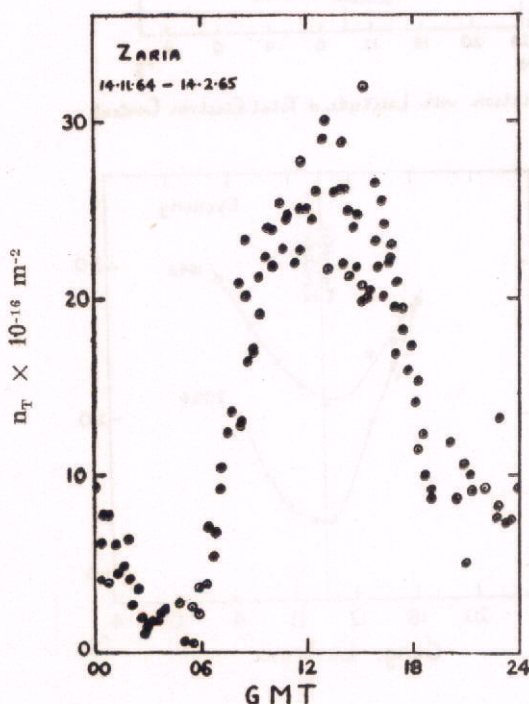
Fig. 1 — Diurnal variation of total electron content n_T
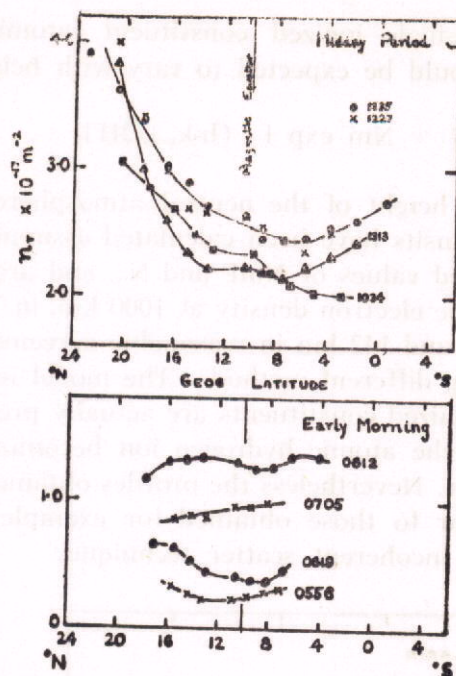
Fig. 2 —   Variation with Latitude of Total Electron Content
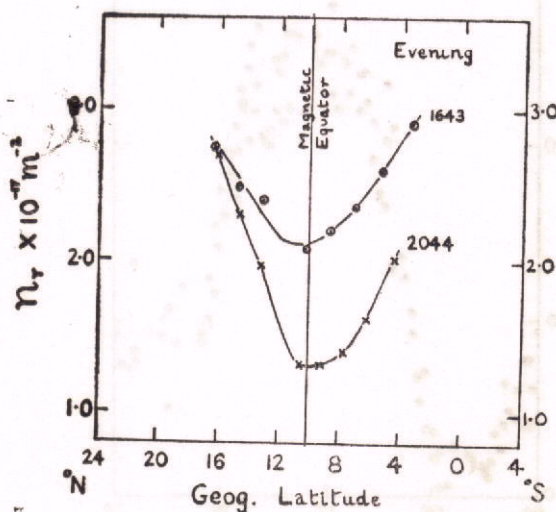
Fig. 3 —   VARIATION WITH LATITUDE OF TOTAL ELECTRON
                          CONTENT n_T

TABLE I

Values of the scale height, H, and of the electron concentration, N_{1000}, at 1000 km altitude calculated from N_T and NmF assuming a distribution $N = N_o \exp(-\frac{1}{2}Z)$ above hmF.

Data	G.M.T.	NmF (per cm³)	hmF (Km)	N_T (10^{-17} m^{-2})	N_e (10^{-17} m^{-2}) up to hmF	N_u (10^{-17} m^{-2})	H (km)	N_{1000} (per cm³)
8.12.64	1100	61 × 10¹	330	2.47	0.84	1.63	142	4.4 × 10⁴
5.12.64	1100	77 × 10⁴	380	2.20	1.22	0.98	63	0.34 × 10⁴
2.12.64	1200	75.5 × 10⁴	330	2.27	0.91	1.36	91	1.36 × 10⁴
9.02.65	1400	61 × 10⁴	325	2.12	0.76	1.36	115	2.3 × 10⁴
31.01.65	1600	98.5 × 10⁴	300	2.04	0.71	1.30	66	0.29 × 10⁴
22.01.65	1700	96 × 10⁴	310	2.22	0.68	1.54	80	0.96 × 10⁴

SECOND ORDER CORRECTION ON ELECTRON CONTENT MEASUREMENTS WITH FARADAY ROTATION TECHNIQUE*

by

F. de Mendonça, J.L.R. Muzzio and F. Walter

C.N.A.E. — São José dos Campos — S.P. — Brazil

Determination of the total electron content ($I = \int N dh$) of the ionosphere by means of the application of Faraday rotation technique on signals received from satellite beacons has been performed since the launching of Sputnik 1, by many investigators, see for instance the list of references in the paper by Garriott and Mendonça[1]. Most computations utilizing Faraday techniques has been done using single frequencies and lately two closely spaced frequencies such as the ones transmitted by the beacon satellites BE-B and BE-C in 40 and 41 MHz (see Fig. 1).

FARADAY ROTATION RECORDING

Satellite : S-66
Station : S J dos Campos
Date : 3 Nov. 1964

Closest approach 19 31 39.0 UT
Proximal point 19 31 46.0
QT 19 32 50.0
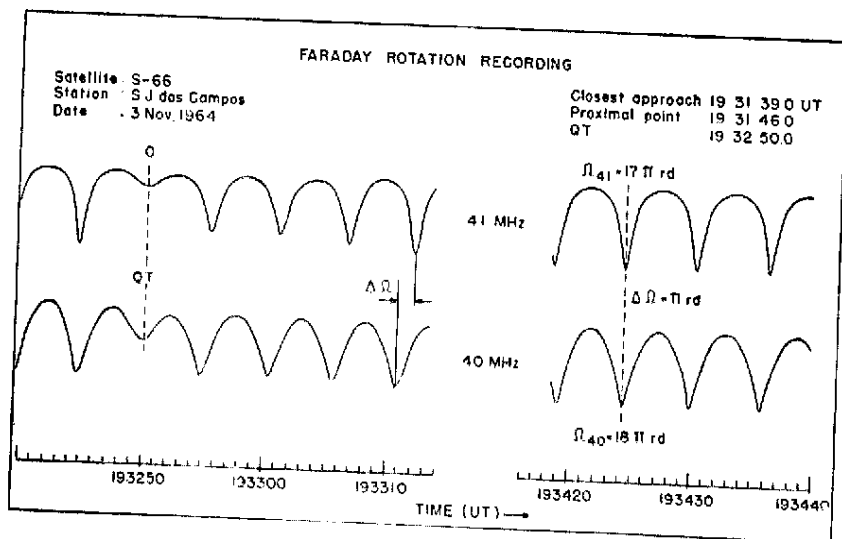
Fig. 1 — Recording of the Faraday rotation of polarization in the 40 and 41 MHz beacons of S-66, showing the quasi transverse (QT) propagation region ($\Omega = 0$) and a case with $\Omega_{40} = 18 \, \Delta\Omega$.

The first order relation

$$\Omega = (K/f^2) \ (H \cos \theta \sec \chi) \ I, \tag{1}$$

which is applicable only in restricted cases, including the absence of horizontal gradients, has been widely used for the determination of I. Ross[2] introduced a second order correction obtaining the relation

$$\Omega = (K/f^2) \ (H \cos \theta \sec \chi) \ (1 + \alpha) \ I_2 \tag{2}$$

where

$$\alpha = (X^*/2) \ [\beta + (\beta - 1) \ G] \tag{3}$$

The factor $G = \tan \theta \ (\tan \theta - Y/Y_L)$ is related to the geometry of the geomagnetic field (Fig. 2).
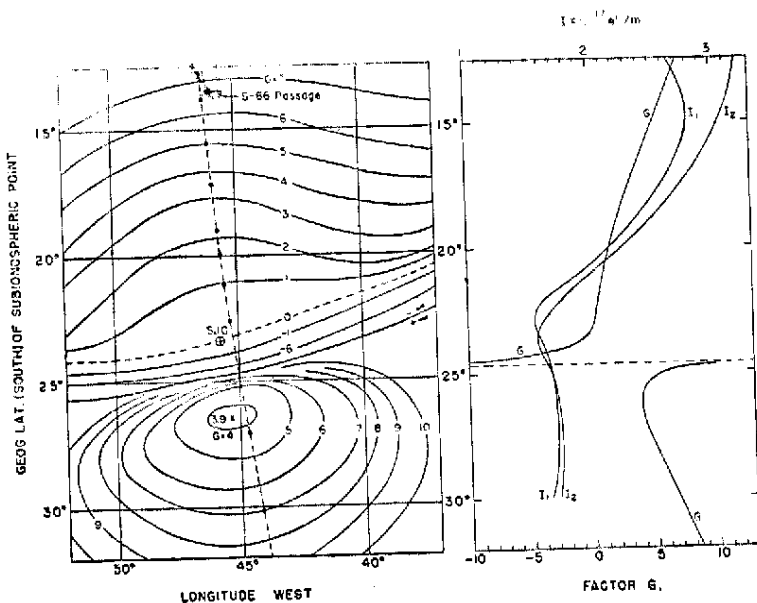
Fig. 2 — Plot of the factor G for ionospheric points at h = 350 km for the São José dos Campos station, including the track of a southbound passage of S-66 on 16 Oct. 1964 with QT at 215435 UT. Also shown are the values of G, I_1 (First order) and I_2 (Second order) for this particular passage of the satellite.

For the case of two closely spaced frequencies one has:

$$d\Omega = -2\Omega \,(df/f)\,(1 + 2\alpha) \tag{4}$$

or

$$\triangle\Omega = 2\Omega \,(n\text{-}1)\,(1 + 2\alpha)$$

Thus one may obtain the correction term $(1 + \alpha)$ from the measured values of Ω and $\triangle\Omega$:

$$\alpha = [1 - 2\,(n\text{-}1)\,\Omega/\triangle\Omega]\,/\,[4(n\text{-}1)\Omega/\triangle\Omega] \tag{5}$$

Combining equations (1), (2) and (5) we have

$$I_2 = (F^2\Omega/KM)\,4\,\Omega\,(n\text{-}1)/[\triangle\Omega + 2\Omega(n\text{-}1)] \tag{6}$$

Hence, with precalculated values of M one can easily obtain values of electron content with the second order correction. The values of α obtained with this procedure (Fig. 3) are naturally much closer to reality than the ones calculated with models and equation (3). We have written a program for our small computer in which we feed the values of the satellite position, Ω, $\triangle\Omega$ and height of the ionospheric point, and obtain the output values of I_1 and I_2 for the sub-ionospheric point, including dip angle, the factor M and G. A few passages are plotted in Fig. 4.

Note that if $n = f_2/f_1 = 1.025$ in equation (5) we get

$$(1 + \alpha) = 0.500 + 10.0\,\triangle\Omega/\Omega$$

and that $\alpha = 0$ when $\Omega = 20\,\triangle\Omega$. In this situation one has $I_1 = I_2$ At our low latitude station we have observed extreme cases in which a variation of π rd in $\triangle\Omega$ corresponded to a variation of only 6 π rd in Ω. The first order results are such that the over estimation in I for some areas tend to cancel the variation of electron content through the equatorial anomaly. Thus one should be cautious in drawing conclusions from the first order results. The full paper to be published will include comparisons between results obtained with Faraday and Doppler methods.
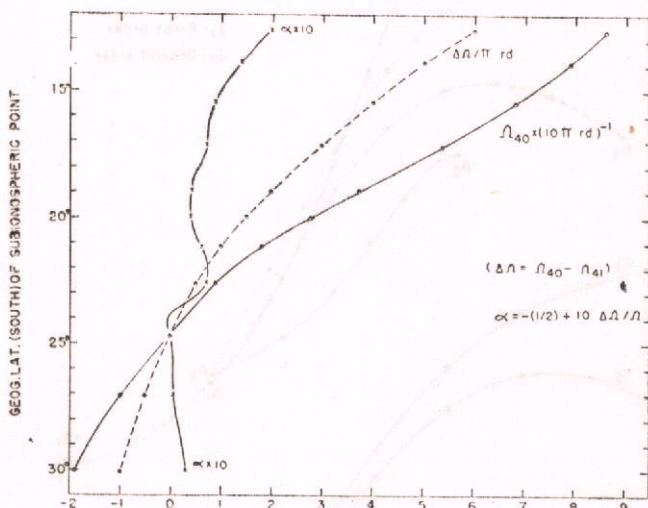
Fig. 3 — Plot of the values of α, $\triangle\Omega$ and Ω for the satellite passage of Fig. 2. Note that when $\triangle\Omega$ varies by π rd from 5 to 6 π rd, Ω varies only by 7 π rd from 79 to 86 π rd.

Fig. 4 — Plots of I and L for a few passages of the satellite S-66 (BE-B). Note the parts where L ≈ I, i.e., $\alpha = 0$ and also the tendency of over-estimation in L, masking the equatorial anomaly in I.

Reference:

1) Garriott, O.K. and F. de Mendonça, J. Geophys. Res., 68, 4917, Sept. 1963.

2) Ross, W. J. Geophys. Res., 70, 597, Feb. 1965.
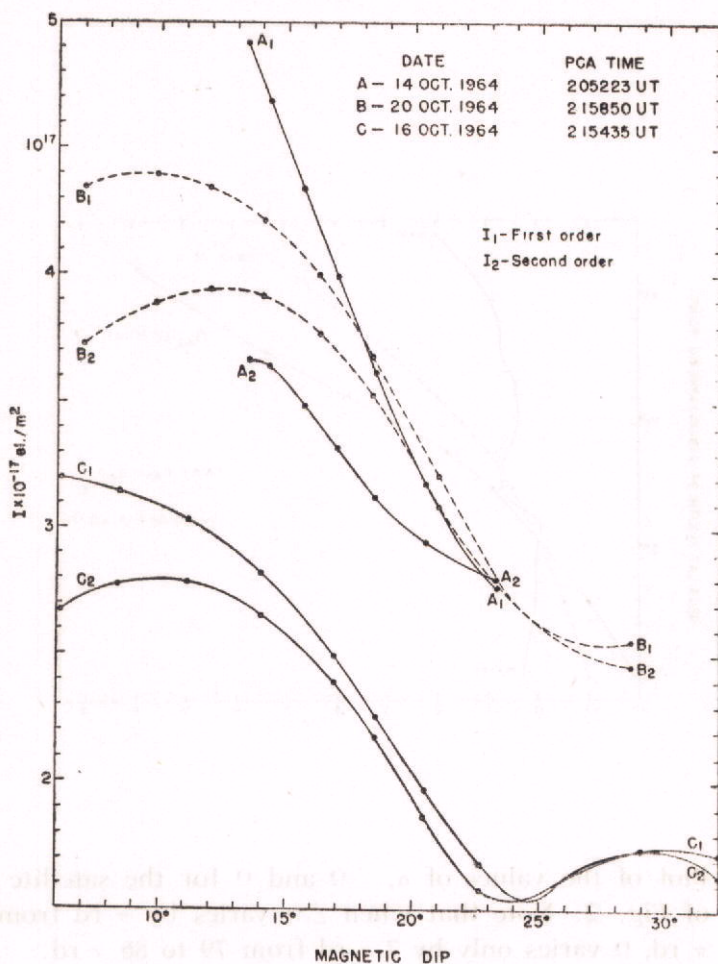
Fig. 4 — Plots of I_1 and I_2 for a few passages of the satellite S-66
(BE-B). Note the parts where $I_1 \approx I_2$, i.e., $\alpha \approx 0$ and also
the tendency of over estimation in I_1 masking the equatorial
anomaly in I.

Reference:

1) Garriott, O. K. and F. de Mendonça, J. Geophys. Res., **68**, 4917, Sept. 1963.

2) Ross, W., J. Geophys. Res., **70**, 597, Feb. 1965.

INCOHERENT SCATTER MEASUREMENTS OF EQUATORIAL
F-REGION PARAMETERS DURING THE SUNRISE PERIOD

by

Robert Cohen
Jicamarca Radar Observatory, Lima, Peru

and

Willian B. Hanson
Southwest Center for Advanced Studies, Dallas, Texas

Using the incoherent scatter technique the parameters N, T_e and T_i have been measured as functions of height and time between 180 and 500 km during the sunrise period. By applying a theoretical treatment due to Hanson, the electron production function, q, and the heat and radiation losses, Q_1 and Q_2, as well as the heating efficiency, ε, have been calculated from these parameters. A value for these quantities has been obtained for three heights, with an average ε of about 2.4 eV per fast electron over that height interval. (The variations in that parameter over the height range may not be significant in Figure 4). The heat loss by airglow radiation and that lost in heating are noted from Fig. 4 to become comparable at the highest height (375 km).
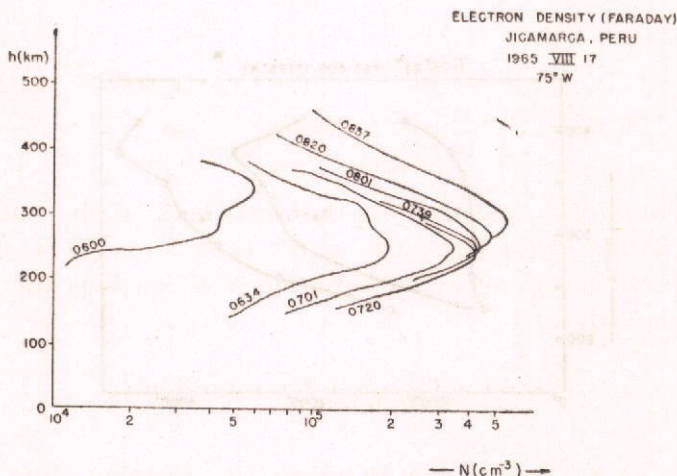
Fig. 1 — Electron density profiles obtained by the Faraday technique at the times (75°W) indicated alongside each curve.

JICAMARCA, PER
1965 ⅧⅠ 17
07ʰ34ᵐ (75° W)
h = 380 km
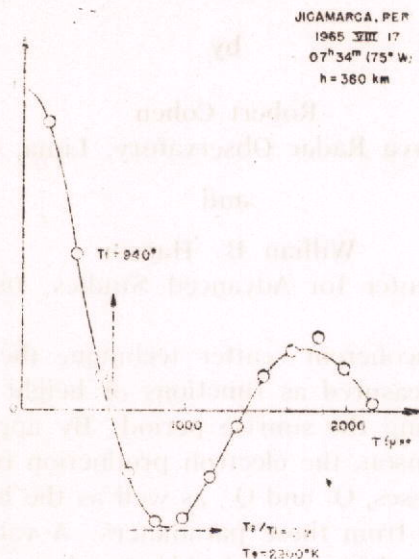
Fig. 2 — A typical measurement of the autocorrelation function, resulting in the T_e and T_i determination as indicated.
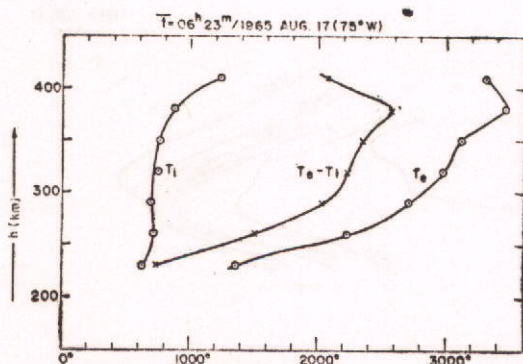
Fig. 3 — The T_e, T_e-T_i variations with height determined from experimental measurements such as Fig. 2.

1985 XIII 17   07ʰ12ᵐ (75° W)   JICAMARCA, PERU
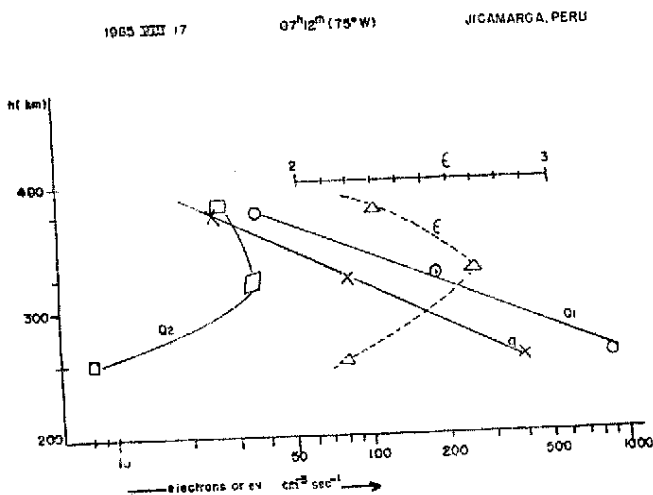
Fig 4 -- Height variations of the derived parameters.

ELECTRON DENSITY STUDIES AT JICAMARCA

by

J. P. McClure

Jicamarca Radar Observatory, Lima, Peru

The incoherent scatter radar located near the magnetic dip equator at Lima, Peru, has been used to study electron density, electron and ion temperatures, and ion composition. Electron density observations will be presented here. The other parameters will be discuted in the following companion paper by D. T. Farley.

At Jicamarca, electron density profiles can be obtained up to heights of several thousand kilometers. The densities up to 600 km is usually measured by observing the Faraday rotation of the scattered signal. Above this height the density is measured by observing the total power of the scattered signal. Several hundred kilometers of overlap are generally used when fitting Faraday and power profiles together.

All necessary comments about the data are made in the figure captions. Figure 1 shows the data for 1-2 and 3 February 1965. Figures 2 to 6 show the electron density data and the total electron content for 17-18 and 19 June 1965. Finally, figure 7 shows the electron density data for 17-18 and 19 August 1965, the days when the electron and ion temperature and ion composition measurements in the companion paper by Farley were made.
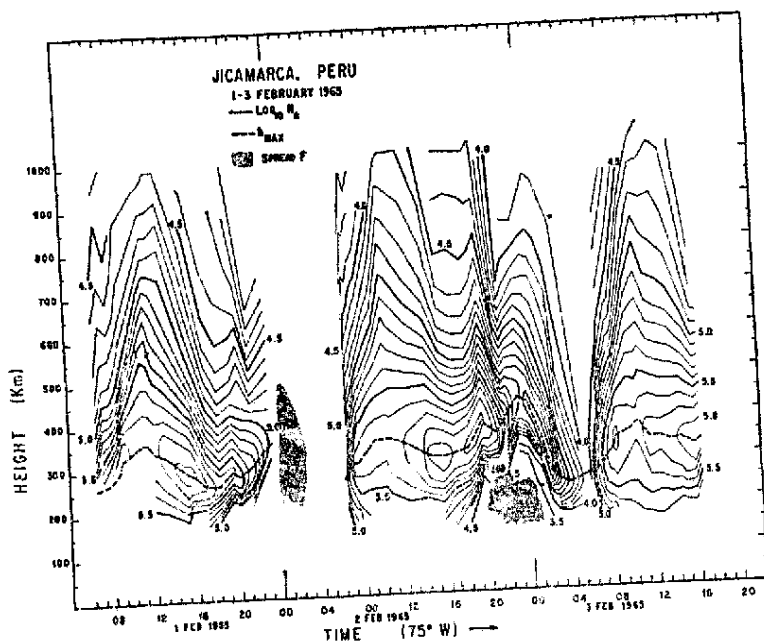
Fig. 1 — Electron density contours for 1-2 and 3 February 1965. Vertical motion of the entire F layer is seen to be very similar between 1800 and 2400 on both 1 and 2 February.
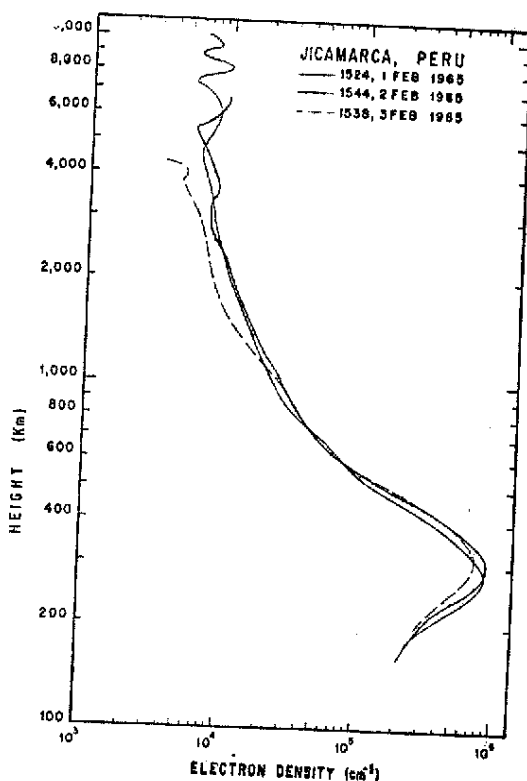
Fig. 2 — Electron density profiles near 1530 local time for 1-2 and 3 February 1965. We see that the equatorial profile was near ly the same at midafternoon on these three magnetically quiet days.
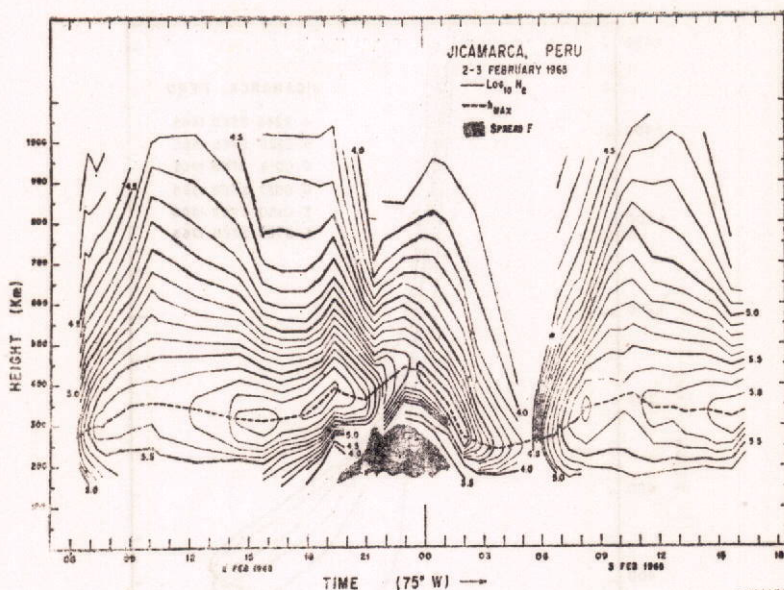
Fig. 3 — Electron density contours for 2-3 February 1965. On an expanded time scale we may see more clearly the vertical motions of the F layer. Between 0000 and 0200 on 3 February the F layer is seen to drop 200 km with no change in electron density.
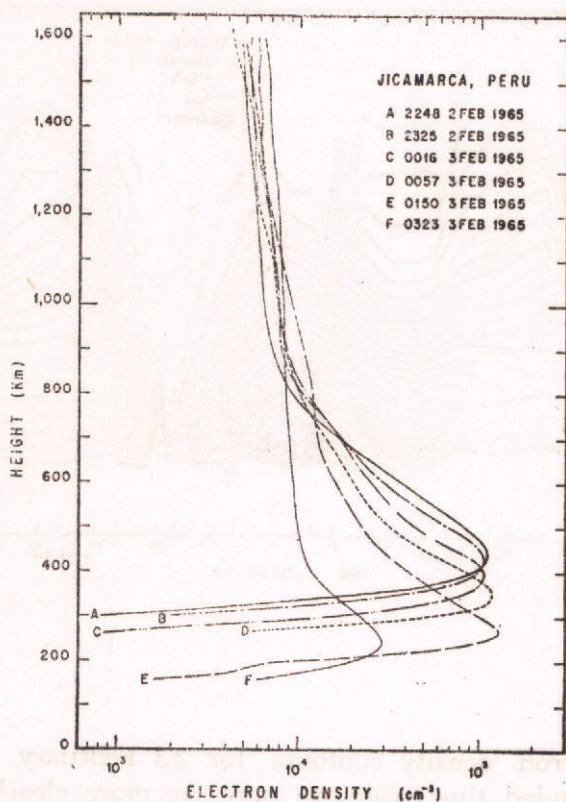
Fig. 4 — Six individual profiles which illustrate the vertical motion of the F layer.
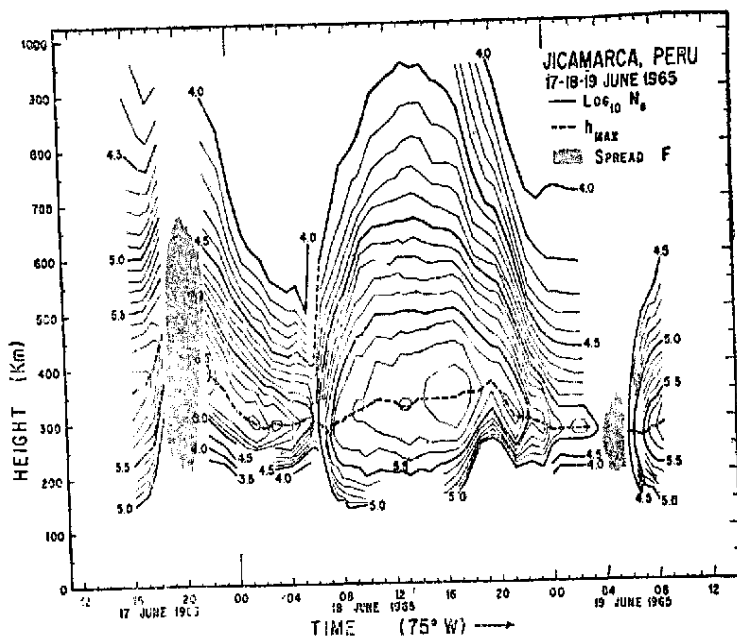
Fig. 5 — Electron density contours for 17-18 and 19 June 1965. The spread F observed at 0400 on 19 June was not preceded by vertical ionospheric motion, in contrast with all the other examples shown here.
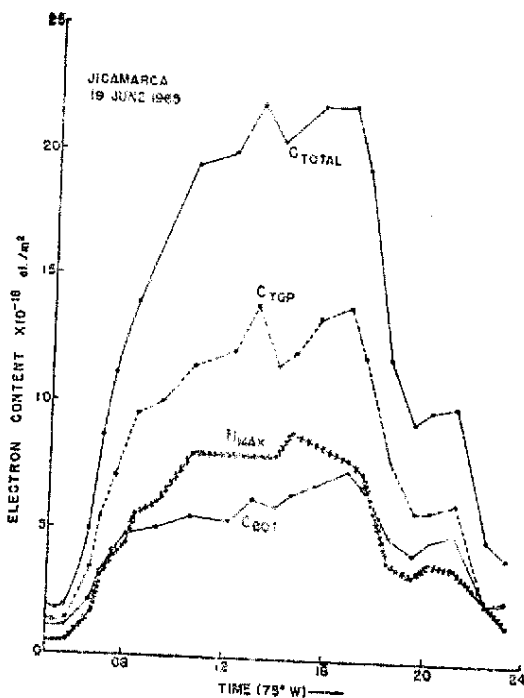
Fig. 6 — Total electron content. This information is contained in the contour plots of Figure 5, but is shown explicitly here for easy comparison with satellite electron content results. More of these plots will be shown in a later paper.
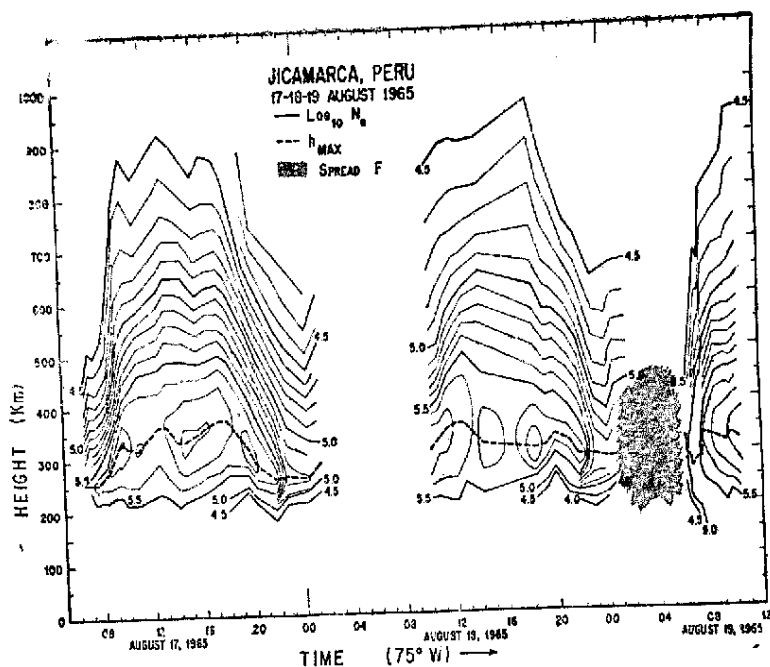
Fig. 7 — Electron density contours for 17-18 and 19 August, 1965. The spread F on 19 August began without vertical motion of the lower part of the F region, but there is evidence of lifting above the F region maximum just before it began. The temperature and composition measurements summarized in the following paper by D. T. Farley were made on these days.

TEMPERATURE AND COMPOSITION MEASUREMENTS

AT JICAMARCA

by

D. T. Farley

Jicamarca Radar Observatory, Lima, Peru

A series of measurements of the temperature and composition of the ionosphere were made, using the incoherent scatter technique, during the period 17-19 August, 1965 at Jicamarca. The quality of the data obtained is believed to be good. The altitude range covered was 200-1000 km.

The limited results so far available can be summarized as follows:

1) The concentration of H plus above 500 km was of the order of $1 - 2 \times 10^4$ cm^{-3} and was nearly independent of altitude and time of day.

2) The concentration of H$_e$ plus was less than 10% of the total density at all times and at all heights.

3) The altitude at which N [H plus] = N [0 plus] was about 900-1000 km during the day, but dropped to 600-700 km at night.

4) During most of the day the ion temperature was of the order of 900-1100° K in the altitude range 200-500 km. It then rose sharply to at least 2000° K at 1000 km.

5) The electron temperature at midday had a maximum of about 2000°-2500° K near 250 km. With increasing altitude the electron temperature at first fell, reaching equilibrium with the ion temperature at about 350 km, and then rose again as the ion temperature increased.

6) At night the ionosphere above 200 km was very nearly isothermal, with both T_e and T_i dropping to values of 600-800° K.

7) During the day the observed temperatures and scale heights did not correspond, whereas at night they very nearly did.
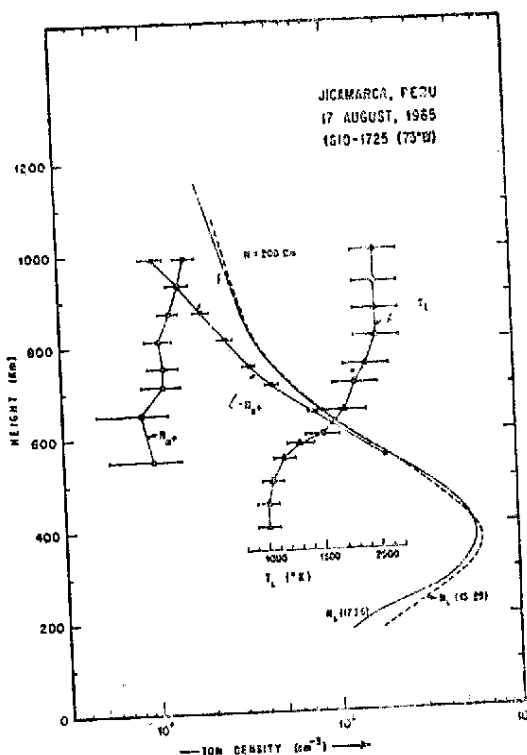
Fig. 1 — A daytime measurement of composition and ion temperature. The concentration of He plus was less than 10% at all heights shown.
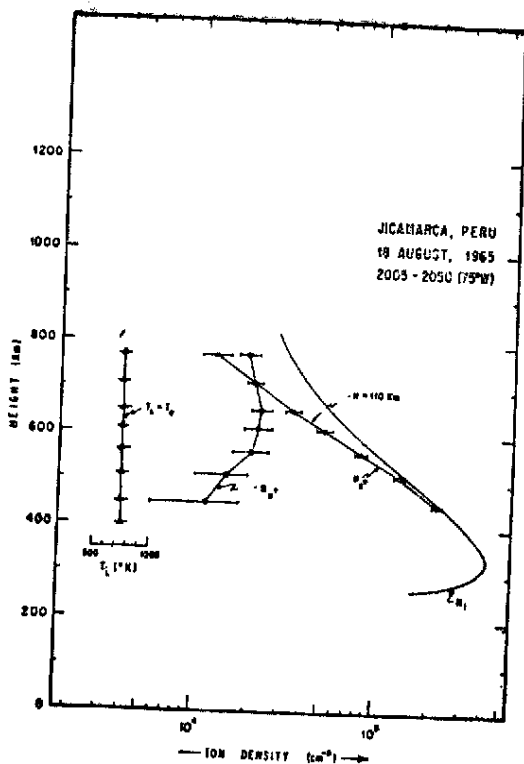
Fig. 2 — A nighttime measurement of composition and electron and ion temperatures. The concentration of He plus was less than 10% at all heights shown.

Fig. 3 — (same as Fig. 2).

plotted in Fig. 4. The functions plotted is the autocorrel-
ation for a shifted in the signal. This functions
is just the Fourier transform of the signal spectrum. The
good agreement between the theoretical curves and the
experimental data shows that the uncertainty in the composi-
tion is about 2%, and in the temperature perhaps ± 10%.
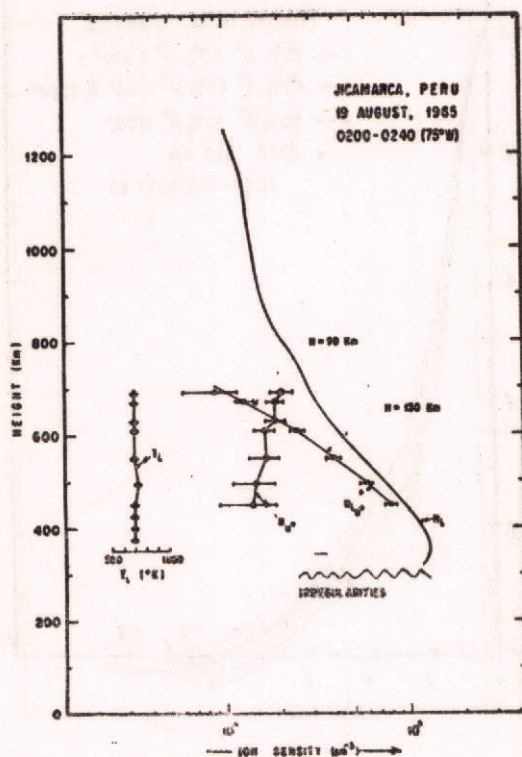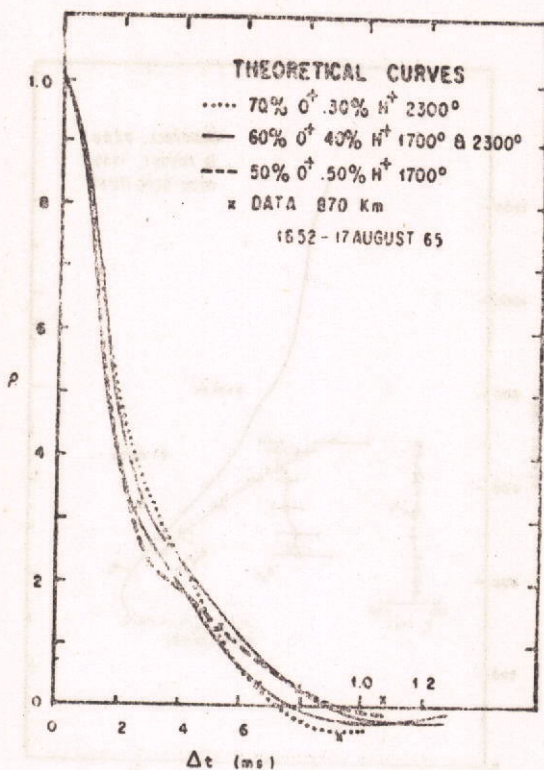
Fig. 4 — A sample set of data used in determining one of the points plotted in Fig. 1. The functions plotted is the autocorrelation function ρ ($\triangle t$) of the received signal. This functions is just the Fourier transform of the signal spectrum. The good agreement between the theoretical curves and the experimental data shows that the uncertainty in the composition is about $\pm$ 5%, and in the temperature perhaps $\pm$ 10%.
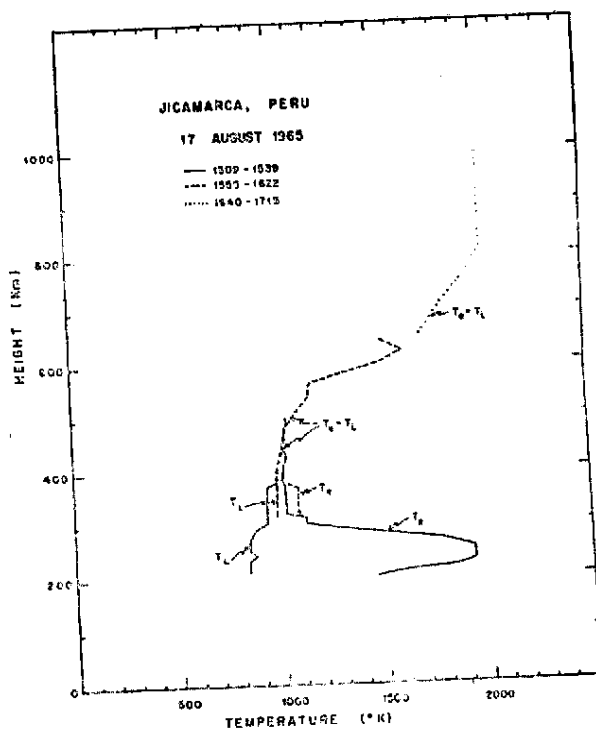
Fig. 5 — A daytime profile of electron and ion temperatures.
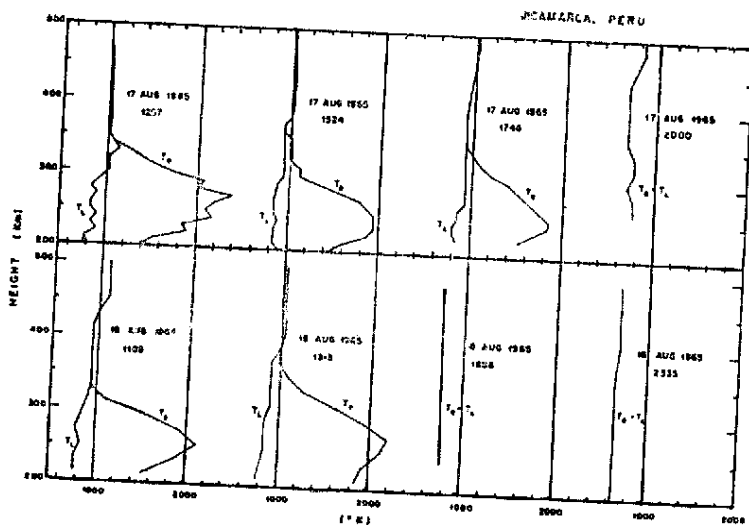
Fig. 6 — A series of low altitude electron and ion temperatures profiles.

SUNRISE STRATIFICATION IN THE EQUATORIAL F-REGION

by

R. B. Norton

CRPL, Boulder, Colorado

Ionograms taken at stations near the magnetic equator occasionally show a transient stratification during sunrise. It is the purpose of this paper first to describe these observations and then to present a simple interpretation of them.

These stratifications can be put in one of two groups depending on the presunrise layer and the subsequent behavior of the stratification. The first group corresponds to a presunrise layer existing at rather greater than usual altitudes with a critical frequency above about 5 MHz. This stratification begins at low frequency but increases rapidly until it merges with the foF2 (see Fig. 1). It usually lasts about one hour, but may last as long as an hour and a half. The second group corresponds to a presunrise layer existing at a lower than usual altitude with a critical frequency of less than about 3 MHz. In this case the stratification begins near the critical frequency and remains fairly constant in frequency while foF2 increases rapidly (see Fig. 2). The stratification weakens and then disappears after a total lifetime of about 15-30 minutes.

The ionograms taken at Huancayo foi each day between April 1957 — March 1958 and April 1954 — March 1955 have been investigated for the occurrence of the sunrise stratification. About three dozen examples were found for sunspot maximum and about half a dozen at sunspot minimum. However, of these examples, only about one dozen at sunspot maximum and only one or two at sunspot minimum were well developed. Although they occur throughout the year, the stratifications occurred most frequently in June and July. During the same period no stratifications of this sort were found on the Washington ionograms, thus suggesting that this phenomenon is peculiar to the equatorial region. No obvious correlation of the occurrence of the stratification with magnetic activity was found.
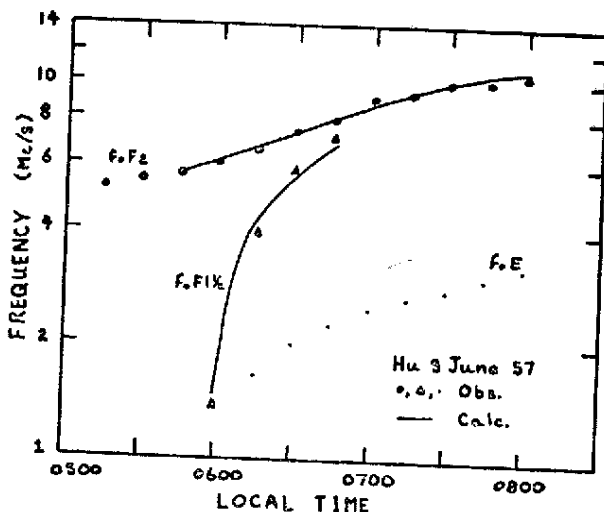
Fig. 1 — An example of group 1. The critical frequency of foE,
foF1 ½ and foF2 plotted versus local time for Huancayo, 3
June 1957 and compared with calculations based on photo-
chemistry;

$$\beta = 3 \times 10^{-4} \ sec^{-1} \quad and \quad q = 400 \ cm^{-3} \ sec^{-1}.$$

Our interpretation of the stratification is very simple and
involves only photochemistry. We suggest that to a good approxima-
tion the stratification results from the addition of the residual layer
with the new ionization which is formed at sunrise. In the case of the
first group the new ionization is formed below the residual layer and
for the second group the new ionization is formed primarily above the
residual layer. As is clear from the comparisons of critical frequencies
in Fig. 1 and 2 and of electron density profiles at fixed times in Fig.
3 and 4, this theory explains the sunrise data very well. Even the curve
for 0600 is a good average fit to the data. However, the stratification
in this case is very transient and has already disappeared in the calculat-
ed profiles. The agreement could be greatly improved by using a more
realistic discription to the solar flux than used in this calculation and
by adjusting the parameters slightly.
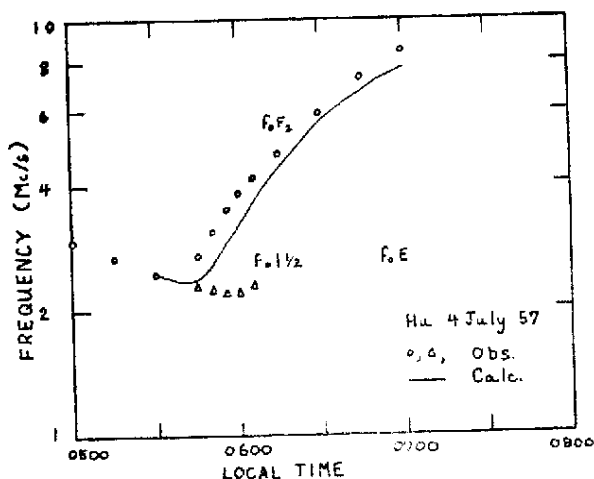
Fig. 2 — An exemple of group 2. The critical frequencies foE, fo1½ and foF2 plotted versus local time for Huancayo (4 July 1957) and compared with calculations based on photochemistry;

$\beta = 2 \times 10^{-4}$ sec^{-1} and $q = 400$ cm^3 sec^{-1}.
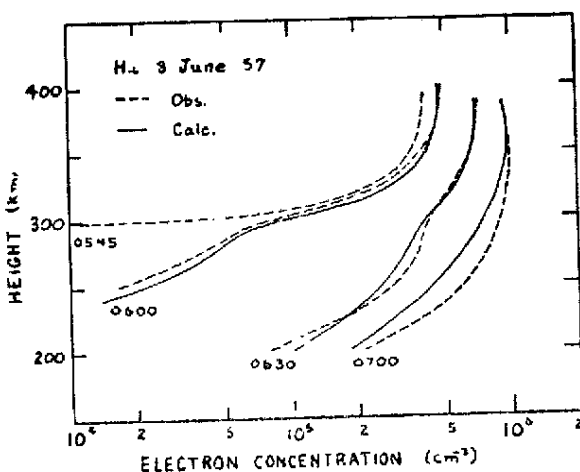
Fig. 3 — An example of group 1. The electron density for fixed times plotted versus height for Huancayo 3 June 1957 and compared with calculations based on photochemistry; $\beta = 3 \times 10^{-4}$ sec^{-1} and $q = 400$ cm^{-3} sec^{-1}.
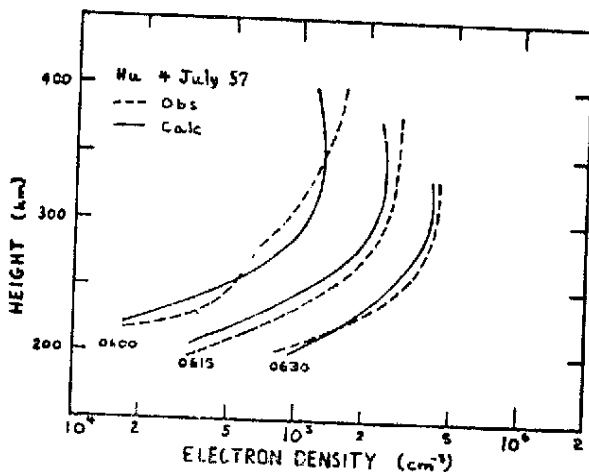
Fig. 4 — An example of group 2. The electron density for fixed times plotted versus height for Huancayo, 4 July 1957 and compared with calculations based on photochemistry; $\beta = 2 \times 10^{-4}$ sec^{-1} and q = 400 cm^{-3} sec^{-1}.

The photochemical rates used in these calculations can be specified by their values at 300 km; the loss rate was about 3×10^{-4} sec^{-1} and the production rate was about 600 cm^{-3} sec^{-1} for the example in the first group (Fig. 1 and 3) and slightly smaller for the second group (Fig. 2 and 4).

PHOTOCHEMICAL RATES IN THE EQUATORIAL F2-REGION

FROM THE FEBRUARY 1962 ECLIPSE

by

R. B. Norton and T. E. VanZandt

CRPL, Boulder, Colorado

A temporary sounding station was located on Canton Island (2.5°S and 171.4°W; dip 9°) February 1962 in order to obtain ionograms during a solar eclipse at a time of low sunspot activity. The eclipse occurred on 4 February 1962 when the 10 cm flux index was 100. Although the ionograms were difficult to interpret because of sporadic E and a multitude of stratifications, they have been reduced to give electron density profiles which have been subsequently analysed to obtain photochemical rates.

The various critical frequencies are illustrated in Fig. 1. Besides the usual E, F1 and F2 critical frequencies an extra E region cusp occurred primarily in the first part of the eclipse and an F1½ in the latter part. During much of the eclipse, especially around totality, sporadic E blanketed the E and sometimes the F1 layers. The dashed lines in Fig. 1 represent a model of foE for times when the E layer was blanketed. Figure 2 shows the electron density as a function of time for a few fixed heights.

The data at 260 km was analysed to give $\beta = 3 \times 10^{-4}$ sec^{-1} and $q = 200$ cm^{-3} sec^{-1}. The Danger Island eclipse data[1] gave $\beta = 9.6 \times 10^{-4}$ sec^{-1} and $q = 1080$ cm^{-3} sec^{-1}, but occurred during a perior of considerable sunspot activity (10 cm index of 220). The ratio of the β's for these two eclipses is 2.5; the ratio of the N$_2$ density taken from Harris and Priester[2] for the appropriate time and 10 cm flux index is 2.6. The ratio of q's is 5.4, but includes both changes in neutral atmosphere and solar flux. If we assume that the Harris and Priester model is substantially correct then the ratio of atomic oxygen should be 1.4 which implies that the ratio of solar ionizing fluxes for the two
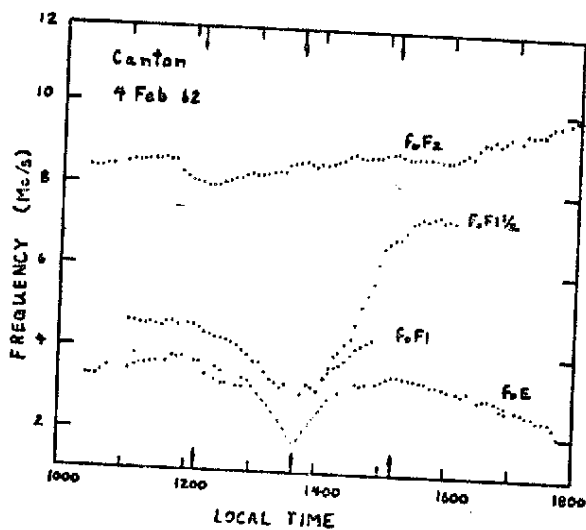
Fig. 1 — Critical frequencies plotted versus time. The eclipse times are indicated by the arrows.
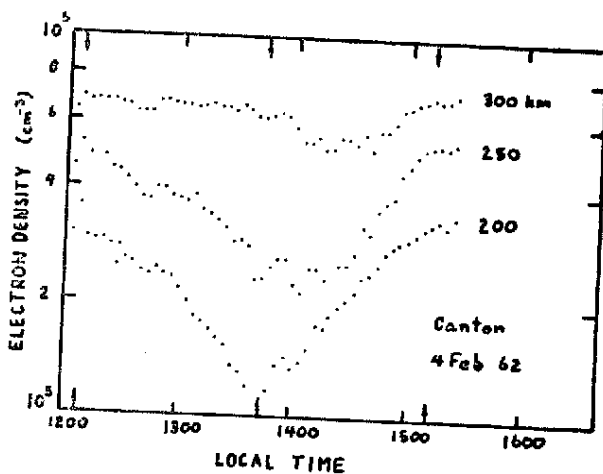
Fig. 2 — Electron density at fixed heights plotted versus time. The eclipse times are indicated by the arrows.

References

1 — VanZandt T. E., Norton R. B. and Stonehocker G. H. — NASA Techinical Note D-1444, 1962.

2 — Harris I. and Priester W. — J. Geophys. Research, **65**, 2003, 1960.

DIFFUSIVE EQUILIBRIUM AND THE EQUATORIAL
ANOMALY IN ELECTRON DENSITY

by

T. E. VanZandt and R. B. Norton
CRPL, Boulder, Colorado

and

H. Rishbeth
Radio and Space Research Station
Slough, Bucks, England

Theoretical three-ion diffusive equilibrium profiles were fitted to the shell-aligned electron density profiles for a pass of the topside sounder Alouette on 17 February 1963 at about 1600 LT.
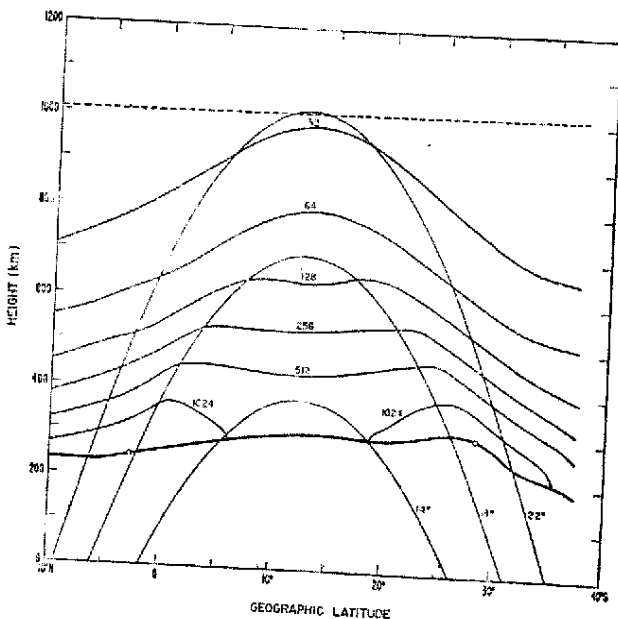
Fig. 1 — Contours of constant electron density (labeled in electrons cm⁻³ x 10⁻³). Since the densities differ by a factors of two, the distance between them is the scale height, vertical or shell-alined. The intersections of apex shells with the plane of orbit are shown.

The fit was very good for $T = 840 \pm 70°$ K; the height where [He plus] = [0 plus] was 610 ± 20 km, and at that height, [H plus]/[0 plus] = 0.3. The field line through the inflection point of the equatorial ledge had an apex of about 700 km. It is argued that the ledge normally can be pronounced only when it lies in a light ion region. It is shown that the equatorial ledge is an inward facing lip in the level contours inside the equatorial dome.

The discrepancy between this ion composition and those observed by Ariel in 1962 and Jicamarca Radar Observatory in 1964-65 inferred a solar cycle effect.
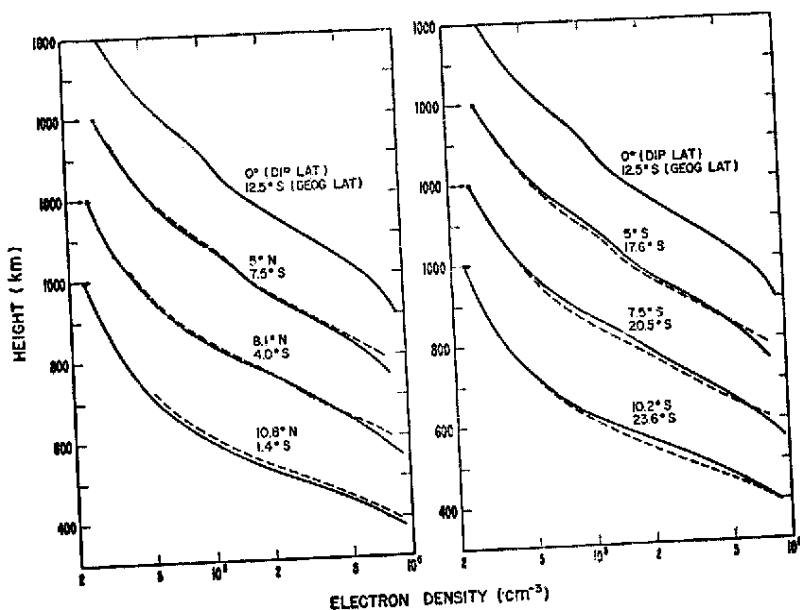
Fig. 2 — Vertical profiles of electron concentration at various dips. N and S. The disappearance of the ledge as it enters the 0 plus region can be clearly seen.
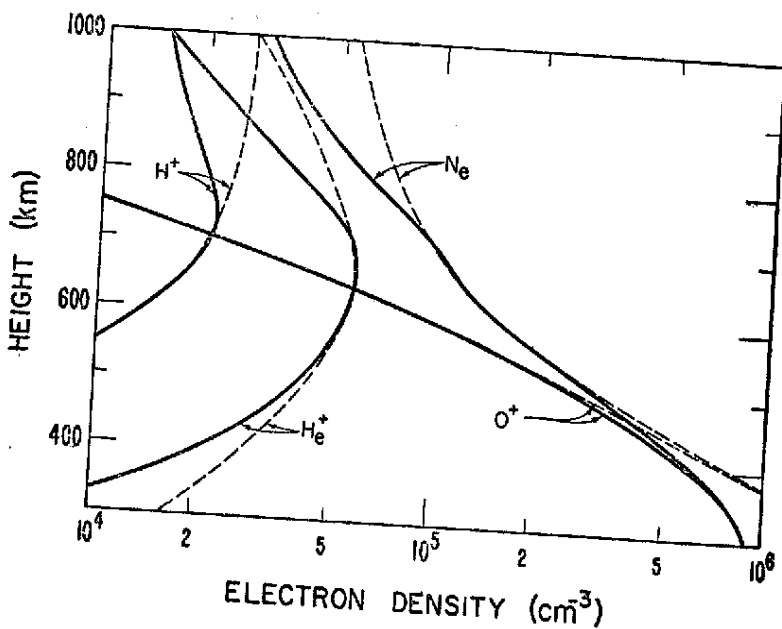
Fig. 3 — The inferred ion composition. The dashed curve is the field aligned distribution and the solid curve is the vertical distribution at the equator.

THE EFFECT OF IONIZATION TRANSPORT ON

THE EQUATORIAL F-REGION

by

W. B. Hanson and R. J. Moffett

Southwest Center for Advanced Studies

Dallas, Texas, U.S.A.

A full time-dependent solution is presentend for the plasma continuity equation

$$\delta N/\delta t = P - L \ \text{Div} \ \varphi$$

in the vicinity of the equatorial F region. The production and loss terms (P and L) are assumed to be due respectively to solar-ultraviolet radiation and to a linear loss mechanism which is characterized by the scale height of molecular nitrogen. It is further assumed that the concentration of oxygen ions is equal to the electron concentration N; such a restriction limits the validity of the derived values of N at high altitudes where light ions may predominate, but will not appreciably affect the applicability of the solution near the F2 peak. The plasma flux ψ, represents the net motion of either ions or electrons due to both electrodynamic drifts and diffusive processes. The particle velocities associated with small currents which flow perpendicular to the magnetic field are neglected in ψ, but the Biot-Savart forces associated with these currents are included in the equations.

Figure 1 represents the solution obtained for a set of atmospheric parameters chosen to represent conditions near sunspot maximum. In effect, the electron concentration contours show the values of N which would be achieved in a magnetic tube of force which diverges with a constant equatorial velocity of 10 m/sec. The equatorial crossing distance of the tube changes from 200 km to 2200 km during the course of this movement, with a total time lapse of 2 x 10⁵ seconds. The solar conditions and the atmospheric parameters are held constant

at their noon values during this period. Even with rather severe
restriction the solution appears to represent with reasonable fidelity
the observed meridional distribution of electrons during midday. The
contours shown in Fig. 2 represent a similar solution obtained for
typical sunspot minimum atmospheric parameters.

Fig. 1 —

S.S. MAXIMUM CONDITIONS: $T_i = T_e/2 = 1500°$ K

AT 400 km: $P = 1.8 \times 10^2$ cm^{-3} sec^{-1} $\beta = 8.0 \times 10^{-3}$ sec^{-1} $\frac{(N_m)_{max}}{(N_m)_{eq}} = 1.6$

$D_a = 1.3 \times 10^{11}$ cm^2 sec^{-1} $n(O) = 2 \times 10^8$ cm^{-3}

$V_o = 10$ m/sec independent of altitude

Fig. 2 —

S.S. MINIMUM CONDITIONS $T_i = T_e/2 = 850°$ K

AT 400 km: $P = 6.0 \times 10^0$ cm^{-3} sec^{-1} $\beta = 1.0 \times 10^{-6}$ sec^{-1} $\frac{(N_m)_{max}}{(N_m)_{eq}} = 2.2$

$D_a = 8.4 \times 10^{11}$ cm^2 sec^{-1} $n(O) = 2 \times 10^7$ cm^{-3}

$V_o = 10$ m/sec independent of altitude
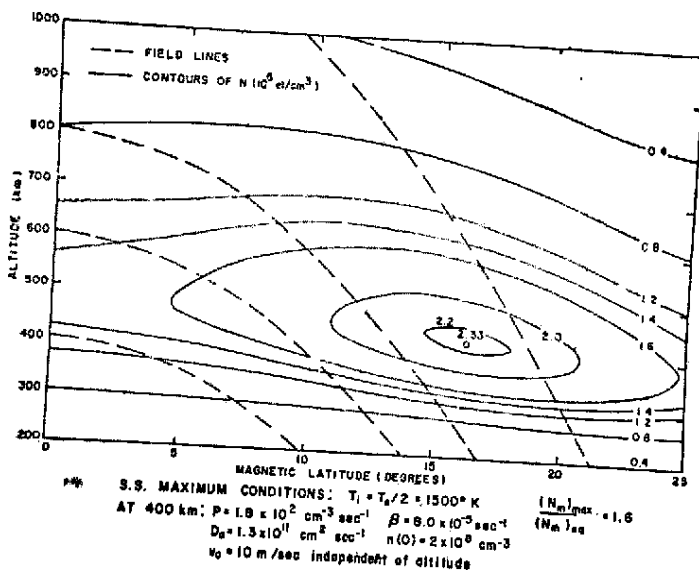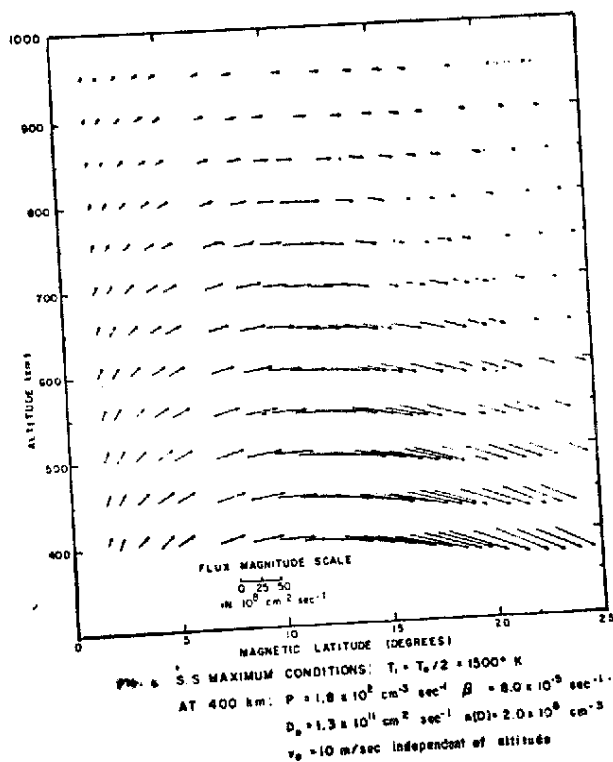
Fig. 3 — Demonstrates dramatically the plasma fountain originally postulated by Martin to explain the Appleton peaks in NmF2. The vector field of the plasma flux has been plotted for the solution presented in Fig. 1.
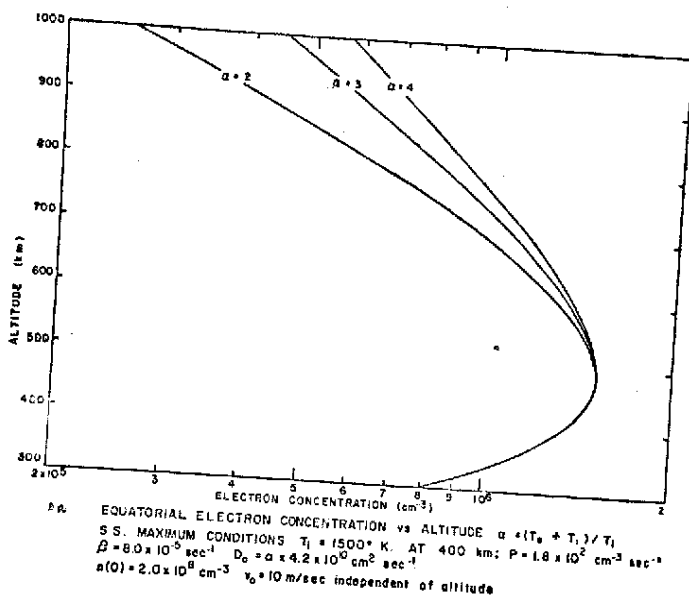
Fig.4 — Shows the equatorial values of N obtained for sunspot maximum conditions, for different values of $(T_e + T_i)/T_i$ and a vertical drift velocity at the equator of 10 m/sec. While large changes in the electron temperature produce drastic differences in N above the F2 peak, they have little effect on N below this altitude. This situation also obtains values of N at higher latitudes which are not shown in the figure.
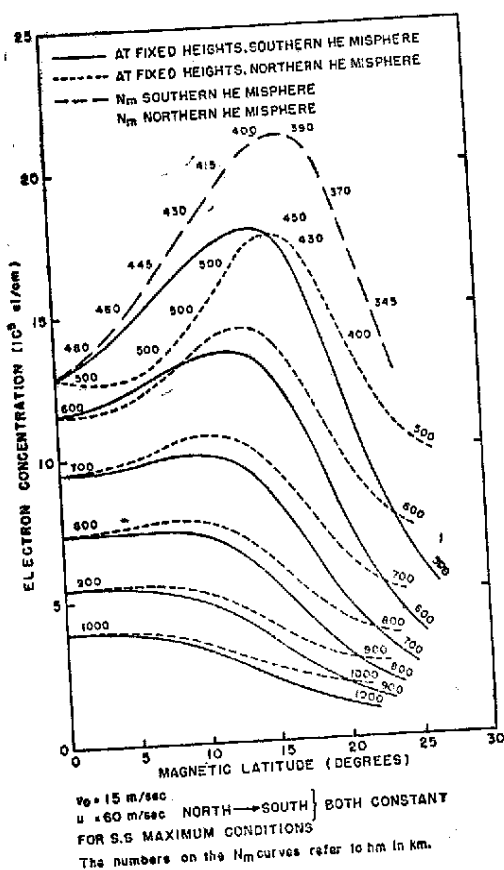
Fig. 5 — Shows an asymmetric ionosphere produced by the combined effects of a vertical equatorial drift of 15 m/sec and a north-south neutral air velocity of 60 m/sec. This north-south wind has two main effects on N which tend to cancel each other. The fact that plasma produced in the Northern hemisphere is blown to the south to be re-combined will cause N to be larger in the south. The wind tends to raise the F- peak in the Northern hemisphere and lower it in the Southern hemisphere, however, so that re-combination proceeds more rapidly in the south. The net result of this competition produces the fixed height contours shown in Fig. 5 where it can be seen that NmF2 is of the order of 10 percent larger in the Southern hemisphere.

The time-dependent capabilities of the technique are clearly seen in Fig. 6, which shows the build up of N from a value of zero everywhere when the sun (P) was "turned on" to an equilibrium condition. The solution applies to the distribution along the field line which crosses the equator at 700 km.

Fig. 6 —

S.S. MAXIMUM CONDITIONS
INITIAL N = 0
EQUATORIAL Z = 700 km
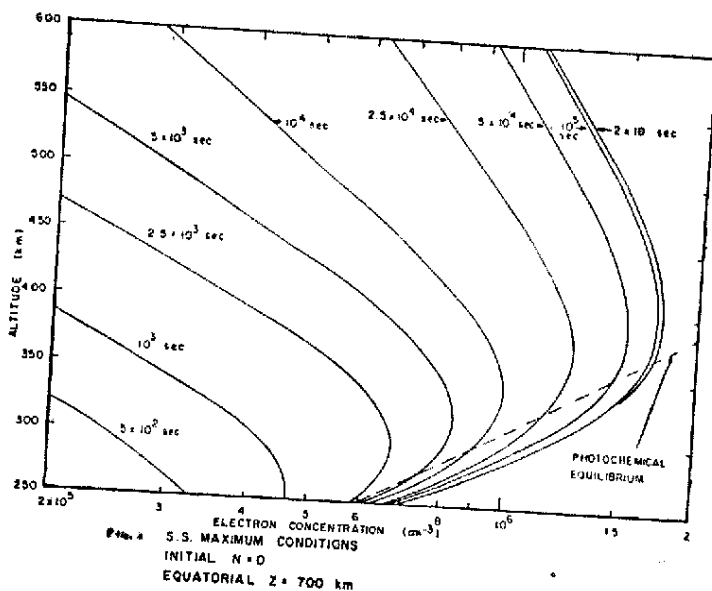
DIFFUSION AND ELECTROMAGNETIC DRIFT IN THE

EQUATORIAL F2 REGION

by

E. N. Bramley and M. Peart

Radio and Space Research Station

Slough, Bucks, England

Calculations of the equilibrium electron density distribution in the F2 region of the equatorial ionosphere are described. The effect of photoionization, loss, diffusion along geomagnetic field lines, and an electromagnetic drift of arbitrary magnitude are included. The work is an extension of previous calculations in which the drift was included as a perturbation effect only. It is found that under representative daytime ionospheric conditions an upward drift of a few meters per second is sufficient to produce an equatorial anomaly which is quantitatively similar to that observed experimentally.

Note on Symbols and Parameter Values

Symbols

H	Scale height of ionizable gas (used as unit of lenght)
a	geocentric distance of level of peak production ($z = 0$) at the equator ($\emptyset = 0$) for overhead sun.
q_0	peak photo ionization rate at $z = 0$ and $\emptyset = 0$
d_0	diffusion rate (D/H^2) for $z = 0$
β	linear loss coefficient: $\beta = \beta_0 \ \exp(-kz)$
ω	upward drift speed at $z = 0$, $\emptyset = 0$. .

$$P = q_0 \ d_0, \quad L = \beta_0 \ d_0, \quad W = \omega/d_0,$$

Values Adopted

$a = 80$, $H = 82$ km (corresponding to sunspot maximum conditions)

$k = 2$ (i.e. scale height of β is taken to be $H/2$)

$d_0 = 5 \times 10^{-5}$ sec^{-1}

$P = 2 \times 10^7$ cm^{-3}, $L = 500$, $W = 1$ and 5

The values W = 1 and 5 correspond for the above value of d₀ to upward drift speeds of 4.1 and 20.5 m sec⁻¹ respectively at the reference level at the equator.
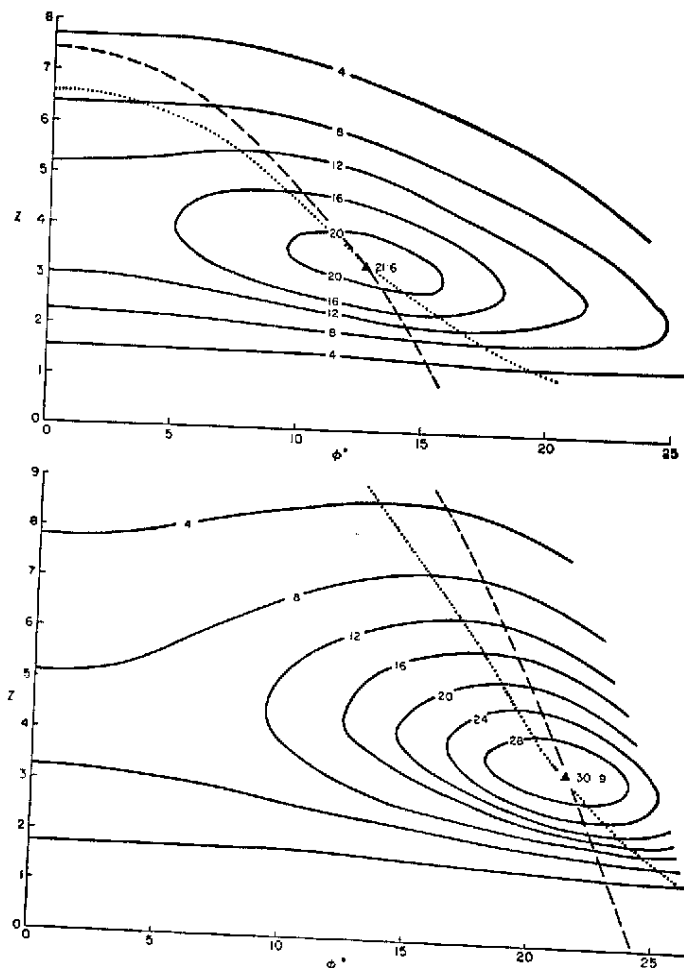
Fig. 1 — Contours of electron density (in units of 10^5 cm⁻³) as a function of latitude and height. The height is measured in units of 1 scale height of the ionizable gas (82 km) above a reference level of 180 km. The vertical drift speed at the reference level is 4.1 m sec⁻¹ for the top figure and 20.5 m sec⁻¹ for the bottom one.
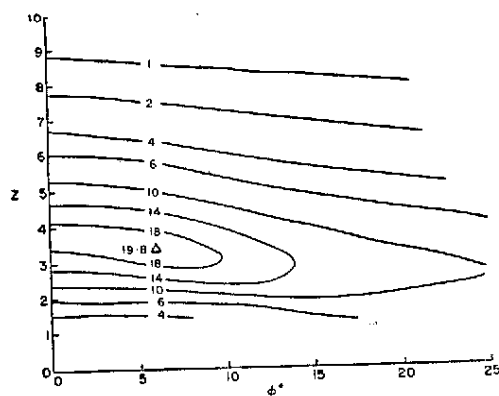
Fig. 2 — Same as Fig. 1 with no vertical drift.

GEOMAGNETIC CONTROL OF THE EQUATORIAL TOPSIDE IONO-
SPHERE AND ITS ASSOCIATED CURRENT SYSTEM

by

Richard A. Goldberg

Goddard Space Flight Center — NASA

Greenbelt, Maryland, U.S.A.

A detailed study of the momentum transport equation for charged gaseous fluids moving through a neutral gas suggests that the equatorial geomagnetic anomaly is simply the natural steady state electron density distribution one would expect under the influence of gravitational, electric, and magnetic fields and production and loss, when interaction with the neutral medium is negligible[1]. Figure 1 demonstrates the type of comparison one obtains between the calculated and observed topside constant height electron density profiles for an isothermal atmosphere[2]. Furthermore, the agreement between measurement and theory can be extended down to the F2 layer density peak when a more realistic model is included for the vertical temperature distribution of electrons and ions[3].

The distribution illustrated in Fig. 1 is supported by the longitudinal component of the F region current system, as given by the following equation[1]:

$$(-1/Nr)\,(\delta N/\delta\theta) - (1/\tau r)\,(\delta\tau/\delta\theta) = (\mu M / 4\pi k\tau)\,(\cos\theta/r^2)j\Phi \qquad (1)$$

where N is electron number concentration, τ is the average of the electron and ion temperatures, (r, θ, Φ) are the spherical polar coordinates, $j\Phi$ is the longitudinal component of current density per unit particle, i.e.

$$\Phi = e\,(v_i - v_e) \qquad (2)$$

where e is electron charge and v_i, v_e are ion and electron velocities respectively. Finally, M_i, μ_o and k are physical constants.
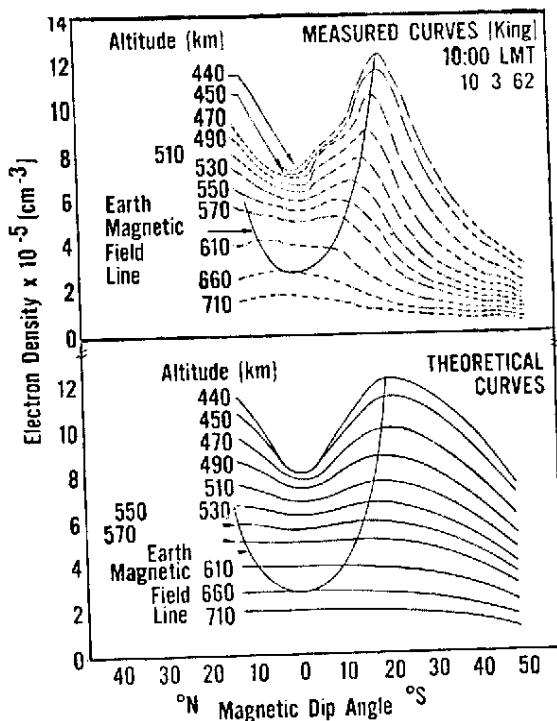
Fig. 1 — Comparison of theoretical curves, using the momentum transport equations for electrons and ions, with Alouette observations.

If we consider equation (1), and assume that $\delta_T/\delta\theta \ll \delta N/\delta\theta$ we see that $j\Phi$ is directly proportional to $(1/N)\delta N/\delta\theta$, and thus, the current density is directly proportional to the north-south slope of density $\delta N/\delta\theta$. We see that there can be no gradient in the north-south direction, and hence no anomaly, when $j\Phi$ is absent.

The ion-electron velocity difference latitudinal profiles at constant height for the model illustrated in Fig. 1 can be calculated using equation (1) and are shown in Fig. 2. We note that the anomaly requires an easterly flow within its crests, and a westerly pattern beyond

its crests, the crest marking the focus of the current system. This is a similar conclusion to that from theories making use of the continuity equation and assuming a vertical upward drift (and hence eastward electric field) at the equator. These theories also find that a westward electric field (or current) is incapable of producing the anomaly.

The current system represented in Fig. 2 is extremely small, many orders of magnitude below that calculated for the E region. Nevertheless, it bears a striking resemblance to the E region system qualitatively. Furthermore, preliminary studies indicate a strong correlation between variations in the E region current system magnitude and the measured slopes of the geomagnetic anomaly (ratio of crest to trough), the measure of the F region current system. This suggests that the tidal forces and other effects responsible for E region behavior may also control the destiny of the F region density distribution.
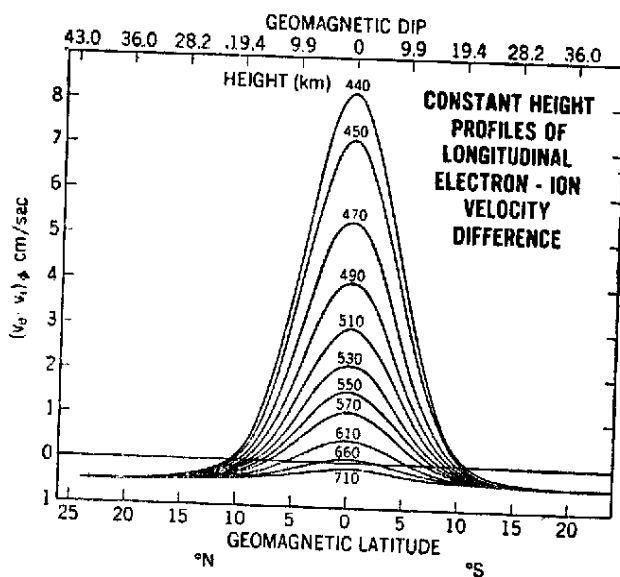
Fig. 2 — Constant height profiles of longitudinal ion-electron velocity difference calculated theoretically from the momentum transport equations for electrons and ions.

References

(1) Goldberg R.A. — The Equatorial Geomagnetic Anomaly and its Associated Current System — J. Geophys. Res. (in Press) 1965.

(2) Goldberg, R. A., P. C. Kendall and E. R. Schmerling — Geomagnetic Control of Electron Density in the F region of the Ionosphere — J. Geophys. Res., **69, 417-427,** 1964.

(3) Goldberg, R. A. — The Effect of a Variable Electron Temperature on the Equatorial Electron Density Distribution in the Upper Ionosphere. — J. Geophys. Res. **70,** 655-665, 1965.

THEORY OF RESONANCES IN IONOGRAMS TAKEN BY SOUNDERS ABOVE THE IONOSPHERE*

by

J. P. Dougherty

and

J. J. Monaghan**

Department of Applied Mathematics and Theoretical Physics,
University of Cambridge

This paper describes a theory of the resonant effects observed by sounding equipment on the ionospheric satellite "Alouette". The model consists of an oscillating dipole immersed in a uniform hot plasma with uniform magnetic field. A formal expression for the electric field throughout space is readily constructed. In simple cases (zero temperature and either no magnetic field or infinite light velocity) this reduces to an integral which can be evaluated analytically and the resonance shown explicitly. In general we try to locate the frequencies at which resonance will occur without evaluating the field. This can be done by the "pinching-poles" technique used in quantum field theory.

The results show that resonances would occur at the following frequencies: the plasma frequency, ω_p; the gyrofrequency of the electrons, Ω_e and its harmonics $n\Omega_e$, the "hybrid" frequency $(\omega_p^2 + \Omega_e^2)^{1/2}$, and the "zero range" frequencies, which satisfy $\omega^2 \pm \Omega_e - \omega_p^2 = 0$. Some idea of the relative importance of these resonances can also be gained for the theory. The fundamental of the gyrofrequency series, and the zero range frequencies, would give only weak resonances. The series $\omega = n\Omega_e$ has a complicated structure, and is really the superposition of four series, some of which are slightly shifted from the exact harmonics.

SUMMARY OF THE SESSION

by

T. E. VanZandt

CRPL — Boulder, Colorado

and

W. B. Hanson

Southwest Center for Advanced Studies

Dallas, Texas, U.S.A.

King showed that maps displaying contours of foF2 vs. latitude and local time (that is, at a given U. T.) can be described in terms of ridges of foF2, and that the equatorial anomaly ridge is most intense when it is joined by a mid-latitude ridge during the day. He also suggested that the anomaly forms below hmaxF2 at sunrise and moves upwards until it becomes evident as the equatorial anomaly after it moves through hmaxF2.

Vila studied the morphology at the equatorial anomaly in Africa using ground-based and airborne ionosondes. From the times and places of occurrence of the regular F1½ layer he suggests that it is caused by diffusion of photo-electrons along the field lines.

Lyon and Olatunji presented a thorough study of the morphology of the ionosphere at Ibadan over a sunspot cycle.

Rastogi showed that the behavior of the F2 layer at Natal is different from that at other equatorial stations. He suggested that this is correlated with the large angle between the dip equator and parallels of latitude at Natal.

McClure, Cohen and Farley presented very importante preliminary results from the Jicamarca Radio Observatory. Large vertical motions were observed at night. Ion and electron temperatures and ion composition were measured. It was shown that the variations of T_e at sunrise are consistent with the theory.

Skinner, Hunter and Mendonça discussed the measurements of total electron content using satellite beacons.

Rastogi discussed the morphology of lunar tides and Yonezawa analized the seasonal non-seasonal, and semi-annual variations of foF2.

Three papers were presented based on analysis of the Alouette data in the equatorial region. VanZandt, Norton and Rishbeth found that a change in

ion composition from 0 plus to He plus occurred at an altitude of approximately 600 km over a rather wide region near the equator. It was also found that the plasma temperature was constant throughout this region. They further pointed out that the "ledges" found on equatorial topside profiles were much more likely to be observed in the light ion region than in the heavy ion region because a given small change in N corresponds to a much greater range change when the scale height is large.

Thomas, Chan, Colin and Rycroft plotted vertical scale height profiles at fixed height through the equatorial region and showed that at low latitudes two symmetric maxima in real height appeared, while at high altitudes two similarly placed minima occurred. They presented an equation from which it is possible to recover the scale height along field lines from the measured vertical and horizontal scale lengths.

Somayajulu noted that the top of the equatorial "dome" is closely related to the transition altitude from 0 plus to He plus ions and suggested that there may be some causal relationship.

The photochemistry of the F-layer during an eclipse was discussed by Norton and VanZandt. They showed that good agreement between the electron concentrations observed during the February eclipse in 1962 and the calculated behavior could be obtained using reasonable values for the atmospheric para-meters and ionizing radiation intensity. Good agreement was also obtained with eclipse data taken during sunspot maximum. The fact that commonly accepted model atmospheres were used in these calculations lends considerable support to the validity of these models, and to their dependence on sunspot number. It appears possible to provide a natural explanation of the morning maximum in NmF2 in terms of photochemistry alone without invoking any ionization transport effects.

Norton also gave evidence that the transient sunrise F1½ layer is the consequence of photoionization below an exceptionally high nighttime F2 layer.

Two papers were presented, one by Bramley and Peart, and one by Hanson and Moffett, which demonstrated that the main features of the daytime equatorial F region can be produced by the action of solar-ultraviolet produc-tion, diffusion, a linear loss process, and electrodynamic drift. The vertical drift process is shown to be an essential feature, with and upward component of 5 m/sec to 20 m/sec being required to obtain Appleton's peaks in the observed range of amplitude and latitude. Hanson and Moffett also demonstrated that a 10 percent asymmetry in NmF2 between the Northern and Southern hemispheres can be produced by a north-south wind of 60 m/sec blowing across the equator. The enhancement occurs in the hemisphere toward which the wind is blowing. They also showed the time dependent nature of the electron concentration profile during the transient phase after a production term is suddenly turned on.

A further step in describing the distribution of plasma above F2 peak which results from diffusive equilibrium along magnetic field lines and which is associated with a given equatorial N (h) profile was presented by Goldberg. He presented calculations of the current system which produces the Biot-Savart forces necessary to maintain the derived plasma distribution under the action of gravity, pressure gradients, and the presence of the earth's magnetic field. This current system is uniquely specified for a given equatorial profile, provided that T_e, T_i, and m_i are left unchanged.

Dougherty and Monaghan discussed the origin of the plasma resonances which are observed with the Alouette satellite in terms of the dispersion relationship for the electric field of an oscillating dipole immersed in a uniform hot plasma. The frequencies of interest are those which propagate with essentially zero group velocity, i. e., the excitations must remain in the vicinity of the satellite in order to be detected. For directions perpendicular to the magnetic field a series of solutions for real ω and k are found. Each solution has three points at which the group velocity is zero, the choice of a set of these zeros defines series of plasma resonance frequencies. It appears that the set of frequencies with k of the order of the reciprocal electron Larmor radius does not agree satisfactorily with the observed frequencies. The choice then must be made between very large k values corresponding to very small dimensions, or more probably to very small k values which would be dictated by the antenna dimensions. Unfortunately, the solutions become rather complicated for small k, and it is difficult to obtain the results with high accuracy. In addition to these perpendicular resonances, it is also possible to excite the plasma frequency, which propagates parallel to the magnetic field.

V — F-REGION DISTURBANCES AND IRREGULARITIES

V — F-REGION DISTURBANCES AND IRREGULARITIES

(Discussion Leader: J. P. Dougherty)

Review Paper

by

Robert Cohen

Jicamarca Radar Observatory, Lima, Peru

The ionospheric F-region is characterized not only by electron density variations that are relatively smooth module scale height, but also small fluctuations in the electron density which vary with space and time. These can be described by the function.

$$\delta N = \delta N (x, y, z; t)$$

The fluctuations of this sort that are always present give rise to the weak scattering of radio waves known as incoherent scatter, but occasionally the fluctuations tend to become organized with respect to the magnetic field lines in such a way that they produce what are known as field-aligned irregularities of electron density. These irregularities produce a strong scattering of radio waves which are incident to the field lines in a perpendicular orientation, and for that reason they are referred to as being "aspect sensitive".

The spatial properties of the irregularities at any instant can best be described by means of an autocorrelation function,

$$\rho(r) \propto \exp (-r/l)$$

where l is known as the scale size, and tends to be large in the field direction compared to the directions transverse to the field.

The irregularities present at a given moment can be described by a spectrum of scale sizes, and the interaction of radio waves that scatter from the irregularities to given coherent echoes at normal incidence to the field lines is determined by the Fourier component of this distribution comparable to the wave length of the exploring wave. The larger irregularities, on the other hand, are the determining factor for the forward scattering of radio waves that is experience on receiving scintillating radio signals from sources in space. The

fact that scintillations have been correlated with radar scattering from the same medium is indicative of the possibility that both large and small scale irregularities can coexist in the spectral distribution, and it is possible that the large irregularities result in the ultimate formation of the smaller ones.

In the equatorial region, as contrasted with temperate latitudes, both the large and small irregularities occur less frequently during times of magnetic activity, and as at other latitudes, they occur most commonly at night. There is appreciable experimental evidence that both the small and large irreguarities are aligned with the earth's magnetic field.

The large or "thick" irregularities are frequently referred to as "wave-guide" irregularities because of their ducting property, first inferred from the appearance of equatorial ionograms. Now that it has been possible to orbit an ionosonde in their midst, this waveguide propagation has enabled their localization in space. Although the presence of large irregularities was recognized from scintillation studies, it has been difficult by that technique to establish specific spatial properties regarding them, such as their height of occurrence. The in situ measurements by the S-27 and S-48 topside sounders, on the other hand, are a powerful tool in obtaining detailed spatial characteristics of the waveguides.

On equatorial bottomside ionograms, the thin irregularities and the thick irregularities manifest themselves as "equatorial spread-F" and "temperate latitude spread-F" configurations, respectively. Some ionograms are complicated combinations of these configurations being the result of coexistent irregularities of both kinds.

A significant observation with S-27 is the discovery that patches of the thin, scattering irregularities are at times distributed along magnetic field aligned sheets. However, they are propably not patches of **overdense** ionization, as stated in references.

The spatial distribution of the thin irregularities as obtained from topside observations during a six month period beginning in September, 1962 is shown in Fig. 1. There is no indication of equatorial irregularities present during the afternoon hours, but there are sometimes irregularities present in the morning hours. This feature of the sunspot minimum period had earlier been noted from ground-based ionosonde observations.

The distribution of waveguide irregularities is sometimes obscured by the presence of the thin irregularities, so it may not be significant that few of these are noted from the topside near the equator, (Fig. 2). However, for the period around sunspot maximum, bottomside sounders indicate a more plentiful equatorial distribution of presumably waveguide irregularities giving rise to frequency spreading (Fig. 3).
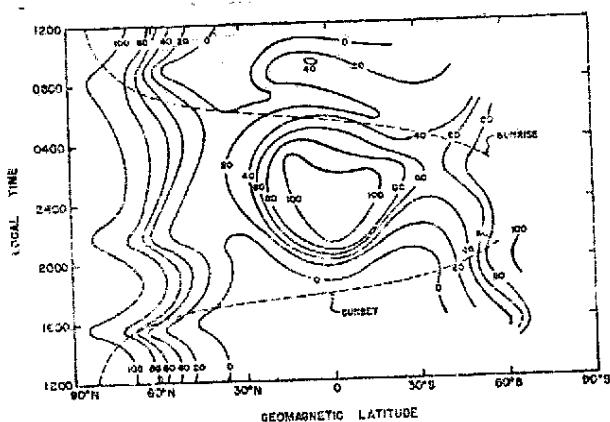
Fig. 1 — Spatial distribution of percentage occurrence of aspect-sensitive F region irregularities as observed from S-27 from September, 1962 to March, 1963.
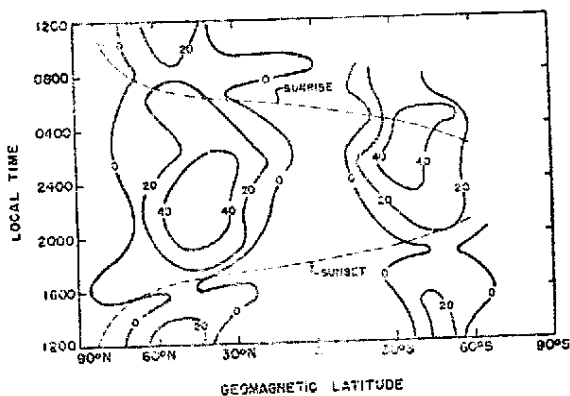
Fig. 2 — Spatial distribution for waveguide irregularities observed in the same way as Fig. 1.
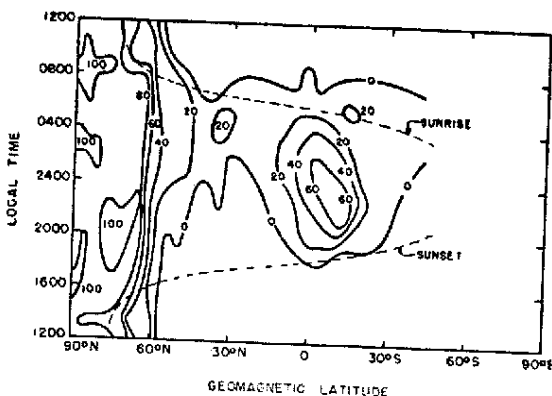
Fig. 3 — Spatial distribution of waveguide irregularities deduced from frequency spreading obtained on ground-based ionosondes during sunspot maximum.

It is perhaps an understatement to conclude that the equatorial F region irregularities are little understood theoretically, and this is also the situation with respect to those encountered at other latitudes. It is probable that the irregularities result from various plasma instabilities, since turbulence is unlikely at the heights where they occur. However, it has so far been difficult to establish just what state of the ionospheric plasma is conducive to the instabilities involved. It is possible that gravity waves produce the very large irregularities that are noted as large-scale perturbations of the electron density profiles, otherwise known as "travelling disturbances".

One theoretical analysis for the equatorial case has shown that pre-existent scattering irregularities below hmax will be amplified in intensity by a rise in height of the F layer in which they are embedded. F-region drifts are probably significant in the understanding of the irregularities and their formation, as is the motion of the irregularities and their patches. Such drifts and motions are discussed in the accompanying review paper by Kent on section VI of this report.

The irregularities in the equatorial F region tend to be more highly elongated than those encountered at other latitudes. Axial ratios of scale sizes range from 10 to 1 or more. The spectrum of irregularity scale sizes transverse to the magnetic field lines reported by various workers ranges from several meters to several thousand meters, while their length along the field lines is estimated to extend from at least several kilometers to the many thousands

of kilometers associated with the conjugate ducting observed from the topside. The ducts observed in this way may be identical with those that propagate whistlers.

Insofar as time variations and lifetimes of irregularities, it has been suggested that they may be formed at sunset and persist through the night. However, there are observations at 18 MHz indicating that individual patches have lifetimes varying from 10 to 150 minutes, with an average value of about 20 minutes. For patches of irregularities observed by the study of radio-star scintillations, the internal structure of the patch did not change appreciably during its motion across the observing point.

During the high sunspot activity of the IGY, irregularities over Peru were common except during May, June and July of 1958. However, over Africa the seasonal variation at low sunspot activity seems to be just the opposite, and there is less variation at sunspot maximum.

The thickness of irregularity patches has been variously estimated as ranging between limits of 10 to 400 km, with comparable east-west and north-south extents.

SATELLITE SCINTILLATIONS FROM LOW TO HIGH LATITUDES

by

J. Aarons, B. Ramsey and H. Silverman

Air Force Cambridge Research Laboratories

Bedford, Massachusetts, U.S.A.

In order to investigate the latitude dependence of scintillation index at 40 MHz three sites were instrumented for an intensive study during the period April 20-30, 1965. The sites were Arecibo, Puerto Rico at 19° N, Sagamore Hill, Mass. at 42° N and Thule Greenland at 78° N; all were close to the 70° W meridian.

Using the high inclination satellite, S 66, records were made of 40 MHz and 41 MHz transmissions. Two time periods were analysed, 1400-1700 E.S.T. and 0200-0430 E.S.T.

Figure 1 (Rev. 2717) is a tracing of records from the three stations. Portions A and B show little or no scintillation at Arecibo or Sagamore Hill; they are for identical time periods. The "closest approach" records of 1 C show no scintillation; however the scintillation at 1613-1614 recorded at Sagamore Hill and those simultaneously observed at Thule show high indices as the satellite sub-ionospheric latitude approaches the auroral zone.

Sub-satellite positions are plotted in the map Fig. 1 although it should be noted that only simultaneity of sub-ionospheric latitude should be considered. For a qualitative view however the motion from a completely scintillating high latitude signal to a non-scintillating low latitude is readily seen.

A similar pattern is observed in Fig. 2 with the difference being that scintillations are observed farther to the north than in Fig. 1. An entirely new set of record is shown in Fig. 3 which display a record (Rev. 2669) taken on April 22, 1965 where medium level scintillations (25-50%) are observed from 0° to 60° of latitude. The scintillation index is defined as follows:

$$\text{Scintillation Index} = (S_{max} - S_{min})/(S_{max} + S_{min})$$
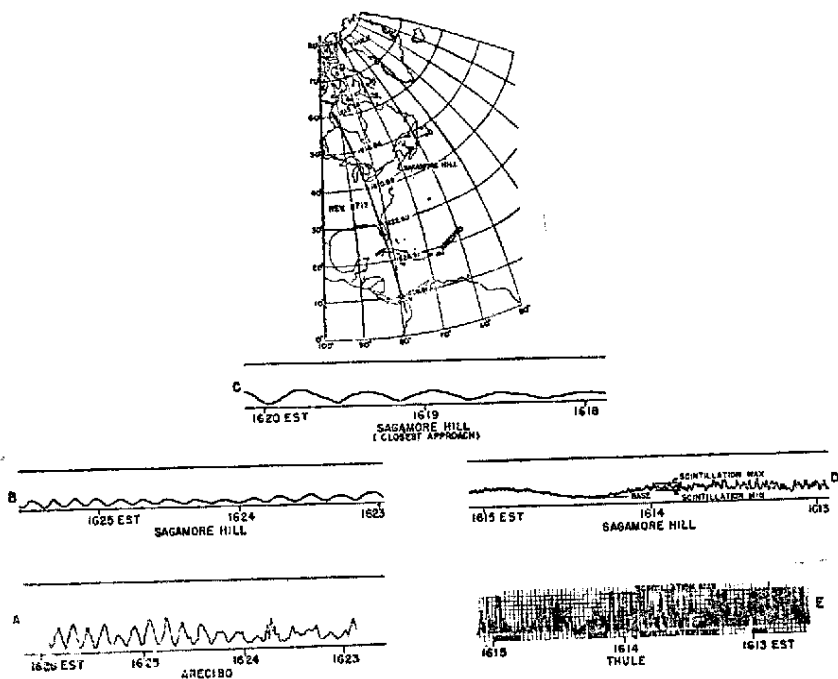
SiMULTANEOUS OBSERVATIONS OF S 66 ON APRIL 25, 1965 ON 41 Mc
FROM ARECIBO - SAGAMORE HILL AND SAGAMORE HILL - THULE.
AN "OVERHEAD" PASS AT SAGAMORE HILL IS INCLUDED.

Fig. 1 — Map in the top show sub-satellite positions. Portions C, B and A (left side) show little or no scintillations. Graphs D and E on the right side for Sagamore Hill and Thule show indices of scintillation.
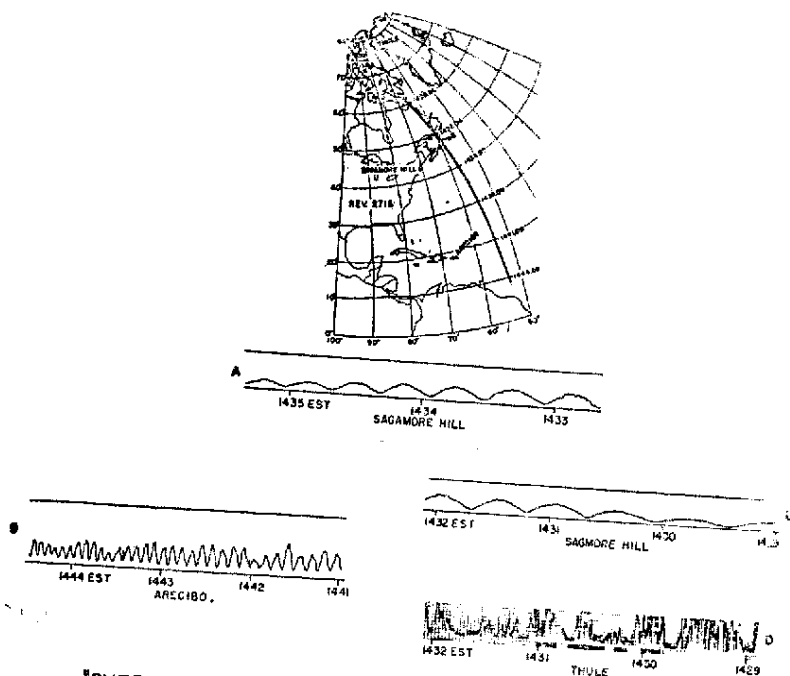
"OVERHEAD" RECORDS OF S 66 ON APRIL 25, 1965 (REV 2716) ON 41 Mc AT ARECIBO (A) AND SAGAMORE HILL (B). SIMULTANEOUS OBSERVATIONS AT SAGAMORE HILL (C) AND THULE (D)

Fig. 2 — Shows a similar pattern to Fig. 1 but with scintillations observed farther to the north.
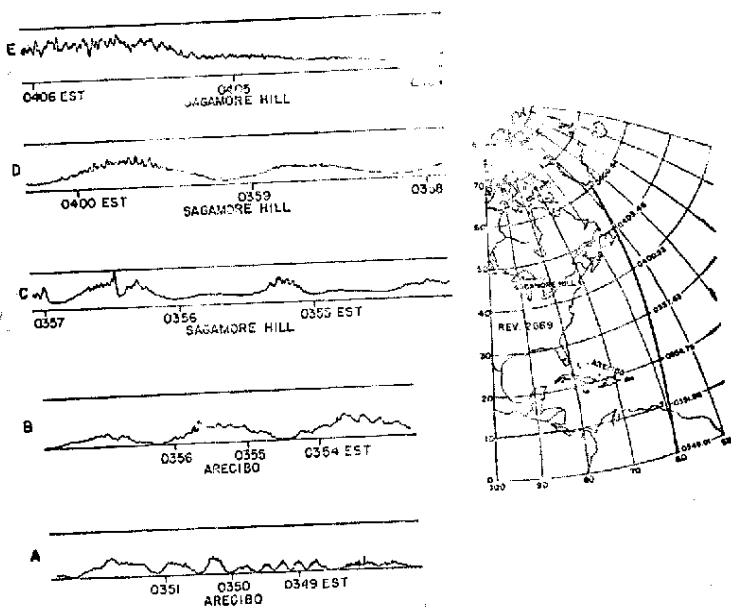
MEDIUM LEVEL SCINTILLATIONS NOTED ON REV. 2669 ON APRIL 22, 1965 (S 66) ON 40 & 41 Mc. AT 41 Mc MEDIUM LEVEL SCINTILLATIONS ARE GENERALLY NOTED DURING THIS TIME PERIOD

Fig. 3 — Scintillations observed from 0° to 60° latitude.

If the signal reaches base level as (shown in Fig. 1E) then 100% scintillation index is noted.

The latitude structure that is revealed for these time periods during geomagnetically quiet days is as follows:

The daytime scintillation structure is for scintillations of the "curtain" variety (involving a boundary near the auroral zone) to be absent during the day at low and middle latitudes but to be present at

auroral latitudes. During the post midnight hours when both a low gradient of critical frequencies and low critical frequencies exist over a long range of low to middle latitudes an irregularity structure is observed over a wide range of latitudes. For the period studied and for the latitudes observed the amplitude of the index was constant. The southern range extended to the geographical equator; however adequate statistical results are not available for the very low geographical latitudes.

SATELLITE SCINTILLATION OBSERVATIONS DURING LOCAL SUMMER AT LOW SOUTH GEOMAGNETIC LATITUDES

by

S. M. Radicella and A. H. C. de Ragone

Universidad Nacional de Tucumán, Argentina

Records, in a total of 200, taken at Tucuman (26.9° S, 64.5° W) during local summer, of the 40 MHz signals of the satellite Explorer XXII (S-66) have been analyzed in order to provide elements for studies of occurrence and importance of scintillation at low latitudes. A well defined diurnal variation, with the largest scintillation activity around local midnight was observed, as found by other investigators. Very few cases of scintillation were observed (Fig. 1) at noon hours.

DIURNAL VARIATION OF SCINTILLATION OCCURRENCE AT 40 MHz (S-66 SATELLITE) TUCUMAN LOCAL SUMMER, 1964-1965.
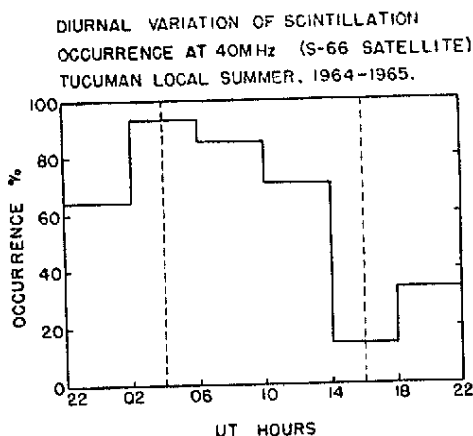
Fig. 1

In order to study the latitudinal variation, 29 transits of the satellite were analyzed in detail for the interval of time from 2200 to 0200 LMT, avoiding in this way the diurnal variation of the latitudinal behavior. A strong increase of the occurrence of scintillation appears

north of the observing site while to the south the occurrence remains constant (Fig. 2). At the limits of the latitude interval under consideration it is observed that the occurrence of scintillation activity is greatly decreased. The same data has been analyzed excluding satellite passages with elevation angles smaller than 20°, however no important differences have been obtained in the results with this procedure (Fig. 3).
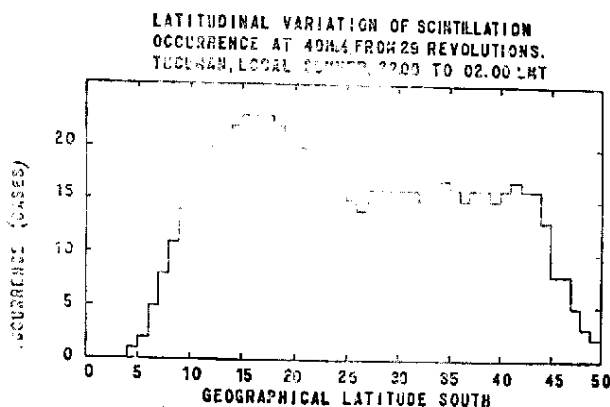
Fig. 2
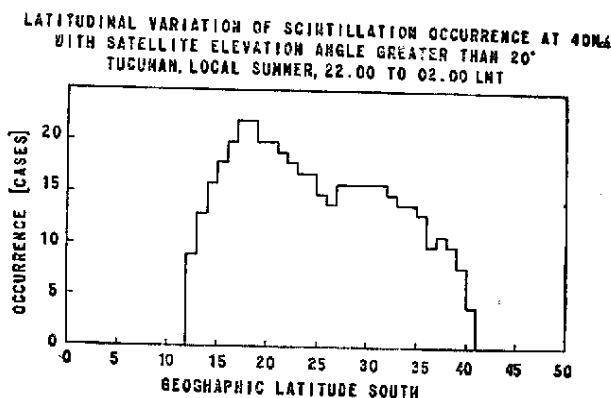
Fig. 3

In the analysis of scintillation reported herein, two indices have been defined considering separately the relative amplitude and the rate of fading of the scintillation (Fig. 4). The occurrence of scintillation for the different values of the two indices for all elevation angles has

been studied. The most important observation that can be made is the fact that during the interval of time under consideration, both amplitude and fading rate of scintillation are predominantely high (Fig. 5 and 6). No evidence of any longitudinal variation has been found.

A=3   R=3

A=2, R=2
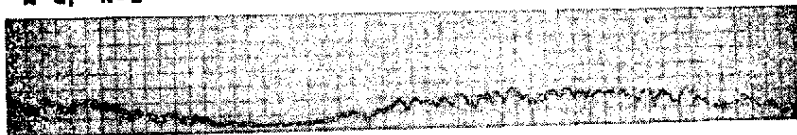
A=1, R=1
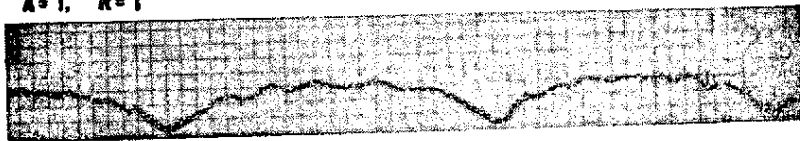
NO SCINTILLATION
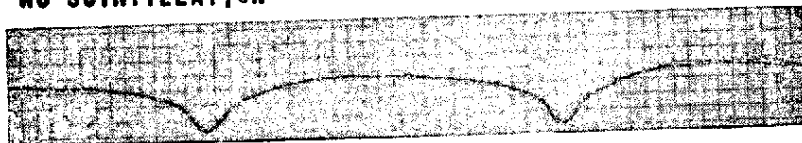
TUCUMAN 22.00-02.00 LMT

Fig. 4 — A display of scintillations on the signals of S-66 showing the indices for amplitude (A) and fading rate (R).
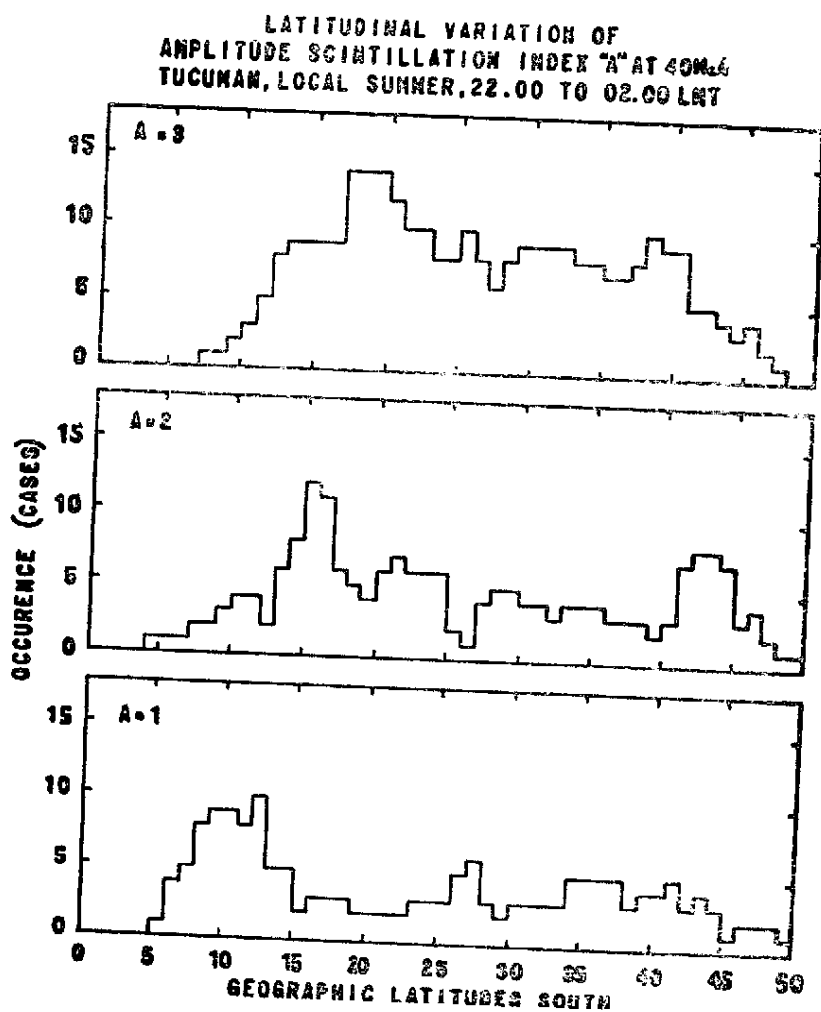
Fig. 5 — Amplitude index A variation.

LATITUDINAL VARIATION OF
RATE SCINTILLATION INDEX "R" AT 40 H c/s
TUCUMAN LOCAL SUMMER, 22.00 TO 02.00 LMT.
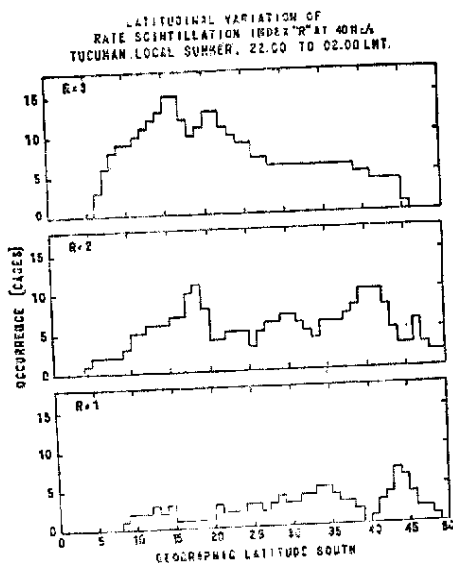
Fig. 6 — Rate of fading index R variation.

The observed latitudinal variation can be explained by an increase of scintillation activity towards the equator and a decrease of activity (both to the north and to the south of the station) due do the decrease of the value of the angle between the direction of the wave propagation and the direction of the magnetic field line, as suggested by Mawdsley.

IONOSPHERIC STUDIES USING THE TRACKING BEAGON ON THE "EARLY BIRD" SYNCHRONOUS SATELLITE

by

J. R. Koster

University of Ghana, Legon, Accra, Ghana

Continuous recordings were made of the 136 MHz signal from "Early Bird" for a period of 81 days between 24 May and 12 August 1965 at Accra, Ghana. Yagi antennas were used and the signal amplitude was recorded. These recordings were used to study scintillation occurrence (Figs. 1 and 2).
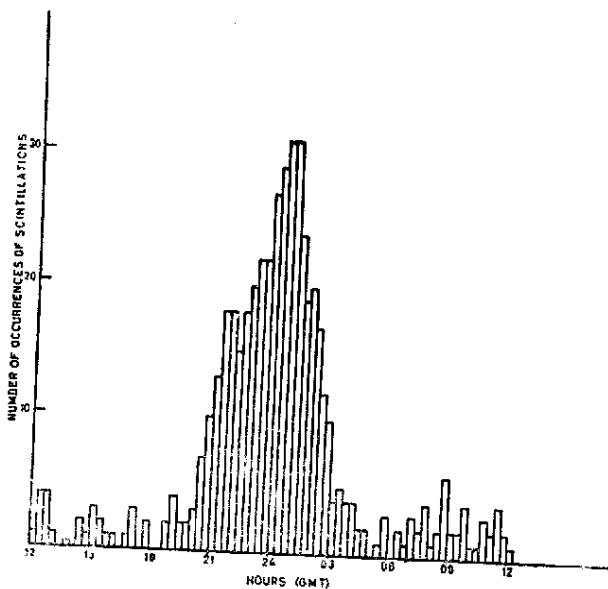
Fig. 1 — Number of occurrence of scintillation in each twenty-minute interval of the day during the 81 days of the observations.
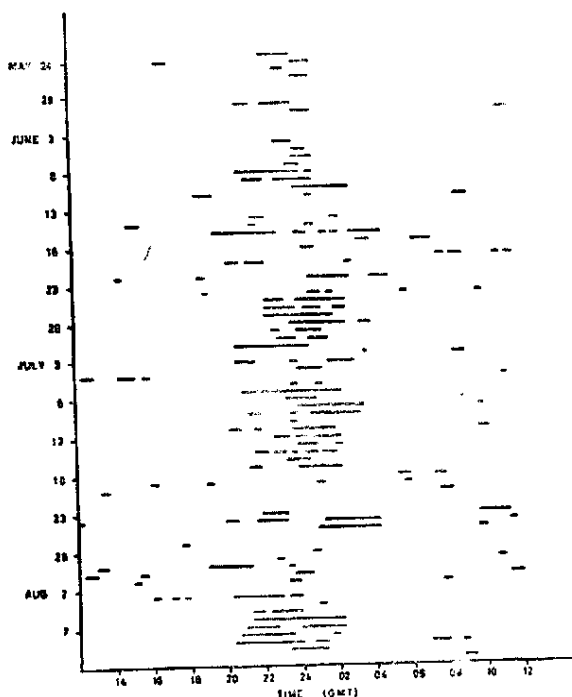
Fig. 2 — Time and duration of all occurrences of scintillation during the 81 day observing period.

The results confirm previous finding of the diurnal variation of scintillation, with a pronounced peak at midnight. The average time of scintillation was less than 30 minutes during daytime versus 95 minutes at nighttime. Amplitudes of scintillation were also smaller during the day. With respect to polarization it was noted that the, correlation between signals received on crossed antenass was not significantly less than that received on parallel ones. The amplitude of scintillations was found to have nearly a Raleigh distribution. The size of the irregularities was such that the mean E-W size of the pattern on the ground was 232 meters, the axial ratio of the correlation ellipse was found to be 60 to 1. The value of the eccentricity of the ellipse was

determined utilizing a 21 km baseline and was found to be 0.99986 ± 0.00030. Mean velocity over the ground was 78 m/sec towards the east. (See Figs. 3 and 4).
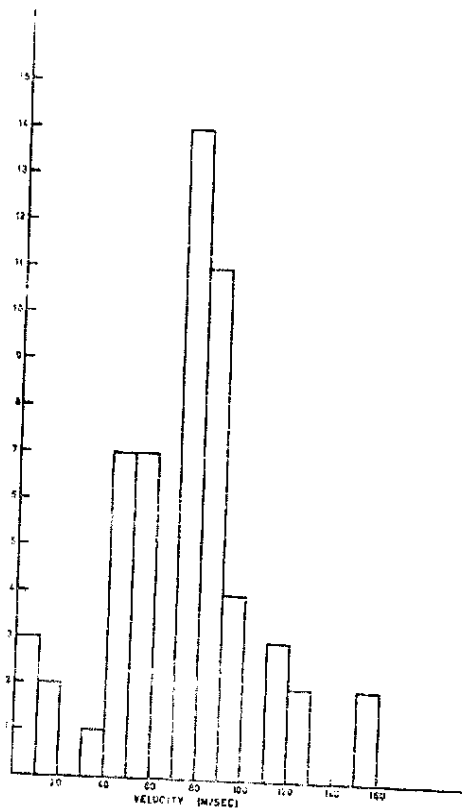
Fig. 3 — The E-W velocity distribution for the 62 records analyzed.
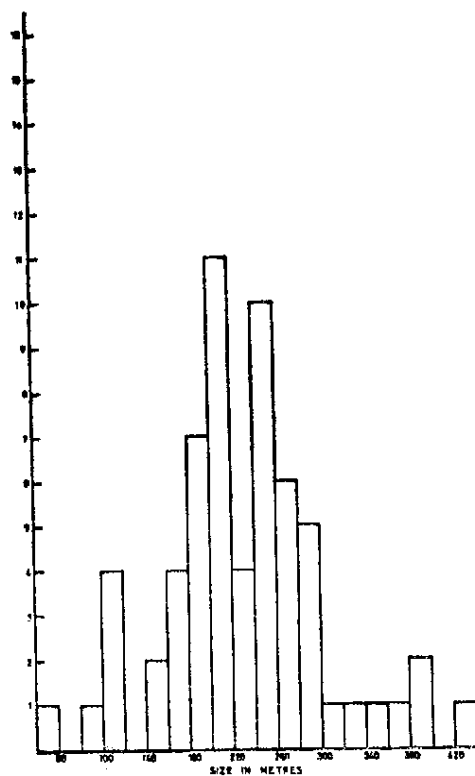
Fig. 4 — The distribution of size of irregularities found from the full correlation analysis of 62 records.

By monitoring the Faraday polarization rotation of the electric field vector of the carrier beacon, one can measure continuously the total electron content between the satellite and the observer. A total daily rotation of about 70° ocurred. (See Fig. 5).
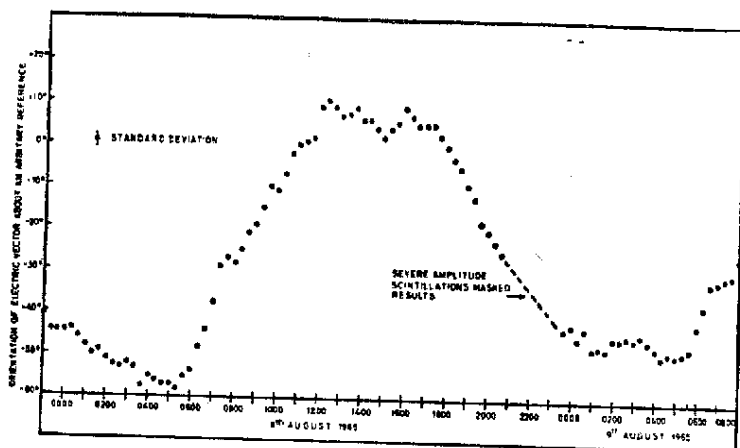
Fig. 5 — A plot of the Faraday rotation of the electric field vector as a function of time for a period of 32 hours.

SOME FEATURES OF EQUATORIAL SPREAD-F AT LA PAZ

by

G. R. Mejia

Laboratório de Física Cósmica

Universidad Mayor de San Andres

La Paz — Bolivia

The phenomenon of Spread-F near the geomagnetic equator shows two basic configurations known as (a) Equatorial type or frequency spreading component and (b) Temperate Latitude type or range spreading component.

Data from five stations about the geomagnetic equator in the American zone have been used. Monthly means of the percentage of occurrence of Spread-F for both types were calculated. A solar control effect in the occurrence appears to exist. Simultaneous percentages of incidence of Spread-F and nighttime Sporadic E are studied and the sudden disappearance of the Es at 18-19 hours period seems to have some correlation with the onset of Spread-F.

The frequency of occurrence of Spread-F is shown to be more prevalent at sunspot minimum that at sunspot maximum at La Paz. The geomagnetic activity is clearly shown in both types of Spread-F at La Paz and Huancayo.

The results are described in the captions of the following five figures.
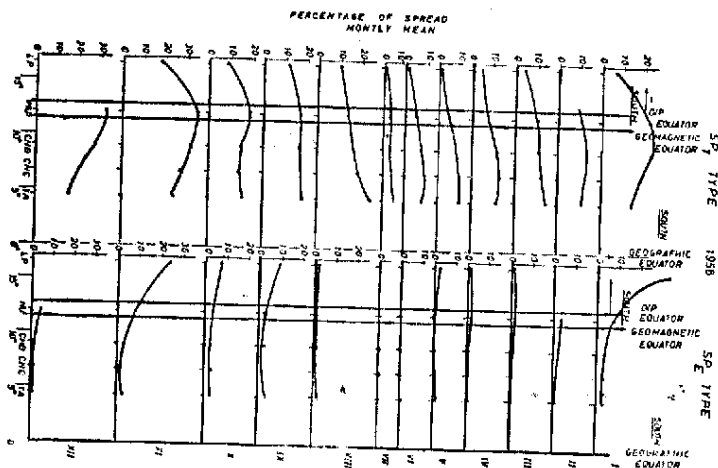
Fig. 1 — The 1958 year monthly mean for the frequency spreading
(SP$_E$) and range spreading (SP$_T$) components are plotted
from data of five stations located near the Geomagnetic
Equator. Their coordinates are shown in Table I. It is easy
to deduce from it that the monthly mean maximum in both
components shows some type of solar control in its latitude
variation.

TABLE 1

Station	Symbol	GEOGRAPHIC		GEOMAGNETIC		
		Lat.	Long.	Lat.	Long.	Dip
La Paz	LP	16°32'S	68°03'W	05. 0 S	000. 9°	−05°
Huancayo	HU	12°03'S	75°20'W	00. 6" S	358. 8°	02"
Chimbote	CHB	09°04'S	78°35'W	02. 2" N	350. 4°	06°
Chiclayo	CHC	06°48'S	79°49'W	04. 4" N	349. 2°	10°
Talara	TA	04°34'S	81°15'W	06. 6" N	347. 7°	13°
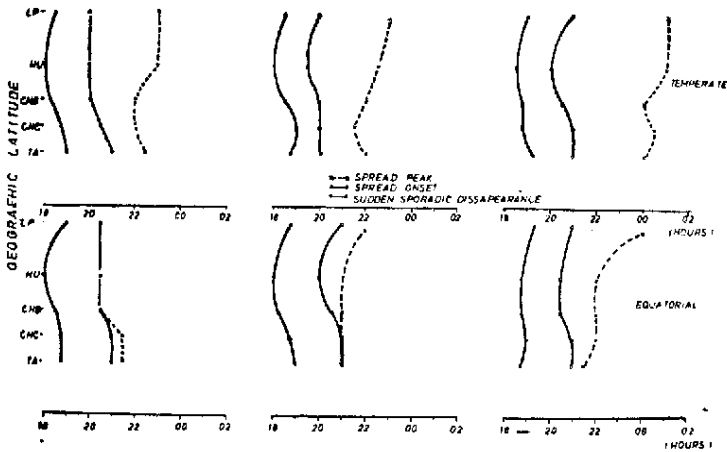
Fig. 2 — The curves with filled circles represent the maximum in the sudden Sporadic E disappearance time distribution, the curves with open circles represent the onset time in Spread-F; and the dashed curves represent the maximum spread time along the stations. There seems to be a positive time correlation between the Es disappearance and the onset of the spread, quite similar to the one between the increase on the height of F layer and the onset of the spread-F, because in both cases there are about two hours delay times.
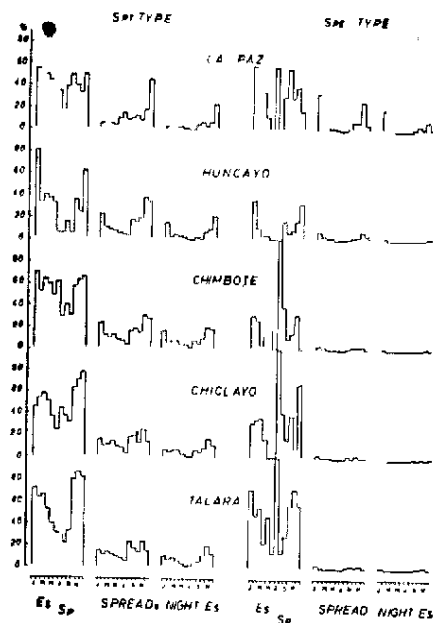
Fig. 3 — Monthly mean histograms showing spread-F, simultaneous Es occurrence and Es to SP relation. Huancayo has lower percentage in the Es/SP relation in both components of the spread. The higher percentage reached during the month of July and for the SP_E type is due to the fact that there were a few cases of spread (half an hour cases) and all of them had simultaneous Es occurrence.
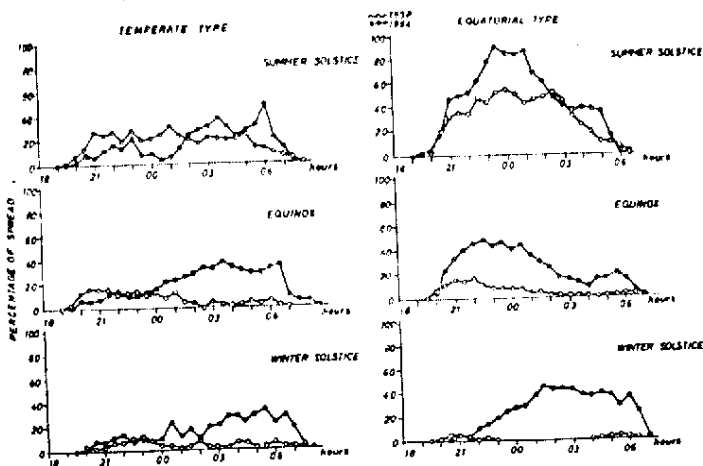
Fig. 4 — Solstice and Equinox percentages in incidence of Spread-F during 1958, maximum solar activity, and 1964, minimum solar activity. The SP_T diurnal variation shows a greater percentage of occurrence for the early hours of the morning during 1964 and during the last hours of the night during 1958. For the SP_E type this is not shown. Also a higher decrease in percentage occurs during the high than in the low solar activity years.
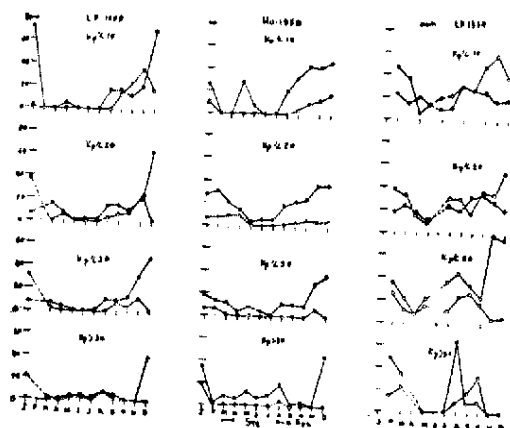
Fig. 5 — The percentage in the incidence of Spread-F is plotted for different values of Kp (Geomagnetic index) for La Paz and Huancayo (1958) and La Paz (1964). The magnetic negative effect on the spread occurrence is clearly shown in both types. Dots corresponds to the range spreading component and circles to the frequency spreading component.

NOTE: a) The Solstice and equinox periods are taken in the following way:

Summer Solstice: Nov., Dec., Jan. and Feb.

Winter Solstice : May, Jun., Jul. and Aug.

Equinox   : Mar., Apr., Sept. and Oct.

b) The f plot representation was used. On it the SP_T and SP_E configurations are represented with a dashed and full line respectively parallels to the frequency axis.

c) The percentage in the occurrence of the components of spread-F is calculated dividing the number of hour cases and half an hour cases with SP_T or SP_E to the total number of hour and half an hour cases.

EQUATORIAL SPREAD-F AT IBADAN

by

Arthur J. Lyon

University of Ibadan, Nigeria

Solar-cycle Variation

Figure 1 shows the variation with sunspot number of F, the occurrence frequency of equatorial spread-F at Ibadan. F represents the percentage of occurrences of intense spread-F showing no signs of group retardation between 1900 hours and 6000 inclusive. The data are annual means from 1959 to 1964, and show a steady decrease from about 50% at sunspot maximum to about 30% at sunspot minimum.

Fig. 1 (a) — Variation of spread-F occurrence frequency, F, with sunspot number.
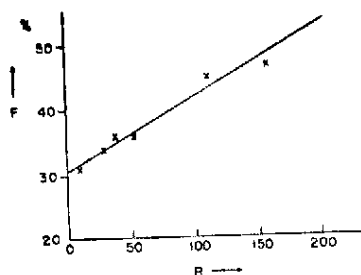
(b) — Diurnal variation of F in summer at sunspot maximum, F is the percentage occurrence of intense equatorial spread-F between 19h and 06h inclusive.
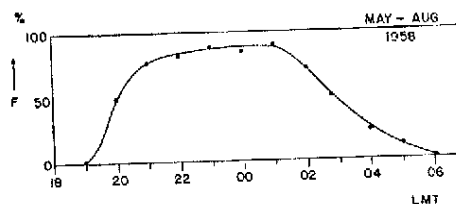
Annual Variation

Figure 2 shows the variation of F through the year, averaged from 1952-64, and also that of midnight h'F. Both show a marked increase in local summer.
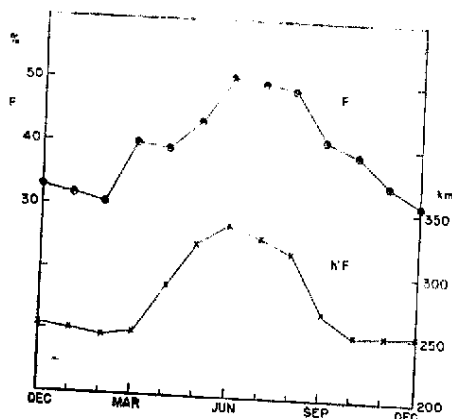
Fig. 2 — Annual variations (a) of spread-F occurrence frequency, F, throughout the night and (b) of midnight h'F.

Estimation of Electron Density

Because of the high incidence of intense equatorial spread-F, when no critical frequency can be measured, the practice has been adopted as Ibadan, since 1958, of scaling a top frequency less half the gyrofrequency (0.4 MHz at Ibadan) in a manner similar to that used for foEs. These measurements have been qualified by the letters QF, and have been included in the monthly medians tabulated in Ibadan bulletins.

This procedure has been adopted in the belief that the top frequency gives at least an approximate indication of the critical frequency of the underlying ionization. Figure 3 suggests a tentative justification of this belief. Many cases occur where one or two hours have intense equatorial spread-F while the adjacent hour on either side do not. It is then possible to compare interpolated values of critical frequency with the QF values. The figure shows a mass plot of "QF" values against

corresponding "INT" (interpolated) values. The points lie about equally on either side of the line drawn at 45° to the axes. This suggests that QF values correspond roughly, on the average, to the unobservable critical frequency. In individual cases however the difference may be quite large, and reliance cannot be placed on individual "QF" values.
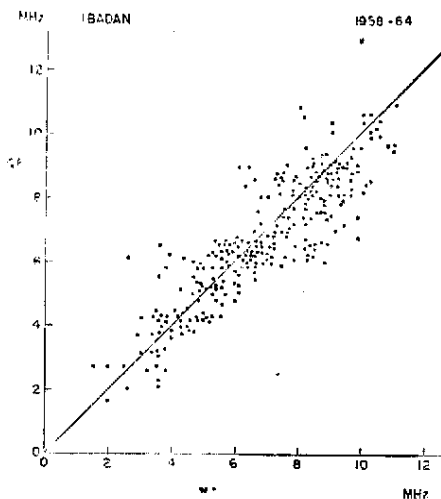
Fig. 3 — A mass plot of top frequency of spread-F (ordinary wave, denoted by symbol QF) against corresponding interpolated values (denoted by "INT").

CORRELATION OF SPREAD-F AND MAGNETIC ACTIVITY
AT NAIROBI

by

R. F. Kelleher

University College Nairobi, Kenya

The occurrence of spread-F at Nairobi has been calculated for the International Quiet and Disturbed days during the period March 1964-February 1965. The simple expedient was adopted of counting the number of times foF2 reading in the ionogram reduction sheets is qualified by F, JF, UF, or is entirely replaced by F. No distinction has been attempted between types of spreading.

Fig. 1 shows the results for the whole year. The occurrence is slightly higher on disturbed days. The seasonal variations (Figs. 2-5) show that the periods before and after midnight behave in opposite sense with respect to magnetic activity. The maximum occurrence of spread-F is in June, and the minimum is in December.
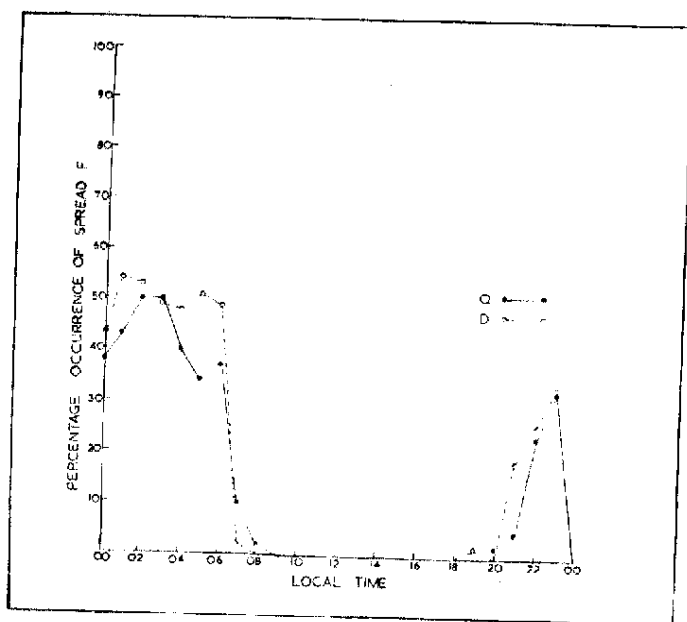
Fig. 1 — Percentage of occurrence of spread-F versus local time for quiet and disturbed days for the whole year.
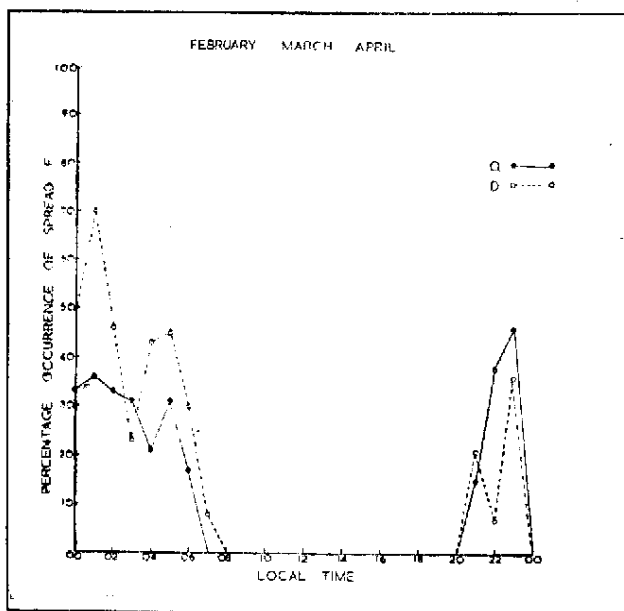
Fig. 2 — Same as Fig. 1 for Feb., Mar. and Apr.
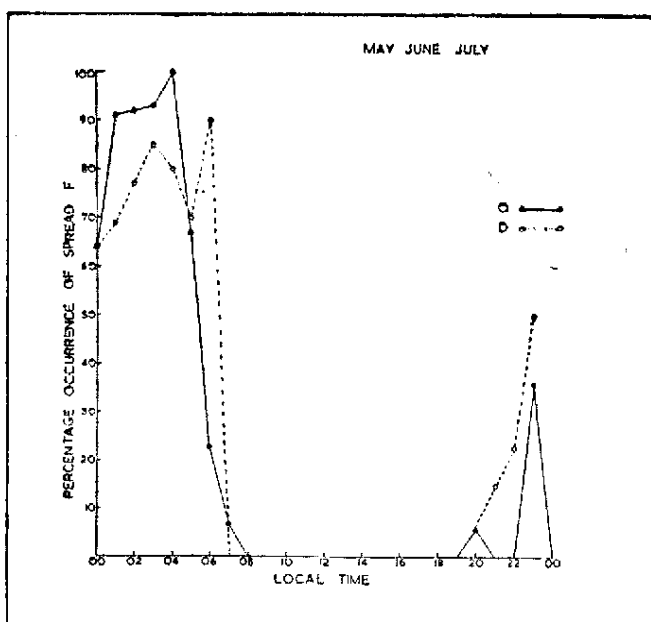
Fig. 3 — Same as Fig. 1 for May, Jun. and Jul.
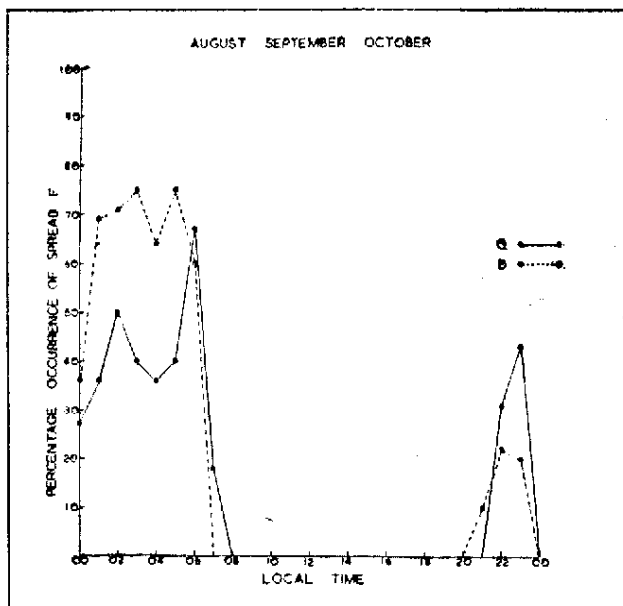
Fig. 4 — Same as Fig. 1 for Aug., Sep. and Oct.
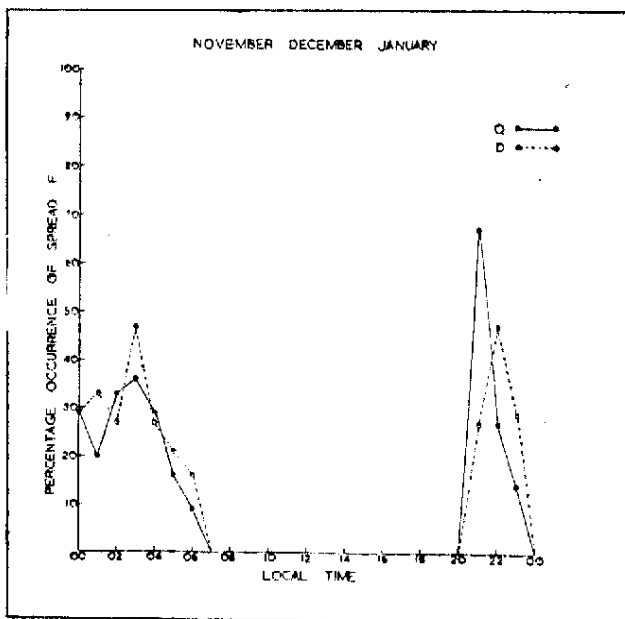
Fig. 5 — Same as Fig. 1 for Nov., Dec. and Jan.

THE SIZE OF LOW LATITUDE IONOSPHERIC IRREGULARITIES

AS DETERMINED BY THE ANGULAR DIAMETER OF

DISCRETE SOURCES

by

Jules Aarons and Donald Guidice

Air Force Cambridge Research Laboratories

Bedford, Mass., U.S.A.

Several methods have been used to measure the size of the irregularities producing ionospheric scintillation. The most frequently used technique is to measure the size of the shadow pattern on the ground by spaced receivers using radio stars or satellites as the sources of radio frequency energy.

Another technique is to utilize the angular diameter of the discrete sources to determine irregularity size. A large angular diameter source does not scintillate; a small source does. The phenomenon is directly analogous to the optical portion of the spectrum where stars scintillate but planets do not.

Using the 1000 foot diameter spherical antenna at Arecibo, Puerto Rico (19° N, Magnetic Latitude 32° N) we have taken drifts and "cuts" (in declination and in right ascension) of sources varying in angular diameter from less than 1' to greater than 29'. All observations were done in the time period 2200-0500. Eight sources were observed with angular diameters less than 5'; one source, 3C157, had an angular diameter 29' while another source 3C392 had a diameter of 16'.

Figure 1 shows the source 3C123, whose diameter was less than 1', scintillating at the four observed frequencies 22.3 MHz, 26.7 MHz, 33.45 MHz and 38.75 MHz. Scintillations are correlated at all four frequencies leading to the conclusion that weak scattering was taking place throughout the spectrum observed. Figure 2 (3C157) shows no scintillations during the scan across the 29' extended source.
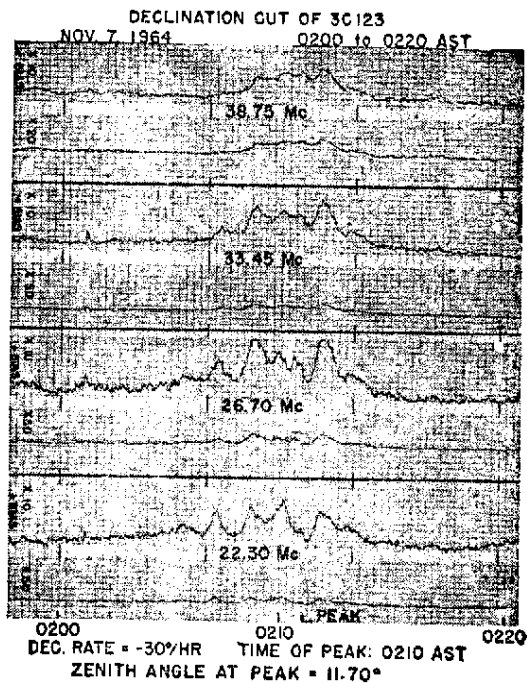
Fig. 1 — Declination scan of 3C123, a source of narrow angular diameter (1'). Scintillations of long period (30 seconds - 1 minute) are well correlated indicating weak scattering.
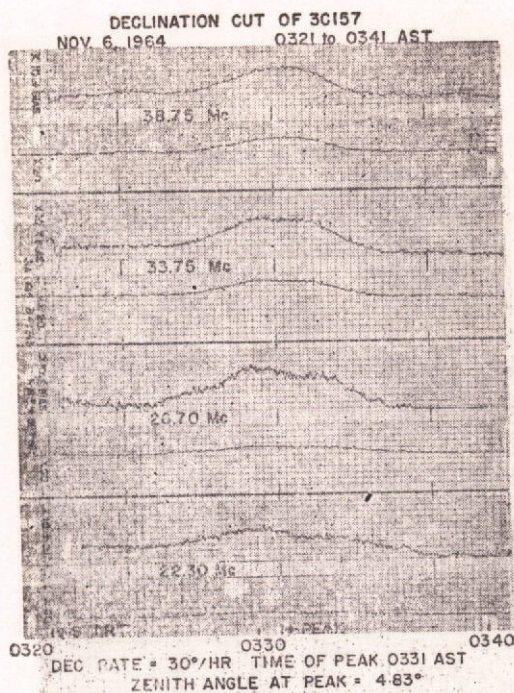
Fig. 2 — No scintillations are observed in these recordings of the extended source 3C157 (29').

Since it is possible to have irregularities in the distribution of irregularities from day to day, we have compared two records taken consecutively, 3C353 a source of 4' diameter (Figure 3) and 3C392, an extended source of 16' angular diameter (Figure 4); the former scintillates and the latter does not.
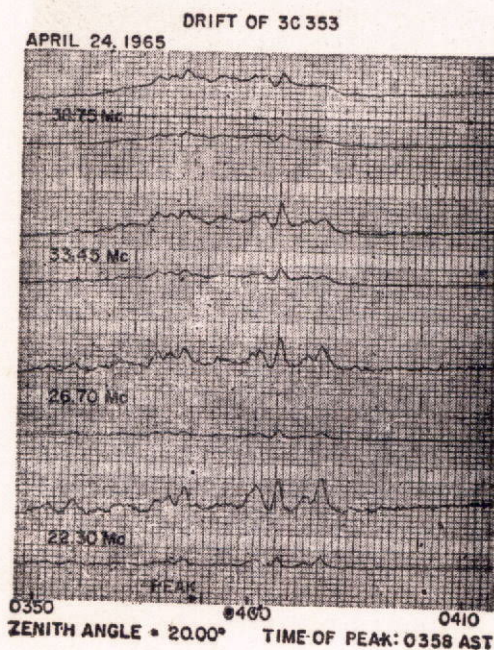
Fig. 3 — Scintillations of 3C353 (4') are shown in this drift taken immediately before the drift of Fig. 4.
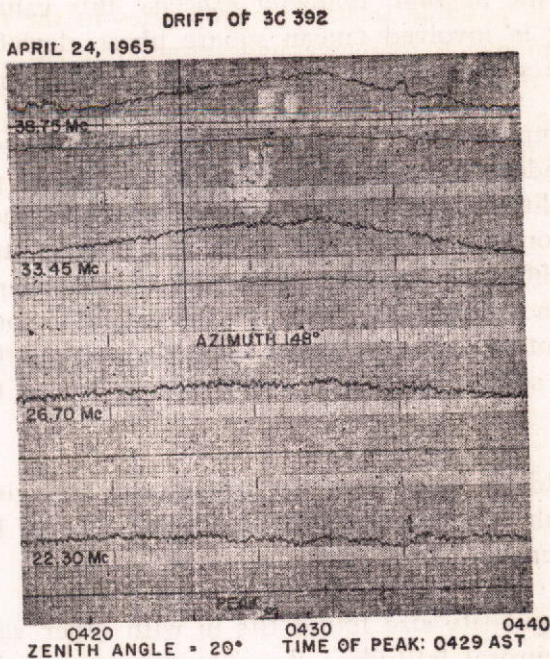
Fig. 4 — No scintillations have been noted in this extended source of 16' (3C392). This is the smallest source which failed to produce scintillations in the study.

If one tabulates the angular diameter of sources in the Cambridge University 3C catalogue, source sizes show a gap between 4'-5' and 6'; no detectable sources between these diameters were available at Arecibo for our sensitivity in this frequency range.

If 10'-12' is used as the angular diameter of a radio star source where scintillations index shows a decrease to 1/e of its value, and if 400 km is used as the height of the scintillation layer, then we get 1 km for the size of the irregularity using the terminology of Hewish.

The irregularity size is found from the formula $\theta = L/Z$, where θ is the angular diameter measured in radians, L is the size of the irregularity and Z is the distance to the irregularity.

When the angular diameter exceeds this value and if only weak scattering is involved (mean square phase deviations less than one radian) the source will show decreased scintillations.

In a simple manner one can consider portions of the extended source acting independently, each producing a shadow pattern on the ground. The addition of the shadow patterns wipes out the scintillations. The scattering concept of Lawrence, Little and Chivers states that when the phase path difference between the length of the generator of one of the scattered cones (from one "end" of the extended source) and that included by the other cone (measured along the same path) exceeds one radian then the source scintillations will fall to 1/e of the value of a point source.

It should be noted that the irregularity size given is for the nighttime ionosphere at the latitude of Arecibo, Puerto Rico, and it is the shorter dimension.

The irregularity size found fits in with other values found in middle and subauroral latitudes; the sizes may very well be different from the "cloud" type of scintillations seen during the day in short patches.

SOME CHARACTERISTICS OF IONOSPHERIC IRREGULARITIES

AT IBADAN

by

R. W. Morriss and A. J. Lyon

University of Ibadan, Ibadan, Nigeria

From the analysis of ionospheric drift data the mean axial ratio of the irregularities, their orientation and the parameter V_c can also be obtained. The following are preliminary results on these parameters from work still in progress.

Axial ratios appear to be somewhat greater at sunspot maximum than at sunspot minimum, greater by day than by night, and greater in the F layer. The following table gives values derived from the data analysed so far.

Table I

Axial Ratios at Ibadan

	sunspot minimum		sunspot maximum
	Day	Night	
E-region	4.6	2.6	5.6
F-region	4.9	3.7	6.9

The orientation of the irregularities is predominantly towards magnetic north with a standard deviation of order of $\pm 10°$. The values of the ratio V_c/V are very variable but the average value is about 0.7, rather similar to that observed at sunspot maximum.

All these results are still being studied and they should be treated with caution.

THE PROCESSES OF STIMULATED EMISSION AS POSSIBLE

ORIGIN OF IONOSPHERIC IRREGULARITIES

by

G. Tisnado

Instituto Geofisico del Peru

(abstract not available)

.

SUMMARY OF THE SESSION

by

J. R. Koster

University of Ghana, Legon, Accra, Ghana

The session on F region irregularities reflected the somewhat unsatisfactory state of our knowledge of this aspect of ionospheric behavior. It has been known for decades that radio waves reflected from the ionosphere show irregular fading, giving evidence of the presence of small irregularities in the electron density of the ionosphere at all times. A much more severe type of irregularity gives rise to the so called "spread-F" echoes observed on ionosondes, as well as violent radio star and satellite scintillations. These are known to be particularly severe at the equator. For a number of years more and more information has been accumulating on the spatial and temporal distribution of these irregularities, as well as their scattering properties, and the shape, size and velocity of the diffraction pattern which they produce on the ground. But we still do not have satisfactory explanation of why these irregularities exist at all in the F region of the ionosphere. The present session added still more material to the accumulation of experimental data mentioned above — but a satisfactory theory, as usual, was conspicuously absent. Hence it is my duty to summarize the new experimental data, and to bewail the continued absence of a theory.

Spatial Distribution of Irregularities

Most new information on spatial distribution came from the American zone. The Bolivian group studied the distribution of Spread-F echoes across the equator at five strategically located stations. Satellite scintillation results from Tucuman confirmed the existence of a relatively narrow belt of intense scattering near the equator, and a much wider distribution of lesser irregularities — the latter giving maximum scintillation when observed in a direction to the magnetic field lines. Evidence from the Air Force Cambridge group shows that these irregularities are distributed all the way to the polar regions.

Temporal Distribution

The evidence on the temporal distribution of F region irregularities largely confirmed what was already known, but added little hitherto unknown information to the total picture. The analysis of Nairobi ionograms indicated

that the latter is a typical middle-latitude station in this respect. From further analysis of South American and Nigerian data the already known difference in seasonal behavior between the American and African zones was confirmed.

Character of the Diffraction Pattern on the Ground

Here again a few new details were added to an already fairly clear picture. The intense irregularities are field-aligned, and measurements in Ghana using the "Early Bird" synchronous satellite show that the elongation of the diffraction pattern on the ground is 60 to 1 or more, and that the transverse size is of the order of a few hundred meters. Using radio stars of differing angular diameters, the Air Force Cambridge group deduced sizes of the order of one kilometer. Irregularities observed by reflection of HF waves have smaller elongations. Axial ratios of about 5 are reported at Ibadan, about 3 at Nairobi, and about 8 at Tamale. There is some evidence from Nigeria of moderate variations in size with time of day and sunspot cycle, but the changes are moderate, and there is some doubt about their significance.

Satellite Observations of Ionospheric Ducts

One of the new contributions to this field was the announcement of observations of ducts capable of directing radio waves along field lines in the ionosphere. Sizes are found to be of the order of 2 km by 10^4 km, and electron density variations of the order of 3 to 8% occur, but it is yet unknown whether these are enhancements or reductions in electron content relative to the ambient medium. The information presented came from the analysis of only one month's data, and it seems certain that further new and interesting information will be forthcoming.

Theoretical Considerations

Only one theoretical paper was given in the session — an attempt to explain the origin of these intense irregularities by a process of stimulated emission. Discussion indicated, however, that the mechanism falls short by several orders of magnitude. So we are left with our mounting volume of experimental information and the complete lack of a unifying theory to explain the observations and guide further experimentation. We invite the plasma physicists to devote themselves to this problem as a matter of urgency during the coming years, so that some order may emerge from the experimental chaos.

VI — IONOSPHERIC DRIFTS

VI — IONOSPHERIC DRIFTS

(Discussion leader: Robert Cohen)

Review Paper

by

G. S. Kent

University of the West Indies, Jamaica

Abstract

A brief account is given of the various techniques which are used in ionospheric drift measurements, and their limitations, together with an outline of the methods of analysis. A survey is then given of the experimental results for the F-region, discussing the world-wide distribution and behavior of the harmonic components of the drift. These results are interpreted in terms of the commonly accepted theories and some special problems of interest, which occur in the equatorial regions, are described. A similar survey is given for the D and E-regions, emphasising the lack of data in the equatorial region and the need for more varied experimental techniques.

Introduction

Any survey of ionospheric drifts has to contend with three problems. These are:

The scarcity of observing stations,

The multiplicity of observing techniques, and

The complexity of the data obtained.

Let us consider these in the order shown.

Viewed on a world-wide scale, there are in fact a large number of stations which have made measurements on ionospheric drifts. When one considers, however, a small latitude belt this number is drastically reduced. In the present case there a.e only two stations, within 20° of the magnetic equator, which have made sufficient routine measurements for anything like a complete drifts picture to be obtained. These are Ibadan and Waltair, with magnetic latitudes of 3°S and 10°N respectively. Inside this belt there are, in addition, several other stations, such as Singapore (Magnetic latitude 10°S), Accra (Magnetic latitude 5°S) and Huancayo (Magnetic latitude 1°S) which have considerably added to our picture of the drift system. However the additional information gained in this may has almost as often revealed where are gaps in our knowledge as it has helped fill in those gaps. Outside the belt there are many more stations, and the results from these will be discussed later when we consider the world-wide pattern of drifts.

Table I

Principal methods of measuring ionospheric drifts

Method of Observation	Region Observed	Phenomenon Observed
Meteor trail	85-100 km.	Neutral air movements
Luminescent trail from rocket	80-150 km.	Neutral air movements
Mitra spaced receiver	100-130 and 160-350 km.	Small ionospheric irregularities
Radio star scintillation	F-region	Individual irregularities
Backscatter and Doppler shift	Sporadic-E and F-region	Larger irregularities and patches of irregularities
Spaced ionosondes	Sporadic-E and F-region	Patches of irregularities and travelling disturbances.

A list of observing techniques is shown in Table I., together with the ionosphere regions and the probable media which they observe. The main problem in combining results obtained by different methods is to know how justified one is in assuming that they are observing the same phenomena. There is the obvious distinction between measurements made on the neutral atmosphere and those on ionization. In the F region the movements usually observed are in, and probably mainly controlled by, the ionized constituent. The influence of the neutral air on this motion is probably slight although still under debate. In the E region the collision frequency is sufficiently high for

the neutral air molecules to set in motion the ionized particles. The motions of the neutral and ionized particles are therefore strongly correlated, though not necessarily the same. There is the less obvious problem of what a measurement of an irregularity in electron density actually mean in terms of the movement of the plasma. We have to consider the possibility that the velocity of the irregularity may be different from that of the plasma and even that it may simply be a wave motion inside the medium. As we shall see, this is quite often likely to be the case.

Most of the measurements so far made at the equator have been on the ionized constituent, and there is a very definite need for observations to be made using meteors and rockets. In this survey, we shall consider some of the results obtained in other latitudes by these methods, as they show some of the limitations of the radio methods and, in particular, indicate that the E region has a much more complicated wind structure than was formarly thought.

The third difficulty in a drifts survey is to interpret the results. The majority of drift measurements have been made using the Mitra (1949) three antenna technique. The full analysis of the records obtained may be made using the Briggs, Phillips and Shinn (1950) method and its refinements (Phillips and Spencer, 1955). This analysis is tedious and slow and, when large quantities of data have been reduced, various approximations have been used, which may not always give accurate results. Apart from the difficulties of reduction there is the problem of the interpretation of the results obtained. The most common way is to divide them into North-South and East-West components and then to Fourier analyse these into steady drifts and harmonic components with periods of 24, 12, 8 hours etc. Polar plots of the variation of these with time of day and season may then be drawn. Results obtained in this way seem subject to a great deal of variability due both to sampling fluctuation and to the different observational techniques and reduction methods. In addition, in order to be able to present results analysed in this way, a very complete experimental program has to be carried out. Very often this is limited by the physical phenomenon itself. For example, measurement of the drift velocity of equatorial Spread-F may only be carried out at night, making it impossible to calculate harmonic components. A further problem in the interpretation of the results arises when one tries to fix the height to which any set of drift measurements refer. Usually this is taken as the actual height of reflection. This is probably an over simplification of the problem; it is believed that the fading is imposed on the wave just below the height of reflection (Ratcliffe 1959) and this is the justification for the normal assumption. The best scattering mechanism is still far from clear and the assumption should be treated with some reserve.

In this survey, we shall consider, first, drifts in the F- region. The experimental results for this appear more consistent and the interpretation

simpler than for the E-region. In addition, as far as equatorial stations are concerned, there are considerably more F-region than E-region results. We shall not consider, in detail, measurements made on the Sporadic-E layer as these are discussed in Section III of this Report.

F-Region Experimental Results And Theory

The world-wide picture — space antenna observations: Figure 1 shows a plot against latitude, of the relative importance of the first three harmonic components for F-region drifts (taken from Rao and Rao, 1962, 1963 and 1964; Purslow, 1958; Skinner, Wright and Lyon, 1962; Mitra, Vij and Dasgrupta, 1960; Shimazaki, 1960; Briggs, 1960). The results shown here are all based on observations made using the Mitra method, and the values for the steady, the 24 hour and the 12 hour components have been estimated in terms of their relative importance, expressed, rather simply, as a fraction of the total observed drift. Perhaps the most obvious characteristic is the variability of the values, showing that only the most general conclusions may be drawn. The following are the most outstanding:

a) Near the equator the drift is dominated by the 24 hour component.

b) Near 30° magnetic latitude north or south, the 24 hour component is very small and the steady component is dominant.

c) The importance of the semi-diurnal component increases with distance from the equator.

In Fig. 2 the steady and the diurnal drifts have been repplotted in terms of their north-south and east-west components. The first of these has been expressed as towards or away from the equator in order to include both northern and southern latitude stations. The semi-diurnal drift has not been replotted as there is little consistency to be found between results from different stations. The 24 hour component has been shown (Fig. 2) in terms of its peak amplitude and its direction at midnight. Again there is considerable scatter but some regularities emerge:

1) The steady component averages about 20 m/sec. Its direction is east and away from the equator in low latitude and west and towards the equator in high latitudes.

2) The 24 hour component has values approaching 100 m/sec at the equator. Its direction at midnight is towards the east and away from the equator at low latitudes. Considerable doubt however exists on its north-south behavior very close to the equator. Owing to the elongation of the drifting

irregularities, it has not been measured successfully at any station closer than about 10° of latitude. At the equator, one would by symmetry expect little or no north-south component; this makes the high values, observed at Waltair and Singapore, as shown in the fourth graph, rather difficult to understand. The latitude variation of the east-west component is very clear, it decreases to a minimum at about 30° north and beyond this its direction is reversed.
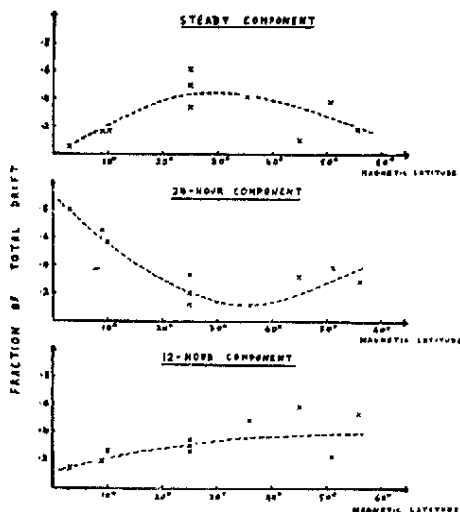
Fig I. Variation with latitude of the relative importance of the harmonic components of F-region drifts.

The semi-diurnal component has not been split into its north-south and east-west components. On the average however it is found that —

— At low latitudes: East-West component > North-South

— At high latitudes: East-West component < North-South

Values for the velocity vary between 5 and 50 meters per second. A further relationship, not shown in these figures, is the direction of rotation of the drift vector during the day. This varies with season but, in general, the rotation is clockwise in the northern hemisphere and anti-clockwise in the southern.

The theories which seek to explain the harmonically varying components of the movements are generally based on the idea, initially developed by Martyn (1955), that they are due to electrostatic fields in the dynamo region

below. These electric fields are produced by the currents in the E-region
and are communicated to the F-region along the highly conducting lines of
force. Maeda (1955, 1959, 1962) has estimated the electrostatic field for the
known dynamo currents and deduced the F-region drift pattern.   This pattern
for the horizontal component of the velocities is shown in Fig. 3. Various
features of this pattern agree well with the main experimental results:

— The variation at the equator is largely diurnal and is west by day
and east by night.

— The diurnal component decreases with distance from the equator,
then it reverses and increases again towards the poles.

— In mid-latitudes there is a strong semi-diurnal component.

— In mid-latitudes there is a strong north-south component of drift.

Beyond this the correspondence is not exact and certain differences appear. In
particular near the equator, the north-south component is expected to be low,
contrary to the experimental evidence.
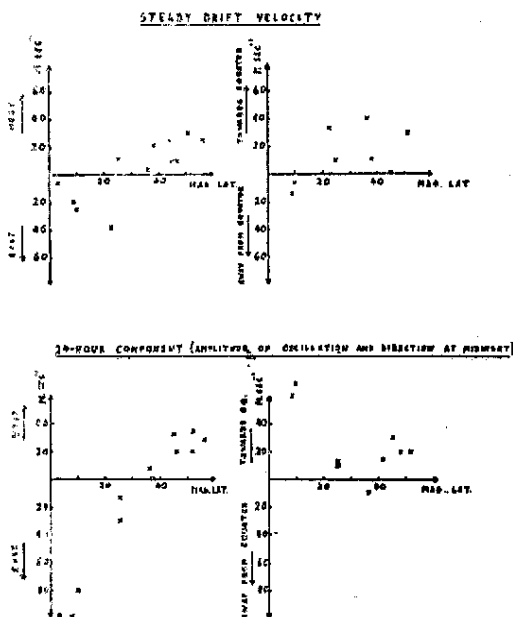
Fig 2.   Latitude variation of the
components of F-region drifts.
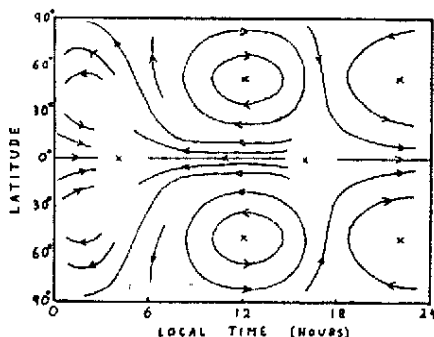
Fig 3.   World-wide pattern of
F-region drifts based on
the S$_q$ current system
(after Maeda, 1962).

The magnitudes of the velocities are not shown in Fig. 3. According to Maeda, these should be highest at the equator, where values of at least 100 m/sec would be expected. A minimum occurs at about 45° latitude and values increase again to about 50 m/sec at the poles. This general behavior is again substantially in agreement with experiment.

Other experimental results on F-region drift velocities: Two other important methods of studying F region drift velocities are by the use of radio-star scintillation and by the study of travelling ionospheric disturbances.

Radio star scintillation observations suffer from the disadvantage that the diffraction pattern on the ground is usually found to be highly elongated (Jones, 1960; Koster, 1963). This means that the measurement of the north-south component of drift is very uncertain and results are usually not to be trusted. Even in the East-West direction the results do not agree well with those obtained by the normal Mitra reflection technique. For example, at Jodrell Bank (Chivers, 1961) there is a steady westerly wind of about 75 meters per second, and in the auroral regions (Harang, 1963) very high values of the order of 500 meters per second are found. At the equator (Koster, 1963) the agreement is much better.   The difference is perhaps not surprising as the irregularities causing the scintillation occur at the same height or above those on which the ordinary Mitra drift measurements are made.   The nature and cause of the irregularities is still far from clear.

Travelling disturbances in the F-region appear on an ionogram as a split or a cusp on the h(f) record. By studying the motions of these cusps on spaced ionosondes, measurements have been made on the drift velocities of the disturbances, which are found to have dimensions of several thousand kilometers (Munro, 1958; Thomas, 1959; Heisler, 1962). The main characteristic of the motion is a strong north-south component of about 150 meters per second. The direction may vary with season, but in winter in either hemisphere is towards the equator. There is, in addition, a weaker velocity component in the east-west direction which changes diurnally. The north-south velocity is much higher than that obtained by the Mitr$_a$ method; Heisler has suggested that the observed motion is the combination of the movement of a perturbation originating near the winter pole and travelling towards the equator, and the mainly east-west movementes of the medium through which it is travelling. Observations of these perturbations in low latitudes are lacking and, in particular, it is not certain whether they actually cross the equator.

A wave structure is suggested for these disturbances by the fact that it is possible to measure both a phase and a group velocity for them (Heisler and Whitehead, 1961), the phase velocity being about half that of the group velocity quoted above. One explanation for these disturbances is in terms of gravity waves (Hines, 1960). These are atmospheric waves propagated in a similar way to a tidal oscillation. They have however shorter periods of the order of minutes or a few hours. They are probably generated close to the ground and travelling upwards, are responsible for much of the observed wind structure in the E-region. Those with pediods of the order of ten minutes are supposed to leak through the E-region into the F-region where they are observed as travelling disturbances. Certain difficulties lie in a comparison of the theoretical phase and group velocities with those observed experimentally. Heisler and Whitehead (1961) suggest that the disturbances observed experimentally may in fact be due to movements induced in the F-region, by the electric fields generated in the E-region by the gravity waves rather than by actual neutral air movements in the F-region.

Special Equatorial Problems and Results: — Here we shall discuss four problems of special interest in the equatorial region.

1) The east-west drifts very close to the magnetic equator: Martin (1955) suggested that near the magnetic equator the east-west drift velocity should have a value of the order of 200 meters per second. Measurements made at Ibadan (Skinner, Lyon and Wright 1962) and Waltair (Rao and Rao, 1963) do not give values as high as this. Osborne and Skinner using drift measurements made at Tamale (Magnetic Latitude 0.3°S) quote daytime apparent velocities as high as 250 meters per second. This implies a very rapid change in the drift velocity close to the magnetic equator. This result is an isolated one and even here a complete analysis has not been published. It is clearly an experiment which needs to be repeated to confirm or disprove these very high drift velocities.

2) The north-south component of drift in the equatorial belt: The behavior of the north-south component of velocity near the equator has been discussed before. On Martyn's theory and from considerations of symmetry, no north-south component would on the average be expected very close to the magnetic equator. Results from Waltair (Rao and Rao, 1963) and Singapore (Purslow, 1958) indicate a considerable component at a magnetic latitude of only 10°. Measurements on this have not been made at Ibadan (Magnetic Latitude 3°S) owing to the difficulties encoutered with the highly elongated ground diffraction pattern. It would seem that, with a large north-south antenna spacing, this problem could be overcome and some measurements made in order to explain this anomally. The elongation of the irregularities is itself of interest At Ibadan, the axis ratio of the ground pattern is found to be at least ten. At Waltair, this value has fallen to less then three, a surprisingly large change for only a ten degree shift in latitude.

3) Equatorial Spread-F and Scintillation Measurements: Some consistent measurements have been made on the movements of Spread-F (Calvert, Davies, Stiltner and Brown, 1962), and the irregularities responsible for radio star scintillation (Koster, 1963). These show eastward drift velocities decreasing during the night from about 120 meters per second at 2100 to 70 meters per second at 0600. Calvert et. al. have shown in addition that there is a strong dependence of the velocity on sunspot period. Perhaps the most curious feature of the irregularities is the extreme stability of the irregularities. Both scintillation and ordinary drifts measurements yield a parameter V_c which is a measure of the random velocity of movement. Koster obtained values for the ratio of V_3 to the drift velocity V of less than 0.1, indicating very low random velocities. Studies of the occurrence of Spread-F at widely separated stations imply that either the causative agent or the Spread-F itself may drift several thousand kilometers and still be recognisable.

The direction obtained for V (in an E-W direction only) is the same as that obtained by the Mitra technique and its magnitude is very similar (Skinner, Lyon and Wright, 1962). The decrease in velocity during the night is however different, as is the low random velocity. These discrepancies require to be examined and also a more careful study made of what exactly is being measured in the two case.

A further difference occurs in the size and shape of the irregularities observed by scintallation methods. The east-west sizes are considerably larger than those observed by the reflection techniques and the elongation appears very much greater, so far no reliable estimate has probably been made of this (Kent and Koster, 1964).

4) Vertical velocities: Measurements on the vertical velocities of irregularities are much less commonly made than those on the horizontal velocities. Such measurements usually require an examination of Doppler shifts

and arc more thoublesome but they are clearly required to give a complete picture of the drift. Clemesh$_a$ (1964), in Accra (Magnetic latitude 5°S) has observed the motion of Spread-F patches at a frequency of 18 MHz. As would be expected, these drift are to the east with velocities of the order of 100 meters per second. In addition he has observed Doppler shifts which he attributes to a vertically downward motion of the irregularities with velocities as high as 70 meters per second. It is not certain whether this is a movement of the irregularities inside the patch or of the patch as a whole. In either case it is an interesting phenomenon and more work on the measurement of these vertical velocities is required.

In this section very little has been said about seasonal variation or dependence on magnetic activity. These have been observed and are often very complex. At Ibadan (3°S) there is a 50% variation in the east-west drift velocity during the year with a maximum in the December solstice; at Waltair (10°N), there is a similar variation but the maximum occurs in the autumn (Skinner, Lyon and Wright, 1962; Rao and Rao, 1963). High magnetic activity appears to reduce the drift velocity at Ibadan, this is contrary to what is observed in high latitude (Briggs, 1960).

D and E-Region Drifts

The world-wide picture: — E-region drifts have been mainly studied until recently by two methods. These are the Mitra spaced antenna and the meteor echo techniques, the former measuring movements of irregularities in ionization and the latter neutral air movements. In the last few years, these two methods have been supplemented, mostly in temperate latitudes, by extensive observations using trails from rockets. The picture obtained is however, still far from clear; the principal reasons for this are as follows:

— As the E-region is largely a daytime phenomenon, the Mitra method can only be used at night when Sporadic-E clouds, are present. Such measurements are not necessarily at the same height, or not the same phenomenon, and results obtained from combining daytime and nighttime observations made respectively on the normal E-layer and on a Sporadic-E layer must be considered with some reserve. No completely reliable estimate can therefore be made of either the steady component or the diurnal component of drift.

— Meteor observations have shown that there exists a marked variation of the main drift components with height, making it difficult to combine measurements made on different occasions, unless the heights are known accurately.

— Recent rocket observations have shown the existance of large rotating disk shaped irregularities with high wind shear velocities. These are attribut-

ed to the gravity waves mentioned earlier, and their presence puts a large irregular component on top of any regular variation which is being sought for.

In view of these, and the additional complication of combining measurements on neutral air and ionized irregularities, it is difficult to give a systematic world-wide picture of the D and E-region drifts. Instead, one tends to catologue the regularities which have been noted and to discuss their limitations:

a) The harmonic components: — Steady, 24-hour and 12-hour components exist at all latitudes. Near the equator the 24-hour component predominates, in higher latitudes the 12-hour component is most important; some values for these are shown in Table 2 (taken from Rao and Rao, 1961; Shimazaki, 1960; Henderson, 1962; Greenhow and Neufeld, 1955, 1956). The gradual change from the 24-hour to the 12-hour component can be seen clearly. The steady component is appreciable at all latitudes, its direction is usually towards the equator and to the east. Polar plots of the harmonic components appear elliptical at the equator and much less so at higher latitudes; the direction of rotation is clockwise in the northern hemisphere and anticlockwise in the southern. The 24-hour and the 12-hour components as found by the radio and the meteor techniques are similar (Greenhow and Neufeld, 1956; Jones, 1958) and the movements are usually ascribed to atmospheric tides. The mechanism by which the tides operate, the reason for the predominance of a solar tide over a lunar one and the similar amplitudes of the diurnal and the semi-diurnal components is still the subject of discussion (Haurwitz, 1964). It is probable that the primary cause is solar heating action in the mesosphere together with a fairly weak 12-hour resonance period in the atmosphere.

Table II

Harmonic components of E-region drifts in different latitudes

Station	Method		Steady	24-hour	12 hour		
Waltair	Spaced	NS	-25	30	35	meters	sec⁻¹
(10°N)	Antenna	EW	5	80	10	,,	,,
Yamagawa	Spaced	NS	-20	30	35	,,	,,
(25°N)	Antenna	EW	35	20	30	,,	,,
Lower Hutt	Spaced	NS	15	10	10	,,	,,
(45°S)	Antenna	FW	5	30	20	,,	,,
Jodrell Bank	Meteor	NS	-15	10	25	,,	,,
(51°N)		EW	5	10	25	,,	,,

Explanations for the steady zonal wind which is observed are in terms of an equilibrium, set up between the combined effects of a temperature gradient, the Coriolis force due to the earths rotation and gravity. The deductions are in fairly good agreement with the experimentally observed winds. (Hines, 1965).

b) The variation with height: — Variation of the amplitude and phase of the tidal winds with height have been observed, using both the radio and the meteor echo technique. (Rao and Rao, 1964; Jones, 1964; Greenhow and Neufeld, 1956; Elford, 1959). An increase of velocity with height is found, with gradients of the order of one meter per second per kilometer. The phase of the components also changes with height. The comparison of these variations with tidal theory is still under discussion (Hines, 1965).

c) Irregular winds and gravity waves: — Drift measurements in the E-region obtained by any method show a large scatter and in addition the radio measurements show high values of V_c. Recent rocket results (Manring, Bedinger and Knowlich, 1962; Blamont and De Jager, 1962; Edmunds, Justus and Kurts, 1963; Kampfe, Smith and Brown, 1962; Rosenberg and Edwards, 1964; Jarret, Megratten and Rees, 1963) have contributed considerably to a clarification of this picture. Such measurements are necessarily isolated, but the use of chemiluminescent trails enables movements to be followed throughout a night. These measurements show, that in between 80 and 150 kilometers there exist large flat cells which rotate clockwise, when viewed form above, with periods of several hours. The horizontal scale of these movements is still uncertain, but is probably of the order of 100 kilometers. Along a vertical axis the wind direction reverses about every five kilometers at the lower end of this height range, and every twenty kilometers at the upper end. As mentioned earlier, these are attributed to gravity waves (Hines, 1960, 1965) generated near the ground. These waves can be shown theoretically to have a relationship between the direction of energy flow and the phase velocity, such that, when the energy flow is upwards, the apparent phase velocity is downwards. The experimental measurements have so far confirmed this picture. The velocities of the associated winds are high in a horizontal plane with values of the order of 100 meters per second and they are found to increase with height. In a vertical direction the velocities appear to be much less.

Turbulence does not appear to be important in the E-region; rocket results show that it ceases rather abruptly between 100 and 110 kilometers. In the D-region however it is significant, as is shown by the high apparent rate of diffusion of meteor trails (Greenhow, 1959).

Equatorial D and E-region results: — Drift measurements in the Equatorial D and E- regions are very few indeed, being confined almost entirely to Waltair. At Waltair it is found (Rao and Rao, 1961) that the diurnal component predominates, with a much stronger east-west than north-south velocity. The

maximum drift speed is in the neighborhood of 800 meters per second and is westward by day and eastward by night. Values for (V_c/V) are high, averaging about 0.7. The variation of drift with time is primarily solar but a weak lunar tide (Ramana and Rao, 1962) is also present. The nighttime data used for this analysis is presumably based on measurements made on the Sporadic-E layer.

At Ibadan (Skinner and Wright, 1962) results are only available for the daytime. A velocity of 60 meters per second to the west is found during the day, a reversal in direction occurring at about 0900 local time. This agrees well with the Waltair result, but as there is no nighttime data a detailed analysis, cannot be made.

Towards the edge of the equatorial belt it is likely that the drift velocity decreases somewhat. At Puerto Rico, magnetic latitude 32°N, the mean drift velocity is about 40 meters per second (Keneshea, Gardner and Pfister, 1965) and (V_c/V) is greater than unity, although at Ymagava (Magnetic latitude 25°N) the drift velocity is almost as high as at Waltair (Rao an Rao, 1965). No measurements are published that have been taken on the magnetic equator, but a rather surprising result (Ramanathan, private communication) appears to be obtained at Trivandrum (Magnetic latitude 0°). Here, during the day, there is a very large drift velocity to the west, of the order of 200 meters per second. This is very similar to the results obtained by Osborne and Skinner (1963) at Tamale for the F-region and more work is evidently required on this.

Mention should be made here, of the work, carried out in Lima on Equatorial Sporadic-E (Bowles, Cohen, Ochs and Balsley, 1960; Cohen and Bowles, 1963). Using very high frequencies (50 MHz) they have observed echoes which they attribute to plane wave irregularities in the electrojet. These move with velocities of over 300 meters per second, principally in a westerly direction. High frequency (5 MHz) observations on Equatorial Sporadic-E (Skinner and Wright, 1962) show much lower velocities, of the order of 60 m/sec. Although these observations are probably not made on identical phenomena, and neither may be measuring a true drift of ionization, the discrepancy still has to be explained. Some results on this will be presented in a separate paper.

Conclusion

The principal conclusion to be drawn from this survey is that there exists a lack of stations and results within the equatorial belt. There are considerable gaps in our knowledge, one of the most important being the way in which the drift velocities behave in the vicinity of the equator itself. Information on north-south drift components is extremely slight and more detailed work on this is also required. All measurements published so far have been

made on the ionized constituent. Meteor and rocket observations would be very valuable, both in filling in the parameters, such as the North-South component, which are difficult to measure by radio techniques, and also to study the relation between neutral air and ionization movements. Considerable research is still required into the nature of what is being measured in any particular drifts experiment, whether it is a true movement of ionization or a wave motion. At the moment, it can be said that we understand certain aspects of these phenomena, but that a clear synthesis will need much additional experimental observations.

References

Blamont J. E. De Jager, C.	1962	J. Geophys. Res. **67,** 3113.
Bowles, K. L. Cohen, R. Ochs, G. R. Balsley, B. B.	1960	J. Geophys. Res. **65,** 1863.
Briggs, B. H.	1960	Some Ionospheric Results Obtained During The International Geophysical Year — Elsevier Publishing Company. P. 297.
Briggs, B. H. Phillips, G. J. Shinn, D. H.	1950	Proc. Phys. Soc. (Lond) **B 68,** 106.
Calvert, W. Davies, K. Stiltner, E. Brown, J. T.	1962	Procedings of the International Conference on the Ionosphere. London, July, 1962.
Chivers, H. J. A.	1961	J. Atmos. Terr. Phys. **21,** 221
Clemesha, B. R.	1964	J. Atmos. Terr. Phys. **26,** 91
Cohen, R. Bowles, K. L.	1963	J. Geophys. Res. **68,** 2303.
Edwards, H. B. Justus, C. G. Kurts, D. C.	1963	J. Geophys. Res. **68,** 6062.
Elford, W. G.	1959	J. Atmos. Terr. Phys. **15,** 132.
Greenhow, J. S.	1959	J. Atmos. Terr. Phys. **64,** 2208.

Greenhow, J. S. Neufeld, E. L.	1955	Phil. Mag. **46**, 549.
Greenhow, J. S. Neufeld, E. L.	1956	Phil. Mag. **1**, 1157.
Harang, L.		J. Atmos Terr. Phys. **25**, 109.
Haurwitz, B.	1964	World Meteorological Organisation, Technical Note No. 58. WMO-no. 146. TP. 69.
Henderson, C. L.	1962	Proceedings of the International Conference on the Ionosphere. London, July, 1962. Inst. of Phys. and the Physical Society. p. 342.
Heisler, L. H.	1962	J. Atmos. Terr. Phys. **25**, 71.
Heisler, L. H. Whitehead, J. D.	1961	Aust. J. Phys. **14**, 481.
Hines, C. O.	1960	Can. J. Phys. **38**, 1441.
Hines, C. O.	1965	Physics of the Earths Upper Atmosphere — Prentice-Hall. Chapter 6.
Jarrett, A. H. Megratten, G. J. Smith, F. J.	1963	Plan. Spa. Sci. **11**, 1319.
Jones, I. L.	1958	J. Atmos. Terr. Phys. **12**, 68.
Jones, I. L.	1960	J. Atmos. Terr. Phys. **19**, 26.
Kampe, Aufm. H. J. Smith, M. E. Brown, R. M.	1962	J. Geo. Res. **67**, 4243.
Keneshea, T. J. Gardner, M. E. Pfister, W. J.	1965	J. Atmos. Terr. Phys. **27**, 7.
Kent, G. S. Koster, J. R.	1964	AGARD conference on Spread-F in Copenhagen
Koster, J. R.	1963	J. Geo. Res. **68**, 2570.
Maeda, H.	1955	J. Geomag. Geoelec. Kyoto. **7**, 121.
Maeda, H.	1959	J. Geomag. Geoelec. Kyoto. **10**, 66.
Maeda, H.	1962	Procedings of the International Conference on the Ionosphere. London, July, 1962. Institute of Physics and the Physical Society. p. 187.

Manring, E.
Bedinger, J.
Knoflich, H.   1962   J. Geophys. Res. **67**, 3923.

Martyn, D. F.   1955   Physics of the Ionosphere-Physical Society,
                                London, p. 260.

Mitra, S. N.   1949   Proc. Inst. Elec. Engs. (London) Part 3. **96**,
                                441.

Mitra, S. N.
Vij, K. K.
Dasgrupta, P. D.   1960   J. Atmos. Terr. Phys. **19**, 172.

Munro, G. H.   1958   Aust. J. Phys. **11**, 91.

Osborne, O. G.
Skinner, N. J.   1963   J. Geo. Res. **68**, 2441.

Phillips, G. J.
Spencer, M.   1955   Proc. Phys. Soc. (London), B **68**, 481.

Purslow, B. W.   1958   Nature, **181**, 35.

Ramana, K. V. V.
Rao, B. R.   1962   J. Atmos. Terr. Phys. **23**, 221.

Rao, R. R.
Rao, B. R.   1961   J. Atmos. Terr. Phys. **22**, 81.

Rao, P. B.
Rao, B. R.   1962   Procedings of the International Conference on
                                the Ionosphere. London, July, 1962.
                                Institute of Physics and the Physical Society.
                                p. 363.

Rao, A. S.
Rao, B. R.   1963   J. Atmos. Terr. Phys. **25**, 249.

Rao, G. L. N.
Rao, B. R.   1964   J. Atmos. Terr. Phys. **26**, 213.

Rao, G. L. N.
Rao, B. R.   1964   J. Atmos. Terr. Phys. **26**, 628.

Ratcliffe, J. A.   1956   Rep. Prog. Phys. **19**, 188.

Rosenberg, N. W.
Edwards, H. D.   1964   J. Geo. Res. **69**, 2819.

Shimazaki, T.   1960   Some Ionospheric Results Obtained During the
                                International Geophysical Year — Elsevier
                                Publishing Company. p. 345.

Skinner, N. J.   1962   Ionospheric Sporadic-E — Pergamon Press,
Wright, R. W.   London.

Skinner, N. J.   1962   Proceedings of the International Conference
Wright, R. W.   on the Ionosphere. London, July, 1962.
Lyon, A. J.   Institute of Physics and the Physical Society.
                          p. 301.

Thomas, L.   1959   J. Atmos. Terr. Phys. **14, 123**.

A NEW METHOD OF APPLYING THE

CORRELATION ANALYSIS

by

R. F. Kelleher

Physics Department

University College Nairobi, Kenya

The correlation analysis of Briggs et al.[1], as extended by Phillips and Spencer[2], is one of the principal methods of examing fading records to obtain information about the properties of ground diffraction patterns. From plots of the auto and cross correlation functions, velocities V_c' and V are obtained in each of three directions, and from these six parameters the velocity, size, shape and rate of change of the pattern can be determined.

It is common to derive the values of V_c' from the cross correlations corresponding to zero time-shift. It would seem better however, to confine the analysis to the maximum value of cross correlation alone since the errors involved are then smaller. This is particularly important when dealing with patterns which have a small size in one or more directions (as frequently happens with the highly elongated patterns common in equatorial regions) because the instantaneous cross correlation will be low and the individual auto-correlations will probably give very different values for the corresponding time-shift.

In this note we derive the equation to be used in the maximum correlation method. This equation was obtained in a different way by Briggs et al. The discussions is limited to a one-dimensional pattern.

The nomenclature follows the standard practice. If the distance between two receiving points is ξ_0, the different velocities are found from the relationships

$$V' = \xi_0/\tau' \quad , \quad V_c' = \xi_0/\tau_c' \quad , \quad V_m = \xi_0/\tau_m$$

We derive first the normal equations connecting V' and V_c' with V and V_c.

Original Equations

The principal assumption in correlation analysis is that the overall correlation can be represented in quadratic form. That is,

$$e\ (\xi,\tau) = F\ (\tau^2 + \xi^2 - 2c\xi\tau) = F\ (g) \qquad (1)$$

where $F\ (g)$ is a monotonically decreasing function with a maximum value of 1. Now the autocorrelation has the form

$$e\ (0,\ \tau) = F\ (a\ \tau^2)$$

and the instantaneous spatial correlation

$$a\ \tau_c'^2 = b\ \xi_0^2 \quad \text{or} \quad b = a/V_c'^2$$

We now consider the separation ξ_0 and find the value of τ, (τ'), which makes the correlation a maximum. This will occur when g is a minimum. Differentiating

$$\delta g/\delta\tau = 2a\tau - 2c\xi_0 = 0$$

and therefore

$$\tau' = (c/a)\ \xi_0 \quad \text{or} \quad c = a/V'$$

Thus,

$$e = F\ \{a[\tau^2 + (\xi/V')^2 - 2\xi\tau/V']\}$$

Now suppose that ξ and τ are connected by the relationship $\xi = K\tau$ (one receiving point is moving with a velocity K) so that

$$e = F\ \{a\ \tau^2[1 + K/V_c')^2 - 2K/V']\} = F\ (a\tau^2 h)$$

The correlation will fall most slowly with time when $K = V$, the drift velocity. Now,

$$\delta h/\delta K = (2K/V'^2_c) - 2/V'$$

and so,

$$V \, V' = V'^2_c$$

Thus when $K = V$ we have

$$e = F \, [b \, (V'^2_c - V^2)]$$

But the fading is now due entirely to the randon component and so

$$e = F \, [b \, V^2_c]$$

Therefore

$$V_c^2 = V'^2_c - V^2$$

We now establish the connection between τ_m, the time shift on the autocorrelation curve corresponding to the maximum value of cross correlation, and the parameters τ' and τ_c'.

From equation (1) with $\xi = V'\tau$ we get:

$$e = F \, \{a \, \tau'^2[(V'/Vc_c)^2 - 1]\}$$

We thus have

$$\tau_m^2 = \tau'^2 \, [(V'/V'_c)^2 - 1]$$

and

$$(\tau_c')^2 = \tau_m^2 + \tau'^2$$

Then the value of τ_c' can be determined from τ_m and τ' and the analysis proceeds as before. Also this last expression can be rewritten utilizing the inicial relationships of the velocities, then:

$$(1/V'_c)^2 = (1/V_m)^2 + (1/V')^2$$

It is easy to see that $V'_c \leqslant V'$. This approach therefore eliminates the familliar difficult case which arises sometimes in the normal analysis, when $V'_c < V$.

References

1) — B. H. Briggs, G. J. Phillips D. H. Shinn — Proc. Phys. Soc. **63B**, 106, 1950.

2) — G. J. Phillips and M. Spencer — Proc. Phys. Soc. **68B**, 481, 1955.

THE APPLICATION OF THE BRIGGS-SPENCER METHOD FOR THE CALCULATION OF IONOSPHERE DRIFT PARAMETERS TO THE EQUATORIAL SITUATION

by

R. W. Morriss and A. J. Lyon

University of Ibadan, Ibadan, Nigeria

The method given by Briggs and Spencer[1] for calculating drift velocities from spaced antenna data uses the time delays of similar fades and their standard deviation. Contrary to the statement by the authors, it seems that the method also gives unique values for the axial ratio and orientation of the characteristic ellipses and for the quantity V_c.

In the equatorial situation, where the characteristic ellipses are rather elongated and directed along the field lines, or nearly so, the formulas required can be simplified considerably. The inclusion of standard deviations make it possible to estimate the standard errors of all the derived parameters.

The configuration of the antennas used at Ibadan and the notation for the time delays, are shown in Fig. 1. T_x is the time delay between the west and south antennas position if a feature reaches S after W, and similarly for T_y and T_z. Clearly,

$$T_z = T_y - T_x$$

and we define T as

$$T = T_y + T_z$$

The standard deviations are denoted by σ, σ_x, σ_y, σ_z and the mean time delays by T^*, T^*_x, T^*_y, and T^*_z. We then define

$$W = (T^*)^2 (\sigma/0.61)^2 \; ; \; Z = (T^*)^2 (\sigma_z/0.61)^2$$

and similarly for X and Y. Only four independent quantities are determined from the observed similar fades, for example: σ, T^*, σ_z and T^*_z.
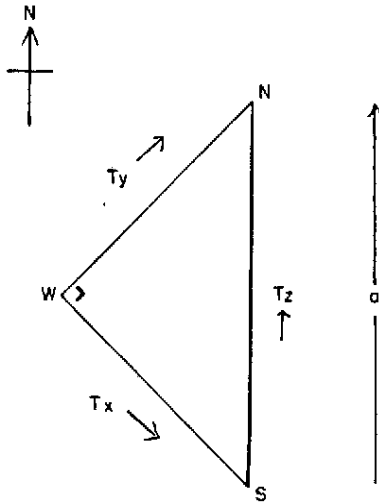
Fig. 1 — Configuration of the three antennas used for drifts measurements at Ibadan, and notation for time delays.

If the irregularities are assumed to be exactly field aligned, the eastward and northward componentes of drift velocity are given respectively by

$$V_{E_0} = T^*/W, \text{ and } V_{N_0} = aT^*_z/Z$$

where a is the distance N-S; and the axial ratio is given by

$$r = (W/Z)^{1/2}$$

The standard errors of V_{E_0} and V_{N_0} are given by

$$S_E/V_{E_0} = n^{-1/2} f (\sigma/T^*), \quad S_N/V_{N_0} = n^{-1/2} f (\sigma_z/T^*_z)$$

rather uncertain, and the assumption $\delta = 0$ may be equally good. If the estimated δ is adopted the drift velocities become

$$V_N = (a/Z)\{T^*_z - (1-1/r^2) \tan \delta . T^*\}$$

$$V_E = (a/W)\{T^* - (r^2-1) \tan \delta . T^*_z\}$$

These equations are particulary useful in assessing the uncertainty in V_E and V_N associated with the inevitable uncertainty in δ.

The Briggs-Spencer method has the following advantages over the full correlation analysis more commonly adopted:

(a) — It is much simpler both in scaling from the records and in the subsequent computations. The various calculations required are readily programed for a computer.

(b) — The standard errors of all computed parameters are readily assessed.

(c) — By making use of clearly identifiable features in the fading pattern the method may give a better representation of the behavior of distinct irregularities.

Reference

B. H. Briggs and M. Spencer, "The Physics of the Ionosphere", p. 119, Physical Society, 1955.

A MODEL FOR THE INTERPRETATION OF SOME IONOSPHERIC DRIFT MEASUREMENTS

by

G. S. Kent

University of the West Indies, Jamaica

On this paper a model is described for the interpretation of ionospheric drift measurements, made by the spaced receiver method, when the wave scattered from the ionosphere has a frequency considerably above that of the plasma frequency of the scattering region. In the analysis associated with this method of measuring ionospheric drifts, the correlation function $\rho\ (\xi,\ \tau)$ of the diffraction pattern f (x, t) formed on the ground, as shown in Fig. 1, is usually determined in terms of its shape, size and drift velocity V_a. In addition to these, there is another function which arises from the analysis, namely the characteristic random velocity V_c, which is a measure of the way in which the diffraction changes its form as it drifts. Usually V_c is left uninterpreted and the object of this paper is to show how this may, under certain circunstances be related to the random velocities of the irregularities causing the scattering.
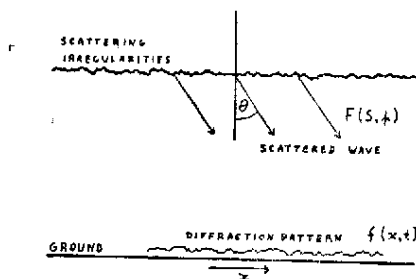
Fig 1. The scattering geometry.

A two-dimensional model is considered, in which the scattering irregularities are weak and lie in a medium whose refractive index is close to unity. They are supposed to have a steady drift velocity V_1, together with superimposed random velocities whose root mean square value is V_m; this model is shown in Fig. 2. The scattered spectrum $F(s, h)$ in terms of angle and frequency is then calculated, using a simple angular scattering function and the Doppler shifts produced by motions of the irregularities.

The diffraction pattern on the ground is expressed in terms of the drift velocity V_0, the characteristic random velocity V_c and the size ξ_0 of the pattern along its minor axis, the major axis being taken to be infinitely large. Using the well-known Fourier Transform relationship connecting the autocorrelation function $\rho\ (\xi, \tau)$ of the diffraction patter to the power spectrum $|F(s,h)|^2$, the former is transformed to give the equivalent power spectrum. This spectrum is then equated to that derived from the ionospheric model described above.
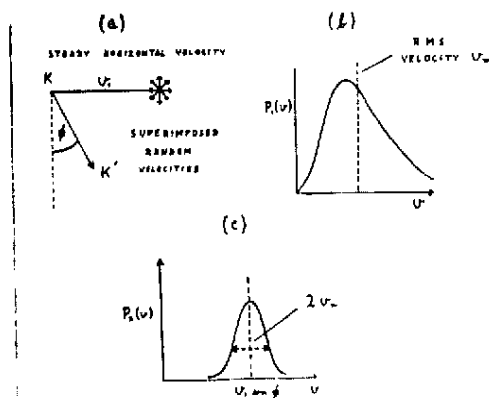
Fig 2. The ionospheric model.
(a) The directions of the velocities.
(b) The distribution of random velocities.
(c) The resolved velocity distribution along KK'.

The relationship may depend on the geometrical arrangement of the transmitter and receiver, but under the conditions of the normal spaced antenna experiment, in which the transmitter and receiver are adjacent as shown in Fig. 3, the following equations are obtained.

$$V_1 \quad = \quad V_o/2$$

$$\text{and} \quad V_m \quad = \quad (V_c/\xi_o)/\pi\sqrt{2}$$

The first equation is the one normally used in drifts analysis. The second one is new and it should be noted that V_m is related not to V_c but to (V_c/ξ_o) where V_c is the characteristic random velocity and ξ_o is the pattern size.
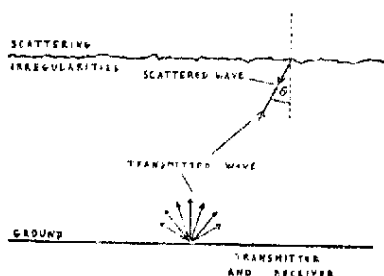
Fig 3. The scattering geometry for ionospheric drifts measurements.

PRELIMINARY RESULTS OF DIFFRACTION

PATTERN MEASUREMENTS AT NAIROBI

by

R. F. Kelleher and P. Miall

Physics Department, University College Nairobi, Kenya

In conformance with the IQSY program, a three-receiver fading-amplitude experiment on a frequency of 2.15 MHz has been set up in Nairobi. The antenna spacing is 100 m.

The records are analysed by the correlation techniques of Briggs et al.[1] and Phillips and Spencer[2], using a computer program developed by G. F. Fooks[3] of the Radio and Space Research Station at Slough. The values of τ'_c are calculated from the relationship:

$$\tau'_c = \tau^2_m + \tau'^2$$

where the three time shifts are those shown in Fig. 1. The results therefore depend only on the position and value of the maximum cross-correlation and should be subject to smaller errors than those derived using a value of τ'_c obtained from the instantaneous cross-correlation. This is important when dealing with small dimension diffraction patterns for which the instantaneous correlations is low.

A preliminary look at the results for Nairobi give medium values of the diffraction pattern parameters as

	r	P_χ (%)	V_c/V	d (m)
E	3.0	27	1.3	82
F	3.2	25	1.0	42

where P_χ is the percentage number of occasions when the major axis of the characteristic ellipse lies within $\pm$ 20° of the magnetic meridian,

and d is the lenght of the semi-minor axis. The F-Region results should be treated with great caution as the number of records is low.
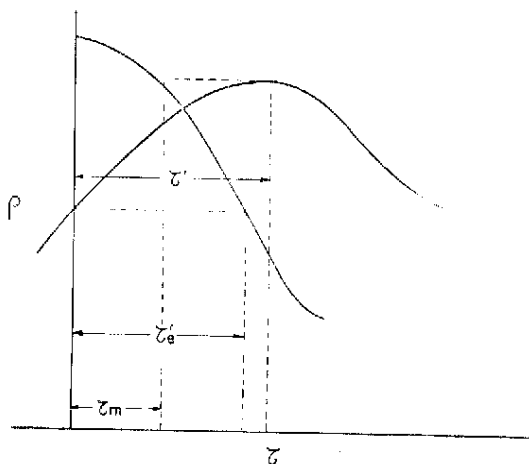
Fig. 1 —

Time shifts in correlation analysis

      The axial ratios appear to be higher than those found at Singapore (where the median value is $r = 1.7$), though there is less tendency for the irregularities to lie in the direction of the magnetic field. There is some indication that at Nairobi the axial ratios increase with the height of reflection.

      The drift directions in the E-Region are predominantly towards the north and west during daylight hours, and towards the south and east at night.

References

1.   Briggs, B. H., G. J. Phillips and D. H. Shinn — Proc. Phys. Soc., **63 B**, 1950

2.   Phillips, G. J. and M. Spencer — Proc. Phys. Soc., **68 B**, 1955.

3.   Fooks, G. F. — J. Atmos. Terr. Phys., **27**, 979, Sept. 1965.

SOME DRIFTS MEASUREMENTS MADE NEAR THE

MAGNETIC EQUATOR IN GHANA

by

J. R. Koster

University of Ghana, Legon, Accra, Ghana

A series of drift measurements at Tamale, Ghana (dip latitude 0.5°S) were made by Skinner, over a three week period in February and March, 1962. Over 160 of these records were subjected to the full correlation analysis by Mr. S. K. Katsriku of the University of Ghana. The main results are:

E-region

Axial ratio of pattern on ground: 5.5

Orientation — along field lines: $\pm$ 0.5°

Size of pattern (i.e. distance over which the correlation function falls to 0.5): 50m

> Velocity: Westward by day, with mean speed of 67 m/sec
> Maximum true velocity 115 m/s (West of 0900 UT)
> Apparent velocity as high as 210 MHz.

> $V/V_c = 1.3$. Hence apparent velocities are about 60% higher than true velocities.

F-region

Orientation — along field lines: $\pm$ 0.4°

Axial ratio of pattern on ground: 7

Size of pattern (mean during daytime): 46m

Velocity: Nighttime mean: 70 m/sec
          Daytime mean: 115 m/sec
          Maximum: 200 m/sec (West of 0900 UT)

$V/V_c = 1.9$. Hence apparent velocities are about 25 to 30% higher than true velocities.

These values of velocity are considerably higher than those reported by stations somewhat further from the dip equator, and suggest that more measurements are worth making.

PRELIMINARY RESULTS OF IONOSPHERE WIND

MEASUREMENTS AT THUMBA

by

M. R. Deshpande and R. G. Rastogi

Physical Research Laboratory, Ahmedabad, India

Measurements of horizontal drifts in the E and F regions of the ionosphere over Thumba (Geog.-Lat. 2.5°S, Geog.-Long. 76.9°E, magnetic dip 0.6°S) have been made since January 1964. The present article describes the magnitude (V) and direction (θ) of the drifts derived according to the method of similar fades. The direction of the drift is predominantly westward, there being a small indication of eastward drift during winter season (Fig. 1). The N-S component is very small during any of the seasons.
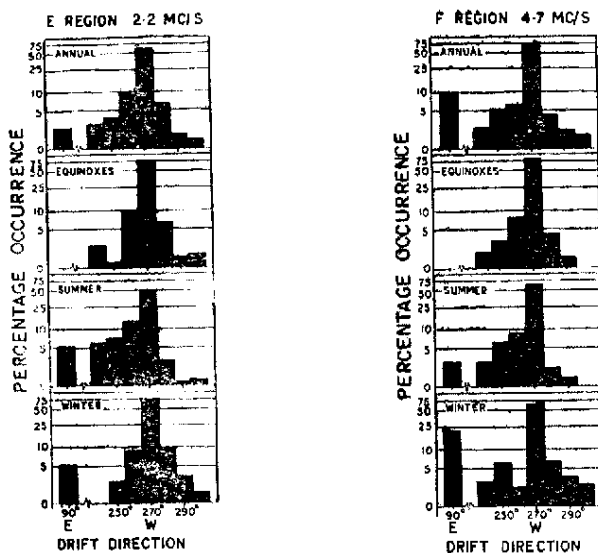
Fig. 1 — Histograms of drift direction in the E and F regions of the ionosphere over Thumba during different seasons of the year.

The annual mean drift speed is 132 m/sec for E region and 161 m/sec for the F region. There is no significant seasonal variation in the drift speed (Fig. 2). The daily variation of the drift speed indicates a morning peak at about 0900 hr in the E region and at about 1000-1100 hr for the F region. There is an indication of evening peak for both E and F region (Fig. 3). The peak value of monthly average drift speed is about 250 m/sec for the E region and about 300 m/sec for the F region.

The observations indicates that the irregularities in the ionosphere over Thumba are highly elongated in N-S direction, the drift is predominantly along E-W direction towards West. The drift speed values are much higher than those observed at higher latitudes. A close association between the horizontal drifts in the ionosphere over Thumba and the electrojet currents is suggested.
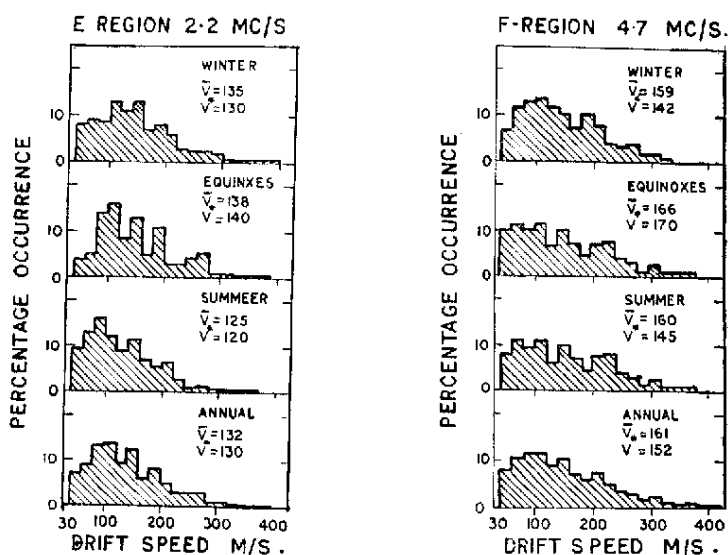
Fig. 2 — Histograms of drift speed in E and F regions of the ionosphere over Thumba during different seasons of the year.
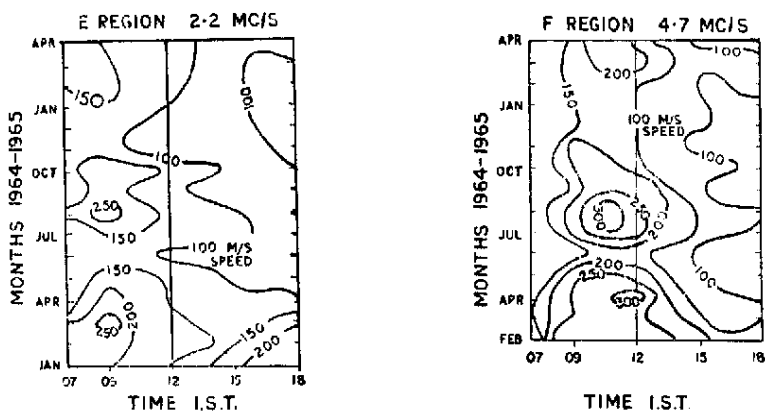
Fig. 3 — Contour diagrams showing the drift speed in E and F regions of the ionosphere over Thumba at different times of the day during different months of the year.

IONOSPHERIC DRIFT MEASUREMENTS AT SINGAPORE

by

V . A. W. Harrison

Radio and Space Research Station

Slough, England

Measurements of the magnitude and direction of the horizontal drift of ionization in the E and F-Regions of the ionosphere have been made at the Radio and Space Research Station, Singapore (Magnetic Latitude 9°S). These have been made by three close-spaced receiver method and the records analysed by the method of similar fades to find the diurnal (Figs. 1 and 2) and seasonal (Figs. 3 and 4) variations of drift. The correlation on the daytime east-west components with sunspot number (Fig. 5) and magnetic activity (Fig. 6) has also been examined.

A few records have been submitted to full correlation analysis. These show the elongation of the correlation ellipse to be about 1.7: 1 for both regions with major axis approximately north-south and the ratio V_c/V to be about unity.

DAY   5 MONTH MEDIANS   NIGHT.

SEASONAL VARIATIONS IN THE F REGION FOR 1960.
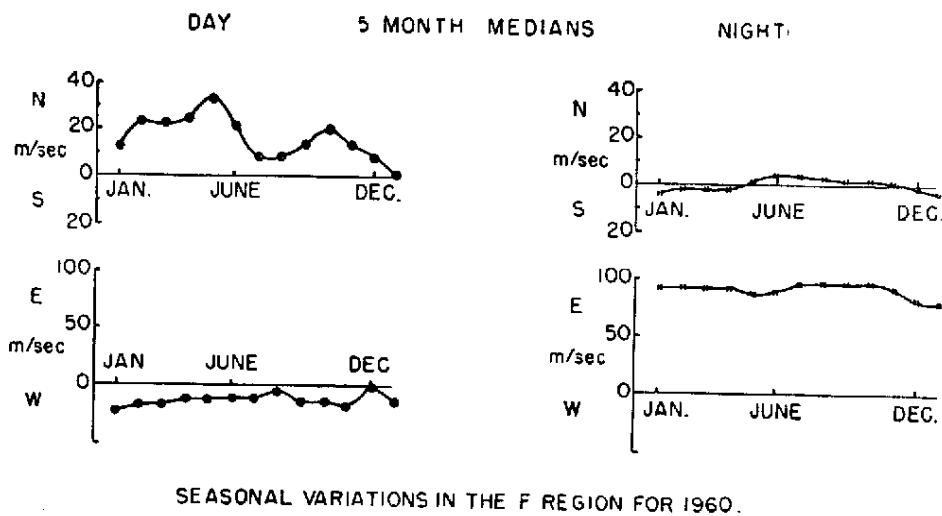
Fig. 4 — Components of the seasonal variation of the day and night-time drifts in the F region for 1960.

CORRELATION COEFFICIENT

Day between measurement of sunspot number and drift.

CORRELATION OF DRIFT VELOCITY WITH SUNSPOT NUMBER

CORRELATION COEFFICIENT

Day between measurement of Ap and drift

CORRELATION OF DRIFT VELOCITY WITH MAGNETIC INDEX Ap.
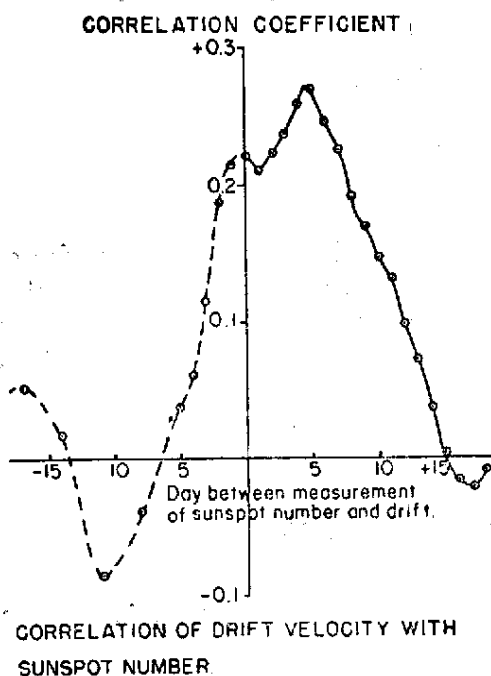
Fig. 5 — The correlation of the daytime E-W components with sunspot number. Note the positive correlation with time lag of 3-5 days.
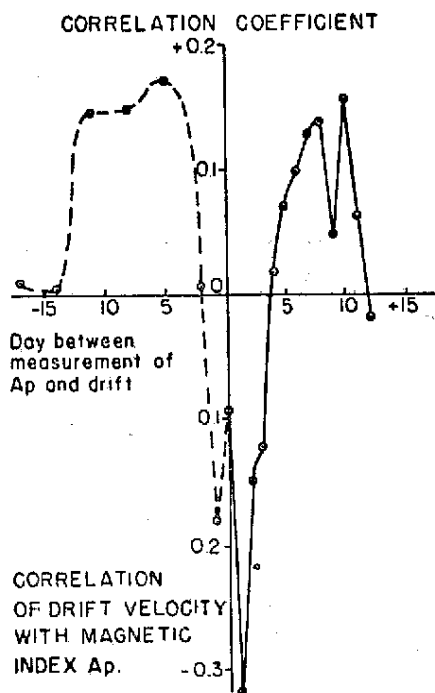
Fig. 6 — The correlation of the daytime E-W components with magnetic activity. Note the negative correlation with zero time lag.

SOME RESULTS OF IONOSPHERIC DRIFT

MEASUREMENTS AT IBADAN

by

R. W. Morriss and A. J. Lyon

Introduction

During the I.Q.S.Y. measurements have been made, as far as possible, hourly on Wednesday and Thursday of each week and also every day during the World Geophysical Intervals. From October 1964 the Briggs-Spencer method has been used in its simple form as explained in the accompanying paper to obtain the eastward drift component V_{Eo}. Two equinox seasons have now been analysed by this method.

The Eastward Component, V_E

Figure 1 shows a mass plot of values obtained on 21 days in the autumnal equinox period of 1964 including most of the days of the World Geophysical Interval in October. The circles indicate the median values and a smooth curve has been fitted to these by visual estimation. Despite the considerable scatter of individual points the median points follow a quite regular pattern. As was also found in the sunspot maximum observations of Skinner et al.[1], the velocities are predominantly westwards by night. The change-over takes place between 0600 and 0700 LT in the morning, and between 2000 and 2100 in the evening. The average magnitude of the velocity in the daytime is 43 m/sec, and during the night (0000-0500) is 55 m/sec. There appears to be a clear maximum in the daytime velocity of about 50 m/sec westwards occurring between 0900 and 1000. Figure 2 (a) compares the median curve of Fig. 1 with a corresponding curve for equinox at sunspot maximum. This is based on results for September 1957 and March 1958 due to Skinner et al. (unpublished). The agreement in general form between the curve is remarkably good. They appear to be

almost exactly in phase, and the sunspot maximum curve shows a small maximum near 1000LT, similar to that on the sunspot minimum curve. The magnitudes however are considerably higher at sunspot maximum, reaching about 100 m/sec eastwards at night and have a daytime average of 76 m/sec westwards. It would appear therefore that drift velocities at sunspot maximum are almost twice that at sunspot minimum.

Figure 2 (b) shows the median diurnal variation for a similar series of days near the March equinox 1964, and the equinox curve for 1957/58 is repeated for comparison. The general shape of the March curve is clearly very similar to the October one and the magnitudes are also very similar.
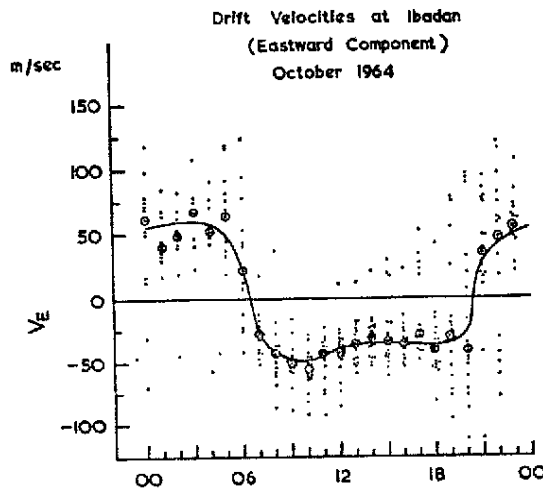
Fig. 1 — Mass plot showing diurnal variation of eastward component of drift velocity at Ibadan in October 1964. The circles indicate hourly median values.
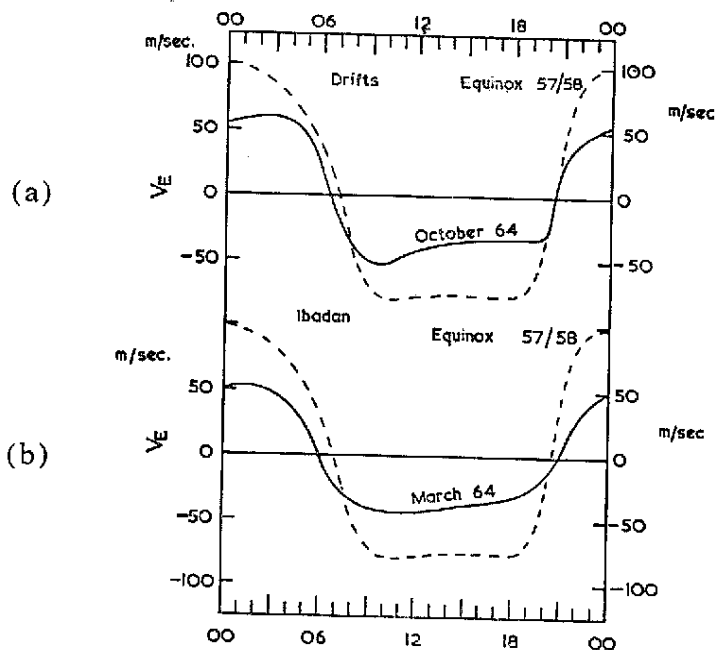
Fig. 2 — Comparison of diurnal variations of eastward drift velocity at sunspot maximum (broken curves) and sunspot minimum (continuous curves). The data are for Ibadan during equinox months, and the curves have been drawn to run smoothly through the hourly median points, as in Fig. 1.

Reliability of the Results

The standard error of V_{E_0} is readily calculated by the formula given in the accompanying paper. Figure 3 shows the values of V_{E_0} obtained on a particular day together with their standard errors, which are typically of the order of ± 5 to ± 10 m/sec.

The standard deviations of the values on different days at a given hour are much greater than this, as is clear from the large scatter

on the mass plot in Fig. 1. In this case the standard deviations are about ± 20 m/sec by day and ± 40 m/sec by night, and somewhat larger values have been obtained in other seasons. If the standard errors quoted above are realistic it is clear that these standard deviations are almost entirely due to real variability of the drift velocity from day and not to errors of measurement.

It should be noted that the diurnal variation of V_{Eo} is frequently much more irregular than that shown in Fig. 3, and reversals of sign during the day or night are by no means uncommom.
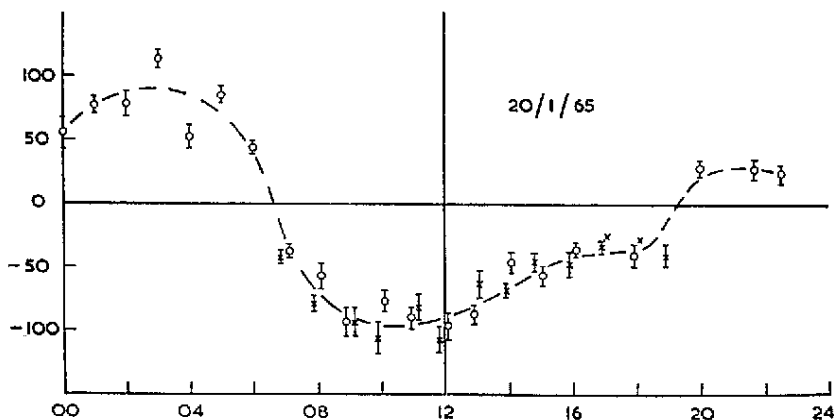
Fig. 3 — Diurnal variation of eastward component of drift velocity at Ibadan on a single day. Circles are for the F region and crosses for the E region. The error bars have been computed assuming the irregularities to be accurately field aligned.

Reference

N. J. Skinner, A. J. Lyon and R. W. H. Wright, "The Ionosphere", Institute of Physics and Physical Society, p. 301, 1963.

TRIANGULATION MEASUREMENTS OF DRIFTING PATCHES OF EQUATORIAL F REGION IRREGULARITIES

by

Robert Cohen

Jicamarca Radar Observatory,

Lima, Peru

Studies of "Equatorial Spread F" configurations have demonstrated that these can be understood by the calculation of the propagation delays experienced en route by rays scattering from the associated irregularities as a function of frequency. The configurations obtained have three characteristic forms depending on whether the irregularity patch is located at the base of the F layer, or is embedded in the F layer below hmax or above hmax.

By the analysis of each ionogram it is possible to establish the height of the patch and its distance east or west of the ionosonde, since the propagation is limited to the equatorial plane by the aspect sensitivity of the scattering. From a series of such ionograms, one can determine the velocity of the irregularity patch, but it is impossible to establish whether the sucessive positions of the patch and the associated velocities are eastward or westward, since all of the determinations are symmetric in this regard. However, using ionosondes located in each case at 1° north of the dip equator at Jicamarca and Huancayo, Peru, separated by 160 km, it is possible to triangulate the positions of the patch and hence sense the motion. For the limited number of cases studied to date, it is apparent that it is accompanied by a downward movement of the patch.

Fig. 1 — Two examples of the triangulation measurements of the motion of a patch of F region irregularities. Points marked o are those measured from Jicamarca, and x refers to those measured from Huancayo. Velocities are 26 and 67 m/sec, at 2000 and 0200 hours, respectively.
(Other illustrations used are in Calvert and Cohen, JGR **66**, 3125-3140, Oct., 1961).
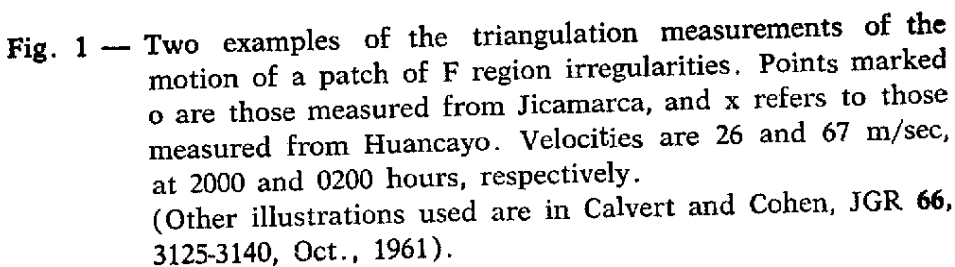
EVIDENCE FOR A NIGHTTIME WESTWARD CURRENT IN THE EQUATORIAL E-REGION

by

B. B. Balsley
Central Radio Propagation Laboratory, Colorado

and

Jicamarca Radar Observatory, Lima, Peru.

It has been well established that during the daytime at the magnetic equator there is a strong, eastward current known as the equatorial electrojet, corresponding to a westward flow of electrons and the associated electron-density irregularities. A nighttime current system flowing in the opposite direction at the equator has been postulated, but is difficult to observe with magnetometers.

Recently, power spectra of echoes from nighttime E- region irregularities above Jicamarca have been obtained which indicate frequency-shifts, i.e., motions of irregularities that are opposite to those obtained during the daytime. Insofar as these motions of irregularities are indicative of the motion of the plasma in which they are embedded, this would imply an eastward motion of the electron, or a westward current at night. This interpretation seems reasonable, since the theoretical explanation of the nighttime irregularities is probably analogous to that for the daytime ones. See Figs. 1 and 2.

Thus a reversal of current must occur sometime after sunset, and the 2000 hours minimum of VHF signal strength scattered by the equatorial E Region in propagation from Arequipa to Trujillo, Peru during 1958 may be further evidence of this reversal.
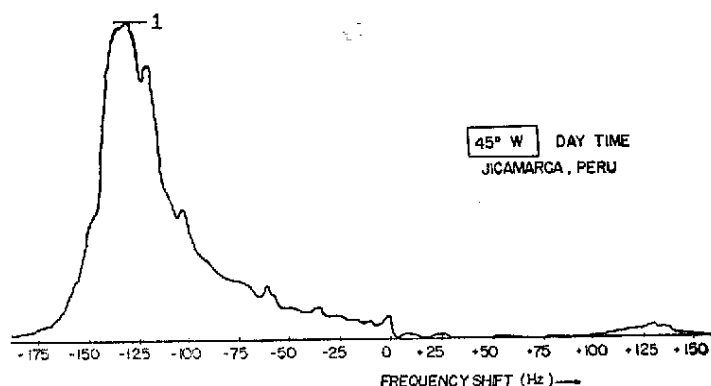
Fig. 1 — Power spectrum obtained during daytime from electrojet irregularities viewed at 45° West of Jicamarca, Peru at a frequency of 49.92 MHz. (Maximum value of signal spectrum normalized to unity on relative scale).
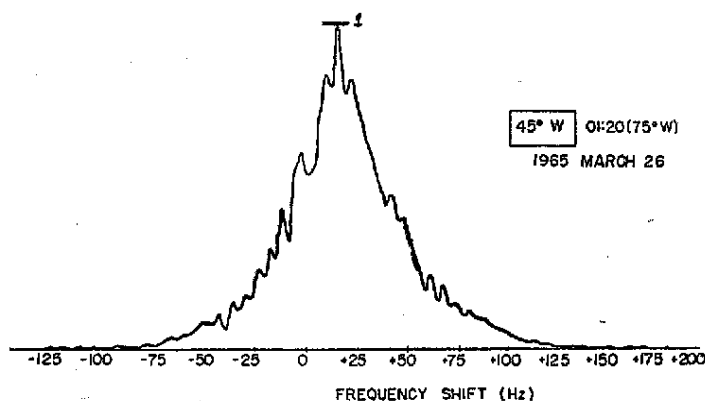
Fig. 2 — Power spectrum obtained during nighttime in the same way as for Fig. 1.

SUMMARY OF THE SESSION

by

R. G. Rastogi

Physical Research Laboratory, Amedabad, India

A review of the present knowledge of ionospheric drifts was given by Dr. G. S. Kent. it was gratifying to learn of new observation; of ionospheric drifts at equatorial stations, viz. Singapore, Thumba, Nairobi, Ibadan and Tamale.

The daily variations of the drift speed and direction at all of these stations was shown to be very similar for both the E and F region. It was accepted that the F region drifts would be affected by the underlying sporadic E region but it was felt that the observed daily variation of F region drift is characteristic of the layer.

At all the stations, the north-south component of the drift was found to be smaller than the east-west component. The measurements of N-S components at stations very close to the magnetic equator were not considered significant due to extreme elongation of the irregularities in the north-south direction.

The direction of drift in the E as well as the F regions is mainly westward during the day and eastward during the night, the change-over taking place at times close to the dawn and dusk. The drift speed is found to be larger in the F than in the E region at all the stations.

There has been very little seasonal variation of the drift observed in E or F regions at the equatorial stations.

The drift speeds in E or F regions at Tamale (dip 1°S) are shown to be greater than the corresponding values at Ibadan (dip 6°S) indicating that within the equatorial region the drift speed increases towards the equator. Very high values of drift speed at Thumba (0.6°S) indicate that the excessive drift region over the equator may be quite narrow.

The measurements of drift at Ibadan during two epochs of solar activity indicate that the speed increases with an increase of suspot number in approximately the same ratio as the increase of the daily range of the horizontal

magnetic field. A positive correlation has been found between the daytime E-W drift at Singapore and sunspot numbers with a time delay of 3 to 5 days. The drift speed at Singapore is found to be negatively correlated with the magnetic activity.

Fuller analysis of the fading records show that the mean orientation of the irregularities at Tamale is along the N-S direction within an error of 4-10 degree. The elongation of the correlation ellipse is found to be 1.7 at Singapore, about 5 at Ibadan and about 8 to 10 at Tamale.

Kelleher has suggested a modification of Phillips and Spencer's full correlation analysis whereby the error introduced due to the slight differences in the autocorrelograms at the three antennas are reduced. Morriss and Lyon have suggested that some index of reliability should be given to the results of analysis and have applied Briggs and Spencer's method using time delays and their standard deviations for the equatorial stations where the irregularities are highly elongated.

Prof. Maeda suggested that the effect of magnetic activity on the ionospheric drift should be further examined. He also suggested that experiments should be undertaken to study the relation between the neutral and electron drifts in the ionosphere.

Prof. Wright suggested that the latitudinal variation of the elongation of the irregularities should be examined and more equatorial stations should be established to determine the width of the excessive drift region over the magnetic equator.

VII — EXOSPHERE

VII — EXOSPHERE

(Discussion leader: William B. Hanson)

Review Paper

The Electron Distribution in the Earth's Exosphere

by

J. O. Thomas

Imperial College, University of London

It is generally agreed that the main constituent of the earth's atmosphere at great heights above the earth is hydrogen. Hydrogen ions are formed by the reaction:

$$O \text{ plus} + H \rightarrow H \text{ plus} + O$$

as was first pointed out by Dungey. The relative equilibrium concentrations in the exosphere are determined largely by the importance of this reaction near the base of the neutral particle exosphere where the cross-section for collision between ions and neutrals is relatively high. The base of the exosphere near 1000 km above the ground is the most probable level of origin for protons entering the exosphere from below after formation by the reaction referred to above. Thus the relative abundances of 0 plus and H plus (and also of He plus) ions at the base of the exosphere controls the electron and ion distribution throughout the exosphere. The proton number density is given by the chemical equilibrium expression given by Hanson and Ortenburger[1] in 1961:

$$[H \text{ plus}] = (9/8) [H] [0 \text{ plus}]/[0]$$

These workers also showed that conjugate F2 peaks are only weakly coupled with the protons in the protonsphere.

The structure of the lower exosphere has been discussed by a large number of workers. Detailed references are given by Angerami and Thomas[2].

Some important equations (given with the usual nomenclature as used in that paper) are present below.

For the electron density N_e on a line of force we have

$$\frac{N_e(s)}{N_{eo}} = \frac{T_{eo}}{T_e(s)} \left[(1/\eta) \sum_i \eta_i \exp \frac{z}{H_i} \right]^{1/(1+C)}$$

The suffix zero refers to values at the critical or base level in the exosphere (≈ 1000 km) on the line of force; z is the geopotencial altitude, $H_i = kT_{io}/m_i g_o$; $C = T_{eo}/T_{io}$; $i = 1, 2, 3$, for 0 plus, He plus and H plus respectively and

$$\eta = \eta_1 + \eta_2 + \eta_3; \; \eta_1 = 1, \; \eta_2 = \frac{n[He\ plus]}{n[0\ plus]} \; etc.$$

so that η_2 is the number density of He plus normalized to that of 0 plus at the base of the exosphere.

For $T_e = T_i$ the power which the quantity in the square bracket is raised becomes ½.

The densities of two ions will be equal at transition levels given by

$$z_{ij} = H_{ij}/(H_i - H_j) \ln(\eta_j/\eta_i)$$

Figure 1 shows data on the electron density to distances of $\approx 5R_e$ as obtained from whistler studies. Figure 1 is taken from Thomas and Dufour[a] in which detailed source of references to the various curves are given. At approximately $3.5R_e$ during "average" conditions, the electron density decreases suddenly by a factor of ten in a distance of about $R_e/10$. The "knee" has been observed by Carpenter using whistler data and also by Gringauz During storms the knee moves nearer the earth ($R_e \approx 2$). A diffusive equilibrium theory is believed to apply up to, but not beyond the knee. For distances equal to or greater than $4R_e$, collisionless plasma theory must be used.

It has been shown [a] that good agreement between theory and experiment (see Fig. 2) can be obtained if a proper allowance is made for the latitudinal dependence of the ionic abundances at the base of the exosphere. The agreement between experimental $N_e(h)$ profiles and theoretical profiles computed using a diffusive equilibrium theory and observational data from Alouette I and from Ariel I requires that the proton abundance at 1000 km

decrease with latitude as shown in Fig. 3. The general shape of the proton distribution given is Fig. 3 has been verified by recent experiments.

In Figures 4 and 5 the proton distribution resulting from the calculations of Thomas and Dufour [3] are combined with the Ariel 1 data to give a complete picture of the ion relative abundances at 1000 km which are consistent with the Alouette 1 and Ariel 1 observation and would give the observed whistler electron density profiles.

EXPERIMENTAL EXOSPHERIC ELECTRON DENSITY PROFILES

a STOREY (1953)
b ALLCOCK (1959)
c CARPENTER (1963)
d SMITH (1960), (1961)
e POPE (1961), (1962)
f BOWLES (1962)
g SCHMELOVSKY (1960)
h SCHOUTE-VANNECK & MUIR (1963)
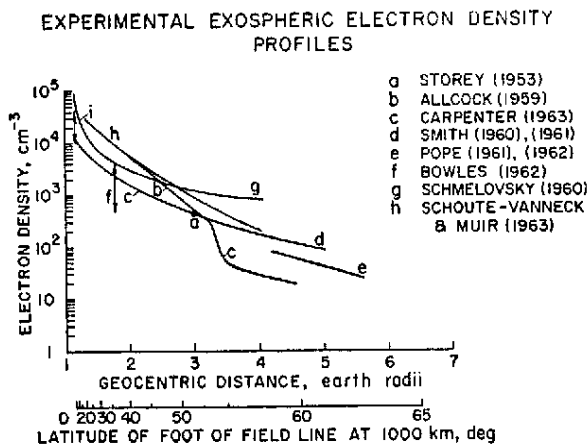
Fig. 1 — Examples of experimental observations of exospheric electron density in the equatorial plane. The arrow, f, represents a range of values obtained by the incoherent scatter technique. The other data are derived from whistler observations made at different times under a wide variety of solar and magnetic conditions. The arrow, i, approximates the region in which the Alouette I observations of electron density for 1,000 km lie. Detailed references to the original sources are given in Thomas and Dufour[3].

EXPERIMENTAL AND THEORETICAL EXOSPHERIC
ELECTRON DISTRIBUTIONS
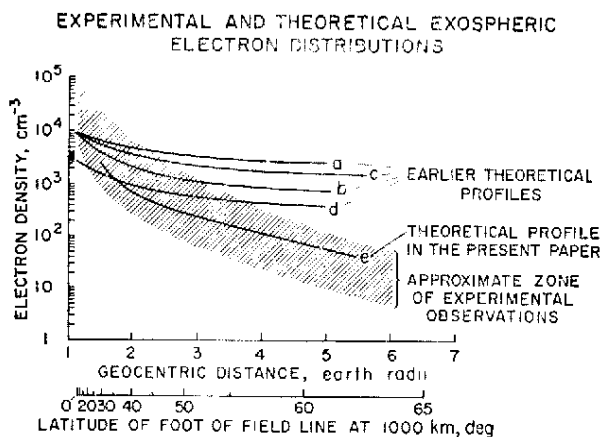
Fig. 2 — Comparison of experimental and theoretical electron density distributions in the whistler medium. The shaded area represents approximately the zone in which the experimental profiles of Fig. 1 lie. Curves a and b were taken from Bates and Patterson, curve c from Dungey and curve d from Johnson. The electron density distribution given by Johnson applies along a line of force. The equatorial profile, d, was obtained using a constant density at the reference-level. Detailed references are given in the paper by Thomas and Dufour[3].

PREDICTED LATITUDINAL DISTRIBUTION
OF PROTONS AT 1000 km
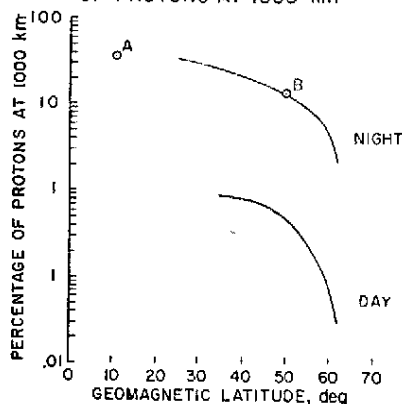
Fig. 3 — Theoretically predicted abundance of H plus ions at 1000 km as a function of magnetic latitude near 1500 and 0300 LMT calculated for the summer of 1962 — the period in which the published Ariel I data were recorded. The experimental points A and B derived from the Ariel transition altitude (He plus → H plus) data lie very close to the theoretical curve calculated in the way described in Thomas and Dufour[3].

IONIC RELATIVE ABUNDANCES AT 1000 km
LATITUDINAL VARIATIONS
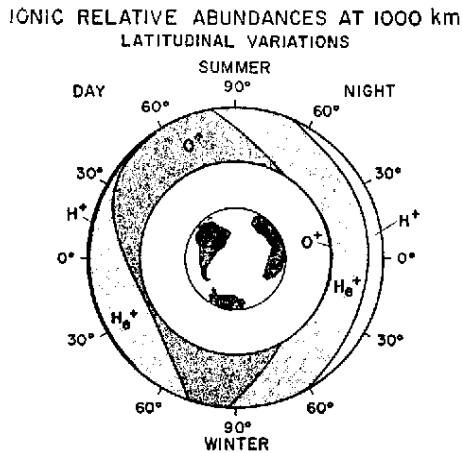
Fig. 4 — Exospheric ionic relative abundances at 1,000 km for different latitudes for typical daytime and nighttime conditions in summer and winter in a sunspot minimum solar epoch. The relative abundance of 0 plus, He plus and H plus ions at any latitude is given by the radial width of the shaded area corresponding to each ion. The picture presented is a composite one, consistent with the experimental results obtained from Alouette 1, Ariel I and from whistlers.

IONIC RELATIVE ABUNDANCES AT 1000 km.
DIURNAL VARIATION, SUMMER

Fig. 5 — Diurnal variation in the summer exospheric ionic composition at 1,000 km, at 50° N geomagnetic latitude, during a sunspot minimum solar epoch. The picture presented is a composite one, consistent with the experimental results obtained from Alouette I, Ariel I and from whistlers.

References

(1) Hanson, W. B., and I. B. Ortenberger, J. Geophys. Res., **66**, 1425, 1961.

(2) Angerami, J. J. and J. O. Thomas, J. Geophys. Res., **69**, 4737, 1964.

(3) Thomas, J. O. and S. W. Dufour, Nature, **206**, 567, 1965.

THE ELECTROM DENSITY IN THE MAGNETOSPHERE

by

J. J. Angerami[*] and D. L. Carpenter

Stanford University, Stanford, California, U.S.A.

Analysis of nose whistlers recorded at Eights Station Antartica, shows that the electron density in the equatorial plane decrease smoothly with geocentric distance, except for a very sharp decrease of more than one order of magnitude at about 4 R_E. This change is called[1] the "knee" of the distribution and marks the equatorial crossing of the field-aligned boundary which separates the magnetosphere in two distinct regions.

The inner region (Plamasphere) is characterized by densities in excess of 10 electrons per cubic centimeter and by mean free paths that are short compared to the length of the field line linking the conjugate ionospheres. The relative abundance of collisions leads to an isotropic distribution of velocities and a hydrostatic support of ionization along the geomagnetic field.
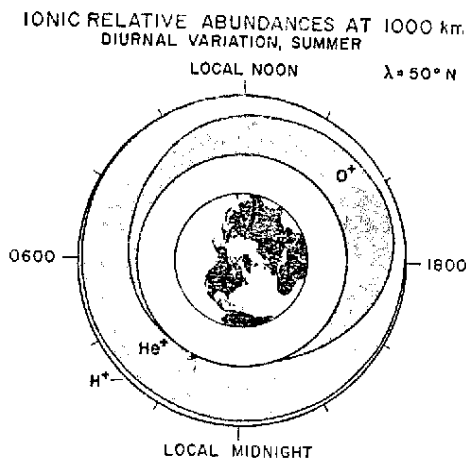
In the outer region, because the densities are lower and the temperatures are higher (around 3000°K), the mean free path is larger than the length of the line of force joining the conjugate ionospheres. Thus the distributions of electrons along a line of force is governed not by hydrostatic equilibrium, but rather by ballistic motions of the ions coming from below[2].

The experimental data is shown by plots of electron density in the equatorial plane versus geocentric distance, and plots of electron content in tubes of force (with 1 cm² cross section at 1000 km, and limited by this level and the equatorial plane) versus dipole latitude at 1000 km.

(*) On leave from Escola Politécnica da Universidade de São Paulo, Brasil.

A full account of this work will be published in the J. Geophys. Research, in early 1966. Details on the diurnal and magnetic activity variations of the knee, as well as plasma motions on the magnetosphere can be found in a companion paper by D. L. Carpenter, to be published in the same Journal.
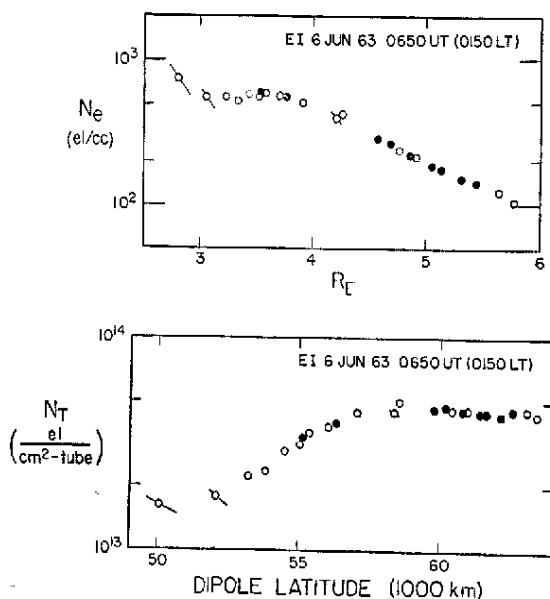
Fig. 1 — The upper figure is the equatorial profile corresponding to a night of very low magnetic activity ($K_p \approx 0$), causing the "knee" to be removed beyond 5.8 R_E (geocentric). Note the flattening of the profile below 3.8 R_E and the gradual decrease from this point up to 5.8 R_E. All points in the plot come from the same whistler, with 24 independent components. The bottom figure shows the same data in terms of tube content versus dipole latitude at 1000 km. This content should not be confused with the content measured by Doppler shift from satellites. From 50° to 57° the content increases, mainly due to increase in volume of the tubes of force. Above 57° the decrease in density compensates the increase in volume and the content levels off.

Fig. 2 — Four different equatorial profiles corresponding to post-midnight hours when the magnetic activity is moderate (K_p in the range 2 to 4). Note the sharpness and repeatability of the "knee" both in position and density. The continuous line represents the profile of Fig. 1 and is shown as a references.

● ○ EI 7 JUL 63 0650 UT (0150 LT)
▲ △ EI 8 JUL 63 ~0700 UT (~0200 LT)
■ □ EI 4 AUG 63 0850 UT (0350 LT)
▼ ▽ EI 5 AUG 63 0550, 0850 UT (0050, 0350 LT)

N_e
(el/cc)

R_E

● ○ EI 7 JUL 63 0650 UT (0150 LT)
▲ △ EI 8 JUL 63 ~0700 UT (~0200 LT)
■ □ EI 4 AUG 63 0850 UT (0350 LT)
▼ ▽ EI 5 AUG 63 0550, 0850 UT (0050, 0350 LT)

N_T
$\left(\dfrac{el}{cm^2\text{-tube}}\right)$

DIPOLE LATITUDE (1000 km)
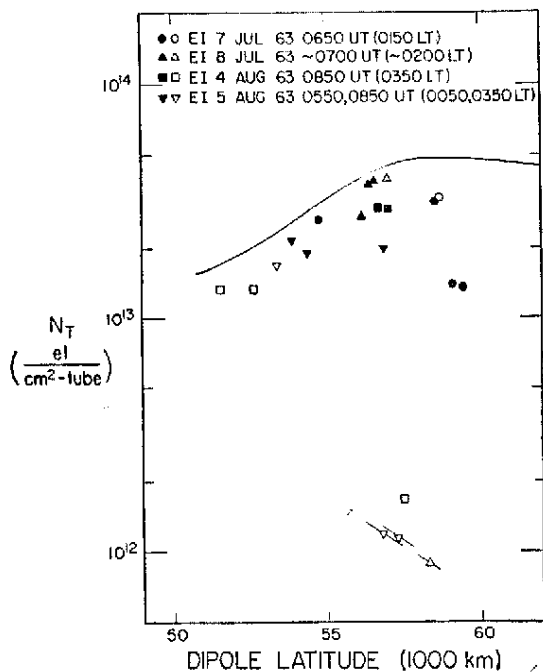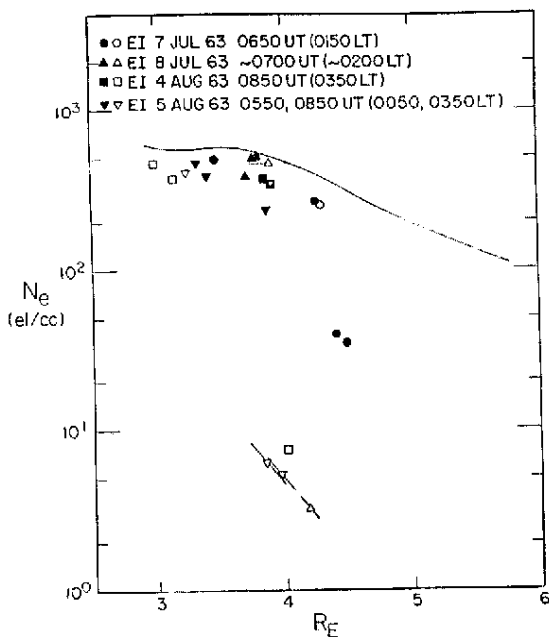
Fig. 3 — The same data of Fig. 2 shown as electron tube content versus dipole latitude at 1000 km. Note that the tubes of force in the region beyond the "knee" are virtually "empty" ($\approx 1/20$) as compared to the neighboring tubes in the inner region.
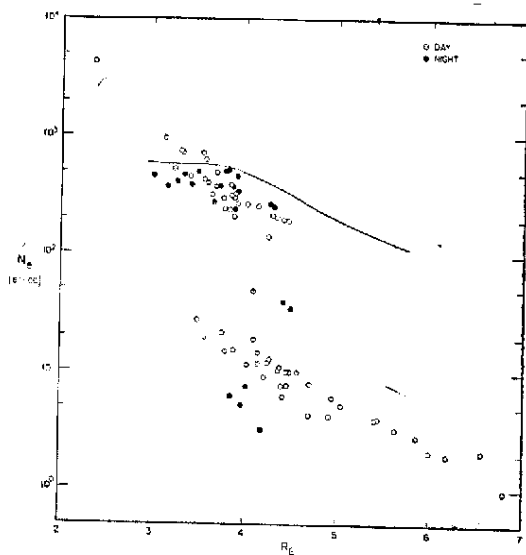
Fig. 4 — Electron density in the equatorial plane, including the night-
time data of Fig. 2 and daytime points from 11 different
days with K_p in the range 2 to 4, in the period July-August,
1963. Note that inside the "knee" at 4 R_E the day and night-
time densities area are about the same. Towards lower altitudes
the nighttime data follows the reference profile, although
the daytime points lie above it. This is evidence of a day-
night variation which tends to increase downwards. Just
beyond the "knee" the densities at night are lower than at
daytime. The profile outside the "knee" is well defined in
daytime up to 7 R_E, where the density reaches 1 el/cm^3. The
uncertainty of this value, due to various factors (such as
distortion of the magnetic field by the solar wind, thermal
effects on whistler propagation, etc.) is not greater than a
factor of $\pm$ 2.
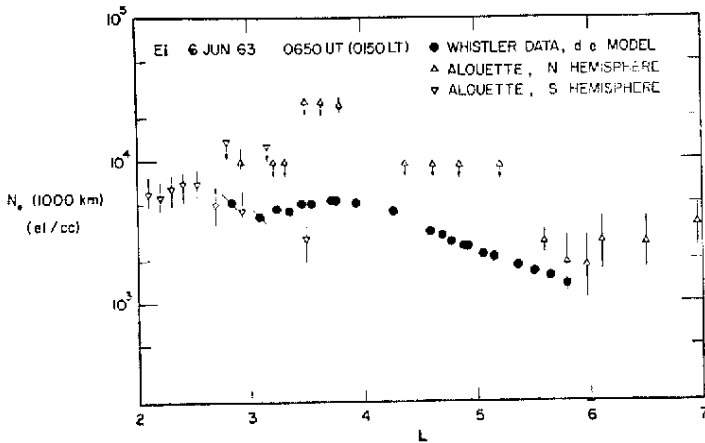
Fig. 5 — Comparison of whistler and Alouette measurements indicates the applicability of diffusive equilibrium along the lines of force in the region inside the "knee", at nighttime. The filled circles were determined from the equatorial profile of Fig. 1, assuming diffusive equilibrium along the magnetic field lines[3] with a uniform temperature of 1200°K and H plus concentration of 40% at 1000 Km. The times of the Alouette recordings were within 30 minutes of the whistler measurements.
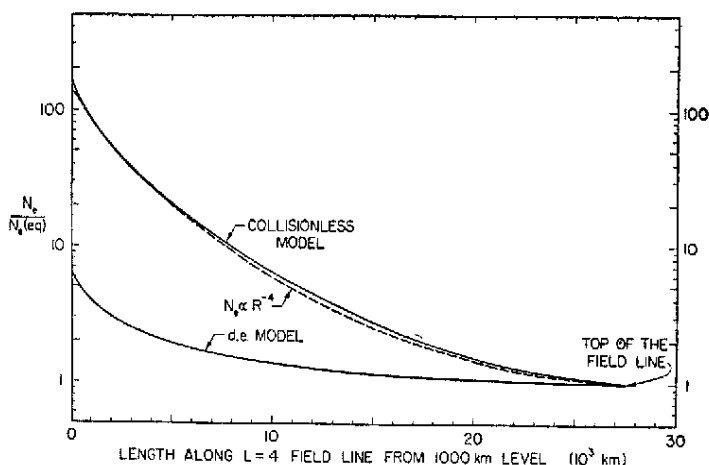
Fig. 6 — The relative variation of electron density along a line of force crossing the equator at $4R_E$. The diffusive equilibrium model is applicable in the region inside the "knee". The collisionless model[2] describes well the variation of electron density along the lines of force in the tenuous region outside the "knee". As the plot shows, the empirical model $N_e \propto R^{-4}$ is a good approximation for the collisionless model.

References

(1) Carpenter, D. L., Whistler Evidence of a "Knee" in the Magnetospheric Ionization Density Profile, J. Geophys. Res. 68, 1675-1682, 1963.

(2) Eviatar, A., A. M. Lenchek and S. F. Singer, Distribution of Density in an Ion-Exosphere of a Non-Rotating Planet, The Physics of Fluids, 1964.

EXOSPHERIC ELECTRON DENSITY PROFILES OBTAINED FROM

INCOHERENT SCATTERING MEASUREMENTS

by

D. T. Farley

Jicamarca Radar Observatory, Lima, Peru

During the period 1-3 February 1965, continuous measurements of electron density up to altitudes above 4000 km were obtained at Jicamarca. Between 3000 and 5000 km, the densities were always somewhat less that 10^1 cm^{-3}, with a variation of about a factor of two throughout the day. The measurements were very consistent on successive days, and the accuracy of the profiles at 4000 km is estimated to be ± 20% or better. The results are consistent with various whistler measurements made at different times, and are presented in the following four figures.

Fig. 1 — Three profiles of electron density taken at nearly the same time on three sucessive days.
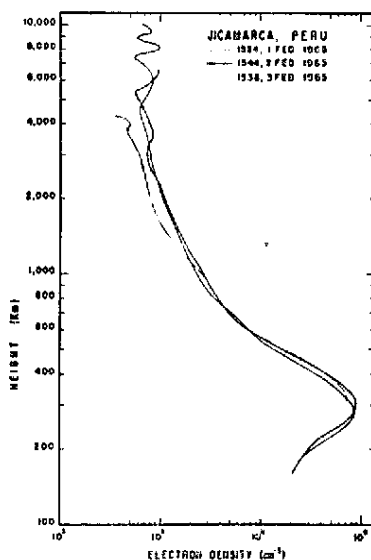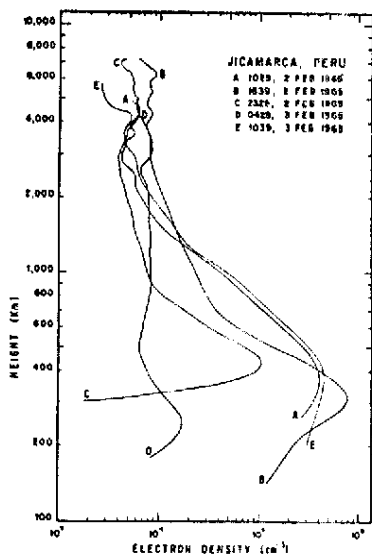
Fig. 2 — A series of electron density profiles taken throughout a 24-hour period. Each observation was taken over an interval of 40-60 minutes, beginning with the time indicated.
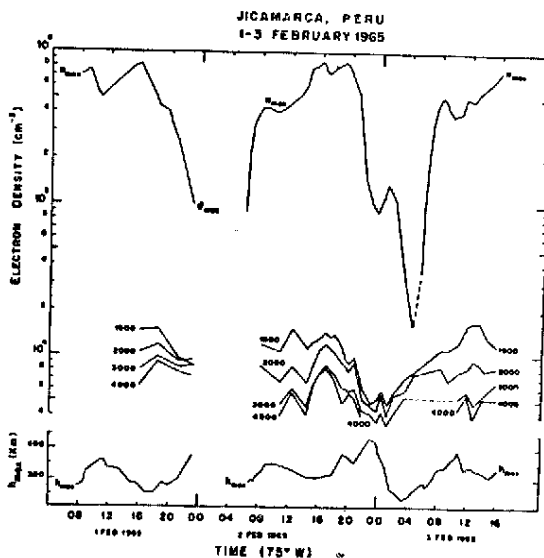
Fig. 3 — The variation of exospheric electron densities at a constant height. The height, in kilometers, corresponding to each curve is indicated. The behavior of Nmax and hmax are shown for comparison.
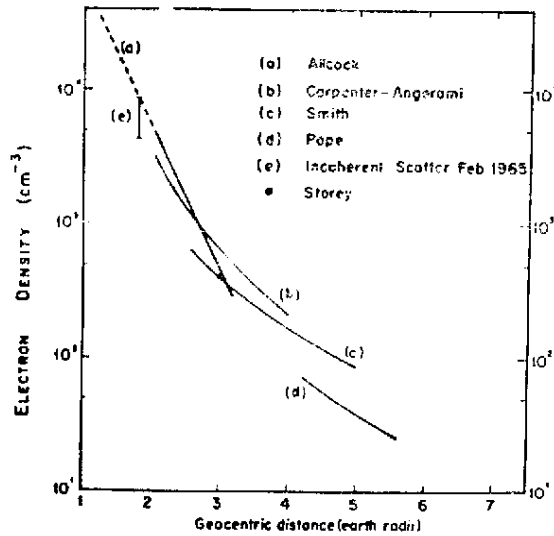
Fig. 4 — Comparison of electron densities obtained at Jicamarca with those obtained from some whistler measurements. This figure is adapted from Fig. 8 of Carpenter and Smith (Revs. of Geophys., **2**, 415, 1964).

MEASUREMENTS OF 1 TO 4 MEV TRAPPED PROTONS IN THE EQUATORIAL MAGNETOSPHERE

by

G. C. Theodoridis and F. R. Paolini

American Science and Engineering, Inc., Cambridge
Massachusetts, U.S.A.

and

L. Katz and D. Smart

Air Force Cambridge Research Laboratories
Bedford, Massachusetts, U.S.A.

A Blue Scout Junior vertical probre launched on 30 March 1965 from Cape Kennedy reached a peak altitude of about 16,500 km. It crossed magnetic shells with L from about 2 to 3.7, at magnetic latitudes from 40° to the magnetic equator. The probe carried instruments to measure the flux energy spectra, and pitch angle distributions of trapped protons and electrons in various energy ranges.

The data presented in this paper concern protons between 1 and 4 Mev and were obtained from a solid state spectrometer. This instrument consisted of two ORTEC solid state detectors each with a depletion depth of about 200 microns. Pulses recorded in the first detector alone, in anticoincidence with pulses from the second detector, correspond to protons of energy below 5 Mev which are stopped in the first detector and therefore produce a pulse proportional to their total energy. Spectral information was derived by pulse height analysis.

The field of view of the detector was a cone with half angle of 3.3°. The spectrometer output was sampled 60 times per second and the probe spin frequency was about 3 rotations per second. Thus pitch angle distributions with good angular resolution could also be obtained.

Figure 1 gives a summary of recorded perpendicular intensities of protons above 1 Mev along the path of the rocket. Intensities are plotted versus the magnetic shell parameter L. The figure includes also the corresponding values of the magnetic field B and the geomagnetic latitude λ.

Complete integral spectra over the energy range from about 1 to 4 Mev have been obtained for magnetic shells above L $\approx$ 2.5. Two such spectra are shown in Fig. 2. Within the accuracy of the measurements, obtained spectra agreed with an exponential energy dependence exp ($-$ E/E$^\circ$). In the sampled region the slope parameter E$_0$ assumed values between approximately 0.4 and 0.6 Mev.
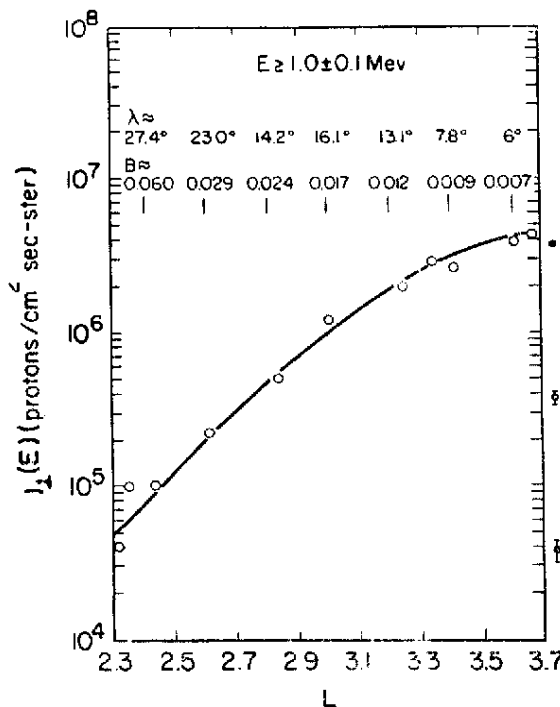
Fig. 1 — Perpendicular proton intensities above 1 Mev measured along the rocket trajectory.
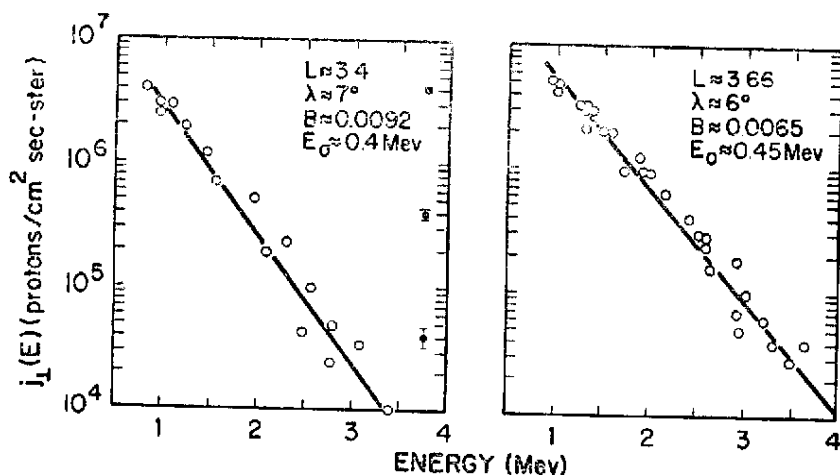
Fig. 2 — Integral energy spectra of protons between 1 and 4 Mev.

Figure 3 gives pitch angle distributions for protons of energy above 1 Mev at two points along the rocket trajetory. Due to the nearly perpendicular orientation of the probe spin axis with respect to the local magnetic field vector a complete scanning of pitch angles was possible during the largest part of the trajectory.

On the basis of pitch angle distributions measured near the equator, information can be derived about perpendicular intensities at points situated at higher magnetic latitudes on the same magnetic shell. Using perpendicular intensities derived in this manner from measured pitch angle distributions, and perpendicular intensities directly record-ed along the rocket path, contours of intensity versus L at constant λ can be constructed. Some of these are given in Fig. 4. Isoiñtensity contours presented in Fig. 5 were derived from the intensity curves of Fig. 4, in the polar geomagnetic coordinates R and λ.
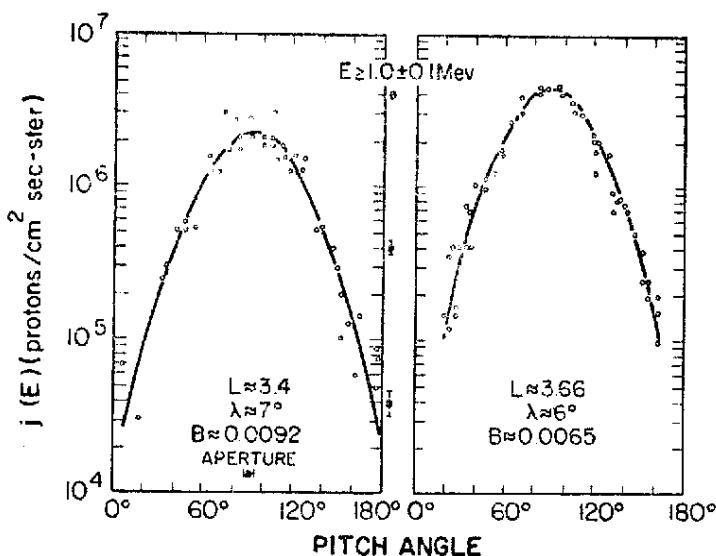
Fig. 3 — Proton pitch angle distributions.
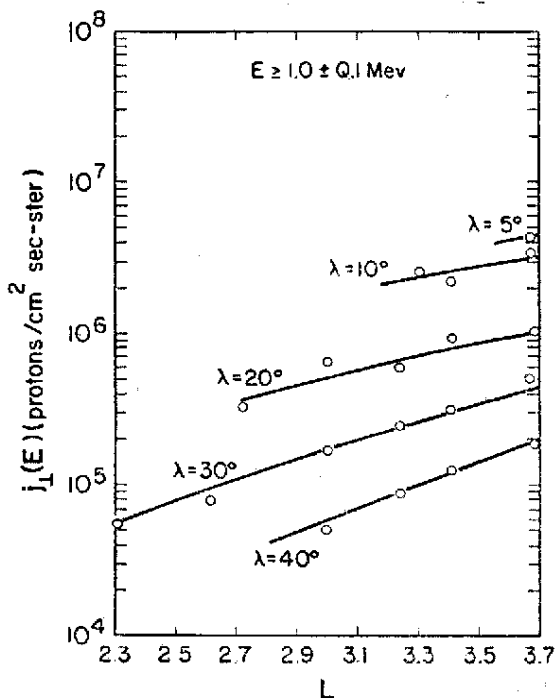
Fig. 4 — Proton perpendicular intensities above 1 Mev at various L and λ as derived from unidirectional intensities and pitch angle distributions measured along the rocket trajectory.
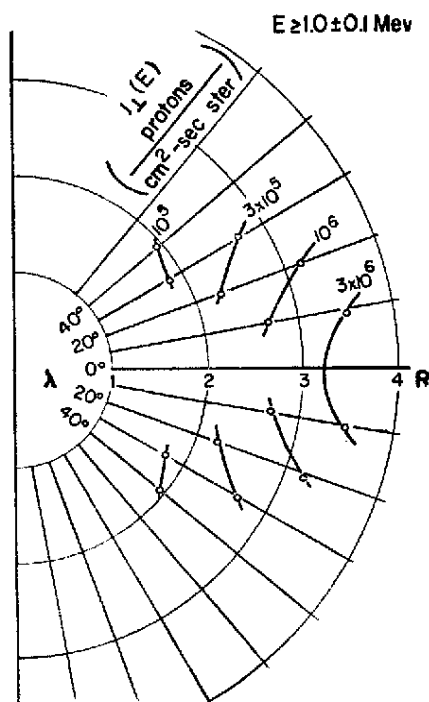
Fig. 5 — Isointensity contours of protons above 1 mev.

Proton data obtained by Davis and Williamson, with Explorer XII agree well with the intensity levels of protons above 1 Mev around L≈3 reported here. Spectral slopes in this region are in agreement as well. In summary, low energy proton perpendicular intensities up to about 5 x 10⁶/cm² sec sr were observed at L≈3 to 3.5 near the magnetic equator. Measured pitch angle distributions were used to derive the perpendicular intensities at higher magnetic latitudes. Integral spectra between about 1 and 4 Mev exhibit an exponential energy dependence with a slope E_0 0.4 to 0.6 Mev.

EXPLORER XX OBSERVATIONS AT CONJUGATE DUCTS

by

T. E. VanZandt, B. T. Loftus and W. Calvert

NBS, CRPL, Boulder, Colorado, U.S.A.

Conjugate ducting is observed frequently on Explorer XX (Fixed-Frequency Topside Sounder) records. Several ducts are shown in Fig. 1; they range from 3 to 20 km in N-S dimensions.
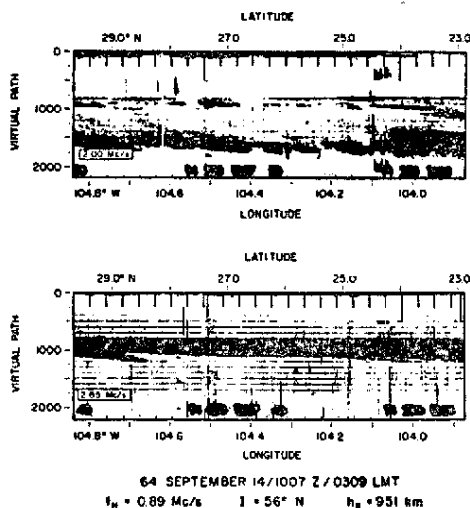
Fig. 1 — A typical record with conjugate ducts, at times of 1006/52, 1007/01, 1007/51, 1007/52 and 1008/00 (HRMI/SEc). Multiple echoes can be seen at 1007/52 on the 2.85 MHz record, at 800, 500, and 200 km of virtual range. The last multiple has a time delay of 317 msec on a path of 95,000 km.

Figure 2 shows the geographical and diurnal variation of the ducts observed in the American zone during September 1964. From the September and October data we conclude that during the autumnal equinox season of 1964, ducting was common from 0200 to 0900 hours and rare from 1000 to 1800 LT. We do not yet have enough data for the 1800 to 0200 LT hour period. It will be interesting to find the time of onset of ducting.
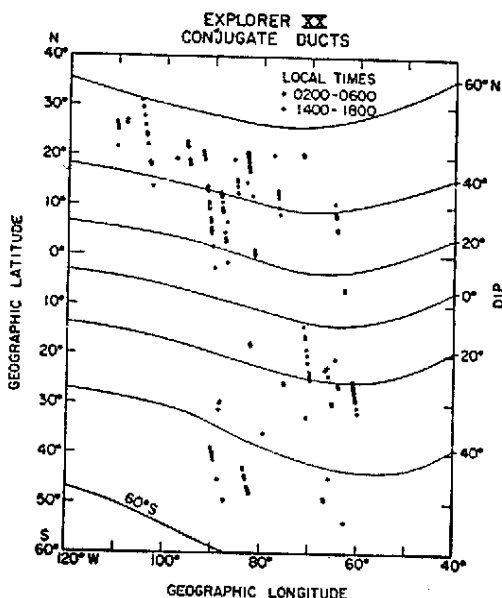
Fig. 2 — The locations of conjugate ducts observed during September 1964. Curves of constant dip are also shown.

The rate of occurrence of conjugate ducts on Hawaii records during the same period was an order of magnitude smaller.

The most striking feature at Fig. 2 is the abrupt decrease in occurrence at a dip of about 55° (or apex radius ≈ 1.75 earth radii). Conjugate ducts are observed monthly on 1.50 MHz, less often on 2.00 MHz, rarely on 2.85 MHz, and never on 3.72 MHz. However, most of the occurrences of conjugate ducting on 2.85 MHz were near the 55°

cutoff. Since the $\triangle N$ at the apex of the line of force necessary for ducting is a rapidly increasing function of frequency, and since N is a rapidly decreasing function of the apex height, this implies that $\triangle N/N$ at a fixed height increases with latitude up to the 55° cutoff and then decrease poleward.

These observations provide the parameters for design of experiments to observe conjugate ducting from the ground. The transmitter should be locate at a dip of less than 55° and should be operated at a frequency of 3 MHz or less. Of course, these limits may vary with seasons or sunspot number, but it is very unlikely that ducting could be observed at a dip of 70° on $\approx$ 10 MHz.

OBSERVATION OF COHERENT RADIO SCATTER FROM IRREGULARITIES 6000 KM ABOVE THE MAGNETIC EQUATOR

by

Robert Cohen and Kenneth L. Bowles

Jicamarca Radio Observatory, Lima, Peru

During some nights in April and May, 1964 remarkably strong echoes were observed above Jicamarca at a range of 6000 km. They were obtained only at night, and their intensity varied in time. The echo intensity increased and decreased in times comparable to the 15 minute integration interval. During several intervals when especially strong echoes were visible on an oscilloscope, they were noted to fade slowly, at about a 1 cycle per second frequency. The half-width of the region from which the echoes were obtained was about 400 km, an the central ranges observed did not vary more than about 500 km from the nominal 6000 km, previously mentioned. See Figs. 1 and 2.

JICAMARCA, PERU
1964 APRIL 8
2136 - 2149 (75°W)
49.92 MHz
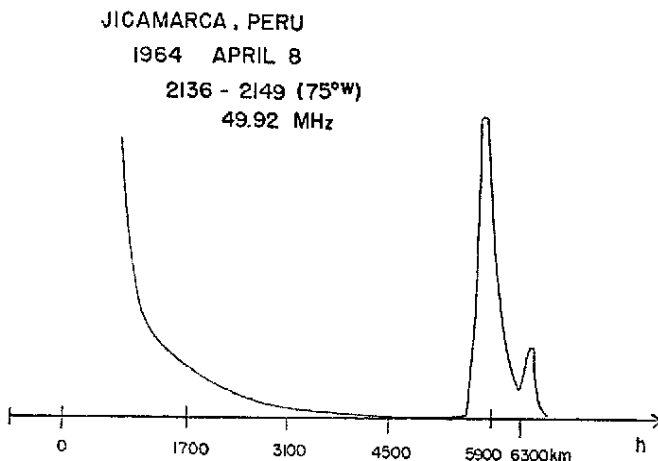
Fig. 1 — The detected voltage received as a function of radar range on the night of 8 April 1964. The tail of the F-layer is shown at the left. The remainder of the F-region echoes have been blanked out.

JICAMARCA, PERU
1964 MAY 21
00^{h}06^m (75^{ow})
49.92 M Hz

O ⊢ 450 km
150
pulse
resolution
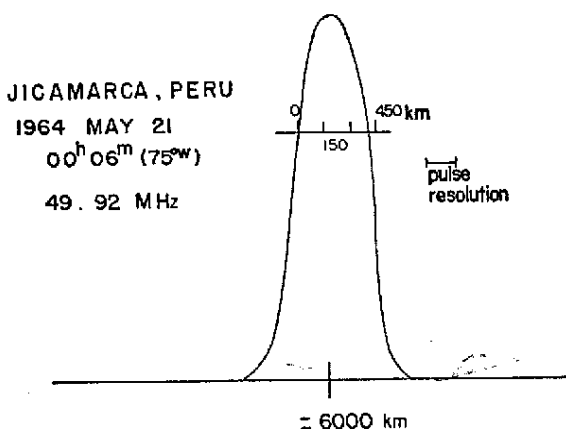
≈ 6000 km

F. 2 — Details of the echo-intensity versus height on 21 May 1964.

It is presumably impossible to achieve orthogonality between the Jicamarca antenna beam and magnetic field lines 6000 km above Jicamarca, and the angle between them is estimated at about 87°. The echoes presumably originated from field-aligned or horizontally aligned irregularities, and have not been observed since the months cited. The presence of coherent echoes indicated that there was an irregularity structure in the 6000 km region comparable to the 6-meter wave length of the exploring radar.

SYNCHROTRON RADIATION MEASUREMENTS AT JICAMARCA

by

D. T. Farley

Jicamarca Radar Observatory, Lima, Peru

On August 25-26, 1965 the amount of synchrotron radiation reaching the earth at a frequency of 50 MHz was measured. One quarter of the large crossed dipole array at Jicamarca was used as the antenna. The beam-width was about 2°. The signals from the two orthogonal linear polarizations were fed into separate receivers. Assuming the synchrotron radiation to be linearly polarized, with the plane of polarization at an angle α to the plane of polarization corresponding to receiver A, the voltage imputs to receivers A and B can be represented as follows:

$$V_A = V_{NA} + V_s (\cos \alpha) + \gamma V_{NB}$$

$$V_B = V_{NB} + V_s (\sin \alpha) + \gamma V_{NA}$$

where V_{NA} and V_{NB} are uncorrelated signals due to the randomly polarized cosmic noise, and V_s is the synchrotron noise. The terms involving γ arise from the crosstalk due to lack of complete orthogonality between the antenna polarizations.

After phase detection, the A and B signals are digitized and multiplied together, and the results are summed (see Fig. 1). The uncorrelated signals average to zero after sufficient integration, and we obtain

$$(V_A V_B)^* = \gamma [(V_{NA}^2)^* + (V_{NB}^2)^*] + (V_s^2)^* \cos \alpha \sin \alpha$$

To measure small amounts of synchrotron radiation, it is obviously crucial to have α as small as possible. In this experiment γ was determined to be about 10^{-3}, implying an isolation of the order of 60 db between the two polarization. The observed synchrotron radi-

ation, expressed in terms of temperature, was about $35° \pm 5°K$ at 50 MHz. A significant fraction of this is presumably a residual effect of the Starfish nuclear test of 9 July 1962. However, in future measurements, it may be possible to determine the background radiation from the natural Van Allen belts, as suggested originally by Dyce and Nakada[1]. With the present experimental arrangement, it should be possible to measure synchrotron radiation levels as low as 5-10°K (see Fig. 2).
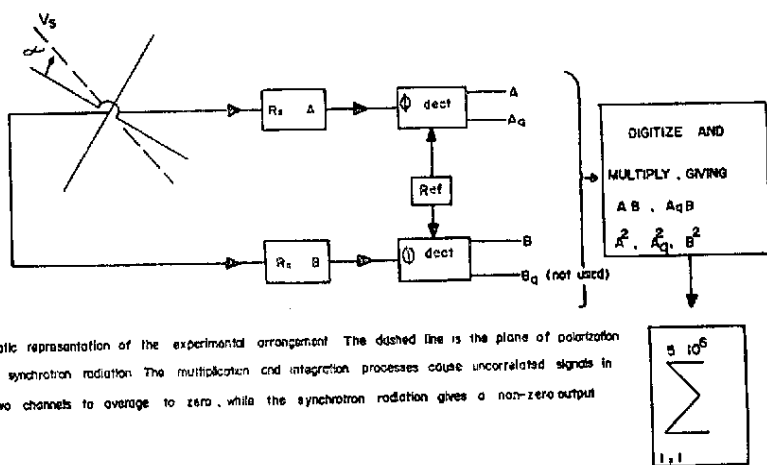
FIGURE 1 Schematic representation of the experimental arrangement. The dashed line is the plane of polarization of the synchrotron radiation The multiplication and integration processes cause uncorrelated signals in the two channels to average to zero, while the synchrotron radiation gives a non-zero output
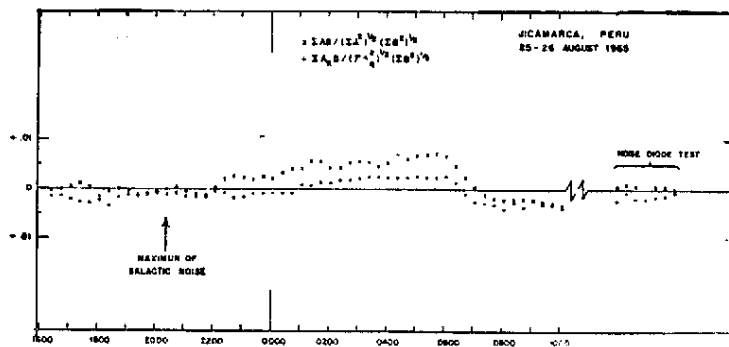
Fig. 2 — Synchrotron radiation observations. The maximum value of the galactic noise at 2000 hrs. was about 45,000°K, whereas the minimum value at 0600 hrs. was about 5000°K. The measurements near 2000 hrs. show that γ, the voltage cross-talk ratio, was of order 10^{-3} or less. The observations near 0600 hrs. give a value of synchrotron noise power of about 35 K. Note the Faraday rotation occurring after sunrise as the ionosphere builds up.

Reference

(1) R. B. Dyce and M. P. Nakada, J. Geophys. Res., **64**, 1163-1168, 1959.

OBSERVATIONS OF SOLAR COSMIC RAY EVENTS DURING

SOLAR MINIMUM

by

A. D. Goedeke, A. J. Masley and G. W. Adams

Space Sciences Department

Douglas Missile and Space Systems Division,

Santa Monica, California

Since February, 1962, numerous increase of solar cosmic ray intensities have been observed directly by polar orbiting satellites and space probes, and indirectly by riometers located at high geomagnetic latitudes. About 30 events have been recorded to date, 10 of which were well defined solar cosmic ray events and were observed by the Douglas riometers located at McMurdo Sound, Antartica and the conjugate point as Shepherd Bay, N. W. T., Canada.

Many of the events were not associated with solar activity. There is some evidence of a 27-day recurrence tendency and that the sun may be continually accelerating low-energy protons from one main active region. These low energy, low intensity events have steep energy spectra with few protons above 10 MeV. They are normally below the threshold of riometer detection, even at very high polar latitudes.

In addition to the proton events, three solar electron events were conclusively identified by Iowa detectors on Mariner IV. This is the first direct evidence for the existence of solar accelerated electrons. The electrons had energies greater than 40 kev with steeply falling energy spectra.

Table I below shows the observed solar cosmic ray intensity enhancements since February 1962. The check-marks identify those events conclusively identified as typical solar cosmic ray events. These events had high enough intensities and energies to be well observed by high latitude riometers.

The unchecked events were low intensity, low energy events below the threshold of riometer detection. The three electron events observed by Van Allen on Mariner IV are not shown.

TABLE I

Solar Cosmic Ray Increases

	FEB 2, 1962		JUL 21, 1963
	FEB 12	√	SEP 14
√	FEB 20	√	SEP 20
√	OCT 23	√	SEP 26
√	FEB 9, 1963		OCT 30
	MAR 9	√	MAR 16, 1964
	APR 5		JAN 8, 1965
√	APR 15	√	FEB 5
√	APR 30		APR 17
	MAY 27		MAY 27
	JUN 14		JUN 1
	JUN 25		JUN 12
			JUN 28
			JUL 3
			JUL 13

Of the 10 solar cosmic ray events we have observed, one was due to a recurring region; 3 to flares east of central meridian; and 6 to flares west of central meridian, although the total number of flares greater or equal to class 2 was somewhat higher for the east side. The east side events were smeared out low intensity events lasting several days. The events for which delay times could be determined were all west side events with delays of 1 to 2 hours, which is the approximate rectilinear travel time of 30 MeV protons. These characteristics are similar to those observed for solar maximum events. In contrast to the similarities between events near solar maximum and solar minimum, some of the differences are: (1) the frequency of occurrence of riometer identifiable events is about 1 event per 4 months near solar minimum, compared to 1 event per month near solar maximum; (2) the peak intensities for the large solar minimum events are down by about 10^4 compared to the largest solar minimum events; and (3) although many of the solar maximum events had substancial intensities for protons in excess of 40 MeV, the solar minimum events reach galactic background at 40-100 MeV. Comments are made on captions of Figs. 1 and 2.

Because of the absence of adequate detection techniques during the previous period of solar minimum, it is highly probable that of the events since February 1962, only 5 could have been recorded.

SOLAR COSMIC RAY SPECTRA
SOLAR MINIMUM
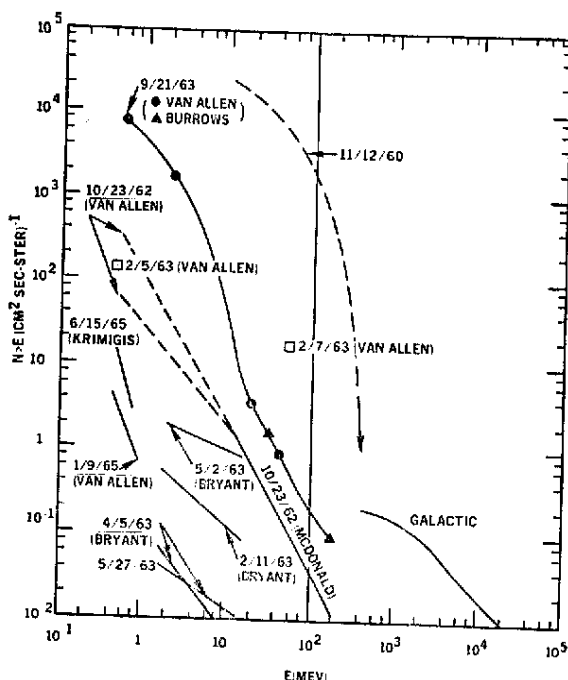
Fig. 1 — Solar proton energy spectra for solar minimum events. The spectra of the November 12, 1960 solar cosmic ray event is shown for comparison. This plot is the Olgivie, et. al. (1962) rocket spectrum adjusted to the maximum intensity of the event. The September 21, 1963 data are from Injun I (Van Allen, 1964) and from Alouette (Burrows, et. al., 1964). The October 23 plot is from a differential spectrum furnished by McDonald (1963) and the two > 500KeV points are from Mariner II (Van Allen, 1963). The two data points denoted by squares are for the February 5, 1965 event and are from Van Allen (1965). The spectra for the February 11, April 5, May 2, and May 27, 1963 events are from Bryant, et al. (1965). The January 9, 1965 event is from Van Allen 1965), and the June 15, 1965 spectrum is from Krimigis (private communication).
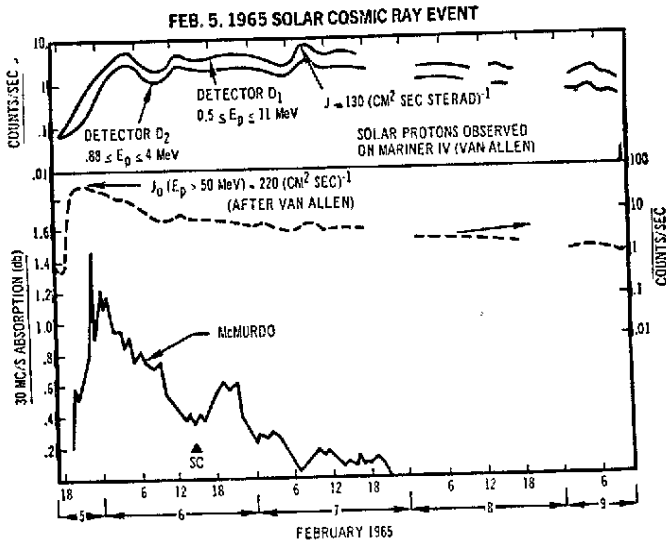
Fig. 2 — Solar cosmic ray event of February 5, 1965-This figure shows the counting rate profiles of the Iowa detectors D_1, D_2, and B, on Mariner IV (Van Allen, et. al., S.U.I. Report 65-5) along with the McMurdo 30 MHz absorption profile. The dashed curve is the counting rate profile of detector B (high energy). The first increase was observed at 1840 UT $\pm$ 10 minutes on Feb. 5, agreeing well with the start time identified by the riometers. The peak omnidirectional intensity by protons with energies greater than 50 MeV was about 220 cm^{-2} sec^{-1} and occurred at about 2200 UT, agreeing closely with the time of peak absorption at McMurdo. There were several relative maxima in the directional intensity of $0.5 \leqslant E_p \leqslant 11$ MeV protrons as seen in the figure. The greatest value was ≈ 130 (cm^2 sec sr)$^{-1}$ at about 0900 UT on February 7.

SUMMARY OF THE SESSION

by

J. P. Dougherty

Department of Applied Mathematics and Theoretical Physics

University of Cambridge, England

A review and seven paper weve given under the title exosphere. There was some discussion of the choice of title, and of the role of exospheric or magnetospheric studies in the equatorial context, but our task here is only to summarize the papers presented.

In his review, Dr. J. O. Thomas outlined the present knowledge of the ionized part of the atmosphere from above the F region (say 1.000 km) to about 5 earth radii, and the theoretical interpretation. For the vast majority of the particles (the thermal ones) a good description is obtained by treating each flux tube separately and supposing the plasma it contains to be in diffusive equilibrium under gravitational, centrifugal and electrostatic forces. The distribution of the electron and the three species of positive ions (H plus, He plus, O plus) throughout space can be calculated if sufficient data is given at a reference level (say 1.000 km). This data is itself still subject to some uncertainty, but information is now being gathered by topside sounders and other means. Whistlers also give independent observations of the electron density, mainly, in the equatorial plane.

On the shell $L \simeq 4$ there is a rapid decline in the electron density and the temperature begins to increase with L. It appears that diffusive equilibrium breaks down for the magnetosphere outside this shell, but this phenomenon is not yet understood in detail.

Many other phenomena, for example whistler guidance, low frequency emissions and Van Allen belts, occur in this region, but were not surveyed in any detail since it was not proposed to spend much time on them at this meeting.

The first four research papers concerned the distribution of electrons and ions in the region of diffusive equilibrium; the remaining three dealt with observations of highly energetic particles. In the first paper Thomas described some of his more recent calculations which extend and improve the theoretical picture mentioned in the review. The rate at which the electron density diminishes with increasing distance has been observed to be greater than predicted by simple theories, but this difficulty is resolved if one introduces a

latitudinal variation of the relative abundances of the three ions as measured at the base level, and a similar variation of temperature at that level. The lighter ions must be more abundant at lower latitudes. This seems indeed to be the case, according to observations by the Alouette and Ariel I satellites.

Mr. J. Angerami's paper suggested that the rapid decline in electron density at L $\simeq$ 4 (known as the "knee") might be explained by supposing that at that level the mean free path of protons is comparable with the distance, measured along the line of force between conjugate points. Below that level, the gas may be treated as a simple fluid with isotropic pressure. Above it the pressure may become anisotropic, or equivalently the particles may all be treated by the well known adiabatic invariant, and a distribution of pitch angles must be specified. It is claimed that this difference in behavior can bring about the "knee".

There followed papers giving observations of electron density at the Jicamarca Observatory. Dr. D. T. Farley described recent electron density profiles to heights of 5000 km, taken by incoherent scatter. The results are in good agreement with whistler measurements. Consistent and clean profiles are obtained, and these are believed to be of good accuracy. Dr. R. Cohen described a remarkable phenomenon as yet quite unexplained, in which a patch of strong irregularities, perhaps roughly similar to spread-F, has occasionally been observed at a height of 6000 km. Some discussion followed, but nobody seemed to have a ready explanation.

Turning to the papers on high energy particles, we should recall that the magnetosphere contains the natural radiation known as the Van Allen belts, the inner belt including protons with up to hundreds of MeV energy, as well as electrons, while the outer mainly of electrons at rather lower energy. This radiation is "trapped" by the earth's magnetic field. In addition, energetic particles may be introduced artificially by a high-altitude nuclear explosion. Such an explosion took place on July 9, 1962. Electrons were trapped on a shell L $\simeq$ 1.2. Their synchroton radiation may be observed by an equatorial station such as Jicamarca, as we heard in detail at the First Symposium in Peru.

Farley reported briefly on results arising from a search for such radiation during the recent manned space flight. The purpose of these observations was to report the occurrence of any such explosion, for the safety of the astronauts, a contingency which did not in fact, arise. However, it was of interest to note that a weak residue of the 1962 radiation is still observable. It also appears that the instrumentation at Jicamarca is now such that the synchroton radiation from the natural Van Allen belts may be measurable soon, provided no further high altitude explosion takes place.

Dr. G. C. Theodoridis presented a paper on some new observations of

flown fairly close to the equator, to a height L $\simeq$ 3.7. It explored the distribution of moderately energetic protons in the range 1 to 4 MeV in a region corresponding roughly to the minimum between the two main belts. The energy spectrum and pitch angle distribution of the protons was recorded, this information may be used to trace the distribution along the lines of force to higher latitudes. Reasonable agreement with the results of other flights was obtained.

Finally Dr. D. Goedeke reported a study of solar cosmic ray events at sunspot minimum. These events are very much weaker than those at sunspot maximum, but it appears that they are not noticeably less frequent.
Another interesting observation was that the onset of such an event was recorded simultaneously by a station on the earth (in the polar cap) and by instruments on the Mariner 4 space probe, which at that time was approaching Mars. This indicates that the stream of solar protons must have been very broad.

VIII — AIRGLOW

VIII — AIRGLOW

(Discussion leader: S. Silverman)

Review Paper

by

F. E. Roach

Central Radio Propagation Laboratory — ESSA, Boulder

Colorado, U.S.A.

The luminescence of the upper atmosphere known as the night airglow has been historically distinguished from the aurora in that the excitation of the emitting atoms or molecules is primarily due to *in situ* reactions rather than extraneous events.

The distribution is based upon the concept of auroral excitation by energetic particles proceeding into the atmosphere under the influence of the geomagnetic field.

There are several different airglows in both the spectroscopic and physical senses. In the so called "chemical kitchen" (70 km to 100 km) emissions are known to be due to hydroxyl (OH), sodium (the D-lines), atomic oxigen (the 5577A lines) and molecular oxygen (the Herzberg bands). There is also a "continuum" of unknown origin which seems to extend throughout the visible spectrum. The 70 to 100 km airglows, especially 5577A and the continuum, combine into an annular type layer visible, for example, to astronauts who see it tangentially with significantly extended path length, thirty-five fold as compared with the zenith path as seen from the earth's surface.

Of particular interest to students of equatorial aeronomy is the 6300A emission from atomic oxygen which seems to originate in the F region of the ionosphere (see Figure 1 for partial energy level diagram of atomic oxygen). The association of this radiation with the rate of recombination in the F region has been established by a series of investigations due in large part to the late Daniel Barbier and collaborators. In two flights from France to South Africa it was shown that the zenith brightness of 6300 A displays two maxima

symmetrical with respect to the magnetic equator strikingly similar to the variation of the ionospheric parameter foF2 which has come to be known as the equatorial anomaly, (see Figs. 2 and 3).

The temporal variations in the brightness of 6300 A in equatorial regions have been shown to be proportional to the rate of recombination in the F-region.

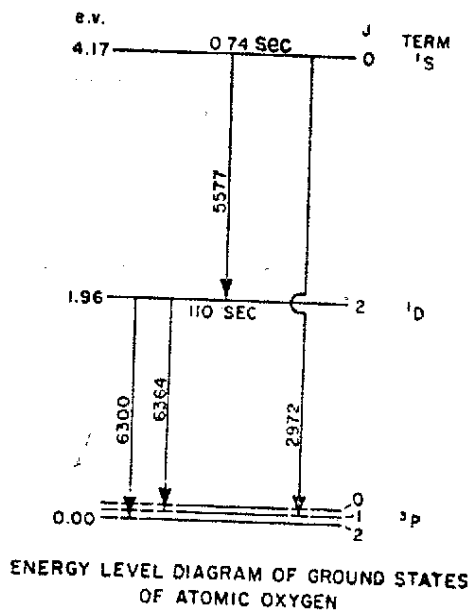ENERGY LEVEL DIAGRAM OF GROUND STATES
OF ATOMIC OXYGEN

Fig. 1 — Energy Level Diagram of Ground States of Atomic Oxygen.
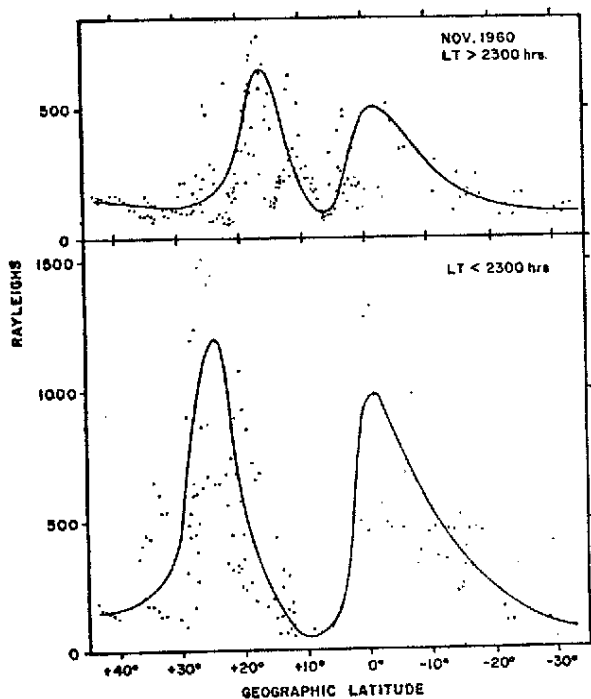
Fig. 2 — Zenith brightness of 6300 A as a function of geographic latitude based on a flight from France to South Africa by Barbier, Weill and collaborators in November 1960.
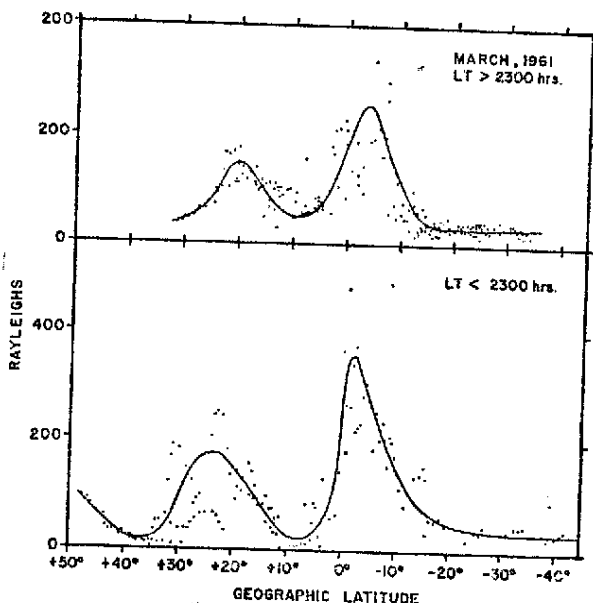
Fig. 3 — Zenith brightness of 6300 A as a function of geographic latitude based on flight from France to South Africa by Barbier, Weill and collaborators in November 1961.

The relationship can be derived from basic physical consideration if the excitation and the recombination are both taken as due to reactions of the type:

$$0 \text{ plus } + 0_2 \rightarrow 0_2 \text{ plus } + 0$$
$$0_2 \text{ plus } + e \rightarrow 0 + 0 \; (^1D_o + {}^1S)$$
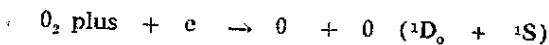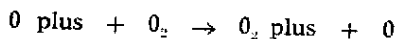
6300A or 5577A

The reactions are, as indicated, energetically capable of exciting atomic oxygen to either the D or the S level and can thus produce either the 6300 A or the 5577 A radiation. It is observed that the equatorial temporal variations in 6300 A are accompanied by concomitant variations in 5577 A with ratio of intensities I [6300]/I [5577] of about 4/1. Another pair of reactions which may contribute to the recombination and to the 6300 A but not 5577 A optical emission is

0   plus + N_2 → NO plus + N

NO plus + e → N   + 0 (^{1}D) ← 6300 A
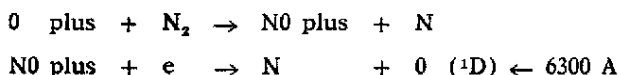
The observation of equatorial airglow contributes not only to our knowledge of F-region recombination processes but also to both the vertical and horizontal structure of the equatorial ionosphere. This is due to a semi-empirical relationship (now known as the Barbier formula) which puts the recombination rate in terms of two parameters (foF2 and h'F) which are measured routinely by students of ionograms:

$$Q_{6300} = A + B (foF2)^2 . \exp [-(h'F-200)/H]$$

where H is a scale height referred to the neutral atmosphere. The success of the formula in predicting 6300A brightness is illustrated in Fig. 4. One of the consequences of the relationship is that it permits the study of a relatively large ionospheric sample covered with good resolution by a single photometer at a given station in contrast with an ionospheric sounder which includes the zenith with poor angular resolution. Although both foF2 and h'F are involved in the Barbier's formula the more powerful term is usually the exponential term involving h'F. In Figs. 5 and 6 are shown photometric maps of 6300 A from observations made in Hawaii. In Fig. 5 we note that the isophotes delineate an "arc" which is oriented along a magnetic parallel. Figure 6 illustrates a situation, often observed, in which considerable detailed photometric structure occurs. The closely spaced isophote lines imply strong local gradients in foF2 and h'F, chiefly the latter. Variations in h'F of many tens of kilometers over a horizontal distance of a few tens of km indicate a highly corrugated ionospheric structure. Under conditions such as those of Fig. 6 the ionograms become very complex but their interpretations can be rationalized in part, at least, by their study along with that of the photometric isophote maps.
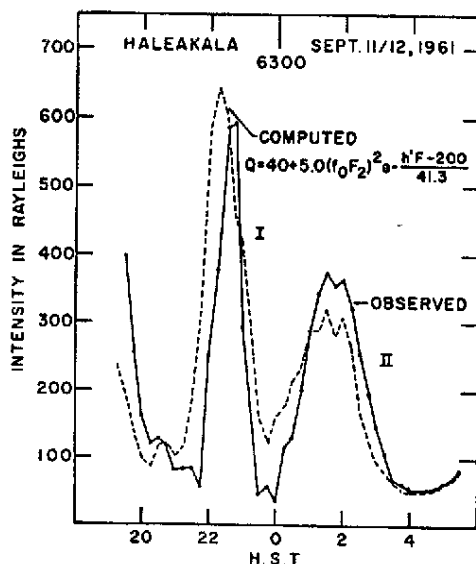
Fig. 4 — Temporal variation in the Zenith brightness of 6300 A at Haleakala (Maui, Hawaii) for 11-12 Sept. 1961. Dashed curve illustrate the calculated brightness for comparison with the solid curve (observed).
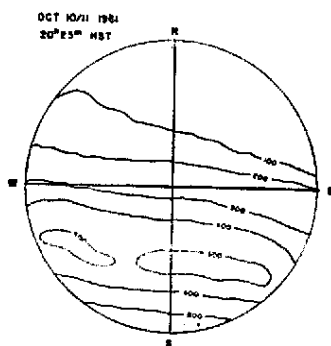
Fig. 5 — Isophote map showing existence of a 6300 A are from observations at Haleakala (Maui, Hawaii).
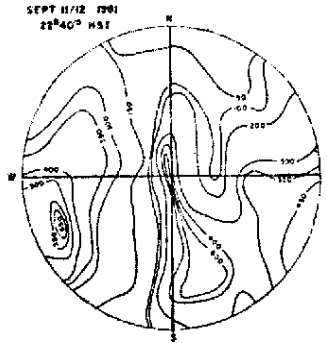
Fig. 6 — Isophote map showing detailed structure of 6300 A patterns.

References

1. Barbier, D., G. Weill and J. C. Glaume, Ann Geophys. **17**, 305, 1961.

2. Barbier, D., F. E. Roach and W. R. Steiger, J. Res. NBS, **660**, 145, 1962.

RECENT RESULTS OBTAINED BY D. BARBIER

IN THE EQUATORIAL AIRGLOW

by

G. Weill

Institut d'Astrophysique de Paris, France

(Paper not available)

SOME RECENT STUDIES OF TROPICAL AIRGLOW

ENHANCEMENT

by

T.E. VanZandt, W. R. Steiger, F. E. Roach, V. L. Peterson

and R. B. Norton

NBS — Boulder Laboratories, Boulder, Colorado

It is shown that the Barbier formula assumes:

1 — No deactivation of O (^{1}D);

2 — The rate of loss of electron is proportional to the electron concentration;

3 — The neutral temperature is independent of height and time;

4 — The normalized electron concentration, $N(h)/N_m$ is a function of $(h-h_m)$ only, and

5 — h is given by h'F + constant.

It is then shown that the Barbier formula can be improved to

$$Q = B \ \beta_0 \ \exp \ [-(h_m-h_0)/H] \ N_m \ H$$

where B is a constant, β is the linear loss coefficient at h, and H is the scale height of O_2. This formula relaxes assumptions (3) and (4) to:

3'. The neutral temperature is independent of height.

4'. The normalized electron concentration is a function of $[(h-h_m)/H]$ only.

Also, assumption (5) can be improved by

5'. $h_m = h'$ (f = 0.815 foF2)   or
      h_m = a function of M 3000

It is shown that at Maui, Hawaii, the emission calculated using the full theory of emission and electron concentration profiles inferred from ionograms agrees well with the observed emission (Fig. 1). However, there is a small amount of emission (0-100 Rayleighs) which is uncounted for by the theory.
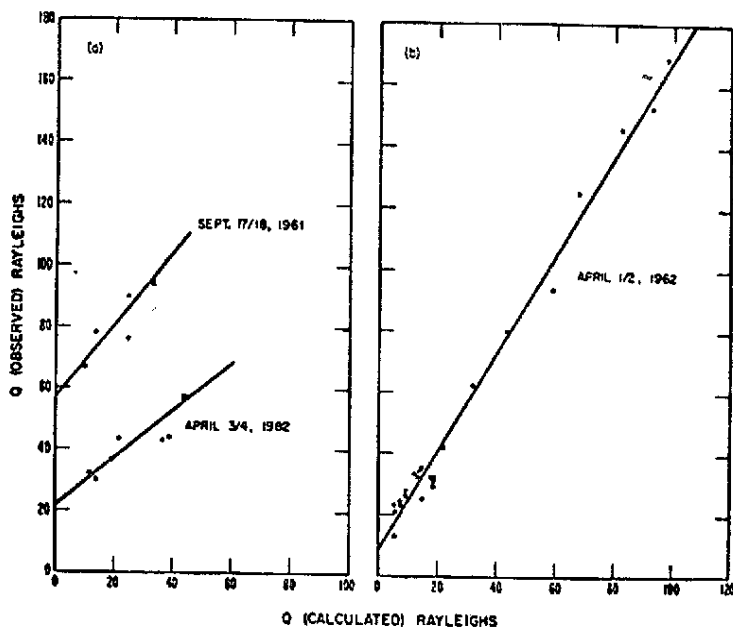
Fig. 1 — Calculated versus observed emissions for Maui, Hawaii.

From a comparison of sweeps of the 6300 and 5577A emission it is inferred that the ratio [n? of excitations of O (¹D) per recombination] / [ditto O (¹S)] lies between 3 and 4.

Maps of the vertical intensity of tropical atomic oxygen airglow enhancements are described. Frequently, the enhancements are in the form of NS fingers, with very little enhancement between. The fingers are often only 200 km apart. They last for 2-3 hours, disappear, and then frequently resurge, in almost the same locations several hours later. The enhancements in the zenith at Maui are mostly due to changes in height of the ionosphere. This implies a strongly corrugated ionosphere during enhancements.

THE 6300 A [OI] AIRGLOW EMISSION: CALCULATED

INTENSITIES FOR THE AMERICAS

by

S . M . Radicella

Universidad de Tucumán, Argentina

(Paper not available)

SOME RELATIONS BETWEEN THE NOCTURNAL VARIATION OF

AIRGLOW 5577 A AND foF2 AT LOW LATITUDES

by

P. D. Amgreji

Physical Research Laboratory, Ahmedabad 9, India

The mean nocturnal variation of 5577 A green airglow intensity at Indian stations during IGY-IGC are compared. The stations Srinagar (34°N), Naini Tal (29°N) and Mt Abu (25°N) show a gradual increase of the intensity until midnight followed by a steady decline. The stations at Poona (19° N) and on the ship Soya (5°N to 5°S during its journey in the Indian Ocean) showed two maxima near 2100 and 0300 hours. The double maxima in the nocturnal variation are found to be less separated with increasing latitude and finally converge to a single maximum at about midnight at 30°N latitude suggesting meridional movements of the green airglow cell. The general trend of the nocturnal variations of the airglow intensity and of foF2 are similar.
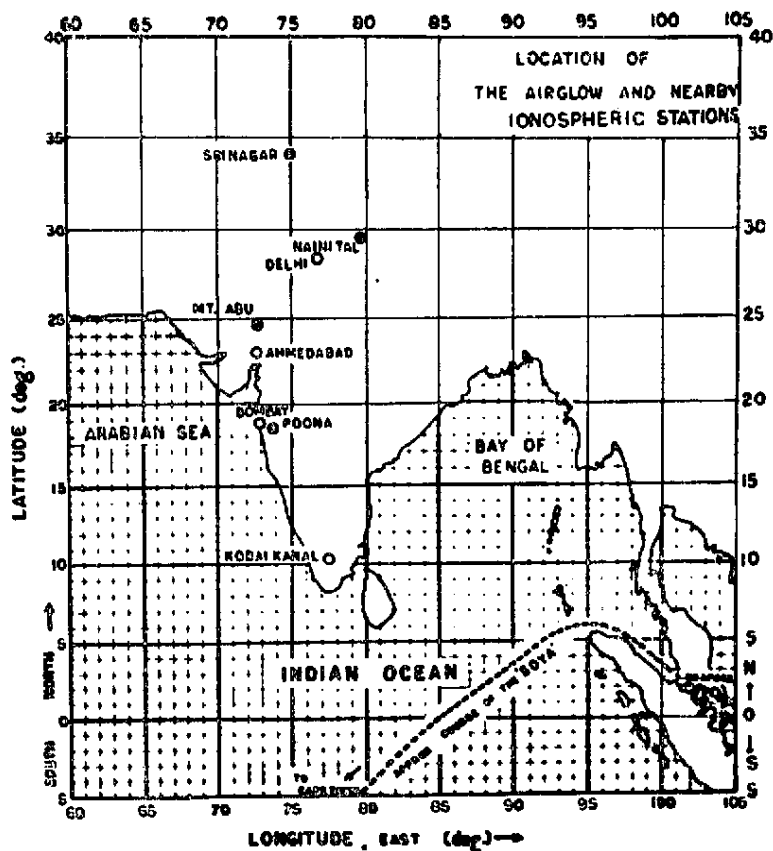
Fig. 1 — The locations of airglow (filled circles) and ionospheric (open circles) stations in India.
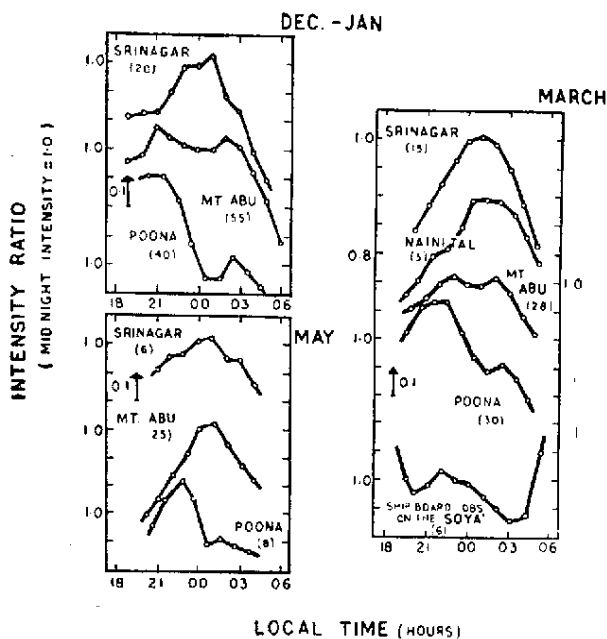
Fig. 2 — Mean nocturnal variations of the nightglow 5577 A emission at various latitudes in the Indian zone during IGY-IGC.
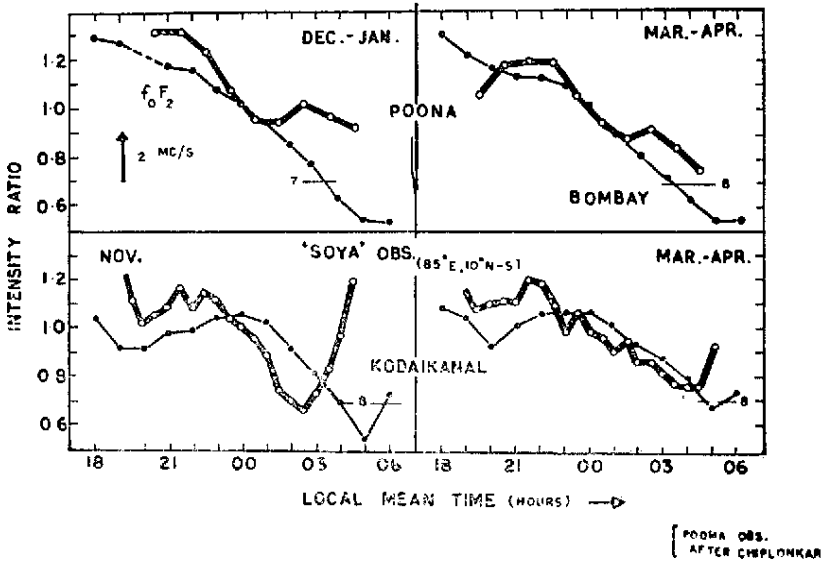
Fig. 3 — The mean nocturnal variation of the airglow 5577 A emission
(open circles) and foF2 (filled circles) at Poona and on
board the Soya.
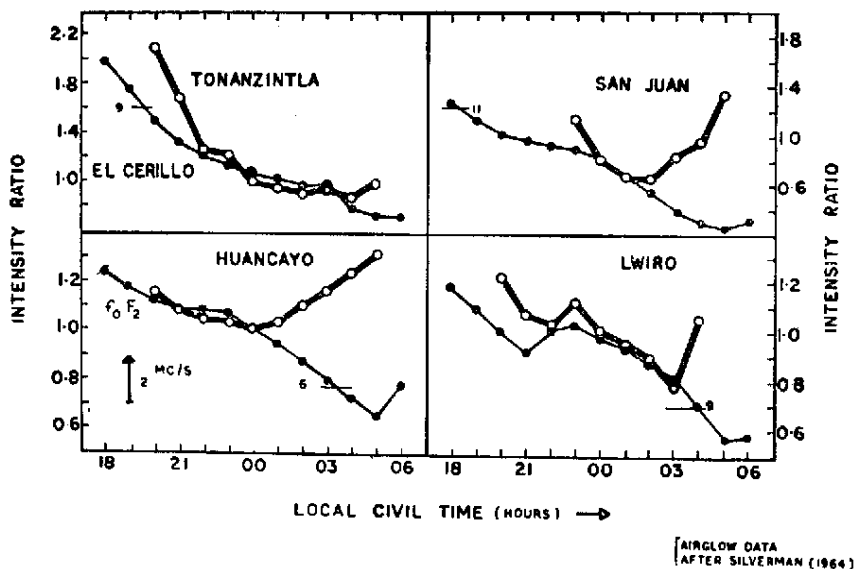
Fig. 4 — The mean nocturnal variation of the airglow 5577 A emission (open circles) and foF2 (filled circles) at several equatorial and near equatorial stations.

AIRBORNE NIGHT AIRGLOW MEASUREMENTS IN THE SOUTH ATLANTIC MAGNETIC ANOMALY*

by

T. P. Markham

Air Force Cambridge Research Laboratories

and

R. E. Anctil

Lowell Technological Institute

It has been suggested by Cole (J.G.R., **66**, 3064, 1961) and Gledhill and Van Rooten (Nature, **196,** 973-975, 1962) that the precipitation of electrons in the South Atlantic anomaly region should result in a considerable enhancement of the airglow emissions in this region. Measurements of the night airglow 5577 A and 6300 A [OI] lines were made in the South Atlantic magnetic anomaly from an Air Force KC-135 Aircraft. The data does not show any intensity enhancement over that found outside the anomaly region.

WORLD-WIDE OPTICAL EFFECTS IN THE

EARLY HOURS OF SC STORMS

by

G. Weill and J. Christophe-Glaume

Institut d'Astrophysique de Paris, France

The occurrence of bright auroral displays and the expansion of the auroral zone towards the equator during the main phase of geomagnetic storms have long been recognized. Two distinct optical effects which occur during the initial phase of the storms were recently identified.

a) At SC time an aurora of moderate intensity develops at the auroral zone and rapidly expands towards the poles. Seen from inside the zone the display has the characteristic spectral features of aurora, intensities in the kR range, and a blanket like appearance. The intensity peaks approximately 45 minutes after SC. This effect does not extend appreciably outside the zone.

b) At middle and low latitude stations a synchronous effect is observed on airglow. The effect is conspicuous on the 5577 A [OI] line intensity, while the other airglow radiations are not appreciably enhanced. Peak effect intensities, of the order of 20 Rayleighs, are reached 45 and 70 minutes after the SC at Haute Provence and Tamanrasset respectively.

About two hours after the SC the intensity of 5577 A [OI] increases again and is known to correlate with $\triangle H$ during the main phase.

THE 5577 [OI] AIRGLOW EMISSION INTENSITY DURING THE HOURS IMMEDIATELY PRECEDING AND FOLLOWING THE SUDDEN COMMENCEMENT OF A MAGNETIC STORM

by

S. M. Silverman

Air Force Cambridge Research Laboratories

Bedford, Mass., U.S.A.

and

W. F. Bellew

Northeastern University, Boston, Mass., U.S.A.

A preliminary study of more than 30 cases at Sacramento Peak, New Mexico confirms the existence of an increase in the 5577 A [OI] airglow emission intensity following the sudden commencement of a magnetic storm noted by Glaume (Annales de Géophysique, 1965). The delay time of the intensity maximum is of the order of one hour following the SC similar to that observed at Haute Provence and Tamanrasset, and the intensity increase is of the same order of magnitude. In contra distinction to the other stations, however, our data indicate that the effect begins some hours prior to the onset of the SC. Data from other stations is needed to define the phenomenon more definitely.

SUMMARY OF THE SESSION

by

S. M. Radicella

Universidad Nacional de Tucumán, Argentina

Seven papers were presented in this session. These were devoted primarily to the study of either the tropical arc of the 6300 A red line emission or the 5577 A green line emission.

Dr. G. Weill presented the last results obtained by the late Dr. D. Barbier of the behavior of the red line in equatorial and sub-equatorial regions in Africa and also some modifications of the original Barbier formula that empirically relates airglow emissions and ionospheric parameters. With the improved equation a better fit is obtained. On the same line Dr. VanZandt presented a paper by himself, Steiger, Roach, Peterson and Norton where it is shown that the Barbier formula can be improved by using, among other factors, a better ionospheric height parameter, either hmax or M (3000). These authors have observed that at Maui the photometer is looking at a very dynamic and corrugated ionosphere and mention the importance of the comparison between the fine structure of the red line emission and the features that appear on the ionograms. Radicella had shown some results on the possibility of predicting the red line behavior on a world wide basis using ionospheric data and the original Barbier formula.

Weill and Christophe-Glaume and also Silverman and Bellew found a very interesting phenomenon: the increase of the 5577A green line emission following a magnetic sudden commencement. This increase is of the order of ten percent and its duration is of some hours. A latitudinal variation of the phenomenon may occur. A paper by Markham and Anctil presented by Dr. Silverman shows that no increase of the intensity of airglow emissions is observed in the region of the South Atlantic magnetic anomaly.

Dr. Rastogi presented a paper by Amgreji where a possible correlation between green line emission and foF2 data for stations in India is discussed. An apparent latitudinal movement of the green line airglow was found by Amgreji.

IX — LOW LATITUDE CURRENT SYSTEM INCLUDING THE

ELECTROJET AND MAGNETIC VARIATIONS

IX — LOW LATITUDE CURRENT SYSTEM INCLUDING THE

ELECTROJET AND MAGNETIC VARIATIONS

(Discussion leader: A. T. Price)

REVIEW ON CURRENT SYSTEMS

by

S. Matsushita

HAO, CRPL and UC, Boulder, Colorado, U.S.A.

Sq Current Systems

As known very well, the external (overhead) and the internal (induced within the earth) current systems are responsible for Sq variation. Cain and Neilson (1963) obtained an external Sq current diagram by U. S. Weather Bureau machine-mapping technique using spherical harmonic coefficients given by Chapman (1919) (see Fig. 1). By the so-called numerical method Price and Wilkins (1963) showed Sq current systems during the Second Polar Year. Using the spherical harmonic method (or analytical method) Matsushita and Maeda (1965) have showed recently Sq current systems during the IGY. A global presentation of a worldwide yearly average external current system viewed from the magnetic equatorial plane at the 0000, 0600, 1200, and 1800 hours meridians is shown in Fig. 2.

Figure 3 presents external Sq current systems near noon in three longitudinal zones for each season with respect to geographic latitude (ordinate) and dip latitude (thin solid curves). The vertical straight lines indicate the noon meridian in each zone, which corresponds to 30°E, 150°E, and 90°W geographic longitude. This diagram shows longitudinal and hemispheric inequalities and gives an idea of how the daytime external Sq current and equatorial electrojet shift during one complete rotation of the earth. The longitudinal inequality of the electrojet seems to be caused by longitudinal differences involved in Cowling and other tensor components of electric conductivity and tidal wind systems. The hemispheric asymmetry was also discussed by Van Sabben (1964).
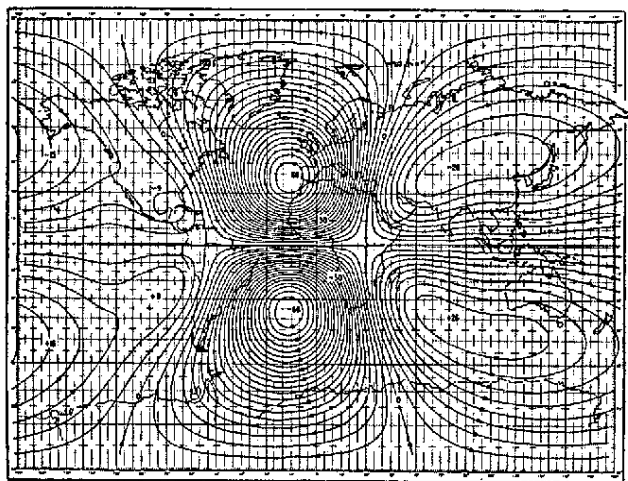
Fig. 1 — The external Sq current system for the mean equinox of 1902. Values of current flow are in kiloamperes with a contour interval of 3000 amperes (Cain and Nielson, 1963).

EXTERNAL SOLAR CURRENT SYSTEMS
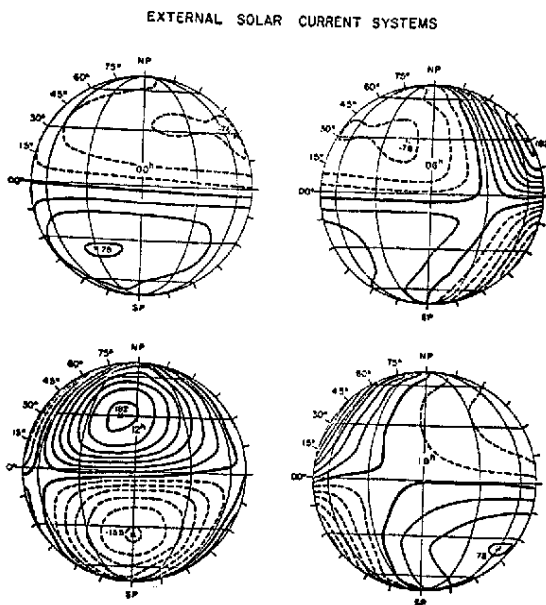
Fig. 2 — A worldwide yearly average external current system during the IGY. The current intensity between two consecutive lines is 25 x 10³ amperes, and the thick solid curves indicate the zero-intensity lines. The thin solid and broken curves show counterclockwise and clockwise current vortices, respectively. The numbers near the cross marks are the total current intensity of these vortices in units of 10³ amperes (Matsushita, 1965).

EXTERNAL Sq CURRENT SYSTEMS NEAR NOON AT EACH ZONE
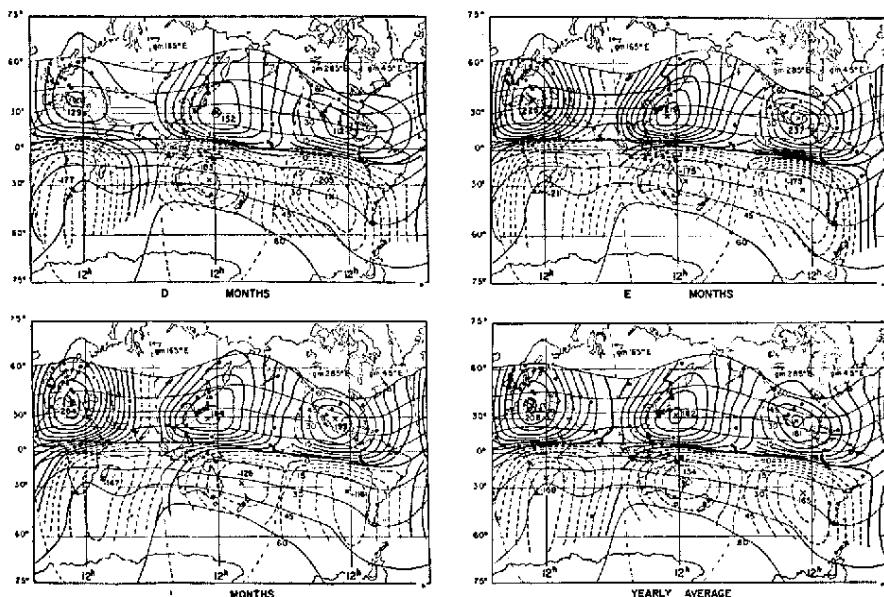
Fig. 3 — External Sq current systems near noon in three longitudinal zones, which are divided with respect to geomagnetic longitudes, 165°, 285°, and 45°E, during D months (January, February, November, and December), E months (March, April, September, and October), J months (May through August) and yearly average, 1958. The current intensity between two consecutive lines is 25 x 10³ amperes and the numbers near the cross marks are the total current intensity in units of 10³ amperes.

Kato (1963) discussed Joule heating caused by the equatorial electrojet and suggested that the electron temperature is raised above the neutral particle temperature by several tens of degrees. Electrical conductivity anomalies in the earth's crust in Peru were discussed by Schmucker et. al. (1964); the Z component shows peculiar variations, and coastal edge effects are apparent.

Rocket observations of the equatorial electrojet over Thumba, India, were made by Maynard et. al. (1965). Figure 4 shows the result at 1000 local standard time on January 27, 1964; the total change in field between apogee (170 km) and 100 km below apogee was about 90 gammas. Somewhat less than one-half of this change, 35 to 45 gammas, should be apparent on ground

records; Trivandrum showed about 30 gamma change. Figure 5-a shows a rocket observation result over Woomera (30°56'S, 136°31,E) at 1137 Australian central standard time on March 12, 1964, and Fig. 5-b shows another rocket observation over Wallops Island (38°N, 75°W) in June and October, 1964.
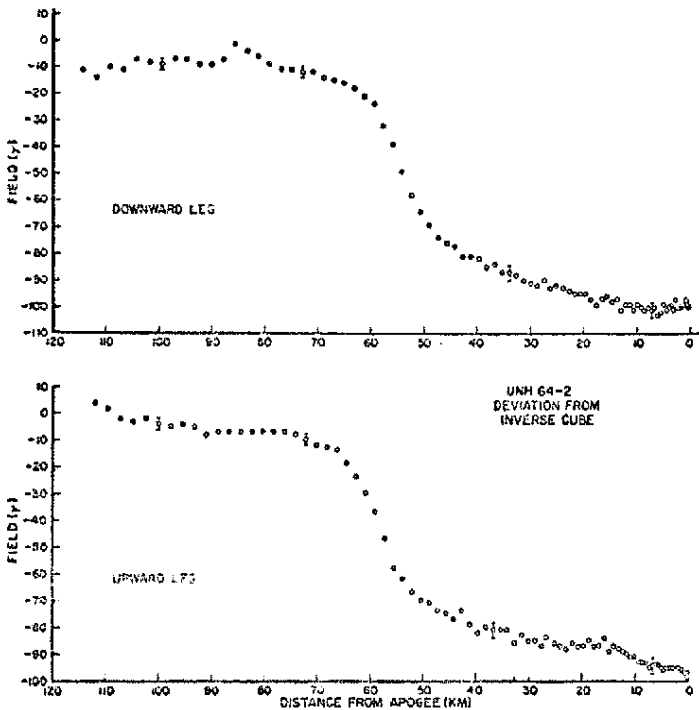
Fig. 4 — The difference between the measured field and Finch and Leaton field in gammas plotted with respect to the distance from apogee (170 km) in kilometers (Maynard et. al., 1965).
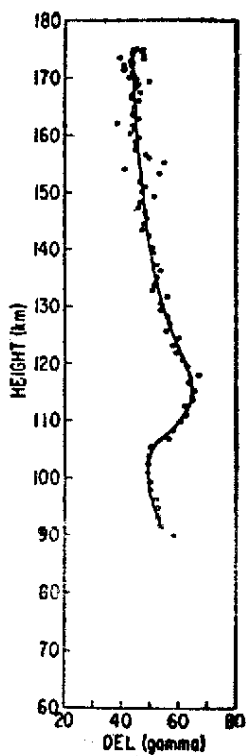
Fig. 5-a — Magnetic discontinuity detected by a rocket observation over Woomera (Burrows and Hall, 1965).
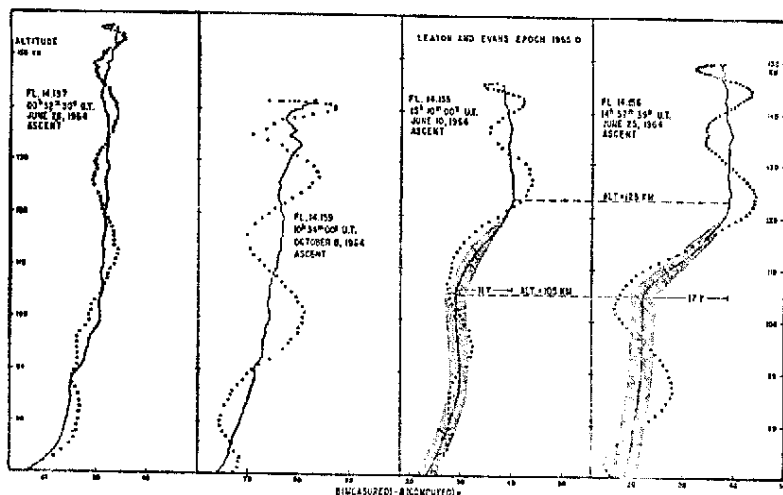
Fig. 5-b — Plots of altitude versus the measured total field minus the comput
ed total field for the ascent portions of all flights; data points taken
at intervals of approximately one second. Solid lines represent the
data corrected for effects due to vehide precession (Davis et. al.,
1965).

L Variations and Current Systems

There are several reports of lunar variations. Onwumechilli (1964) and
Rao and Raja Rao (1963) discussed extraordinary L tides at magnetic equatorial
sessions, and Rastogi (1963, 1964) studied longitudinal inequalities of L vari-
ations. Matsushita (1964) obtained L variations of three magnetic components
at Huancayo during the period from 1922 through 1947. Rao and Rao (1965)
showed L horizontal drifts in the E and F2 region over Waltair, India. The
NS and EW components of the drift in the E region were 7.2 sin (2t + 185°) m/s
and 9.6 sin (2t + 73°) m/s, respectively; these seem to be much larger than
expected from magnetic data.

Concerning the lunar current systems, Matsushita and Maeda (1965)
studied all avaible results of lunar analysis of geomagnetic data from a total
of 37 stations and showed external and internal current systems. Figure 6

presents the external L current systems for a mean lunation during an average activity period for three seasons, which are viewed from the magnetic equatorial plane at 1200 lunar time meridian; these are compared also with solar current systems in Fig. 6.
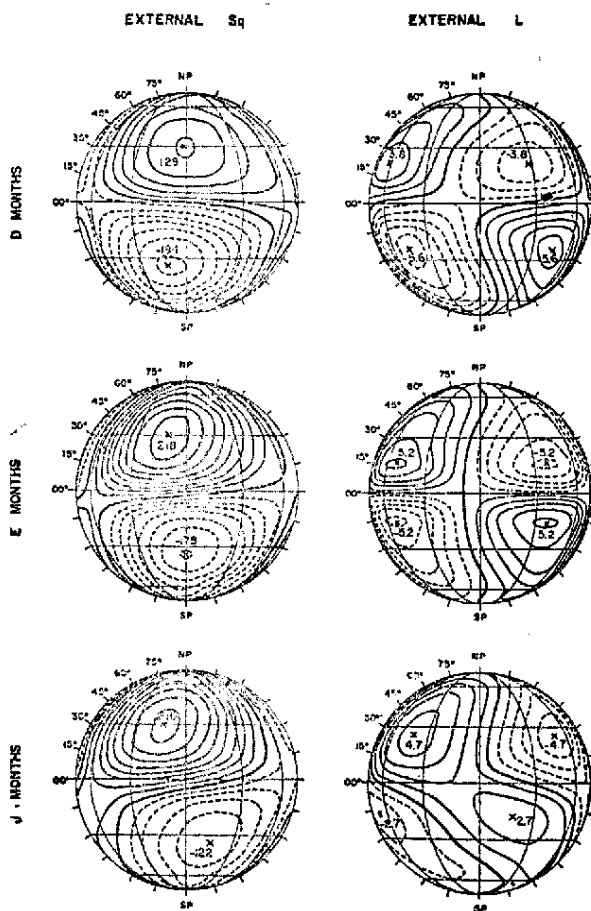
Fig. 6 — The external L current systems for a mean lunation (right) and the external Sq (left) average worldwide in three seasons viewed from the magnetic equatorial plane at 12 h meridian. The numbers near the cross marks are the total current intensity of counter-clockwise (solid curves) and clockwise (broken curves) vortices in units of 10^3 amperes. The current intensity between two consecutive lines is 10^3 amperes for L and 25×10^3 amperes for Sq.

References

Sq Variations:

Burrows, K., and S. H. Hall, Rocket Measurements of the Geomagnetic Field above Woomera, South Australia, J. G. R., **70**, 2149 — 2158, 1965.

Cain, J. C., and J. R. Neilson, Automatic Mapping of the Geomagnetic Field, J. G. R., **68**, 4689-4696, 1963.

Chapman, S., The Solar and Lunar Diurnal Variation of the Earth's Magnetism, Phil. Trans. Roy. Soc. London, A, **218**, 1 — 118, 1919.

Davis, T. N., J. D. Stolarik, and J. P. Heppner, Rocket Measurements of Sq Currents at Mid-latitude, NASA Goddard Space Flight Center Rept., X-612-65-226, 1965.

Kato, S., Joule Heating at the Magnetic Equator, Planet. Space Sci., **11**, 1297-1302, 1963.

Matsushita, S., Global Presentation of the External Sq and L Current Systems, J. G. R., **70**, 1965.

Matsushita, S., and H. Maeda, On the Geomagnetic Solar Quiet Daily Variation Field During the IGY, J. G. R., **70**, 2535-2558, 1965.

Maynard, N. C., L. J. Cahill, Jr., and T. S. G. Sastry, Preliminary Results of Measurements of the Equatorial Electrojet over India, J. G. R., **70**, 1241-1245, 1965.

Price, A. T., and G. A. Wilkins, New Methods for the Analysis of Geomagnetic Fields and their Application to the Sq Field of 1932-3, Phil. Trans. Roy. Soc London, A, **256**, 31-98, 1963.

Schmucker, U., O. Hartmann, A. A. Giesecke, Jr., M. Casaverde, and S. E. Forbush, Electrical Conductivity Anomalies in the Earth's Crust in Peru, Annual Rept. D. T. M., Carnegie Inst., 354-362, 1964.

Van Sabben, D., North-South Asymmetry of Sq, J. A. T. P., **26**, 1187-1195, 1964.

L Variations:

Matsushita, S., Lunar Tides in the Ionosphere, Handbuch der Physik, 49/I, Springer, Verlag, Heidelberg, 1964.

Matsushita, S., and H. Maeda, On the Geomagnetic Daily Lunar Variation Field, J. G. R., **70**, 2559-2578, 1965.

Onwumechilli, A., On the Existence of Days with Extraordinary Geomagnetic Lunar Tide, J. A. T. P., **26,** 729-748, 1964.

Rao, A. S., and B. R. Rao, Lunar Daily Variations of Horizontal Drifts in the E and F2-region, J. A. T. P., **27,** 661-663, 1965.

Rao, K. N., and K. S. Raja Rao, Quiet Day Magnetic Variations Near the Magnetic Equator, Nature, **200,** 460-461, 1963.

Rastogi, R. G., Longitudinal Inequalities in the Lunar Tide and in Sudden Commencement in H Near the Magnetic Equator, J.A T.P., **25,** 343-397, 1963.

Rastogi, R. G., Lunar Tidal Oscillations in the Solar Daily Range of H at Equatorial Stations During IGY-IGC, J.G.R., **69,** 1020-1024, 1964.

REVIEW ON MAGNETIC VARIATIONS

by

S. Matsushita

HAO, CRPL and UC, Boulder, Colorado, U.S.A.

Colorado, U.S.A.

Definition

We need to define a few subject matters in order to avoid confusion among researchers. Some workers define Sq as an absolutely quiet daily variation which is free from the effects caused by solar winds and the magnetosphere. This definition is convenient in discussions of theoretical models, but is difficult to obtain from actual data. Practically speaking Sq can be derived from relatively quiet days in an averaged form as Chapman and Bartels (1940) and Price and Stone (1964) discussed. We can assume that except at high latitudes, thus obtained variation is fairly free from solar wind and magnetosphere effects. We may discuss a quiet-day variation (which can not be called as Sq) from observed data at an individual station on an individual day. In other words, "Sq" indicates an average behavior of quiet-day variation, and an individual "quiet day" variation has a possibility to include disturbance effects slightly larger than Sq variation has. To obtain Sq, five international quiet days are not very favorable as Matsushita and Maeda (1965) discussed.

The so-called equatorial electrojet is a part of the external current system which is reponsible for Sq or quiet-day magnetic variations: the enhancement of the current is caused by a special situation of electric conductivity over the magnetic equatorial zone. To discuss the jet using geomagnetic data however, workers often separated the jet from the middle-latitude current system. This is again a practical method: to discuss day-to-day, seasonal, and sunspot-activity variations of the jet, we should not forget that the jet is a part of the middle-latitude current system (Mayaud, 1963).

There are several equatorial parameters such as geographic, geomagnetic and magnetic equators (de Alvarez, 1963). The best equator to explain geomagnetic variations was discussed many years ago by several workers, such as Hasegawa and Ota (1950). This subject has been revived recently. Chernosky et al. (1964) showed several of the equatorial parameters: dip 0°, horizontal intensity maximum, total intensity minimum, cosmic ray minimum, equinoctial solar perpendicular and so on, as shown in Fig. 1. Price and Wilkins (1963) used mean magnetic latitude, namely an average of geomagnetic and magnetic

latitudes, and Onwumechilli (1964) discussed an effective equator, such as "mean normal equator" or "two-to-one equator". Since we can not get rid of the longitudinal effect whichever one we take, it seems to be simpler to stick with dip latitudes and to obtain longitudinal inequalities which are mainly caused by tidal winds controlled by geographic latitudes and partly caused by differences of main magnetic field intensity, hence electric conductivity, and by induction effects in the ionosphere and below the ground.
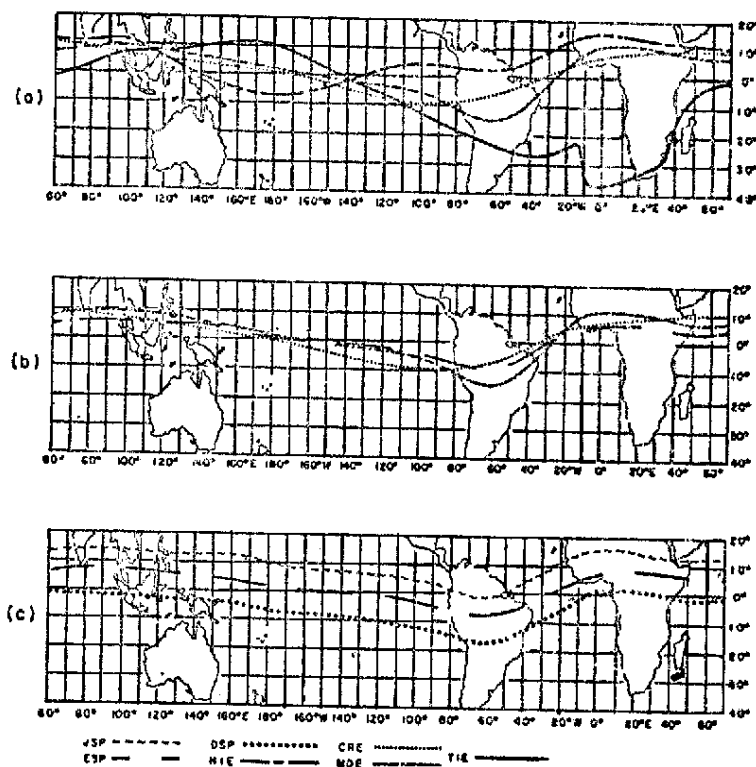
Fig. 1 — Equatorial loci of magnetic field parameters as obtained or derived from U. S. Navy Hydrographic Office charts and cosmic ray minima showing: (a) relationship of magnetic dip equator (MDE), horizontal intensity maximum (HIE), total intensity minimum (TIE), and cosmic ray minimum (CRE); (b) similarity of magnetic dip equator (MDE), cosmic ray minimum (CRE), and equinoctial solar perpendicular (ESP); and (c) seasonal shift in points of perpendicularity derived from parameters related to solar noon altitude and geomagnetic inclination at times of June solstice (JSP), equinox (ESP), and December solstice (DSP). (Chernosky et al., 1964).

Magnetic Variations

Daily and seasonal changes of quiet-day magnetic variations were discussed by Godivier and Crenn (1965) for Tchad, by Ogbuehi and Onwumechilli (1964) for Nigeria, by Osborne (1964) for Peru and by Yacob and Khanna (1963) for India. Daily, seasonal, and sunspot-number variations of H and Z along and near the jet in India, Africa, and the Pacific were studied by Chapman and Raja Rao (1965). A solar control of Sq (H) at Alibag was discussed by Yacob and Prabhavalkar (1965). A detailed study of Sq variations during the IGY was made by Price and Stone (1964) and Matsushita and Maeda (1965).

Recent analysis of stratospheric winds showed an equatorial oscillation of about 26 months, whose largest amplitude is at about 25 km. Stacey and Wescott (1963) suggested that these stratospheric oscillations reach up to ionospheric heights and showed that monthly mean values of H at Alibag and Apia indicate 26 or 27 month periodicity. However, a spectral analysis of the monthly average daily amplitude of H at Huancayo made by London and Matsushita (1963) shows a peak at 6 months indicating an equinoctial maximum; nothing is evident in the neighborhood of 26 months (see Fig. 2). Shapiro and Ward (1964) reached the same conclusion.
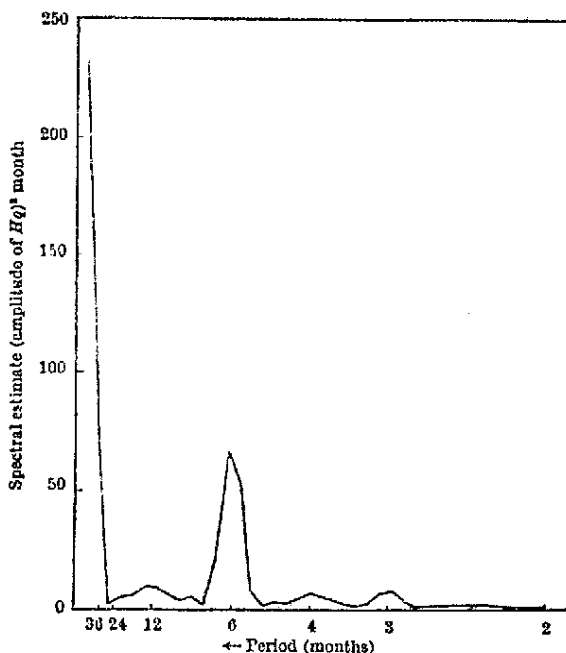

Fig. 2 — Spectral estimate of the monthly average daily emplitude of H at Huancayo, Peru (1922-1959), (London and Matsushita, 1963).

References

Chapman, S. and J. Bartels, **Geomagnetism**, Clarendon Press, Oxford 1940.

Chapman, S. and K. S. Raja Rao; The H and Z Variations Along and Near the Equatorial Electrojet in India, Africa and the Pacific; J. A. T. P., **27**, 559-581, 1965.

Chernosky, E. J., J. M. Collins, and M. P. Hagan, Equatorial Loci of the Earth's Magnetic Field and Cosmic Ray Parameters, Environmetal Res. Papers n° 5, AFCRL-64-174, 1964.

De Alvarez, M. G., Definitions of the Geomagnetic Equator, Geofísica International, Mexico, **3**, 43-48, 1963.

Godivier, R., and Y. Crenn, Electrojet Equatorial an Tchad, Ann. Geophysics, **21**, 143-155, 1965.

Hasegawa, M. and M. Ota, On the Magnetic Field of Sq in the Middle and Lower Latitudes During the Second Polar Year, Trans. Oslo Meeting IATME Bull, **13**, 426-430, 1950.

London, J. and S. Matsushita, Periodicities of the Geomagnetic Variation Field at Huancayo, Peru, Nature, **198**, 374, 1963.

Matsushita, S. and H. Maeda, On the Geomagnetic Solar Quiet Daily Variation Field During the IGY, J. G. R., **70**, 2535-2558, 1965.

Mayaud, P. N., Electrojet Equatorial et Activité Magnétique, Ann. Géophysic, **19**, 164-179 1963.

Ogbuehi, P. O. and A. Onwumechilli, Daily and Seasonal Changes in the Equatorial Electrojet in Nigeria, J. A. T. P., **26**, 889-898, 1964.

Onwumechilli, A., The Effective Equator for Geomagnetic Sq Variations, J. G. R., **69**, 5063-5073, 1964.

Osborne, D. G., Daily and Seasonal Changes of the Equatorial Electrojet in Peru, J. A. T. P., **26**, 1097-1105, 1964.

Price, A. T. and D. J. Stone, The Quiet-day Magnetic Variations During the IGY, Ann. IGY, Pergamon Press, **35**, 64-269, 1964.

Shapiro, R., and F. Ward, Possibility of a 26 or 27 Month Periodicity in the Equatorial Geomagnetic Field, Nature, **201**, 909, 1964.

Stacey, and Wescott, (see London and Matsushita, 1963).

Yacob, A., and K. B. Khanna, Geomagnetic Sq Variations and Parameters of the Electrojet for 1958, 1959, Indian J. Geophys., **14**, 470-477, 1963.

Yacob, A. and A. S. Prabhavalkar, Solar Control of the Amplitude and Phase of the Yearly Mean Sq (H) at Alibag for the Period 1909 to 1960, J. A. T. P., **27**, 73-80, 1965.

THE ANALYSIS OF THE Sq-FIELD IN EQUATORIAL REGIONS

by

G. A. Wilkins

H. M. Nautical Almanac Office, England

Techniques for the interpolation of the components of the Sq-field variations over the earth at any instant of universal time, for the determination of a potential function that represents both the north (X) and east (Y) components, and for the separation of the potential into parts of external and internal origin were described by Price and Wilkins (1963). These techniques were applied to the Sq-field in the J-months of the second International Polar Year (1932-3) but, although the broad features indicated in the maps are believed to be substantially correct, the maps do not show correctly the field in equatorial regions for the following reasons:

     a) The available data did not suggest that the line of maximum range of the horizontal component lies along the magnetic dip equator in all longitudes as is now generally believed;

     b) The mesh used in the analysis was too coarse in the equatorial regions to allow a proper representation of the equatorial peak at midday;

     c) Much of the detail given by the numerical results is not shown in the diagrams reproduced in the paper; in particular the maps of the equipotentials fail to show clearly that the electrojet lies well within the northern current system at each epoch; and

     d) No special attemps (apart from averaging over the twenty international quiet days of each season) were made to eliminate the effects of the L and SD-fields.

The experience gained in that study (which was largely carried out in 1950-1) suggests that the following points should be borne in mind in studies of the Sq-field in equatorial regions:

a) There are no clear criteria by which the effects of the so-called "normal Sq" and "electrojet" can be distinguished, and for most studies of the electrojet effect it seems desirable to consider the field over a range of at least 20° in latitude on each side of the dip equator;

b) The field shows complex changes with latitude, longitude and universal time, and it is unlikely that it can be adequately represented by a small number of parameters; similarly any general interpretations based on only a few characteristics of the observations at a small number of stations are likely to be misleading;

c) The variations in both **X** and **Y** (or **H** and **D**) should be considered together on a regional basis and used to determine the equipotencial lines for the field; such a representation shows clearly the significant changes in direction, as well as intensity, of the field;

d) The variations in the vertical component (**Z**) play a dominating role in the separation of the field into parts of external and internal origin; their peculiar and irregular behavior makes this a difficult task and careful study of the Z-variations over the region is required. Since the rates of change of the field with both time and position are much larger than in temperate latitudes, the relative ratios of the external and internal parts may not be the same as that obtained in early spherical harmonic analyses of the Sq-field.

The method of spherical harmonic analysis is not by itself suitable for analysing the field in equatorial regions since many terms (at least 80) are required to fit adequately the variations at midday at the dip equator. The methods of Price and Wilkins can be used on a regional basis, but a reasonable approximation to the world-wide field must be included if a satisfactory separation of the potential is to be obtained. Alternatively these methods could be applied to the difference between the observed field and an arbitrary, synthetic field based on a spherical harmonic analysis (to low order) of the field in temperate latitudes.

The external current system responsible for the Sq-variations appears to lie in the E-layer of the ionosphere at a height (approximately 105 km) that is small in comparison with the radius of the earth; the equipotentials of the external field therefore correspond closely to

the current lines of the ionospheric system, and can be used to estimate the variations in integrated current density over the layer. Reliable determination of the current function and of the way in which it changes with latitude, longitude and universal time will require a better distribution of observations than is now available, and may demand the development of new techniques for the analysis of the data.

Reference

Price, A. T., and G. A. Wilkins. Phil. Trans. Roy. Soc. London, ser. A, n.° 1066, vol. **256,** pp. 31-98, 12 December 1963.

IONOSPHERIC CURRENTS AND MAGNETIC FIELDS

by

Denis G. Osborne

University College, Dar es Salaam,

Tanzania

This paper surveys the information given by a magnetic station about ionospheric currents. Some applications are made to interpret magnetic data in equatorial regions.

The Northward field, X, due to a uniform sheet of eastward current is given by

$$X = a \, I_y \quad \text{(gamma)}$$

where a is a constant and I_y is the current intensity in the eastward direction in A/km. For an ionospheric current sheet at 100 km with an induced image current at -600 km we have $a \approx 1$ as shown by Chapman and Bartels (1940). The earth's curvature has only a small effect on the calculated value for a. If the eastward current intensity varies with northward distance linearly, as shown in Fig. 1, the same relation holds with I_y as the intensity at the overhead point. Approximately 70% of the field X due to an infinite uniform current sheet at 100 km comes from current flowing in an ionospheric element 400 km square with sides north and east, centered above the magnetometer. It follows that a magnetometer records current fluctuations in approximately this area of the ionosphere.

The Eastward field, Y, is given similarly by

$$Y = a \, I_x,$$

where x represents northward direction. If the earth rotates under a quasi static current system the rate of change of a component with time is a measure of its eastward space gradient. Thus

$$dY/dt = (dy/dt) (dY/dt) = a (dy/dt) dI_x/dy$$

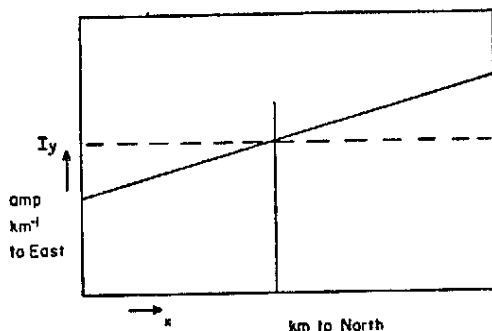The rotation speed dy/dt is about 1,600 km/hour at the equator.

Figure I: Eastward current intensity against distance north.

The Vertical field, Z, contrasts with the horizontal components It is due to differences in ionospheric currents rather than their mean value; it senses currents at a distance from the magnetometer rather than overhead; and it measures the difference between external and internal contributions rather than their sum. Small differences in the earth conductivity can produce large differences in the expected vertical field. For the current model in Fig. 1:

$$Z = bdI_y/dx = cdX/dx$$

where **b** and **c** are constants.

The vertical field due to both components of current may be written in terms of current gradients or field gradients as:

$$Z = X_x - Z_y = c (dX/dx) - cdY/dy = b (dI_y/dx) - bdI_x/dy$$

Magnetometer values for X, Y and Z thus give information about the currents I_x, I_y and about their space gradients. To extract this information from magnetograms it is necessary to choose a base-line of supposed minimum ionospheric current and to choose measures of hourly values and range. There is need for an agreed recommend-

ation on these definitions to facilitate comparison of results between different investigators. (Definitions were given when the paper was presented but were discussed at another conference session. The proposed definitions are not repeated here to avoid confusion).

Equatorial applications are illustrated by four examples.

1. A recognition of the extent of the ionospheric system detected by a magnetometer is important for comparisons between radio and magnetic data: for example of Es with H.

2. An examination of the observed maximum gradients dX/dx and dY/dy in Peru suggests that for these $Z_x/Z_y \approx 100$ and that $Z_y < 1$ gamma, contrary to the suggestions of Knapp and Gettemy (1963).

3. Forbush and Casaverde (1961) give values for magnetic variation in Peru. The value for D suggest that a net current flows into the equatorial electrojet from the north in the mornings, and out of the jet to the south in the afternoons.

4. The values for H and D from Peru enable currents entering and leaving ionospheric current element in the electrojet region to be calculated. These are represented by a, b, c, d, in Fig. 2. It is found that $a + b + c \neq d$, such that an excess of current enters the elements in the morning and leaves it in the afternoon. Subsequent discussion suggested that this apparent contradiction may be explained as an induction effect. To do this would seem necessary to suppose induction currents that give different values of the constant **a** for the X and Y components.
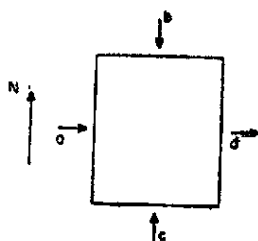

Figure 2 :   a + b + c ≠ d, showing unbalance of currents in ionospheric element.

References

Chapman, S. and J. Bartels, "Geomagnetism", Oxford University Press, 1940

Forbush, S.E. and M. Casaverde, "Equatorial Electrojet in Peru", Institute of Washington, Publication 620, 1961.

Knapp, D. G. and J. W. Gettemy, J. of Geophys. Res., **68**. 2411, 1961.

A THREE DIMENSIONAL MODEL OF DENSITY DISTRIBUTION OF IONOSPHERIC CURRENT CAUSING PART OF QUIET DAY GEOMAGNETIC VARIATIONS

by

A. Onwumechilli

Department of Physics, University of Ibadan, Nigeria

A three dimensional current density distribution depending on two coordinates is described. Let the axes of the cartesian coordinates (x, y, z) point to the north, east and downward respectively and let the current flow west to east. The variation of current intensity (A/km) in the x-direction is represented by

$$J_x = J_{xo} \, a^2(a^2 + \alpha \, x^2)/(a^2 + x^2) \tag{1}$$

Here J_{xo} is the intensity at $x = 0$, $y = 0$, a is a constant length and α is a dimensionless constant. If α is negative the current has a return path in the horizontal plane. See Figs. 1-3.

The vertical variation of intensity can be represented by a similar equation. Combining both equations, we get that current density in A km^{-2} is given by

$$J = J_o \, [a^2(a^2 + \alpha x^2)/(a^2 + x^2)^2] \, [b^2(b^2 + \beta \, z^2)/(b^2 + z^2)^2] \tag{2}$$

This equation implies that the density is constant along any line parallel to the y-axis and depicts current lines as infinitely long in the eastward y direction. In low latitudes say, the model is applicable around noon when the Sq current is very nearly eastward. The width 2 w, and thickness 2 d, are given by

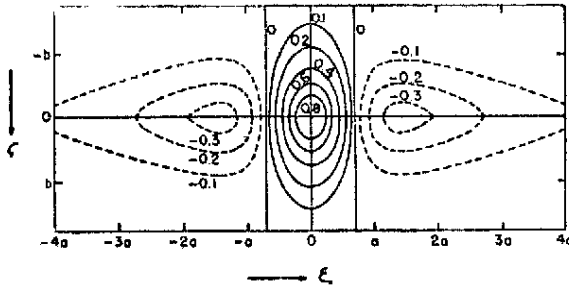$$2w = (2 a / \sqrt{-\alpha}) \text{ and } 2d = (2 b / \sqrt{-\beta}) \tag{3}$$

Fig. 1 — Contours of equal density in units of J/J_o for the case of equal **a** and **b** and with $\alpha = -2$, $\beta = 0$. Solid lines for eastward current and broken lines for westward current.
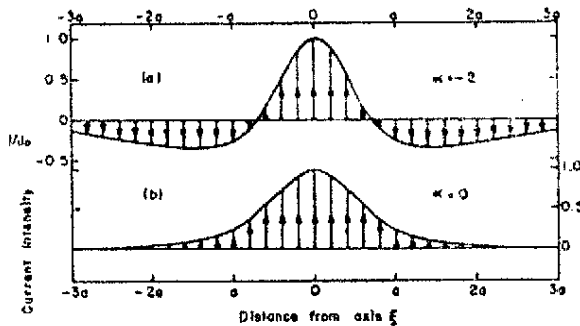

Fig. 2 — Illustrating two kinds of current flow covered by the three-dimensional model: (a) for negative α the return current is antiparallel to the forward current and (b), for positive and zero α the current is unidirectional.
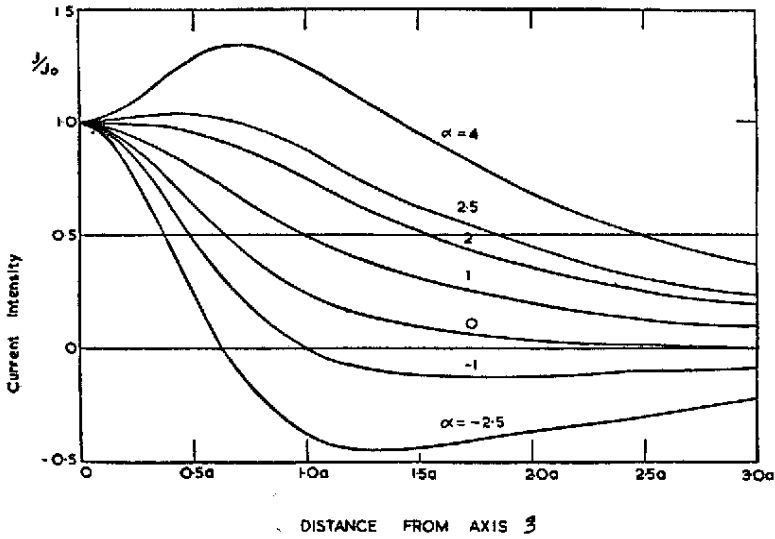
Fig. 3 — Eastward current intensity as a function of distance from the axis for the current model, for some values of α.

THE MAGNETIC FIELD OF A CURRENT MODEL FOR PART OF

GEOMAGNETIC Sq VARIATION

by

A. Onwumechilli

Department of Physics

University of Ibadan, Nigeria

The magnetic field due to a three-dimensional model of density distribution of ionospheric electrical current is derived. Working approximations are obtained and discussed. Examples are given to illustrate its application and to show that it fits the electrojet and the worldwide Sq (X) at the equinox near noon.

Figure 1 shows how well the field of the model fits Sq (X) obtained from a worldwide net of stations on the 22 September 1958.
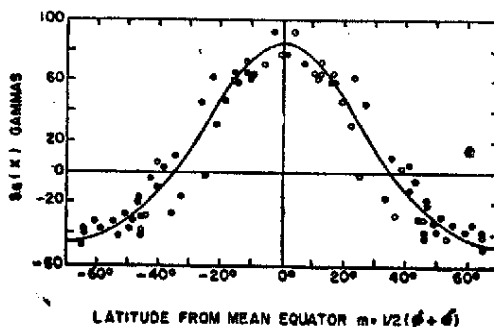

Fig. 1 — Showing how the field of the three-dimensional model fits the worldwide Sq (X) on 22 September 1958.

Earlier analysis of electrojet field measurements used the simple uniform band model. For comparing the present with the earlier model, two sets of electrojet data have been fitted with both models. Measurements made in Nigeria during September equinox 1962 have been fitted in Figs. 2 and 3. Figures 4 and 5 are for measurements in Peru. Undoubtedly the new model is to be preferred to the uniform band model.

The model has also been used to fit one vertical current density measurement made in India by Cahill et al. (Fig. 6). Here too the performance of the model is satisfactory.

Fig. 2 — Showing the extent to which the uniform current band model fits electrojet field derived from observations (circles) in Nigeria at equinox 1962 (after Ogbuehi, 1964).

Fig. 3 — Showing how the field of the three-dimensional model fits observed jet X and Z respectively (points) during equinox 1962 in Nigeria (Ogbuehi, 1964).
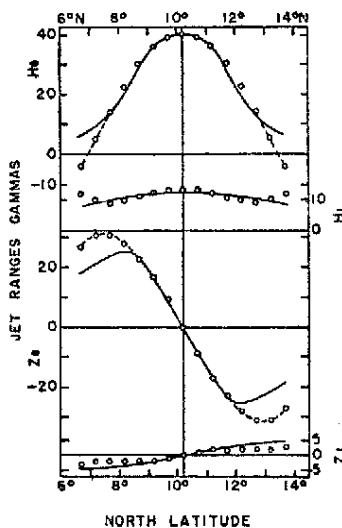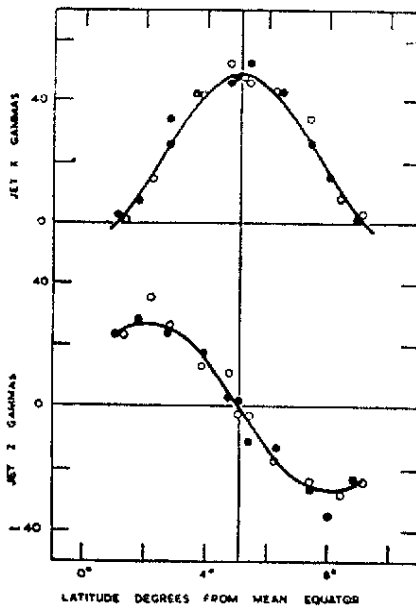
Fig. 4 — Showing the extent to which the uniform current band model fits electrojet field derived from observations (points) in Peru at equinox 1957 (after Forbush and Casaverde, 1961).
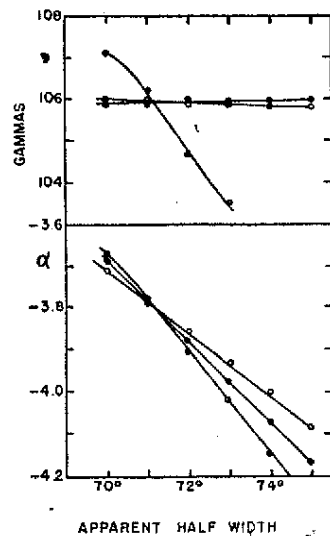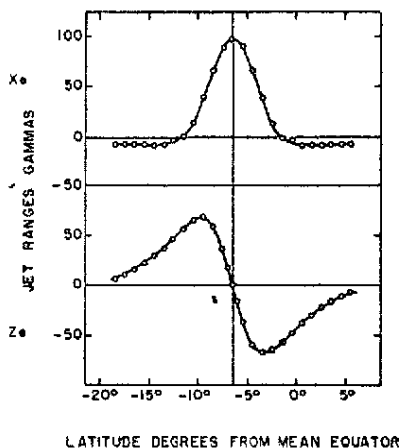
Fig. 5 — Showing how the field model fits electrojet field derived from observations (points) in Peru at equinox 1957.
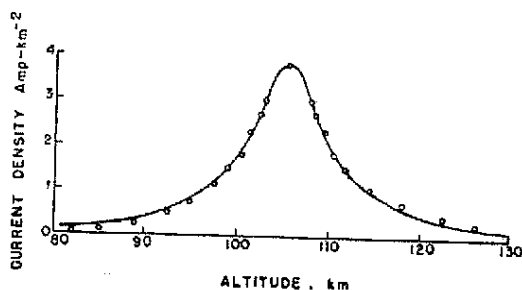
Fig. 6 — Showing how the new model fits vertical current density profile of the electrojet in India.

References

1. Forbush, S.E., and M. Casaverde — Carnegie Inst. Wash. Publ. 620, (1961).

2. Ogbuehi, P. O. and Onwumechilli — J. Atmosph. Terr. Phys. **26**, 889-898, (1964).

3. Maynard, M.C., L.J. Cahill, Jr., and T.S.G. Sastry, J. Geophys. Res., **70**, 1241-1245, (1965).

SUNSPOT ACTIVITY EFFECT ON Sq

by

S. Matsushita

HAO, CRPL and UC, Boulder, Colorado, U.S.A.

The magnetic potential of the Sq field can be shown as

$$\Omega = C + R \, \Sigma \, \Sigma \, C^m_n \cos (m \lambda + \alpha^m_n) \, P^m_n \, (\theta)$$

where λ is the local angular time measured from midnight, θ is dip colatitude, R is the earth's radius, and P^m_n is the Schmidt's function. The coefficients C^m_n were given by various workers for different sunspot periods; Schuster (1889) for 1870, Chapman (1919) for 1902 and 1905, Benkova (1940) for 1933, Hasegawa and Ota (1950) for 1932-1933, and Matsushita an Maeda (1965) for 1958. The main terms of the external origin C^m_n, which are equal to $0.715 \, C^m_n$, were plotted with respect to the sunspot number and the electron density of the E region (see Fig. 1). Here foE was approximated by $(4.38 \times 10^{-3} \, S + 3.0)$, where S is the sunspot number.

To show an average behavior of the external Sq field, a weight mean $(4 \, C^1_2 + 2 \, C^2_3 + C^3_4)/7$ was also plotted in addition to the main terms: diurnal coefficient C^1_2, semi-diurnal coefficient C^2_3, 8 hour period coefficient C^3_4, and a main seasonal term C^1_1. All these values show a fairly good linear distribution and are approximated by straight lines as are indicated in Fig. 1.

The distribution of C^3_4 is approximately C^3_4 (in gammas) $= 1.28 \times 10^{-5} \, N_e$.

In other words the 8 hour period term is proportional to the electron density N_e, hence to electric conductivity. The distributions of other terms show that the value of this coefficient increases more than the increase of N_e or electric conductivity. A probable explanation of this result is an increase of wind speed due to the temperature increa-

se caused by solar activity. In the case of $(4\,\mathbf{C}^1_2 + 2\,\mathbf{C}^2_3 + \mathbf{C}^3_4)/7$. the ratio of the coefficient for the IGY to the coefficient for the Second Polar Year is 2.14 which is 1.37 times larger than the ratio of N_e in these years. In other words the tidal wind speed during the IGY is about 1.4 times larger than that during the Second Polar Year. An estimation of main coefficients for the IQSY based on the current sunspot number is also shown in Fig. 1.
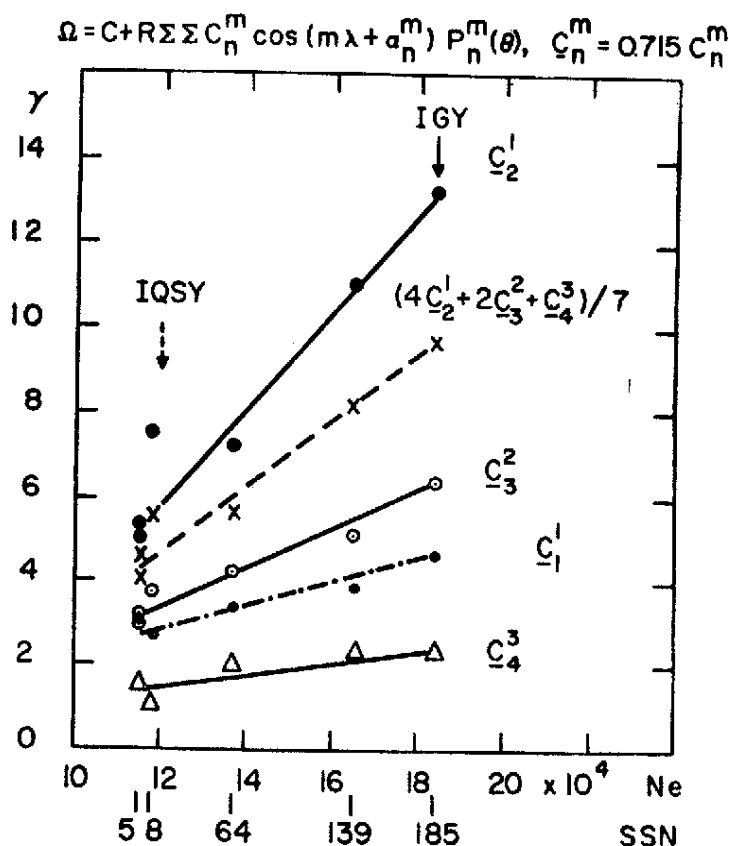

Fig. 1 — Main terms of external origin plotted with respect to sunspot number and electron density in the E region. Also plotted is a weight mean (dashed line).

In the expression $I = I_0 (1 + mS \times 10^{-4})$ given by Chapman and Bartels (1940), $m = 72$ was obtained from the present result of $(4 C^1_2 + 2 C^2_3 + C^3_4)/7$. Van Sabben (1964) obtained $m = 83$ from his study of current intensities. In the recent studies of the equatorial electrojet, Chapman and Raja Rao (1965) gave $m = 78$ at Huancayo for 1922-1932 and 72 for 1933-1943, and Yacob and Prabhavalker (1965) gave $m = 74$ for the diurnal component of H at Alibag for 1905-1960. The sunspot activity effect on Sq current system seems to be generally the same as the effect on the daily amplitude of H in the magnetic equatorial zone.

The ratios of the Sq current intensity in summer to winter and in summer to equinoxes are about 2.5 and 1.4 during the sunspot minimum period (Chapman and Bartels, 1940) and 1.6 and 1.0 during the IGY (a very large sunspot maximum period).

References

Chapman, S., The Solar and Lunar Diurnal Variation of the Earth's Magnetism, Phil, Trans. Roy. Soc., London, A, 218, 1-118, 1919.

Chapman, S., and V. Bartels, **Geomagnetism**, Clarendon Press, Oxford 1940.

Chapman, S., and K. S. Raja Rao, The H and Z Variations Along and Near the Equatorial Electrojet in India, Africa, and the Pacific, J.A.T.P., **27**, 559-581, 1965.

Benkova, N. P., Spherical Harmonic Analysis of the Sq Variations, May-August 1933, Terrest. Mag. Atmosph. Elec. **45**, 425-432, 1940.

Hasegawa, M. and M. Ota, On the Magnetic Field of Sq in the Middle and Lower Latitudes During the Second Polar Year, Trans. Oslo Meeting, IATME Bull.13, 426-430, 1950.

Matsushita, S. and H. Maeda, On the Geomagnetic Solar Quiet Daily Variation Field During the IGY; J.G.R., **70**, 2535-2558, 1965.

Schuster, A., The Diurnal Variation of Terrestrial Magnetism, Phil. Trans. Roy. Soc. London, A, **180**, 467-518, 1889.

Van Sabben, D., North-south Asymmetry of Sq, J.A.T.P., **26**, 1187-1195, 1964.

Yacob, A., and A. S. Prabhavalkar, Solar Control of the Amplitude and Phase of the Yearly Mean Sq (H) at Alibag for the Period 1909 to 1960, J.A.T.P., **27**, 73-80, 1965.

SOME CORRELATION STUDIES IN EQUATORIAL GEOMAGNETISM

by

Denis G. Osborne

University College, Dar Es Salaam, Tanzania

A brief survey is given of recent correlation studies associated with the equatorial electrojet. Some implications of these studies are considered.

The daily horizontal range at the magnetic dip equator may be taken as the sum of a normal contribution (supposedly the range beside the jet) and a jet contribution. Forbush and Casaverde (1961) reported that for Peru the values of these different contributions vary independently from day to day even on quiet days. Subsequent calculations of correlation coefficients between daily ranges have confirmed this independence. A similar result was obtained using values of ranges for Ghana by Osborne (1962) and is shown in the scatter diagram of Fig. 1. Preliminary values for East Africa give a similar low correlation between these parameters. Hence the additional range due to the jet, and the range at a station just beside the jet, are essentially independent as they vary from day to day.
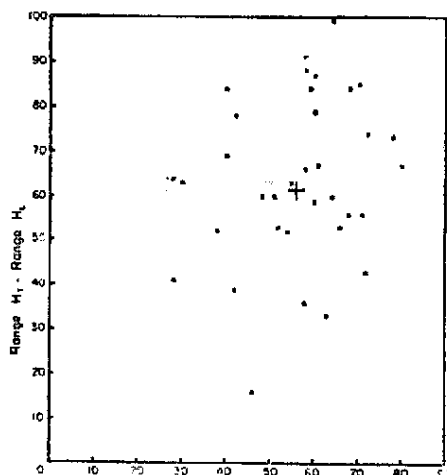

Fig. 1 — Scatter diagram of Normal and Jet ranges for 36 days in Ghana.

Osborne (1965) gives correlation coefficients between daily ranges at seven stations between latitudes of -12.1 and $+64.9$ degrees, taken for twenty days in each of three seasons. Table I shows the means of these seasonal coefficients for selected stations, the value J indicating a jet strength defined as the difference between the range at Huancayo and Talara, and the code letters referring to magnetic observatories in the American sector having the latitudes shown. These values indicate either a large westward drift of current over the northern hemisphere on days when the jet is large, or the drawing in of current to the jet from the northern loop of the quiet day current system on large jet days. This second possibility must cast suspicion on the use of fields just beside the jet as indicative of an undisturbed normal field. It is shown also in this paper that the electrojet in Peru is independent of the position of the northern focus of the quiet day current system. There is some possibility that these calculations are affected by a universal time contribution to the daily variation in the American sector and it would be advisable to repeat them for the European or Pacific sectors and to seek for correlations between jet parameters and ranges in the same geographic hemisphere as the path of the electrojet.

Table I

Correlation coefficients between ranges at

stations shown, values X 100.

Station	Hu	Ta	JS	Tu	Fı
Latitude (degrees)	-12.1	-04.6	18.4	32.4	38.2
Correlation with range at Hu	x	55	-40	-04	-38
Correlation with range "J"	88	08	-47	01	-36

Osborne (1964) showed that the difference between vertical ranges at stations under the jet were correlated very closely with the jet strength, indicating that the variability in vertical range is indicative of a variability in position of the jet axis. However this high correlation requires also that the horizontal ranges on both sides of the electrojet should vary together. Thus the electrojet appears to be an independently varying current embedded in a system of coherent currents. This type of correlation again merits further study.

Wescott, DeWitt and Akasofu (1963) examined the Sq variation in geomagnetically conjugate areas. They give a table showing the position of the northern focus relative to San Juan and of the southern focus relative to Trelew on different days. The northern focus is south of Trelew on 5 of these 22 days. The northern focus is south of San Juan on 9 days, and the southern focus is south of Trelew on all of these 9 days. This is strong evidence that the foci of the northern and southern loops are displaced north or south together on different days.

An examination was made of the correlation between apparent F region drift velocities and magnetic fields in the jet region by Osborne and Skinner (1963). These suggest that the difference field due to the jet is related to F region drift, but this suggestion still waits for further observational test and for theoretical explanation.

In deriving this last relation values were used for different times of the day. Since all the parameters varied fairly regularly with local time the actual correlation coefficients were of little importance, and the information sought was of the form "A is correlated more closely with B than with C".

Recent tentative studies in East Africa suggest that there may be a significant correlation between daytime and nighttime field variability in the equatorial region. These may prove a means of studying these nighttime fields, and of discriminating between their possible causes in local nighttime ionospheric effects or induced currents from distant daytime ionospheric currents on the far side of the earth.

References

Forbush, S. E. and
M. Casaverde   1961   "Equatorial Electrojet in Peru" Carnegie
                                  Inst. Wash., Publ. 620.

Osborne, D. G.   1962   J. Atmosph. Terr. Phys., **24,** 491.

Osborne, D. G.   1964   J. Atmosph. Terr. Phys., **26,** 1097

Osborne, D. G.   1965   J. Atmosph. Terr. Phys., in press.

Osborne, D. G. and
N. J. Skinner   1963   J. Geophys. Research, **68,** 2439.

Wescott, E. M., R.
N. De-Witt and S.
I. Akasofu   1963   J. Geophys. Research, **68,** 6377.

MAGNETIC VARIATION IN EAST AFRICA

by

A. N. Hunter
University College, Nairobi, Kenya

and

D. G. Osborne
University College, Dar es Salaam, Tanzania

A magnetic observatory has been operated in Nairobi (see Table I) since February 1964. Figs. 1-3 show the diurnal variation of the horizontal component H averaged over quiet and disturbed days for the three seasons. Disturbance features include a rise in the early morning hours and a minimum in the early evening. Fig. 4 shows the monthly means of daily ranges on quiet days grouped by seasons. It is surprising that the maximum daily range occurs in northern winter but this may be due to limited observational data.

TABLE I

Station coordinates

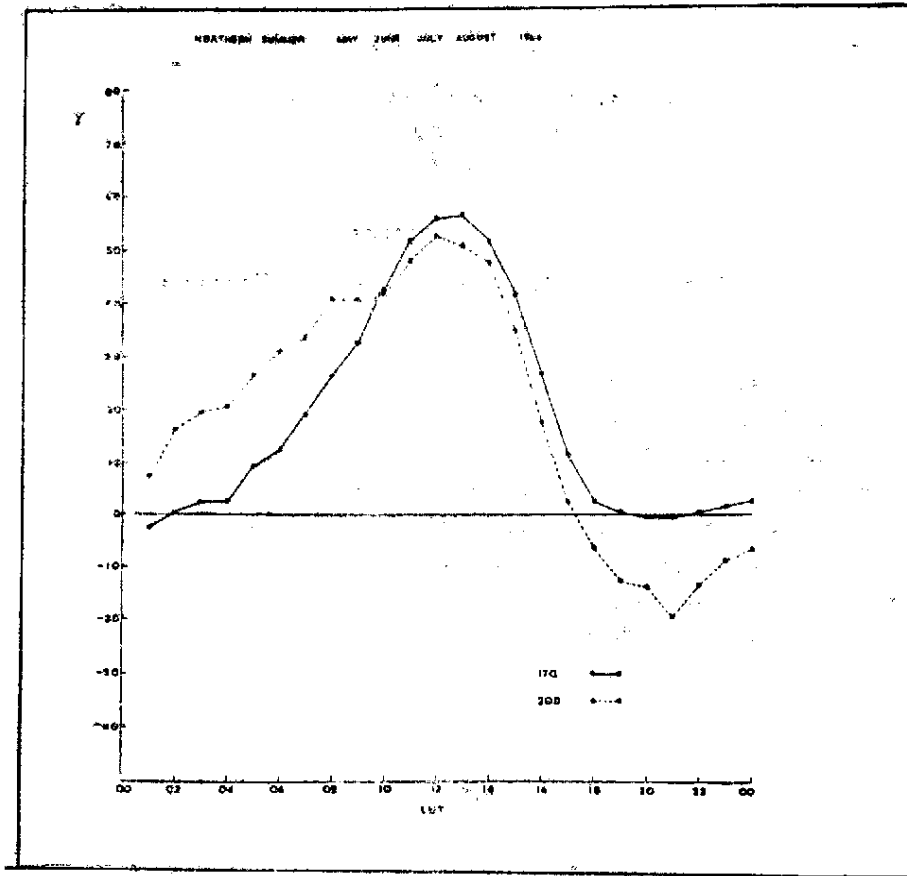| Station	Geographic		Magnetic dip angle
Nairobi	01.3°S	36.8°E	26.9 S
Addis Ababa	09.2°N	38.6°E	01.2 S

Fig. 1 — Diurnal variations of the horizontal component H average for quiet and disturbed days in northern summer.
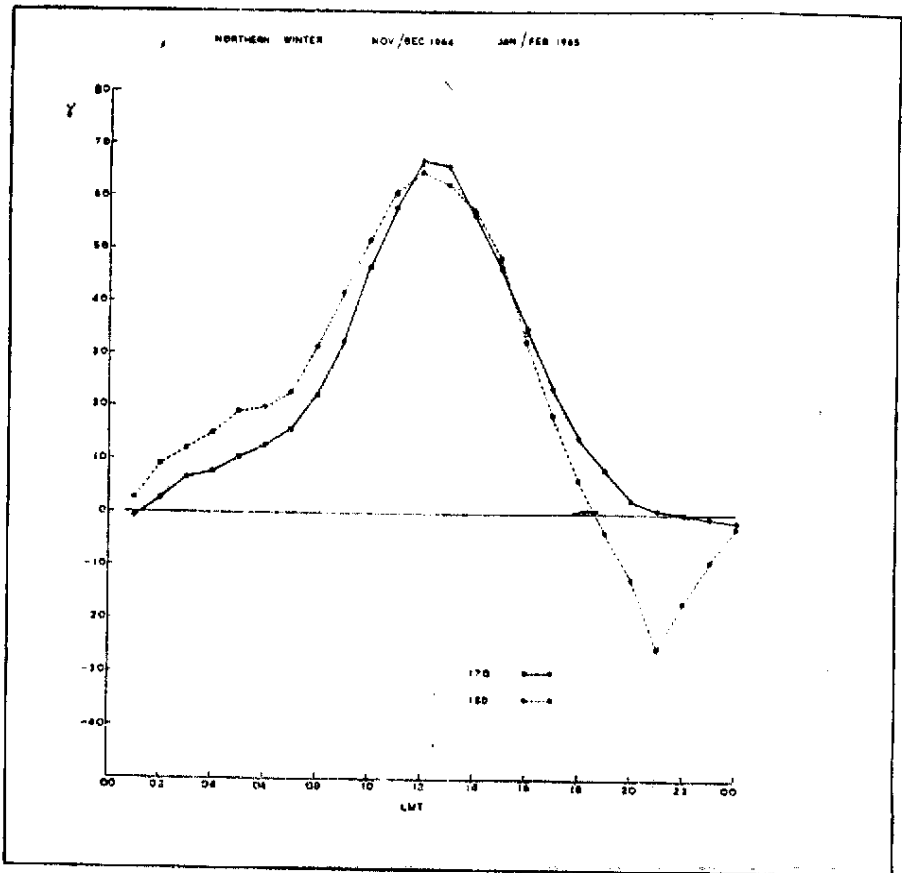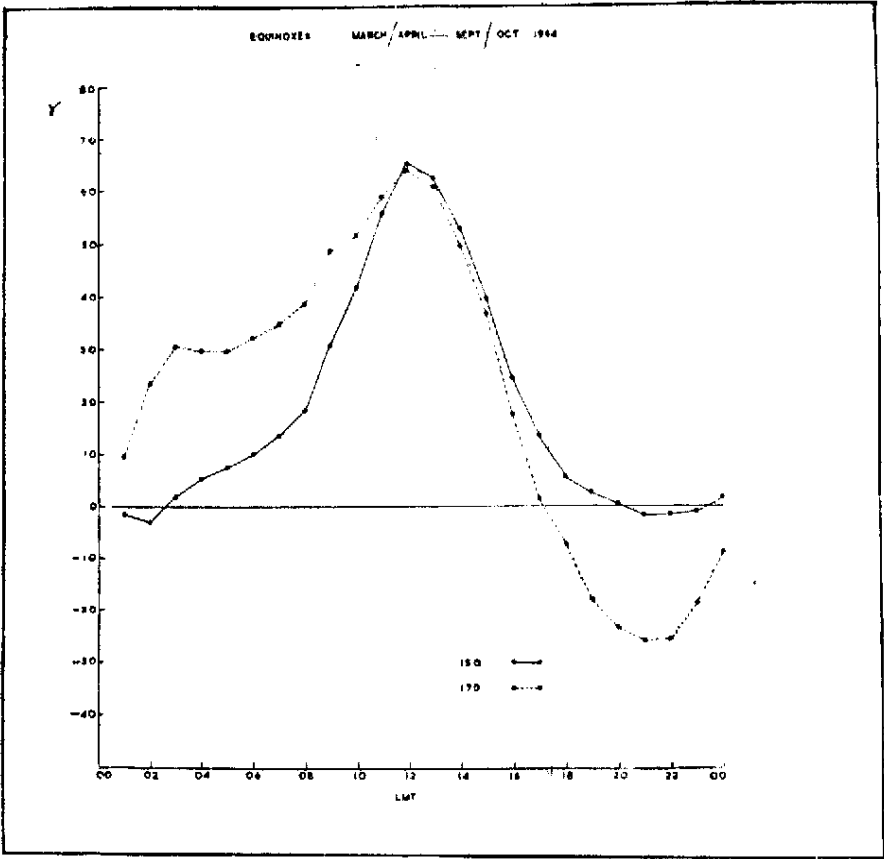
Fig. 2 — Same as Fig. 1 for northern winter.

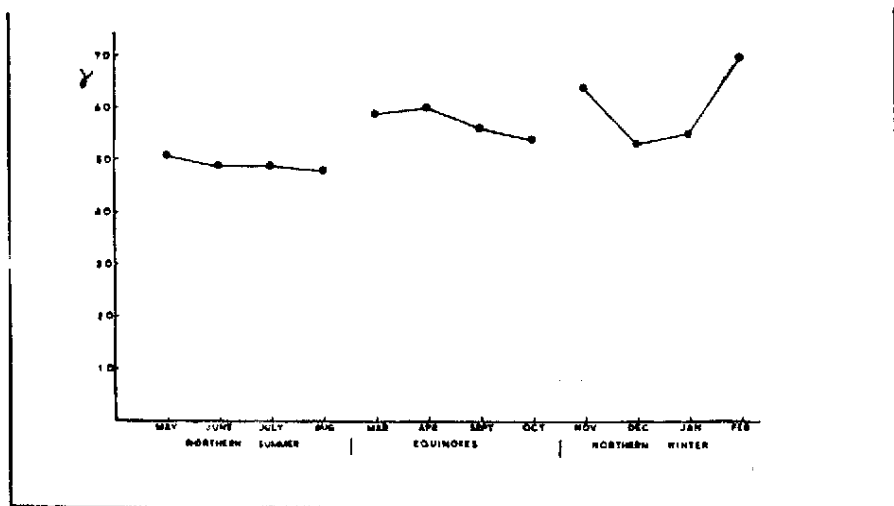Fig. 3 — Same as Fig. 1 for the equinoxes.

Fig. 4 — Monthly means of daily ranges on quiet days grouped by seasons.

Comparisons have been made with the horizontal variation at Addis Ababa for the four months February to May. 1964, the only months for which data from Addis Ababa was available. Figs. 5 and 6 show the variation at both places on quiet and disturbed days in the period. The mean daily range on quiet days at Nairobi is just under 60 gammas, that at Addis Ababa just under 80 gammas. The range at Nairobi is large relative to that of Addis Ababa (Hunter and Desai, 1965). Morning and evening disturbance effects are similar at the two stations but are more pronounced at Nairobi than at Addis Ababa.
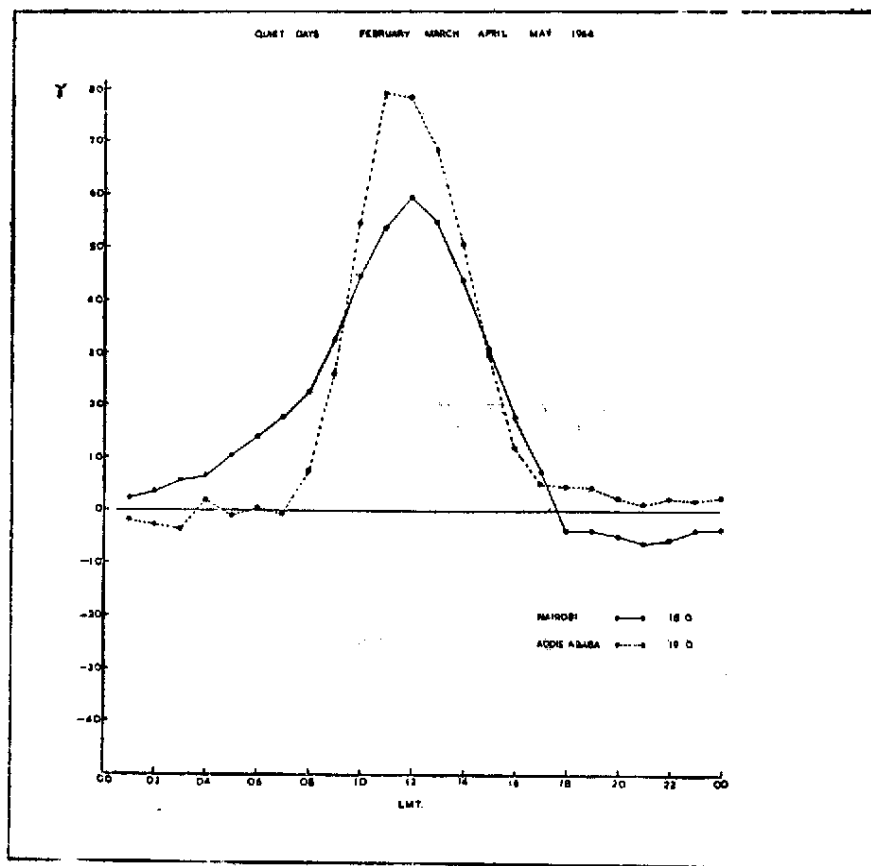
Fig. 5 — Comparison between the horizontal variations in Nairobi and
        Addis Ababa during quiet days.
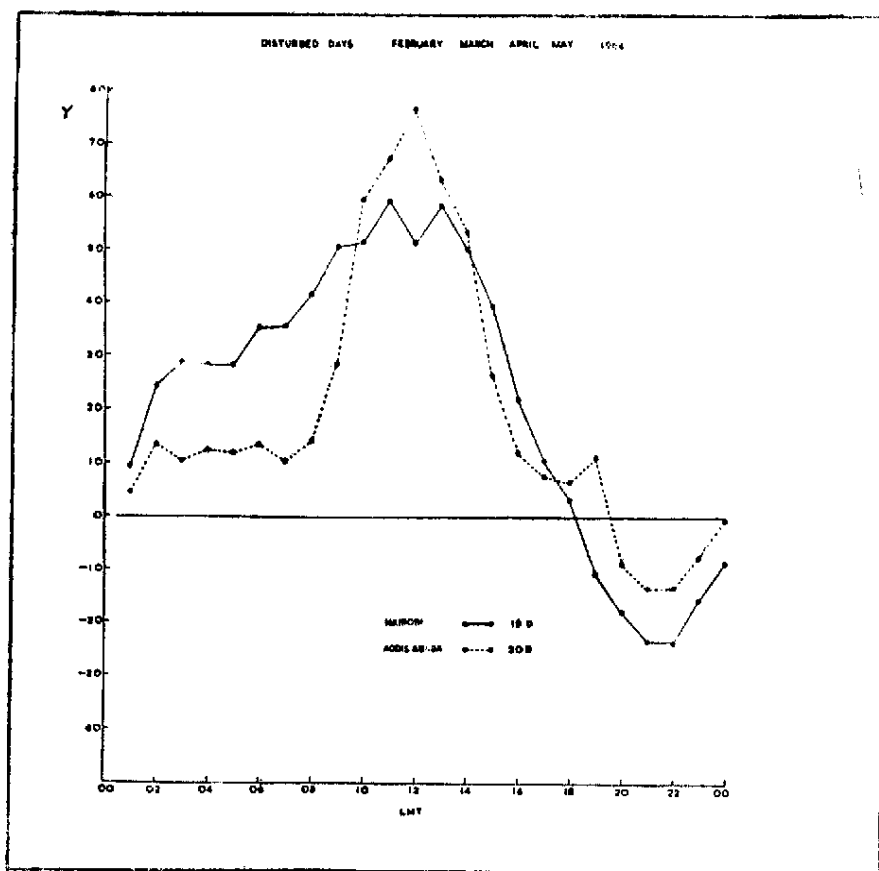
Fig. 6 — Same as Fig. 5 for disturbed days.

The correlation between chosen parameters at Nairobi and Addis Ababa was studied for the twenty quiet days. Hourly values and daily ranges were calculated using the definition given by Osborne (1963) with the same local time of UT plus 3 hours at the two stations. A base value B was defined as the mean for the hours 2400 and 0100 on the night preceding a quiet day (for which the range was measured) and B' as the mean value for the hours 2400 and 0100 on the following

night. Table II shows five linear correlation coefficients between selected parameters. The first two coefficients are similar to those found for similar by situated stations in Ghana and Peru. The third value, shows a low and insignificant correlation between base values on quiet days, although it had been expected that nighttime variability in the horizontal field would be due to distant features such as the equatorial ring current and would be similar at both stations. The lack of coherence in the variations suggests that there is an appreciable local nighttime field. The significant values for these last two coefficients suggests that this method of analysis can yield information about nighttime currents in the electrojet region.

The results in this paper show the importance of continuing these observations in East Africa.

TABLE II

Correlation Coefficients

R refers to daily range of horizontal component

B refers to base value, defined in text, subscripts

a and n refer to Addis Ababa an Nairobi.

R_a	:	R_n	0.53
$(R_a - R_n)$	:	R_n	-0.22
B'_a	:	B'_n	0.20
$(R_a - R_n)$	:	$(B_a - B_n)$	-0.47
$(R_a - R_n)$	:	$(B'_a - B'_n)$	0.40

References

Hunter, A. N. and

Desai   1965   Nature, In press

Osborne, D. G.   1963   J. of Geophys. Res., **68**, 2435.

ELECTROJET PARAMETERS

by

Rosemary Hutton

Ahmadu Bello University, Nigeria

Using data from eight South American observatories varying in latitude approximately 18° on either side of the dip equator, the latitudinal variations of the magnetic elements have been examined for each hour from 0600 to 1800 hours for 30 Quiet Days during the IGY.

The principal deductions which may be made from a study of the $\triangle$ H latitudinal variations ($\triangle$ representing the departure from the mean midnight value) are as follows: —

1) The form of the overhead current in the equatorial zone appears to change considerably both during the course of a single day and also from one day to another, even though these are successive Quiet Days (cf. Figs. 1a-1f). Frequently, a dual jet effect is observed in the early morning and late afternoon hours.

2) The maximum current strength, as represented by $\triangle H_{max}$, also varies considerably from day to day — for example, in the case of the three days illustrated, its values are: —

Date	$\triangle H_{max}$
28/7/58	152 gamma
29/7/58	160 gamma
30/7/58	220 gamma

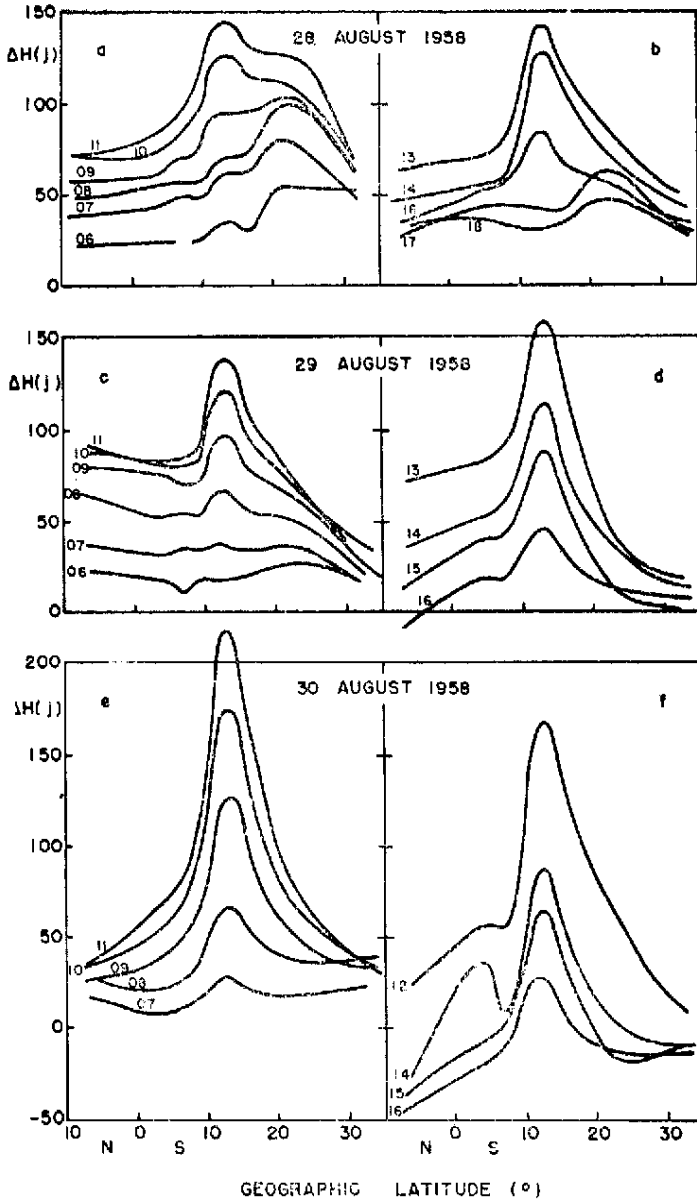On the average, however, the equinoctial values of $\triangle H_{max}$ are greater than at other times of the year.

Fig. 1 (a-f) — The △H latitudinal variations in South America for 3
successive Quiet Days during the IGY.

3) The equatorial current attains its daily maximum value at approximately 1100 hours at a mean latitude in Peru of 13°S, i.e., within the accuracy of this estimation on the magnetic dip equator. At other times of the day, the position of maximum current may occur slightly to the north or south of the dip equator; there is also some support for the suggestion of a small day to day variability in the position of maximum daily current.

4) For certain purposes, it may be useful to consider the equatorial current system as consisting of the superposition of the normal non-equatorial Sq current and a jet current, i.e., $\triangle H = \triangle H_N + \triangle H_J$. The strength of this additional current, $\triangle H_J$, is found to correlate well with the strength of the normal current, $\triangle H_N$, at the dip equator, on any one day, provided allowance is made, as illustrated in Fig. 2, for the fact that the space gradients of $\triangle H$ outside the equatorial region may at times be considerable. The high correlation — in most cases significant at $< 1\%$ level — strongly supports the hypothesis that the equatorial currents form an integral part of the worldwide Sq current system.

Examination of the ratio $\triangle H_J / \triangle H_N$ suggests, however, that the degree of equatorial enhancement varies from approximately 60% in the December solstice to almost 100% in the June solstice and equinoxes.
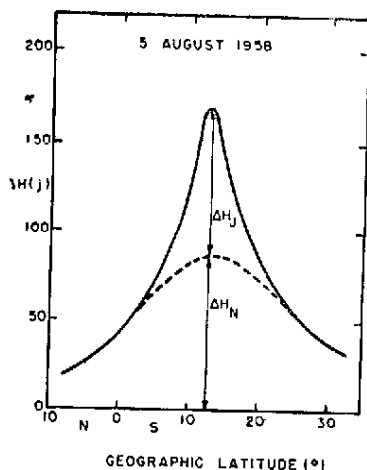

Fig. 2 — Illustrating the method used for determining the degree of enhancement of the world wide Sq current at the dip equator.

5) **Attempts** to use the $\triangle H$ latitudinal variations **to obtain an** estima-tion of the width of the jet region do not seem **to be as** successful as the use of the $\triangle Z$ latitudinal variations which will be reported elsewhere.

DAILY CHANGES IN THE EQUATORIAL ELECTROJET OVER INDIA DURING THE EQUINOX OF 1958

by

A. Onwumechilli and P. O. Ogbuehi

Department of Physics, University of Ibadan, Nigeria

The new current model described in previous papers in this session has been used to study day-to-day changes is the equatorial electrojet in India. The preliminary results for 21 Quiet Days ($Cp \leq 1.0$) in September 1958 are shown in the Fig. 1. These indicate that the current parameters vary from one day to the next.

Preliminary calculations show that the peak intensities of the electrojet and the worldwide Sq current are negatively correlated. This rather surprising result is being further studied.
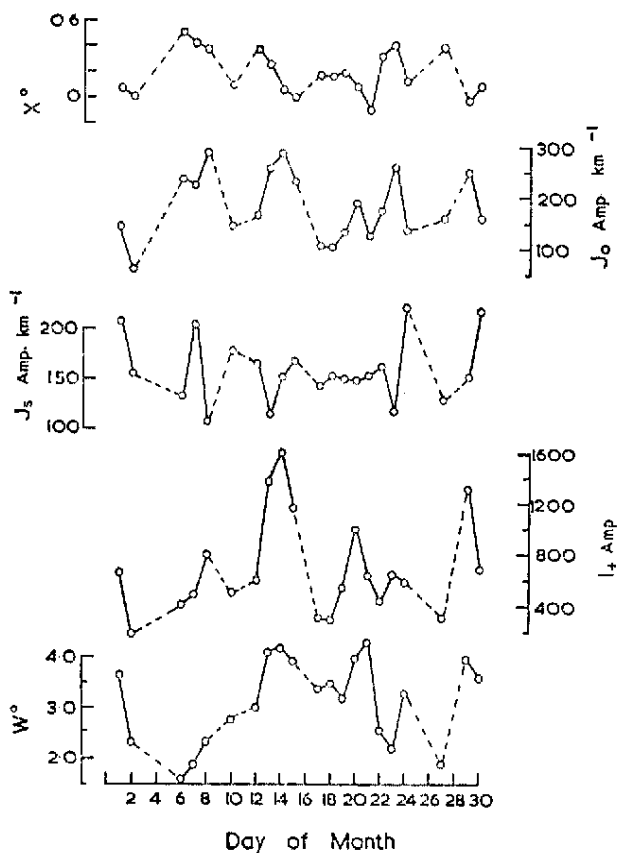
Fig. 1 — Showing the daily changes, in the electrojet and worldwide Sq current parameters: distance of electrojet axis from dip equator, X°; peak electrojet intensity, J_o; peak Sq intensity J_s; total eastward electrojet current, I_T; electrojet half-width, W°. Consecutive days have been joined by continuous lines and non-consecutive days by broken lines.

SOME RECENT ANALYSIS OF THE MAGNETIC FIELD OF

THE EQUATORIAL ELECTROJET

by

A. Onwumechilli and P. O. Ogbuehi

Department of Physics

University of Ibadan, Nigeria

The aim of the paper is to reanalyze different ground based measurements of the magnetic field of the equatorial electrojet using the same methods of analysis. An evaluation of some methods of analysis is attempted and the preferable methods are used. The model used for ionospheric currents has been described in previous papers.

The measurements analyzed were made in Peru during the equinoxes in 1957 and in Nigeria during December 1956, and May to October 1962. The preliminary results are given in Table I. A comparison of rows 1 and 2 shows that the electrojet is wider and more intense in Peru than in Nigeria. Rows 3 and 4 indicate that the electrojet may be slightly wider in local summer (June) than at equinox. That the electrojet is more intense at equinox is confirmed. The large reduction in current intensity from 1956 to 1962 is due to reduction in solar activity.

One difference still remains in the differents sets of data. The daily ranges of the magnetic elements were differently defined in each set of measurements. The effects of this on the results is being looked into.

The depth of the induced electrojet current below the ground has been estimated. For the September equinox measurements in Nigeria, the width was found to be 4.8° of latitude. This is to be compared to the value 5.5° suggested by Chapman for the worldwide Sq current.

For each set of data, α came out negative. This implies that the electrojet current has a return path of its own, separate from that of the rest of the Sq current system. In the light of this result, the relationship between the electrojet and the rest of the Sq current system is being further investigated.

TABLE I

Parameters of the equatorial electrojet in Peru and Nigeria

N°	Location	Epoch	α	Width (km)	J_o $(A\ km^{-1})$	East Jet Current Ampere (A)
1	Nigeria	Dec. 1956	-1.57	530	194	56100
2	Peru	Equinoxes 1957	-1.26	920	236	114000
3	Nigeria	June 1962	-3.41	920	83	46100
4	Nigeria	September 1962	-2.20	790	104	46700

THE EFFECTIVE CONDUCTIVITY OF THE EQUATORIAL

IONOSPHERE FOR THE Sq CURRENT SYSTEM

by

A. T. Price

The relation between j and E for currents flowing in any ionopheric layer is given by the equations below, assuming the total vertical component of current is inhibited by polarization at the base of the ionosphere. Letting j_o and j_φ represent currents in the θ and φ directions respectively, we have:

$$j_o = k_{oo} E_o + k_{o\varphi} E_\varphi$$
$$j_\varphi = -k_{o\varphi} E_o + k_{\varphi\varphi} E_\varphi,$$

where the layer conductivities depend on many parameters, such as number density of particles, collision and gyro frequencies etc., and specially on the main magnetic field, being very sensitive to the dip angle where this is small.

The integrated values C_{oo} of k_{oo} etc. through the ionosphere up to 600 km height as functions of θ are of the general form shown in Fig. 1, though the overall magnitudes may vary at different times from those shown. The $C_{\varphi\varphi}$ has a maximum at the dip equator equal to the integral of the Cowling conductivity k_3, but begins to fall rapidly from this value at about 2° distance. At first sight, this would seem to explain the concentration of Sq currents at the dip equator, which constitutes the equatorial electrojet. Closer examination suggests this is not entirely true, and it does not explain several features such as the variations of Sq at the equator with longitude, since k_3 varies only very slightly with longitude.

Rocket experiments indicate that the currents flow at about 110 km height. At this height $k_{\varphi\varphi}$ has a much sharper maximum than $C_{\varphi\varphi}$ and so could not account for the width of the electrojet. Also at

this height $k_{0\varphi}$ rises from zero to a sharp maximum at about $0.5°$ (say 60 km) from the equator, and then decreases, though not as rapidly as $k_{\varphi\varphi}$, and in this region $|k_{0\varphi}| > k_{\varphi\varphi}$.   Hence $k_{0\varphi}$ must have a profound effect on the current distribution.
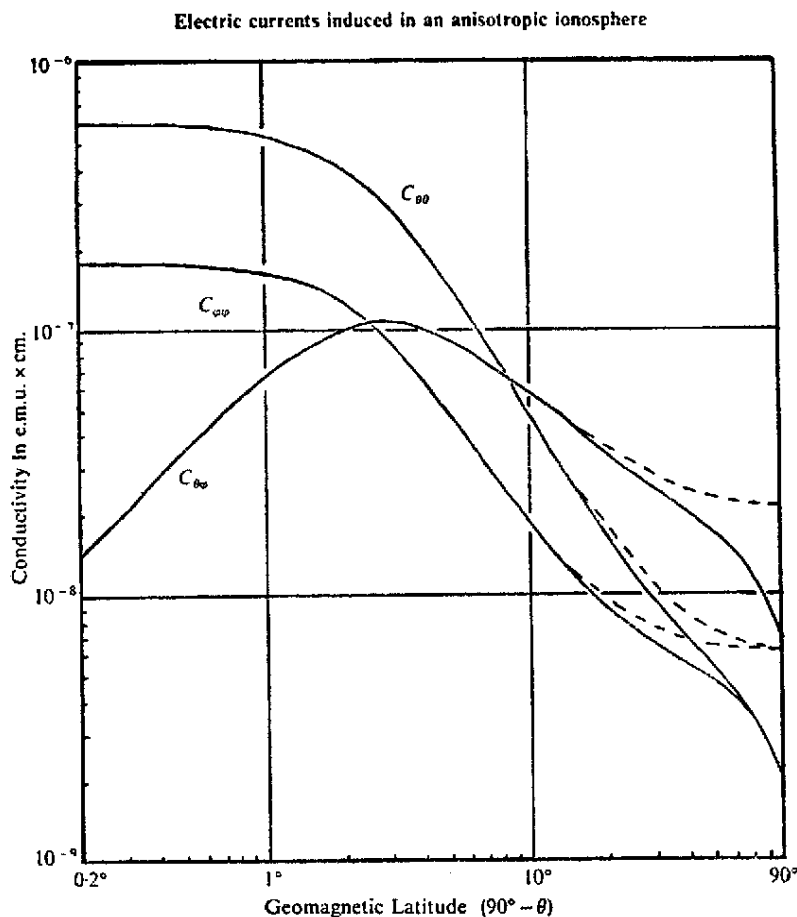
Electric currents induced in an anisotropic ionosphere

Fig. 1 — The integrated layer conductivities $C_{\theta\theta}$, $C_{\theta\varphi}$, $C_{\varphi\varphi}$ (Note **both** scales are logarithmic).

An electromotive force E_φ will set up a horizontal Hall current $k_{o\varphi} E_\varphi$ in the θ (southward) direction, north of the equator and in the northward direction south of the equator. This current will be at least partially inhibited because of the zero value of $k_{o\varphi}$ at the equator and the low values a few degrees north or south. This means that the horizontal as well as the vertical component of the Hall current is nearly extinguished so that the effective conductivity becomes k_3 for the region. This region will normally be a band of about 5" width, but in special circumstances could be much wider, which may explain the large ranges of Sq observed in East Africa, and also the changes of intensity of the jet with longitude.

The above equation can be solved to obtain

$$E_o = R_{oo} \, j_o + R_{o\varphi} \, j\varphi$$

$$E_\varphi = -R_{o\varphi} \, j_o + R_{\varphi\varphi} \, j\varphi$$

where in particular

$$R_{o\varphi} = - k_{o\varphi}/(k_{oo} \, k_{\varphi\varphi} + k^2_{o\varphi}),$$

and for a simple dipole field $|R_{o\varphi}|$ reduces to k_3^{-1}. These resistance coefficients are plotted as functions of θ in Fig. 2. This again shows that, if the θ component j_o is zero in any region, the effective conductivity is k_3.

If the horizontal Hall current is not completely extinquished at the equator there will be a tendency for the jet current to cross and recross the equator, which seems to occur at certain stations like Huancayo.

Is should also be noted that the layer conductivities are affected by the field of the jet itself. If the strength of the jet increases the numerical value of the magnetic dip on either side will be decreased, and in consequence the width of the jet should increase.
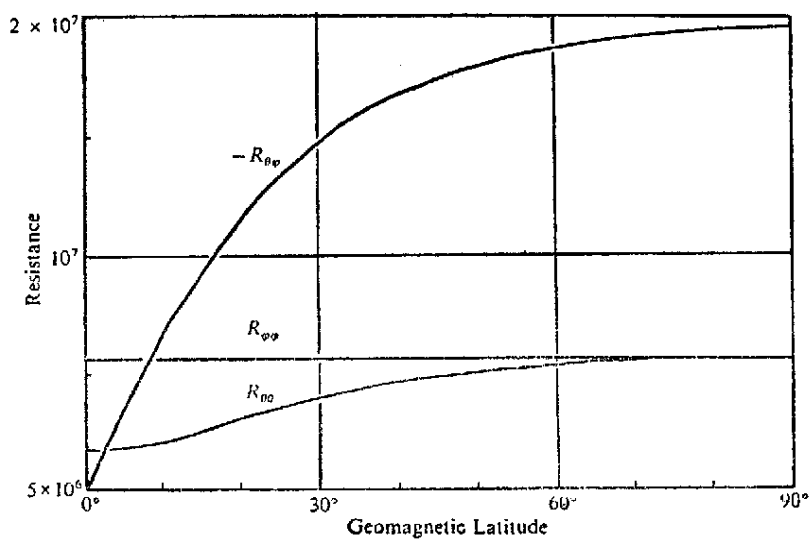
Fig. 2 — Components of the resistance tensor $R_{\theta\theta}$, $R_{\theta\varphi}$, $R_{\varphi\varphi}$ (Scales are both linear).

CONDUCTIVITY STRUCTURE OF THE EQUATORIAL

IONOSPHERE

by

Ken-Ichi Maeda

Kyoto University, Japan

The ionospheric conductivity governing the dynamo current is represented by three elements, σ_{xx}, σ_{xy} and σ_{yy}, which relate current with the electric field by the following equations.

$$
\begin{bmatrix} I_x \\ I_y \end{bmatrix} = \begin{bmatrix} \sigma_{xx} & \sigma_{xy} \\ -\sigma_{xy} & \sigma_{yy} \end{bmatrix} \begin{bmatrix} E_y \\ E_x \end{bmatrix},
$$

where x is southward positive and y is eastward positive. It was believed that σ_{yy} is the only controling element for the narrow belt centering at the magnetic dip equator. This point is examined and it was found that σ_{xy} should not be ignored except in the very narrow zone with the dip angle of $\pm$ 20' and is even greater than σ_{yy} at about 1° dip angle. Figures 1, 2 and 3 show σ_{xx}, σ_{xy} and σ_{yy}. After a simple treatment of the dynamo equation shown above, it can be said that the the current function and current density are proportional to σ_{yx} + $\sigma_{xy}^2/\sigma_{yx}$. This quantity is plotted against height in Fig 4. From this figure we can see that $\sigma_{yy} + \sigma_{xy}^2/\sigma_{xx}$ is almost independent of the dip angle and the slight second peak exists from about 130 to 140 km. The curves were obtained from a model in which the electron density increases monotonously from the E to the F layers. If there is a so-called E-F valley at around 120 to 130 km, the second peak will become more clear.

If the problem is concerned with the pattern of dynamo current flow and the structure of electric field, the situations is not so simple. In Fig. 5 classification of height range is shown. The relative order of magnitude of σ_{xx}, σ_{xy} and σ_{yy} is shown for each of the height

ranges and the effective conductivity t$_0$ govern the current is a'so shown. In the height ranges 1, 2 and 3, the current pattern is of equatorial type although is differs slightly for each range. However, in the range 4 (hatched area) the current pattern differs much from the other three ranges, because σ_{xx}, σ_{xy} and σ_{yy} are all comparative.

The dependency of $\sigma_{yy} + \sigma_{xy}^2/\sigma_{xx}$ on the permanent geomagnetic field (B) can be seen by the following relations, noting Fig. 5:

$$\sigma_{xx} \propto B^0 \quad , \quad \sigma_{xy} \propto B^{-2} \text{ and } \sigma_{yy} \propto B^{-1},$$
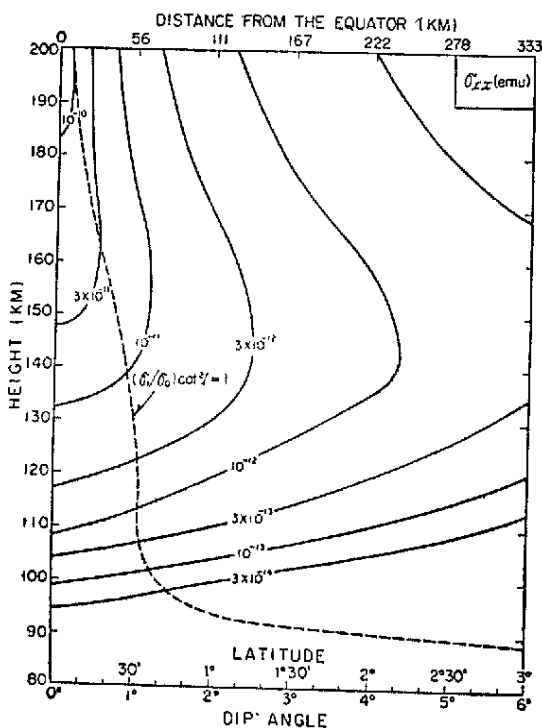
Fig. 1 — Contour map of σ_{xx} (emu) plotted on height-dip angle coordinates. Latitude and distance from the equator are shown on abscissa.
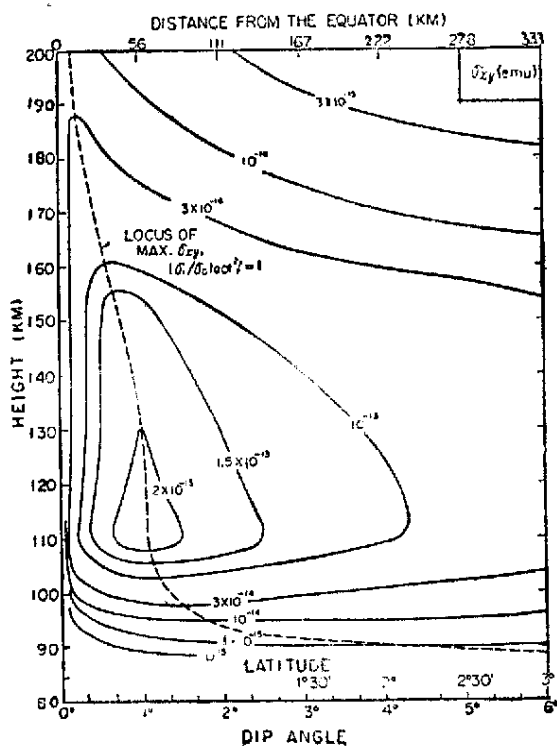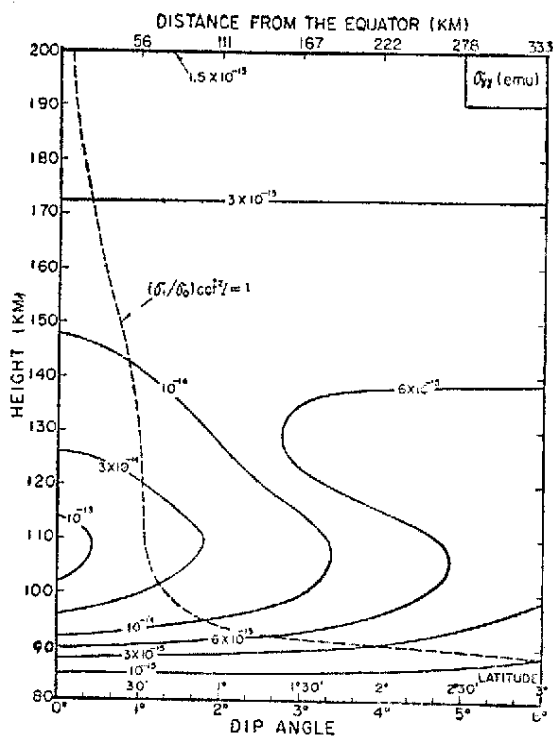
Fig. 2 — Contour map of σ_{xy} (emu)
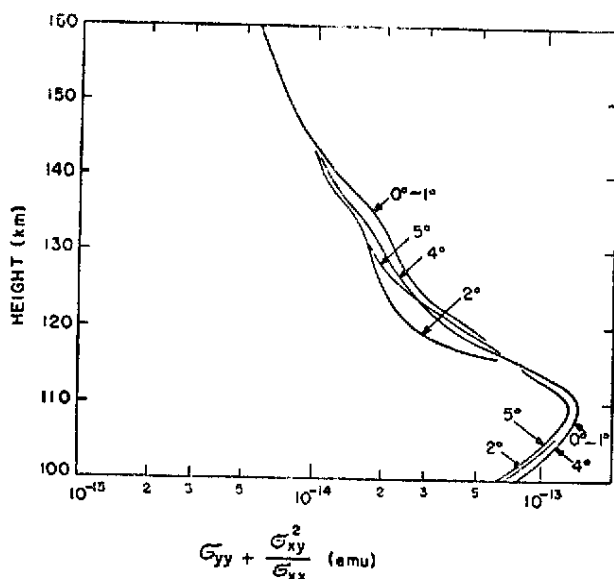
Fig. 3 — Contour map of σ_{yy} (emu)

Fig. 4 — $\sigma_{yy} + \sigma_{xy}{}^2/\sigma_{xx}$ versus height. Dip angle is shown on each curve.
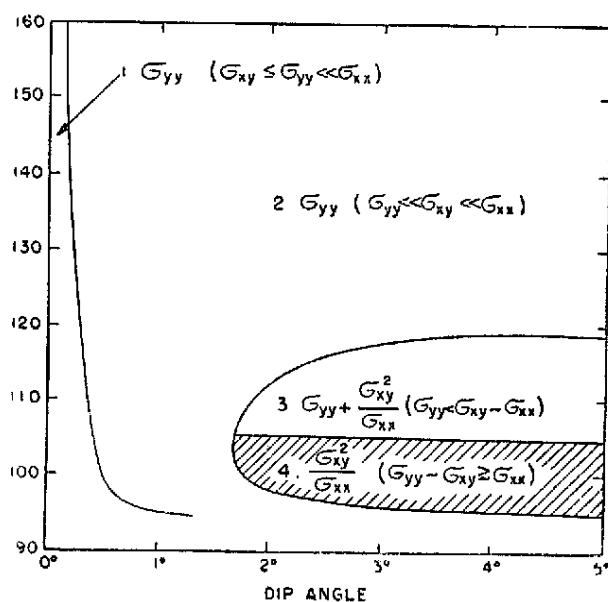

Fig. 5 — Classification of height range as a function of dip angle.

NIGHTTIME CONDUCTIVITY OF THE

EQUATORIAL IONOSPHERE

by

Hiroshi Kamiyama

Geophysical Institute, Tohoku University

Sendai, Japan

One of the features of the equatorial anomaly in the geomagnetic field is that its diurnal variation is enhanced only during daytime (Chapman, 1951). This was well explained by the anomalous increase in electrical conductivity of the ionosphere over the dip-equator (Hirono, 1952; Baker and Martyn, 1953). However, it has not been accounted for that the nighttime variations in the equator are not significantly different from those at adjacent latitudes.

In this illustrated abstract we shall try to explain this fact by the characteristics of the nighttime electrical conductivity of the ionosphere. The most essential tensor component of the conductivity responsible for the equatorial electrojet may be σ_{yy} which is a function of σ_0, σ_1, and σ_0 and I, where I denotes the dip angle and σ_0, σ_1, σ_2 are the parallel, transverse, and Hall conductivity, respectively. At the dip equator where I = 0 we have:

$$\sigma_{yy} = \sigma_1 + \sigma_2^2/\sigma_1$$

From the estimation of the collision frequencies for electrons and ions it is shown that the parallel conductivity σ_0 is essentially contributed from electrons. The Hall conductivity is easily found to be also proportional to electron density, if the electrical neutrality is assumed in any part of the ionosphere. On the other hand, the transverse conductivity σ_1 in the dynamic region is proportional to the sum of the concentrations of positive and negative ions. From the examination of the equilibrium between negative ion density and electron density during the night

when the photodissociation is absent, it is seen that the negative ion-electron ratio λ is almost inversely proportional to electron density, λ being more than unity at the level of 100 km when electron density is reduced to the order of 10^3 cm^{-3}. For example, the values tabulated below are found for the selected cases (refer to Figs. 1 and 2).

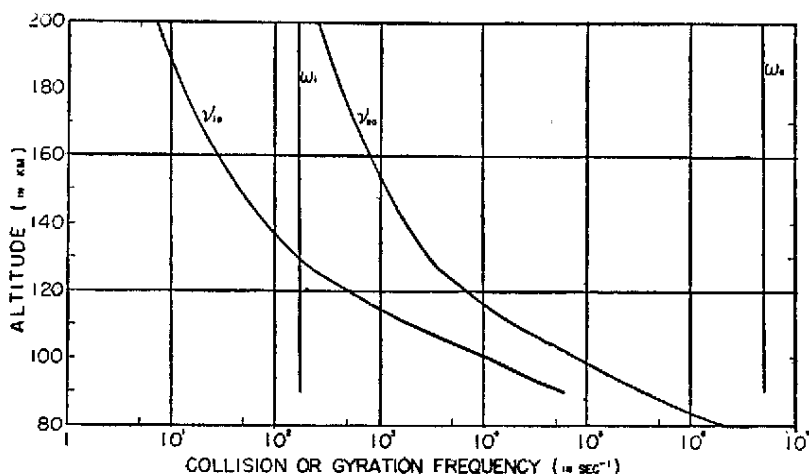| Electron density (cm^{-3})	height (km)	σ_0 (e.m.u.)	σ_1 (e.m.u.)	σ_2 (e.m.u.)
$n_e = 10^5$	100	3.0×10^{-13}	1.8×10^{-16}	5.5×10^{-16}
	125	5.0×10^{-12}	2.0×10^{-15}	5.0×10^{-15}
$n_e = 10^3$	100	3.0×10^{-15}	6.5×10^{-18}	5.5×10^{-17}
(nighttime)	125	5.0×10^{-14}	4.5×10^{-17}	5.0×10^{-17}

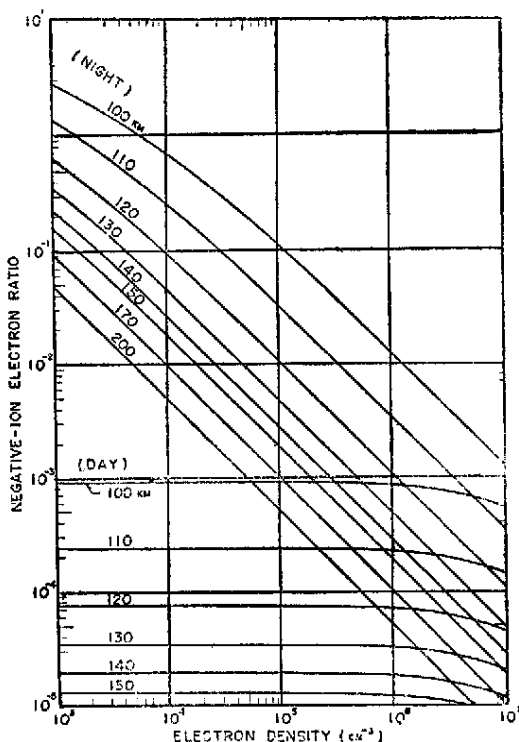Fig. 1 — Frequencies of collision and gyration for electrons and ions as a function of height.

Fig. 2 — The ratio (λ) of negative ion density to electron density as a function of electron density at various heights.

These values lead to a less pronounced equatorial anomaly in σ_{yy} for lower electron density during the night (see Figs. 3 and 4). With an appropriate electron density profile, the ratio of the height-integration of σ_{yy} at the dip equator to that at the latitude of 4°, is found to be about 10 during daytime whereas it is only about 1.5 during nighttime (see Fig. 5). It is pointed out that the equatorial electrojet during daytime is located below the current sheet which is not very variable with latitude. Apart from the dip equator, the east-west current depends on σ_{xy} as well as σ_{yy}. The maximum of σ_{yy} is found, in general, at a level between 120 km and 130 km, where as σ_{xy} attains to its maximum at a level between 100 km and 110 km.

Therefore two current sheets could be found for a suitable distribution of electron density.
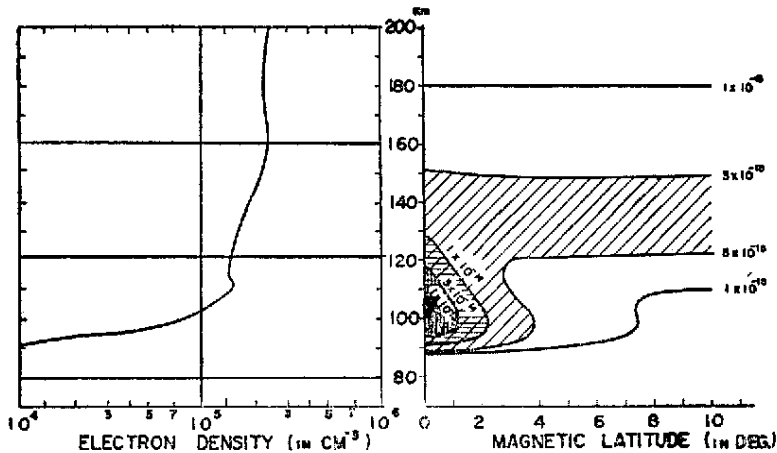

Fig. 3 — Profile of the conductive sheet (right) deduced from a model of the ionosphere during daytime (left). Conductivity is indicated in emu.
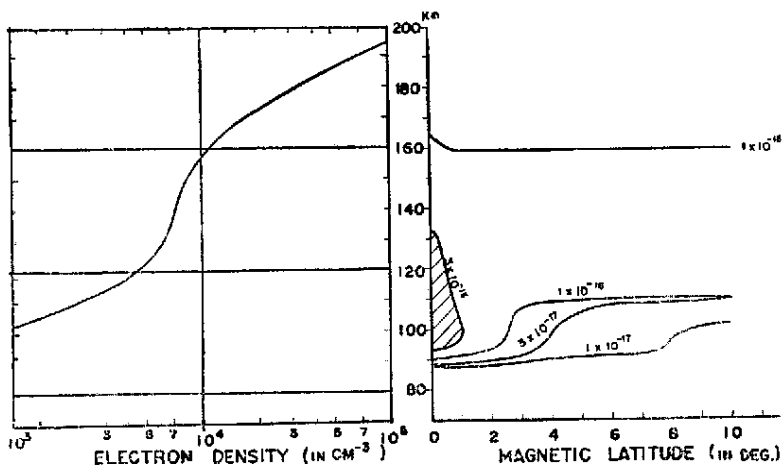

Fig. 4 — Profile of the conductive sheet (right) deduced from a model of the ionosphere during the night (left). Conductivity is indicated in emu.
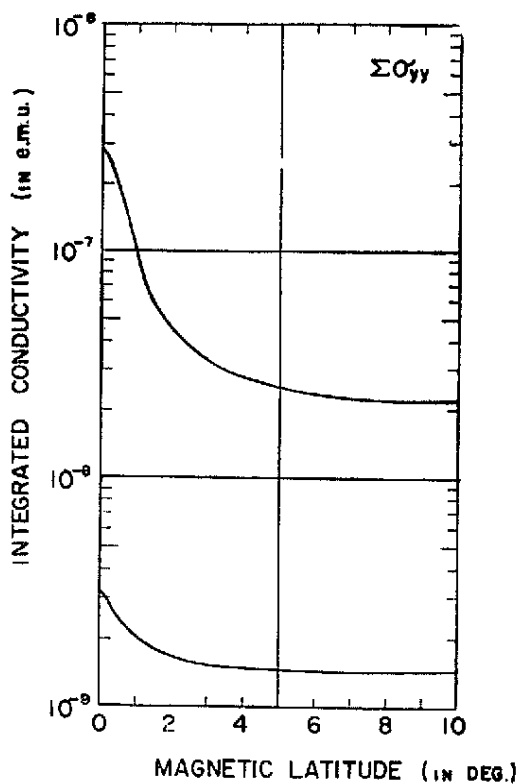
Fig. 5 — Latitudinal distribution of integrated σ_{yy} up to 200 km. The upper curve is for daytime (Fig. 3) and the lower curve is for nighttime (Fig. 4).

PRELIMINARY RESULTS OF MEASUREMENTS OF Sq CURRENTS

AND THE EQUATORIAL ELECTROJET NEAR PERU

by

N. C. Maynard and L. J. Cahill, Jr.

University of New Hampshire, Durham, N.H., U.S.A.

Four Nike-Apache sounding rockets were launched from the USNS Croatan off the coast of Peru during March, 1965, as part of the recent NASA Mobile Launch Expedition. The rockets were instrumented with a nuclear free precession magnetometer to measure the total intensity of the earth's magnetic field, a DC Langmuir probe to measure relative electron density, a barometer switch for trajectory determination, and a magnetic aspect sensor. Preliminary magnetometer results from two of these flights are presented.

Flight UNH 65-5 was launched from the Croatan at 1100 hours local time on 12 March 1965, from the position 11°25'S, 81°20'W, near the dip equator and near the center of the electrojet. The trajectory was computed to fit the baro-switch operation times at 70.000 feet and peak altitude was calculated to 173 km. Using the coefficients of Leaton and Evans, the theoretical field was computed over an approximate trajectory. The difference curve between the measured and computed fields, plotted as a function of altitude, shows a change of slope at about 95 km and again at about 130 km. The maximum current appears to be located at 108 km. The total change in field is about 120 gammas which compares with 60 to 70 gammas for similar midday flights in India. (Fig. 1).
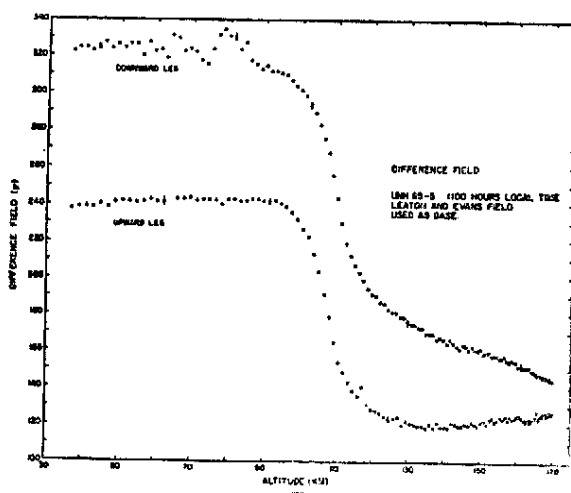
Fig. 1 — The difference between the measured field and the calculated field, plotted against altitude for UNH 65-5. The long sloping tail above 130 km on the downward leg is believed to be the result of inaccuracy of the preliminary trajectory used in calculating the theoretical field. Similarly the gradual rise above 140 km on the upward leg is also attributed to this factor. The wide fluctuations below 85 km on the downward leg are apparently caused by overturning of the rocket spin axis.

Flight UNH 65-2 was launched at 1136 hours local time on 9 March 1965 from the position 03°07'S, 84°22'W. This was more than 8°N of the magnetic dip equator and hence well to the north of the equatorial electrojet. For initial analysis, time of peak altitude was taken as the time of minimum magnetic field. The radar tracking data in the early portion of the flight were also used in computing a trajectory. Peak altitude was determined to be 161.8 km. The theoretical field was computed over an approximate trajectory, using the same range as established for UNH 65-5, and using the **Leaton and Evans** coefficients. The difference curve between the measured and theoretical fields indicates that the Sq current measured is more

diffuse than the electrojet, extending from 93 km up to about 130 km (upward leg data). A change of slope between 105 and 110 km on the upward leg (100 and 105 km on the downward leg) apparently is not due to precession and suggests a double-layered current structure with the peak of the lower layer at 100 km and of the upper layer at 118 km (upward leg data). Total magnetic change due to the current layers was about 45 gammas. (Fig. 2).
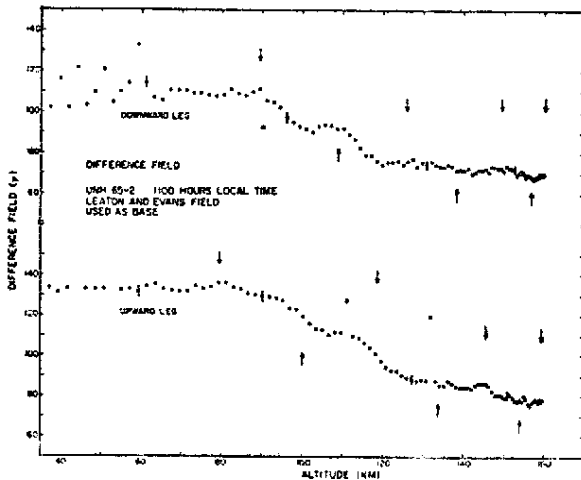

Fig. 2 — The difference between the measured field and the calculated field as a function of altitude for UNH 65-2. The arrows above the curves denote maxima in the effect from rocket precession, while those below the curves indicate minima. The shift downward in altitude of the effect of the Sq current on the downward leg is thought to be to preliminary trajectory errors. The fluctuations below 65 km on the downward leg are due to overturning of the rocket spin axis.

For the two days of the flights, magnetograms from the Peruvian stations at Huanuco and Cañete (above and below the electrojet center respectively) show that the rockets were launched near the peak of the diurnal variation on each day, and that the earth's magnetic field was reasonably quiet (see Fig. 3).
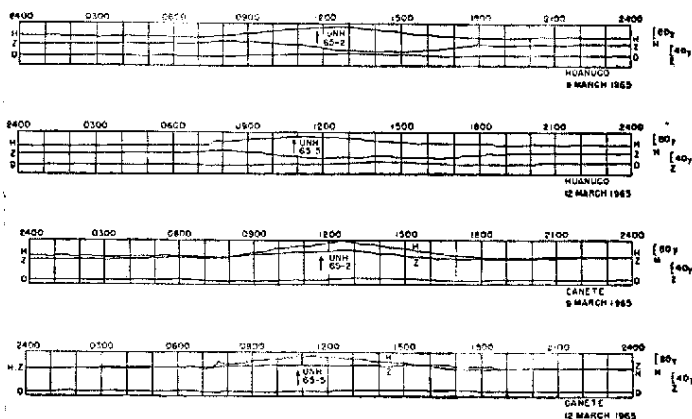

Fig. 3 — Magnetograms from the magnetic observatories at Huanuco and Cañete in Peru, for the days of the two launchings. Time of launch for each flight is denoted on the respective magnetogram.

AIRBORNE MEASUREMENTS ON THE EQUATORIAL ELECTROJET

by

George J. Gassmann

Air Force Cambridge Research Laboratories

Bedford, Mass., U.S.A.

and

R. A. Wagner

Lowell Tech. Institute, Boston, Mass., U.S.A.

During 29 crossings of the geomagnetic dip equator near 80° W longitude near the Peruvian coast, airborne equipment obtained cross-sections of the geomagnetic field intensity and of ionospheric characteristics in February and July 1964. Straight line flights covered from 3 to 12 degrees in latitude at an altitude of about 11 km above sea level and at a speed of 800 km per hour (Fig. 1). The magnetic intensities for each of the flight lines were obtained from ground charts as relatively smooth curves. Variations from this base trend were adjusted to the intensity simultaneously recorded at Huancayo at this dip latitude for most flights. Influences of the aircraft's magnetic field were evaluated inasmuch as this was possible. The magnetic anomalies due to the electrojet and the amplitudes of the Esq echoes show fair correlation of details and fair to good correlation of large scale features.

From the records obtained in the flights it is interpreted that the width and position of the electrojet vary considerably from hour to hour and from day to day. The data suggest that the electrojet during certain days in February was separated into two or more parallel streaks. Examination of the data relative to the coastal

crossings indicated magnetic effects which are attributed to strong
electric currents in the ocean. These currents are suggested to be a
sector of the Sq current systems but somewhat stranger than antecipated.
An interpretation of these ocean electric current systems relative to the
western hemisphere indicates a concentration of current flow adjacent
to the coast of South America which is dependent upon the local time
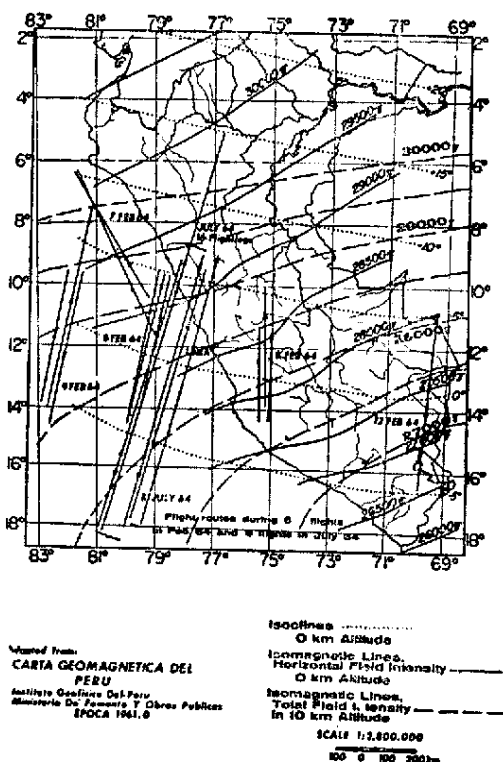of day. The results are illustrated in the following four figures.

Fig. 1 — Chart of the geomagnetic field intensity and dip in Peru
after Casaverde and Giesecke showing the aircraft flight
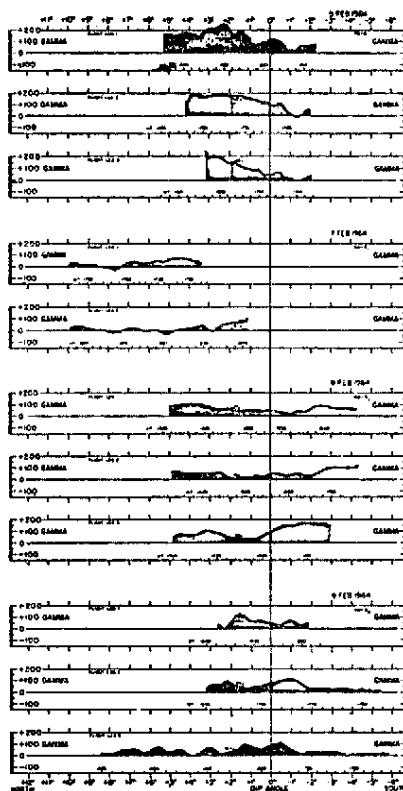paths.

Fig. 2 — Magnetic field intensities obtained on some of the February flights showing derivation of the measured and corrected total field intensity from the "normal" values obtained from the charts.
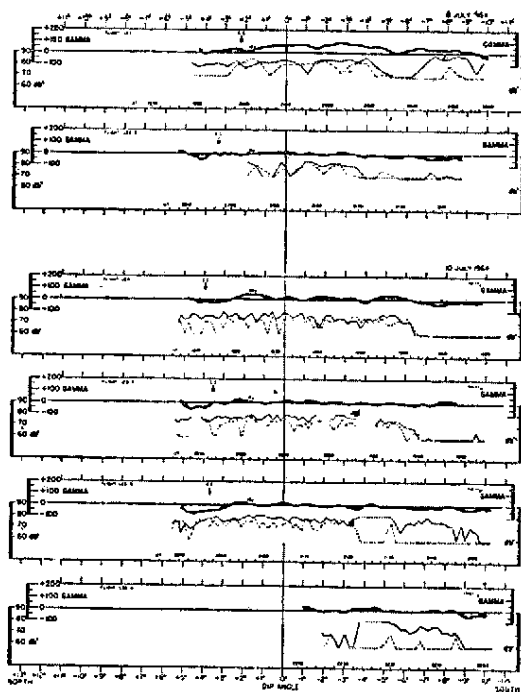
Fig. 3 — Magnetic field intensities obtained on some of the July
flights showing deviation (shaded area) of the measured
and corrected total field intensity from the "normal" values
obtained from the chart together with ionospheric signal
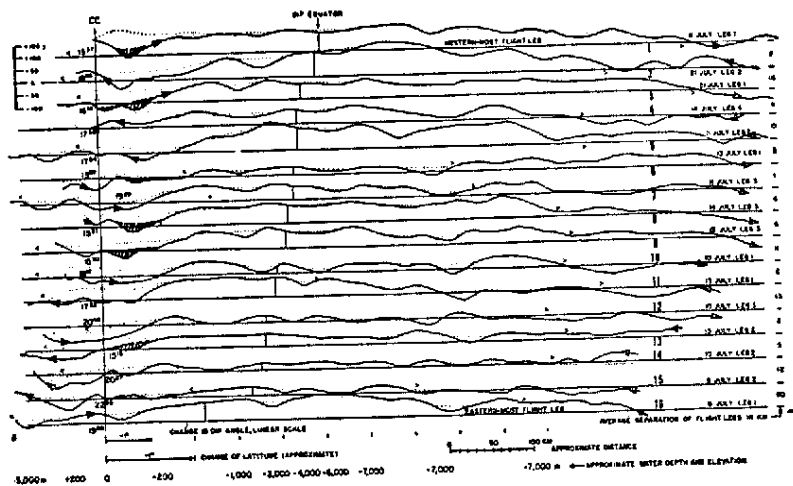reflection intensity (solid and dashed lines).

Fig. 4 — Magnetic total field intensities obtained on the July flights aligned relative to the coastal crossings (CC) in sequence from west to east. The dotted and dashed lines indicate the attempt to recognize and separate permanent and variable anomalies below the aircraft.
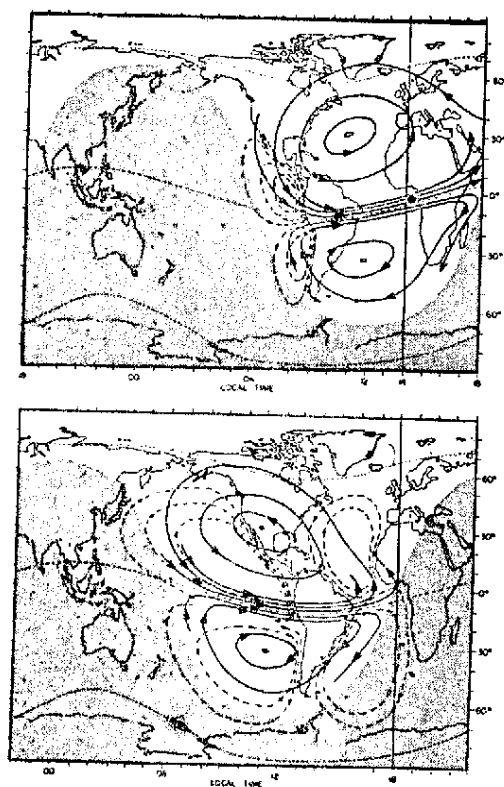
Fig. 5 — Two daytime systems interpreted from the data obtained in these measurements and the flow lines imposed by the shore lines. The ocean current are shown by the dotted lines and the overhead current by the solid lines.

MEASUREMENT OF MAGNETIC FIELD INCLINATION IN THE EQUATORIAL F REGION BY FARADAY ROTATION OF INCOHERENT SCATTER ECHOES

by

Robert Cohen

Jicamarca Radar Observatory, Lima, Peru

The differential Faraday rotation is proportional to (NB $\cos \theta$), where N is the electron density, B is the magnetic field intensity, and θ is the angle between B and the propagation vector of the wave. Existing magnetic field models do not provide a sufficiently accurate estimate of θ when θ is near 90°, since in that case the rotation rate is very sensitive to the exact value of the angle. Consequently, for the spatial region above the Jicamarca Radar Observatory (11.95° S; 76.87° W; dip 2°), an experimental determination of B $\cos \theta$ has been made by comparing Faraday records with electron density profiles deduced from top and bottom side ionograms and incoherent scatter power. In particular, the observed maximum rates of Faraday rotation have been compared on many occasions with ionosonde measurements of Nmax.

The average value of (B $\cos \theta$) so obtained provides a precise and convenient absolute calibration for the incoherent scatter records; furthermore, by employing existing estimates of B, it can be used to find θ and hence the magnetic field inclination in space. Through such comparison, the field inclination has been measured for heights up to 800 km at two antenna positions separated 3.36° in the magnetic north-south direction. In each position, the field inclination near Hmax is consistent with that indenpendently determined from the spectrum of the incoherent scatter signal. The predictions of five magnetic field models are compared with these results. See Figs. 1, 2 and 3.
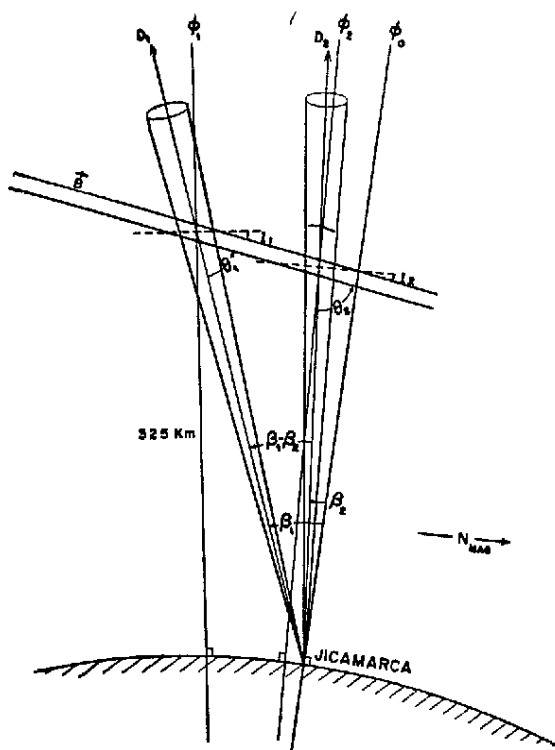
Fig. 1 — Schematic diagram of antenna-beam configuration compared with magnetic field lines above Jicamarca, Peru for the two antenna beam positions that have been employed in calibrating the Faraday rotation and in measuring the magnetic field inclination.
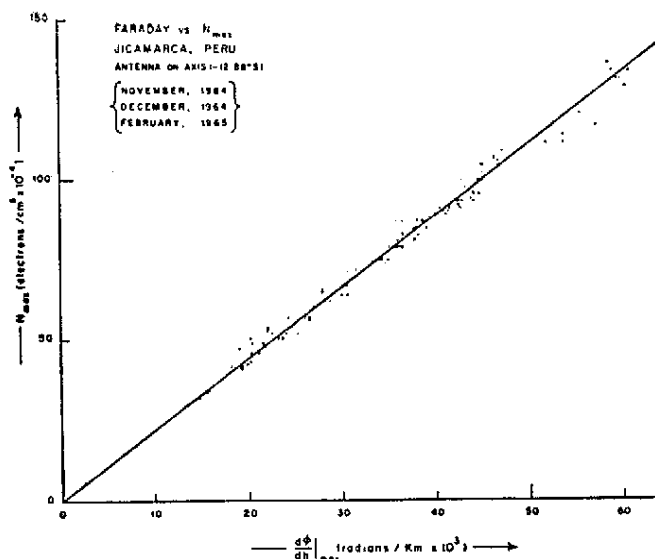
Fig. 2 — Comparisons of Nmax deduced from ionosonde observations with the maximum rotation rate measured simultaneously with the Faraday technique.
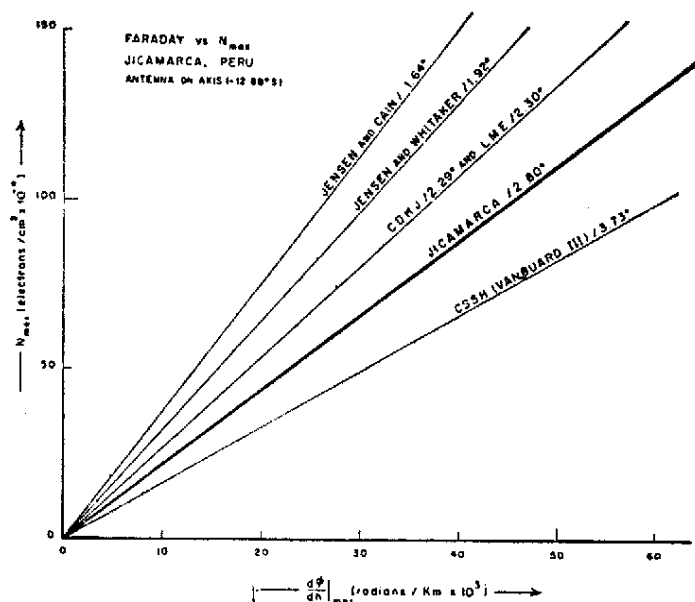
Fig. 3 — Comparison of the calibration at 325 km deduced from Fig. 2 with the calibrations that would have been obtained had the inclinations predicted by various magnetic-field models been the case.

DETERMINATION OF THE DIP EQUATOR USING THE

SATELLITE EXPLORER XX

by

T. E. VanZandt

National Bureau of Standard, CRPL, Boulder, Colorado, U.S.A.

During the daytime, the h'(t) traces on the Explorer XX records (Calvert, Knecht, and VanZandt, 1964) often exhibit a hump near the dip equator (Fig. 1). When the hump is symmetrical, it is likely that the center of symmetry of the hump is at the local dip equator. This would be true if the plasma were in diffusive equilibrium along the field lines. Any process which might move the center of symmetry by perturbing diffusive equilibrium would make the hump asymmetrical.
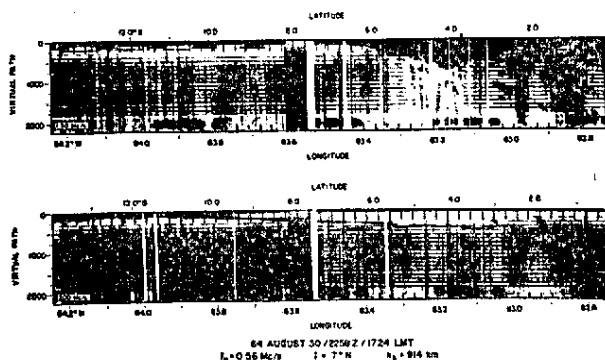

Fig. 1 — Explorer XX records on 1.50 and 2.00 MHz. The time delay τ (expressed in vertical path $= c\tau/2$ km) is measured downwards from the top of the records. The horizontal scale is time or geographical position. These records are four minutes long. The center of symmetry of the equatorial ionosphere is on the left at a latitude of about 12°S, as indicated by the z-trace in the upper record and the x-trace in the lower one.

From Explorer XX data obtained in September 1964, eight determinations of the center of symmetry have been made (Fig. 2). On these occasions the satellite was between about 900 and 1000 km. These locations of the dip equator agree well with recent spherical harmonic analyses of the field. There remains a small discrepancy (0.3°-0.4° of latitude), but the number of points are two few and their error bars are too large to say whether the Explorer XX determinations may be more accurate than the spherical harmonic analyses.

The movement of the center of the hump when the hump is asymmetrical may be of use in studying the perturbations of diffusive equilibrium, that is, in inferring the velocity of plasma flow across the equator.
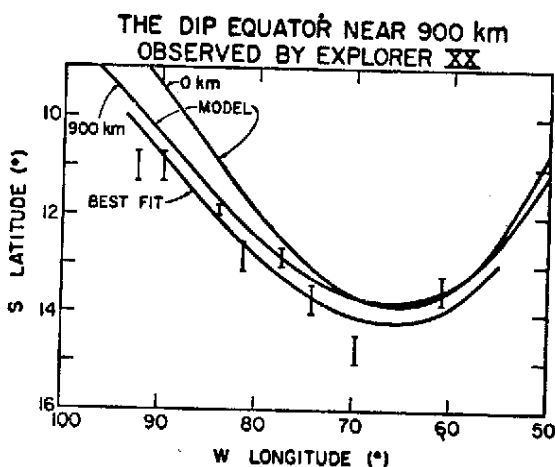

Fig. 2 — Shown are eight points determined from Explorer XX records, the dip equator at 0 and 900 km computed with Cain's 1965 spherical harmonic coefficients, and a "best fit" to the Explorer XX data, obtained by moving the 900 km curve 04° southward.

SUMMARY OF THE SESSION

by

P. O. Ogbuehi

University of Ibadan, Nigeria

and

D. G. Osborne

University College, Dar es Salaam, Tanzania

Papers

The session was presided over by Professor A. T. Price. The introductory review was given by Dr. S. Matsushita and papers were presented by the following authors: Cahill, Cohen, Gassmann, Hunter, Hutton, Kamiyami, Maeda, Maynard, Ogbuehi, Onwumechilli, Osborne, Price, VanZandt, Wagner and Wilkins.

Definitions

The introductory review and several papers in the session provoked discussion on questions of definition. Some of these were questions of arbitrary choice, others involved matters of physical significance. The rival merits of different **coordinate systems** were discussed. It was generally recognized that both dip and geographic equators had controls on geomagnetic variations in low latitudes, but it was felt that magnetic dip latitude and geographic longitude were appropriate for most studies of equatorial phenomena. Magnetic dip latitude is defined as

$$\tan^{-1} (\tfrac{1}{2} \tan \mathrm{Dip})$$

and must be distinguished from the geomagnetic (dipole) latitude. Some allowance may be needed for differences between the position of the magnetic

dip equator in the E region and at ground level and satellite measurements may help in determining its position when greater precision has been achieved. The variation of dip angle with altitude can be determined also by comparing Faraday rotation and ionosonde measurements.

By definition the **mean solar quiet day variation, Sq,** is the average magnetic variation over several quiet days. It is an operational definition and it is impossible to eliminate completely the effects of disturbance in order to obtain an "**ideal Sq**". The term Sq should not be referred to behavior on individual days, but it is appropriate to talk of the quiet day and of quiet day magnetic variation or the quiet day current system for individual cases.

It is generally accepted that the **equatorial electrojet** is part of the quiet day current system. The jet is considered as that part of the current responsible for the increased horizontal field variation in a narrow belt near the dip equator. The picture is that of an intense eastward electrojet current set up as a result of the crowding of current lines into the narrow belt of high conductivity at the dip equator. For purposes of some analyses the measured field variations may be separated into electrojet and world-wide parts.

The definition of **daily range** for a magnetic element was discussed and the importance of an agreed recommendation made clear. Discussion on this point was deferred until later in the conference.

New Information

Remarkably few new experimental results were reported. In East Africa the daily horizontal range at Nairobi, ten degrees in latitude south of the magnetic dip equator, is not very much less than that at Addis Ababa on the dip equator. In discussion it was reported that there is a similar slow change of range with latitude in India and it is possible that the electrojet current is much wider in the East Africa — India sector than it is elsewhere. A plot of horizontal field against latitude at different times on individual days for the South American sector suggests that there is considerable variability in the form of the jet.

Recent rocket measurements of ionospheric currents near Peru located a strong current at about 110 km in the electrojet region. It was suggested that there is evidence for two current layers just outside the electrojet zone. Studies with an airborne magnetometer in a plane flying across the electrojet region in South America gave a suggestion that the electrojet is split into two or more parallel filaments of current on certain days.

All of these experimental data are tentative and require further observation. The ideas suggested by them and the obvious complexity of the electrojet behavior should stimulate further work.

Data Analysis

A number of studies of the electrojet using measurements of ground level magnetic fields were reported. These confirmed that the width, intensity and axis position of the electrojet vary considerably from day to day. Correlation studies show that for different hours of the same day the electrojet and world-wide current intensities at the dip equator are positively correlated. On the other hand the maximum current intensities on different days attributed to the electrojet and those observed at other latitudes are negatively correlated. These statements are not necessarily contradictory. Some of these studies indicate that the electrojet may be embedded completely in the northern or southern loops of the quiet day current system. Studies of correlation coefficients between daily ranges for stations at different latitudes also suggest an anomalous behavior beside the electrojet, in agreement with studies on individual days reported already. A reduction in current strength beside the jet may be due to current choosing the high conductivity jet belt in preference to neighboring paths.

One paper stressed the importances of a study of data from a world-wide network of stations before deducing information about the equatorial electrojet. In discussion the need for fitting large scale analytic programs to detailed local observations was emphasized. Another paper gave consideration to the relationship between the variation of all three magnetic components and the overhead current system. It is probable that present data could yield much information on the relationship between the electrojet and the rest of the quiet day current system and further investigations are needed.

Currents

A new model for current distribution in ionospheric currents was proposed. The predictions of the model give a satisfactory variation with latitude of the magnetic field components of the world-wide Sq current system. Its predictions for the electrojet current are good. The model gives a better fit with observed variations than the older simple model of uniform current band.

Conductivities

Three papers on ionospheric conductivity showed the complexity of ionospheric conditions in the electrojet region. The Cowling conductivity is specially important at the dip equator but the layer Hall conductivity at about 110 km height rises from a minimum at this equator to maxima about half a degree north or south and then decreases rapidly. It was again suggested that the width of the electrojet is determined by the latitude variation of the Hall conductivity rather than the Cowling conductivity. This led to a prediction that the jet may be much wider where the dip and geographic equators are parallel than it is elsewhere.

Estimates for ionospheric conductivity at night in the equatorial region are very low. However induced currents on the night side of the earth due to ionospheric currents on the day side could produce nighttime fields at the magnetic dip equator. These may explain the seemingly significant correlations between day and night fields reported for preliminary studies in East Africa.

Theoretical conductivity contours may help to suggest a pattern for current density distributions in electrojet models.

Conclusions

Questions of definition can be sources of fruitless argument. It should be stressed that authors need to define their terms clearly in any paper. It ought to be possible to reach agreement on the meaning of certain words or phrases so that these can be used as a short-hand notation. Agreed recommendations on such terms as magnetic equator and measures of daily range should be sought, but agreement is likely to be reached more quickly if the need for differing usage in different studies is clearly recognized.

If the analysis of Sq variations on a world-wide scale is to be applied to the electrojet, there is need for a much smaller mesh in equatorial regions. Detailed local studies need to be made and for these it is necessary to use more stations than in previous studies, covering a wider range of latitudes and (in one or two cases at least) a fairly close spacing to test longitudinal differences. It is important that all three components should be analized. Detailed study of local electrojet phenomena requires the consideration of information from distant stations.

In order to allow comparisons between measurements in different places, efforts should be made to get data from equatorial magnetic stations sent to the World Data Centers as quickly as possible.

X — MAGNETIC AND IONOSPHERIC STORMS

X — MAGNETIC AND IONOSPHERIC STORMS

(Discussion leaders: S. Matsushita and S. Chapman)

Review Paper:

Magnetic Storms

by

S. Chapman

High Altitude Observatory

Boulder, Colorado, U.S.A.

During magnetic storms an additional disturbance (D) magnetic field is superposed on the normal field of the earth, namely on the main field produced within the earth plus the field of the Sq (and L) currents that cause the daily magnetic variations on quiet days.

The D field is caused by at least three different types of electric currents. One type is generated by a flux of charged particles from the sun, mainly protons and electrons, substantially equal in number density and mean speed. Almost all these charged particles are deflected away from the earth by the geomagnetic field; their pressure encloses the field in a cavity — the magnetosphere — within the charged flux. A thin surface layer at the inner boundary of this flux carries an electric current system, corresponding to the slightly different modes of deflection of the positive particles and the electrons. This current system and its magnetic field are denoted by DCF (D for disturbance, CF for charged flux). The DCF currents inscrease the geomagnetic intensity at the earth's surface, particulary in the horizontal or northward component. Many magnetic storms begin with a sudden increase of the field by a sudden enhancemente of the charged flux: this is seen as a sudden commencement (SSC) of the storm.

Often this increase is nullified within an hour or a few hours, and the surface field intensity becomes reduced below normal. This decrease, which is the major feature of many magnetic storms, is ascribed to the growth of a westward current flowing partly or completely around the earth, within the magnetospheric cavity in the solar flux. This current and its magnetic field are denoted by DR (D for disturbance, R for ring current). The growth of this current is not yet understood, but one explanation (Akasofu and McIlwain, 1963; Akasofu, 1964 a, b) ascribes it to a flux of uncharged particles from the sun (UF: U for uncharged, F for flux). Such particles can cross the cavity

boundary without hindrance and flow onwards into the earth's atmosphere; there many will collide with particles of the atmosphere and lose an electron. Then the residual particle — in most cases a proton — becomes subject to the influence of the geomagnetic field, and a member of the Van Allen belt of energetic charged particles. These spiral around the geomagnetic field lines (somewhat distorted by the D field), and oscillate back and forth along them; they also drift, the positive particles to the westward, producing a westward electric current; electrons in the belts drift eastward, likewise contributing to a westward electric current. This is identified as the DR current. Its radius from the earth's center may be a few or several earth radii; the net decrease of field intensity at the earth's surface is proportional to the kinetic energy of the particles in the belt; the particles in the lower range of energy, of a few kev, are most numerous and contribute most of the DR current.

Sometimes the magnetic data suggest that the DR current that grows (and later decays) during a magnetic storm does not completely encircle the earth (Akasofu and Chapmam, 1964); and this is not surprising, if the ring current is built up by uncharged particles. These will travel straight onward towards the earth until they become ionized by collision; hence there must be a gap in the ring current on the night side of the earth, where the earth precludes direct passage of the uncharged particles. But the drift of the particles, after they become charged, must then tend to accumulate positive charge at the western end and negative charge at the eastern end. This charge will flow northwards and southwards along the magnetic field lines, and the transferred charge will produce an electric field that causes electric current to flow in the ionosphere to neutralize the charge distribution. This current will flow partly westward over the night hemisphere, but mainly eastward over the more conducting sunlit part of the ionosphere. These ionospheric currents reduce the DR field over the sunlit hemisphere below its value over the night hemisphere.

The third main current system that contributes to the D field is strongest in the polar ionosphere around both magnetic axis poles, where charged particles from the Van Allen belts and their DR current distributions enter the atmosphere and produce the aurora. It is suggested that positive and negative particles, mainly protons and electrons, set up charge distributions in the polar caps, by entering at slightly different polar latitudes. The electric forces thus set up in the polar regions, generally near the auroral zones, drive a system of currents flowing most strongly in high latitudes along the auroral zone. The concentrated currents there are called auroral electrojets. They complete their circuit by current flow over the polar caps and over the great interzonal belt between the auroral zones. There may also be some flow from one hemisphere to the other along field lines. This current system and its field are denoted by DP, D for disturbance and P for polar.

Thus the DCF currents flow far outside the ionosphere. The DR currents may flow wholly outside the ionosphere, or partly outside and partly inside. The DP currents probably flow mainly, if not wholly, in the ionosphere.

The world distribution of electrical conductivity over the ionosphere must directly influence the DP currents, and it will likewise influence any part of the DR current system that may flow in the ionosphere; it can influence the DCF part of the D field at the earth's surface only in connection with currents caused in the ionosphere by electromagnetic induction, when the DCF field is changing.

The ionosphere will partly shield the surface from outside field changes such as those of the DCF and DR currents. If the ionosphere were everywhere uniformly and isotropically conducting, a sudden increase in the charged flux (CF) and in the DCF currents and field would induce shielding westward currents flowing around latitude parallels. The great difference of conductivity as between day and night will prevent the induction of symmetric latitudinal currents; the currents induced will be more complex, but some daytime enhancement along the dip equator seems inevitable.

Sometimes DP currents appear at or very soon after the sudden commencement of a magnetic storm; in such a case their effect may exceed and conceal any DCF induction effects near the equatorial electrojet. Storm commencements in relation to the electrojet have been considered by various authors (Ferraro, Parkinson and Unthank, 1951; Sugiura, 1953; Forbush and Vestine, 1955; Obayashi and Jacobs, 1957); cf. Fig. 1. However, so far as I know, electromagnetic induction effects in the ionosphere in and near the region of the equatorial electrojet have not been studied systematically for sudden storm commencements chosen for the absence of DP currents — and these are the only cases where interpretation may be relatively simple. Ashour and Price (1948) have considered important problems of ionospheric electromagnetic induction associated with magnetic storms, but without special consideration of the equatorial electrojet belt.

The existence of a partial ring current system has only recently been proposed (Akasofu and Chapman, 1964), and the influence of the equatorial ionospheric belt of high electric conductivity upon its magnetic field has not yet been considered quantitatively. The DR current will enter the ionosphere north and south of the equator, mainly in latitudes rather high except during magnetic storms of such great intensity as to produce low latitude auroras. Nevertheless it may prove possible to detect an equatorial electrojet influence on the DR field during intervals between polar substorms, when the DP current system is absent. Hitherto it has seemed that the DR field shows no equatorial electrojet anomaly (Chapman, 1951; Sugiura and Chapman, 1960). The DP current system is the one most obviously subject to equatorial influence, and the electrojet influence on the D field has been studied (e.g., Akasofu and Chapman, 1963), in connection with the fluctuating DP currents. If the DP auroral electrojet currents is westward, its return flow in low latitudes is eastward, and enhances the Sq eastward electrojet present during the hours of sunlight. Many examples of this are available in the records. Westward auroral

electrojets tend to be located mainly on the night side of the earth, which
reduces the equatorial electrojet influence upon the D field.   This is because
during the night the ionization in the E layer, which is the layer in which there
is enhancement of electrical conductivity along the dip equator, dies away.
Hence only that part of the interzonal return current of westward auroral
electrojets that can extend into the sunlit hemisphere can be affected by the
equatorial electrojet. This eastward DP return current along the electrojet can
at times be intense (Fig. 2). Eastward auroral electrojets tend to occur in
the post-noon sector of the sunlit hemisphere, and although they are generally
weaker than westward auroral electrojets, their westward return current is
more favorably located to flow preferentially along the dip equator. Examples
of this are available, showing that sometimes the westward DP return current
can reverse the eastward direction of Sq current flow along and near the dip
equator (e.g., this seems to occur at Koror on Nov. 7, 1957, soon after 11 h
local time).   This is most likely to occur during a great magnetic storm, when
the aurora and its electrojet is in an unusually low latitude, and consequently
unusually near the dip equator.
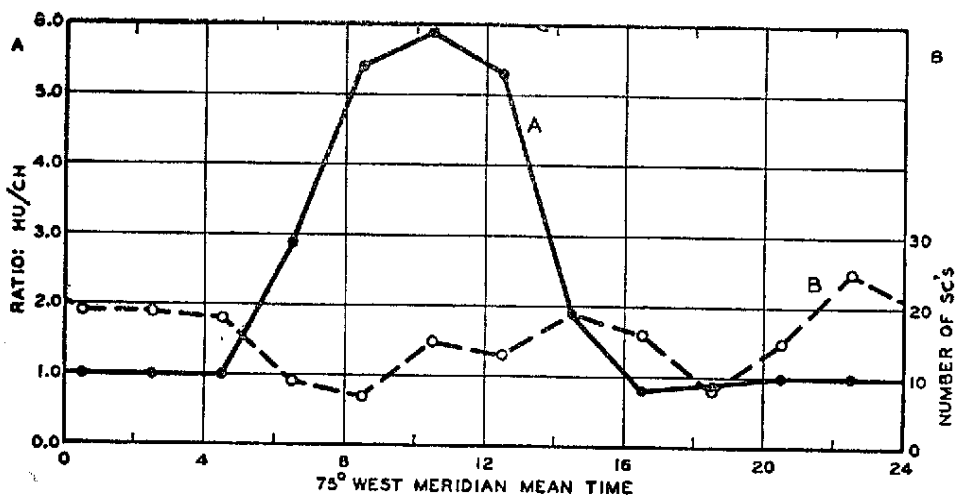
Fig. 1 — Enhancement of the in H under the equatorial electrojet.   The full
curve indicates the daily variation of the ratio of the amplitude of
Sc's at Huancayo to the amplitude of the corresponding Sc's at Chelten-
ham, for 183 Sc's, 1922-46.   This shows the daytime enhancement of
the Sc in H at Huancayo. The broken line gives the daily variation
of the frequency of these Sc's, relative to local time (which is
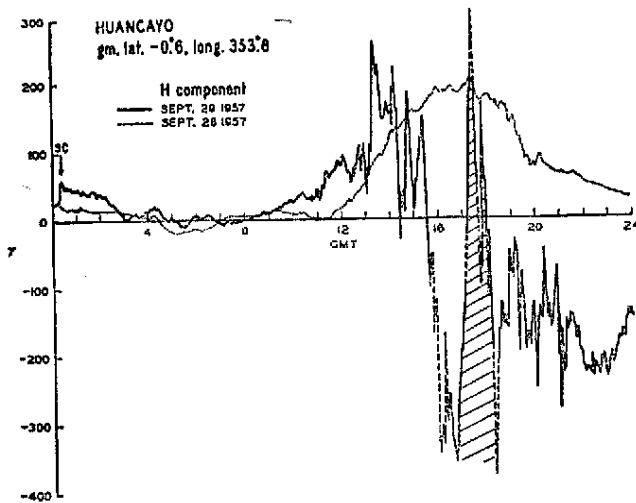approximately the same at the two stations). (Sugiura 1953; Fig. 1).

Fig. 2 — The Huancayo H records for 1957 September 28 (a quiet day) and 29 (including part of a great magnetic storm); on the 28th the record shows Sq, and the beginning of Sq is shown also on the 29th. Then the great storm began, with first a DCF increase and then a much larger decrease (DR). On this, between 1600 and 1900 GMT, is superposed the effect of an intense eastward return current of a westward auroral electrojet; despite the big H reduction caused by the DR current near the height of the main phase, the DP return current brings H above the normal maximum value around local noon. At this time the DP current much enhances the normal eastward Sq current along the electrojet. (Akasofu and Chapman, 1963; Fig. 4).

References

(1) Akasofu, S. - I., (a) A source of the energy for geomagnetic storms and auroras, Planet. Space Sci., **12**, 801-833, 1964.

(2) Akasofu, S. - I., (b) The neutral hydrogen flux in the solar plasma flow — I, Planet. Space Sci., **12**, 905-913, 1964.

(3) Akasofu, S. - I., and Chapman, S., The sudden commencement of geomagnetic storms, Vrania, Spain, **250**, 1-35, 1960.

(4) Akasofu, S. - I. and Chapman, S., The enhancement of the equatorial electrojet during polar magnetic substorms, J. Geophys. Res., **68, 2375-2382,** 1963.

(5) Akasofu, S. - I. and Chapman, S., On the asymmetric development of magnetic storm fields in low and middle latitudes, Planet. Space Sci., **12,** 607-626, 1964.

(6) Akasofu, S. - I. and McIlwain, C. E., Energetic neutral hydrogen atoms as a source of the ring current particles, Trans. Amer. Geophys. Union, **44, 883,** 1963.

(7) Ashour, A. A. and Price, A. T., The induction of electric currents in a non-uniform ionosphere, Proc. Roy. Soc., A, **195,** 198-224, 1948.

(8) Chapman, S., The normality of geomagnetic disturbances at Huancayo, Geofis. P. e App., **19,** 151-158, 1951.

(9) Ferraro, V. C. A., Parkinson, W. C. and Unthank, H. W., Sudden commencements and sudden impulses in geomagnetism, Cheltenham (Md.), Tucson, San Juan, Honolulu, Huancayo, and Watheroo; J. Geophys. Res., **56,** 177-195, 1951.

(10) Forbush, S. E. and Vestine, E. H., Daytime enhancement of size of sudden commencements and initial phase of magnetic storms at Huancayo, J. Geophys. Res., **60,** 299-316, 1955.

(11) Obayashi, T. and Jacobs, J. A., Sudden commencements of magnetic storms and atmospheric dynamo action, J. Geophys. Res., **62,** 589-616, 1957.

(12) Sugiura, M., The solar diurnal variation in the amplitude of sudden commencements of magnetic storms at the geomagnetic equator, J. Geophys. Res., **58,** 558-559, 1953.

(13) Sugiura, M. and Chapman, S., The average morphology of geomagnetic storms with sudden commencement, Abh. d. Akad. d. Wiss. in Göttingen, Math. — Phys. Klasse, Sonderheft **4,** 1960.

(14) Vestine, E. H., The immediate source of the field of magnetic storms, J. Geophys. Res., **58,** 560-562, 1953.

BRIEF REMARKS ON STORMS

by

S. Matsushita

HAO, CRPL and UC, Boulder, Colorado, U.S.A.

There are many reports of the enhancement of the horizontal component during the daylight hours in the magnetic equatorial zone at sudden commencements and impulses, solar daily disturbance variations (DS), and solar flares; for example, Bhargava and Subrahmanyan (1964), Matsushita (1964) and Rastogi et al. (1965). This enhancement is caused by the high conductivity in the magnetic equatorial zone. Ashour and Ferraro (1964) discussed the induction of electric currents in an anisotropic equatorial ionosphere, and Ferris and Price (1965) showed a slightly different method of analysis concerning this subject. The frequent occurrence of the preceding reverse impulse type sudden commencement (named $^-$SC) during the daylight hours in the magnetic equatorial zone, which is shown in Fig. 1 may be explained by the induction effect.
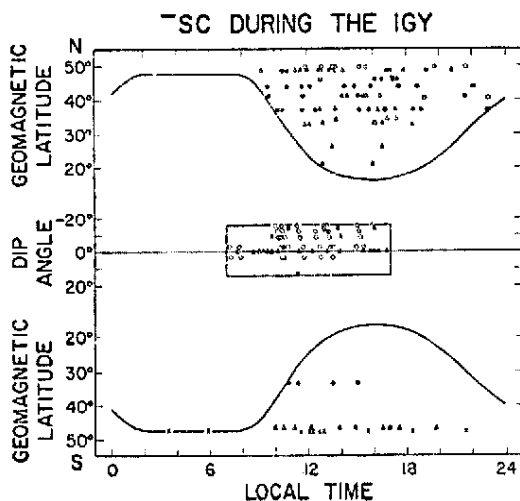
Fig. 1 — Occurrences of $^-$SC at worldwide IGY stations between the geomagnetic latitudes 50°N and 50°S are shown against the local time of occurrence and the latitude of the station (the dip angles in the magnetic equatorial zone). The solid circles, triangles, crosses, and open circles indicate the following four longitudinal zones: Europe and Africa (gm 50°E-140°E), Asia and Australia (gm 140°E-320°E); and Northwest and South America (gm 320°E-50°E), (Matsushita, 1964).

Figure 2 shows observed world-wide pattern of the horizontal vectors of geomagnetic changes caused by the Starfish explosion on 9 July 1962. A large southward vector change in the magnetic equatorial zone during the daylight hours, shown in Fig. 2, seems to be caused by a westward jet current of positive particles due to the explosion (Maeda et al. 1964).

Forbush (1964) made a detailed study of ring current effects from magnetic data and discussed solar cycle and seasonal variations of the effect and application for investigating secular change of the earth's main magnetic field.

Theoretical models of magnetic storm were reviewed by Matsushita (1964); none of them is very satisfactory, we need to study them in the future in more details. Concerning ionospheric storms there is also no satisfactory theory.
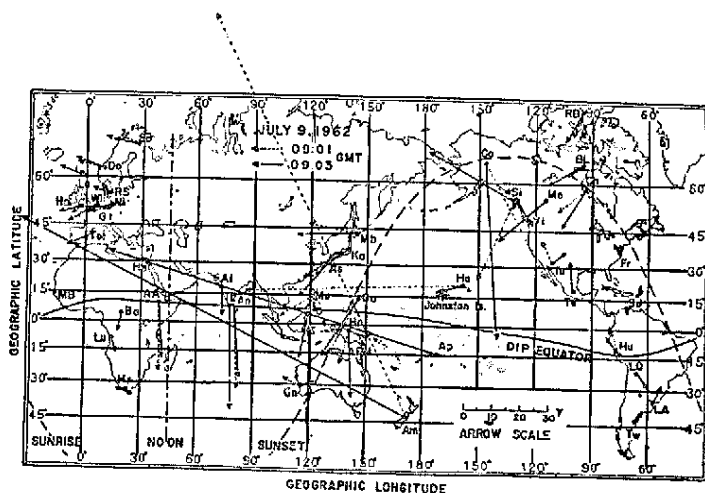
Fig. 2 — Observed worldwide pattern of the horizontal vectors of geomagnetic changes at 0901 and 0903 UT on 9 July, 1962, (Maeda et al. 1964).

References

Ashour, A.A. and V.C.A. Ferraro, The induction of electric currents in an anisotropic ionosphere with a belt of high conductivity running along the equator, J.A.T.P., **26**, 509-523, 1964.

Bhargava, B.N. and R.V. Subrahmanyan, Geomagnetic disturbances associated with equatorial, electrojet, J.A.T.P., **26**, 879-888, 1964.

Ferris, G.A., and A.T. Price, Electric currents induced in an anisotropic ionosphere, Geophys. J. Roy. Astron. Soc. **9**, 285-308, 1965.

Forbush, S.E., The geomagnetic field of the equatorial ring current its solar cycle and seasonal variations and application for investigating secular change of the earth's magnetic field, Annual Rept. D.T.M., Carnegie Inst. 351-354, 1964.

Maeda, H., A.J. Shirgaokar, M. Yasuhara, and S. Matsushita, On the geomagnetic effect of the Starfish high-altitude nuclear explosion, J.G.R., **69**, 917-945, 1964.

Matsushita, S., Geomagnetic storms and related phenomena, Res. in Geophysics, edited by H. Odishaw, MIT Press, **I**, 455-483, 1964.

Rastogi, R.G., N.D. Kaushida, and N.B. Trivedi, Solar flare crocket and sudden commencement in H within the equatorial electrojet region, J.A.T.P., **27**, 663-668, 1965.

KOROR DATA AND MAGNETIC BAYS IN LOW LATITUDES

by

David G. Knapp

Environmental Science Services Administration

U.S. Coast and Geodetic Survey

The strong midday enhancement of most types of perturbation at stations along the dip equator provides an independent means of scrutinizing the associated conductive strip, and this phenomenon promises the advantage that its proximate cause, unlike the driving mechanism of Sq, may be independent ou longitude. From a rather cursory inspection of records at several low-latitude observatorics including some of those in the immediate vicinity of the dip equator, it appears that the low-latitude perturbation effects in H are similar and simultaneous in different longitudes; and if this is so, they cannot be regarded as mere fluctuations in the Sq system.

A straightforward way to account for this coherence is to suppose (a) that the magnetic perturbations represent a band of zonal perturbation currents in the ionosphere, flowing all around the earth, but redistributed in the midday segment so as to concentrate along the dip equator; and (b) that these are secondary currents in a transformer action, the primary currents being generated in a higher level, perhaps in the Van Allen radiation belts.

This study is mainly concerned with the high degree of coherence between the vertical and horizontal components of bays at Koror, and with the moderate midday enhancement of the ratio $\triangle Z/\triangle H$ lor the bays. It is suggested that the nighttime Z fluctuations at Koror are accounted for by inhomogeneity of the induced subsurface current as modified by the island effect. If the ocean and the earth's crust had zero conductivity, the $\triangle Z/\triangle H$ ratio should drop to zero at night. It does not do so. The diurnal curve of $\triangle Z/\triangle H$ does show a slight midday rise that is attributed to the dip-equator concentration, but it appears

that this rise is not a simple measure of the zenith distance of the electrojet, because the known 28 km northward drift of the dip equator between the IGY and the IQSY is not accompanied by a corresponding increase in the midday enhancement of $\triangle Z/\triangle H$.

The paper includes a suggestion as to the reason for the fact the equatorial enhancement of the daily variation of H is usually found to be less than that of the perturbation fields.

Curves are shown in Figs. 1-4 of the daily variation of the $\triangle Z/\triangle H$ ratio for Koror bays. A curiosity of the curves is the suggestion they contain a premidnight rise, perhaps comparable with the midday salient, though the number of bays scaled (540 thus far) is not enough to establish this with any assurance. The scarcity of measurable night-time bays is a factor in this.
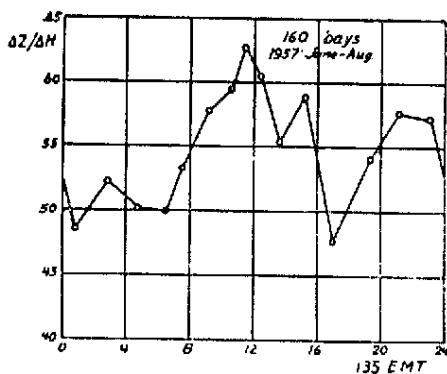
Fig. 1 — Ratio of vertical to horizontal amplitude of bays at Koror, for Jun.-Dec. 1957. Note small amplitude of the midday peak.
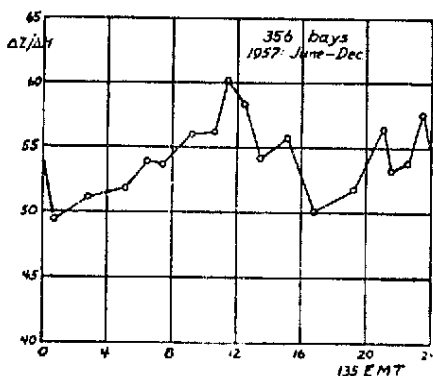
Fig. 2 — Ratio of vertical to horizontal amplitude of bays at Koror, for Sept.-Dec. 1957.
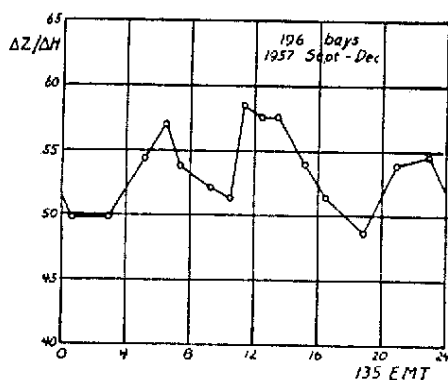
Fig. 3 — Ratio of vertical to horizontal amplitude of bays at Koror,
        for Sept.-Dec. 1957.
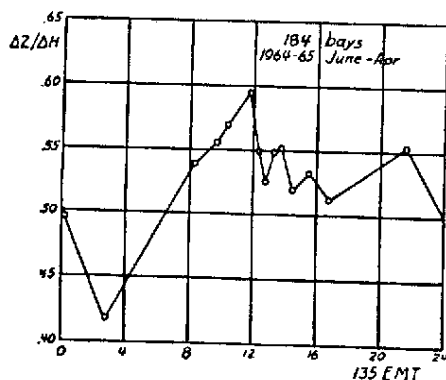
Fig. 4 — Ratio of vertical to horizontal amplitude of bays at Koror,
        for Jun. 1964 to Apr. 1965.

PRELIMINARY REPORT ON SOME GEOMAGNETIC EVENTS

RECORDED UNDER THE ELECTROJET IN PERU

by

Mateo Casaverde and Alberto Giesecke

Instituto Geofisico del Peru, Peru

The present report is a preliminary one of two on the many geomagnetic events recorded during the different surveys carried out in Peru in the last three years. The results of these experiments may answer a few of the many questions which have arisen during the discussions on the equatorial electrojet at the Symposium.

The records obtained at the 8 to 10 stations offers for the first time a good spatial resolution on the variation recorded on the magnetic equator. Fig. 1 shows the locations of the ten sites: Huancayo (HU), Ayacucho (AYO), Abancay (ABA), Cuzco (CUZ), Ccapana (CCA), Sicuani (SIC), Pucavá (PUC), Cabanillas (CAB), Arequipa (ARE) and Ayanguera (AYA). The dip varies from $+ 2°$ down to $- 6°$ for these stations. Fig. 2 shows a magnetically quiet day variation (24 Aug. 1963) in the three components D, H and Z, which shows the current concentration of the equatorial electrojet. The curves reveal a consistent change of the daily ranges along the profile across the southern and central portion of the electrojet. The steady increase of the noon maximum in H from AYA, 400 km south of the dip equator, to CUZ right on the dip equator, shows clearly the effect of the electrojet which is superimposed on the normal Sq. Table I shows the daily ranges for H and Z; the dip angle and the distance of each station from the dip equator.

If we define the width of the electrojet as the distance between the points of inflection of the Z range variation, positive as well as negative, we find from a previous report (Forbush and Casaverde) an approximate half width of 300 km; which would correspond to the

sunspot maximum. From Table I, we find for the most southern station, which is about 400 km from the dip equator, the highest range for Z (45 gammas). This would suggest that the half width of the electrojet is equal or greater than 400 km for the sunspot minimum than during the sunspot maximum.
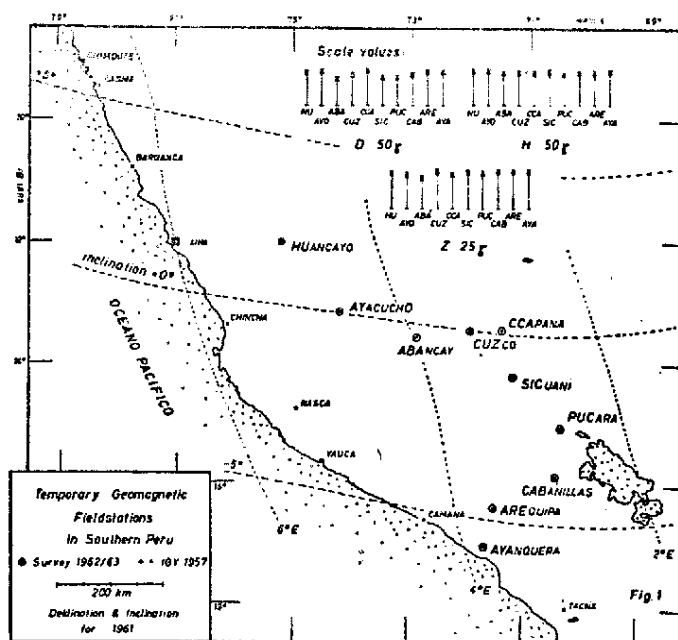

Fig. 1 — Location of geomagnetic stations during the 1963 survey. Scale values for variographs, are included.
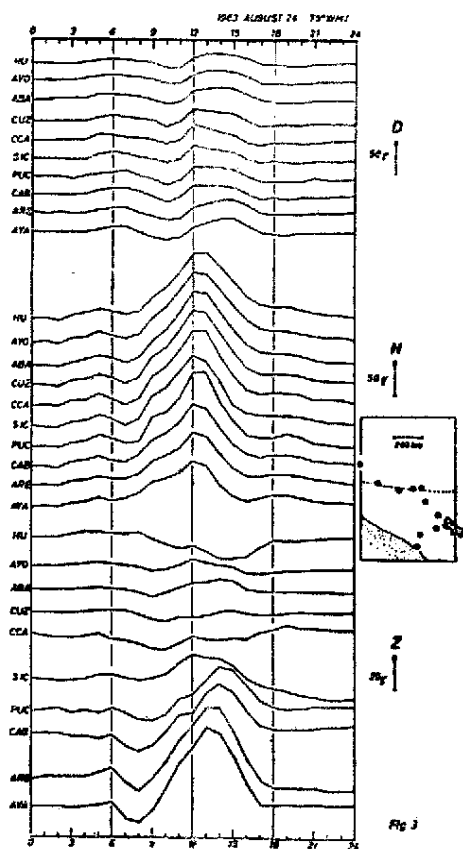
Fig. 2 — Quiet diurnal variation for D, H and Z on 24 August 1963.

Table 1

Total daily ranges for H (γ^H_T) and Z (γ^Z_T) for 24 Aug. 1963.
Magnetic dip (I), distance in km from the dip equator.

STATION	γ^H_T	γ^Z_T	I	Distance from I = 0°
	(gammas)	(gammas)		(km)
HU	105	−7	2°	115 North
AYO	110	3	0	—
ABA	120	5	−0,5	—
CCA	120	0	0	—
CUZ	120	−2	0	—
SIC	100	14	−1,3	80 South
PUC	105	12	−2.8	170 South
CAB	80	18	−4.0	250 South
ARE	70	35	−4.8	320 South
AYA	60	45	−6.0	400 South

During IGY it was found, with stations along the coast in Peru, as reported by other workers in Africa and South Pacific, an asymmetry in the Z range distribution below the electrojet with higher values — twice as much — toward the south. This same result was found during the present survey discarding the possibility of any ocean effect. SIC has a γ^Z_T twice as much as HU, being both stations about the same distance from the dip equator.

Figure 3 shows the SC and a few hours of the most intense storm of 1963, which started at 0915 (75°W MT) on September 21, lasting for about two days. The storm was recorded at all field stations, except that ABA and CCA were not operating. The H ranges of the SC as well as the following short period variations increase gradually toward the magnetic equator. This indicates a similar equatorial concentrations of the overhead currents as described for the daily long

period variations. However, the Z variations show different variations from place to place and do not reflect at all the external electrojet field. These anomalies are related to internal conductivity anomalies which is a matter of additional surveys being carried out in southern Peru The D variations show a very interesting feature in contrast to the long period diurnal variation. This may be an effect of some other current systems at higher levels than the electrojet.
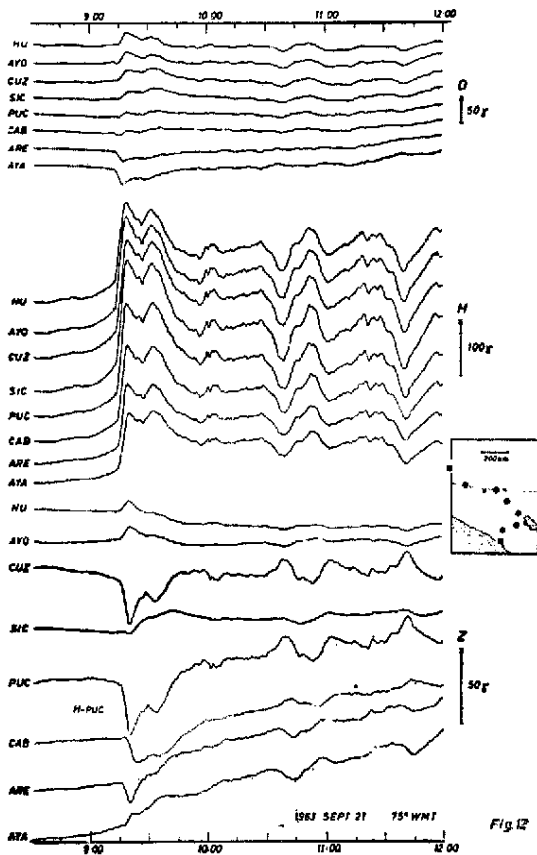
Fig. 3 — Sudden Storm Commencement for D, H and Z on 21 Sept. 1963.

Reference

Forbush, S.E. and M. Casaverde, Equatorial Electrojet in Peru, Carnegie Institute of Washington, Pub. 620, 1961.

THE 22-YEAR VARIATION IN THE OCCURRENCE OF

GEOMAGNETICALLY DISTURBED DAYS

by

Edwin J. Chernosky
Air Force Cambridge Research Laboratories
Bedford, Mass., U.S.A.

It is known that magnetic activity varies in some relation to the phase of the eleven-year solar cycle in which it occurs. In this paper a study is made for a relation of the occurrence of magnetic activity to the 22-year sunspot cycle. The 22-year cycle is based upon the alternating change in the sequence of the magnetic polarity of pairs of sunspot from one eleven-year period to the next. Sunspots generally occur in pairs with their connecting axis in an east-west direction. The eastern most spot of each group in one hemisphere will have one polarity during that eleven year period and the opposite during the following eleven-years. The northern and southern hemisphere of the sun show characteristics opposite to each other.

To make this study, the International Magnetic Character Figure C, ranging from 0.0 to 2.0 is used to describe the magnetic activity of each day. Days having values of C from 1.0 to 2.0 were considered as disturbed. Eighty years of data or 29,219 days from 1884-1963 were used. The eighty years were arranged in 20 groups according to the year of the sunspot magnetism cycle in which they occurred. Twenty years instead of 22 years were used to form the cyclic period since some of the sunspot number cycles were less than 11 years in length. The additional years were included in the year of cycle minimum adjacent to each other. See Fig. 1.

Mean values of each of the 20 groups, each including from 3 to 6 years, were used to show the cycle trends during the two number-cycles represented and for intercomparison of the two number-cycles.

The annual variations within each group were evaluated using average for each ninth group. Instead of 20 year-groups however these were combined from consecutive pairs to give 10 year-groups and more representative samples (Fig. 2).

REPRESENTATION OF SUNSPOT-MAGNETISM CYCLE IN GEOMAGNETIC ACTIVITY LEVEL AND DISTURBED DAY OCCURRENCE (1884-1963)
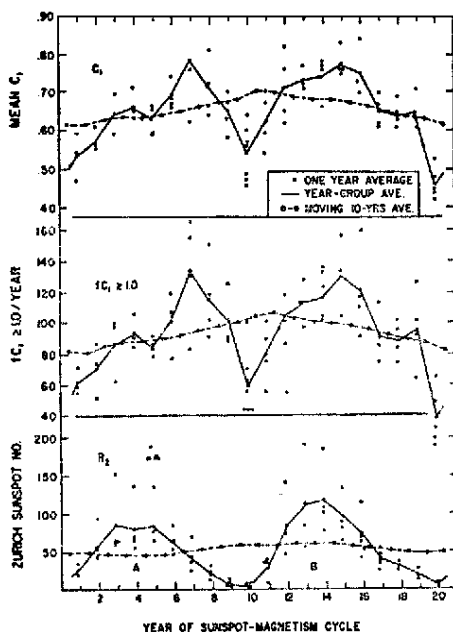
Fig. 1 — Annual values and their averages grouped according to the sunspot-magnetism cycle showing cyclic trends in magnetic activity, number of disturbed days and sunspot number. The sunspot-magnetism cycle in terrestrial magnetic activity is indicated by the dashed lines of the upper two graphs.
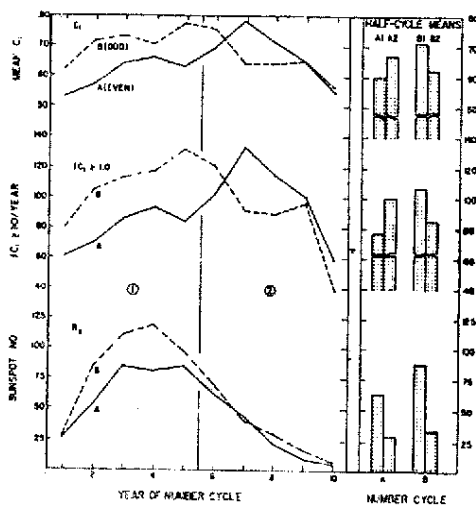
Fig. 2 — A comparison of magnetic activity, number of disturbed days and sunspot number from one cycle to another. The change in level of terrestrial magnetic activity for each half of each cycle is shown by the bar graphs at the right and indicates the nature of the sunspot-magnetism cycle in this aspect.

The analysis of the annual means represented by the 20 year-groups showed that even numbered Zurich 11-year cycles were more active in the last half of the cycle than in the first half. For the Zurich odd-numbered cycles, the first half of the cycle was more active. This change is one indication of the 22-year cycle in terrestrial magnetic activity.

The annual variation shows two periods of maximum activity each year near the times of equinox. The semi-annual peaks are very weak at the minimum ending the odd-numbered cycles and the post-minimum period beginning the following even-numbered cycle. The semi-annual peaks are strongly evidenced at the maximum ending the

even-numbered cycles and the post-minimum period beginning the odd cycles. In individual calendar years the semi-annual variation is usually more clearly shown by the frequencies of occurrence of distributed days than by the monthly mean C_i figure. See Fig. 3.
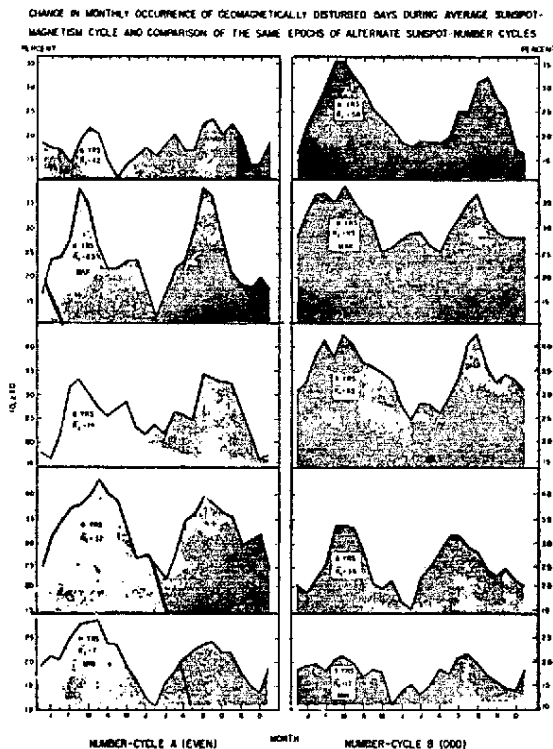
Fig. 3 — The change in the annual variation of magnetic disturbance as shown by the occurrence of magnetically disturbed days for ten epochs of the sunspot-magnetism cycle. Read down from top left to bottom to follow the change. The same epochs of consecutive cycles compared side by side.

It is not certain whether this change in characteristics at alternate solar minimum is due to varying deflection or intensity of the solar emission affecting the earth or is a cyclic modification of the terrestrial environment. There is good indication that there is a 22-year cycle variation in terrestrial magnetic activity and this is a factor which need to be considered in further evaluation of solar cycle trends of equatorial and other measurements.

THE ORIGIN OF FLUCTUATIONS IN THE EQUATORIAL ELECTROJET: A NEW TYPE OF GEOMAGNETIC VARIATION

by

Atsuhiro Nishida, Noboru Iwasaki and Takesi Nagata

Geophysical Institute, University of Tokyo, Japan

The enhanced Sq variation at the geomagnetic equator is frequently marred by large irregular fluctuations whose magnitude occasionally reaches the amplitude of the Sq variation. In the present paper, the world-wide morphology of all types of equatorial fluctuations (except micropulsations) which are detected in 40 days' sample period during the IGY are presented, and their origin is investigated. Part of these fluctuations can be identified as geomagnetic variations of the known kind, namely, sfe, ssc and positive and negative si. The majority of them, however, show peculiar characteristics which cannot be explained in terms of the nature of the known variations.

These remaining fluctuations seem to belong to a new class of the geomagnetic variation. They appear at the equator as decreases in the horizontal component with a maximum magnitude of about 200 γ, and with a time scale ranging from half an hour to several hours. Simultaneously with the fluctuation in the equatorial field, variations of the identical form appear over a wide area, which is centered at about 1800 hours meridian and is wider than the hemisphere (see Figs. 1 and 2). When the equivalent current system is drawn for these fluctuations, it is found that the direction of the current flow is independent of latitude below the geomagnetic latitude of about 75°, and all these currents flow through the polar cap (see Fig. 3). These fluctuations appear quite frequently, and in the sample period around the vernal equinox of 1958, they are almost always present.
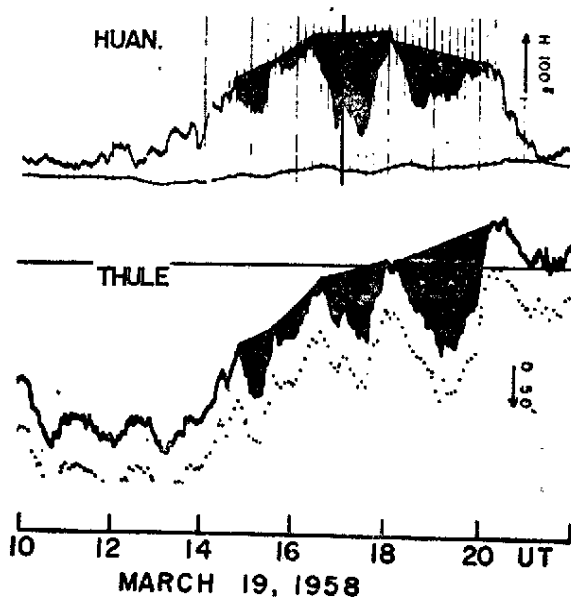
Fig. 1 — Comparison of magnetograms from equatorial (Huancayo) and polar (Thule) stations. The variation of the new type appears in phase in both records. The blackened part is the decrease in the new type variation from the normal record on a very quiet day.
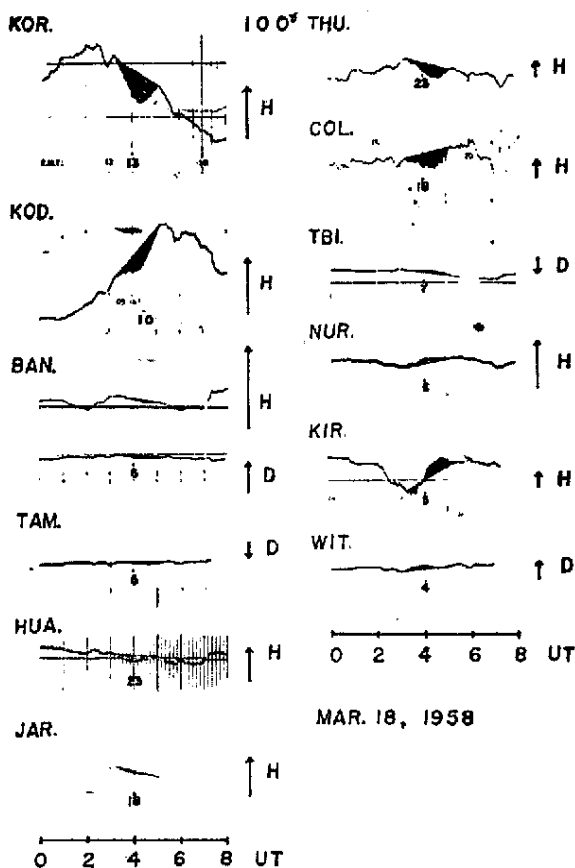
Fig. 2 — Samples of magnetograms from widely distributed stations, showing the new type variations. Except in a region where negative bays are sometimes superposed, an excellent coherence can be seen.
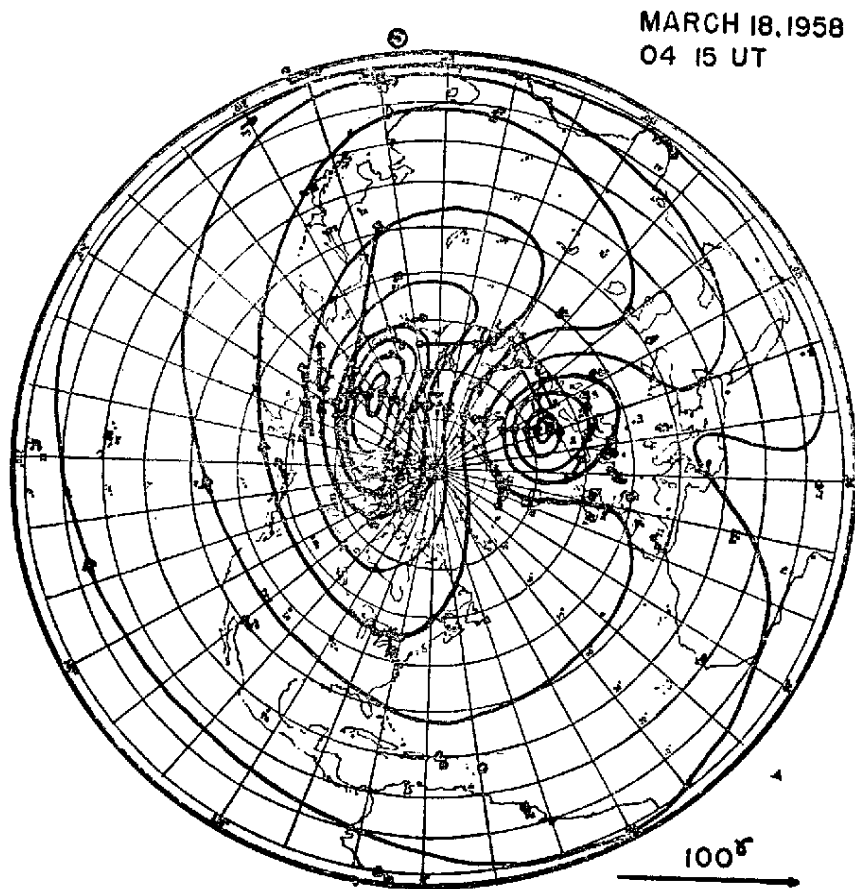
Fig. 3 — Equivalent current system for the case shown in Fig. 2.

The magnitude of the electric potential associated with these fluctuations is around 50 kv across the current vortex. Thus, this new type of geomagnetic variations seems to testify the presence of a large scale magnetospheric convection of a transient nature, which is as intense as the one associated with the viscous-like interaction with the solar wind.

IONOSPHERIC PARAMETERS FOR NAIROBI FOR MAGNETICALLY DISTURBED AND QUIET DAYS

by

R. F. Kelleher

Physics Department, University College Nairobi, Kenya

An examination has been made of certain ionospheric parameters obtained from routine hourly vertical soundings at Nairobi. The present results give median values for the International Quiet and Disturbed Days during the period March 1964 to February 1965.

The results are shown in Fig. 1-6 and suggest that (at least in sunspot minimum years) Nairobi lies in an intermediate region where geomagnetic control is small.
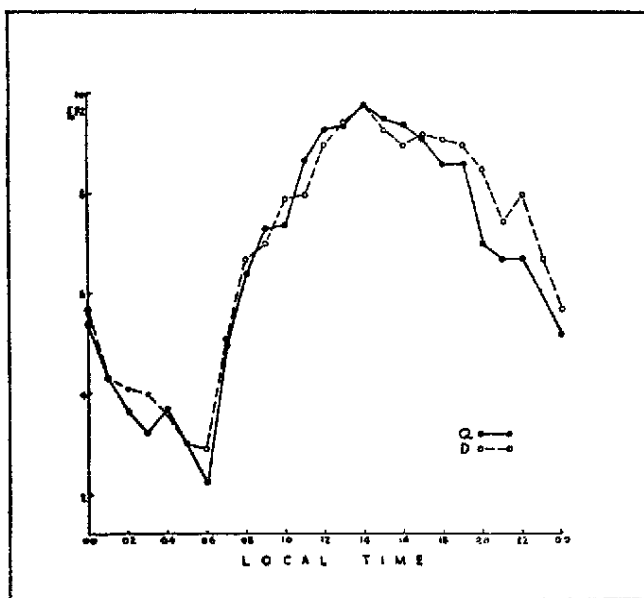
Fig. 1 — Shows the foF2 data for quiet and disturbed days. It can be seem that there is little difference between the two sets of days, though the critical frequency is slightly higher under disturbed conditions for hours after about 1600 LT.
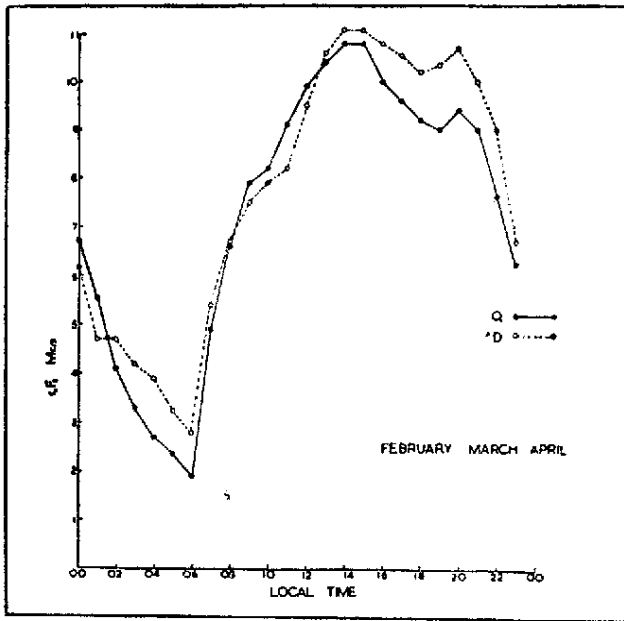
Fig. 2 — Show seasonal results (Feb., Mar. and Apr.). An interesting feature is the secondary peak occurring between 1900-2300 LT, which is anhanced by magnetic activity and is particularly pronounced in local summer (Fig. 5).
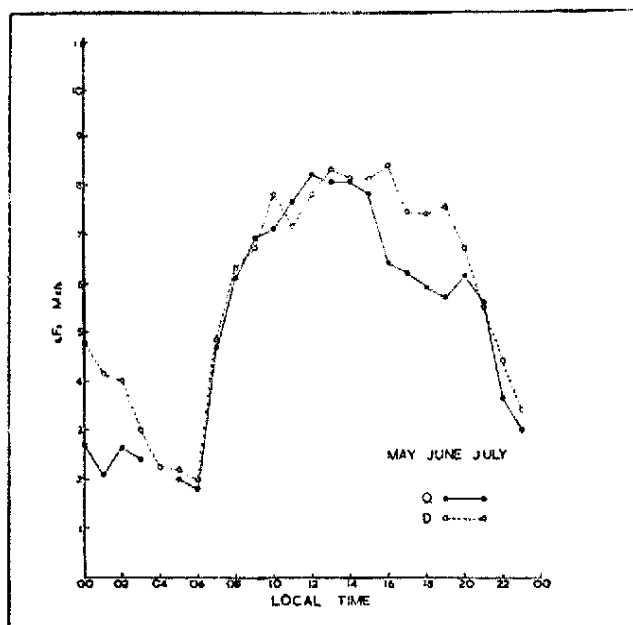
Fig. 3 — Same as Fig. 2 for May, June and July.

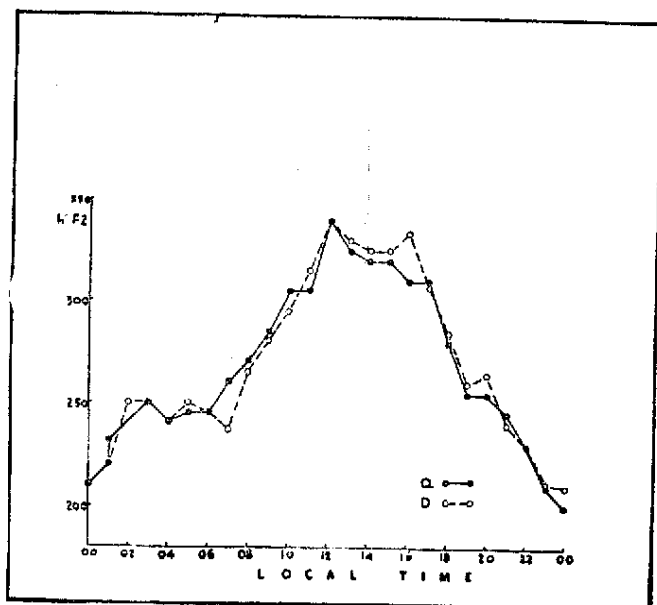Fig. 4 — Same as Fig. 2 for Aug., Sept. and Oct.
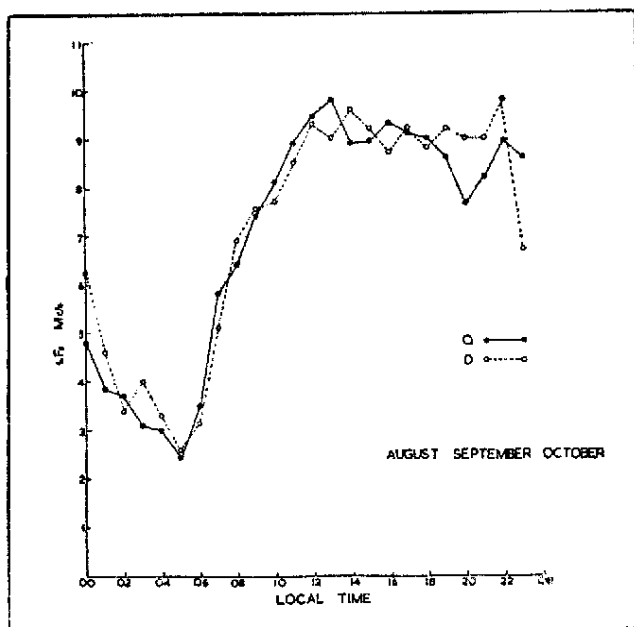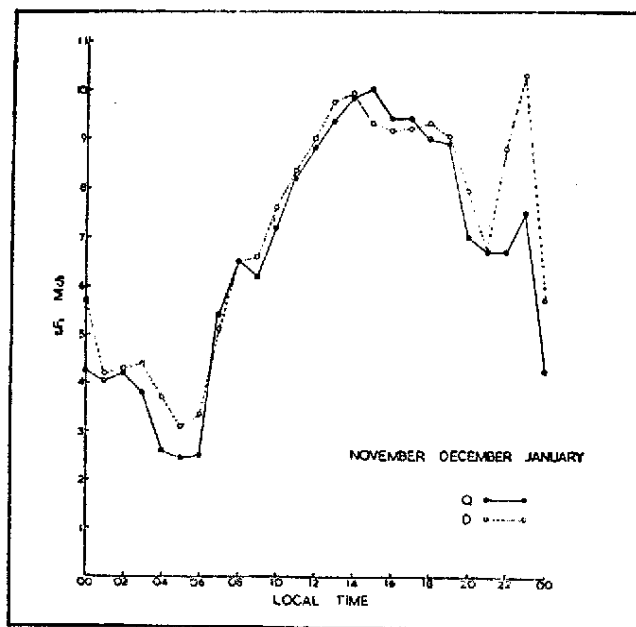
Fig. 5 — Same as Fig. 2 for Nov., Dec and Jan.

Fig. 6 — Plot of the parameters h'F2. Here also the differences between quiet and disturbed days are small. It is likewise found that the probability of occurrence of a sharp F1 cusp is largely unaffected by magnetic activity.

SOME FEATURES OF EQUATORIAL IONOSPHERIC STORMS

by

E. O. Olatunji

Ibadan University, Nigeria

Ionospheric disturbance effects in the equatorial F2 layer are examined in the next five figures. Data obtained from ionograms and total columnar electron content measurements are used to elucidate some features which have to be considered if one it to understand storm mechanisms.

A storm event in the topside ionosphere reveals an inversion of storm effect at great altitudes; and suggests a reduced transport of ionization from the magnetic equatorial belt during a disturbance.
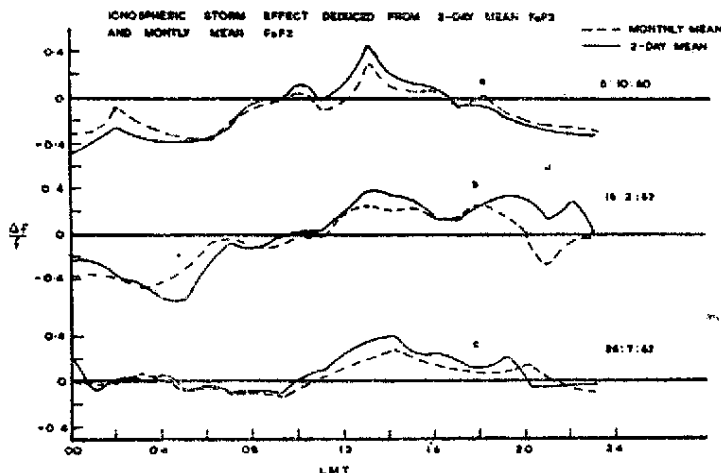
Fig. 1 — Shows the results of ionospheric storms deduced from 2-day mean foF2 (solid lines) and monthly mean of foF2 (dashed lines).
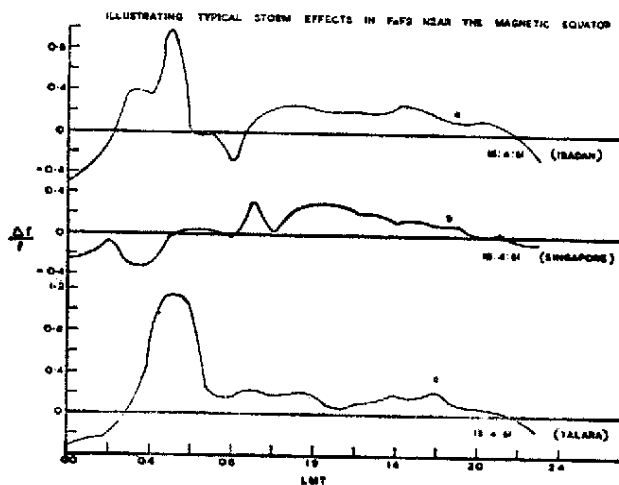
Fig. 2 — Examination of foF2 for three equatorial stations in separated longitude zones shows a tendency towards a daytime increase and nighttime decrease of ionization density relative to quiet days.
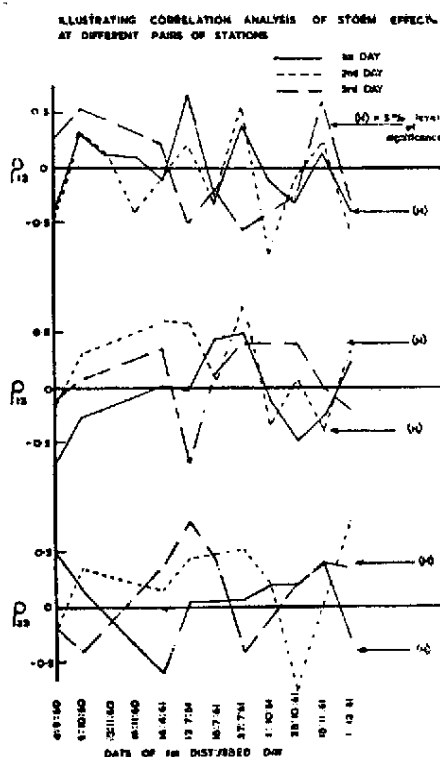
Fig. 3 — Illustrates the correlation analysis of storm effects at different pairs of stations (see Fig. 2). Differences in behavior at different stations for a given storm, and for storms at a fixed station are clearly exhibited.
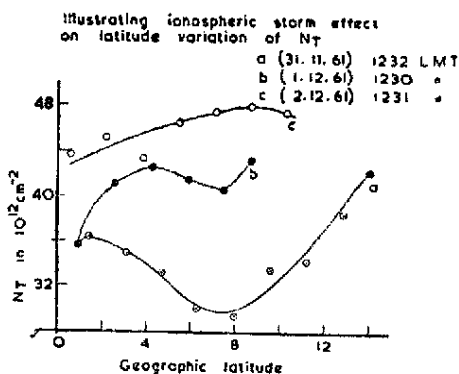
Fig. 4 — A daytime increase of the total columnar ionization during a storms is shown to be a regular feature. In the great majority of cases, hmF2 is not altered by a sotrm. The increase in ionization density occurs mostly in the topside ionosphere.
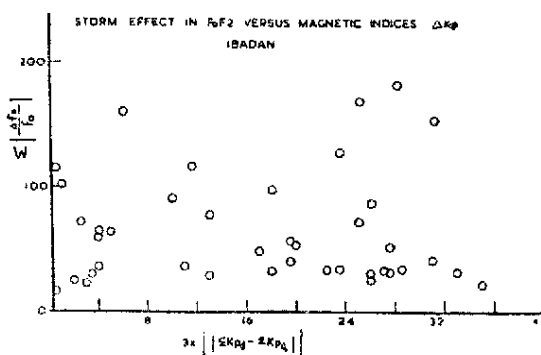

Fig. 5 — Time and intensity relationships between ionospheric and magnetic disturbances are examined. Both time and intensity relations raise difficulties in reconciling storm theory and evidence.

ENHANCEMENT OF MAGNETIC DISTURBANCES OVER THE

MAGNETIC EQUATOR DURING THE NIGHTTIME HOURS

by

R.G. Rastogi, N.D. Kaushita and N.B. Trivedi

Physical Research Laboratory, Ahmedabad, India

The amplitudes of sudden commencement of magnetic storms (SSC) during the daylight hours and of solar flare effects (sfe) in horizontal field, H, show a pronounced maximum over the magnetic equator. The deviation of vertical field, $\triangle Z$, are positive south of the equator and negative north of the equator, the sign changing at a place very close to the magnetic equator. SSC in H during the nighttime for the stations in American Zone show significant enhancement near the magnetic equator. The change in sign of $\triangle Z$ happens at a dip of about 7°N (Fig. 1).
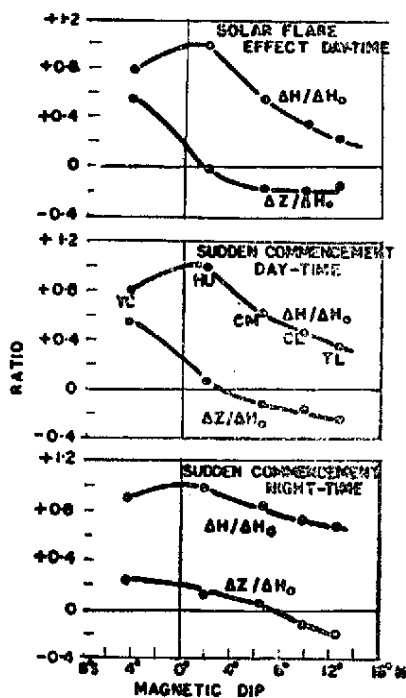

Fig. 1 — Variations with magnetic dip of the ratios of $\triangle H$ and $\triangle Z$ at different stations with respect to $\triangle H_o$ at Huancayo for the daytime sudden commencement storms and solar flare effects and for the nighttime sudden commencements at Peruvian stations.

Nighttime fluctuations in H at Huancayo and San Juan show excellent similarity with each other (Fig. 2). Mean ratio of $\triangle$H at Huancayo to $\triangle$H at San Juan has a value of about 9.0 for midday and 1.7 for midnight hours (Fig. 3). Comparing magnetograms at Huancayo, Yanca, Chimbote, Chiclayo and Talara, one finds very close similarities in the fluctuations, i.e., the amplitude decreasing progressively from Huancayo to Talara (Fig. 4). The average deviation in H at Talara (13°N dip) is about 0.65 to that at Huancayo (2°N dip) indicating a sharp enhancement of $\triangle$H at the magnetic equator even during the nighttime hours (Fig. 5).

It is concluded that the significant equatorial enhancements of the amplitudes of SSC and post disturbance fluctuations in H during the nighttime indicates the existence of some electrojet currents over the magnetic equator during the nighttime hours also
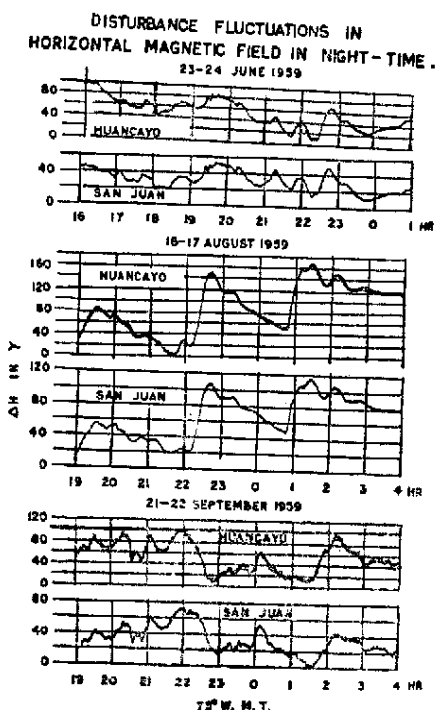

Fig. 2 — Tracings of H magnetograms at Huancayo and San Juan during nighttime disturbances.
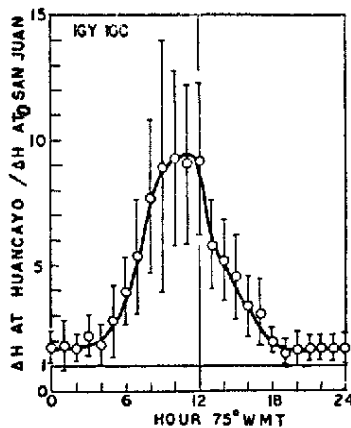
Fig. 3 — Daily variation of the ratio of deviations in H at Huancayo and at San Juan.
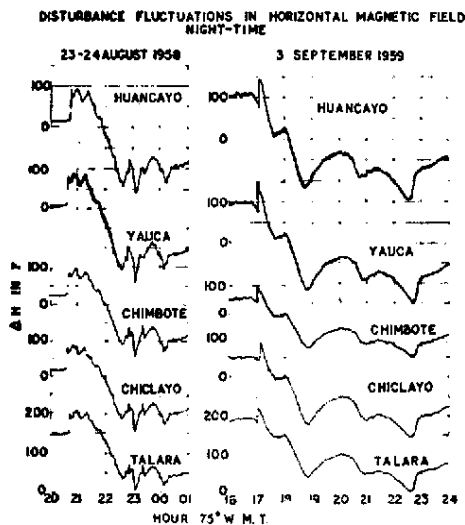

Fig. 4 — Tracings of H magnetograms at the Peruvian chain of stations during nighttime disturbances.
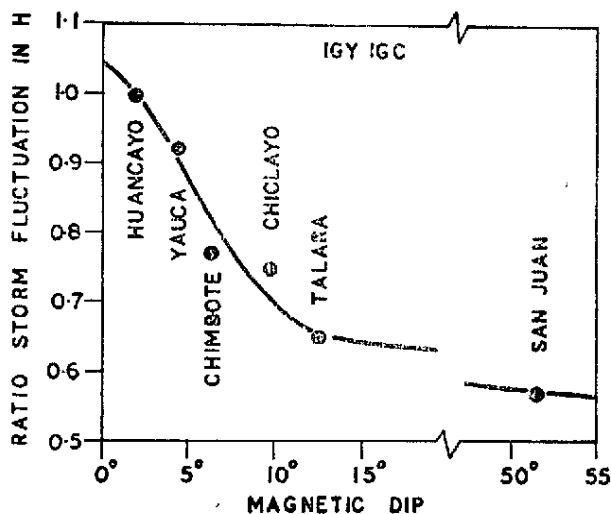
Fig. 5 — Latitudinal variation of deviations in H during the night-time disturbances.

ABNORMAL DISTURBANCE DAILY VARIATION AT

HUANCAYO DURING IGY-IGC

by

R. G. Rastogi and G. Rajaram

Physical Research Laboratories, Ahmedabad, India

It is well known that noon foF2 at equatorial stations during any of the seasons increases with increasing magnetic activity. Further the daytime values of foF2 are greater on Disturbed than on Quiet Days.

During the IGY-IGC period, values of noon foF2 at Huancayo are shown to decrease with increasing K index during the December solstices, while during the June solstices foF2 is positively correlated with K index. The mean foF2 on International Quiet Days are greater than on International Disturbed Days during the daytime hours of December solstices of IGY-IGC.

Comparing the daily variations of foF2 on Q and D days during the two solstices at different stations along 75°W meridian zone, the abnormal decrease of foF2 during D days is found only at the equatorial stations of Huancayo, Chimbote, Chiclayo and Talara during the December solstices (Fig. 1).

Comparing the variations of foF2 at Huancayo over the years 1953 to 1961, the decreases of foF2 on D days of December solstices, is seen only during the years of maximum solar activity, i.e., 1957-1960 (Fig. 2).

Comparing the variations of foF2 on Q and D days during the December solstice at the equatorial stations along different longitudes, viz. Huancayo, Ibadan and Kodaikanal, it is a found that the abnormal SD (foF2) occurs only at Huancayo (Fig. 3).
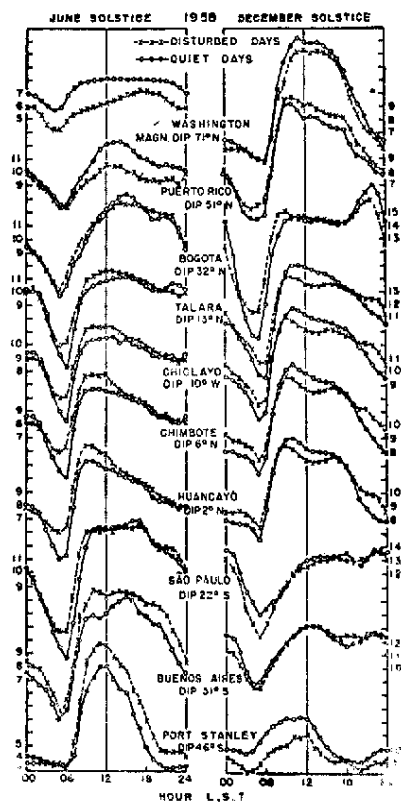
Fig. 1 — Average daily variation of foF2 at International Quiet and
Disturbed Days of June and December solstices of 1958 at
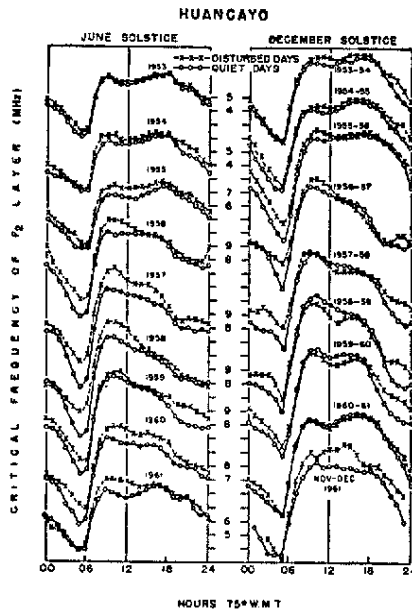various stations in the American Zone.

Fig. 2 — Average daily variation of foF2 at Huancayo on International
Quiet (o) and Disturbed (x) Days of June and December
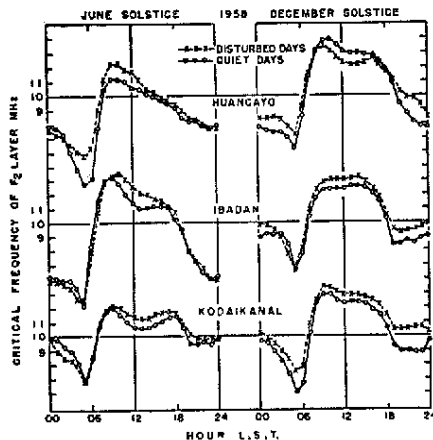solstices in the years 1953-1961.

Fig. 3 — Average daily variation of foF2 at Huancayo, Ibadan and
Kodaikanal in June and December solstices of 1958.

It is concluded that during the December solstices (when the Earth is nearest to the Sun) of the maximum solar activity period some causes come into operation which have the effect of decreasing foF2 near the magnetic equator in the American Zone, where the horizontal magnetic field is the minimum. It is suggested that this cause may be the precipitation of the corpuscular radiation into the F2 region heights during the magnetically active periods of the maximum sunspot years.

SUMMARY OF THE SESSION

by

E. J. Chernosky

Air Force Cambridge Research Laboratories

Bedford, Mass., U.S.A.

At the session on **Magnetic and Ionospheric Storms** nine papers were presented after reviews by Professor Chapman on Magnetic Storms and Dr Matsushita on Ionospheric Storms.

In examining magnetic bays on the Koror records Knapp found that they were possibly coherent in different longitudes at the low latitudes. He assumes that this possible coherence is due to zonal perturbations in the ionosphere flowing all around the earth at low latitudes. One explanation of this required that the magnetic perturbations represent a band of zonal perturbations flowing all around the earth but redistributed in the midday segment so as to concentrate along the dip equator.

Examination of the $\triangle Z / \triangle H$ ratios for the Koror data for some 540 bays showed a midday peak with a possible late night secondary maximum. Nighttime bays are infrequent however and more data are needed to complete this study. It is to be noted that these data are concerned only with bays or transient departures from the normal diurnal variations and the following paper does so as well.

Nishida, Iwasaka and Nagata examined departures of high and low latitude station traces from a normal curve. These departures, from one-half to several hours in length perhaps, were evaluated over a period of 40 days in the 1953 data. While some of the variations can be identified as solar flare effects, storms sudden commencements, and positive and negative sudden increases, the majority cannot be so explained. They appear at the equator as negative departures, in the horizontal component having a maximum amplitude of 200 γ, and possibly are bays. Simultaeously with the equatorial departures very similar variations appear over a wide area which is wider than the hemisphere. From the equivalent current system for these fluctuations it is found that the direction of current flow is independent of latitude below geomag. lat. 75° and all these currents flow through the polar cap. During the vernal equinox period examined the departures were almost always present.

The median values from routine hourly soundings at Nairobi were studied for the magnetically 5 quiet and 5 disturbed days for the period March 1964 through February 1965. There is little difference between the median values for the quiet and the disturbed days although the critical frequency is less than one megacycle lower on the quiet days for most night hours (after about 1600 LMT) and less than ½ megacycle higher during daylight hours over the entire period. A secondary peak shows up during local summer between 1900 and 2300 hours which seems to be enhanced by magnetic activity. The probability of occurrence of an F1 cusp is largely unaffected by magnetic activity. From February to April quiet days are fairly consistently below the disturbed days for foF2, except in the morning daylight hours. Differences in h'F2 were less than 20 km between the quiet and disturbed days. Kelleher felt that at least in sunspot minimum years Nairobi lies in an intermediate region where geomagnetic control is small.

Olatunji could find no relation to Kp and Ap for ionospheric storms recorded at Talara, Ibadan, and Singapore. There was some indication that ionospheric storms began from a half to nine hours later than magnetic storms in 1960 and 1961.

Rastogi showed that the IGY-IGC period the noon values of foF2 at Huancayo decreased with increasing K index during the December solstices while during the June solstice foF2 is positively correlated with K.

The abnormal decrease of foF2 during disturbed days is found only at the equatorial stations of Huancayo, Chimbote, Chiclayo, and Talara, during the December solstice for the stations along the 75°W meridian. For the years 1953-1961 this decrease was only seen during maximum solar activity. Comparing the variations at different longitudes it is found that the abnormal S_D occurs only at Huancayo.

Rastogi suggested that the agency responsible for this is a precipitation of the solar corpuscular radiation into the weaker horizontal force of the American zone.

Rastogi also showed the daytime enhancement of the sudden commencement at Huancayo over that at San Juan as did Sugiura. Nighttime fluctuations in H at Huancayo and San Juan compared very well. The fluctuation at the Peruvian stations of Huancayo, Yauca, Chimbote, Chiclayo, and Talara, are very similar, the amplitude decreasing as one moves north to Talara from Huancayo. At Talara the average deviation of H is 0.65 times that of Huancayo.

Rastogi concluded that the significant equatorial enhancement of SSC and the post disturbance fluctuations in H during the nighttime indicates the

existence of some electrojet currents over the magnetic equator during the nighttime hours also.

Casaverde showed that the D and H diurnal changes were essentially the same across the equatorial zone on quiet days with only Z showing change. At the onset of a sudden commencement storm only H remained the same across the equatorial electrojet in Peru, the D and Z onsets being different on opposite sides of the electrojet. The electrojet appears to be nearer 800 km wide at sunspot minimum as compared with 600 km at sunspot maximum.

In considering data taken at sunspot minima it should be noted at what minima these data are taken. There appears to be a 22-year sunspot cycle in terrestrial magnetic activity insofar as the semi-annual equinoctial maxima are concerned as one example. The equinoctial maxima are strong at and following one sunspot cycle maxima while at the following sunspot cycle minima they are poorly defined. It was also reported that the cycle trends are such that they are greater in the last half of one cycle and in the first half of the following cycle

XI — LOW LATITUDE MAGNETIC PULSATIONS

XI — LOW LATITUDE MAGNETIC PULSATIONS

(Discussion leader: J. R. Heirtzler)

Review Paper

EQUATORIAL STUDIES OF RAPID FLUCTUATIONS

IN THE EARTH'S MAGNETIC FIELD

by

W. H. Campbell

NBS — CRPL, Boulder, Colorado

Introduction

This paper concerns naturally occurring ultra low frequency electromagnetic field variation in the range of 3,5 to 0.003 cycles per second (1/3 sec to 300 sec periods). Such phenomena are investigated to understand processes transpiring in the local ionosphere and the distant magnetosphere. Even though some of the signals in the equatorial region have unique characteristics which could best resolve source propagation mechanisms, the equatorial studies in these frequencies has thus far lagged behind the middle and low latitudes, probably as a result of the greater scarcity of geophysical laboratories in that region.

The purpose of this paper is to summarize what has been accomplished to date at the very low latitudes and to describe the needed areas for further endeavor. Four pulsation types which show rather different characteristics will be discussed separately in this review. Although spatial and temporal variations in amplitude make it improbable that such a spectrum of signals as shown Fig. 1 could be recorded, it illustrates the size, range, and names of signals followed in this study.
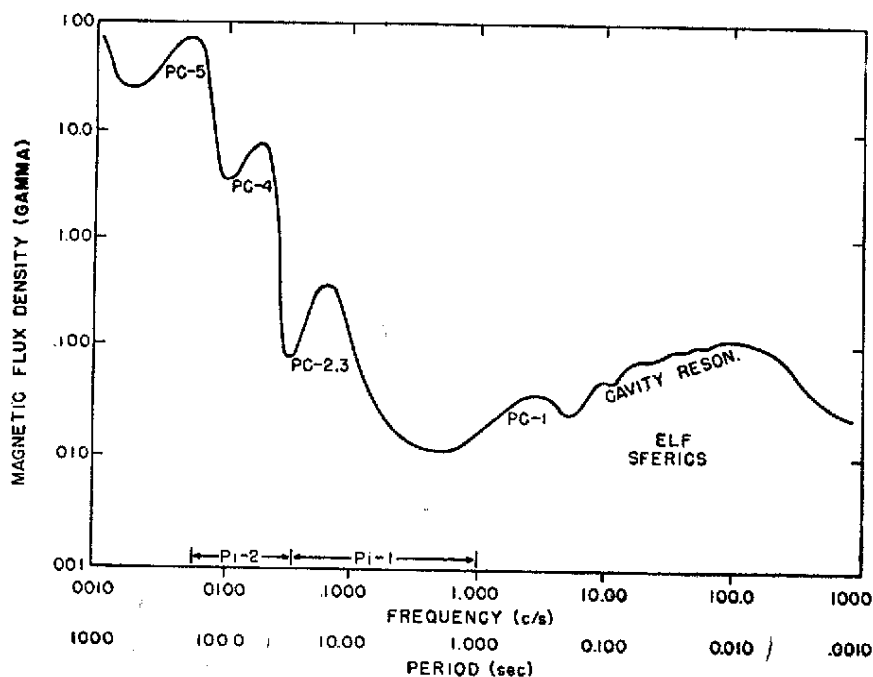
Fig. 1 — Identification of spectra of pulsations in the lower frequencies.

The Regular Pulsations Near 1 Sec Period   (Pc-1)

These curious pulsations are generally found in the frequency range of 3.5 to 0.3 c/s; typical amplitudes are 10 to 100 mγ. The fluctuations are generally found in groups of about one-half hour duration, often occurring singly and, on occasion, lasting half-a-day. There is a beat-like appearance in the amplitude traces that, in part, results from the typical overlapping rising frequency emission structure evident on frequence-time displays.

There seems to be a general linear relationship of the recurrence period of the emission (Trec) and the average period (t mid) so that Trec (sec) $\cong$ 85 t mid (sec). The maximum occurrence time, near midday at auroral latitudes decreases to pre-dawn hours at the middle latitudes. Equatorial and polar occurrences are rarer than at other latitudes; presently diurnal patterns at such places are unreported. The local time variation of the mid-frequency appears to be similar at middle and high latitudes with higher frequencies in the night

hours and low frequencies during the day; the same would be expected at the equator. The few samples of polarization show the magnetic flux density vector counter clockwise in a plane perpendicular to the earth field at the boreal auroral zone and randomly oriented at northern mid-latitudes; measurements have not been reported at the equator. The events have a high probability of occurrence 5 to 7 days following large Kp indices of solar terrestrial disturbances. No dependence of amplitude upon concurrent ionospheric conditions is yet evidenced. High latitude conjugate station signals generally show a 0.8 to 0.9 correlation. Stations separated by more than 500 km in the middle and high latitudes of one hemisphere are uncorrelated in activity although isolated cases of extreme distribution have occurred.

One study of an equatorial event with the group of Pacific stations illustrated in Figure 2 showed a 180° phase shift in the recurrence structure at Kauai and Tongatapu; Canton, near the equator, seemed to exhibit the summation of the other stations.
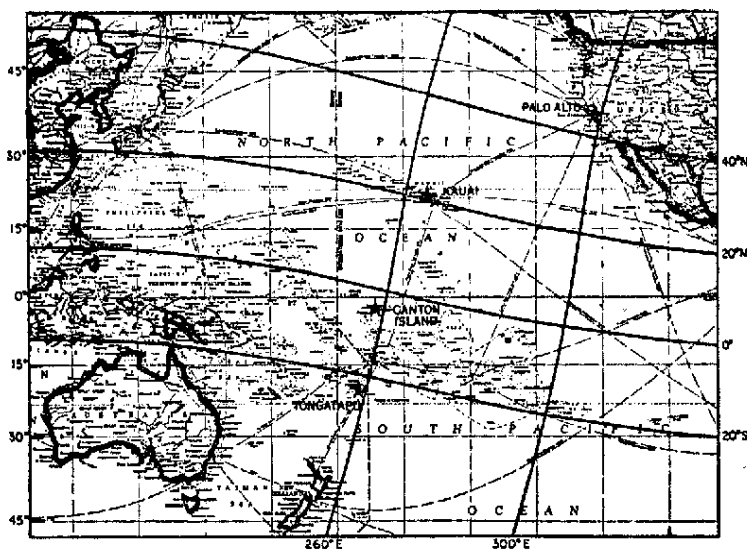

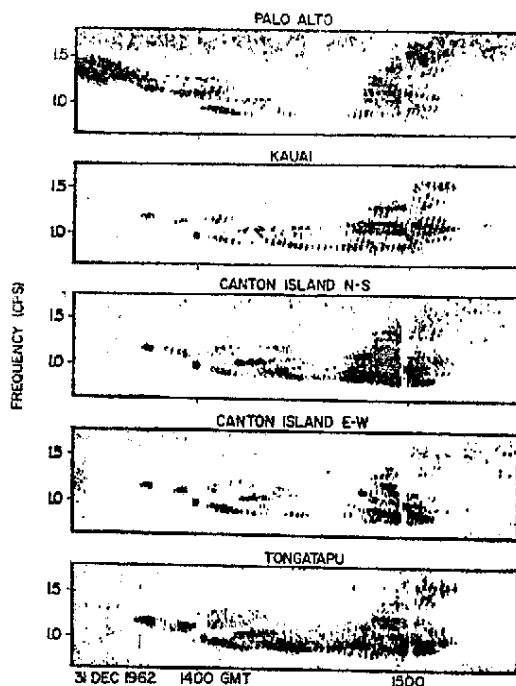Fig. 2a — Group of Pacific stations where measurements were made.

Fig. 2b — Pc-1 pulsations spectra at Kauai, Canton, and Tongatapu (from Tepley, 1964).

There have only been guesses as to the originating source of these pulsations. The resonance type features of the event and the high latitude conjugate station coincidence encourage the presently popular hydromagnetic models of the phenomenon of propagation along the high L field lines. It is typically assumed that the energy comes from the solar wind and that necessary conditions for resonant propagation in the magnetosphere must be established several days after the onset of the solar terrestrial disturbance. Ionospheric absorption of the energy in these frequencies is predicted by most models but has escaped measurement.

Equatorial studies of these events has scarcely begun. Even the most rudimentary features are unreported. A major contribution to the understanding of the phenomenon can be made by determining the method of arrival of the fluctuations into equatorial regions.

Regular Pulsations Near 20 Sec Period (Pc-2,3)

These are rather sinusoidal pulsations with typical amplitudes reaching 1/3 gamma in size. They are generally observed in the period range of 5 to 40 seconds with a beat-like appearance. A diurnal variation of the oscillatory period is observed at middle and high latitudes which typically rises to 20 or 25 seconds in the daytime hours, and falls to about 5 or 10 seconds at night; the variation range varies gradually over many days. Saito (1962) indicates that a similar distribution of periods should be expected at equatorial stations; a better study is needed here. The occurrence frequency has been reported as a day type (Fig. 3). At middle and high latitudes the times of maximum have been justified by variations in ionospheric conditions. The interesting differences at equatorial stations, shown in Fig. 4 need interpretation.
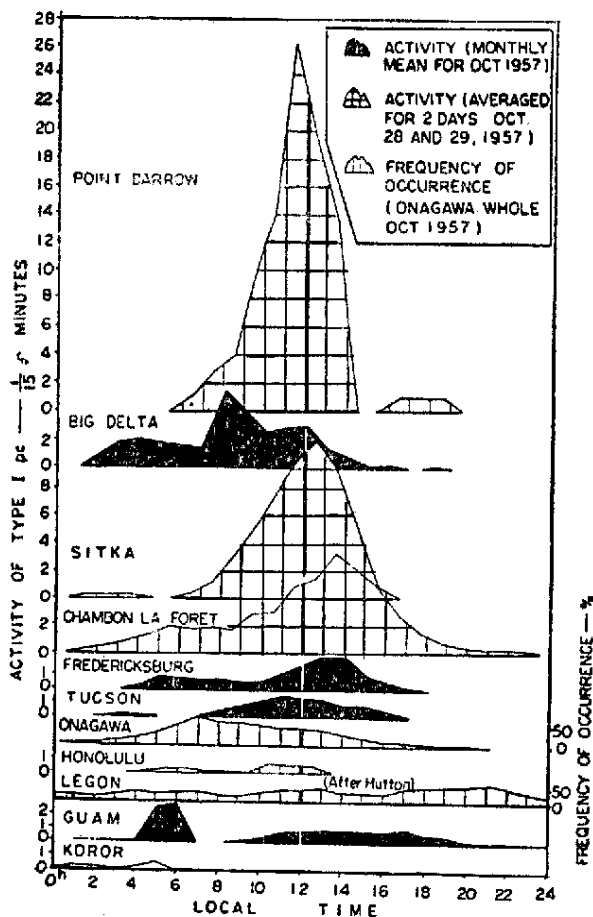

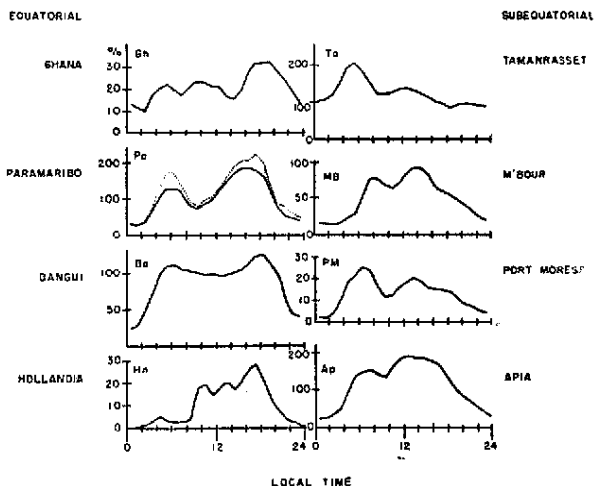Fig. 3 — The dayside enhancement of Pc-2 and 3 activity (from Saito, 1962).

Fig. 4 — Equatorial and subequatorial diurnal variation of Pc-2 and 3 activity (from Romaña, 1962).

The large amplitude pulsations appear simultaneously at widely spaced locations. Fig. 5 illustrates an amplitude distribution of 3 events versus latitude; unfortunately it was night or early morning at Guam and Koror for this sample. More effort on the distribution study is needed, particularly at electrojet maximum and disappearance times.
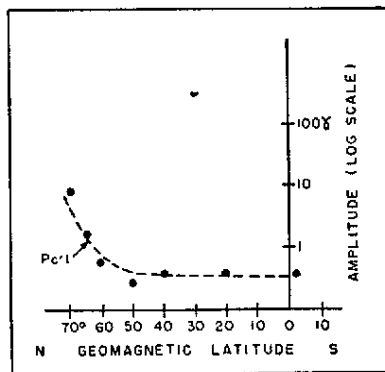

Fig. 5 — Latitudinal variation of Pc-2 and 3 amplitude (from Jacobs and Sinno, 1960).

The vertical component of the field is typically reported to be small and the field is generally largest in the magnetic N-S direction. Polarization and phase studies are unusually scarce and have not been made at the equator.

The excellent correlation of daily amplitude values with magnetic disturbance indices places the phenomenon clearly with the solar-terrestrial disturbance family. It is generally assumed that the pulsations also have a hydromagnetic origin. Nevertheless, the positive dependence on ionospheric conditions have greatly enccu.aged the consideration of associated ionospheric currents extending a high latitude effect to the equatorial region.

Regular Pulsations With Periods of the Order of Minutes (Pc-4, 5)

Two distinct period groups with typical periods between 45 to 70 sec (Pc 4) and 250 to 600 sec (Pc 5) have been identified at various world stations. Presently, many characteristics of these two groups seem sufficiently similar to allow them to be discussed jointly. Long period damped oscillations will be considered a part of these groups.

The Pc 4 have been reported as day type pulsations; occurrence maxima are found near noon hours at all latitudes. The longer period pulsations seem to have a gradual transition from a single morning peak activity at high latitudes to a double morning and evening maximum at the lower latitudes; the equatorial reports need confirmation, however. In Fig. 6 the seasonal pattern of Pc-4 at Manila shows the equatorial peaks of activity near noon hours and minimal activity during the solstices, generally similar to the middle and high latitude behavior. Fig. 7 illustrates an increasing occurrence at Ghana with decreasing solar activity.
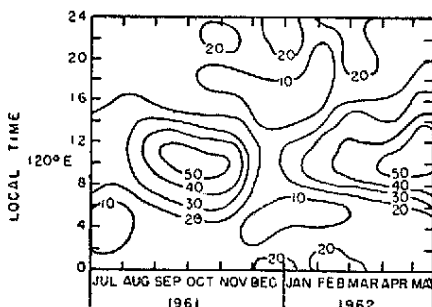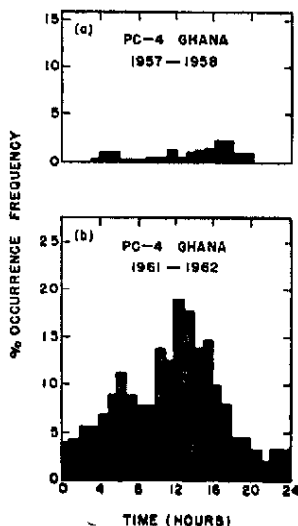

Fig. 6 — Monthly occurrence pattern of Pc-2 and 3 at Manila (from Glover, 1963).

Fig. 7 — Diurnal variation of Pc-4 at Ghana in 1957/58 (top) and 1961/62 (bottom) (from Hutton 1965).

The periods of both Pc-4 and Pc-5 activity are longer in the nighttime than at daytime; they are reported to be shortest around June solstice (45 and 400 sec) and longest at December solstice (70 and 450 sec).

There is a latitudinal variation in the plane of polarization of the pulsations, illustrated in Fig. 8, showing the oscillations perpendicular to the geomagnetic field lines at high latitudes but parallel at equatorial locations.
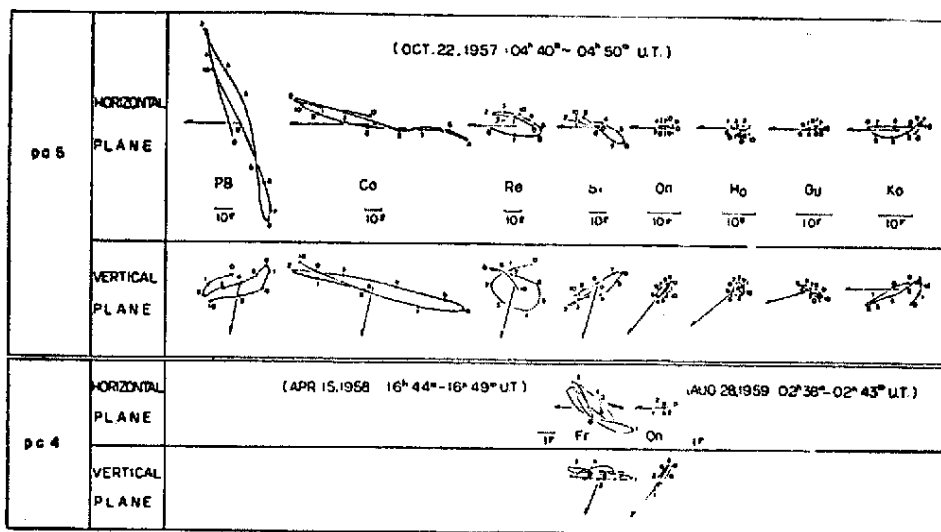

Fig. 8 — Pc-4 and 5 field directions at different latitudes (from Saito, 1964).

Figure 9 illustrates a sample of simultaneous pulsations at various world locations. Fig. 10 illustrates the latitudinal amplitude distribution of the field components. Note the equatorial enhancement; it was midday at Koror. Curiously, the field component parallel to the main field has comparable amplitudes both near the auroral zone and at the equator. Fig. 11 shows the average amplitude at Koror to that at Honolulu or Kakioka in local time at Koror. There is a clear daytime enhancement for these nine cases of Pc-5. Fig. 12 shows the average amplitudes of the H component of each station (normalized to College) plotted against local time.

Characteristics of Large Amplitude Geomagnetic Pulsations
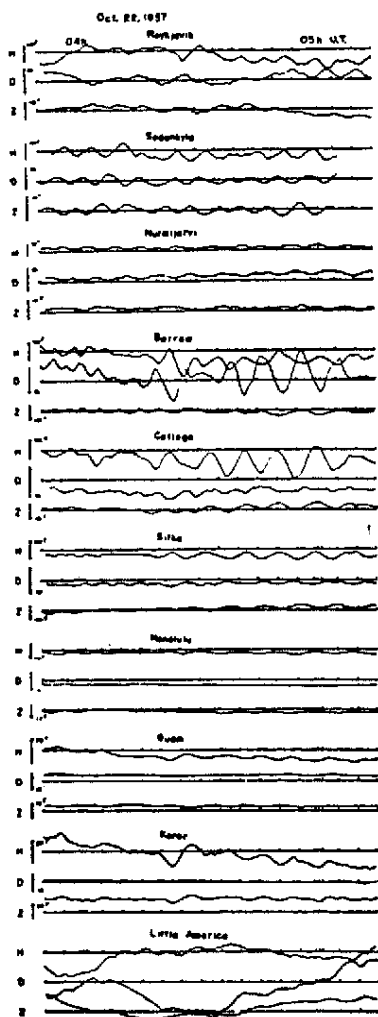

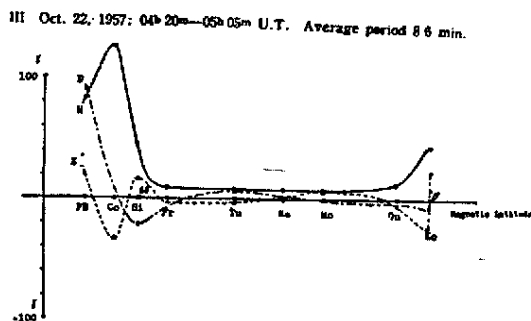Fig. 9 — Pc-5 event on world magnetograms (from Matuura, 1961).

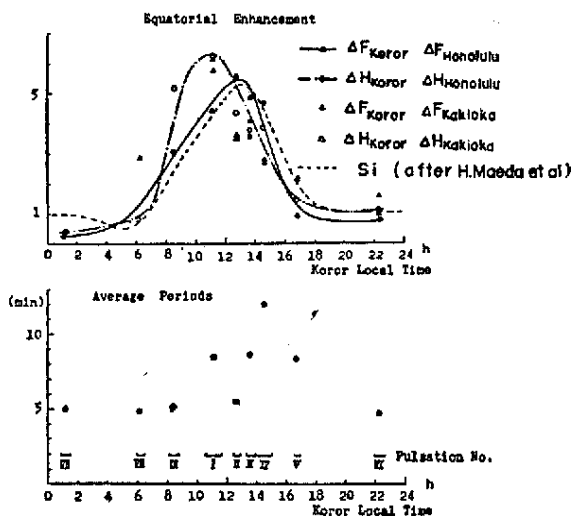Fig. 10 — Amplitude variation versus latitude for Pc-5 event (from Matuura).

Fig. 11 — Local time variation of equatorial enhancement factor for averaged
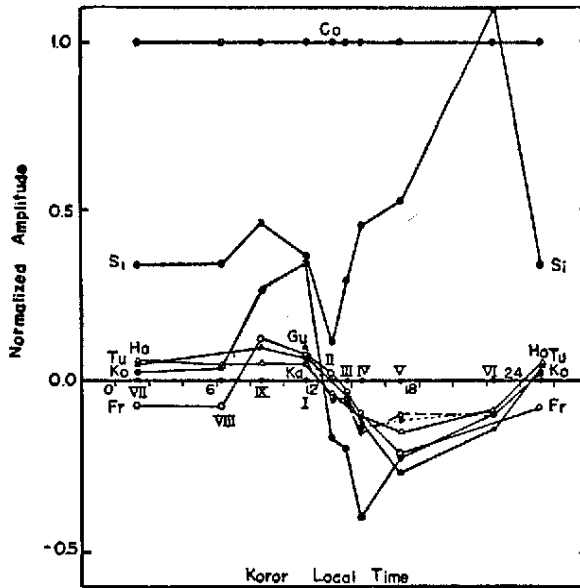amplitudes and periods for Pc-5 event (from Matuura, 1961).

Fig. 12 — Local time variation of the amplitudes (from Matuura, 1961).

At non-equatorial latitudes the field fluctuations are, on occasions, identified with measurable ionospheric phenomena. Example of concurrent pulsations in auroral particle precipitation, luminosity variations and electron density, are available. On rare occasions satellite observations of pulsations have been identified with surface pulsations. Most recently the characteristic period of Pc-4 and 5 have been found to vary with satellite drag. The activity level of Pc-3 and 4 has been shown to have correllation coefficients of 0.8 and 0.6 respectively with direct measurements of solar wind velocity.

Hydromagnetic type oscillations of the earth's field lines analogous to elastic string vibrations have been used to explain some of the high latitude occurrence and polarization features. Activity at polar conjugate stations is used to verify such models. If all surface observations are measures of arriving hydromagnetic waves, the observed equatorial enhancement certainly needs clarification. The question is whether a Pc-5 current system, such as that shown in Fig. 13, exists in the ionosphere or is merely a convenient description of surface values.
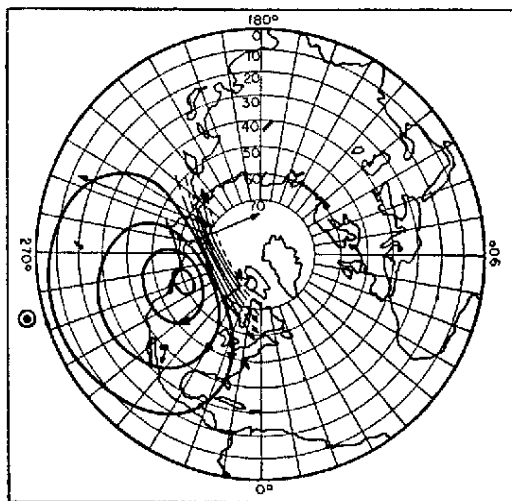
Fig. 13 — Equivalent current system for Pc-5   (from Jacobs and Sinno, 1960).

Pulsations With Irregular Forms

There are certainly many events with transitional features between rather pure sinusoidal pulsations and quite irregular random period rapid variations; in this paper the two groups are only clearly separated for convenience of discussion. The frequency components are from several cycles per second to several per hour; amplitudes vary from several hundred gammas to the lower limit of the recording system.

At the higher latitudes these fluctuations are a measure of the solar terrestrial disturbance, some of which have been termed polar magnetic substorms (Akasofu and Chapman, 1963). They have a clear association with ionospheric phenomena. They have been identified with the aurora itself as well as the bombarding electrons and the ionospheric absorption and reflection. Great similarities and some difference have been found in events measured at conjugately located stations.

Associated with the auroral electrojet the events at high latitudes occur most frequently with the typical nighttime negative magnetic bays. They are found also during the afternoon positive bay events. Studies at middle latitudes tied the occurrence of the fluctuations to a closing of the ionospheric current loops. A day-side enhancement has been found.

At the equator the variations are most numerous during the daytime hours (Fig. 14). The night-time events only appeared during disturbed Kp conditions Fig. 15 shows the diurnal variation in ratio (r) of the fluctuation H to Z components with higher values at night than in day. This inferred that greatly different types of currents systems were involved at such times. Fig. 16 shows the dependence of "r" on duration period of the fluctuation, which though not clearly explained, may imply an induced current effect. About 90% of the events at Ibadan have been identified at other observatories within the auroral zone and along the equator, (see Table I). The amplitude of the fluctuations at the equator is quite dependent on the magnitude of the electrojet current there. The ability to identify similar signals at distant stations was related to the amplitude of the variations and therefore dependent upon the equatorial Sq magnitude.
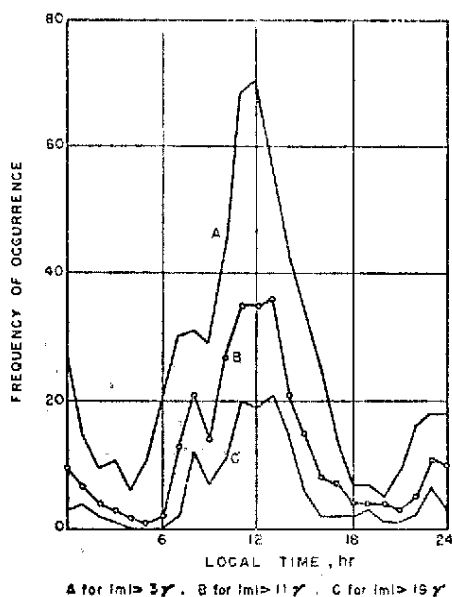

Fig. 14 — Occurrence frequency of irregular fluctuations in Nigeria (from Onwumechilli, 1960).
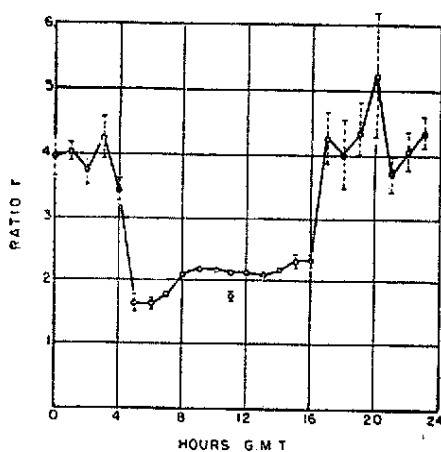
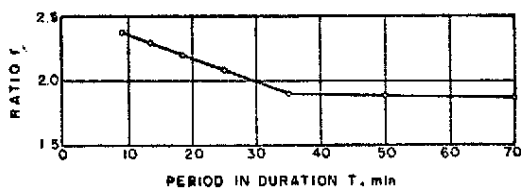Fig. 15 — Diurnal variation of amplitude ratio H/Z for irregular fluctuations in Nigeria (from Onwumechilli, 1959).

Fig. 16 — Variation of ratio H/Z with period of irregular variations (from Onwumechilli, 1959).

TABLE 1

Percentage of fluctuations at Ibadan that are identifiable at other observatories. The observatories are arranged in order of latitude from North to South.

Station	Identifiable	Unidentifiable	all	% Identifiable
Tromso	42	7	49	86
College	169	.61	230	73
Eskdalemuir	588	11	599	98
L'Aquila	551	28	579	95
San Fernando	823	88	911	90
M'Bour	904	22	926	98
Guam	1252	163	1415	88
Addis Ababa	1277	45	1322	97
Korror	1140	183	1323	86
Korror, Guam	2392	346	2738	87
Port Moresby	326	150	476	68
Huancayo	1248	281	1529	82

Figure 17 illustrates the latitude variation of enhancement in Nigeria and its comparison to the H daily range. The strong dependence of the amplitude of the fluctuations on the strength of Sq implied that these variations were actually variations of Sq itself. If this be so, then these minute variations will become a sharper tool for dissecting the dimentions of the electrojet itself. In addition, there do occur events on a fine time scale which are unique to, or appear earlier in, one auroral zone. If the electrojet is to be identified with only the northern or southern Sq system, it may be possible to use hemispherical identification of an irregular pulsation to tag the Sq of the electrojet. Similarly, if there is a night side closing of induced current in the earth as Price suggests, the irregular pulsations might possibly be used as tracers for this system.
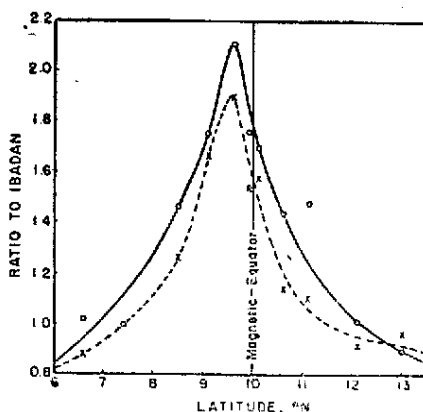
Fig. 17 — Equatorial enhancement of daily amplitude ratio of irregular fluctuations (from Onwumechilli and Ogbuchi, 1962).

Concluding Remarks

In summary, it appears that less is known of the equatorial continuous pulsations than of the irregular fluctuations and less of the higher frequencies than the lower. The typical question to be resolved seems to be how much of the observed signal can be traced to ionospheric currents. Many of the regular, sinusoidal pulsations should be studied as hydromagnetic waves and measurements made of the wave polarization planes, phase velocities, and arrival directions. Possibilities of cross field line propagation, radially to the low latitude region from magnetospheric equator and ducted propagation beneath an Alfven velocity maximum from the auroral zone to the low latitudes both need further investigation. There is still considerable opportunity for significant micropulsation studies at the equator.

References

Glover, F. N., Recent Magnetic Observations in the Philippines, J Geophys. Res., **68**, 2385-2394, 1963.

Hutton, R., Equatorial Effects, Radio Sci., **69**, 1169-1177, 1965.

Jacobs, J A. and K. Sinno, World-wide Characteristics Micropulsations, Geophysic. J. Roy. Astron. Soc., **3**, 333-353, 1960.

Matuura, N., Characterstics of Large Amplitude Geomagnetic Pulsations, Rept. Ionos. Space Res. Japan, **15**, 192-214, 1961.

Onwumechilli, A., The Relation between H and Z Variation near the Equatorial Electrojet, J. Atmos. Terr, Phys., **16**, 274-282, 1959.

Onwumechilli, A., Fluctuations in the Geomagnetic Horizontal Field near the Magnetic Equator, J. Atmos. Terr. Phys., **17**, 286-294, 1960.

Onwumechilli, A. and P. O. Ogbuchi, Fluctuations in the Geomagnetic Horizontal Field, J Atmos. Terr. Phys., **24**, 173-190, 1962.

Romaña, A., Concerning some Features of the Curves of Occurrence Frequency of Pc's at Observations in the Equatorial Zone, Geomagnetica, Nat. Met. Service, Lisbon, 217-227, 1962. (D.R.B., Canada Translation T 3 Sq by E. R. Hope).

Saito, T., Statistical Studies on Three Types of Geomagnetic Continuous Pulsations, Sci. Rept. Tohoku Univ., Serv. 5, Geophys. 14, n° 3, 81-106, 1962.

Saito, T., Mechanisms of Geomagnetic Continuous Pulsations and Physical States of the Exosphere, J. Geomag. Geoelect., **16**, 115-151, 1964.

Tepley, L, Low Latitude Observations of Fine Structured Hydromagnetic Emissions, J. Geophys. Res., **69**, 2273-2290, 1964.

RAPID GEOMAGNETIC ACTIVITY AT VERY LOW LATITUDE

CONJUGATE STATIONS

by

J. R. Heirtzler[1], F. de Mendonça[2] and H. Montes[1]

Introduction

There has been increasing evidence to indicate that micro-pulsation activity is due to ionosphere current systems. However most measurements have been confined to mid and high latitudes, with certain of the high latitude measurements being made simultaneously at high latitude conjugate points. To supplement these measurements we recorded rapid magnetic activity at very low latitude (equatorial) conjugate points on a line of force that has its maximum altitude in the F-layer. We utilized a pair of such conjugate points in eastern Brazil, located near the towns of Amapá and Barbacena (Fig. 1). The point conjugate to Amapá lies about 100 km west of Barbacena. The two points are separated by about 3000 km as measured along the surface of the earth.

As a joint project between Lamont Geological Observatory and C.N.A.E. two mobile field installations were used at the two towns during December, 1964. Each installation used a rubidium-vapor magnetometer. For 15 days recordings were made with a full scale (5") span of 3 gammas and a chart speed of 40 iph, then for another 7 days with a full scale span of 30 gammas and a chart speed of 6 iph. Timing accuracy was kept to within about 3 seconds by frequently synchronizing a local time marker with WWV, and the magnetic field

---
[1] Lamont Geological Observatory, Columbia Univ., Palisades, N.Y.
[2] Comissão Nacional de Atividades Espaciais, Brasil

strength had a relative accuracy of better than 0.05 gammas. To indicate simultaneous activity in mid-latitudes we will show the simultaneous records from a rubidium magnetometer at Lebanon State Forest in the state of New Jersey. At Lebanon the dip of the field is 72 degrees down, at Amapá is it 25 degrees down, and at Barbacena it is 19 degrees up, according to world dip charts.
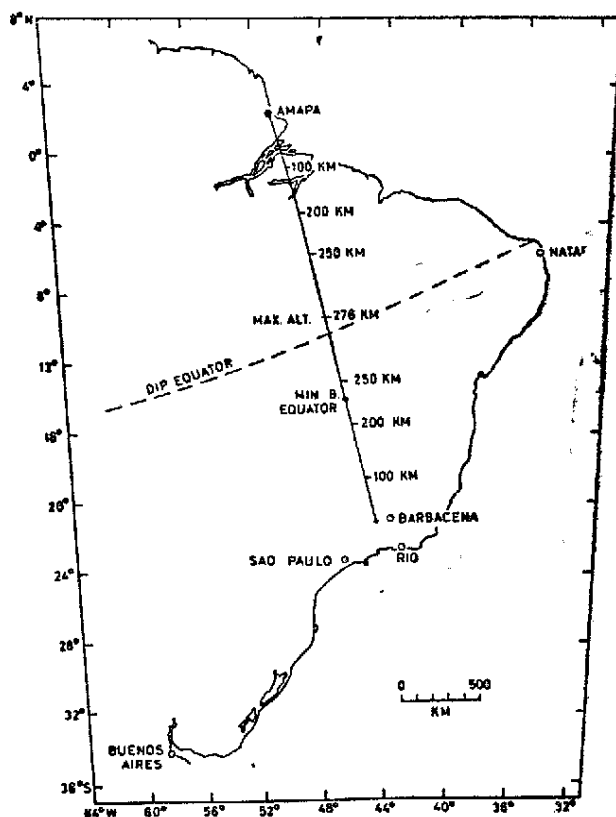

Fig. 1 — Position of line of force passing through Amapá.

While the main measurements reported here were made at conjugate points we suspect that the type of activity observed at each of these two stations was characteristic of an appreciable geographic area centered about those respective points.

Cross Spectral Determinations

The time during which measurements were made was very quiet magnetically. The Fredericksburg K-index did not exceed 3 during the time that we have data. Frequently that index was 0 and for one day the sum of K was only 1.

Figure 2 shows a 24-hour batch of data from the conjugate stations. Although one cannot see micropulsation activity on the time and gamma scales used, it is possible to see many small irregular disturbances with periods less than one hour that are quite similar and nearly simultaneous at the two places. It is somewhat more difficult to see the detailed similarity during midday when there is a large Sq effect.
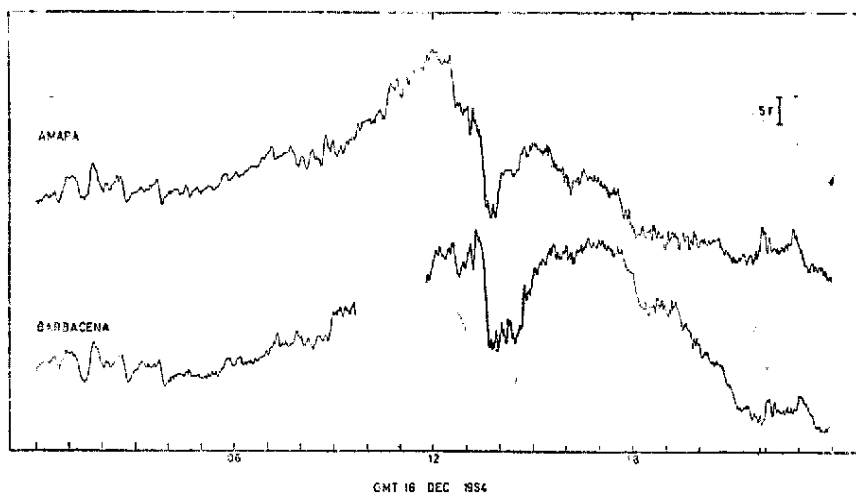

CMT 16 DEC 1964

Fig. 2 — Total magnetic field intensity records for one day at the conjugate stations. There is a data gap in the Barbacena record.

To study the statistical properties of the magnetic activity the records were digitized and cross spectral determinations made by the covariance method. For one of the more active days we chose three one hour intervals and cross spectral determinations were made between each pair of stations for each hour. Figures 3, 4, 5 and 6 show some of the spectra. Fig. 7 shows a sample of record on an expanded time scale.
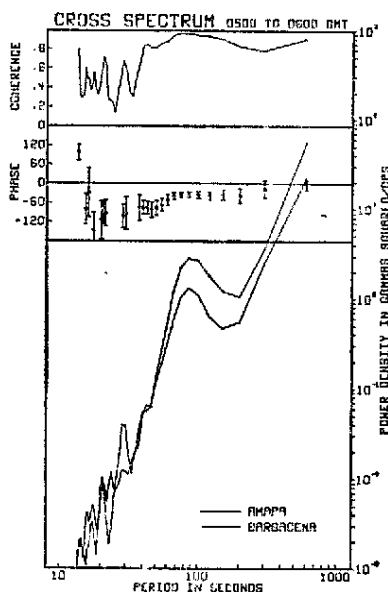

Fig. 3 — Spectral results for 05-06 GMT (02-03 LMT). For periods between 40 and 1000 sec (some long period data not shown) the activity is highly coherent. The most significant spectral peak is at 80 sec. Characteristically rapid magnetic activity is greater at Amapá than at Barbacena but still greater at Lebanon. For this hour nearly all phases are negative.

Fig. 4 — Spectra for same time as Fig. 3 but between Amapá and Lebanon. The same spectral peak is evident in the Lebanon data and, except over this peak, coherence is low. For the most part the phases show an erratic behavior.
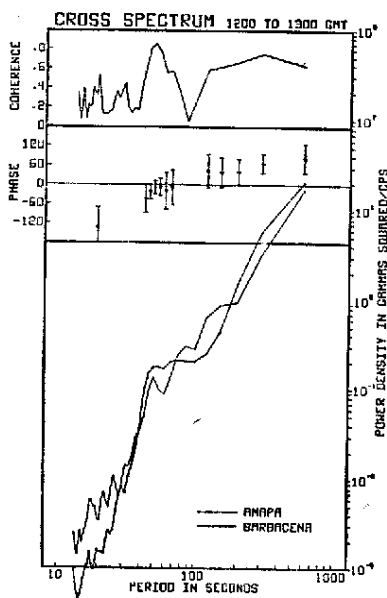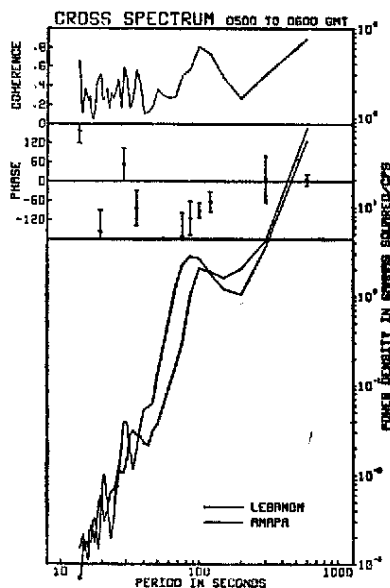

Fig. 5 — Spectra for 12-13 GMT (09-10 LMT). Coherence is much worse than 05-06 GMT except over the minor spectral peak at 50 sec period. Amapá-Lebanon spectral data for the same time is less coherent.
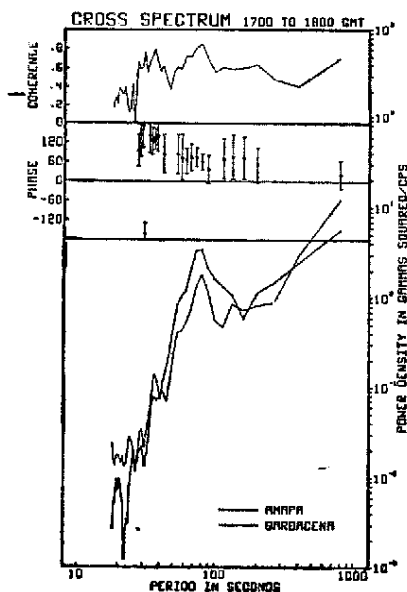
Fig. 6 — Amapá-Barbacena spectra for 17-18 GMT (14-15 LMT). Phase lags are positive and activity at all stations is greater than in the previous time intervals. Notice that the spectral peak at 80 sec period is only moderately coherent and has a phase lag of about 60 degrees (0.25 min in time). The amplitude ratios Barbacena: Amapá: Lebanon are about 1.0: 1.3:2:2 for the 80 sec activity.
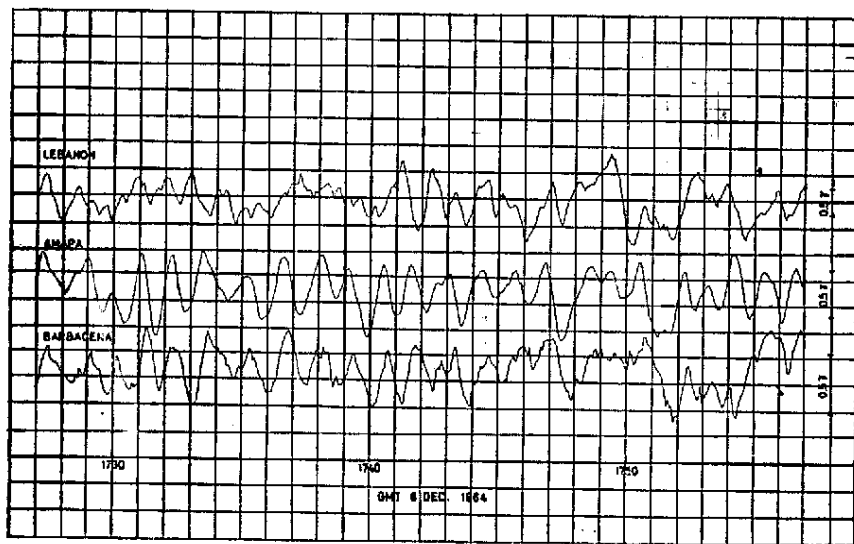

Fig. 7 — Records obtained during the time interval analysed in Fig. 6. This is relatively high amplitude activity that is only moderately coherent between Amapá and Lebanon. Periods greater than about 300 sec have been filtered out with zero phase shift filter.

Another Statistical Measure

To study the statistics of the activity for a period of many days we resort to a less accurate but less laborious procedure. We examined the records on the 10 min mark over a period of 12 days for Amapá. If there were as least two cycles of regular activity in the period range 10-200 sec and with at least 0.2 gamma amplitude, a notation of time and period were made. An analysis of these events is given in Figs. 8, 9 and 10.
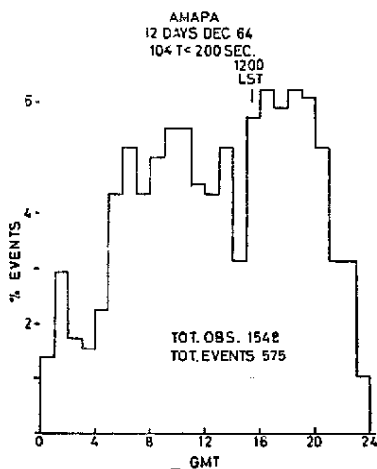
Fig. 8 — Diurnal frequency of occurrence of all events.

Fig. 9 — Period distributions of all events. The high value of 50-70 sec and the low value of 70-90 sec is probably not of special significance but simply results from the arbitrary period intervals used for classification. However the general shape of the distribution shows that events in the 30-110 sec period range are more easily detected by eye than periods outside this range.
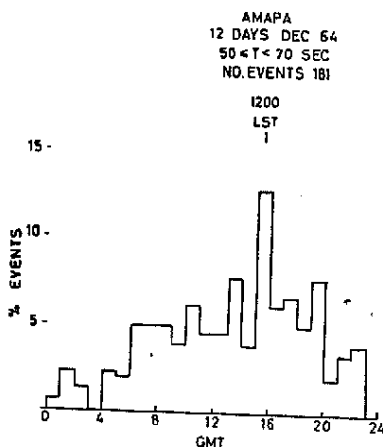
AMAPA
12 DAYS DEC 64
50 < T < 70 SEC
NO. EVENTS 181
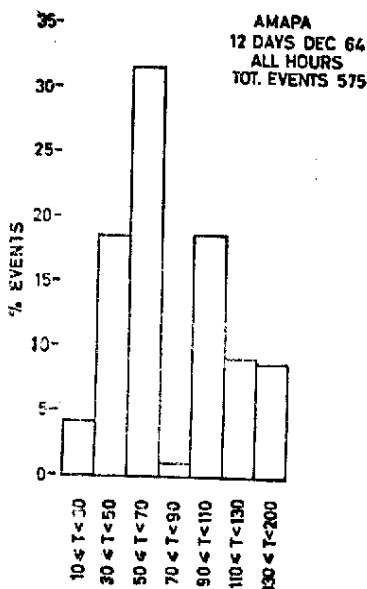
Fig. 10 — Distribution of 50-70 sec period events as a function of time of day. It is clear that these events may occur at any time of day but may be seen on the records more frequently at local noon. At mid-latitudes it is most common for the events to occur 00-06 solar time (Davidson, 1964). The early morning occurrence of these events has been found at other equatorial stations (Hutton, private communication).

Summary and Conclusions

For the conjugate stations used the micropulsation activity and small amplitude more irregular background activity is remarkably similar and frequently very coherent. Similarities which exist when magnetometer are only within a few hundred km of each other in mid-latitudes are frequently found for equatorial conjugate stations separated by 3000 km. Our limited data confirms an observation made with spaced magnetometers at mid-latitudes (Davidson, in preparation) namely that the coherence is not as great under the stronger part of the Sq current system as at other times of day.

Herron (in press) has shown that a diurnal pattern is usually observed in the phase differences between closely spaced micropulsation

recorders. We believe that the tendency of Amapa to lead in the morning and to lag in the evening is significant (it conforms to Herron's midlatitude observations where the station nearer the dark hemisphere usually leads in phase) but because the stations are in opposite geomagnetic hemispheres and on somewhat different meridians we hesitate to base firm conclusions on the phase observations.

We feel that this work has clearly illustrated the simple fact, that 40-1000 sec micropulsation activity in low latitude regions of the opposite hemispheres at least during December is remarkably similar, even in small detail, although it may be shifted in phase.

During the time of our observations we found that certain events with 50-70 sec period were most common and had their maximum frequency of occurrence at local noon. From the limited data available we were not able to identify the 0600 and the 1800 LMT maximum in the frequency of occurrence found by Hutton (1962) for Legon. Our results resemble more the annual mean of the diurnal frequency of occurrence found by Glover (1963), for stations in the Philippines. We believe, however, that frequency of occurrence diagrams can be a misleading way to illustrate micropulsation statistics because they do not show whether the activity noted is coherent over any large area. We feel that a proper analysis of micropulsation activity shows spectral peaks on a background curve and rapid activity should be divided into micropulsations spectral peak (which are usually coherent over large areas) and background (which usually is incoherent, or coherent at other times of day).

One is tempted to relegate the true and coherent micropulsations activity to the fringes of the Sq current system because of the lower coherencies for spectral peaks found near midday. In a similar way one is tempted to associate the micropulsation background activity with the stronger parts of the Sq current system since frequency of occurrence diagrams tend to peak near midday and, at least for mid-latitudes, the spectral power of the micropulsation background rises and falls with the strength of the Sq (Davidson, in preparation). (We have not yet examined that relationship for the conjugate stations of Amapá and Barbacena).

Our measurements were made during the December solstice when the sun was far south and the average Sq foci skewed in a similar direction. Indeed, the great similarity of the coherent micropulsations leads us to think that they were beneath a current in a single hemisphere.

Jacobs and Sinno (1960) proposed a micropulsation current system with return flow through the auroral zone. Our observations could be interpreted as due to such a system. In 1964 Jacobs and Watanabe suggested that this current is driven by symmetric but oppositely directed motions of the ends of a line of force, at conjugate points. Since we were, in effect, measuring only the horizontal components of field strength and the components would not be expected to change sign across the Sq equator our measurements yielded no direct information about that theory.

Magnetic measurements of all three components of field strength, made at various seasons of the year at these conjugate stations should give definitive results on the micropulsation current system in equatorial latitudes.

References

Davidson, Maurice J., "Average Diurnal Characteristics of Geomagnetic Power Spectrums in the Period Range 4.5 to 1000 Seconds", J.G.R., **69**, 23, pp. 5116-5119, Dec. 1, 1964.

Glover, F.N., "Recent Magnetic Observations in the Philippines", J.G.R. **68**, 9, 2385, May 1, 1963.

Herron, Thomas J., "Phase Characteristics of Geomagnetic Micropulsations", in press.

Hutton, V. Rosemary S., "Equatorial Micropulsations", J. Phy. Soc. Japan, **17**, Suppl. A.-II, 20-23, 1962.

Jacobs, J.A., and T. Watanabe, "A Model of Geomagnetic Micropulsations with Long Periods", Canad. J. of Phys., **42**, 200-207, Jan. 1964.

ÉTUDE EXPÉRIMENTALE DES VARIATIONS MAGNÉTIQUES

RAPIDES AU VOISINAGE DE L'EQUATEUR (ADDIS-ABEBA)

J. Roquet

Institut de Physique du Globe de Paris, France

En collaboration avec le Directeur de l'Observatoire d'Addis Abéba nous avons récemment mis en station un dispositif d'enregistrement des variations magnétiques rapides. Analogue aux dispositifs en service en France, il permet l'utilisation de deux bandes passantes ($\gtrless$ 10 sec); les vitesses respectives de déroulement sont de 30 mm/min et 6 mm/min et les sensibilités d'environ 3 to 10 milligammas/mm. Une sensibilité beaucoup plus élevé est prévue à Addis pour la première bande, en vue de son utilisation lors de la saison non orageuse.

Les premiérs enregistrements obtenue ont été systématiquement comparés aux enregistrements magnétiques de Garchy pour les périodes > 10 sec et, pour les périodes < 10 sec, à des enregistrements telluriques; dans ce cas, l'amplitude des variations magnétiques correspondantes est obtenue au moyen des coefficients de correspondance magnéto-tellurique déterminés par H. Fournier.

Pulsations < 10 sec
(enregistrées du 11/2 au 3/4/1965)

Pc 1 — Quinze cas ont été enregistrés pendant cette période à Garchy; l'amplitude a parfois attemt 25 milligammas. **Aucum** d'entre eux n'a été enregistré à Addis. Un cas, de nature douteuse, a été observé à Addis sans qu'il le soit à Garchy.

Pi 1 — Les microstructures moyennes de Pi 2 (type spt de Yanagihara) sont presque toujours observées simultanement aux deux stations. Mais, sur 62 cas de microstructure fine de Pi 2 (type Troitskaya) observés à Garchy, 2 seulement ont été observé à Addis (Figs. 1 et 2).
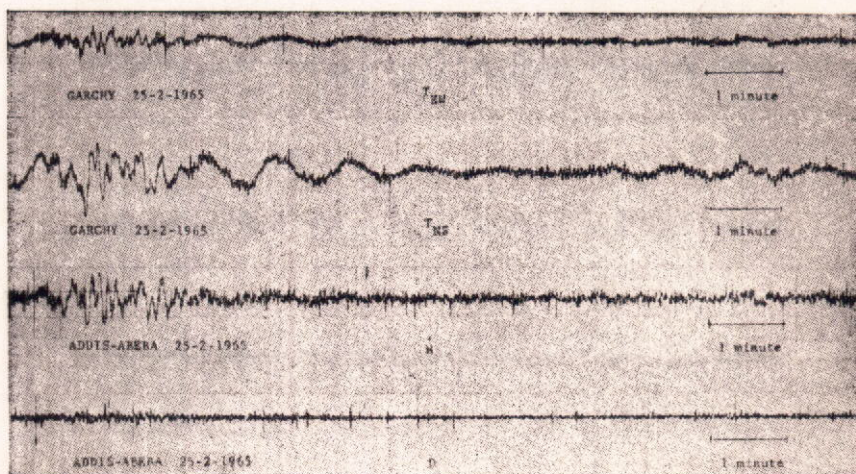
Fig. 1 — On observe (25 février) une miscrostruture moyenne (4 à 12 sec) qui présente une bonne correspondance à Garchy (T_{NS}) et Addis Abeba (H). La microstructure fine (1 à 2 sec) existe à Garchy sur le deux composantes; un bruit de fond assez forte existe sur H à Addis, mais le phenomene (d'amplitude faible) est visible sur D (voir, en particulier les deux dernier tiers de l'enregistrement).
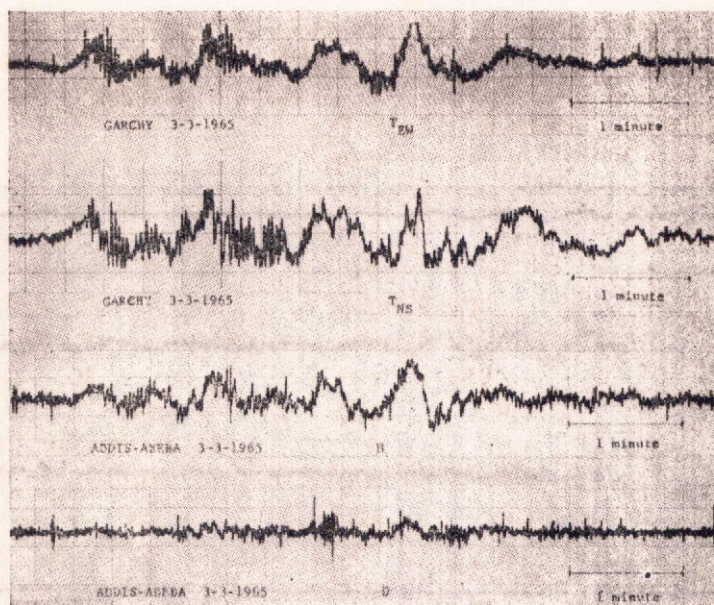
Fig. 2 — La microstructure moyenne (3 mars) est bien marquée à
         Garchy sur le deux composantes ; elle est nette sur H à Addis
         mais faible sur D. La microstructure fine, nettement mar-
         quée à Garchy sur les deux composantes, n'apparaît que sur
         H à Addis et les oscillations sont moins nombreuses.

Pulsations > 10 sec
(enregistrées du 15/5 au 15/6/1965).

Tous les cas observés à Garchy peuvent être retrouvés facile-
ment à Addis dans certaines limites très larges d'heure locale (3 h de
longitude entre les deux stations).

Le Tableau I donne des amplitudes maxima journalières des
Pc 3 aux deux stations. Le Tableau II donne un exemple d'une compa-
raison amplitude par amplitude des oscillations observées pour des
Pc4. Il apparaît que Pc 3 et Pc 4 ont des amplitudes du même ordres
sur H, mais sont plus faibles à Addis sur D.

Enfin tous les trains de Pi 2 sont communs aux deux stations.
le rapport des amplitudes entre les deux stations (voir Tableaux III
pour quelques examples) est variable.

TABLEAU I

AMPLITUDES MAXIMA JOURNALIERES DES PC 3

	H		D	
	ADDIS-ABEBA	GARCHY	ADDIS-ABEBA	GARCHY
15 Mai 1965	0,5 γ	0,35 γ	X	0,1 γ
16	X	1,05	X	0,4
17	X	1,5	X	1,2
18	0,6	0,1	0,25 γ	0,6
19	0,9	0,7	0,25	1,2
20	Pc 3 rares		P_C 3 rares	
21	Pc 3 rares		P_C 3 rares	
22	Pc 3 rares		P_C 3 rares	
23	0,95	1,15	0,1	1,05
24	0,15	0,4	0,07	0,4
25	0,65	0,35	0,2	0,9
26	0,4	0,15	0,1	0,25
27	0,8	X	0,15	0,9
28	0,6	0,3	0,2	0,75
29	0,5	0,15	0,15	0,6
30	0,3	0,3	0,15	0,4
31	Pc 3 rares		Pc 3 rares	
1 er Juin 1965	Pc 3 rares		Pc 3 rares	
2	0,45	0,35	0,15	0,2
3	0,2	X	0,1	0,35
4	0,45	0,5	0,2	0,3
5	0,45	0,5	0,2	X
6	0,5	0,75	0,15	0,7
7	0,5	0,45	0,15	0,5
8	0,2	0,2	0,07	0,25
9	Pc 3 rares		Pc 3 rares	
10	0,55	0,35	0,1	0,25
11	0,3	0,4	0,15	0,5
12	0,25	0,4	0,1	0,45
13	Pc 3 rares		Pc 3 rares	
14	Pc 3 rares		Pc 3 rares	
15	orage magnétique		orage magnétique	

X : lacunes dans l'enregistrement

TABLEAU II

AMPLITUDES (en γ) de Pc 4 — 13 Juin 1965 (début à 09h 29m T. U.)

H	ADDIS-ABEBA :	1,15 0,7 0,85 1,7 1,1 0,8 0,3 0,4 1,15 0,8 1,4 2,1 1,0 1,05 0,7 1,6 1,2
	GARCHY :	0,85 0,6 0,65 0,55 0,55 0,6 0,3 0,4 0,55 0,7 0,6 0,8 0,6 0,55 0,75 0,7 0,6
D	ADDIS-ABEBA :	0,15 — — — — — — 0,1 — 0,15 — 0,1 0,25 0,15
	GARCHY :	0,8 0,6 0,5 0,35 0,2 0,4 0,3 0,4 0,35 0,9 0,7 0,5 0,6 0,55 0,85 0,7 0,45

TABLEAU III

AMPLITUDES (en γ) de Pi 2

23 Mai 1965 (début à 22h 13m T.U.)

H	ADDIS-ABEBA :	—	—	1,1	1,5	1,15	1,4	1,7	2,2	1,9	1,3	—	1,3	2,1	—	—	1,5	1,45	1,8	1,05
	GARCHY :	—	—	1,5	1,1	0,8	0,9	1,2	1,7	1,35	0,95	0,85	1,1	1,5	—	—	—	1,3	0,7	1,4 0,8
D	ADDIS-ABEBA :	—	—	0,4	0,5	0,4	0,4	0,5	0,5	0,5	0,4	0,4	0,4	0,5	—	—	0,35	0,35	0,4	**0,2**
	GARCHY :	—	—	1,7	1,5	1,1	1,9	2,0	2,3	2,4	0,9	1,45	2,3	0,95	—	—	3,2	1,3	0,7	0,75

23 Mai 1965 (début à 23h 03m T.U.)

H	ADDIS-ABEBA :	—	0,7	0,65	0,65	1,35	1,3	1,0	0,7	0,8	0,4
	GARCHY :	—	0,8	0,6	0,65	1,3	1,1	0,8	0,5	0,5	0,45
D	ADDIS-ABEBA :	—	0,2	0,25	0,2	0,35	0,3	0,25	0,25	0,2	0,1
	GARCHY :	—	1,2	1,2	0,6	1,05	1,2	0,9	0,4	0,4	—

4 Juin 1965 (début à 23h 46m T.U.)

H	ADDIS-ABEBA :	—	0,3	0,5	0,2	0,45	1,3	0,7	0,8	0,9	0,45	0,2	0,2	0,4	0,6	0,05	0,3	0,5	0,5	
	GARCHY :	—	0,8	0,7	—	—	2,1	1,3	1,1	1,1	1,05	0,65	0,5	0,65	—	0,65	0,5	0,3		
D	ADDIS-ABEBA :	—	0,1	0,15	0,15	0,25	0,45	0,35	0,35	0,25	0,2	0,1	0,05	0,15	0,10	0,03	0,05	0,15	0,15	
	GARCHY :	—	1,1	1,15	—	—	2,6	2,1	1,9	1,6	0,95	0,9	1,3	1,15	—	1,05	0,8	0,3		

Conclusion

Une amplification des pulsations par l'electrojet équatorial n'a pas été mise en èvidence dans cette comparaison portant sur une periode limitée. L'anoindrissement considérable, a l'équateur, des pulsations de très courte période pourrait résulter de deux mécanismes entière·ment différents :

1) des conditions d'excitation très peu favorables pour les P_C 1.

2) une absorption ionosphérique très intense pour la micro-structure fine des Pi 2 (Pi 1).

SUMMARY OF THE SESSION

by

Rosemary Hutton

Ahmadu Bello University, Zaria, Nigeria

The session on Low Latitude Magnetic Pulsations was probably the briefest session at this Symposium. The chairman, for this topic, was Dr Heirtzler and the review paper was given by Dr Campbell; only two papers on recent work were presented. This should not be regarded, however, as indicative of either a lack of interest in equatorial micropulsation studies or of a lack of significant problems which may be invesgated in the equatorial region.

In his review, Dr. Campbell showed how certain well- planned studies of irregular pulsations of period grater than 60 seconds had already revealed a close relationship between the amplitude of this type of activity at a particular equatorial station and the instantaneous values of the Sq current strength at that station; he pojnted out the need for supplementation of existing studies of regular pulsations of period 10-60 seconds and for the explanation of the anomalous behavior of this phenomena in the equatorial region during the IGY. He also stressed the need for studies of regular pulsations of period less than 10 seconds, as there is practically no published work for this type of activity at equatorial stations.

It is encouraging to note that both the projects reported at this session were undertaken as a direct results of recommendations made at previous scientific meetings. The low latitude conjugate point micropulsation study at two Brazilian stations arose from a recommendation made at the first Equatorial Symposium in 1962 and the study of rapid variation at Addis Ababa was recommended by IAGA at the Berkeley meeting of IUGG in 1963. In both cases, individual pulsation events at two stations have been compared. The conjugate point study showed that even for stations 3000 km apart, there was a remarkably close correspondance in activity of period in the range 50-1000 seconds. The suggestion that the degree of coherence might be slightly less when the Sq current is stronger merits further study. The comparison of pulsations at Addis Ababa, with corresponding pulsations observed in France suggested that there was reasonable correspondence between equatorial and mid-latitude pulsational activity for periods greater than 4 or 5 seconds, but that the shorter period regular and irregular pulsations observed at mid-latitudes were not detectable at the equator. In the discussion, which followed, it was suggested that the amplitude of the Pc 4 pulsations at the two stations should be examined further to see

whether there might be some indication of enhancement of this type of activity around mid-day. It was also noted that Pc 1, of mean period about 1.5 seconds and amplitude as great as 2 gammas had been observed at a Nigeria station in April of this year.

During informal discussions, attended by eight delegates, it was noted that, in addition to the work reported at this Symposium, an encouraging number of new micropulsation studies are now in progress at other equatorial stations. Reports of analysis of the recordings which are being made in Peru are awaited with interest. Some preliminary analysis has already been made of rapid variations recorded at the University of Ceylon and studies in this field are, at the present time, being initiated at universities in Uganda and Nigeria, and also at the CNAE Station at Natal (Brazil). It is also hoped that some rapid variation studies will be resumed in Ghana in the near future.

In view of the additional facilities now available for equatorial micropulsation recording, it might be useful to those who are becoming engaged in this field of study at equatorial stations, to point out the direction in which it was felt future research should be oriented. There is still a need for basic information, such as magnitude and occurrence frequency, of the various types of phenomena which may be detected in the equatorial region — this type of information is of somewhat restricted use by itself, but it can and should be obtained by each equatorial station from its own recordings. To obtain some understanding of the physical nature of the origin of the various types of micropulsation however, two methods of approach have beem recommended. Firstly, it is suggested that the relationship between rapid magnetic variations and time varying ionospheric parameters should be determined. Secondly, simultaneous observations from two or more stations, both across and along the dip equator and also in the electrojet region and outside, are essential for the separation of those events of hydromagnetic origin from those associated with ionospheric currents — this latter group should show some enhancement near the dip equator around mid-day.

The operation of a network of recording stations is probably too ambitious a project for most equatorial stations to consider attempting by themselves. It is of such interest, however, that it is to be hoped that a co-operative study, involving several organizations, may materialize as a result of the discussions at this Symposium.

AUTHOR INDEX